UNIVERSIDAD COMPLUTENSE DE MADRID
FACULTAD DE CIENCIAS QUÍMICAS
Departamento de Química Orgánica I

HIGH AFFINITY EXTTF-BASED RECEPTORS FOR FULLERENES

MEMORIA PARA OPTAR AL GRADO DE DOCTOR
PRESENTADA POR

Beatriz Helena Isla Mata

Bajo la dirección de los doctores

Nazario Martín Léon
Emilio M. Pérez

Madrid, 2013

UNIVERSIDAD COMPLUTENSE DE MADRID
FACULTAD DE CIENCIAS QUÍMICAS
Departamento de Química Orgánica

HIGH AFFINITY exTTF-BASED RECEPTORS FOR FULLERENES

TESIS DOCTORAL

Beatriz Helena Isla Mata

Madrid, 2013

HIGH AFFINITY exTTF-BASED RECEPTORS FOR FULLERENES

Directores:

Dr. Nazario Martín León

Dr. Emilio M. Pérez

Memoria que para optar al grado de

DOCTOR EN CIENCIAS QUÍMICAS

presenta

Beatriz Helena Isla Mata

MADRID

Septiembre, 2013

Agradecimientos

El presente trabajo ha sido realizado en el Departamento de Química Orgánica de la Universidad Complutense de Madrid, bajo la dirección del Profesor Nazario Martín y el Doctor Emilio M. Pérez. Quisiera agradecer a mis directores y al anterior Ministerio de Educación la concesión de una Beca predoctoral del programa nacional de Formación de Profesorado Universitario que ha hecho posible la realización del presente trabajo.

Un agradecimiento especial a todas las personas que han participado en los trabajos que presento en esta tesis: dentro del grupo de investigación, además de a mis directores, quiero agradecer muy especialmente a los Doctores David Canevet y Fulvio Brunetti por trabajar conmigo y todo lo que he aprendido trabajando con ellos, también a mis compañeros María Gallego y Alberto de Juan; por todos sus cálculos teóricos y su importante aportación a los trabajos al Profesor Enrique Ortí, Doctor Rafael Viruela y a Juan Aragó del ICMol de la Universidad de Valencia; por la medidas fotofísicas al Profesor Dirk M. Guldi y al Doctor Bruno Grimm de la Universidad de Erlangen; al Profesor Javier de Mendoza, al Doctor Carles Bo y a la Doctora Elisa Huerta del ICIQ por permitirme participar con ellos en el desarrollo de receptores basados en CTV, a Elisa especialmente por permitirme ser su padawan y por todo lo que me enseñó durante el comienzo de mi tesis, que a mi parecer ha sido determinante; agradecimientos también a la Universidad de la Habana al Profesor Roberto Cao y al Doctor Roberto Cao Jr., al Doctor Roberto Cao Jr. por abrirme el campo de las nanopartículas y por ser un compañero de mesa verdaderamente chévere.

También merecen un reconocimiento todos los colaboradores que no aparecen en las publicaciones: el CAI de RMN de la Complutense por su magnífico trabajo, su eficiencia y su disposición; el servicio de masas de la Universidad Autónoma; los distintos servicios del Centro Nacional de Microscopía que tanta paciencia han tenido en AFM, SEM y TEM, y todos los servicios de asistencia a la investigación que tanto nos ayudan cuando son bien llevados.

Mi agradecimiento también a mis anfitriones en las estancias fuera de la Complutense, al Profesor Javier de Mendoza por mi mes en el ICIQ en Tarragona al principio de mi tesis y al Profesor Ben L. Feringa en la Universidad de Groningen por su cercanía durante mi estancia breve, que además me ha permitido solicitar una mención europea y aprender muchísimo sobre el funcionamiento de un grupo de tan alto nivel. También hicieron como anfitriones muchos compañeros de estos laboratorios, por tenerlo más reciente quiero mencionar los nombres de algunos de los compañeros de Groningen: gracias a Paula de Mendoza por hacer de anfitriona, a Martín Fañanás por ser un apoyo divertido, a Kuang-Yen Chen (Peter) por estar siempre dispuesto a ayudar, a Matea Vlatkovic por su cariño, a Claudia Poloni, Wiktor, Bea, Jiawen, Arjen, Nop y a todos los que hicieron mi estancia más agradable. Tampoco puedo dejar sin mencionar a Enrique Cequier y de nuevo a Elisa por toda su paciencia y ayuda en el ICIQ.

Este trabajo ha estado enmarcado en un ecosistema muy especial de fauna muy variada, mis agradecimientos también a todos los que han pasado durante estos años por el laboratorio de Nazario, en orden cronológico según recuerdo: Salvatore, Martita, Agustín, Noemí, José Santos, Juan Luis Murcia, Fatimuchi, Antonio, Raúl, Carmen La Brava, Oobelto, Pierre-Antoine, todos los que se me olvidan por esas fechas y los profes, a los nuevos (para mí) Javi, Sonia, Alberto Muchachito, el breve paso de André, los vecinos del Q02 y del Q23, especialmente a mi superamiga Helena (Jelen), porque por independiente que intente ser siempre hace falta una superamiga en estos andares.

La presente tesis ha sido terminada y escrita en IMDEA Nanociencia, una vez fuera de mi medio natural en la Complutense quiero incluir en este apartado a mis últimos compañeros de edificio, de planta y de laboratorio, una pena no haber coincidido por más tiempo Sofía. Espero que todo os vaya fenomenal en este sitio tan silencioso.

Reitero el agradecimiento a mis directores, Nazario y Emilio, por su dedicación y esfuerzo, que me han ayudado a convertirme en investigadora para el resto de mi vida. Quiero agradecer en especial al Emilio del pasado, al que molaba tanto que me enseñó todo desde cero y tenía todo el tiempo del mundo, ha sido una gran oportunidad ser tu primera doctoranda y andar en ese laboratorio codo con codo, espero haberlo aprovechado lo suficiente.

Fuera de la Universidad he de agradecer muy especialmente a Juan Pablo, mi pareja, por la financiación durante mi primer año de tesis, el comienzo de este trabajo y mi llegada a la investigación no hubiese sido posible sin él. Muchas gracias por aquel voto de confianza y por los que me sigues dando. También mencionar en la financiación la ayuda de mis padres, gracias también por enseñarme la importancia de conseguir un trabajo que realmente me guste.

REFERENCES, ABBREVIATIONS AND ACRONYMS

Bibliographic citations have been placed as footnotes in the pages where they were first cited in the section and at the end of each section or chapter; they were added independently at every section or chapter, so they are duplicated in different chapters when necessary

Throughout this manuscript, abbreviations and acronyms recommended by the American Chemical Society in the Organic Chemistry area (revised in the *Journal of Organic Chemistry* on January **2013**; http://pubs.acs.org/paragonplus/submission/joceah/joceah_authguide.pdf) have been employed. In addition, those indicated below have also been used.

A	Acceptor
AFM	Atomic Force Microscopy
D	Donor
Eox	Oxidation potentional
Ered	Reduction potentional
ESR	Electron spin resonance
LESR	Ligth-induced electron spin resonance
exTTF	π-extended tetrathiafulvalene
Fc	Ferrocene
FLG	Few layers graphene
MEH-PPV	Poly[2-methoxy-5-(2 ethylhexyloxy)-1,4 phenylenevinylene]
MDMO-PPV	Poly[2-methoxy-5-(3',7'-dimethyloctyloxy)-1,4-phenylenevinylene]
P3HT	Poly-3-hexylthiophene
PSC	Photosynthetic reaction centre
PCBM	1-(3-methoxycarbonylpropil)-1-phenyl[6,6] methanofullerene
Upy	2-ureido-4-[1H]-pyrimidone
CTV	Cyclotriveratrylene
NDI	Naphthalenediimide
St-PMMA	Syndiotactic poly (methyl methacrylate)

ULGA	Ultralight graphene aerogel
PAH	Polycyclic aromatic hydrocarbon
PBI	Perylene bisimides
PET	Photoinduced electron transfer
IC_{50}	Inhibitory concentration 50
TTF	Tetrathiafulvalene
IPR	Isolated pentagon rule
ISC	Intersystem crossing
NLO	Non-linear optics
Pc	Phthalocyanine
0D	Zerodimensional
1D	Unidimensional
2D	Bidimensional
3D	Tridimensional
EnT	Energy transfer
TCAQ	Tetracyanoanthraquinodimethane
DLS	Dynamic light scattering
TOCSY	Total Correlation Spectroscopy
PCBA	[6,6]Pheny C_{61}butyric acic
PhCl	Chlorobenzene
oDCB	*o*-dichlorobenzene
DIAD	Diisopropyl azodicarboxylate
SPR	Surface plasmon resonance
NP	Nanoparticle
TEM	Transmission electron microscopy
MUA	Mercaptundecanoic acid
HA	Hemagglutinin

SA	Sialic acid
EDX	Energy dispersive X-ray spectroscopy
CVD	Chemical vapour deposition
RGO	Reduction of graphene oxide
TGA	Thermogravimetric analysis
FWHM	Full width at half maximum
Trux	Truxene
BSSE	Basis set superposition error
CP	Counterpoise

TABLE OF CONTENTS

According to RD 1393/2007 and 99/2011 the present thesis has been written in English in a publications format. A review about the field and the related previous work of the group has been placed at the beginning. There is a brief general objectives section, after which you can find the seven publications gathered in four chapters according to the different projects. The chapters dedicated to publications contain the corresponding publications content, which was enriched with available supporting information and some short explanatory sub-sections when necessary. After these chapters, a conciliatory general discussion is placed. This section was used to clarify common aspects in the different publications and to perform a comparative of the obtained results. To avoid unnecessary repetitions the objectives, general discussion and conclusions sections have been kept to a minimum. You can also find Spanish and English summaries at the end.

1. INTRODUCTION

1.1. FULLERENES

Fullerenes are molecular allotropes of carbon built up of fused pentagonal and hexagonal rings. The pentagons, absent in graphite, provide curvature. [60]fullerene was discovered by H. W. Kroto, R. F. Curl, and R. E. Smalley in 1985[1] while simulating the conditions under which carbon nucleates in the atmosphere of red giant stars. Using a laser to vaporize graphite rods in an atmosphere of helium gas, these scientist and their assistants obtained cage-like molecules composed of 60 carbon atoms (C_{60}) joined together by single and double bonds to form a hollow sphere with 12 pentagonal and 20 hexagonal faces—a design that resembles a football, or soccer ball. Conditions could be found to get C_{60} signal in mass spectra as dominant, and Kroto and Smalley concluded that the stability of C_{60} stems from its spherical geometry.[1] The C_{60} molecule was coined as buckminsterfullerene after the American architect R. Buckminster Fuller, whose geodesic dome is constructed on the same structural principles (Figure 1). H. W. Kroto, R. F. Curl, and R. E. Smalley were awarded with the Nobel Prize of Chemistry in 1996 for the discovery of fullerenes.[2] In an example of the human ability for prediction, before the discovery of buckminsterfullerene, there were efforts to find new three-dimensional superaromatic π-systems. In 1970 Osawa first proposed the spherical I_h-symmetry football structure of C_{60}, and there were some theoretical papers in which some calculations on C_{60} were reported.[3]

[1] H. W. Kroto, J. R. Heath, S. C. O'Brien, R. F. Curl and R. E. Smalley, *Nature* **1985,** *318*, 162-163.
[2](a) R. F. Curl, *Angew. Chem., Int. Ed. Engl.* **1997,** *36*, 1566-1576; H. Kroto, *Angew. Chem., Int. Ed. Engl.* **1997,** *36*, 1578-1593; (b) R. E. Smalley, *Angew. Chem., Int. Ed. Engl.* **1997,** *36*, 1594-1601.
[3] A. Hirsch and M. Brettreich, Parent Fullerenes. In *Fullerenes*, Wiley-VCH Verlag GmbH & Co. KGaA: 2005; pp 1-48.

The first important breakthrough in fullerene science occurred in 1990, when the astrophysicist Wolfgang Krätschmer and Donald Huffman prepared fullerene C_{60} for the first time in multigram amounts,[4] thus making it available for the scientific community.

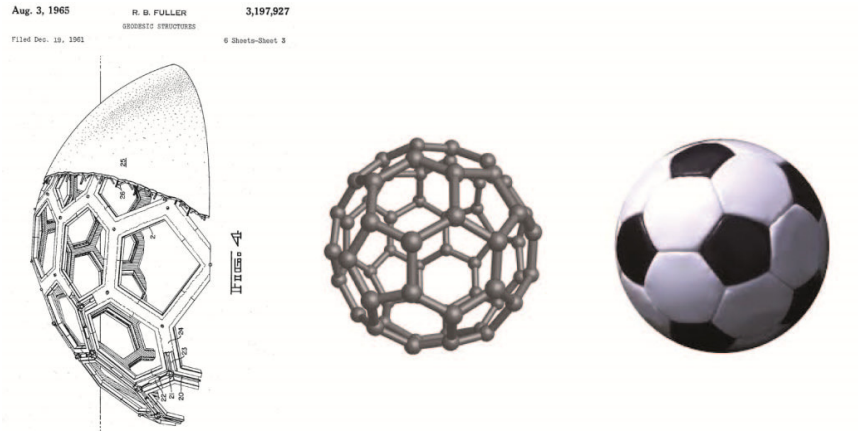

Figura 1. Patent drawing of geodesic domes of Buckminster Fuller,[5] 1961 (left); structure of fullerene C_{60}; and soccer ball (right).

The discovery of fullerenes has been followed by the different carbon allotropes such as carbon nanotubes by S. Iijima in 1991,[6] and graphene by A. K. Geim and K. S. Novoselov in 2004,[7] and all of them sparked the interest of the scientific community, becoming very active areas of research, especially in the field of new materials, and possible biomedical applications.[8]

1.1.1. Physical and spectroscopic properties

The high degree of symmetry and the arrangement of the molecular orbitals are key issues for a number of interesting chemical and physical properties of the fullerenes. Focusing in [60]fullerene, the smallest stable fullerene, it consists of 60 carbon atoms arranged in a sphere of 7.1 Å diameter. In its structure all the pentagonal rings are isolated by hexagons (Isolated Pentagon Rule, IPR), and the covalent bonds between two hexagons ([6,6] bonds) are shorter than the bonds between pentagon and hexagon ([5,6] bonds). The next higher stable fullerene is C_{70},[9] which satisfies IPR and possesses an equatorial belt formed by fused hexagons. It consists in 70 carbon atoms and it is formed by 12 pentagonal rings and 25 hexagonal rings. The pentagons in the structure create destabilization and allow the spherical geometry, which distributes the strain.[3]

---

[4] W. Kratschmer, L. D. Lamb, K. Fostiropoulos and D. R. Huffman, *Nature* **1990,** *347*, 354-358.
[5] R.Buckminster Fuller GEODESIC STRUCTURES (OCR). US 3197927, 1965.
[6] (a) S. Iijima, *Nature* **1991,** *354*, 56-58; D. S. Bethune, C. H. Klang, M. S. de Vries, G. Gorman, R. Savoy, J. Vazquez and R. Beyers, *Nature* **1993,** *363*, 605-607; (b) S. Iijima and T. Ichihashi, *Nature* **1993,** *363*, 603-605.
[7] (a) K. S. Novoselov, A. K. Geim, S. V. Morozov, D. Jiang, Y. Zhang, S. V. Dubonos, I. V. Grigorieva and A. A. Firsov, *Science* **2004,** *306*, 666-669; (b) A. K. Geim and K. S. Novoselov, *Nat Mater* **2007,** *6*, 183-191.
[8] J. L. Delgado, M. A. Herranz and N. Martín, *J. Mater. Chem.* **2008,** *18*, 1417-1426.
[9] H. Ajie, M. M. Alvarez, S. J. Anz, R. D. Beck, F. Diederich, K. Fostiropoulos, D. R. Huffman, W. Kraetschmer, Y. Rubin and et al., *J. Phys. Chem.* **1990,** *94*, 8630-8633.

There are two special properties in the [60]fullerene structure: i) all twelve pentagons are isolated by hexagons; and ii) the called [6,6] bonds, that means the bonds at the junctions of two hexagons, are shorter than the [5,6] bonds, the bonds at the junction of a hexagon and a pentagon. This bond-length alternation shows that in the most stable Kekulé structure, the double bonds are located in the [6,6] bonds and there are no double bonds in the pentagonal rings. The formation of IPR structures enhances the sphericity of the molecules and hence, this spherical shape is able to distribute the strain. Due to the curvature of the buckminsterfullerene molecule each carbon atom presents peculiar $sp^{2.3}$ hybridization and fullerene behave as an electron deficient polyene, with the most reactive positions placed in the [6,6] bonds.

Fullerenes are soluble in some organic solvents, primarily aromatic solvents and carbon disufide, and insoluble in polar and H-bonding solvents. Their solubility plays an important role in the chemistry of fullerenes.

Fullerenes C_{60} and C_{70} are moderate chromophores, with strong absorption between 190 and 410 nm, as a result of allowed transitions, and some absorption in the region between 410 and 620 nm, as a result of orbital forbidden single-singlet transitions (Figure 2). The latter are responsible of the characteristic colour of these fullerenes in solution (purple for C_{60}, and red for C_{70}).

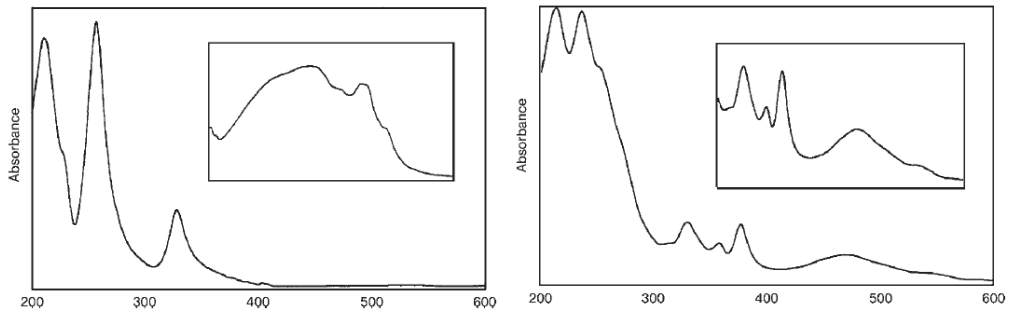

Figure 2. Left: Electronic absorption spectrum of C_{60} in hexane, inset shows 420-470 nm region; Right: Electronic absorption spectrum of C_{70} in hexane, inset shows 300-600 nm region.[3]

The properties found in NMR experiment were a unique signal in ^{13}C NMR spectrum of C_{60} due to the icosahedral symmetry (δ = 143.2 ppm), and five signals in the case of C_{70}.[9] It was important for its first detection that C_{60} has only four active vibrational bands in IR,[4] due to its icosahedral symmetry. In the case of C_{70} the IR spectra is more complex.

1.1.2. Electronic and Photophysical properties

The peculiar electronic properties of fullerenes make them attractive from the photophysical point of view. Photophysical properties have been extensively reviewed.[10] Some of the main properties of C_{60}, which make buckminsterfullerene interesting for different applications, are the following:

- It is a good electron acceptor
- Its LUMO allows for the reversible addition of up to 6 electrons
- It has a low reorganization energy
- It is relatively inert.

Upon irradiation of C_{60} with visible or UV light, an excited singlet state (S1) is reached, which decays very fast via intersystem crossing (ISC, quantum yield ϕ_T > 99%)[11] to the energetically lower triplet excited state (T1). These states are susceptible to various deactivation processes. In the case of dyads, with a covalently linked electron donor, photoinduced electron or energy transfer can take place. The solvent polarity plays an important role in these processes: polar solvents favour electron transfer, since they stabilize the polar charge-separated state. In multicomponent arrays, when there is a face-to-face arrangement of C_{60} with the electron donor, photoinduced electron transfer occurs even in non-polar solvents.[12]

Upon light irradiation and in the presence of oxygen, C_{60} generates excited singlet molecular oxygen with high efficiency by bimolecular quenching (Figure 3).[10a, 11] The photogeneration of singlet oxygen, a highly reactive species involved in oxidative cellular processes, could allow for the development of C_{60}-based photodynamic therapy agents.[13] Moreover, the fact that C_{60} is relatively inert under mild conditions, has made functionalized fullerenes potential candidates for a variety of medicinal applications.[14]

$$C_{60} \xrightarrow{h\nu} {}^1C_{60}^{\cdot} \xrightarrow{ISC} {}^3C_{60}^{\cdot} \xrightarrow[O_2]{EnT} {}^1O_2^{\cdot}$$

Figure 3. Photosensitization process of oxygen via a triplet-singlet electron-exchange energy transfer process.

---

[10] (a) J. W. Arbogast, A. P. Darmanyan, C. S. Foote, F. N. Diederich, R. L. Whetten, Y. Rubin, M. M. Alvarez and S. J. Anz, *J. Phys. Chem.* **1991,** *95*, 11-12; (b) T. W. Ebbesen, K. Tanigaki and S. Kuroshima, *Chem. Phys. Lett.* **1991,** *181*, 501-504; (c) D. M. Guldi and M. Prato, *Acc. Chem. Res.* **2000,** *33*, 695-703.

[11] R. R. Hung and J. J. Grabowski, *J. Phys. Chem.* **1991,** *95*, 6073-6075.

[12] (a) P. A. Liddell, J. P. Sumida, A. N. Macpherson, L. Noss, G. R. Seely, K. N. Clark, A. L. Moore, T. A. Moore and D. Gust, *Photochem. Photobiol.* **1994,** *60*, 537-541; (b) N. Armaroli, G. Marconi, L. Echegoyen, J.-P. Bourgeois and F. Diederich, *Chem. Eur. J.* **2000,** *6*, 1629-1645.

[13] T. Da Ros and M. Prato, *Chem. Commun.* **1999,** *0*, 663-669.

[14] (a) A. W. Jensen, S. R. Wilson and D. I. Schuster, *Biorg. Med. Chem.* **1996,** *4*, 767-779; (b) K. M. Kadish and R. S. Ruoff, *Fullerenes: Chemistry, Physics, and Technology*. Wiley: 2000.

Fullerene C_{60} is a good electron acceptor,[10c, 14b, 15] and its triply-degenerate low-lying LUMO allows for the reversible addition of up to six electrons.[14b, 16] This was supported by cyclic voltammetry measurements carried out with C_{60} in solution as we can see in figure 4, which shows its facile and stepwise reduction.[17] All the reductions are one-electron transfer processes, and even the hexaanion is stable and exhibits reversible behavior on the voltammetry time scale.[14b, 18] A peculiar characteristic is that there are six equally-spaced reduction waves, and this is regarded as a clear manifestation for conditions that guarantee the optimal delocalization of electrons. These properties have led to the synthesis of a large number of donor-acceptor systems in which C_{60} acts as an electron acceptor. Remarkably, small reorganization energies are associated with the reduction of C_{60} and its derivatives. Under optimal conditions, small reorganization energy leads to optimal charge-separation kinetics, and a deceleration of charge-recombination rates. That is, charge-recombination in these systems occurs more slowly than photoelectron transfer which results in the generation of relatively long-lived charge-separated states. Thus, donor-acceptor arrays containing fullerene have been proposed as models for photosynthesis and as energy storage systems.[14b, 15b, 19]

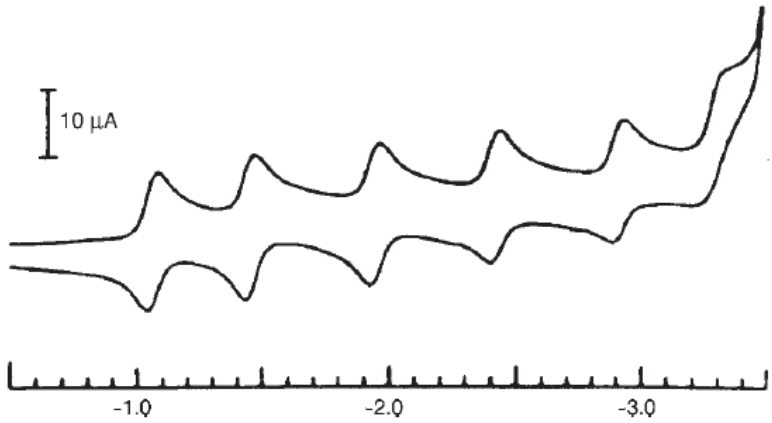

Figure 4. Cyclic voltammogram of C_{60} in acetonitrile–toluene with $TBAPF_6$ as supporting electrolyte at −10 °C using CV at a 100 mV s^{-1} scan rate (mV vs Fc/Fc^{+}).[18]

Related to its electronic features the structural similarity between C_{60} in the ground, excited, or reduced state is remarkable. This fact implies that the structural rigidity of the fullerene core allows a high degree of delocalization of charge density.

[15] (a) N. Martín, L. Sánchez, B. Illescas and I. Pérez, *Chem. Rev.* **1998,** *98*, 2527-2548; (b) H. Imahori and Y. Sakata, *Eur. J. Org. Chem.* **1999,** *1999*, 2445-2457; (c) D. M. Guldi, *Chem. Commun.* **2000,** *0*, 321-327.
[16] (a) R. C. Haddon, L. E. Brus and K. Raghavachari, *Chem. Phys. Lett.* **1986,** *125*, 459-464; (b) P. D. Hale, *J. Am. Chem. Soc.* **1986,** *108*, 6087-6088.
[17] Q. Xie, E. Perez-Cordero and L. Echegoyen, *J. Am. Chem. Soc.* **1992,** *114*, 3978-3980.
[18] L. Echegoyen and L. E. Echegoyen, *Acc. Chem. Res.* **1998,** *31*, 593-601.
[19] (a) H. Imahori and Y. Sakata, *Adv. Mater.* **1997,** *9*, 537-546; (b) D. Gust, T. A. Moore and A. L. Moore, *Acc. Chem. Res.* **2000,** *34*, 40-48; (c) D. M. Guldi, *Chem. Soc. Rev.* **2002,** *31*, 22-36.

Besides as an electron acceptor, C_{60} has been used in several different fields, including: superconductivity,[20] ferromagnetism,[21] as a building block in NLO materials,[22] and in materials with biological activity.[13-14] For the purpose of this introduction, we will focus in applications in the field of optoelectronic devices.[23]

1.1.3. Photovoltaic applications

Photoinduced electron transfer is a fundamental process in nature since it governs photosynthesis in plants and bacteria. The human being needs to face the energy problem, and designing new molecular materials capable to harvest and transform solar energy into chemical or electrical power represents one of the more promising alternatives.

Owing to its unique photophysical and electrochemical features, fullerene C_{60} is the electron acceptor of choice for most organic photovoltaic devices. Photoinduced electron transfer processes from suitable electron donors to fullerenes have been studied, and the design of a wide variety of donor-acceptor systems, acting as artificial photosynthetic centres, represents one of the most active research areas in fullerene chemistry.

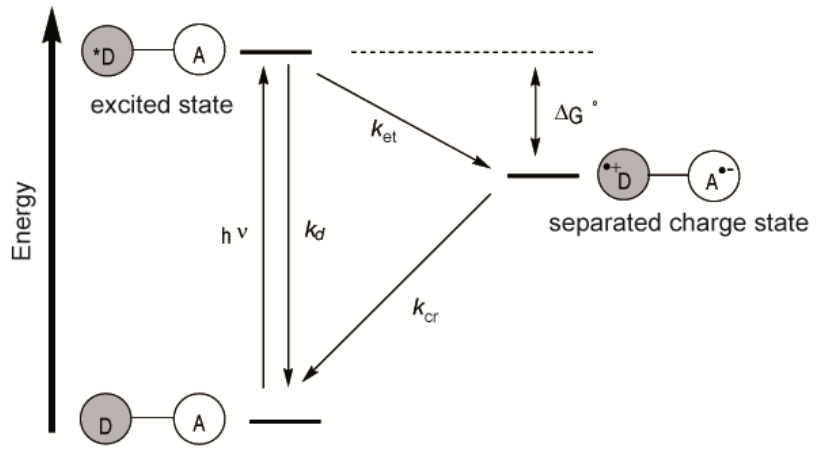

Figure 5. Photoinduced electron transfer process in a donor-acceptor system.

[20] (a) A. F. Hebard, M. J. Rosseinsky, R. C. Haddon, D. W. Murphy, S. H. Glarum, T. T. M. Palstra, A. P. Ramirez and A. R. Kortan, *Nature* **1991,** *350*, 600-601; (b) A. R. Kortan, N. Kopylov, S. Glarum, E. M. Gyorgy, A. P. Ramirez, R. M. Fleming, F. A. Thiel and R. C. Haddon, *Nature* **1992,** *355*, 529-532; (c) J. H. Schon, C. Kloc and B. Batlogg, *Nature* **2000,** *408*, 549-552.

[21] P.-M. Allemand, K. C. Khemani, A. Koch, F. Wudl, K. Holczer, S. Donovan, G. Grúner and J. D. Thompson, *Science* **1991,** *253*, 301-302.

[22] L. W. Tutt and A. Kost, *Nature* **1992,** *356*, 225-226.

[23] (a) Gust, Moore and Moore; C. J. Brabec, N. S. Sariciftci and J. C. Hummelen, *Adv. Funct. Mater.* **2001,** *11*, 15-26; (b) A. Cravino and N. S. Sariciftci, *J. Mater. Chem.* **2002,** *12*, 1931-1943; (c) D. M. Guldi and N. Martín, *J. Mater. Chem.* **2002,** *12*, 1978-1992; (d) M. Prato and N. Martín, *J. Mater. Chem.* **2002,** *12*, 7-ix-7-ix; (e) N. Martín, L. Sánchez, M. a. Á. Herranz, B. Illescas and D. M. Guldi, *Acc. Chem. Res.* **2007,** *40*, 1015-1024; (f) J. L. Delgado, P.-A. Bouit, S. Filippone, M. a. A. Herranz and N. Martín, *Chem. Commun.* **2010,** *46*, 4853-4865.

There are some aspects that the design of a photovoltaic device must take into account. In figure 5 the different processes upon irradiation are shown. The absorption of light by D-A system provokes a singlet excited state, where the energy is localized in the donor. Ideally, the rate of non-productive deactivation pathway (k_d) should be significantly smaller than the rate of electron transfer (k_{et}), giving rise to a charge-separated state which will relax back to the ground state by means of a charge recombination process (k_{cr}). The energy contained in the charge-separated state must be as large as possible to get more chemical potential from light; hence, ΔG^o must be as small as possible.

Different strategies have been used for the design of new devices that incorporate fullerene as electron acceptor, from the use of pristine C_{60} or derivatives as electron acceptors to the design of donor-acceptor systems, such as molecular dyads, triads, etc., in which the electroactive units are connected by covalent or supramolecular bonds.[15a]

- **From pristine C_{60} to PCBM.**

Although C_{60} is a useful material for photovoltaic devices, its low solubility in common organic solvents, strong tendency to crystallize (phase separate), and lack of miscibility with π-conjugated polymers make it much less useful for application in composite layers, especially in bulk-heterojunction solar cells, where it often results in phase segregation. This phase segregation decreases the donor-acceptor interaction as well as the charge transport of the photogenerated electron and holes.[24] In order to overcome this problem C_{60} derivatives with solubilizing groups were synthesized. It has become clear that derivative 1-(3-methoxycarbonylpropil)-1-phenyl[6,6] methanofullerene[25] (PCBM, figure 6) was a successful choice. This derivative presents a high solubility in aromatic hydrocarbons and in carbon disulfide.

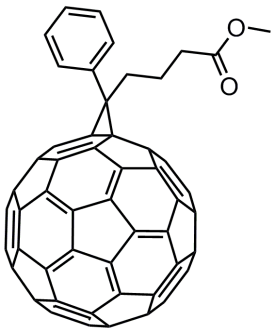

Figure 6. Structure of PCBM.

Homogenous and stable blends were prepared with this derivative and a *p*-phenylenevinylene polymeric electron donor (MEH-PPV) forming the first PCBM-

[24] S. E. Shaheen, C. J. Brabec, N. S. Sariciftci, F. Padinger, T. Fromherz and J. C. Hummelen, *Appl. Phys. Lett.* **2001,** *78*, 841-843.
[25] J. C. Hummelen, B. W. Knight, F. LePeq, F. Wudl, J. Yao and C. L. Wilkins, *J. Org. Chem.* **1995,** *60*, 532-538.

based bulk heterojunction solar cell, which showed a carrier collection efficiency of 29 %.[26] In 2001 a 2.5 % conversion efficiency was reported[24] using poly[2-methoxy-5-(3',7'-dimethyloctyloxy)-1,4-phenylenevinylene] (MDMO-PPV) and PCBM in a 1:4 ratio. The use of chlorobenzene instead of toluene as solvent increased the efficiency by a factor of three due to the changes in the morphology of the device. A couple of years later, using the same poly-*p*-phenylenevinylene and C_{70} PCBM instead of C_{60} PCBM, a 3.0 % conversion efficiency under standard conditions was reported.[27] Using a different polymer, poly-3-hexylthiophene (P3HT), with PCBM, a bulk heterojunction solar cell with conversion efficiency above 5 % was prepared.[28]

- **Donor-fullerene molecular dyads.**

The covalent linkage of electron donors to fullerene by means of flexible or rigid spacers has been the most studied approach, forming dyads, triads, etc. A wide variety of electron donors have been covalently linked to fullerenes, such as porphyrins,[19c, 29] organometallic compounds such as ferrocenes,[30] Ru^{II}bipyridine,[31] carotenes,[32] aniline derivatives,[33] π-conjugated oligomers,[34] phthalocyanines,[35] and tetrathiafulvalenes.[23e] However, not many photovoltaic devices have been prepared and characterized, and thorough studies are required to understand the relationship existing between molecular structure, electron-transfer dynamics, and device function.

[26] G. Yu, J. Gao, J. C. Hummelen, F. Wudl and A. J. Heeger, *Science* **1995,** *270*, 1789-1791.
[27] M. M. Wienk, J. M. Kroon, W. J. H. Verhees, J. Knol, J. C. Hummelen, P. A. van Hal and R. A. J. Janssen, *Angew. Chem. Int. Ed.* **2003,** *42*, 3371-3375.
[28] (a) P. Schilinsky, C. Waldauf and C. J. Brabec, *Appl. Phys. Lett.* **2002,** *81*, 3885-3887; (b) F. Padinger, R. S. Rittberger and N. S. Sariciftci, *Adv. Funct. Mater.* **2003,** *13*, 85-88.
[29] H. Imahori, *J. Phys. Chem. B* **2004,** *108*, 6130-6143.
[30] (a) D. M. Guldi, M. Maggini, G. Scorrano and M. Prato, *J. Am. Chem. Soc.* **1997,** *119*, 974-980; (b) M. Fujitsuka, N. Tsuboya, R. Hamasaki, M. Ito, S. Onodera, O. Ito and Y. Yamamoto, *J. Phys. Chem. A* **2003,** *107*, 1452-1458; (c) D. M. Guldi, C. Luo, N. A. Kotov, T. D. Ros, S. Bosi and M. Prato, *J. Phys. Chem. B* **2003,** *107*, 7293-7298.
[31] (a) D. M. Guldi, M. Maggini, E. Menna, G. Scorrano, P. Ceroni, M. Marcaccio, F. Paolucci and S. Roffia, *Chem. Eur. J.* **2001,** *7*, 1597-1605; (b) J.-F. Nierengarten, N. Armaroli, G. Accorsi, Y. Rio and J.-F. Eckert, *Chem. Eur. J.* **2003,** *9*, 36-41.
[32] S. N. Smirnov, P. A. Liddell, I. V. Vlassiouk, A. Teslja, D. Kuciauskas, C. L. Braun, A. L. Moore, T. A. Moore and D. Gust, *J. Phys. Chem. A* **2003,** *107*, 7567-7573.
[33] R. M. Williams, J. M. Zwier and J. W. Verhoeven, *J. Am. Chem. Soc.* **1995,** *117*, 4093-4099; K. G. Thomas, V. Biju, D. M. Guldi, P. V. Kamat and M. V. George, *J. Phys. Chem. B* **1999,** *103*, 8864-8869.
[34] (a) D. M. Guldi, C. Luo, A. Swartz, R. Gómez, J. L. Segura, N. Martín, C. Brabec and N. S. Sariciftci, *J. Org. Chem.* **2002,** *67*, 1141-1152; (b) D. M. Guldi, A. Swartz, C. Luo, R. Gómez, J. L. Segura and N. Martín, *J. Am. Chem. Soc.* **2002,** *124*, 10875-10886; (c) J. L. Segura, N. Martín and D. M. Guldi, *Chem. Soc. Rev.* **2005,** *34*, 31-47; (d) C. M. Atienza, G. Fernández, L. Sánchez, N. Martín, I. S. Dantas, M. M. Wienk, R. A. J. Janssen, G. M. A. Rahman and D. M. Guldi, *Chem. Commun.* **2006,** *0*, 514-516; (e) G. Fernández, L. Sánchez, D. Veldman, M. M. Wienk, C. Atienza, D. M. Guldi, R. A. J. Janssen and N. Martín, *J. Org. Chem.* **2008,** *73*, 3189-3196.
[35] M. Antonietta Loi, P. Denk, H. Hoppe, H. Neugebauer, C. Winder, D. Meissner, C. Brabec, N. Serdar Sariciftci, A. Gouloumis, P. Vazquez and T. Torres, *J. Mater. Chem.* **2003,** *13*, 700-704.

- **exTTF-based dyads with fullerene**

Our group has reported a vast variety of dyads containing fullerene and tetrathiafulvalene (TTF) derivatives. Unlike other electron donors, TTF and its *p*-quinonoid analogue 2-[9-(1,3-dithiol-2-ylidene)anthracen-10(9H)-ylidene]-1,3-dithiole (exTTF) become aromatic upon oxidation. The aromatization affords thermodynamically stable radical-cationic and dicationic species at relatively low oxidation potentials.[36] This is a crucial factor in the stabilization of the photogenerated radical ion pairs, one of the objectives to improve efficiencies in possible devices. Besides this, TTF derivatives feature some of highest hole mobilities for solution-processed materials.[37]

The first TTF/C_{60} conjugate was reported in 1996,[38] and its photophysical properties in 2000,[39] which showed lifetimes for the charge-separated state of around 2 ns. Lifetimes around 200 ns were found in the case of the analogues with exTTF[40] instead of TTF. This stabilization of the radical ion pairs is rationalized in terms of the aromaticity that is gained during the transformation of the ground state into the radical-cation species.

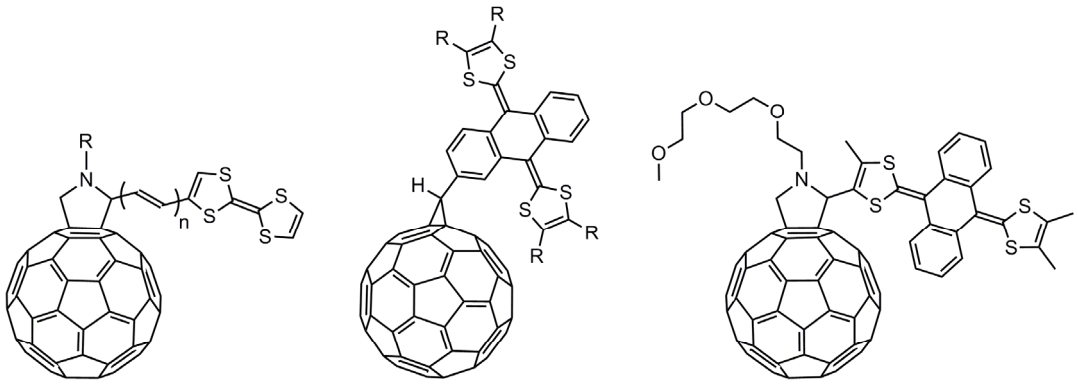

Figure 7. Topologically different C_{60}/TTF and C_{60}/exTTF conjugates and lifetime for the respective radical ion pairs.

[36] (a) Y. Yamashita, Y. Kobayashi and T. Miyashi, *Angew. Chem., Int. Ed. Engl.* **1989,** *28*, 1052-1053; (b) M. R. Bryce, A. J. Moore, M. Hasan, G. J. Ashwell, A. T. Fraser, W. Clegg, M. B. Hursthouse and A. I. Karaulov, *Angew. Chem., Int. Ed. Engl.* **1990,** *29*, 1450-1452; (c) N. Martín, L. Sánchez, C. Seoane, E. Ortí, P. M. Viruela and R. Viruela, *J. Org. Chem.* **1998,** *63*, 1268-1279; (d) C. A. Christensen, A. S. Batsanov and M. R. Bryce, *J. Am. Chem. Soc.* **2006,** *128*, 10484-10490.

[37] (a) N. Gautier, F. Dumur, V. Lloveras, J. Vidal-Gancedo, J. Veciana, C. Rovira and P. Hudhomme, *Angew. Chem. Int. Ed.* **2003,** *42*, 2765-2768; (b) M. Mas-Torrent, P. Hadley, S. T. Bromley, X. Ribas, J. Tarrés, M. Mas, E. Molins, J. Veciana and C. Rovira, *J. Am. Chem. Soc.* **2004,** *126*, 8546-8553.

[38] N. Martín, L. Sánchez, C. Seoane, R. Andreu, J. Garín and J. Orduna, *Tetrahedron Lett.* **1996,** *37*, 5979-5982.

[39] N. Martín, L. Sánchez, M. A. Herranz and D. M. Guldi, *J. Phys. Chem. A* **2000,** *104*, 4648-4657.

[40] M. C. Díaz, M. A. Herranz, B. M. Illescas, N. Martín, N. Godbert, M. R. Bryce, C. Luo, A. Swartz, G. Anderson and D. M. Guldi, *J. Org. Chem.* **2003,** *68*, 7711-7721.

Three main facts prompted the evolution of the next strategy, the supramolecular chemistry of fullerenes: i) the arrangement of the donor-acceptor couples in the photosynthetic reaction centre (PRC)[41] is performed by non-covalent interactions; ii) photoinduced electron transfer between a donor and C_{60} may take place through space; iii) the nanometric organization of p- and n-type materials in photovoltaic devices is expected to facilitate charge mobility, preventing recombination.[42]

1.2. SUPRAMOLECULAR CHEMISTRY

1.2.1. Definition, development, and concepts.

In 1987 the Nobel Prize in Chemistry was awarded jointly to Donald J. Cram, Jean-Marie Lehn and Charles J. Pedersen *"for their development and use of molecules with structure-specific interactions of high selectivity"*. To provide a first approach to supramolecular chemistry it is appropriate to cite Jean Marie Lehn's words from his Nobel lecture: "*Supramolecular chemistry may be defined as chemistry beyond the molecule, bearing on the organized entities of higher complexity that result from the association of two or more chemical species held together by intermolecular forces.[…] One may say that supermolecules are to molecules and the intermolecular bond what molecules are to atoms and the covalent bond.*" Molecular associations have been studied for a long time and the term "supermolecule" was introduced already in the mid-1930's to describe entities of higher organization resulting from the association of coordinatively saturated species.

There are some important events about the origin of this new field of research. For example Charles J. Pedersen first reported alkali metal ions binding crown ether to form highly structured complexes,[43] and J.- M. Lehn, J.- P. Sauvage, and B. Dietrich reported papers about binding properties of cryptands in 1969 (figure 8).[44] Some years later Cram outlined that complexes between organic compounds simulate the substrate selectivity of enzymes.[45]

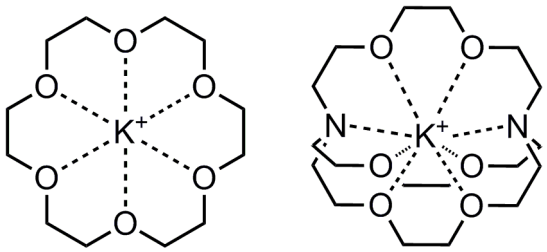

[41] (a) W. Khlbrandt and D. N. Wang, *Nature* **1991,** *350*, 130-134; (b) G. McDermott, S. M. Prince, A. A. Freer, A. M. Hawthornthwaite-Lawless, M. Z. Papiz, R. J. Cogdell and N. W. Isaacs, *Nature* **1995,** *374*, 517-521.
[42] C.-H. Huang, N. D. McClenaghan, A. Kuhn, J. W. Hofstraat and D. M. Bassani, *Org. Lett.* **2005,** *7*, 3409-3412.
[43] C. J. Pedersen, *Journal of the American Chemical Society* **1967,** *89*, 2495-2496; , 7017-7036.
[44] (a) B. Dietrich, J. M. Lehn and J. P. Sauvage, *Tetrahedron Lett.* **1969,** *10*, 2885-2888; (b) B. Dietrich, J. M. Lehn and J. P. Sauvage, *Tetrahedron Lett.* **1969,** *10*, 2889-2892.
[45] D. J. Cram and J. M. Cram, *Science* **1974,** *183*, 803-809.

Figure 8. Complexation of Pedersen's 18-crown-6 (left) and Lehn's [2.2.2] cryptand (right) with K^+.

If we consider supramolecular chemistry in its simplest sense, as involving some kind of noncovalent binding event, we generally consider a molecule as a *host* binding another molecule as a *guest* to form a "host-guest" complex or supermolecule. Usually the larger molecule with *convergent* binding sites is considered the host (Lewis basic donor atoms, hydrogen bond donors, etc.) and the smaller molecule with *divergent* binding sites is considered the guest. These supramolecules or molecular complexes are held together by a range of noncovalent forces, all of which are fundamentally electrostatic in nature:[46] hydrogen bonding, ion pairing, π-acid to π-base interactions, metal to ligand binding, van der Waals attractive forces, etc. (figure 9). Considering a supramolecular system, it is necessary to consider the interplay of all these interactions and effects relating to the host and the guest as well as their surroundings. An approximation of their energies is shown in the table below; it is worth noting that they are all weaker than covalent bonds.

Table 1. Noncovalent interactions and related energies.[47]

Interaction	Strength (kJ mol^{-1})
Ion-ion	200-300
Ion-dipole	50-200
Dipole-dipole	5-50
Hydrogen bonding	4-120
Cation-π	5-80
π–π	0-50
Van der Waals	< 5 but variable with surface area
Solvophobic	Related to solvent-solvent interaction energy

The assembly of small molecules implies a delicate balance between enthalpy (association energy) and entropy (organization penalty).[48] The concepts of

[46] C. A. Hunter, *Angew. Chem. Int. Ed.* **2004,** *43*, 5310-5324.
[47] J. W. Steed and J. L. Atwood, Concepts. In *Supramolecular Chemistry*, John Wiley & Sons, Ltd: 2009; pp 1-48.

cooperativity, macrocyclic effects,[49] complementarity and host preorganization[50] are essential to tweak the equilibrium between enthalpy and entropy to favor association.

Often, more than one type of interaction and/or interaction points are involved in the formation of a host-guest complex. We achieve *positive cooperativity* if the overall stability of the complex is greater than the sum of the energies of interaction of the guest with the binding groups individually (multiplicative interactions). These binding site cooperatives in a supramolecular interaction are a generalization of the chelate effect found in classical coordination chemistry. The chelate effect relates to the observation that metal complexes of bidentate ligands are significantly more stable than unidentate ligands. This chelate effect has a favourable entropy contribution and kinetic effects, and can be used to enhance the thermodynamic stability of a supramolecular complex.

The *macrocyclic effect* is simply the manifestation of increasing *preorganisation*, organisation of the binding sites in space prior to guest binding. The enthalpic penalty associated with host conformational rearrangement has been "paid in advance" during the synthesis of the macrocycle. Macrocycles also present less solvent-accessible surface area. The enthalpic term arises from the fact that macrocyclic hosts are frequently less strongly solvated than their acyclic analogues. Entropically, macrocycles are less conformationally flexible and so lose fewer degrees of freedom upon complexation.

In addition to the degree of host preorganisation, the other main factor in determining the affinity of a host for a guest is *complementarity*. The *principle of complementarity* states that, in order to bind, hosts must have binding sites which can simultaneously contact and attract the binding sites of the guests without generating internal strains or strong nonbonded repulsions. Finally, the overall free energy of complexation represents the difference between the unfavourable reorganisation energy and the favourable binding energy.

Preorganization and complementarity lead to selectivity. This concept is based in the "lock and key" analogy that Emil Fischer used in 1894 to explain the operating mechanism of enzymes.

[48] G. Whitesides, J. Mathias and C. Seto, *Science* **1991,** *254*, 1312-1319.
[49] R. D. Hancock, *J. Chem. Educ.* **1992,** *69*, 615.
[50] D. J. Cram, *Angew. Chem., Int. Ed. Engl.* **1986,** *25*, 1039-1057.

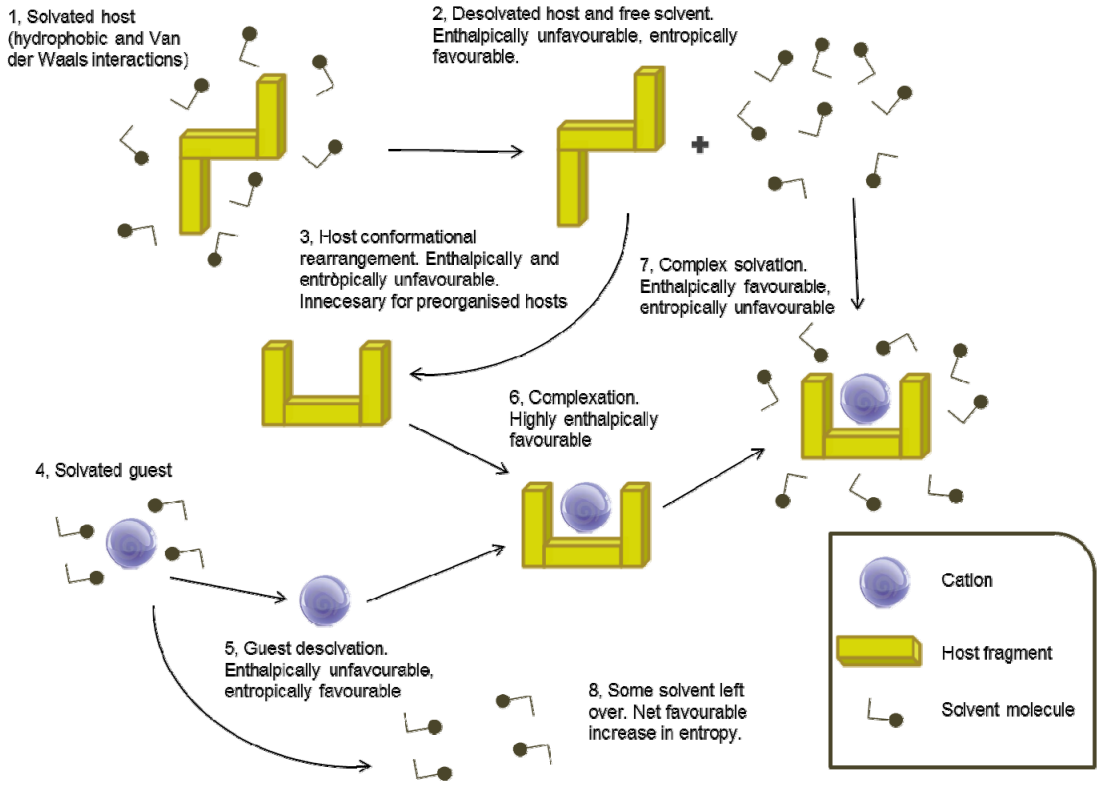

Scheme 1. Example of a complexation process.[47]

1.2.2. Supramolecular polymers

Supramolecular polymers are defined as polymeric arrays of monomeric units that are brought together by reversible noncovalent interactions, resulting in polymeric properties.[51] These self-assembled polymers hold promise as a unique class of novel materials because they combine many of the attractive features of conventional polymers with the tunable properties that result from the reversibility of the bonds between the monomers. Architectural and dynamic parameters that determine polymers properties are a function of the strength of the noncovalent interaction. Thus, the thermal and environmental control over lifetime and bond strength allows us to make many properties tunable in a way not accessible to traditional polymers.

There are many examples of naturally-occurring supramolecular polymers. For example microtubules, microfilaments, and flagella are helical supramolecular polymers formed by proteins by means of noncovalent cooperative interactions.

The first hydrogen-bonded supramolecular polymer was described by Lehn's group in 1990,[52] based in the formation of triply hydrogen-bonded complementary pairs, using uracil derivatives and diaminopyrimidine units. In this case, by the self-assembly of complementary subunits, they were able to engineer the molecular components to form

[51] L. Brunsveld, B. J. B. Folmer, E. W. Meijer and R. P. Sijbesma, *Chem. Rev.* **2001,** *101*, 4071-4098.
[52] C. Fouquey, J.-M. Lehn and A.-M. Levelut, *Adv. Mater.* **1990,** *2*, 254-257.

liquid crystalline supramolecular polymers. A simple empirical rule, derived to predict the binding strength of hydrogen bonded complex, suggest that for a stable supramolecular polymer, at least four hydrogen bonds per backbone unit are needed.[53] Balancing these considerations Meijer and coworkers have prepared a series of hydrogen bonded polymers based on the 2-ureido-4-[1H]-pyrimidone (UPy) moiety (Figure 9). The UPy self-dimerizes by forming four hydrogen bonds with exceptional affinity.[54] These UPy monomers, after functionalization, generate highly viscous solutions in organic media,[55] and this viscous behavior was attributed to the formation of long lived and sufficiently long supramolecular chains.

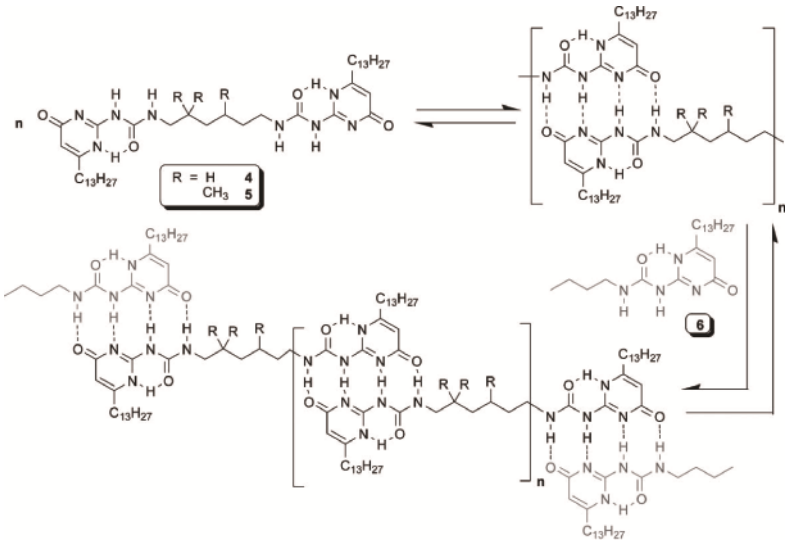

Figure 9. Bifunctional UPy compounds **4** and **5** self-associate in organic solvents, forming linear supramolecular polymers. The chain-stopper **6** can be used to control the statistical chain-length distribution.[55]

The bulk viscoelastic properties of reversible polymers of the kind described above are of interest for possible applications as materials. For example as hot melts and coatings, where a reversible and strongly temperature-dependent rheology is desirable.

Ghadiri's peptide nanotubes are another fascinating class of bio-inspired hydrogen-bonded supramolecular polymers.[56] The properties of these nanotubes can be tuned by changing the aminoacid sequence. The tubes are active against bacterial cell-walls, and have been proved to be effective against bacterial infections in *in vivo* studies on mice.

[53] J. Sartorius and H.-J. Schneider, *Chem. Eur. J.* **1996,** *2*, 1446-1452.
[54] F. H. Beijer, R. P. Sijbesma, H. Kooijman, A. L. Spek and E. W. Meijer, *J. Am. Chem. Soc.* **1998,** *120*, 6761-6769.
[55] R. P. Sijbesma, F. H. Beijer, L. Brunsveld, B. J. B. Folmer, J. H. K. K. Hirschberg, R. F. M. Lange, J. K. L. Lowe and E. W. Meijer, *Science* **1997,** *278*, 1601-1604.
[56] (a) M. R. Ghadiri, J. R. Granja, R. A. Milligan, D. E. McRee and N. Khazanovich, *Nature* **1993,** *366*, 324-327; (b) D. T. Bong, T. D. Clark, J. R. Granja and M. R. Ghadiri, *Angew. Chem. Int. Ed.* **2001,** *40*, 988-1011.

Different noncovalent interactions have been used for the formation of supramolecular polymers. For example Meijer et al. have made use of solvophobic effects to support hydrogen bonding,[57] Rehan et al. reported supramolecular polymers based in metal coordination complexation[58] and, more recently Boris Rybtchinski and colleagues reported an elegant example of useful material that combine π-stacking driven by solvophobic interactions.[59] With the latter they built a recyclable supramolecular membrane that can be used in the size-selective separation of nanoparticles (Figure 10).

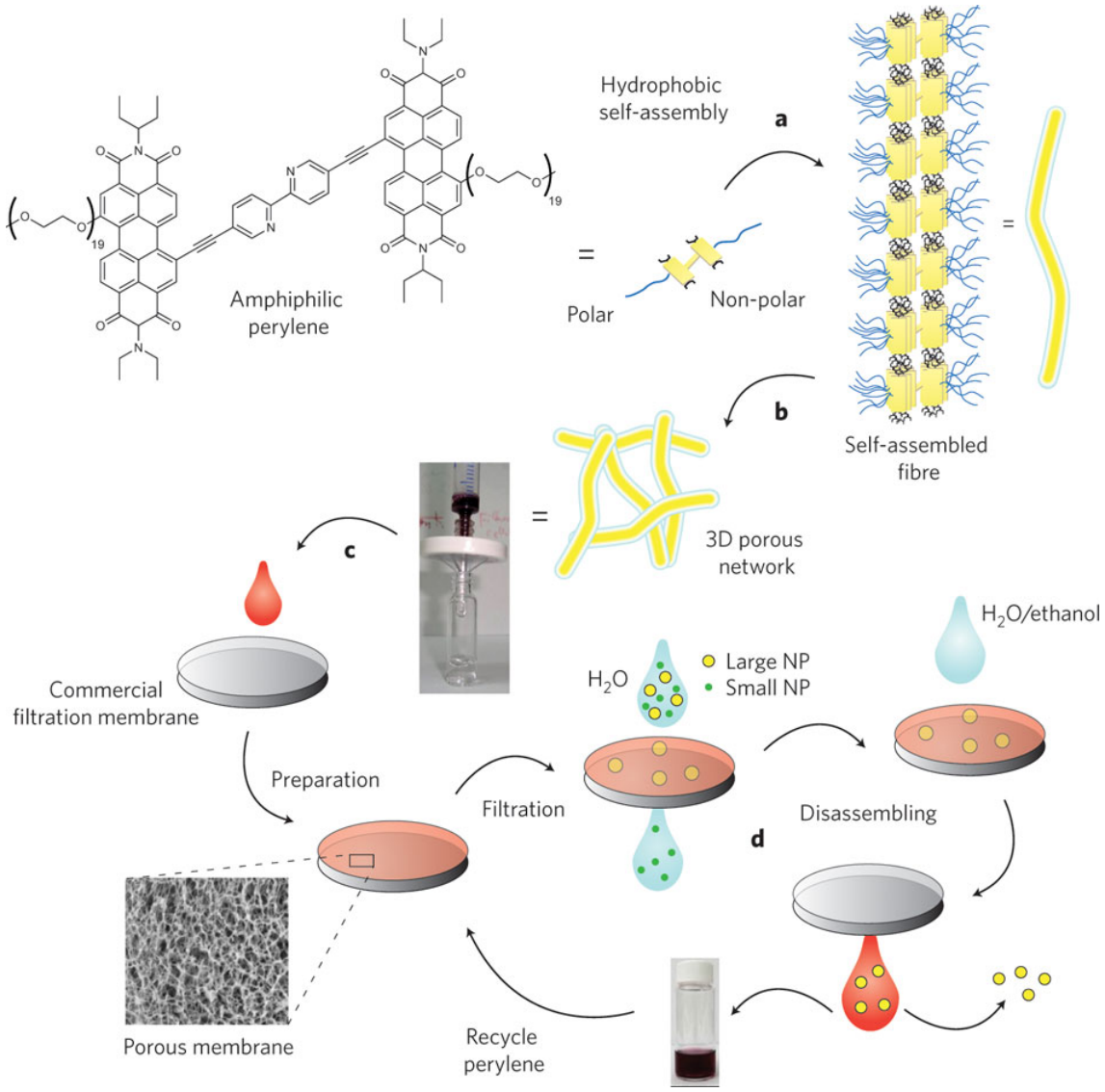

Figure 10. Preparation and use of the supramolecular membrane. **a**, An amphiphilic perylene self-assembles in water into fibres owing to hydrophobic interactions. **b**, The

[57] J. H. K. K. Hirschberg, L. Brunsveld, A. Ramzi, J. A. J. M. Vekemans, R. P. Sijbesma and E. W. Meijer, *Nature* **2000,** *407*, 167-170.
[58] R. Knapp, A. Schott and M. Rehahn, *Macromolecules* **1996,** *29*, 478-480; U. Velten and M. Rehahn, *Chem. Commun.* **1996,** *0*, 2639-2640.
[59] E. Krieg, H. Weissman, E. Shirman, E. Shimoni and B. Rybtchinski, *Nat Nano* **2011,** *6*, 141-146; C. Schmuck, *Nat Nano* **2011,** *6*, 136-137.

fibres entangle to form a 3D network in solution. **c**, When this solution is passed through a commercial microfiltration membrane, the supramolecular network is deposited on the solid support forming a porous membrane. **d**, This membrane can then be used for size-selective filtration. Afterwards the membrane can be dissolved by simply changing the solvent and the material can be recycled numerous times.

In conclusion, a wide variety of strategies can be used to build supramolecular polymers that combine the attractive features of conventional polymers with the unique properties that result from the reversibility of the noncovalent bonds, opening an ample field in materials chemistry.

1.3. SUPRAMOLECULAR CHEMISTRY OF FULLERENES

Nowadays, fullerene derivatives are the benchmark n-type material for the construction of organic photovoltaic devices. The study of the supramolecular chemistry of fullerenes started immediately after macroscopic quantities of fullerene C_{60} became available.[4] This research in supramolecular chemistry of fullerenes is fuelled mainly by the interest in finding new, simpler methods for their purification from fullerite, and in the control of the nanometric organization of electroactive materials, since it could increase the efficiency of the photovoltaic devices.[60]

As we have already seen, designing selective receptors for a specific guest is a challenging topic in supramolecular chemistry.[61, 62] In order to build receptors for fullerenes we have evaluate the peculiar features of this guest. Fullerene behaves as a polyene without further functionality, since it is composed of carbon atoms only, and we have to make the most of its geometry to maximize the host-guest interactions. If we consider the molecular complexation of the pure carbon sphere we have to take into account the impossibility of utilizing directional forces, like hydrogen boding or metal-ligand coordination, which leaves us with π–π stacking, van der Waals, and solvophobic interactions as key factors to consider. Since dispersion forces depend directly on surface area, the basic strategy to optimize the available noncovalent interactions is to increase the surface of the receptor in short contact with the fullerene guest.[63]

The use of directional noncovalent interactions is possible with properly functionalized fullerenes. Therefore, it was developed only once the covalent chemistry of fullerenes to build the desired derivatives was established.

---

[60] (a) P. M. Beaujuge and J. M. J. Fréchet, *J. Am. Chem. Soc.* **2011,** *133*, 20009-20029; (b) Y.-H. Chen, L.-Y. Lin, C.-W. Lu, F. Lin, Z.-Y. Huang, H.-W. Lin, P.-H. Wang, Y.-H. Liu, K.-T. Wong, J. Wen, D. J. Miller and S. B. Darling, *J. Am. Chem. Soc.* **2012,** *134*, 13616-13623.
[61] L. R. MacGillivray and J. L. Atwood, *Angew. Chem. Int. Ed.* **1999,** *38*, 1018-1033.
[62] D. Canevet, E. M. Pérez and N. Martín, *Angew. Chem. Int. Ed.* **2011,** *50*, 9248-9259.
[63] E. M. Pérez and N. Martín, *Chem. Soc. Rev.* **2008,** *37*, 1512-1519.

In this introduction we will focus in the supramolecular chemistry of pristine fullerenes.

1.3.1. Inclusion complexes of fullerenes by classical macrocyclic hosts.

Ringsdorf et al. reported in 1992[64] the first purposely receptors for [60] and [70] fullerenes based on macrocyclic azacrown ether with long alkane chains, forming a lipophilic "cup". In 1994, independently, Atwood[65] and Shinkai[66] found a calix[8]arene receptor (**7** in Figure 11) that demonstrated to be efficient in the precipitation and purification of [60]fullerene from mixtures of fullerenes.

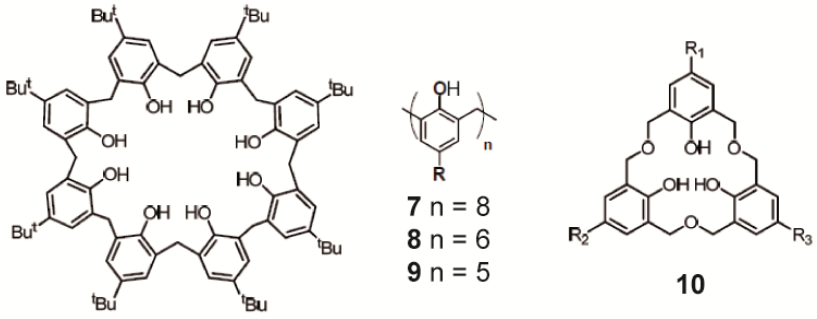

Figure 11. Chemical structure of different calixarene receptors for fullerenes.

This first example with calixarenes gave rise to the development of a wide variety of calixarene-based receptors for C_{60} and C_{70}. The investigation of these hosts demonstrated the fundamental importance of the size of the cavity and functional groups that work as substituent in the design of the receptor. The calix[8]-, [6]-, and [5]- arenes **7**, **8**, and **9**[67] and oxocalixarenes **10**[68] form inclusion complexes with fullerenes, where C_{60} or C_{70} are placed in the cavity of the receptor. Remarkably *p*-homooxacalix[3]arenes reported by Komatsu showed preferential precipitation of C_{70} over C_{60}[68b] in 1:1 mixtures of fullerenes.

Fukuza et al. reported the formation of a 1:1 complex in solution between calix[5]arenes bearing free hydroxyl groups and [60]fullerene.[69] The binding constants were calculated in solution for different solvents through UV-vis titrations, finding the expected isosbestic point for this stoichiometry. They also found a strong dependence of

[64] J. Effing, U. Jonas, L. Jullien, T. Plesnivy, H. Ringsdorf, F. Diederich, C. Thilgen and D. Weinstein, *Angew. Chem., Int. Ed. Engl.* **1992,** *31*, 1599-1602.
[65] J. L. Atwood, G. A. Koutsantonis and C. L. Raston, *Nature* **1994,** *368*, 229-231.
[66] T. Suzuki, K. Nakashima and S. Shinkai, *Chem. Lett.* **1994,** *23*, 699-702.
[67] (a) C. L. Raston, J. L. Atwood, P. J. Nichols and I. B. N. Sudria, *Chem. Commun.* **1996,** *0*, 2615-2616; (b) J. L. Atwood, L. J. Barbour, C. L. Raston and I. B. N. Sudria, *Angew. Chem. Int. Ed.* **1998,** *37*, 981-983; (c) J. L. Atwood, L. J. Barbour, M. W. Heaven and C. L. Raston, *Chem. Commun.* **2003,** *0*, 2270-2271; (d) J. L. Atwood, L. J. Barbour, M. W. Heaven and C. L. Raston, *Angew. Chem. Int. Ed.* **2003,** *42*, 3254-3257.
[68] K. Tsubaki, K. Tanaka, K. Fuji and T. Kinoshita, *Chem. Commun.* **1998,** *0*, 895-896; N. Komatsu, *Org. Biomol. Chem.* **2003,** *1*, 204-209.
[69] T. Haino, M. Yanase and Y. Fukazawa, *Angew. Chem., Int. Ed. Engl.* **1997,** *36*, 259-260.

the solvent, proving the great importance of solvophobic interactions in the association event. However, when they resolved the X ray structure of the complex they found that some of the receptors exhibit a 2:1 stoichiometry in the solid state,[70] with two calixarene units wrapping around the C_{60} surface. This divergence between solid state and solution was observed later in several supramolecular assemblies of fullerenes,[71] and is attributable to the tendency of molecules to pack as tightly as possible in the solid state. This discovery prompted the same group to design different receptors based on bis-calixa[5]renes linked covalently [72] or by means of hydrogen bonds[73] or metal coordination.[74]

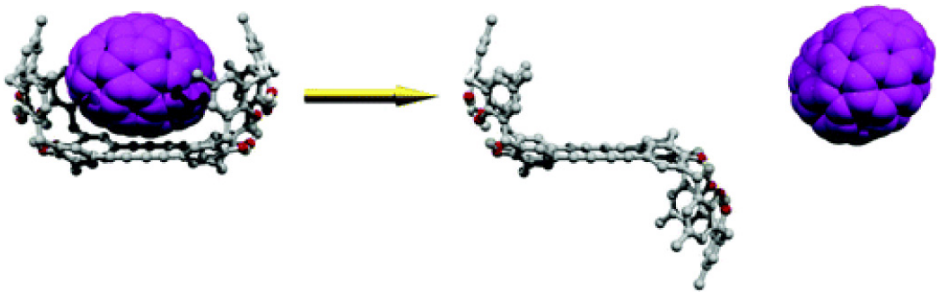

Figure 12. Syn- and anti-isomers of calix[5]arene-based receptor for selective extraction of higher fullerenes (C_{94} and C_{96}).[72b]

They achieved large binding constants with these kinds of receptors, with hosts bridged calix[5]arenes that bind preferentially C_{70} over C_{60} in most of the cases. In figure 12 we can see the syn isomer of the double calix[5]arene selectively captures higher fullerenes from fullerene mixtures. Heating the sample to more than 100 °C stimulates its conformational change to the anti-isomer, bringing liberation of the captured higher fullerenes.[72b] This possibility of associating two curved recognition units as calixarenes to improve the efficiency and selectivity of the receptor for fullerene guest has been tested in literature with other recognition motifs.[75] For example the group of Mendoza achieved an order of magnitude of preference in the binding

[70] T. Haino, M. Yanase and Y. Fukazawa, *Tetrahedron Lett.* **1997,** *38*, 3739-3742.
[71] (a) D. Felder, B. Heinrich, D. Guillon, J.-F. Nicoud and J.-F. Nierengarten, *Chemistry – A European Journal* **2000,** *6*, 3501-3507; (b) S. Mizyed, M. Ashram, D. O. Miller and P. E. Georghiou, *J. Chem. Soc. Perk. Trans. 2* **2001,** *0*, 1916-1919; (c) Y. Rio and J.-F. Nierengarten, *Tetrahedron Lett.* **2002,** *43*, 4321-4324.
[72] (a) T. Haino, M. Yanase and Y. Fukazawa, *Angew. Chem. Int. Ed.* **1998,** *37*, 997-998; (b) T. Haino, Y. Matsumoto and Y. Fukazawa, *J. Am. Chem. Soc.* **2005,** *127*, 8936-8937; (c) T. Haino, C. Fukunaga and Y. Fukazawa, *Org. Lett.* **2006,** *8*, 3545-3548; (d) T. Haino, M. Yanase, C. Fukunaga and Y. Fukazawa, *Tetrahedron* **2006,** *62*, 2025-2035.
[73] M. Yanase, T. Haino and Y. Fukazawa, *Tetrahedron Lett.* **1999,** *40*, 2781-2784.
[74](a) T. Haino, H. Araki, Y. Yamanaka and Y. Fukazawa, *Tetrahedron Lett.* **2001,** *42*, 3203-3206; (b) T. Haino, Y. Yamanaka, H. Araki and Y. Fukazawa, *Chem. Commun.* **2002,** *0*, 402-403.
[75] (a) J. L. Atwood, L. J. Barbour, P. J. Nichols, C. L. Raston and C. A. Sandoval, *Chem. Eur. J.* **1999,** *5*, 990-996; (b) A. Ikeda, M. Yoshimura, H. Udzu, C. Fukuhara and S. Shinkai, *J. Am. Chem. Soc.* **1999,** *121*, 4296-4297; (c) A. Ikeda, H. Udzu, M. Yoshimura and S. Shinkai, *Tetrahedron* **2000,** *56*, 1825-1832.

constants toward C_{70} over C_{60} with a receptor based on a C,C-linked biscalix[4]arene (figure 13).[76]

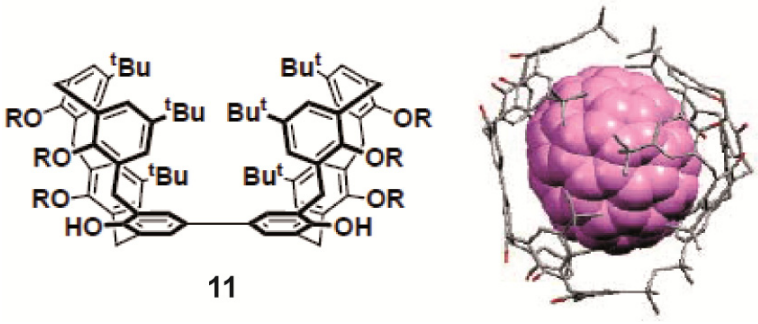

Figure 13. Structure of C,C-linked biscalix[4]arene (left) and molecular model of 1:2 C_{70} complex (right).[76]

Cyclotriveratrylene (CTV) is another classical macrocyclic host and its ability to form inclusion complexes with fullerenes has been studied. In the early nineties Atwood et al. reported the formation of "ball and socket" complexes with C_{60}.[77] Since then several receptors forming 1:1 and 1:2 complexes with fullerenes have been reported.[78] The series of CTV based receptors reported by Matsubara et al. are between them. These receptors are able to bind [60] and [70]fullerenes. They achieved preference of association for C_{60} over C_{70} with one of the receptors consisting of a CTV with aromatic pendants,[78a] and preference for C_{70} over C_{60} with cyclotriveratrylenophanes.[78c] The group of de Mendoza reported CTV derivatives with ureidopyrimidone UPy unit pendants that are able to self-assemble to form capsules through hydrogen bonding in nonpolar solvents in presence of different fullerenes (figure 14).[79] They achieved selective extraction of C_{70} from fullerite with one of these derivatives, which displays a remarkable selectivity for the encapsulation of C_{70} over C_{60}, getting 97% purity C_{70} after only two runs of liquid-solid extractions.[79b] They used the same receptor **12** to achieve C_{84} purification from fullerite only playing with solubility and concentrations, getting 93% purity C_{84} in only one round.[79a]

[76] J. C. Iglesias-Sánchez, A. Fragoso, J. de Mendoza and P. Prados, *Org. Lett.* **2006,** *8*, 2571-2574.
[77] J. W. Steed, P. C. Junk, J. L. Atwood, M. J. Barnes, C. L. Raston and R. S. Burkhalter, *J. Am. Chem. Soc.* **1994,** *116*, 10346-10347.
[78] (a) Felder, Heinrich, Guillon, Nicoud and Nierengarten; H. Matsubara, A. Hasegawa, K. Shiwaku, K. Asano, M. Uno, S. Takahashi and K. Yamamoto, *Chem. Lett.* **1998,** *27*, 923-924; (b) H. Matsubara, T. Shimura, A. Hasegawa, M. Semba, K. Asano and K. Yamamoto, *Chem. Lett.* **1998,** *27*, 1099-1100; (c) H. Matsubara, S.-y. Oguri, K. Asano and K. Yamamoto, *Chem. Lett.* **1999,** *28*, 431-432; (d) J. F. Nierengarten, *Fullerenes, Nanotubes and Carbon Nanostructures* **2005,** *13*, 229-242.
[79] (a) E. Huerta, E. Cequier and J. d. Mendoza, *Chem. Commun.* **2007,** *0*, 5016-5018; (b) E. Huerta, G. A. Metselaar, A. Fragoso, E. Santos, C. Bo and J. de Mendoza, *Angew. Chem. Int. Ed.* **2007,** *46*, 202-205.

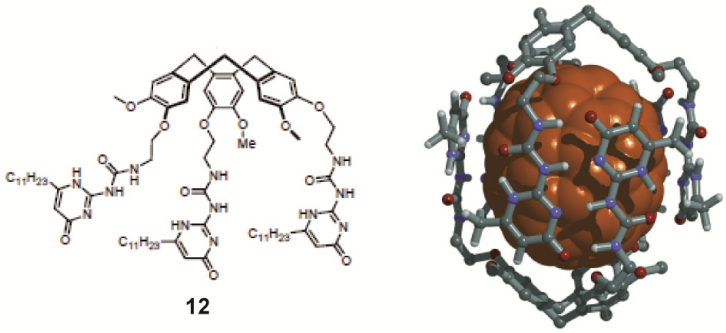

Figure 14. Chemical structure of CTV-UPy receptor (left) and molecular model of 2:1 complex with C_{70}.[79b]

More recently, Chiu et al. have reported a CTV-based molecular cage that allows the isolation of C_{70} with >99% purity from fullerene extracts (figure 15).[80]

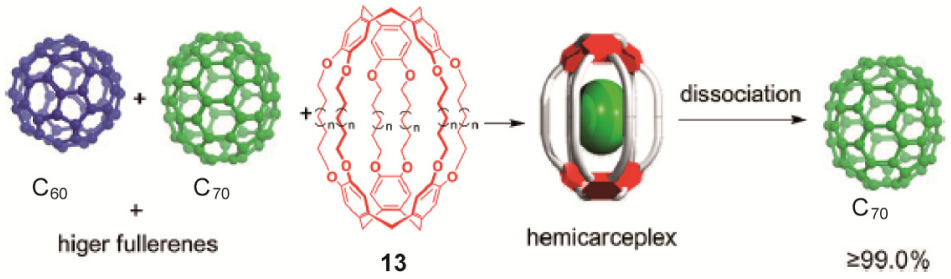

Figure 15. Chemical structure of Chiu's receptor **13** and representation of the extraction process.

1.3.2. Bowl shaped conjugated system

Corannulene is the first known bowl-shaped conjugated system,[81] and the discovery of fullerenes prompted a general interest in this kind of structures. Corannulene has a size nearly identical to that of fullerenes and thus too small to associate with it. Although it forms a stable complex in the gas phase with $(C_{60})^+$,[82] it shows no evidence for complexation either in solution or in the solid state, and chemical derivatization is necessary to observe binding.

The strategy followed by Georghiou and Scott's group[83] was to increase the cavity size adding aromatic rings in the derivatization, while maintaining the original bowl shape of corannulene. Hosts **14** and **15** in figure 16 act as a fullerene receptors with binding constants of log K_a = 2.5 and 3.1 (toluene, room temperature) respectively.

[80] M.-J. Li, C.-H. Huang, C.-C. Lai and S.-H. Chiu, *Org. Lett.* **2012,** *14*, 6146-6149.
[81] W. E. Barth and R. G. Lawton, *J. Am. Chem. Soc.* **1966,** *88*, 380-381.
[82] H. Becker, G. Javahery, S. Petrie, P. C. Cheng, H. Schwarz, L. T. Scott and D. K. Bohme, *J. Am. Chem. Soc.* **1993,** *115*, 11636-11637.
[83] (a) S. Mizyed, P. E. Georghiou, M. Bancu, B. Cuadra, A. K. Rai, P. Cheng and L. T. Scott, *J. Am. Chem. Soc.* **2001,** *123*, 12770-12774; (b) P. E. Georghiou, A. H. Tran, S. Mizyed, M. Bancu and L. T. Scott, *J. Org. Chem.* **2005,** *70*, 6158-6163.

Sygula's[84] group prepared the receptor **16** following a different strategy, the use of two corannulene moieties linked through a rigid aromatic spacer to form a tweezer-like receptor. This "buckycatcher" forms more stable complexes than the receptors bearing a single corannulene with log K_a = 3.9 in toluene at room temperature.

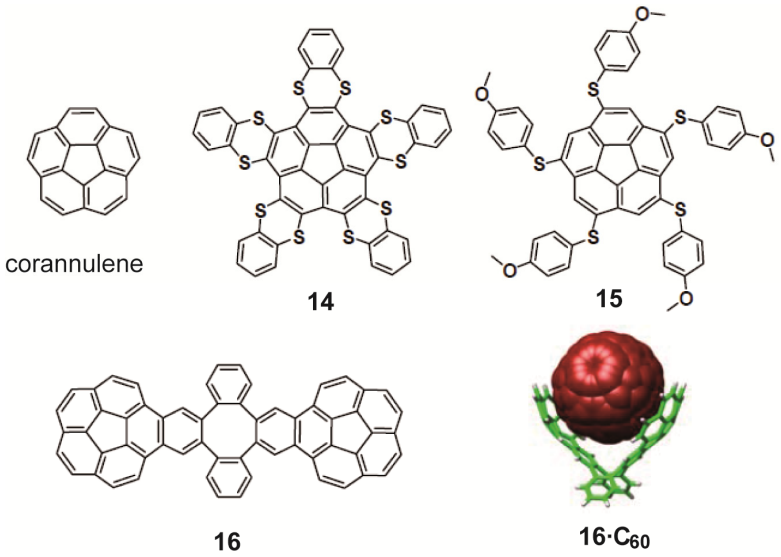

Figure 16. Chemical structure of corannulene and corannulene based receptors. Solid state structure of one of the complex with [60]fullerene is also shown.[83-84]

1.3.3. Carbon nanorings

An inflexible host displays a high degree of preorganization, and preorganization typically results in the formation of a more stable complex. This concept is nicely illustrated with the rational modification of the receptors reported by Kawase and co-workers (figure 17).[85] They first reported the synthesis of cyclic [n]*para*phenylacetylenes **17-20** in 1996.[85a] Nanoring **18** proved to associate [60] and [70] fullerenes with log K_a = 4.2 and 4.3 in benzene at room temperature,[85b, 85c] as measured by UV-vis titrations. They achieved a significant improvement in the association event of fullerenes with compounds **21-24.**[85c, 85g] In these receptors the size of the aromatic surface is increased with naphthylene rings. All those hosts form complexes of remarkable stability with both C_{60} and C_{70}. For example receptor **22** shows log K_a = 5.0 with C_{60} in benzene at room temperature.

[84] A. Sygula, F. R. Fronczek, R. Sygula, P. W. Rabideau and M. M. Olmstead, *J. Am. Chem. Soc.* **2007,** *129*, 3842-3843.

[85] (a) T. Kawase, H. R. Darabi and M. Oda, *Angew. Chem., Int. Ed. Engl.* **1996,** *35*, 2664-2666; (b) T. Kawase, K. Tanaka, N. Fujiwara, H. R. Darabi and M. Oda, *Angew. Chem. Int. Ed.* **2003,** *42*, 1624-1628; (c) T. Kawase, K. Tanaka, Y. Seirai, N. Shiono and M. Oda, *Angew. Chem. Int. Ed.* **2003,** *42*, 5597-5600; (d) T. Kawase, N. Fujiwara, M. Tsutumi, M. Oda, Y. Maeda, T. Wakahara and T. Akasaka, *Angew. Chem. Int. Ed.* **2004,** *43*, 5060-5062; (e) T. Kawase, K. Tanaka, N. Shiono, Y. Seirai and M. Oda, *Angew. Chem. Int. Ed.* **2004,** *43*, 1722-1724; (f) T. Kawase and H. Kurata, *Chem. Rev.* **2006,** *106*, 5250-5273; (g) T. K. a. M. Oda, *Pure Appl. Chem.* **2006,** *78*, 9.

Furthermore, Kawase's nanorings show an unprecedented onion-type association.[85e] They have found **17·20** and **23·24** ring-in-ring inclusion complexes.[86] Given the rigidity of the carbon nanorings, they are capable of binding C_{60} forming onion-type complexes like the ones shown in Figure 17.

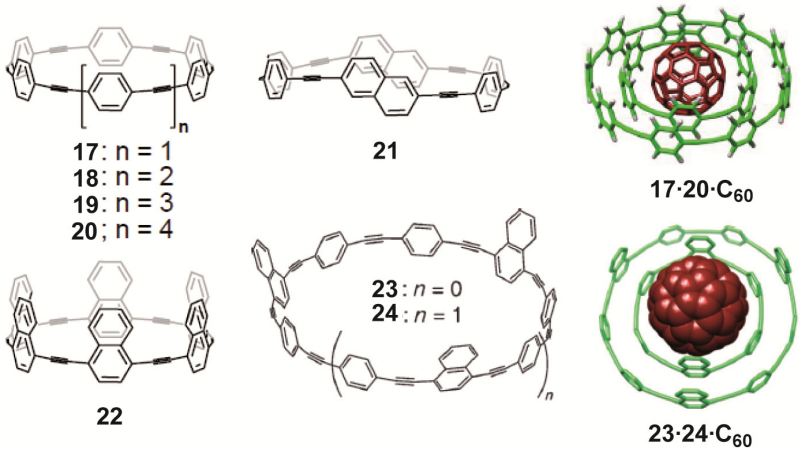

Figure 17. Chemical structures of some of the rigid carbon nanorings reported by Kawase and co-workers. Representation of their onion-like supramolecular structure with C_{60}.[85-86]

1.3.4. Porphyrin based receptors

We have seen that cyclic oligomers consisting of electron-rich aromatic components, such as calixarenes and cyclotriveratrylenes, have been reported as π-hosts for fullerenes. Since metalloporphyrins possess a large π-conjugated system,[87] they can be considered attractive components for the design of host molecules for fullerenes. In fact, a significant portion of the hosts for fullerenes described to date has made use of the porphyrin-fullerene interaction.[88]

The association event between fullerene and porphyrin was first reported in the solid state.[89] The solid state structure of a covalent dyad of [60]fullerene and porphyrin features separations between them of 2.75 Å, indicative of a strong π–π interaction. However, at least two porphyrins are necessary to associate or bind fullerenes in solution. In 1999, Aida and co-workers synthesized a cyclic dimer of a zinc porphyrin

[86] T. Kawase, Y. Nishiyama, T. Nakamura, T. Ebi, K. Matsumoto, H. Kurata and M. Oda, *Angew. Chem. Int. Ed.* **2007,** *46*, 1086-1088.
[87] K. M. Kadish, K. M. Smith and R. Guilard, *The porphyrin handbook: Synthesis and organic chemistry*. Academic Press: 1999.
[88] (a) P. D. W. Boyd, M. C. Hodgson, C. E. F. Rickard, A. G. Oliver, L. Chaker, P. J. Brothers, R. D. Bolskar, F. S. Tham and C. A. Reed, *J. Am. Chem. Soc.* **1999,** *121*, 10487-10495; (b) P. D. W. Boyd and C. A. Reed, *Acc. Chem. Res.* **2004,** *38*, 235-242.
[89] Y. Sun, T. Drovetskaya, R. D. Bolskar, R. Bau, P. D. W. Boyd and C. A. Reed, *J. Org. Chem.* **1997,** *62*, 3642-3649.

(**25**) and studied its abilities to associate fullerene C_{60}.[90] In figure 18 we can see the UV-vis titration that they used to determine a log K_a = 5.8 in benzene at room temperature). We can observe in the spectroscopic titration that the Soret band is bathochromically shifted upon addition of fullerene, forming an isosbestic point around 418 nm, and suggesting electronic interaction between fullerene and porphyrin in the ground state.

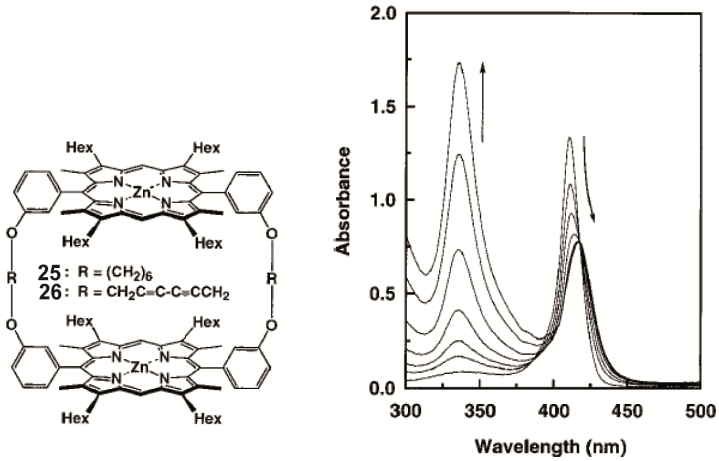

Figure 18. Molecular structure of first zinc porphyrin cyclic dimers and spectroscopic titration of receptor **25** with C_{60} in benzene at room temperature. [**25**] = 1.96 x 10^{-6} M; [C_{60}]/[**25**] = 0, 0.74, 1.48, 2.96, 5.91, 10.35, 14.77.

This finding prompted the Japanese group to design and synthesize a whole family of cyclic metalloporphyrins summarized in the table of figure 19.[91]

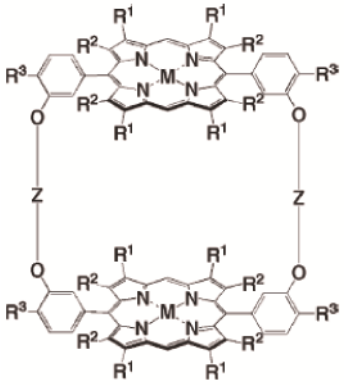

Host	Z	R^1	R^2	R^3	M
27	$-(CH_2)_4-$	H	H	$OC_{12}H_{25}$	$CH_3Rh(III)$
28	$-(CH_2)_5-$	H	H	$OC_{12}H_{25}$	Zn(II)
29	$-(CH_2)_6-$	H	H	$OC_{12}H_{25}$	Zn(II)
30	$-(CH_2)_6-$	C_6H_{13}	CH_3	H	2H
31	$-(CH_2)_6-$	C_6H_{13}	CH_3	H	Co(II)
32	$-(CH_2)_6-$	C_6H_{13}	CH_3	H	$CH_3Rh(III)$
33	$-(CH_2)_6-$	C_6H_{13}	CH_3	H	Ni(II)
34	$-(CH_2)_6-$	C_6H_{13}	CH_3	H	Cu(II)
35	$-(CH_2)_6-$	C_6H_{13}	CH_3	H	Ag(II)
25	$-(CH_2)_6-$	C_6H_{13}	CH_3	H	Zn(II)
36	$-(CH_2)_6-$	C_6H_{13}	C_2H_5	H	Zn(II)
26	$-CH_2C\equiv C-C\equiv CCH_2$	C_6H_{13}	CH_3	H	Zn(II)
37	$-(CH_2)_7-$	H	H	$OC_{12}H_{25}$	Zn(II)
38	$-(CH_2)_6-$	C_6H_{13}	CH_3	H	$CH_3Ir(III)$

Figure 19. Molecular structure of Aida's metalloporphyrins **25-38**.

Through their extensive studies,[92] along with those by other research groups, the field of hosting fullerenes by means of cyclodimeric metalloporphyrins has been well

[90] K. Tashiro, T. Aida, J.-Y. Zheng, K. Kinbara, K. Saigo, S. Sakamoto and K. Yamaguchi, *J. Am. Chem. Soc.* **1999,** *121*, 9477-9478.
[91] K. Tashiro and T. Aida, *Chem. Soc. Rev.* **2007,** *36*, 189-197.

established. A certain conformational flexibility in the linker parts of the host molecule is essential to drive association. As a practical example, host **25** shows log K_a = 5.8 (benzene, 298 K) bearing flexible linkers, while host **26**, a synthetic precursor with rigid linkers, does not show any sign of complexation with fullerenes. In the solid state structure of some of the complexes the porphyrin moieties adopt a nonplanar concave structure. Besides the structure of the linkers between the porphyrins the central metal ions also affect the binding capability of the host molecule toward fullerenes significantly. For example, the binding constant of the Zn porphyrin cyclic dimer **25** is very similar to the free base analogue **30** (log K_a = 5.8 and 5.9 respectively in benzene at room temperature) but the Rh (III) analogue of **25, 32**, binds [60]fullerene with a remarkable log K_a = 7.4 under the same experimental conditions.

Some members of this family of metalloporphyrin-based receptors have been used for the discrimination of fullerenes. For example **29** allows enrichment of a fullerite mixture in higher fullerenes, reaching an overall content of fullerenes other than C_{60} of up to 93 %, starting from only 10 % in the starting mixture, while **37** is able to furnish a 97 % overall content of higher fullerenes.

The iridium derivative **38**[93] of this family that constitutes, to date, the world record in complex stability with fullerene C_{60} with log K_a = 8.1 in 1,2-dichlorobenzene at room temperature. They also performed desymmetrization on a porphyrin ring[94] to insert asymmetry in the system and design chiral hosts for chiral fullerenes (C_{76}, C_{78}, C_{84}). Aida's group finally achieved discrimination between enantiomers with a second generation of chiral hosts, which are more distorted and non-metalated. Through a solid-liquid extraction using this host, they managed to enrich the racemic mixture in (+) or (-) C_{76} with a 7 % *ee* after a single extraction (figure 20).[95]

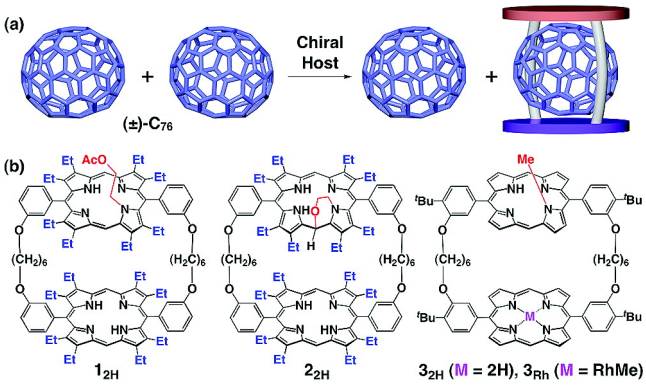

[92] (a) Tashiro, Aida, Zheng, Kinbara, Saigo, Sakamoto and Yamaguchi; K. Tashiro and T. Aida, *Journal of inclusion phenomena and macrocyclic chemistry* **2001,** *41*, 215-217; (b) J.-Y. Zheng, K. Tashiro, Y. Hirabayashi, K. Kinbara, K. Saigo, T. Aida, S. Sakamoto and K. Yamaguchi, *Angew. Chem. Int. Ed.* **2001,** *40*, 1857-1861; (c) K. Tashiro, Y. Hirabayashi, T. Aida, K. Saigo, K. Fujiwara, K. Komatsu, S. Sakamoto and K. Yamaguchi, *J. Am. Chem. Soc.* **2002,** *124*, 12086-12087; (d) Y. Shoji, K. Tashiro and T. Aida, *J. Am. Chem. Soc.* **2004,** *126*, 6570-6571; (e) A. Ouchi, K. Tashiro, K. Yamaguchi, T. Tsuchiya, T. Akasaka and T. Aida, *Angew. Chem. Int. Ed.* **2006,** *45*, 3542-3546.
[93] M. Yanagisawa, K. Tashiro, M. Yamasaki and T. Aida, *J. Am. Chem. Soc.* **2007,** *129*, 11912-11913.
[94] Y. Shoji, K. Tashiro and T. Aida, *J. Am. Chem. Soc.* **2006,** *128*, 10690-10691.
[95] Y. Shoji, K. Tashiro and T. Aida, *J. Am. Chem. Soc.* **2010,** *132*, 5928-5929.

Figure 20. (a) Schematic representation of enantioselective complexation of C_{76} with a chiral host. (b) Molecular structures of chiral hosts.

Anderson and co-workers contributed to the advance of this field increasing the number of interacting porphyrin units within the macrocycle (figure 21). They reported the first example of macrocycle with three porphyrin units.[96] This receptor with more rigid structure shows extremely high binding constants with different fullerenes and a high degree of selectivity toward higher fullerenes, as they nicely illustrated with competition experiments monitored by mass spectrometry.

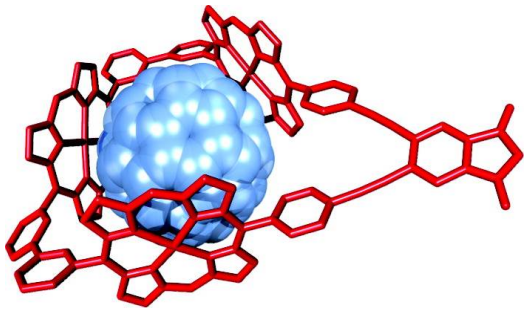

Figure 21. Complex with fullerene of the cyclic porphyrin trimer macrocycle synthesized by Anderson and co-workers.

1.3.5. Supramolecular architectures

There is an extensive bibliography about supramolecular architectures involving noncovalent interactions with fullerenes[91, 62, 23c, 88b, 97]. In the present introduction, we will only overview some of the most noteworthy examples, to illustrate the possibilities in the design of fullerene-containing nanostructured materials. As a beautiful example of handling supramolecular interactions in the design of nanostructured architectures, Aida's group has reported the formation of supramolecular peapods by self-assembly.[98] A suitably functionalized metalloporphyrin host cyclodimerizes and polymerizes *via* hydrogen bond interactions in the presence of C_{60} and C_{70}.

In the preparation of functional materials, Tani's group has reported studies focusing on the self-assembly of macrocyclic dimers[99] by means of N-H hydrogen bonding and π–π interactions. These studies gave rise to an original network that finally was

[96] G. n. Gil-Ramírez, S. D. Karlen, A. Shundo, K. Porfyrakis, Y. Ito, G. A. D. Briggs, J. J. L. Morton and H. L. Anderson, *Org. Lett.* **2010,** *12*, 3544-3547.
[97] T. Kawase, Supramolecular Chemistry of Fullerenes: Host Molecules for Fullerenes on the Basis of π-π Interaction. In *Chemistry of Nanocarbons*, John Wiley & Sons, Ltd: 2010; pp 189-213.
[98] T. Yamaguchi, N. Ishii, K. Tashiro and T. Aida, *J. Am. Chem. Soc.* **2003,** *125*, 13934-13935.
[99] (a) H. Nobukuni, Y. Shimazaki, F. Tani and Y. Naruta, *Angew. Chem. Int. Ed.* **2007,** *46*, 8975-8978; (b) H. Nobukuni, F. Tani, Y. Shimazaki, Y. Naruta, K. Ohkubo, T. Nakanishi, T. Kojima, S. Fukuzumi and S. Seki, *J. Phys. Chem. C* **2009,** *113*, 19694-19699; (c) H. Nobukuni, Y. Shimazaki, H. Uno, Y. Naruta, K. Ohkubo, T. Kojima, S. Fukuzumi, S. Seki, H. Sakai, T. Hasobe and F. Tani, *Chem. Eur. J.* **2010,** *16*, 11611-11623.

described as photoconductive supramolecular peapod, an schematic representation is shown in figure 22. They performed measurements of this linear organization and obtained high conductivity values along the fullerene axis, with significant anysotropy. It is worth noting that they prepared a photoelectrochemical cell capable of converting solar energy with 0.33 % of efficiency.

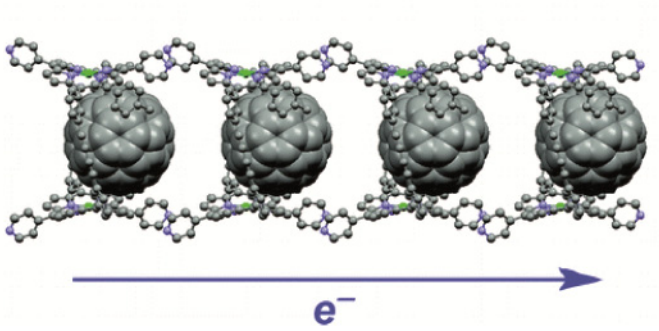

Figure 22. Schematic representation of the photoconductive supramolecular peapod.[99b]

The fabrication of [60]fullerene polymeric array by means of artificial helical nanotube formed by self-assembly of amino acids functionalized naphthalenediimide (NDI), reported by Sanders and co-workers,[100] is also a remarkable example. These helical nanotubes can be filled with C_{60} as an easy tunable kind of receptor for fullerenes (figure 23).[101] More recently, the encapsulation of fullerene in a commodity plastic, syndiotactic poly (methyl methacrylate) (st-PMMA), has been reported.[102] A st-PMMA/fullerene inclusion complex is formed[102b] and can be readily processed into homogeneous films. These improved features open the way for further development of novel fullerene-based nanomaterials with practical applications in optoelectronics.

[100] G. D. Pantoş, P. Pengo and J. K. M. Sanders, *Angew. Chem. Int. Ed.* **2007,** *46*, 194-197.
[101] G. D. Pantoş, J.-L. Wietor and J. K. M. Sanders, *Angew. Chem. Int. Ed.* **2007,** *46*, 2238-2240.
[102] (a) T. Kawauchi, J. Kumaki, A. Kitaura, K. Okoshi, H. Kusanagi, K. Kobayashi, T. Sugai, H. Shinohara and E. Yashima, *Angew. Chem. Int. Ed.* **2008,** *47*, 515-519; (b) S. Qi, H. Iida, L. Liu, S. Irle, W. Hu and E. Yashima, *Angew. Chem.* **2013,** *125*, 1083-1087.

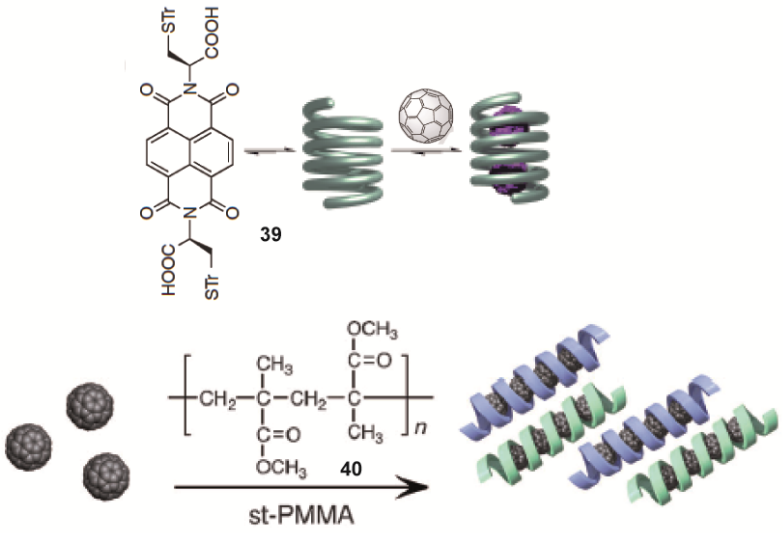

Figure 23. Helical assembles of naphthalenediimide (NDI) **39** (up),[101] and st-PMMA **40** (down) with [60]fullerene.[102b]

In a hydrogen-bonded supramolecular polymer reported by Bassani and coworkers[42] the fullerenes and the oligothiophene moieties are aligned, which results in the improvement of efficiency in light harvesting in the visible region. In a different example, Hummelen and coworkers made use of Upy moieties linked to C_{60} to get donor-donor-acceptor-acceptor (DDAA) hydrogen bonding motif in the monomer, to form self-complementary hydrogen-bonded polymer in an organic solution.[103]

A more complicated example is the use of host-guest interactions of a ditopic calix[5]arene host that encapsulate dumbbell C_{60} moieties, reported by Haino et al.[104] This host has been used to encapsulate C_{60} grafted on to a polymer chain, creating a remarkably stable cross-linkage that can be regulated by the solvent system. With this strategy they achieved an increase in the molecular weight of the polymer, and unique morphological changes to the polymer in its solid state.

Dendritic architectures represent useful building blocks for creating functional materials and dendrimer scaffolds have also been used in the supramolecular chemistry of fullerenes. [60]fullerene molecules have been covalently linked to the periphery of half dendrimer that self-asssembles *via* metal coordination to give rise to the complete globular shape surrounded by 16 fullerenes.[105] In a different example, C_{60} is concentrated on the globular surface of the dendrimer by means of electrostatic interactions with ferrocene moieties attached to its periphery.[106] The authors suggested that such structures could be a candidate to construct molecular batteries.

[103] L. Sánchez, M. T. Rispens and J. C. Hummelen, *Angew. Chem. Int. Ed.* **2002,** *41*, 838-840.
[104] T. Haino, E. Hirai, Y. Fujiwara and K. Kashihara, *Angew. Chem. Int. Ed.* **2010,** *49*, 7899-7903.
[105] (a) N. Armaroli, C. Boudon, D. Felder, J.-P. Gisselbrecht, M. Gross, G. Marconi, J.-F. Nicoud, J.-F. Nierengarten and V. Vicinelli, *Angew. Chem. Int. Ed.* **1999,** *38*, 3730-3733; (b) J.-F. Nierengarten, *Chem. Eur. J.* **2000,** *6*, 3667-3670.
[106] J. Ruiz, C. Pradet, F. Varret and D. Astruc, *Chem. Commun.* **2002,** *0*, 1108-1109.

Complementary hydrogen bonding pairs have also been utilized to form fullerene-funtionalised dendrimers, as reported by Hirsch and co-workers.[107]

In summary, the supramolecular chemistry of fullerenes is a field with a well-developed toolbox that offers easy access to the construction of well-organized nanostructures, which can prove to be of great utility in both material and biological sciences.

1.4. GRAPHENE AND SUPRAMOLECULAR CHEMISTRY OF GRAPHENE

Graphene is the name given to a flat monolayer of carbon atoms tightly packed into a two-dimensional honeycomb lattice. This is the basic building block for graphitic materials of all other dimensionalities; it can be wrapped in 0D to form fullerenes, rolled into 1D to construct nanotubes or stacked in 3D to yield graphite. Graphene, as a strictly 2D crystal, was postulated to be thermodynamically unstable, but Andre Geim and Konstantin Novoselov achieved its isolation in 2004, by simply peeling down graphite with Scotch tape.[7b] The Nobel Prize in Physics 2010 was awarded jointly to Geim and Novoselov *"for groundbreaking experiments regarding the two-dimensional material graphene"*.

Graphene is the thinnest and strongest material reported so far, and exhibits outstanding properties such as excellent conductance of both heat and electricity. Its unique bidimensional structure is responsible for these remarkable properties. The electronic structure of this material rapidly evolves with the number of layers, and the limit between 2D (few layers graphene) and 3D material (graphite) is considered to be at 10 layers.[108]

Electrons in graphene behave as massless Dirac fermions, with electron mobility 100 times greater than silicon. Unsurprisingly, the electronic properties of graphene have been the focus of a significant number of investigations.[109] Graphene has also received the attention of companies. Indeed, graphene has been the focus of over 33,600 research papers and patent applications since 2004 (SciFinder, 10/05/2013).[110] A recent example of a graphene based material is shown in Figure 24. These ultralight and highly compressible aerogels show density as low as 3 mg cm^{-1} and the structure can be fully recovered without fracture even after 90 % compression.[111]

[107] K. Hager, U. Hartnagel and A. Hirsch, *Eur. J. Org. Chem.* **2007,** *2007*, 1942-1956.
[108] B. Partoens and F. M. Peeters, *Physical Review B* **2006,** *74*, 075404.
[109] For reviews, see (a) C. N. R. Rao, A. K. Sood, K. S. Subrahmanyam and A. Govindaraj, *Angew. Chem. Int. Ed.* **2009,** *48*, 7752-7777; (b) P. Avouris, *Nano Lett.* **2010,** *10*, 4285-4294; (c) S. Pang, Y. Hernández, X. Feng and K. Muellen, *Adv. Mater.* **2011,** *23*, 2779-2795; (d) E. Bekyarova, S. Sarkar, F. Wang, M. E. Itkis, I. Kalinina, X. Tian and R. C. Haddon, *Acc. Chem. Res.* **2013,** *46*, 65-76.
[110] N. Savage, *Nature* **2012,** *483*, S30-S31.

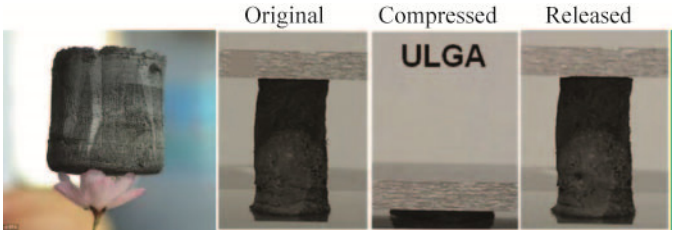

Figure 24. Ultralight graphene aerogel (ULGA). The three digital images at right show the high compressibility of the material.[111]

There are many different methods available for the production of graphene or few layers graphene (FLG).[112] Samples obtained by exfoliating graphite are currently produced with a high degree of purity. The pristine material, regardless of the synthetic method, is insoluble in organic solvents and susceptible of aggregation in aqueous solution. Chemical modification, whether covalent or supramolecular, is therefore required to make graphene processable in order to exploit its outstanding properties for further applications.

There are some general remarks on the chemical reactivity of graphene. The reactivity may occur on the π surface and/or on the edges, but edge atoms are more reactive than those located in the basal plane. This is because the covalent derivatization of graphene involves a rehybridization process from sp^2 to sp^3, which implies the saturation of a double bond and the perturbation of the π-system. Reactions might also occur at defect sites. For supramolecular modifications, we have to take into account the lack of functionality, so we should rely on dispersion forces, as in the case of fullerenes, to interact with graphene's π system.

With regards to the covalent chemistry of pristine graphene, most of the typical reactions of relatively inert conjugated systems such as fullerenes and carbon nanotubes can be applied. For instance, Birch reduction has been considered for the preparation of hydrogenated graphene[113] and photochemical radical additions have also been performed.[114] The addition of aryl diazonium salts to graphene was first introduced by the group of Tour on different types of graphene derivatives obtained from graphite oxide,[115] and later was applied on pristine graphene by them and others groups.[116] The

[111] H. Hu, Z. Zhao, W. Wan, Y. Gogotsi and J. Qiu, *Adv. Mater.* **2013,** *25*, 2219-2223.
[112] S. Guo and S. Dong, *Chem. Soc. Rev.* **2011,** *40*, 2644-2672.
[113] (a) K. S. Subrahmanyam, P. Kumar, U. Maitra, A. Govindaraj, K. P. S. S. Hembram, U. V. Waghmare and C. N. R. Rao, *Proc. Natl. Acad. Sci.* **2011,** *108*, 2674-2677; (b) R. A. Schäfer, J. M. Englert, P. Wehrfritz, W. Bauer, F. Hauke, T. Seyller and A. Hirsch, *Angew. Chem. Int. Ed.* **2013,** *52*, 754-757.
[114] (a) C. E. Hamilton, J. R. Lomeda, Z. Sun, J. M. Tour and A. R. Barron, *Nano Lett.* **2009,** *9*, 3460-3462; (b) H. Liu, S. Ryu, Z. Chen, M. L. Steigerwald, C. Nuckolls and L. E. Brus, *J. Am. Chem. Soc.* **2009,** *131*, 17099-17101.
[115] (a) J. R. Lomeda, C. D. Doyle, D. V. Kosynkin, W.-F. Hwang and J. M. Tour, *J. Am. Chem. Soc.* **2008,** *130*, 16201-16206; (b) Z. Jin, J. R. Lomeda, B. K. Price, W. Lu, Y. Zhu and J. M. Tour, *Chem. Mater.* **2009,** *21*, 3045-3047.
[116] (a) E. Bekyarova, M. E. Itkis, P. Ramesh, C. Berger, M. Sprinkle, W. A. de Heer and R. C. Haddon, *J. Am. Chem. Soc.* **2009,** *131*, 1336-1337; (b) R. Sharma, J. H. Baik, C. J. Perera and M. S. Strano, *Nano*

so-called "click reaction" is a tool for the rapid and efficient attachment of functional groups to various materials including graphene,[117] enhancing pristine graphene's solubility. Friedel-Crafts acylation reaction has been used for the modification of graphene's edges to aid its exfoliation from graphite.[118] The basal planes can also undergo 1,3-dipolar cycloaddition, "Prato reaction", efficiently.[119] The nucleophilic [2+1] cyclopropanation, Bingel-Hirsch reaction, has been carried out in pristine graphene[120] and also aryne [2+2] cycloadditions.[121] Finally [4+2] Diels-Alder cycloaddition reactions have been performed with graphene acting as either diene or dienephile.[122]

The strong Van der Waals interactions between the graphene layers can be compensated for non-covalent adsorption of different species on the surface of graphene.[123] Solvents such as DMF and NMP are the solvents of choice in graphite exfoliation and stabilization of the individual sheets because their surface energies match that of graphene. The possibility of exfoliating graphene in water in the presence of a surfactant stabilizer has been also widely explored.[124]

The exfoliation of graphene has also been achieved with some electroactive molecules. For example Guldi and coworkers have demonstrated a versatile approach to integrate a donor molecule with graphene and to exfoliate graphite at the same time using a zinc phthalocyanine oligomer (ZnPc-PPV) (figure 25).[125] This functionalized graphene was also tested in a photoelectrochemical cell although not optimized. Free-base porphyrins have also been used to achieve the exfoliation of graphite resulting in

---

Lett. **2010,** *10*, 398-405; (c) Z. Sun, S.-i. Kohama, Z. Zhang, J. Lomeda and J. Tour, *Nano Research* **2010,** *3*, 117-125; (d) J. M. Englert, C. Dotzer, G. Yang, M. Schmid, C. Papp, J. M. Gottfried, H.-P. Steinrück, E. Spiecker, F. Hauke and A. Hirsch, *Nat Chem* **2011,** *3*, 279-286.

[117] (a) Z. Jin, T. P. McNicholas, C.-J. Shih, Q. H. Wang, G. L. C. Paulus, A. J. Hilmer, S. Shimizu and M. S. Strano, *Chem. Mater.* **2011,** *23*, 3362-3370; (b) H.-X. Wang, K.-G. Zhou, Y.-L. Xie, J. Zeng, N.-N. Chai, J. Li and H.-L. Zhang, *Chem. Commun.* **2011,** *47*, 5747-5749; (c) M. Castelaín , G. Martínez, P. Merino, J. Á. Martín-Gago , J. L. Segura, G. Ellis and H. J. Salavagione, *Chem. Eur. J.* **2012,** *18*, 4965-4973.

[118] E.-K. Choi, I.-Y. Jeon, S.-Y. Bae, H.-J. Lee, H. S. Shin, L. Dai and J.-B. Baek, *Chem. Commun.* **2010,** *46*, 6320-6322.

[119] (a) M. Quintana, K. Spyrou, M. Grzelczak, W. R. Browne, P. Rudolf and M. Prato, *ACS Nano* **2010,** *4*, 3527-3533; (b) X. Zhang, L. Hou, A. Cnossen, A. C. Coleman, O. Ivashenko, P. Rudolf, B. J. van Wees, W. R. Browne and B. L. Feringa, *Chem. Eur. J.* **2011,** *17*, 8957-8964; (c) M.-E. Ragoussi, J. Malig, G. Katsukis, B. Butz, E. Spiecker, G. de la Torre, T. Torres and D. M. Guldi, *Angew. Chem. Int. Ed.* **2012,** *51*, 6421-6425.

[120] S. P. Economopoulos, G. Rotas, Y. Miyata, H. Shinohara and N. Tagmatarchis, *ACS Nano* **2010,** *4*, 7499-7507.

[121] X. Zhong, J. Jin, S. Li, Z. Niu, W. Hu, R. Li and J. Ma, *Chem. Commun.* **2010,** *46*, 7340-7342.

[122] (a) S. Sarkar, E. Bekyarova, S. Niyogi and R. C. Haddon, *J. Am. Chem. Soc.* **2011,** *133*, 3324-3327; (b) S. Sarkar, E. Bekyarova and R. C. Haddon, *Acc. Chem. Res.* **2012,** *45*, 673-682.

[123] C. Backes, F. Hauke and A. Hirsch, *Adv. Mater.* **2011,** *23*, 2588-2601.

[124] M. Lotya, Y. Hernandez, P. J. King, R. J. Smith, V. Nicolosi, L. S. Karlsson, F. M. Blighe, S. De, Z. Wang, I. T. McGovern, G. S. Duesberg and J. N. Coleman, *J. Am. Chem. Soc.* **2009,** *131*, 3611-3620.

[125] J. Malig, N. Jux, D. Kiessling, J.-J. Cid, P. Vázquez, T. Torres and D. M. Guldi, *Angew. Chem. Int. Ed.* **2011,** *50*, 3561-3565.

nanographene-porphyrin hybrids (figure 25) that reveal efficient charge transfer in the excited state.[126]

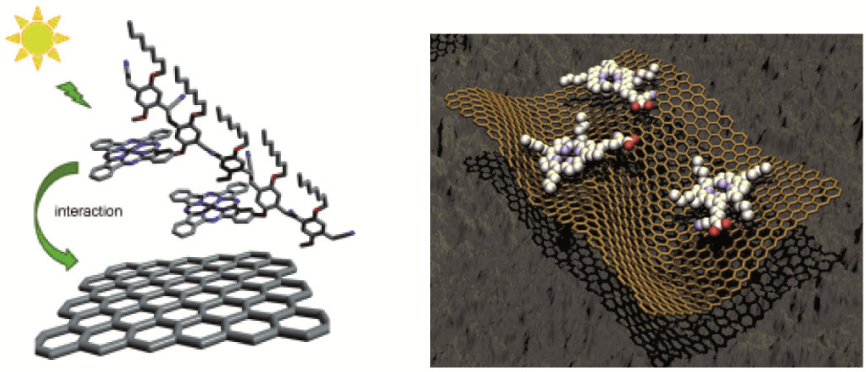

Figure 25. Left: ZnPc-PPV oligomer-graphene hybrid system; right: free-base porphyrin-nanographene hybrid system.

Pyrene derivatives interactions with graphene have been the most investigated option. The supramolecular modification of graphene with pyrene by means of π–π stacking has helped to stabilize graphene in aqueous solutions.[127] The exfoliation of graphite by a positively charged pyrene derivative has been carried out in water to form stable aqueous dispersions of graphene.[128] In an example of multivalent binding, Abruña et al. reported the association of a trivalent pyrene derivative with graphene.[129] This trivalent pyrene was demonstrated to form more stable monolayers than the monovalent pyrene, which is readily desorbed in organic solvents.

Other polycyclic aromatic hydrocarbons (PAHs) have been used for the supramolecular modification and stabilization of graphene layers. The different characteristics of the large aromatic donor and acceptor molecules employed allowed for a rational modification of both the electronic structure and conductivity of graphene sheets.[130] Perylene bisimides PBIs are also suitable for π–π stacking, and are powerful dye-type chromophores that exhibit strong fluorescence. PBIs have been used by Hirsch's group to bind graphene, and its electronic interaction was demonstrated by fluorescence quenching.[131]

Raman spectroscopy has allowed the study of the changes in the electronic structure of graphene due to its interaction with known electron-donors and electron-acceptors.[132]

---

[126] J. Malig, A. W. I. Stephenson, P. Wagner, G. G. Wallace, D. L. Officer and D. M. Guldi, *Chem. Commun.* **2012,** *48*, 8745-8747.
[127] Y. Xu, H. Bai, G. Lu, C. Li and G. Shi, *J. Am. Chem. Soc.* **2008,** *130*, 5856-5857.
[128] J. Malig, C. Romero-Nieto, N. Jux and D. M. Guldi, *Adv. Mater.* **2012,** *24*, 800-805.
[129] J. A. Mann, J. Rodríguez-López, H. D. Abruña and W. R. Dichtel, *J. Am. Chem. Soc.* **2011,** *133*, 17614-17617.
[130] Q. Su, S. Pang, V. Alijani, C. Li, X. Feng and K. Müllen, *Adv. Mater.* **2009,** *21*, 3191-3195.
[131] N. V. Kozhemyakina, J. M. Englert, G. Yang, E. Spiecker, C. D. Schmidt, F. Hauke and A. Hirsch, *Adv. Mater.* **2010,** *22*, 5483-5487.
[132] V. Rakesh, D. Barun, R. Chandra Sekhar and C. N. R. Rao, *J. Phys.: Condens. Matter* **2008,** *20*, 472204.

The Raman G band of few-layer graphene (FLG) changes in the presence of electron donor or acceptor molecules. This band is softened in the presence of electron donor and strengthened with electron acceptor molecules. Additionally, changes in the visible range of the electronic absorption spectrum of graphene have been predicted when electron donor and acceptor molecules are adsorbed onto its surface, if charge transfer takes place.[133] The electrical conductivity is also influenced by association of both types of electroactive molecules: electron-acceptors increase the conductivity and electron-donor molecules decrease the conductivity of few layers graphene

With regards to its use with polymers, pristine graphene has been combined with some of them in the search for materials with improved electronic properties.[134] In fact, graphene have already been used in the performance of organic photovoltaic devices as electron accepting material.[135]

1.5. References

1. H. W. Kroto; J. R. Heath; S. C. O'Brien; R. F. Curl; R. E. Smalley, C_{60}: Buckminsterfullerene. *Nature* **1985,** *318*, 162-163.
2. (a) R. F. Curl, Dawn of Fullerenes: Conjecture and Experiment (Nobel Lecture). *Angew. Chem., Int. Ed. Engl.* **1997,** *36*, 1566-1576;(b) H. Kroto, Symmetry, Space, Stars, and C60 (Nobel Lecture). *Angew. Chem., Int. Ed. Engl.* **1997,** *36*, 1578-1593;(c) R. E. Smalley, Discovering the Fullerenes (Nobel Lecture). *Angew. Chem., Int. Ed. Engl.* **1997,** *36*, 1594-1601.
3. A. Hirsch; M. Brettreich, Parent Fullerenes. In *Fullerenes*, Wiley-VCH Verlag GmbH & Co. KGaA: 2005; pp 1-48.
4. W. Kratschmer; L. D. Lamb; K. Fostiropoulos; D. R. Huffman, Solid C_{60}: a new form of carbon. *Nature* **1990,** *347*, 354-358.
5. R.Buckminster Fuller GEODESIC STRUCTURES (OCR). US 3197927, 1965.
6. (a) S. Iijima, Helical microtubules of graphitic carbon. *Nature* **1991,** *354*, 56-58;(b) D. S. Bethune; C. H. Klang; M. S. de Vries; G. Gorman; R. Savoy; J. Vazquez; R. Beyers, Cobalt-catalysed growth of carbon nanotubes with single-atomic-layer walls. *Nature* **1993,** *363*, 605-607;(c) S. Iijima; T. Ichihashi, Single-shell carbon nanotubes of 1-nm diameter. *Nature* **1993,** *363*, 603-605.
7. (a) K. S. Novoselov; A. K. Geim; S. V. Morozov; D. Jiang; Y. Zhang; S. V. Dubonos; I. V. Grigorieva; A. A. Firsov, Electric Field Effect in Atomically Thin Carbon Films. *Science* **2004,** *306*, 666-669;(b) A. K. Geim; K. S. Novoselov, The rise of graphene. *Nat Mater* **2007,** *6*, 183-191.
8. J. L. Delgado; M. A. Herranz; N. Martín, The nano-forms of carbon. *J. Mater. Chem.* **2008,** *18*, 1417-1426.
9. H. Ajie; M. M. Alvarez; S. J. Anz; R. D. Beck; F. Diederich; K. Fostiropoulos; D. R. Huffman; W. Kraetschmer; Y. Rubin; et al., Characterization of the soluble all-carbon molecules C60 and C70. *J. Phys. Chem.* **1990,** *94*, 8630-8633.
10. (a) J. W. Arbogast; A. P. Darmanyan; C. S. Foote; F. N. Diederich; R. L. Whetten; Y. Rubin; M. M. Alvarez; S. J. Anz, Photophysical properties of sixty atom carbon molecule (C_{60}). *J. Phys. Chem.*

[133] A. K. Manna and S. K. Pati, *Chemistry – An Asian Journal* **2009,** *4*, 855-860.
[134](a) H. Bai, Y. Xu, L. Zhao, C. Li and G. Shi, *Chem. Commun.* **2009,** *0*, 1667-1669; (b) M. Castelaín, H. J. Salavagione, R. Gómez and J. L. Segura, *Chem. Commun.* **2011,** *47*, 7677-7679.
[135] (a) Z. Liu, Q. Liu, Y. Huang, Y. Ma, S. Yin, X. Zhang, W. Sun and Y. Chen, *Adv. Mater.* **2008,** *20*, 3924-3930; (b) Q. Liu, Z. Liu, X. Zhang, L. Yang, N. Zhang, G. Pan, S. Yin, Y. Chen and J. Wei, *Adv. Funct. Mater.* **2009,** *19*, 894-904.

1991, *95*, 11-12;(b) T. W. Ebbesen; K. Tanigaki; S. Kuroshima, Excited-state properties of C_{60}. *Chem. Phys. Lett.* **1991,** *181*, 501-504;(c) D. M. Guldi; M. Prato, Excited-State Properties of C_{60} Fullerene Derivatives. *Acc. Chem. Res.* **2000,** *33*, 695-703.

11. R. R. Hung; J. J. Grabowski, A precise determination of the triplet energy of carbon (C_{60}) by photoacoustic calorimetry. *J. Phys. Chem.* **1991,** *95*, 6073-6075.

12. (a) P. A. Liddell; J. P. Sumida; A. N. Macpherson; L. Noss; G. R. Seely; K. N. Clark; A. L. Moore; T. A. Moore; D. Gust, Preparation and photophysical studies of porphyrin-C_{60} dyads. *Photochem. Photobiol.* **1994,** *60*, 537-541;(b) N. Armaroli; G. Marconi; L. Echegoyen; J.-P. Bourgeois; F. Diederich, Charge-Transfer Interactions in Face-to-Face Porphyrin-Fullerene Systems: Solvent-Dependent Luminescence in the Infrared Spectral Region. *Chem. Eur. J.* **2000,** *6*, 1629-1645.

13. T. Da Ros; M. Prato, Medicinal chemistry with fullerenes and fullerene derivatives. *Chem. Commun.* **1999,** *0*, 663-669.

14. (a) A. W. Jensen; S. R. Wilson; D. I. Schuster, Biological applications of fullerenes. *Biorg. Med. Chem.* **1996,** *4*, 767-779;(b) K. M. Kadish; R. S. Ruoff, *Fullerenes: Chemistry, Physics, and Technology*. Wiley: 2000.

15. (a) N. Martín; L. Sánchez; B. Illescas; I. Pérez, C_{60}-Based Electroactive Organofullerenes. *Chem. Rev.* **1998,** *98*, 2527-2548;(b) H. Imahori; Y. Sakata, Fullerenes as Novel Acceptors in Photosynthetic Electron Transfer. *Eur. J. Org. Chem.* **1999,** *1999*, 2445-2457;(c) D. M. Guldi, Fullerenes: three dimensional electron acceptor materials. *Chem. Commun.* **2000,** *0*, 321-327.

16. (a) R. C. Haddon; L. E. Brus; K. Raghavachari, Electronic structure and bonding in icosahedral C_{60}. *Chem. Phys. Lett.* **1986,** *125*, 459-464;(b) P. D. Hale, Discrete-variational-X.alpha. electronic structure studies of the spherical C_{60} cluster: prediction of ionization potential and electronic transition energy. *J. Am. Chem. Soc.* **1986,** *108*, 6087-6088.

17. Q. Xie; E. Perez-Cordero; L. Echegoyen, Electrochemical detection of C_{60}^{6-} and C_{70}^{6-}: Enhanced stability of fullerides in solution. *J. Am. Chem. Soc.* **1992,** *114*, 3978-3980.

18. L. Echegoyen; L. E. Echegoyen, Electrochemistry of Fullerenes and Their Derivatives. *Acc. Chem. Res.* **1998,** *31*, 593-601.

19. (a) H. Imahori; Y. Sakata, Donor-Linked Fullerenes: Photoinduced electron transfer and its potential application. *Adv. Mater.* **1997,** *9*, 537-546;(b) D. Gust; T. A. Moore; A. L. Moore, Mimicking Photosynthetic Solar Energy Transduction. *Acc. Chem. Res.* **2000,** *34*, 40-48;(c) D. M. Guldi, Fullerene-porphyrin architectures; photosynthetic antenna and reaction center models. *Chem. Soc. Rev.* **2002,** *31*, 22-36.

20. (a) A. F. Hebard; M. J. Rosseinsky; R. C. Haddon; D. W. Murphy; S. H. Glarum; T. T. M. Palstra; A. P. Ramirez; A. R. Kortan, Superconductivity at 18 K in potassium-doped C60. *Nature* **1991,** *350*, 600-601;(b) A. R. Kortan; N. Kopylov; S. Glarum; E. M. Gyorgy; A. P. Ramirez; R. M. Fleming; F. A. Thiel; R. C. Haddon, Superconductivity at 8.4 K in calcium-doped C60. *Nature* **1992,** *355*, 529-532;(c) J. H. Schon; C. Kloc; B. Batlogg, Superconductivity at 52[thinsp]K in hole-doped C60. *Nature* **2000,** *408*, 549-552.

21. P.-M. Allemand; K. C. Khemani; A. Koch; F. Wudl; K. Holczer; S. Donovan; G. Grúner; J. D. Thompson, Organic Molecular Soft Ferromagnetism in a Fullerene C_{60}. *Science* **1991,** *253*, 301-302.

22. L. W. Tutt; A. Kost, Optical limiting performance of C_{60} and C_{70} solutions. *Nature* **1992,** *356*, 225-226.

23. (a) C. J. Brabec; N. S. Sariciftci; J. C. Hummelen, Plastic Solar Cells. *Adv. Funct. Mater.* **2001,** *11*, 15-26;(b) A. Cravino; N. S. Sariciftci, Double-cable polymers for fullerene based organic optoelectronic applications. *J. Mater. Chem.* **2002,** *12*, 1931-1943;(c) D. M. Guldi; N. Martín, Fullerene architectures made to order; biomimetic motifs - design and features. *J. Mater. Chem.* **2002,** *12*, 1978-1992;(d) M. Prato; N. Martín, Editorial. *J. Mater. Chem.* **2002,** *12*, 7-ix-7-ix;(e) N. Martín; L. Sánchez; M. a. Á. Herranz; B. Illescas; D. M. Guldi, Electronic Communication in Tetrathiafulvalene (TTF)/C_{60} Systems: Toward Molecular Solar Energy Conversion Materials? *Acc. Chem. Res.* **2007,** *40*, 1015-1024;(f) J. L. Delgado; P.-A. Bouit; S. Filippone; M. a. A. Herranz; N. Martín, Organic photovoltaics: a chemical approach. *Chem. Commun.* **2010,** *46*, 4853-4865.

24. S. E. Shaheen; C. J. Brabec; N. S. Sariciftci; F. Padinger; T. Fromherz; J. C. Hummelen, 2.5% efficient organic plastic solar cells. *Appl. Phys. Lett.* **2001,** *78*, 841-843.

25. J. C. Hummelen; B. W. Knight; F. LePeq; F. Wudl; J. Yao; C. L. Wilkins, Preparation and Characterization of Fulleroid and Methanofullerene Derivatives. *J. Org. Chem.* **1995,** *60*, 532-538.

26. G. Yu; J. Gao; J. C. Hummelen; F. Wudl; A. J. Heeger, Polymer Photovoltaic Cells: Enhanced Efficiencies via a Network of Internal Donor-Acceptor Heterojunctions. *Science* **1995,** *270*, 1789-1791.
27. M. M. Wienk; J. M. Kroon; W. J. H. Verhees; J. Knol; J. C. Hummelen; P. A. van Hal; R. A. J. Janssen, Efficient Methano[70]fullerene/MDMO-PPV Bulk Heterojunction Photovoltaic Cells. *Angew. Chem. Int. Ed.* **2003,** *42*, 3371-3375.
28. (a) P. Schilinsky; C. Waldauf; C. J. Brabec, Recombination and loss analysis in polythiophene based bulk heterojunction photodetectors. *Appl. Phys. Lett.* **2002,** *81*, 3885-3887;(b) F. Padinger; R. S. Rittberger; N. S. Sariciftci, Effects of Postproduction Treatment on Plastic Solar Cells. *Adv. Funct. Mater.* **2003,** *13*, 85-88.
29. H. Imahori, Giant Multiporphyrin Arrays as Artificial Light-Harvesting Antennas. *J. Phys. Chem. B* **2004,** *108*, 6130-6143.
30. (a) D. M. Guldi; M. Maggini; G. Scorrano; M. Prato, Intramolecular Electron Transfer in Fullerene/Ferrocene Based Donor−Bridge−Acceptor Dyads. *J. Am. Chem. Soc.* **1997,** *119*, 974-980;(b) M. Fujitsuka; N. Tsuboya; R. Hamasaki; M. Ito; S. Onodera; O. Ito; Y. Yamamoto, Solvent Polarity Dependence of Photoinduced Charge Separation and Recombination Processes of Ferrocene−C60 Dyads. *J. Phys. Chem. A* **2003,** *107*, 1452-1458;(c) D. M. Guldi; C. Luo; N. A. Kotov; T. D. Ros; S. Bosi; M. Prato, Zwitterionic Acceptor Moieties: Small Reorganization Energy and Unique Stabilization of Charge Transfer Products†. *J. Phys. Chem. B* **2003,** *107*, 7293-7298.
31. (a) D. M. Guldi; M. Maggini; E. Menna; G. Scorrano; P. Ceroni; M. Marcaccio; F. Paolucci; S. Roffia, A Photosensitizer Dinuclear Ruthenium Complex: Intramolecular Energy Transfer to a Covalently Linked Fullerene Acceptor. *Chem. Eur. J.* **2001,** *7*, 1597-1605;(b) J.-F. Nierengarten; N. Armaroli; G. Accorsi; Y. Rio; J.-F. Eckert, [60]Fullerene: A Versatile Photoactive Core for Dendrimer Chemistry. *Chem. Eur. J.* **2003,** *9*, 36-41.
32. S. N. Smirnov; P. A. Liddell; I. V. Vlassiouk; A. Teslja; D. Kuciauskas; C. L. Braun; A. L. Moore; T. A. Moore; D. Gust, Characterization of the Giant Transient Dipole Generated by Photoinduced Electron Transfer in a Carotene−Porphyrin−Fullerene Molecular Triad. *J. Phys. Chem. A* **2003,** *107*, 7567-7573.
33. (a) R. M. Williams; J. M. Zwier; J. W. Verhoeven, Photoinduced Intramolecular Electron Transfer in a Bridged C_{60} (Acceptor)-Aniline (Donor) System; Photophysical Properties of the First "Active" Fullerene Diad. *J. Am. Chem. Soc.* **1995,** *117*, 4093-4099;(b) K. G. Thomas; V. Biju; D. M. Guldi; P. V. Kamat; M. V. George, Photoinduced Charge Separation and Stabilization in Clusters of a Fullerene−Aniline Dyad. *J. Phys. Chem. B* **1999,** *103*, 8864-8869.
34. (a) D. M. Guldi; C. Luo; A. Swartz; R. Gómez; J. L. Segura; N. Martín; C. Brabec; N. S. Sariciftci, Molecular Engineering of C_{60}-Based Conjugated Oligomer Ensembles: Modulating the Competition between Photoinduced Energy and Electron Transfer Processes. *J. Org. Chem.* **2002,** *67*, 1141-1152;(b) D. M. Guldi; A. Swartz; C. Luo; R. Gómez; J. L. Segura; N. Martín, Rigid Dendritic Donor−Acceptor Ensembles: Control over Energy and Electron Transduction. *J. Am. Chem. Soc.* **2002,** *124*, 10875-10886;(c) J. L. Segura; N. Martín; D. M. Guldi, Materials for organic solar cells: the C_{60}/π-conjugated oligomer approach. *Chem. Soc. Rev.* **2005,** *34*, 31-47;(d) C. M. Atienza; G. Fernández; L. Sánchez; N. Martín; I. S. Dantas; M. M. Wienk; R. A. J. Janssen; G. M. A. Rahman; D. M. Guldi, Light harvesting tetrafullerene nanoarray for organic solar cells. *Chem. Commun.* **2006,** *0*, 514-516;(e) G. Fernández; L. Sánchez; D. Veldman; M. M. Wienk; C. Atienza; D. M. Guldi; R. A. J. Janssen; N. Martín, Tetrafullerene Conjugates for All-Organic Photovoltaics. *J. Org. Chem.* **2008,** *73*, 3189-3196.
35. M. Antonietta Loi; P. Denk; H. Hoppe; H. Neugebauer; C. Winder; D. Meissner; C. Brabec; N. Serdar Sariciftci; A. Gouloumis; P. Vazquez; T. Torres, Long-lived photoinduced charge separation for solar cell applications in phthalocyanine-fulleropyrrolidine dyad thin films. *J. Mater. Chem.* **2003,** *13*, 700-704.
36. (a) Y. Yamashita; Y. Kobayashi; T. Miyashi, p-Quinodimethane Analogues of Tetrathiafulvalene. *Angew. Chem., Int. Ed. Engl.* **1989,** *28*, 1052-1053;(b) M. R. Bryce; A. J. Moore; M. Hasan; G. J. Ashwell; A. T. Fraser; W. Clegg; M. B. Hursthouse; A. I. Karaulov, Electrical and Magnetic Properties and X-Ray Structure of a Highly Conductive 4:1 Complex of Tetracyanoquinodimethane and a Tetrathiafulvalene Derivative. *Angew. Chem., Int. Ed. Engl.* **1990,** *29*, 1450-1452;(c) N. Martín; L. Sánchez; C. Seoane; E. Ortí; P. M. Viruela; R. Viruela, Synthesis, Properties, and Theoretical Characterization of Largely π-Extended Tetrathiafulvalene Derivatives with Quinonoid Structures. *J. Org. Chem.* **1998,** *63*, 1268-1279;(d) C. A. Christensen; A. S. Batsanov; M. R. Bryce, Extreme Conformational Constraints in π-Extended Tetrathiafulvalenes: Unusual Topologies and Redox Behavior of Doubly and Triply Bridged Cyclophanes. *J. Am. Chem. Soc.* **2006,** *128*, 10484-10490.

37. (a) N. Gautier; F. Dumur; V. Lloveras; J. Vidal-Gancedo; J. Veciana; C. Rovira; P. Hudhomme, Intramolecular Electron Transfer Mediated by a Tetrathiafulvalene Bridge in a Purely Organic Mixed-Valence System. *Angew. Chem. Int. Ed.* **2003,** *42*, 2765-2768;(b) M. Mas-Torrent; P. Hadley; S. T. Bromley; X. Ribas; J. Tarrés; M. Mas; E. Molins; J. Veciana; C. Rovira, Correlation between Crystal Structure and Mobility in Organic Field-Effect Transistors Based on Single Crystals of Tetrathiafulvalene Derivatives. *J. Am. Chem. Soc.* **2004,** *126*, 8546-8553.

38. N. Martín; L. Sánchez; C. Seoane; R. Andreu; J. Garín; J. Orduna, Semiconducting charge transfer complexes from [60]Fullerene-tetrathiafulvalene (C_{60}-TTF) systems. *Tetrahedron Lett.* **1996,** *37*, 5979-5982.

39. N. Martín; L. Sánchez; M. A. Herranz; D. M. Guldi, Evidence for Two Separate One-Electron Transfer Events in Excited Fulleropyrrolidine Dyads Containing Tetrathiafulvalene (TTF). *J. Phys. Chem. A* **2000,** *104*, 4648-4657.

40. M. C. Díaz; M. A. Herranz; B. M. Illescas; N. Martín; N. Godbert; M. R. Bryce; C. Luo; A. Swartz; G. Anderson; D. M. Guldi, Probing Charge Separation in Structurally Different C_{60}/exTTF Ensembles. *J. Org. Chem.* **2003,** *68*, 7711-7721.

41. (a) W. Khlbrandt; D. N. Wang, Three-dimensional structure of plant light-harvesting complex determined by electron crystallography. *Nature* **1991,** *350*, 130-134;(b) G. McDermott; S. M. Prince; A. A. Freer; A. M. Hawthornthwaite-Lawless; M. Z. Papiz; R. J. Cogdell; N. W. Isaacs, Crystal structure of an integral membrane light-harvesting complex from photosynthetic bacteria. *Nature* **1995,** *374*, 517-521.

42. C.-H. Huang; N. D. McClenaghan; A. Kuhn; J. W. Hofstraat; D. M. Bassani, Enhanced Photovoltaic Response in Hydrogen-Bonded All-Organic Devices. *Org. Lett.* **2005,** *7*, 3409-3412.

43. (a) C. J. Pedersen, Cyclic polyethers and their complexes with metal salts. *Journal of the American Chemical Society* **1967,** *89*, 2495-2496;(b) C. J. Pedersen, Cyclic polyethers and their complexes with metal salts. *J. Am. Chem. Soc.* **1967,** *89*, 7017-7036.

44. (a) B. Dietrich; J. M. Lehn; J. P. Sauvage, Diaza-polyoxa-macrocycles et macrobicycles. *Tetrahedron Lett.* **1969,** *10*, 2885-2888;(b) B. Dietrich; J. M. Lehn; J. P. Sauvage, Les Cryptates. *Tetrahedron Lett.* **1969,** *10*, 2889-2892.

45. D. J. Cram; J. M. Cram, Host-Guest Chemistry: Complexes between organic compounds simulate the substrate selectivity of enzymes. *Science* **1974,** *183*, 803-809.

46. C. A. Hunter, Quantifying Intermolecular Interactions: Guidelines for the Molecular Recognition Toolbox. *Angew. Chem. Int. Ed.* **2004,** *43*, 5310-5324.

47. J. W. Steed; J. L. Atwood, Concepts. In *Supramolecular Chemistry*, John Wiley & Sons, Ltd: 2009; pp 1-48.

48. G. Whitesides; J. Mathias; C. Seto, Molecular self-assembly and nanochemistry: a chemical strategy for the synthesis of nanostructures. *Science* **1991,** *254*, 1312-1319.

49. R. D. Hancock, Chelate ring size and metal ion selection. The basis of selectivity for metal ions in open-chain ligands and macrocycles. *J. Chem. Educ.* **1992,** *69*, 615.

50. D. J. Cram, Preorganization—From Solvents to Spherands. *Angew. Chem., Int. Ed. Engl.* **1986,** *25*, 1039-1057.

51. L. Brunsveld; B. J. B. Folmer; E. W. Meijer; R. P. Sijbesma, Supramolecular Polymers. *Chem. Rev.* **2001,** *101*, 4071-4098.

52. C. Fouquey; J.-M. Lehn; A.-M. Levelut, Molecular recognition directed self-assembly of supramolecular liquid crystalline polymers from complementary chiral components. *Adv. Mater.* **1990,** *2*, 254-257.

53. J. Sartorius; H.-J. Schneider, A General Scheme Based on Empirical Increments for the Prediction of Hydrogen-Bond Associations of Nucleobases and of Synthetic Host–Guest complexes. *Chem. Eur. J.* **1996,** *2*, 1446-1452.

54. F. H. Beijer; R. P. Sijbesma; H. Kooijman; A. L. Spek; E. W. Meijer, Strong Dimerization of Ureidopyrimidones via Quadruple Hydrogen Bonding. *J. Am. Chem. Soc.* **1998,** *120*, 6761-6769.

55. R. P. Sijbesma; F. H. Beijer; L. Brunsveld; B. J. B. Folmer; J. H. K. K. Hirschberg; R. F. M. Lange; J. K. L. Lowe; E. W. Meijer, Reversible Polymers Formed from Self-Complementary Monomers Using Quadruple Hydrogen Bonding. *Science* **1997,** *278*, 1601-1604.

56. (a) M. R. Ghadiri; J. R. Granja; R. A. Milligan; D. E. McRee; N. Khazanovich, Self-assembling organic nanotubes based on a cyclic peptide architecture. *Nature* **1993,** *366*, 324-327;(b)

D. T. Bong; T. D. Clark; J. R. Granja; M. R. Ghadiri, Self-Assembling Organic Nanotubes. *Angew. Chem. Int. Ed.* **2001,** *40*, 988-1011.

57. J. H. K. K. Hirschberg; L. Brunsveld; A. Ramzi; J. A. J. M. Vekemans; R. P. Sijbesma; E. W. Meijer, Helical self-assembled polymers from cooperative stacking of hydrogen-bonded pairs. *Nature* **2000,** *407*, 167-170.

58. (a) R. Knapp; A. Schott; M. Rehahn, A Novel Synthetic Strategy toward Soluble, Well-Defined Ruthenium(II) Coordination Polymers. *Macromolecules* **1996,** *29*, 478-480;(b) U. Velten; M. Rehahn, First synthesis of soluble, well defined coordination polymers from kinetically unstable copper(I) complexes. *Chem. Commun.* **1996,** *0*, 2639-2640.

59. (a) E. Krieg; H. Weissman; E. Shirman; E. Shimoni; B. Rybtchinski, A recyclable supramolecular membrane for size-selective separation of nanoparticles. *Nat Nano* **2011,** *6*, 141-146;(b) C. Schmuck, Supramolecular structures: Robust materials from weak forces. *Nat Nano* **2011,** *6*, 136-137.

60. (a) P. M. Beaujuge; J. M. J. Fréchet, Molecular Design and Ordering Effects in π-Functional Materials for Transistor and Solar Cell Applications. *J. Am. Chem. Soc.* **2011,** *133*, 20009-20029;(b) Y.-H. Chen; L.-Y. Lin; C.-W. Lu; F. Lin; Z.-Y. Huang; H.-W. Lin; P.-H. Wang; Y.-H. Liu; K.-T. Wong; J. Wen; D. J. Miller; S. B. Darling, Vacuum-Deposited Small-Molecule Organic Solar Cells with High Power Conversion Efficiencies by Judicious Molecular Design and Device Optimization. *J. Am. Chem. Soc.* **2012,** *134*, 13616-13623.

61. L. R. MacGillivray; J. L. Atwood, Structural Classification and General Principles for the Design of Spherical Molecular Hosts. *Angew. Chem. Int. Ed.* **1999,** *38*, 1018-1033.

62. D. Canevet; E. M. Pérez; N. Martín, Wraparound Hosts for Fullerenes: Tailored Macrocycles and Cages. *Angew. Chem. Int. Ed.* **2011,** *50*, 9248-9259.

63. E. M. Pérez; N. Martín, Curves ahead: molecular receptors for fullerenes based on concave-convex complementarity. *Chem. Soc. Rev.* **2008,** *37*, 1512-1519.

64. J. Effing; U. Jonas; L. Jullien; T. Plesnivy; H. Ringsdorf; F. Diederich; C. Thilgen; D. Weinstein, C_{60} and C_{70} in a Basket? – Investigations of Mono- and Multilayers from Azacrown Compounds and Fullerenes. *Angew. Chem., Int. Ed. Engl.* **1992,** *31*, 1599-1602.

65. J. L. Atwood; G. A. Koutsantonis; C. L. Raston, Purification of C_{60} and C_{70} by selective complexation with calixarenes. *Nature* **1994,** *368*, 229-231.

66. T. Suzuki; K. Nakashima; S. Shinkai, Very Convenient and Efficient Purification Method for Fullerene (C₆₀) with 5,11,17,23,29,35,41,47-Octa-<I>tert</I>-butylcalix[8]arene-49,50,51,52,53,54,55,56-octol. *Chem. Lett.* **1994,** *23*, 699-702.

67. (a) C. L. Raston; J. L. Atwood; P. J. Nichols; I. B. N. Sudria, Supramolecular encapsulation of aggregates of C_{60}. *Chem. Commun.* **1996,** *0*, 2615-2616;(b) J. L. Atwood; L. J. Barbour; C. L. Raston; I. B. N. Sudria, C60 and C70 Compounds in the Pincerlike Jaws of Calix[6]arene. *Angew. Chem. Int. Ed.* **1998,** *37*, 981-983;(c) J. L. Atwood; L. J. Barbour; M. W. Heaven; C. L. Raston, Association and orientation of C70 on complexation with calix[5]arene. *Chem. Commun.* **2003,** *0*, 2270-2271;(d) J. L. Atwood; L. J. Barbour; M. W. Heaven; C. L. Raston, Controlling van der Waals Contacts in Complexes of Fullerene C60. *Angew. Chem. Int. Ed.* **2003,** *42*, 3254-3257.

68. (a) K. Tsubaki; K. Tanaka; K. Fuji; T. Kinoshita, Complexation of C60 with hexahomooxacalix[3]arenes and supramolecular structures of complexes in the solid state. *Chem. Commun.* **1998,** *0*, 895-896;(b) N. Komatsu, Preferential precipitation of C70 over C60 with p-halohomooxacalix[3]arenes. *Org. Biomol. Chem.* **2003,** *1*, 204-209.

69. T. Haino; M. Yanase; Y. Fukazawa, New Supramolecular Complex of C_{60} Based on Calix[5]arene—Its Structure in the Crystal and in Solution. *Angew. Chem., Int. Ed. Engl.* **1997,** *36*, 259-260.

70. T. Haino; M. Yanase; Y. Fukazawa, Crystalline supramolecular complexes of C60 with calix[5]arenes. *Tetrahedron Lett.* **1997,** *38*, 3739-3742.

71. (a) D. Felder; B. Heinrich; D. Guillon; J.-F. Nicoud; J.-F. Nierengarten, A Liquid Crystalline Supramolecular Complex of C60 with a Cyclotriveratrylene Derivative. *Chemistry – A European Journal* **2000,** *6*, 3501-3507;(b) S. Mizyed; M. Ashram; D. O. Miller; P. E. Georghiou, Supramolecular complexation of [60]fullerene with hexahomotrioxacalix[3]naphthalenes: a new class of naphthalene-based calixarenes. *J. Chem. Soc. Perk. Trans. 2* **2001,** *0*, 1916-1919;(c) Y. Rio; J.-F. Nierengarten, Water soluble supramolecular cyclotriveratrylene–[60]fullerene complexes with potential for biological applications. *Tetrahedron Lett.* **2002,** *43*, 4321-4324.

72. (a) T. Haino; M. Yanase; Y. Fukazawa, Fullerenes Enclosed in Bridged Calix[5]arenes. *Angew. Chem. Int. Ed.* **1998,** *37*, 997-998;(b) T. Haino; Y. Matsumoto; Y. Fukazawa, Supramolecular Nano Networks Formed by Molecular-Recognition-Directed Self-Assembly of Ditopic Calix[5]arene and Dumbbell [60]Fullerene. *J. Am. Chem. Soc.* **2005,** *127*, 8936-8937;(c) T. Haino; C. Fukunaga; Y. Fukazawa, A New Calix[5]arene-Based Container: Selective Extraction of Higher Fullerenes. *Org. Lett.* **2006,** *8*, 3545-3548;(d) T. Haino; M. Yanase; C. Fukunaga; Y. Fukazawa, Fullerene encapsulation with calix[5]arenes. *Tetrahedron* **2006,** *62*, 2025-2035.

73. M. Yanase; T. Haino; Y. Fukazawa, A self-assembling molecular container for fullerenes. *Tetrahedron Lett.* **1999,** *40*, 2781-2784.

74. (a) T. Haino; H. Araki; Y. Yamanaka; Y. Fukazawa, Fullerene receptor based on calix[5]arene through metal-assisted self-assembly. *Tetrahedron Lett.* **2001,** *42*, 3203-3206;(b) T. Haino; Y. Yamanaka; H. Araki; Y. Fukazawa, Metal-induced regulation of fullerene complexation with double-calix[5]arene. *Chem. Commun.* **2002,** *0*, 402-403.

75. (a) J. L. Atwood; L. J. Barbour; P. J. Nichols; C. L. Raston; C. A. Sandoval, Symmetry-Aligned Supramolecular Encapsulation of C60: [C60⊂(L)2], L=p-Benzylcalix[5]arene or p-Benzylhexahomooxacalix[3]arene. *Chem. Eur. J.* **1999,** *5*, 990-996;(b) A. Ikeda; M. Yoshimura; H. Udzu; C. Fukuhara; S. Shinkai, Inclusion of [60]Fullerene in a Homooxacalix[3]arene-Based Dimeric Capsule Cross-Linked by a PdII−Pyridine Interaction. *J. Am. Chem. Soc.* **1999,** *121*, 4296-4297;(c) A. Ikeda; H. Udzu; M. Yoshimura; S. Shinkai, Inclusion of [60]Fullerene in a Self-assembled Homooxacalix[3]arene-based Dimeric Capsule Constructed by a PdII–pyridine Interaction. The Li+-binding to the Lower Rims can Improve the Inclusion Ability. *Tetrahedron* **2000,** *56*, 1825-1832.

76. J. C. Iglesias-Sánchez; A. Fragoso; J. de Mendoza; P. Prados, Aryl−Aryl Linked Bi-5,5‘-p-tert-butylcalix[4]arene Tweezer for Fullerene Complexation. *Org. Lett.* **2006,** *8*, 2571-2574.

77. J. W. Steed; P. C. Junk; J. L. Atwood; M. J. Barnes; C. L. Raston; R. S. Burkhalter, Ball and Socket Nanostructures: New Supramolecular Chemistry Based on Cyclotriveratrylene. *J. Am. Chem. Soc.* **1994,** *116*, 10346-10347.

78. (a) H. Matsubara; A. Hasegawa; K. Shiwaku; K. Asano; M. Uno; S. Takahashi; K. Yamamoto, Supramolecular Inclusion Complexes of Fullerenes Using Cyclotriveratrylene Derivatives with Aromatic Pendants. *Chem. Lett.* **1998,** *27*, 923-924;(b) H. Matsubara; T. Shimura; A. Hasegawa; M. Semba; K. Asano; K. Yamamoto, Syntheses of Novel Fullerene Tweezers and Their Supramolecular Inclusion Complex of C_{60}. *Chem. Lett.* **1998,** *27*, 1099-1100;(c) H. Matsubara; S.-y. Oguri; K. Asano; K. Yamamoto, Syntheses of Novel Cyclotriveratrylenophane Capsules and Their Supramolecular Complexes of Fullerenes. *Chem. Lett.* **1999,** *28*, 431-432;(d) J. F. Nierengarten, Supramolecular Encapsulation of [60]Fullerene with Dendritic Cyclotriveratrylene Derivatives. *Fullerenes, Nanotubes and Carbon Nanostructures* **2005,** *13*, 229-242.

79. (a) E. Huerta; E. Cequier; J. d. Mendoza, Preferential separation of fullerene[84] from fullerene mixtures by encapsulation. *Chem. Commun.* **2007,** *0*, 5016-5018;(b) E. Huerta; G. A. Metselaar; A. Fragoso; E. Santos; C. Bo; J. de Mendoza, Selective binding and easy separation of C_{70} by nanoscale self-assembled capsules. *Angew. Chem. Int. Ed.* **2007,** *46*, 202-205.

80. M.-J. Li; C.-H. Huang; C.-C. Lai; S.-H. Chiu, Hemicarceplex Formation With a Cyclotriveratrylene-Based Molecular Cage Allows Isolation of High-Purity (≥99.0%) C70 Directly from Fullerene Extracts. *Org. Lett.* **2012,** *14*, 6146-6149.

81. W. E. Barth; R. G. Lawton, Dibenzo[ghi,mno]fluoranthene. *J. Am. Chem. Soc.* **1966,** *88*, 380-381.

82. H. Becker; G. Javahery; S. Petrie; P. C. Cheng; H. Schwarz; L. T. Scott; D. K. Bohme, Gas-phase ion/molecule reactions of corannulene, a fullerene subunit. *J. Am. Chem. Soc.* **1993,** *115*, 11636-11637.

83. (a) S. Mizyed; P. E. Georghiou; M. Bancu; B. Cuadra; A. K. Rai; P. Cheng; L. T. Scott, Embracing C_{60} with Multiarmed Geodesic Partners. *J. Am. Chem. Soc.* **2001,** *123*, 12770-12774;(b) P. E. Georghiou; A. H. Tran; S. Mizyed; M. Bancu; L. T. Scott, Concave Polyarenes with Sulfide-Linked Flaps and Tentacles: New Electron-Rich Hosts for Fullerenes. *J. Org. Chem.* **2005,** *70*, 6158-6163.

84. A. Sygula; F. R. Fronczek; R. Sygula; P. W. Rabideau; M. M. Olmstead, A Double Concave Hydrocarbon Buckycatcher. *J. Am. Chem. Soc.* **2007,** *129*, 3842-3843.

85. (a) T. Kawase; H. R. Darabi; M. Oda, Cyclic [6]- and [8]Paraphenylacetylenes. *Angew. Chem., Int. Ed. Engl.* **1996,** *35*, 2664-2666;(b) T. Kawase; K. Tanaka; N. Fujiwara; H. R. Darabi; M. Oda, Complexation of a Carbon Nanoring with Fullerenes. *Angew. Chem. Int. Ed.* **2003,** *42*, 1624-1628;(c) T.

Kawase; K. Tanaka; Y. Seirai; N. Shiono; M. Oda, Complexation of Carbon Nanorings with Fullerenes: Supramolecular Dynamics and Structural Tuning for a Fullerene Sensor. *Angew. Chem. Int. Ed.* **2003,** *42*, 5597-5600;(d) T. Kawase; N. Fujiwara; M. Tsutumi; M. Oda; Y. Maeda; T. Wakahara; T. Akasaka, Supramolecular Dynamics of Cyclic [6]Paraphenyleneacetylene Complexes with [60]- and [70]Fullerene Derivatives: Electronic and Structural Effects on Complexation. *Angew. Chem. Int. Ed.* **2004,** *43*, 5060-5062;(e) T. Kawase; K. Tanaka; N. Shiono; Y. Seirai; M. Oda, Onion-Type Complexation Based on Carbon Nanorings and a Buckminsterfullerene. *Angew. Chem. Int. Ed.* **2004,** *43*, 1722-1724;(f) T. Kawase; H. Kurata, Ball-, Bowl-, and Belt-Shaped Conjugated Systems and Their Complexing Abilities: Exploration of the Concave−Convex π−π Interaction. *Chem. Rev.* **2006,** *106*, 5250-5273;(g) T. K. a. M. Oda, Complexation of carbon nanorings with fullerenes. *Pure Appl. Chem.* **2006,** *78*, 9.

86. T. Kawase; Y. Nishiyama; T. Nakamura; T. Ebi; K. Matsumoto; H. Kurata; M. Oda, Cyclic [5]Paraphenyleneacetylene: Synthesis, Properties, and Formation of a Ring-in-Ring Complex Showing a Considerably Large Association Constant and Entropy Effect. *Angew. Chem. Int. Ed.* **2007,** *46*, 1086-1088.

87. K. M. Kadish; K. M. Smith; R. Guilard, *The porphyrin handbook: Synthesis and organic chemistry*. Academic Press: 1999.

88. (a) P. D. W. Boyd; M. C. Hodgson; C. E. F. Rickard; A. G. Oliver; L. Chaker; P. J. Brothers; R. D. Bolskar; F. S. Tham; C. A. Reed, Selective Supramolecular Porphyrin/Fullerene Interactions1. *J. Am. Chem. Soc.* **1999,** *121*, 10487-10495;(b) P. D. W. Boyd; C. A. Reed, Fullerene−Porphyrin Constructs. *Acc. Chem. Res.* **2004,** *38*, 235-242.

89. Y. Sun; T. Drovetskaya; R. D. Bolskar; R. Bau; P. D. W. Boyd; C. A. Reed, Fullerides of Pyrrolidine-Functionalized C60. *J. Org. Chem.* **1997,** *62*, 3642-3649.

90. K. Tashiro; T. Aida; J.-Y. Zheng; K. Kinbara; K. Saigo; S. Sakamoto; K. Yamaguchi, A Cyclic Dimer of Metalloporphyrin Forms a Highly Stable Inclusion Complex with C60. *J. Am. Chem. Soc.* **1999,** *121*, 9477-9478.

91. K. Tashiro; T. Aida, Metalloporphyrin hosts for supramolecular chemistry of fullerenes. *Chem. Soc. Rev.* **2007,** *36*, 189-197.

92. (a) K. Tashiro; T. Aida, π-Electronic Charge-Transfer Interactions in Inclusion Complexes of Fullerenens with Cyclic Dimers of Metalloporphyrins. *Journal of inclusion phenomena and macrocyclic chemistry* **2001,** *41*, 215-217;(b) J.-Y. Zheng; K. Tashiro; Y. Hirabayashi; K. Kinbara; K. Saigo; T. Aida; S. Sakamoto; K. Yamaguchi, Cyclic Dimers of Metalloporphyrins as Tunable Hosts for Fullerenes: A Remarkable Effect of Rhodium(III). *Angew. Chem. Int. Ed.* **2001,** *40*, 1857-1861;(c) K. Tashiro; Y. Hirabayashi; T. Aida; K. Saigo; K. Fujiwara; K. Komatsu; S. Sakamoto; K. Yamaguchi, A Supramolecular Oscillator Composed of Carbon Nanocluster C120 and a Rhodium(III) Porphyrin Cyclic Dimer. *J. Am. Chem. Soc.* **2002,** *124*, 12086-12087;(d) Y. Shoji; K. Tashiro; T. Aida, Selective Extraction of Higher Fullerenes Using Cyclic Dimers of Zinc Porphyrins. *J. Am. Chem. Soc.* **2004,** *126*, 6570-6571;(e) A. Ouchi; K. Tashiro; K. Yamaguchi; T. Tsuchiya; T. Akasaka; T. Aida, A Self-Regulatory Host in an Oscillatory Guest Motion: Complexation of Fullerenes with a Short-Spaced Cyclic Dimer of an Organorhodium Porphyrin. *Angew. Chem. Int. Ed.* **2006,** *45*, 3542-3546.

93. M. Yanagisawa; K. Tashiro; M. Yamasaki; T. Aida, Hosting Fullerenes by Dynamic Bond Formation with an Iridium Porphyrin Cyclic Dimer: A "Chemical Friction" for Rotary Guest Motions. *J. Am. Chem. Soc.* **2007,** *129*, 11912-11913.

94. Y. Shoji; K. Tashiro; T. Aida, Sensing of Chiral Fullerenes by a Cyclic Host with an Asymmetrically Distorted π-Electronic Component. *J. Am. Chem. Soc.* **2006,** *128*, 10690-10691.

95. Y. Shoji; K. Tashiro; T. Aida, One-Pot Enantioselective Extraction of Chiral Fullerene C_{76} Using a Cyclic Host Carrying an Asymmetrically Distorted, Highly π-Basic Porphyrin Module. *J. Am. Chem. Soc.* **2010,** *132*, 5928-5929.

96. G. n. Gil-Ramírez; S. D. Karlen; A. Shundo; K. Porfyrakis; Y. Ito; G. A. D. Briggs; J. J. L. Morton; H. L. Anderson, A Cyclic Porphyrin Trimer as a Receptor for Fullerenes. *Org. Lett.* **2010,** *12*, 3544-3547.

97. T. Kawase, Supramolecular Chemistry of Fullerenes: Host Molecules for Fullerenes on the Basis of π-π Interaction. In *Chemistry of Nanocarbons*, John Wiley & Sons, Ltd: 2010; pp 189-213.

98. T. Yamaguchi; N. Ishii; K. Tashiro; T. Aida, Supramolecular Peapods Composed of a Metalloporphyrin Nanotube and Fullerenes. *J. Am. Chem. Soc.* **2003,** *125*, 13934-13935.

99. (a) H. Nobukuni; Y. Shimazaki; F. Tani; Y. Naruta, A Nanotube of Cyclic Porphyrin Dimers Connected by Nonclassical Hydrogen Bonds and Its Inclusion of C60 in a Linear Arrangement. *Angew.*

Chem. Int. Ed. **2007,** *46*, 8975-8978;(b) H. Nobukuni; F. Tani; Y. Shimazaki; Y. Naruta; K. Ohkubo; T. Nakanishi; T. Kojima; S. Fukuzumi; S. Seki, Anisotropic High Electron Mobility and Photodynamics of a Self-Assembled Porphyrin Nanotube Including C60 Molecules. *J. Phys. Chem. C* **2009,** *113*, 19694-19699;(c) H. Nobukuni; Y. Shimazaki; H. Uno; Y. Naruta; K. Ohkubo; T. Kojima; S. Fukuzumi; S. Seki; H. Sakai; T. Hasobe; F. Tani, Supramolecular Structures and Photoelectronic Properties of the Inclusion Complex of a Cyclic Free-Base Porphyrin Dimer and C60. *Chem. Eur. J.* **2010,** *16*, 11611-11623.

100. G. D. Pantoş; P. Pengo; J. K. M. Sanders, Hydrogen-Bonded Helical Organic Nanotubes. *Angew. Chem. Int. Ed.* **2007,** *46*, 194-197.

101. G. D. Pantoş; J.-L. Wietor; J. K. M. Sanders, Filling Helical Nanotubes with C_{60}. *Angew. Chem. Int. Ed.* **2007,** *46*, 2238-2240.

102. (a) T. Kawauchi; J. Kumaki; A. Kitaura; K. Okoshi; H. Kusanagi; K. Kobayashi; T. Sugai; H. Shinohara; E. Yashima, Encapsulation of Fullerenes in a Helical PMMA Cavity Leading to a Robust Processable Complex with a Macromolecular Helicity Memory. *Angew. Chem. Int. Ed.* **2008,** *47*, 515-519;(b) S. Qi; H. Iida; L. Liu; S. Irle; W. Hu; E. Yashima, Electrical Switching Behavior of a [60]Fullerene-Based Molecular Wire Encapsulated in a Syndiotactic Poly(methyl methacrylate) Helical Cavity. *Angew. Chem.* **2013,** *125*, 1083-1087.

103. L. Sánchez; M. T. Rispens; J. C. Hummelen, A Supramolecular Array of Fullerenes by Quadruple Hydrogen Bonding. *Angew. Chem. Int. Ed.* **2002,** *41*, 838-840.

104. T. Haino; E. Hirai; Y. Fujiwara; K. Kashihara, Supramolecular Cross-Linking of [60]Fullerene-Tagged Polyphenylacetylene by the Host–Guest Interaction of Calix[5]arene and [60]Fullerene. *Angew. Chem. Int. Ed.* **2010,** *49*, 7899-7903.

105. (a) N. Armaroli; C. Boudon; D. Felder; J.-P. Gisselbrecht; M. Gross; G. Marconi; J.-F. Nicoud; J.-F. Nierengarten; V. Vicinelli, A Copper(I) Bis-phenanthroline Complex Buried in Fullerene-Functionalized Dendritic Black Boxes. *Angew. Chem. Int. Ed.* **1999,** *38*, 3730-3733;(b) J.-F. Nierengarten, Fullerodendrimers: A New Class of Compounds for Supramolecular Chemistry and Materials Science Applications. *Chem. Eur. J.* **2000,** *6*, 3667-3670.

106. J. Ruiz; C. Pradet; F. Varret; D. Astruc, Molecular batteries: synthesis and characterization of a dendritic 19-electron FeI complex that reduces C60 to its mono-anion. *Chem. Commun.* **2002,** *0*, 1108-1109.

107. K. Hager; U. Hartnagel; A. Hirsch, Supramolecular Dendrimers Self-Assembled from Dendritic Fullerene Ligands and a Homotritopic Hamilton Receptor. *Eur. J. Org. Chem.* **2007,** *2007*, 1942-1956.

108. B. Partoens; F. M. Peeters, From graphene to graphite: Electronic structure around the K point. *Physical Review B* **2006,** *74*, 075404.

109. (a) C. N. R. Rao; A. K. Sood; K. S. Subrahmanyam; A. Govindaraj, Graphene: The New Two-Dimensional Nanomaterial. *Angew. Chem. Int. Ed.* **2009,** *48*, 7752-7777;(b) P. Avouris, Graphene: Electronic and Photonic Properties and Devices. *Nano Lett.* **2010,** *10*, 4285-4294;(c) S. Pang; Y. Hernández; X. Feng; K. Muellen, Graphene as Transparent Electrode Material for Organic Electronics. *Adv. Mater.* **2011,** *23*, 2779-2795;(d) E. Bekyarova; S. Sarkar; F. Wang; M. E. Itkis; I. Kalinina; X. Tian; R. C. Haddon, Effect of Covalent Chemistry on the Electronic Structure and Properties of Carbon Nanotubes and Graphene. *Acc. Chem. Res.* **2013,** *46*, 65-76.

110. N. Savage, Materials science: Super carbon. *Nature* **2012,** *483*, S30-S31.

111. H. Hu; Z. Zhao; W. Wan; Y. Gogotsi; J. Qiu, Ultralight and Highly Compressible Graphene Aerogels. *Adv. Mater.* **2013,** *25*, 2219-2223.

112. S. Guo; S. Dong, Graphene nanosheet: synthesis, molecular engineering, thin film, hybrids, and energy and analytical applications. *Chem. Soc. Rev.* **2011,** *40*, 2644-2672.

113. (a) K. S. Subrahmanyam; P. Kumar; U. Maitra; A. Govindaraj; K. P. S. S. Hembram; U. V. Waghmare; C. N. R. Rao, Chemical storage of hydrogen in few-layer graphene. *Proc. Natl. Acad. Sci.* **2011,** *108*, 2674-2677;(b) R. A. Schäfer; J. M. Englert; P. Wehrfritz; W. Bauer; F. Hauke; T. Seyller; A. Hirsch, On the Way to Graphane—Pronounced Fluorescence of Polyhydrogenated Graphene. *Angew. Chem. Int. Ed.* **2013,** *52*, 754-757.

114. (a) C. E. Hamilton; J. R. Lomeda; Z. Sun; J. M. Tour; A. R. Barron, High-Yield Organic Dispersions of Unfunctionalized Graphene. *Nano Lett.* **2009,** *9*, 3460-3462;(b) H. Liu; S. Ryu; Z. Chen; M. L. Steigerwald; C. Nuckolls; L. E. Brus, Photochemical Reactivity of Graphene. *J. Am. Chem. Soc.* **2009,** *131*, 17099-17101.

115. (a) J. R. Lomeda; C. D. Doyle; D. V. Kosynkin; W.-F. Hwang; J. M. Tour, Diazonium Functionalization of Surfactant-Wrapped Chemically Converted Graphene Sheets. *J. Am. Chem. Soc.*

2008, *130*, 16201-16206;(b) Z. Jin; J. R. Lomeda; B. K. Price; W. Lu; Y. Zhu; J. M. Tour, Mechanically Assisted Exfoliation and Functionalization of Thermally Converted Graphene Sheets. *Chem. Mater.* **2009,** *21*, 3045-3047.

116. (a) E. Bekyarova; M. E. Itkis; P. Ramesh; C. Berger; M. Sprinkle; W. A. de Heer; R. C. Haddon, Chemical Modification of Epitaxial Graphene: Spontaneous Grafting of Aryl Groups. *J. Am. Chem. Soc.* **2009,** *131*, 1336-1337;(b) R. Sharma; J. H. Baik; C. J. Perera; M. S. Strano, Anomalously Large Reactivity of Single Graphene Layers and Edges toward Electron Transfer Chemistries. *Nano Lett.* **2010,** *10*, 398-405;(c) Z. Sun; S.-i. Kohama; Z. Zhang; J. Lomeda; J. Tour, Soluble graphene through edge-selective functionalization. *Nano Research* **2010,** *3*, 117-125;(d) J. M. Englert; C. Dotzer; G. Yang; M. Schmid; C. Papp; J. M. Gottfried; H.-P. Steinrück; E. Spiecker; F. Hauke; A. Hirsch, Covalent bulk functionalization of graphene. *Nat Chem* **2011,** *3*, 279-286.

117. (a) Z. Jin; T. P. McNicholas; C.-J. Shih; Q. H. Wang; G. L. C. Paulus; A. J. Hilmer; S. Shimizu; M. S. Strano, Click Chemistry on Solution-Dispersed Graphene and Monolayer CVD Graphene. *Chem. Mater.* **2011,** *23*, 3362-3370;(b) H.-X. Wang; K.-G. Zhou; Y.-L. Xie; J. Zeng; N.-N. Chai; J. Li; H.-L. Zhang, Photoactive graphene sheets prepared by "click" chemistry. *Chem. Commun.* **2011,** *47*, 5747-5749;(c) M. Castelaín ; G. Martínez; P. Merino; J. Á. Martín-Gago ; J. L. Segura; G. Ellis; H. J. Salavagione, Graphene Functionalisation with a Conjugated Poly(fluorene) by Click Coupling: Striking Electronic Properties in Solution. *Chem. Eur. J.* **2012,** *18*, 4965-4973.

118. E.-K. Choi; I.-Y. Jeon; S.-Y. Bae; H.-J. Lee; H. S. Shin; L. Dai; J.-B. Baek, High-yield exfoliation of three-dimensional graphite into two-dimensional graphene-like sheets. *Chem. Commun.* **2010,** *46*, 6320-6322.

119. (a) M. Quintana; K. Spyrou; M. Grzelczak; W. R. Browne; P. Rudolf; M. Prato, Functionalization of Graphene via 1,3-Dipolar Cycloaddition. *ACS Nano* **2010,** *4*, 3527-3533;(b) X. Zhang; L. Hou; A. Cnossen; A. C. Coleman; O. Ivashenko; P. Rudolf; B. J. van Wees; W. R. Browne; B. L. Feringa, One-Pot Functionalization of Graphene with Porphyrin through Cycloaddition Reactions. *Chem. Eur. J.* **2011,** *17*, 8957-8964;(c) M.-E. Ragoussi; J. Malig; G. Katsukis; B. Butz; E. Spiecker; G. de la Torre; T. Torres; D. M. Guldi, Linking Photo- and Redoxactive Phthalocyanines Covalently to Graphene. *Angew. Chem. Int. Ed.* **2012,** *51*, 6421-6425.

120. S. P. Economopoulos; G. Rotas; Y. Miyata; H. Shinohara; N. Tagmatarchis, Exfoliation and Chemical Modification Using Microwave Irradiation Affording Highly Functionalized Graphene. *ACS Nano* **2010,** *4*, 7499-7507.

121. X. Zhong; J. Jin; S. Li; Z. Niu; W. Hu; R. Li; J. Ma, Aryne cycloaddition: highly efficient chemical modification of graphene. *Chem. Commun.* **2010,** *46*, 7340-7342.

122. (a) S. Sarkar; E. Bekyarova; S. Niyogi; R. C. Haddon, Diels−Alder Chemistry of Graphite and Graphene: Graphene as Diene and Dienophile. *J. Am. Chem. Soc.* **2011,** *133*, 3324-3327;(b) S. Sarkar; E. Bekyarova; R. C. Haddon, Chemistry at the Dirac Point: Diels–Alder Reactivity of Graphene. *Acc. Chem. Res.* **2012,** *45*, 673-682.

123. C. Backes; F. Hauke; A. Hirsch, The Potential of Perylene Bisimide Derivatives for the Solubilization of Carbon Nanotubes and Graphene. *Adv. Mater.* **2011,** *23*, 2588-2601.

124. M. Lotya; Y. Hernandez; P. J. King; R. J. Smith; V. Nicolosi; L. S. Karlsson; F. M. Blighe; S. De; Z. Wang; I. T. McGovern; G. S. Duesberg; J. N. Coleman, Liquid Phase Production of Graphene by Exfoliation of Graphite in Surfactant/Water Solutions. *J. Am. Chem. Soc.* **2009,** *131*, 3611-3620.

125. J. Malig; N. Jux; D. Kiessling; J.-J. Cid; P. Vázquez; T. Torres; D. M. Guldi, Towards Tunable Graphene/Phthalocyanine–PPV Hybrid Systems. *Angew. Chem. Int. Ed.* **2011,** *50*, 3561-3565.

126. J. Malig; A. W. I. Stephenson; P. Wagner; G. G. Wallace; D. L. Officer; D. M. Guldi, Direct exfoliation of graphite with a porphyrin - creating functionalizable nanographene hybrids. *Chem. Commun.* **2012,** *48*, 8745-8747.

127. Y. Xu; H. Bai; G. Lu; C. Li; G. Shi, Flexible Graphene Films via the Filtration of Water-Soluble Noncovalent Functionalized Graphene Sheets. *J. Am. Chem. Soc.* **2008,** *130*, 5856-5857.

128. J. Malig; C. Romero-Nieto; N. Jux; D. M. Guldi, Integrating Water-Soluble Graphene into Porphyrin Nanohybrids. *Adv. Mater.* **2012,** *24*, 800-805.

129. J. A. Mann; J. Rodríguez-López; H. D. Abruña; W. R. Dichtel, Multivalent Binding Motifs for the Noncovalent Functionalization of Graphene. *J. Am. Chem. Soc.* **2011,** *133*, 17614-17617.

130. Q. Su; S. Pang; V. Alijani; C. Li; X. Feng; K. Müllen, Composites of Graphene with Large Aromatic Molecules. *Adv. Mater.* **2009,** *21*, 3191-3195.

131. N. V. Kozhemyakina; J. M. Englert; G. Yang; E. Spiecker; C. D. Schmidt; F. Hauke; A. Hirsch, Non-Covalent Chemistry of Graphene: Electronic Communication with Dendronized Perylene Bisimides. *Adv. Mater.* **2010,** *22*, 5483-5487.
132. V. Rakesh; D. Barun; R. Chandra Sekhar; C. N. R. Rao, Effects of charge transfer interaction of graphene with electron donor and acceptor molecules examined using Raman spectroscopy and cognate techniques. *J. Phys.: Condens. Matter* **2008,** *20*, 472204.
133. A. K. Manna; S. K. Pati, Tuning the Electronic Structure of Graphene by Molecular Charge Transfer: A Computational Study. *Chemistry – An Asian Journal* **2009,** *4*, 855-860.
134. (a) H. Bai; Y. Xu; L. Zhao; C. Li; G. Shi, Non-covalent functionalization of graphene sheets by sulfonated polyaniline. *Chem. Commun.* **2009,** *0*, 1667-1669;(b) M. Castelaín; H. J. Salavagione; R. Gómez; J. L. Segura, Supramolecular assembly of graphene with functionalized poly(fluorene-alt-phenylene): the role of the anthraquinone pendant groups. *Chem. Commun.* **2011,** *47*, 7677-7679.
135. (a) Z. Liu; Q. Liu; Y. Huang; Y. Ma; S. Yin; X. Zhang; W. Sun; Y. Chen, Organic Photovoltaic Devices Based on a Novel Acceptor Material: Graphene. *Adv. Mater.* **2008,** *20*, 3924-3930;(b) Q. Liu; Z. Liu; X. Zhang; L. Yang; N. Zhang; G. Pan; S. Yin; Y. Chen; J. Wei, Polymer Photovoltaic Cells Based on Solution-Processable Graphene and P3HT. *Adv. Funct. Mater.* **2009,** *19*, 894-904.

2. PREVIOUS WORK. SUPRAMOLECULAR CHEMISTRY OF FULLERENES

The photosynthetic apparatus is an important example of a complex ensemble organized by noncovalent interactions in nature. In this photosynthetic process, a highly organized array of electron donor and acceptor moieties is able to transform sunlight into chemical energy by means of a cascade of energy and electron transfer events that operate to convert CO_2 and H_2O into glucose and ATP.[1] Owing to the significance of this complex natural process, big efforts have been dedicated to the construction of chemical structures capable of reproducing it. In order to do that, efficient energy and electron transfer are fundamental in the development of molecular-scale optoelectronics and photonics.

Studies of energy and electron transfer processes in supramolecular systems allow the human being to pave the way for the construction of artificial photosynthetic systems and efficient photovoltaic devices inspired by biomimetic principles. A wide variety of organic electroactive molecules have been utilized in the preparation of models for the study of energy and electron transfer processes, and also for the fabrication of optoelectronic devices, but among the different electron acceptors, [60]fullerene and its derivatives are probably the most successful systems. Therefore, the supramolecular chemistry of fullerenes becomes an interesting tool that scientist must handle to control the nanostructure of fullerene-based devices, taking advantage of the dynamic nature of noncovalent interactions.

The type of noncovalent interactions that we can use depends on the structure of the interacting host and guest. For example, since C_{60} is a spherical polyene without functionality, we are restricted to dispersion-type interactions. Alternatively, we can add the necessary functionality if we would like to use directional interactions such as hydrogen bonds. In the following, we will summarize some of the most prominent examples of hydrogen bonded complexes involving fullerenes.

2.1. Hydrogen bonding in fullerene chemistry

Hydrogen bond arrays are an important tool for self-assembly[2] and were used to achieve the first supramolecular fullerene dimer by Diedrich, Echegoyen and Stoddart in 1999.[3] The considerable attention that the design and synthesis of [60] fullerene

[1] (a) J. P. Abrahams, A. G. W. Leslie, R. Lutter and J. E. Walker, *Nature* **1994,** *370*, 621-628; (b) T. S. Bibby, J. Nield, F. Partensky and J. Barber, *Nature* **2001,** *413*, 590-590.

[2] L. J. Prins, D. N. Reinhoudt and P. Timmerman, *Angew. Chem. Int. Ed.* **2001,** *40*, 2382-2426.

[3] F. Diederich, L. Echegoyen, M. Gómez-López, R. Kessinger and J. Fraser Stoddart, *J. Chem. Soc. Perk. Trans. 2* **1999,** *0*, 1577-1586.

dimers attracted prompted our group to achieve the first rigid non-covalent C_{60}-dimer.[4] In this case the design was based on a 2-ureido-4-pyrimidone moiety, previously reported to form remarkably stable dimers.[5]

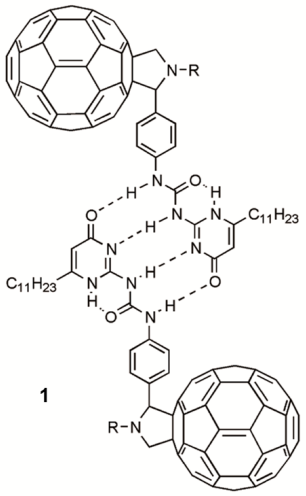

Figure 1. Structure of the C_{60}-dimer and the quadruple hydrogen bond motif.

In this noncovalent C_{60}-dimer both molecular subunits are linked by a self-complementary donor, donor, acceptor, acceptor (DDAA) array of hydrogen bonding motifs. The electrochemical studies of the dimer indicate that there is no mutual interaction in the ground state between the C_{60} units. Nevertheless, the photophysical data of the excited states disclose discernible changes between the monomer and the dimer. This was the first piece of evidence supporting the strong electronic coupling of electroactive units mediated through the highly directional fourfold hydrogen bonding motif. There are plenty of examples in nature where electron transfer is carried out through a network of hydrogen bonds, which makes synthetic hydrogen bonded donor-acceptor assemblies interesting biomimetic model systems. On the other hand, it has been reported that electronic communication through a hydrogen bond interface is greater than in comparable σ- or π-bonding networks.[6]

Considering this precedents, the next step in the use of hydrogen bonds in the supramolecular chemistry of fullerene was to interface strong electron donor units with the C_{60} core. In the context of preparing new donor-acceptor supramolecular pairs, the

[4] J. J. González, S. González, E. M. Priego, C. Luo, D. M. Guldi, J. d. Mendoza and N. Martín, *Chem. Commun.* **2001,** *0*, 163-164.

[5] B. J. B. Folmer, R. P. Sijbesma, H. Kooijman, A. L. Spek and E. W. Meijer, *J. Am. Chem. Soc.* **1999,** *121*, 9001-9007.

[6] (a) J. L. Sessler, B. Wang and A. Harriman, *J. Am. Chem. Soc.* **1993,** *115*, 10418-10419; S. A. W. P. J. de Rege, M. J. Therien, *Science* **1995**, 1409-1413.

integration of tetrathiafulvalene (TTF)[7] and π-conjugated *p*-quinonoid-TTF (exTTF)[8] together with C_{60} appears as a particularly promising approach.

It was considered that two strong, well oriented hydrogen bonds, in combination with ionic interactions, would ensure the formation of stable donor-acceptor dyads. A complementary carboxylate-guanidinium ion pair was used in the design of the ensemble,[9] with a tuned architecture based in different length of spacers and different functional groups, necessary to differentiate between through-bond or through-space character of the electron-transfer. Differences in the fullerene deactivation of fluorescence were not found using either an amide or an ester group in the connection between TTF and guanidinium, this trend indicates that a through-space mechanism might be operative. In the case of spacers of different length, only a 20% increase in fluorescence was observed when rigid biphenyl spacer was used instead of phenyl, while in the case of through-bond mechanism an increase of two orders of magnitude was expected. This confirms a through-space electronic interaction between the two chromophore units in the dyad.

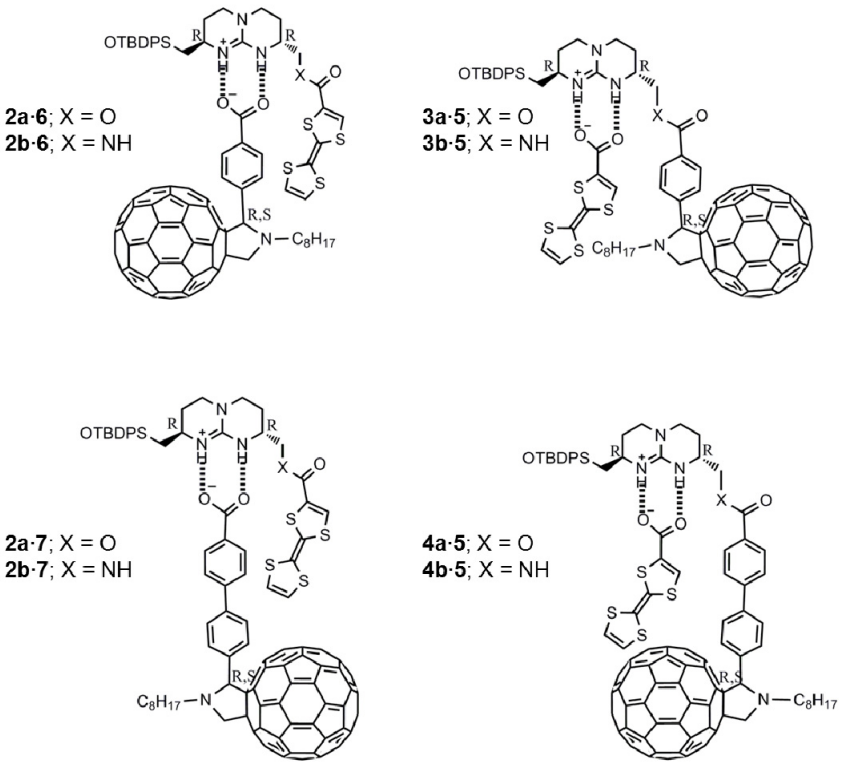

Figure 2. Structures of hydrogen bonded C_{60}·TTF dyads.

[7] J. L. Segura and N. Martín, *Angew. Chem. Int. Ed.* **2001,** *40*, 1372-1409.

[8] M. C. Díaz, B. M. Illescas, N. Martín, R. Viruela, P. M. Viruela, E. Ortí, O. Brede, I. Zilbermann and D. M. Guldi, *Chemistry – A European Journal* **2004,** *10*, 2067-2077.

[9] M. Segura, L. Sánchez, J. de Mendoza, N. Martín and D. M. Guldi, *J. Am. Chem. Soc.* **2003,** *125*, 15093-15100.

With this work it was demonstrated that hydrogen bonding motifs are a useful tool to design photo- and electroactive- donor- acceptor models as novel artificial photosynthetic systems.

To achieve long-lived radical ion-pairs the design of a new hydrogen bonded donor-acceptor assembly with porphyrin as electron donor moiety was carried out. This assembly is composed of a porphyrin amidine donor **8** and fulleropyrrolidine carboxylic acid **9** (Figure 3).[10] The formation of the complex was followed by ^{1}H NMR and fluorescence spectroscopies to determine the association constant, which reached up to log K_a = 7.0 in toluene at room temperature. Transient absorption studies indicated lifetimes of the charge-separated radical-ion-pair states of around 10 μs in THF. This outperforms similar covalent C_{60} conjugates, with charge-separated state lifetimes of around 1 μs, demonstrating the advantages of strong and highly directional hydrogen bonding networks in electron-transfer processes.

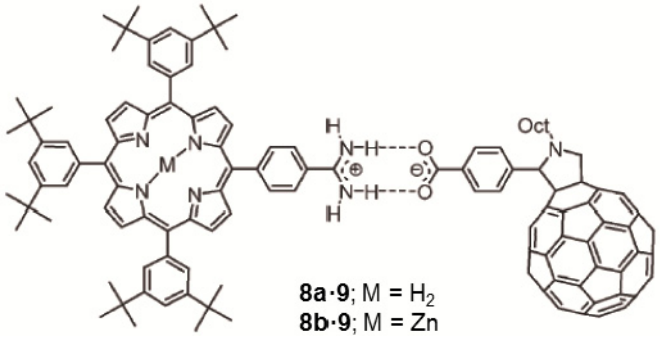

Figure 3. Aminidinium-carboxylate interfaced porphyrin-C_{60} assemblies.

2.2. exTTF as interesting donor unit

TTF and its derivatives have been used as electron donors and as building blocks in many areas of materials chemistry. A π-extended tetrathiafulvalene with *p*-quinodimethane structure (exTTF) is a TTF derivative that incorporates an anthracene spacer between the dithiole rings. In the case of TTF two oxidation waves are found in its electrochemistry, the oxidation to cation radical and dication species occurs sequentially and reversibly at relatively low potentials,[11] and these species ($TTF^{+\cdot}$ and TTF^{2+}) are aromatic and therefore planar, in contrast with the boatlike geometry of the ground state. However, only one quasireversible oxidation wave involving two electrons is found in the case of exTTF, forming a stable dicationic species (Figure 4).

[10] L. Sánchez, M. Sierra, N. Martín, A. J. Myles, T. J. Dale, J. Rebek, W. Seitz and D. M. Guldi, *Angew. Chem. Int. Ed.* **2006,** *45*, 4637-4641.
[11] M. C. Díaz, B. M. Illescas, C. Seoane and N. Martín, *J. Org. Chem.* **2004,** *69*, 4492-4499.

This oxidation involves a big change in the geometry of the exTTF from its nonaromatic neutral butterfly structure to planar aromatic $exTTF^{2+}$.

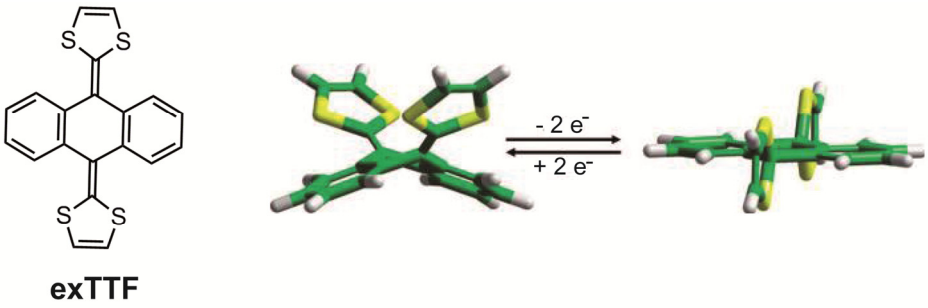

Figure 4. Structure of exTTF, and geometry of the ground state (left) and dicationic state (right) of exTTF.[12]

This planarization in the structure upon oxidation is a very important factor in the stabilization of the charge-separated species $C_{60}^{\cdot+}$ and $exTTF^{\cdot+}$. We have made use of this aromatic stabilization to improve the lifetime of the photolytically generated charge-separated states in exTTF-C_{60} dyads. The covalent combination of exTTF and C_{60} by means of different bridges allows the formation of long-lived charge-separated states with lifetimes ranging from nanoseconds to hundreds of microseconds.[12]

2.3. Supramolecular chemistry of fullerenes including exTTF as electron donor in the structure

The good results in lifetimes with covalent connection between C_{60} and exTTF prompted the group to design supramolecular dyads that involve both species as electron acceptor and donor, respectively. The first attempt was a cyclophane-type crown ether with two exTTF units and a C_{60} derivative with dibenzilammonium salt.[13] In this case, as is shown in the figure below, the crown ether **10** assembles with the dibenzilammonium salt **11**. In the supramolecular sense, the results may be improved. The studies carried out by ^{1}H NMR and fluorescence were in agreement with a binding constant of only log K_a = 1.7 ($CD_3CN/CDCl_3$, 1:1, 298 K).

[12] N. Martín, L. Sánchez, M. a. Á. Herranz, B. Illescas and D. M. Guldi, *Acc. Chem. Res.* **2007,** *40*, 1015-1024.

[13] M. C. Díaz, B. M. Illescas, N. Martín, J. F. Stoddart, M. A. Canales, J. Jiménez-Barbero, G. Sarova and D. M. Guldi, *Tetrahedron* **2006,** *62*, 1998-2002.

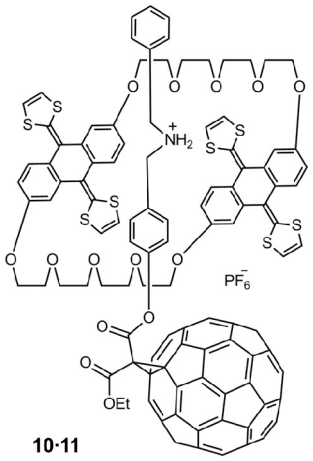

Figure 5. Structure of pseudo-rotaxane formed by exTTF dimer crown ether **10** and dibenzylammoniun-containing C_{60} **11**.

Different designs appear taking into account that photoinduced electron transfer may take place through space, which means we can get electron transfer with both units noncovalently connected. These designs are shown in Figure 6. The crown ether receptor is connected to a C_{60} unit, and the dibenzylammonium salt is connected to the exTTF unit.[14] With these designs, in the case of **(14-H·PF$_6$)·16,** the binding constant was increased to log K_a = 3.3 ($CD_3CN/CDCl_3$, 298 K), almost 2 orders of magnitude larger than in the case of **10·11**. Complexation studies were carried out by means of ^{1}H NMR spectroscopy and fluorescence, getting binding constants between log K_a = 3.0 and log K_a = 4.1(CH_3CN/CH_2Cl_2, 1:1, 298 K).

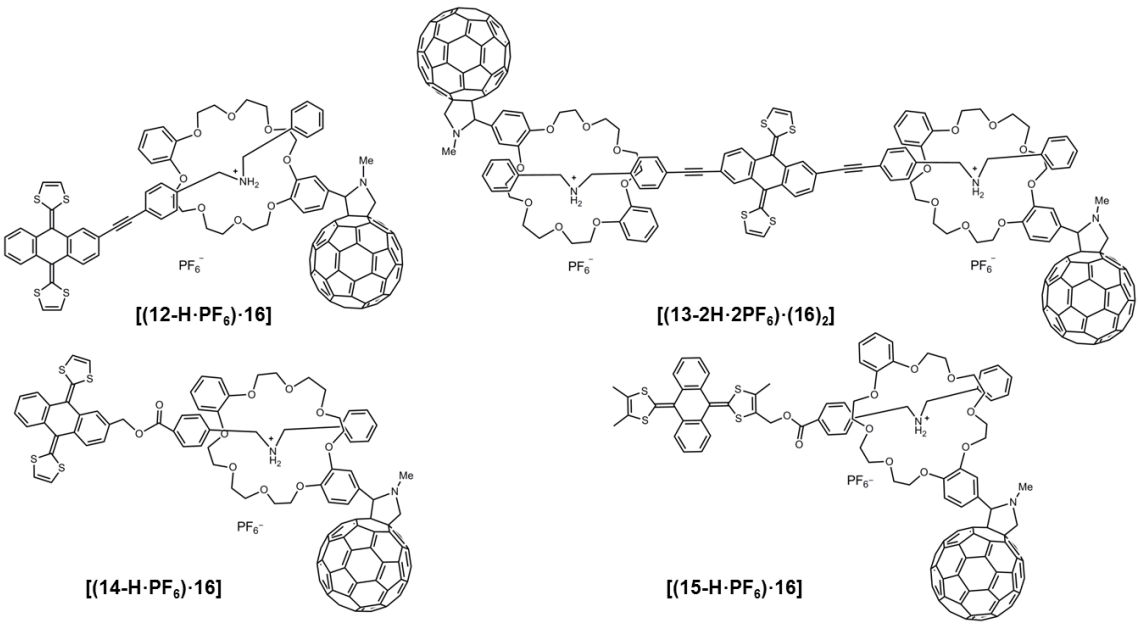

[14] B. M. Illescas, J. Santos, M. C. Díaz, N. Martín, C. M. Atienza and D. M. Guldi, *Eur. J. Org. Chem.* **2007,** *2007*, 5027-5037.

Figure 6. Supramolecular complexes prepared by threading the electron donor into the crown ether-containing [60]fullerene.

If we take a look at the changes in the ^{1}H NMR spectra we can realize that the most important shifts in the signals upon addition of the fullerene derivative are in the ammonium protons. The changes in the ammonium protons confirm the threading of the ammonium salts in the crown ether. For the more insoluble complexes, quenching of the fullerene fluorescence was used to analyze the association constants, and suggested a photoinduced electron transfer process from the donor (exTTF) to the acceptor (C_{60}). UV-vis titrations were not possible because of the absence of significant changes upon addition of fullerene derivative in a dilute solution of each exTTF ammonium salts. Therefore, there are no electronic interactions between both species in the ground state. The voltammograms agree with this conclusion, complexation does not influence significantly the electroactive properties of the components, thus the electroactive units are not spatially close in the complex.

2.4. Exploiting exTTF-fullerene interactions

Considering that fullerene is a polyene without functionality and its spherical geometry, and therefore a very high surface/volume ratio, we investigated the use of dispersion-type forces, dependent on surface, to associate it. The concave shape of exTTF as we can see in the solid-state structure (Figure 4), and its electronic complementarity, indicates it could establish charge-transfer, π–π and Van der Waals interactions with the convex surface of fullerene, making it a promising candidate as a recognition motif for fullerenes. In fact, theoretical calculations in the gas phase predicted an exTTF-C_{60} interaction of approximately 7 kcal mol^{-1}.[15] Nevertheless, experimentally, one single molecule of exTTF does not associate with C_{60}.[16] An attempt to get 1:1 exTTF:C_{60} complex with the electroactive units spatially close was to preorganize the exTTF-C_{60} interaction with a different recognition motif. Our group reported on the preparation and characterization of a supramolecular complex by means of cooperativity between π–π interactions of exTTF with the fullerene surface and H-bonding interactions of crown ether with the ammonium salts.[17] The design is based on a C_{60} derivative with a benzylammonium group **18** that associates with the crown ether containing the exTTF unit in the receptor **17**.

[15] These calculations are unpublished results carried out in collaboration with the group of Prof. Enrique Ortí. T. c. a. u. r. c. o. i. c. w. t. g. o. P. E. Ortí; .

[16] E. M. Pérez, L. Sánchez, G. Fernández and N. Martín, *J. Am. Chem. Soc.* **2006,** *128*, 7172-7173.

[17] J. Santos, B. Grimm, B. M. Illescas, D. M. Guldi and N. Martín, *Chem. Commun.* **2008,** *0*, 5993-5995.

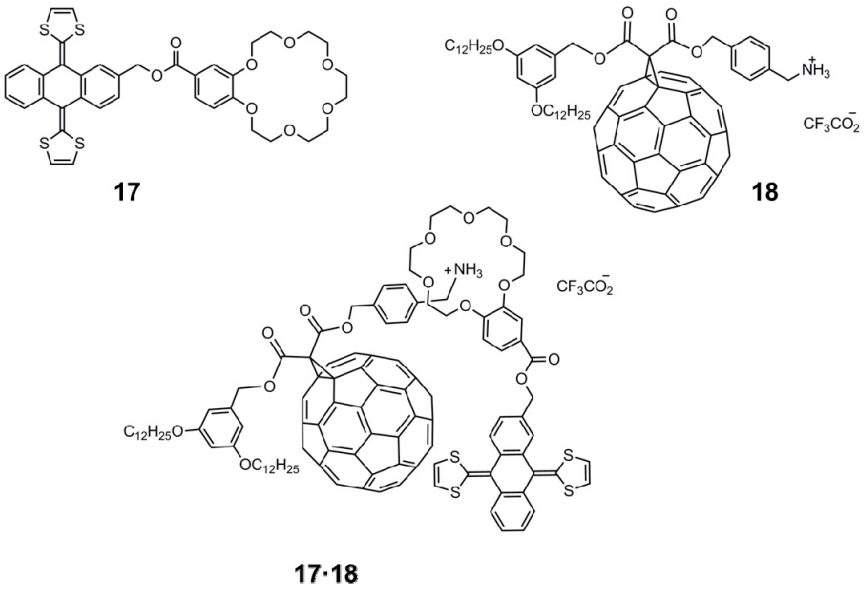

Figure 7. Supramolecular complex and the corresponding exTTF (**17**) and C_{60} (**18**) components.

The result is the donor-acceptor pseudorotaxane supramolecular complex that we can see in the figure. In this case the changes in the absorption spectra upon addition of fullerene component **18** in a solution of the exTTF component **17** are significant and indicate the electronic interaction between the electroactive units in the ground state.

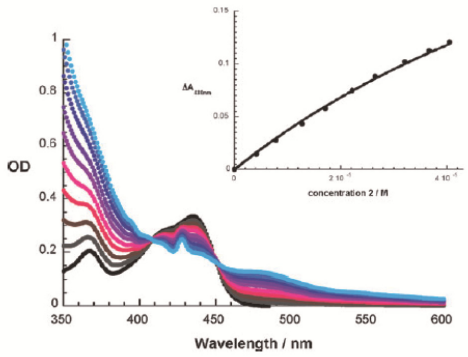

Figure 8. Absorption spectral changes of exTTF component upon addition of fullerene component (until 3 equivalents, chlorobenzene, 298 K). Inset shows ΔAbs at 480 nm as a function of fullerene concentration.

The association event was investigated by UV-vis titration, fluorescence experiments and cyclic voltammetry measurements. Analysis of the UV-vis titration data fits to a 1:1 binding isotherm that affords a log K_a = 6.2 in chlorobenzene at 298 K, three orders of magnitude higher than values obtained for the same ammonium cation with another crown ether receptor lacking the exTTF unit. The fluorescence titrations in different solvents confirm the charge-transfer features. CV measurements also confirm the formation of the complex with a significant shift of the oxidation wave in the complex

compared with **17** and weak changes in the reduction waves compared with **18**. Looking at the binding constants obtained, the authors postulate the significant contribution of charge-transfer and π–π interactions in the complexation process aided by hydrogen bonding. Finally, photophysical measurements show the photoinduced generation of a charge-separated state with a short lifetime of 9.3 ps in chlorobenzene.

Continuing with the idea to create 1:1 exTTF/C_{60} systems, the distorted geometry of exTTF has been used as template to design a new receptor that wraps around the convex surface of the pristine fullerene. Receptor **19** (Figure 9) is composed by two crown ethers linked via ester to an exTTF unit. The crown ethers act as recognition motifs and optimize the stability of the complex.

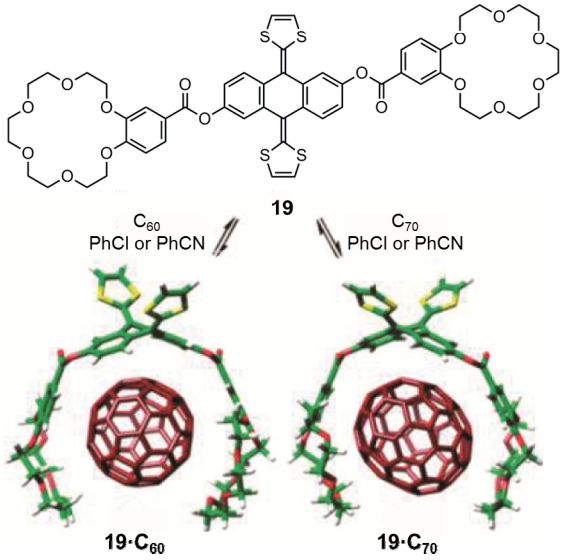

Figure 9. exTTF-bis(crown ether) and its complexes with C_{60} (left) and C_{70} (right).

The binding event was studied through UV-vis titrations observing the typical trends in electronic interaction between exTTF and fullerenes, with the appearance of a broad maximum around 480 nm at the expense of the absorption at 438 nm with an isosbestic point at 460 nm. The analysis of the data indicates a log K_a = 6.7 toward C_{60} in benzonitrile and chlorobenzene at room temperature, one of the highest values for association with fullerene, and a binding constant toward C_{70} even larger, log K_a = 7.4 in benzonitrile at room temperature. The studies of the fluorescence quenching of the receptor confirm these values. The charge-transfer upon addition of fullerene is noticeable in the shift of the maximum of the band around 480 nm in the different solvents and in the emissive features in fluorescence experiments. The lifetime of the charge-separated state determined from a multiwavelength analysis was very short, 45 ps. The large stability of these complexes, some of the most efficient interactions to bind fullerenes, was attributed to cooperative effects from π–π and n-π interactions, where the lone pairs of electrons on the crown-ether oxygen atoms would play a key role.

2.5. exTTF as recognition motif for fullerenes

We have seen in the previous section how secondary hydrogen bond or n-π interactions can be utilized to cooperate with π–π interactions of exTTF motif in the association of fullerenes. We will now move on to see how to exploit exTTF-C_{60} interaction by using basically exTTF as recognition motif. Since one single exTTF unit does not associate fullerene the next step in the design of an exTTF-based receptor for fullerenes was to increase the number of the recognition units in the receptor. The first attempt of this strategy concluded in these simple tweezers composed of two exTTF units linked by an aromatic spacer.[16]

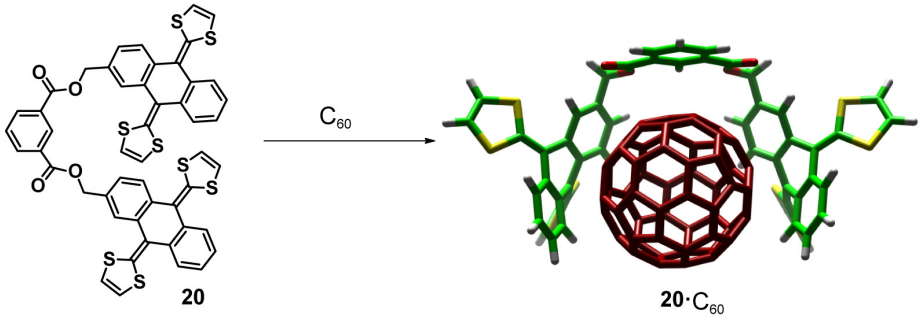

Figure 10. Structure of tweezers-like receptor and model of complex upon addition of C_{60}.

The association event was studied by means of UV-visible titrations. In Figure 11 we can see the changes in the electronic absorption spectra of the receptor upon addition of aliquots of fullerene. It is easy to see the decrease in absorption of the band at 434 nm and the appearance and increase in absorption of a new band at 483 nm assigned to the complex. These changes occur with formation of an isosbestic point at 459 nm. The isosbestic point is suggestive of a 1:1 stoichiometry, which was confirmed by Job's plot analysis. The analysis of the data, fitting these changes to a 1:1 binding isotherm, affords in a log K_a = 3.5 in chlorobenzene at room temperature, which is a good complexation result taking into account the lack of preorganization of **20**.

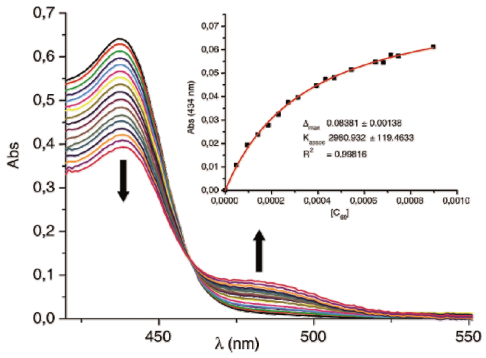

Figure 11. Absorption spectral changes of the receptor **20** (chlorobenzene, 298 K, 2.31 x 10^{-5} M) upon addition of fullerene (chlorobenzene, 298 K, 4.05 x 10^{-3} M). Inset shows the fit of ΔAbs (434 nm) to a 1:1 binding isotherm.

The influence of concave-convex interactions was further investigated with the synthesis of similar tweezers with different recognition motifs to separate the influence of the different contributions to the noncovalent interactions: π–π aromatic interactions, Van der Waals forces, coulombic and concave-convex interactions.[18]

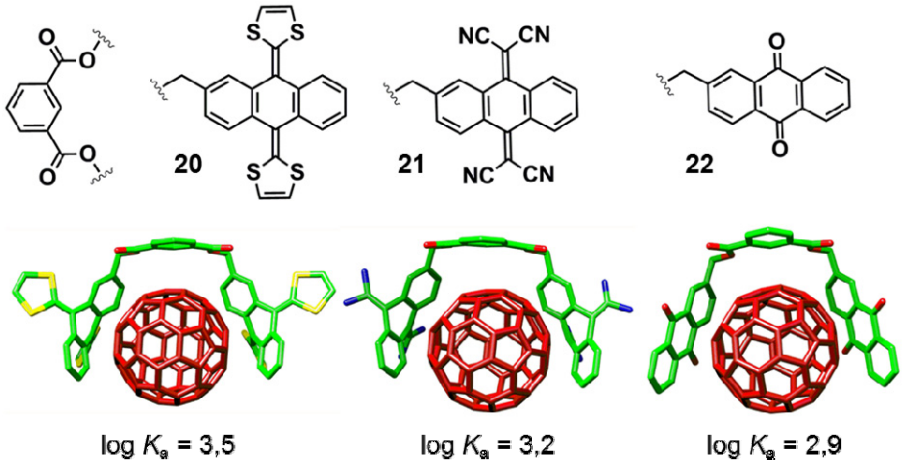

Figure 12. Structures and calculated models of the complexes of different tweezers-like receptors with C_{60}. The different recognition motifs are exTTF, tetracyanoanthraquinodimethane (TCAQ), and anthraquinone respectively. The values of the logarithm of the binding constants are shown below (from ^{1}H NMR titrations, $CHCl_3/CS_2$, 1:1, 298 K).

Receptor **20** incorporates five aromatic rings (for π–π interactions with fullerene), a large concave surface (for Van der Waals and concave-convex interactions), and it is electron rich (for positive electrostatic interactions with the electron poor fullerene); as consequence, **20** is the strongest binder for C_{60}. Receptor **21** has the same number of aromatic rings, a large concave surface, but is electron poor; as consequence its binding constant is smaller, suggesting a noticeable contribution of coulombic interactions. As in the previous case, receptor **22** has the same number of aromatic rings and it is electron poor, but it presents a large planar surface; its binding constant is lower than in the case of receptor **21,** proving the importance of concave-convex complementarity. Finally, it is worth noting that TTF-tweezers, using TTF as recognition unit, do not bind with fullerene. This negative result suggests the importance of a large surface in the receptor to increase Van der Waals interactions.

[18] E. M. Pérez, A. L. Capodilupo, G. Fernández, L. Sánchez, P. M. Viruela, R. Viruela, E. Ortí, M. Bietti and N. Martín, *Chem. Commun.* **2008,** *0*, 4567-4569.

In summary, π–π and Van der Waals interactions are preponderant, coulombic interactions justify the larger binding constant of exTTF tweezers *vs* TCAQ tweezers, and concave-convex complementarity prove its contribution explaining the lower binding constant in anthraquinone receptor toward C_{60}.

The study of the physicochemical properties and the theoretical description of the host-guest interactions were carried out in collaboration with the groups of Professor Dirk M. Guldi and Professor Enrique Ortí respectively.[19] During the UV-vis titrations, as we can see in Figure 11, a new broad band appears around 480 nm upon addition of C_{60} at the expense of the absorption of a band around 434 nm, assigned by calculations to the HOMO→LUMO excitation of exTTF. The absorption maximum of the new band suffers shift depending of the polarity of the solvent, thus a charge-transfer transition arising from the formation of $C_{60}^{\delta-}$exTTF$^{\delta+}$ was evoked, consequence of the strong electronic coupling between the tweezers and the fullerene. The decrease in the band assigned to exTTF excitation was explained with the calculations for the complex form. In the complex this band is present, but with a lower value of oscillator strength. According to calculations the new band around 480 nm was confirmed to be a charge transfer band that involves excitations from HOMO and HOMO -1 in the exTTF units, to the LUMO +4 over C_{60}. There are more than one transition that give origin to this band and involve charge transfer from exTTF units to C_{60} but all of these have very small values in oscillator strength giving rise to our low intensity charge transfer band.

The transient absorption spectroscopy of a mixture of exTTF tweezers and C_{60} reveals the formation of a charge separated state $C_{60}^{\cdot-}$/exTTF$^{\cdot+}$ upon light irradiation, but the lifetime of the charge separated states are very short, in the order of picoseconds, being the product of this charge recombination the singlet ground state. As lifetimes in solution and in the solid state often vary significantly, and other factors frequently play a dominant role in the overall efficiency of the device, these short lifetimes are far from being an unsurpassable obstacle for the application of these systems in optoelectronic devices.

2.6. Truxene instead of anthracene as conjugated core for TTF

With the idea of applications in the construction of nanostructured optoelectronic devices, the search of suitable fragments to form donor-acceptor pairs with fullerene continues. A suitable electron-donor partner should show: good electron donor character, efficient light absorption, and the ability to self-assemble with fullerenes.

It was considered that an increase in the size of the conjugated scaffold and the number of dithiole units would lead to an increase in the noncovalent interactions with fullerenes. To investigate this, we synthesized a new family of π-extended TTF

[19] S. S. Gayathri, M. Wielopolski, E. M. Pérez, G. Fernández, L. Sánchez, R. Viruela, E. Ortí, D. M. Guldi and N. Martín, *Angew. Chem. Int. Ed.* **2009,** *48*, 815-819.

derivatives. The idea was the use of a truxene core decorated with three units of 1,3-dithiol rings,[20] giving rise to truxeneTTF (truxTTF). With this larger conjugated core we expected to increase the absorption in the visible region of the spectrum as an additional benefit.

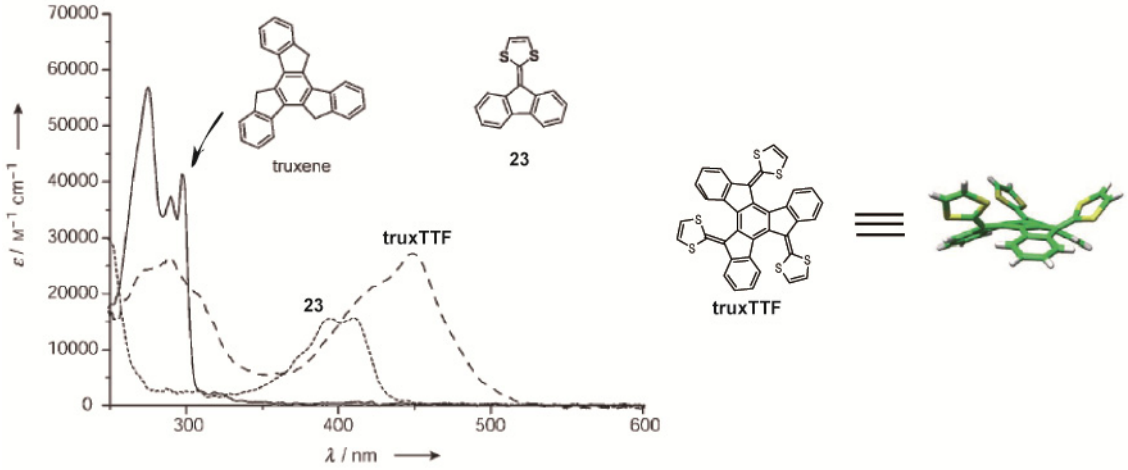

Figure 13. UV-Vis absorption spectra ($CHCl_3$, 298 K) of truxene (solid line), 2-(9H-fluoren-9-ylidene)-1,3-dithiole **23** (dotted line), and **truxeneTTF** (dashed line). The chemical structures and X-ray structure of truxeneTTF are also shown.

As is visible in the solid-state structure (Figure 13), the planar geometry of truxene core is distorted to accommodate de dithiol rings adopting an all-*cis* spherelike geometry. This concave bowl-shaped configuration can maximize van der Waals, concave-convex, and π–π interactions due to its complementarity with the convex surface of fullerene. Despite the loss of planarity the absorption spectra shows shift to red respect to compound **23**, indicating a higher degree of conjugation in the truxeneTTF.

The molecular structure and electronic properties of truxTTF were theoretically investigated, and the band around 431 nm was assigned to intramolecular charge transfer from the dithiole donor units to the truxene core. Its redox behavior was studied by cyclic voltammetry showing complex voltammograms with up to five oxidation waves, suggesting some cooperative effect between the dithiol rings and the truxene core: the first three electrons are extracted mainly from the dithiole rings, while a fourth and fifth electrons can be donated by the truxene core. The ability of truxTTF to associate fullerenes was investigated in solution by ^1H NMR titrations ($CDCl_3/CS_2$, 298 K). The progressive shielding of aromatic signals upon addition of [60] and [70]

[20] E. M. Pérez, M. Sierra, L. Sánchez, M. R. Torres, R. Viruela, P. M. Viruela, E. Ortí and N. Martín, *Angew. Chem. Int. Ed.* **2007,** *46*, 1847-1851.

fullerene fitted successfully to a 1:1 binding isotherm affording log K_a = 3.1 for C_{60} and log K_a = 3.90 for C_{70}. Theoretical calculations were in agreement with these results.

In summary, this basic truxeneTTF structure corresponds to the expectations as an electron donor partner for fullerenes and opens a new door for the manufacture of fullerene-based self-assembled optoelectronic devices. One more advantage of the truxene core comes from its helical chirality and the potential application in the selective molecular recognition for chiral higher fullerenes.

2.7. From host-guest associates to supramolecular architectures

With the exTTF-C_{60} interaction confirmed through all the previous examples of host-guest systems, we decided to investigate whether it could also be applied to the construction of supramolecular materials. As a proof-of-principle we connected covalently an exTTF tweezers-like receptor to a C_{60} unit. Since this monomer is complementary both in a geometrical and electronic sense, we expected this to self-assemble to form polymeric noncovalent linear aggregates, a head-to-tail donor-acceptor supramolecular polymer.[21]

Evidence of association was found in diverse techniques: ^{1}H NMR, UV-vis spectroscopy, dynamic light scattering (DLS), cyclic voltammetry (CV), MALDI-TOF mass spectrometry and atomic force microscopy (AFM).

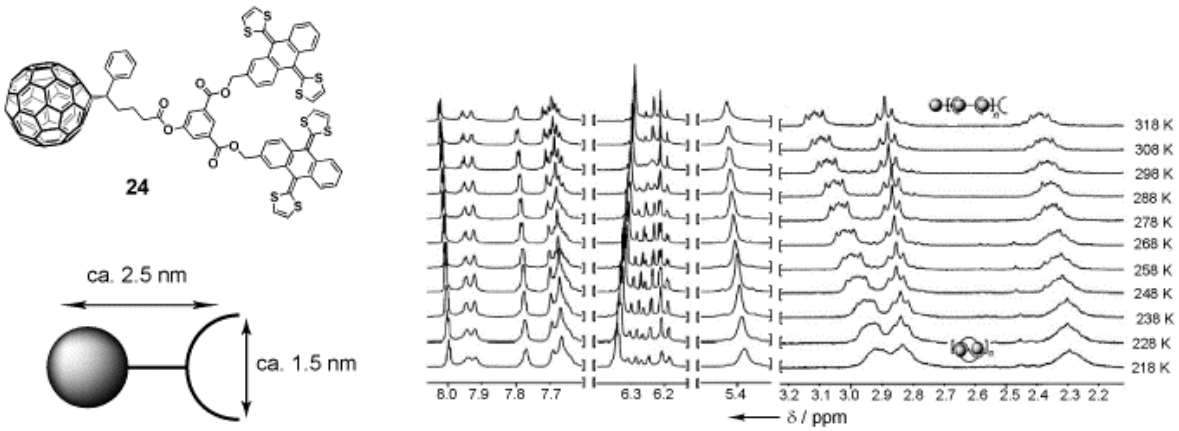

Figure 14. Left; structure and cartoon of monomer **24** C_{60}-exTTF tweezers. Right; Partial ^{1}H NMR spectra of monomer **24** at different temperatures ($CDCl_3$, 300 MHz, 6 mM).

In the ^{1}H NMR spectra of the monomer at different concentrations a slight shielding and more pronounced broadening of most of the signals was observed, that indicates the formation of aggregates of high molecular weight with increasing monomer

[21] G. Fernández, E. M. Pérez, L. Sánchez and N. Martín, *Angew. Chem. Int. Ed.* **2008,** *47*, 1094-1097.

concentration. ^{1}H NMR spectra at different temperatures (Figure 14) were recorded to study the competition between the formation of linear chain and oligomeric cyclization. The upfield shift of the aromatic signals and downfield shift of dithiole signals are indicative of the preferential association of fullerene on the aromatic side of exTTF, as was reported in previous studies of TTF derivatives receptor upon complexation with fullerene.[20] The signals that reveal the preference of cyclic oligomers at low temperature are the methylene signals of the [6,6]-phenyl C_{61} butyric acid (PCBA) unit, which are shielded from 3.1 to 2.9 ppm. These methylene groups have a more important role in this case than in linear chain at room temperature, where these changes were not observed.

Self-association was also investigated through dynamic light scattering (DLS). A broad particle-size distribution was found in solution in DLS with a maximum at hydrodynamic radium of 378 nm. In CV the electronic communication in the ground state was confirmed since the reduction processes become more energetic and irreversible upon concentration.

Besides the NMR, DLS and CV evidence, **24** was also proven to associate in the gas phase, where aggregates up to the pentamer were observed under MALDI-TOF mass spectrometry. Final evidence was found in AFM, where winding, necklace-like aggregates were found.

The good results in the linear supramolecular polymer encouraged the group to design a new monomer with small variations in the synthesis, adding two exTTF tweezers covalently linked to the PCBA moiety. This monomer gave rise to hyper-branched supramolecular polymers.[22] The study of the monomer in solution at different concentrations and at different temperatures by ^{1}H NMR spectroscopy indicates, as was expected, the formation of aggregates and intermolecular binding of the fullerene fragments within the receptor cavity.

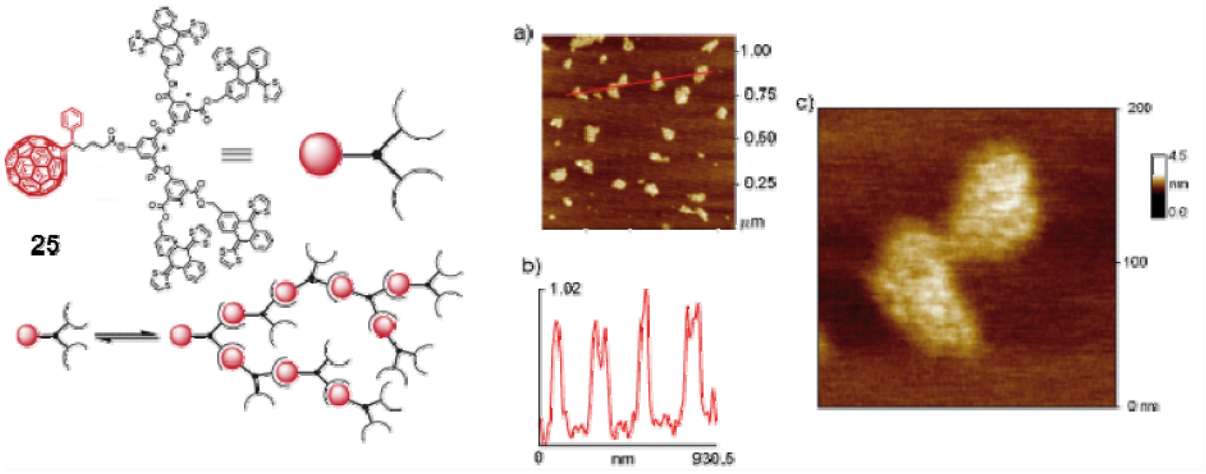

[22] G. Fernández, E. M. Pérez, L. Sánchez and N. Martín, *J. Am. Chem. Soc.* **2008,** *130*, 2410-2411.

Figure 15. Left: chemical structure of the monomer and cartoon representation of the supramolecular hyperbranched polymer. Right: AFM images (tapping mode, air, 298 K) of monomer **25** (a) 1.1 x 1.1 μm; (b) profile along the red line; (c) 200 x 200 nm.

Two sets of hydrodynamic radius were found in DLS experiments, one between 5-15 nm, and another between 785 nm and 1 μm. Cyclic voltammograms indicate, as in the previous case that all redox processes become more energetic and irreversible as the concentration of the monomer increases, pointing to electronic interaction in the ground state. Oligomers up to the hexamer were noticeable in MALDI-TOF spectra. Finally, the AFM images in this case show triangular forms with two of its vertices rounded off (area around 0.2 μm^2) with very regular height, as its visible in the profile (Figure 15b), indicating the expected planar branched oligomers.

The last frontier crossed by the construction of exTTF-based receptors was the reported large dendrimers decorated in their periphery with multiple exTTF units.[23] The synthesis was carried out following a convergent strategy and all the generations were characterized by standard techniques. It is remarkable the self-assemble observed in the dendrimers despite their butterfly-like shape highly distorted from planarity. Evidence of self-assemble was found in gas phase in the MALDI-TOF spectrometry, in solution in DLS and ^{1}H NMR experiments at different concentrations, and on solid supports in the AFM images.

[23] G. Fernández, L. Sánchez, E. M. Pérez and N. Martín, *J. Am. Chem. Soc.* **2008,** *130*, 10674-10683.

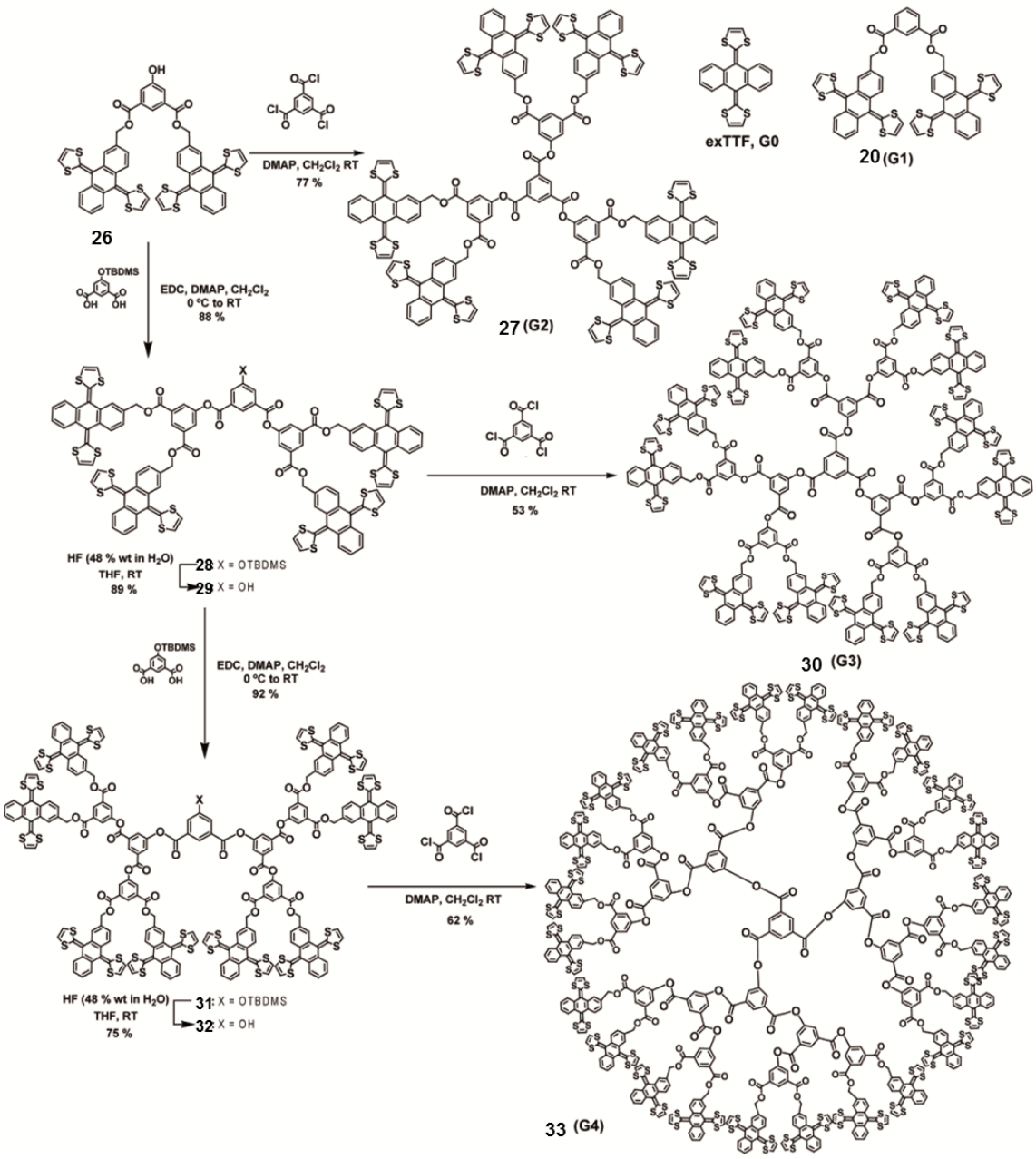

Figure 16. Synthesis of G2 (second generation) to G4 exTTF-based dendrimers and the previously reported G0 and G1 congeners.

The association abilities of these dendrimers towards C_{60} were investigated trough UV-vis titrations (Figure 17) as in the previous exTTF-based receptors, and similar trends in the changes of the absorption spectra were found upon addition of aliquots of C_{60} in a dendrimer solution. There are some important differences as the lack of isosbestic points, indicating the existence of several different stoichiometries. It is important the sigmoidal shape of the binding isotherm, which indicates that the binding process occurs in a cooperative manner, perhaps from the need to disassemble the exTTF units before complexation.

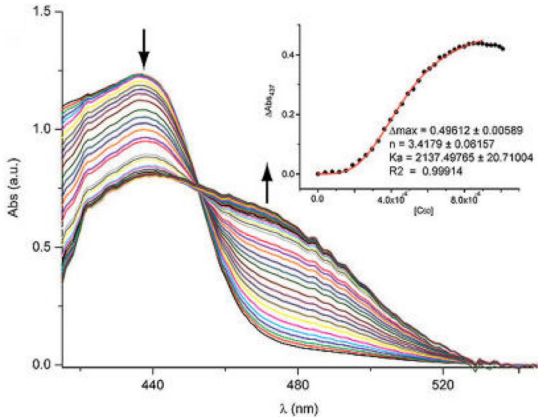

Figure 17. Absorption spectral changes of dendrimer **33** (G4) (chlorobenzene, 298 K) upon addition of fullerene. The absorption spectrum of C_{60} has been subtracted. Inset shows the fit of ΔAbs (437 nm) to the Hill equation.[24]

The redox properties were affected by the complexation process too. A cathodic shift of the reduction waves of C_{60} with respect to pristine fullerene was justified by considering the electron rich environment that the exTTF causes in the proximity of C_{60} in the complex, which makes its reduction more energetic.

2.8. References

1. (a) J. P. Abrahams; A. G. W. Leslie; R. Lutter; J. E. Walker, Structure at 2.8 A resolution of F1-ATPase from bovine heart mitochondria. *Nature* **1994,** *370*, 621-628;(b) T. S. Bibby; J. Nield; F. Partensky; J. Barber, Oxyphotobacteria: Antenna ring around photosystem I. *Nature* **2001,** *413*, 590-590.

2. L. J. Prins; D. N. Reinhoudt; P. Timmerman, Noncovalent Synthesis Using Hydrogen Bonding. *Angew. Chem. Int. Ed.* **2001,** *40*, 2382-2426.

3. F. Diederich; L. Echegoyen; M. Gómez-López; R. Kessinger; J. Fraser Stoddart, The self-assembly of fullerene-containing [2]pseudorotaxanes: formation of a supramolecular C_{60} dimer. *J. Chem. Soc. Perk. Trans. 2* **1999,** *0*, 1577-1586.

4. J. J. González; S. González; E. M. Priego; C. Luo; D. M. Guldi; J. d. Mendoza; N. Martín, A new approach to supramolecular C-dimers based in quadruple hydrogen bonding. *Chem. Commun.* **2001,** *0*, 163-164.

5. B. J. B. Folmer; R. P. Sijbesma; H. Kooijman; A. L. Spek; E. W. Meijer, Cooperative Dynamics in Duplexes of Stacked Hydrogen-Bonded Moieties. *J. Am. Chem. Soc.* **1999,** *121*, 9001-9007.

6. (a) J. L. Sessler; B. Wang; A. Harriman, Long-range photoinduced electron transfer in an associated but non-covalently linked photosynthetic model system. *J. Am. Chem. Soc.* **1993,** *115*, 10418-10419;(b) S. A. W. P. J. de Rege, M. J. Therien, Direct evaluation of electronic coupling mediated by hydrogen bonds: implications for biological electron transfer *Science* **1995**, 1409-1413.

7. J. L. Segura; N. Martín, New Concepts in Tetrathiafulvalene Chemistry. *Angew. Chem. Int. Ed.* **2001,** *40*, 1372-1409.

8. M. C. Díaz; B. M. Illescas; N. Martín; R. Viruela; P. M. Viruela; E. Ortí; O. Brede; I. Zilbermann; D. M. Guldi, Highly Conjugated p-Quinonoid π-Extended Tetrathiafulvalene Derivatives: A Class of Highly Distorted Electron Donors. *Chemistry – A European Journal* **2004,** *10*, 2067-2077.

[24] The applicability of the Hill equation to small molecule self-assembling systems has recently been under discussion. In a careful analysis, G. Ercolani (Gaussian 03, Revision C.02 Gaussian, Inc.: Wallingford CT, 2004.) has argued in favor of the use of the Hill equation only for intermolecular binding of monovalent ligands to a multivalent receptor. Our proposed binding mode fits with this case, since the binding of C_{60} always occurs intermolecularly.

9. M. Segura; L. Sánchez; J. de Mendoza; N. Martín; D. M. Guldi, Hydrogen Bonding Interfaces in Fullerene•TTF Ensembles. *J. Am. Chem. Soc.* **2003,** *125*, 15093-15100.
10. L. Sánchez; M. Sierra; N. Martín; A. J. Myles; T. J. Dale; J. Rebek; W. Seitz; D. M. Guldi, Exceptionally Strong Electronic Communication through Hydrogen Bonds in Porphyrin–C60 Pairs. *Angew. Chem. Int. Ed.* **2006,** *45*, 4637-4641.
11. M. C. Díaz; B. M. Illescas; C. Seoane; N. Martín, Synthesis and Electron-Donor Ability of the First Conjugated π-Extended Tetrathiafulvalene Dimers†. *J. Org. Chem.* **2004,** *69*, 4492-4499.
12. N. Martín; L. Sánchez; M. a. Á. Herranz; B. Illescas; D. M. Guldi, Electronic Communication in Tetrathiafulvalene (TTF)/C_{60} Systems: Toward Molecular Solar Energy Conversion Materials? *Acc. Chem. Res.* **2007,** *40*, 1015-1024.
13. M. C. Díaz; B. M. Illescas; N. Martín; J. F. Stoddart; M. A. Canales; J. Jiménez-Barbero; G. Sarova; D. M. Guldi, Supramolecular pseudo-rotaxane type complexes from π-extended TTF dimer crown ether and C_{60}. *Tetrahedron* **2006,** *62*, 1998-2002.
14. B. M. Illescas; J. Santos; M. C. Díaz; N. Martín; C. M. Atienza; D. M. Guldi, Supramolecular Threaded Complexes from Fullerene–Crown Ether and π-Extended TTF Derivatives. *Eur. J. Org. Chem.* **2007,** *2007*, 5027-5037.
15. T. c. a. u. r. c. o. i. c. w. t. g. o. P. E. Ortí.
16. E. M. Pérez; L. Sánchez; G. Fernández; N. Martín, exTTF as a Building Block for Fullerene Receptors. Unexpected Solvent-Dependent Positive Homotropic Cooperativity. *J. Am. Chem. Soc.* **2006,** *128*, 7172-7173.
17. J. Santos; B. Grimm; B. M. Illescas; D. M. Guldi; N. Martín, Cooperativity between π–π and H-bonding interactions-a supramolecular complex formed by C_{60} and exTTF. *Chem. Commun.* **2008,** *0*, 5993-5995.
18. E. M. Pérez; A. L. Capodilupo; G. Fernández; L. Sánchez; P. M. Viruela; R. Viruela; E. Ortí; M. Bietti; N. Martín, Weighting non-covalent forces in the molecular recognition of C_{60}. Relevance of concave-convex complementarity. *Chem. Commun.* **2008,** *0*, 4567-4569.
19. S. S. Gayathri; M. Wielopolski; E. M. Pérez; G. Fernández; L. Sánchez; R. Viruela; E. Ortí; D. M. Guldi; N. Martín, Discrete supramolecular donor-acceptor complexes. *Angew. Chem. Int. Ed.* **2009,** *48*, 815-819.
20. E. M. Pérez; M. Sierra; L. Sánchez; M. R. Torres; R. Viruela; P. M. Viruela; E. Ortí; N. Martín, Concave Tetrathiafulvalene-Type Donors as Supramolecular Partners for Fullerenes. *Angew. Chem. Int. Ed.* **2007,** *46*, 1847-1851.
21. G. Fernández; E. M. Pérez; L. Sánchez; N. Martín, Self-Organization of Electroactive Materials: A Head-to-Tail Donor–Acceptor Supramolecular Polymer. *Angew. Chem. Int. Ed.* **2008,** *47*, 1094-1097.
22. G. Fernández; E. M. Pérez; L. Sánchez; N. Martín, An Electroactive Dynamically Polydisperse Supramolecular Dendrimer. *J. Am. Chem. Soc.* **2008,** *130*, 2410-2411.
23. G. Fernández; L. Sánchez; E. M. Pérez; N. Martín, Large exTTF-Based Dendrimers. Self-Assembly and Peripheral Cooperative Multiencapsulation of C_{60}. *J. Am. Chem. Soc.* **2008,** *130*, 10674-10683.
24. Gaussian 03, Revision C.02 M. J. T. Frisch, G. W.; Schlegel, H. B.; Scuseria, G. E.; Robb, M. A.; Cheeseman, J. R.; Montgomery, Jr., J. A.; Vreven, T.; Kudin, K. N.; Burant, J. C.; Millam, J. M.; Iyengar, S. S.; Tomasi, J.; Barone, V.; Mennucci, B.; Cossi, M.; Scalmani, G.; Rega, N.; Petersson, G. A.; Nakatsuji, H.; Hada, M.; Ehara, M.; Toyota, K.; Fukuda, R.; Hasegawa, J.; Ishida, M.; Nakajima, T.; Honda, Y.; Kitao, O.; Nakai, H.; Klene, M.; Li, X.; Knox, J. E.; Hratchian, H. P.; Cross, J. B.; Bakken, V.; Adamo, C.; Jaramillo, J.; Gomperts, R.; Stratmann, R. E.; Yazyev, O.; Austin, A. J.; Cammi, R.; Pomelli, C.; Ochterski, J. W.; Ayala, P. Y.; Morokuma, K.; Voth, G. A.; Salvador, P.; Dannenberg, J. J.; Zakrzewski, V. G.; Dapprich, S.; Daniels, A. D.; Strain, M. C.; Farkas, O.; Malick, D. K.; Rabuck, A. D.; Raghavachari, K.; Foresman, J. B.; Ortiz, J. V.; Cui, Q.; Baboul, A. G.; Clifford, S.; Cioslowski, J.; Stefanov, B. B.; Liu, G.; Liashenko, A.; Piskorz, P.; Komaromi, I.; Martin, R. L.; Fox, D. J.; Keith, T.; Al-Laham, M. A.; Peng, C. Y.; Nanayakkara, A.; Challacombe, M.; Gill, P. M. W.; Johnson, B.; Chen, W.; Wong, M. W.; Gonzalez, C.; and Pople, J. A., Gaussian, Inc.: Wallingford CT, 2004.

3. Objectives

The present thesis addresses one main objective: **to design and synthesize new exTTF-based receptors for fullerenes with high affinity**. Within this main objective, we will follow three different strategies:

i) to increase the number of recognition units.
ii) to include preorganization in the design of the receptors.
iii) to expand the π-surface and the number of dithiole rings of the recognition motif.

As part of the study of the properties of these new hosts we will investigate:

iv) the binding events in solution, through UV-vis, fluorescence and NMR titrations; in the gas phase, through mass spectrometry; and in the solid state, through X-ray crystallography and microscopic techniques.
v) the structural, electronic and photophysical properties of the receptors and the supramolecular associates, through a combination of theory and spectroscopy.
vi) the structure-affinity relationships, that is, how changes in the structure of the receptors affect the binding constant towards fullerenes.
vii) the association of some of the receptors to other nanoforms of carbon, in particular graphene.

4. Bis-exTTF macrocyclic receptors.

Helena Isla, María Gallego, Emilio M. Pérez, Rafael Viruela, Enrique Ortí and Nazario Martín, *J. Am. Chem. Soc*. **2010**, *132*, 1772–1773

Bruno Grimm, Helena Isla, Emilio M. Pérez, Nazario Martín and Dirk M. Guldi, *Chem. Commun.,* **2011***, 47,* 7449-7451

David Canevet, María Gallego, Helena Isla, Alberto de Juan, Emilio M. Pérez and Nazario Martín, *J. Am. Chem. Soc*. **2011**, *133*, 3184–3190

4.1. A bis-exTTF macrocyclic receptor that associates C_{60} with micromolar affinity

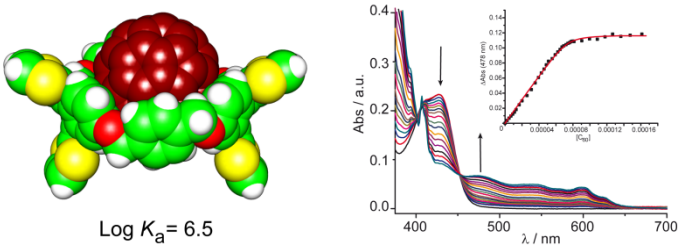

An exTTF-based macrocyclic receptor that associates C_{60} with a binding constant > 10^6 M^{-1} in chlorobenzene at room temperature is described. This represents three orders of magnitude improvement with respect to the previous examples of exTTF-based receptors, and one of the highest binding constants towards C_{60} reported to date.

J. Am. Chem. Soc. **2010**, *132*, 1772–1773

4.1.1. Introduction

The search for molecular receptors for fullerenes is a very active area of research.[1,2,3] Various receptors based on concave recognition motifs like cyclotriveratrylenes,[4,5] corannulenes,[6,7] cyclic paraphenyleneacetylenes,[3,8,9,10] and π-extended tetrathiafulvalene

[1] E. M. Pérez and N. Martín, *Chem. Soc. Rev.* **2008,** *37*, 1512-1519.
[2] K. Tashiro and T. Aida, *Chem. Soc. Rev.* **2007,** *36*, 189-197.
[3] T. Kawase and H. Kurata, *Chem. Rev.* **2006,** *106*, 5250-5273.
[4] J. W. Steed, P. C. Junk, J. L. Atwood, M. J. Barnes, C. L. Raston and R. S. Burkhalter, *J. Am. Chem. Soc.* **1994,** *116*, 10346-10347.
[5] E. Huerta, G. A. Metselaar, A. Fragoso, E. Santos, C. Bo and J. de Mendoza, *Angew. Chem. Int. Ed.* **2007,** *46*, 202-205.
[6] A. Sygula, F. R. Fronczek, R. Sygula, P. W. Rabideau and M. M. Olmstead, *J. Am. Chem. Soc.* **2007,** *129*, 3842-3843.
[7] S. Mizyed, P. E. Georghiou, M. Bancu, B. Cuadra, A. K. Rai, P. Cheng and L. T. Scott, *J. Am. Chem. Soc.* **2001,** *123*, 12770-12774.
[8] T. Kawase, K. Tanaka, N. Shiono, Y. Seirai and M. Oda, *Angew. Chem. Int. Ed.* **2004,** *43*, 1722-1724.
[9] T. Kawase, K. Tanaka, Y. Seirai, N. Shiono and M. Oda, *Angew. Chem. Int. Ed.* **2003,** *42*, 5597-5600.

derivatives[11,12,13,14] have been reported, but to date, hosts that exploit porphyrins as recognizing motifs have dominated the literature both in quantity and binding strength.[2] The highest binding constants among porphyrin-based receptors correspond to Aida´s bisporphyrin macrocyclic receptors. For example, a Zn(II) metalloporphyrin derivative shows a log K_a = 5.8 towards C_{60}, while the free base shows log K_a = 5.9, both in benzene at room temperature.[15] The world-record in complex stability —an Ir(III) metalloporphyrin— shows a log K_a = 8.1 for C_{60} in 1,2-dichlorobenzene (oDCB) at room temperature.[16] It is noteworthy that in the latter case iridium was found to bind a 6,6 junction of the fullerene in a η^2 fashion.

4.1.2. Results and discussion

Making use of the perfect match between the concave aromatic surface of 2-[9-(1,3-dithiol-2-ylidene)anthracen-10(9*H*)-ylidene]-1,3-dithiole (exTTF) and the convex surface of the fullerenes, we reported the first exTTF-based receptor for fullerene, based on a very simple tweezers-like design.[11, 12, 14] This receptor was shown to form complexes with C_{60} of considerable stability considering its lack of preorganization (log K_a = 3.5 in PhCl at room temperature).[14] We would now like to report the design, synthesis, and fullerene binding abilities of macrocycle **4.2**.

[10] T. Kawase, K. Tanaka, N. Fujiwara, H. R. Darabi and M. Oda, *Angew. Chem. Int. Ed.* **2003,** *42*, 1624-1628.
[11] S. S. Gayathri, M. Wielopolski, E. M. Pérez, G. Fernández, L. Sánchez, R. Viruela, E. Ortí, D. M. Guldi and N. Martín, *Angew. Chem. Int. Ed.* **2009,** *48*, 815-819.
[12] E. M. Pérez, A. L. Capodilupo, G. Fernández, L. Sánchez, P. M. Viruela, R. Viruela, E. Ortí, M. Bietti and N. Martín, *Chem. Commun.* **2008,** *0*, 4567-4569.
[13] E. M. Pérez, M. Sierra, L. Sánchez, M. R. Torres, R. Viruela, P. M. Viruela, E. Ortí and N. Martín, *Angew. Chem. Int. Ed.* **2007,** *46*, 1847-1851.
[14] E. M. Pérez, L. Sánchez, G. Fernández and N. Martín, *J. Am. Chem. Soc.* **2006,** *128*, 7172-7173.
[15] J.-Y. Zheng, K. Tashiro, Y. Hirabayashi, K. Kinbara, K. Saigo, T. Aida, S. Sakamoto and K. Yamaguchi, *Angew. Chem. Int. Ed.* **2001,** *40*, 1857-1861.
[16] M. Yanagisawa, K. Tashiro, M. Yamasaki and T. Aida, *J. Am. Chem. Soc.* **2007,** *129*, 11912-11913.

Scheme 1. Synthesis of macrocycle **4.2**.[a]

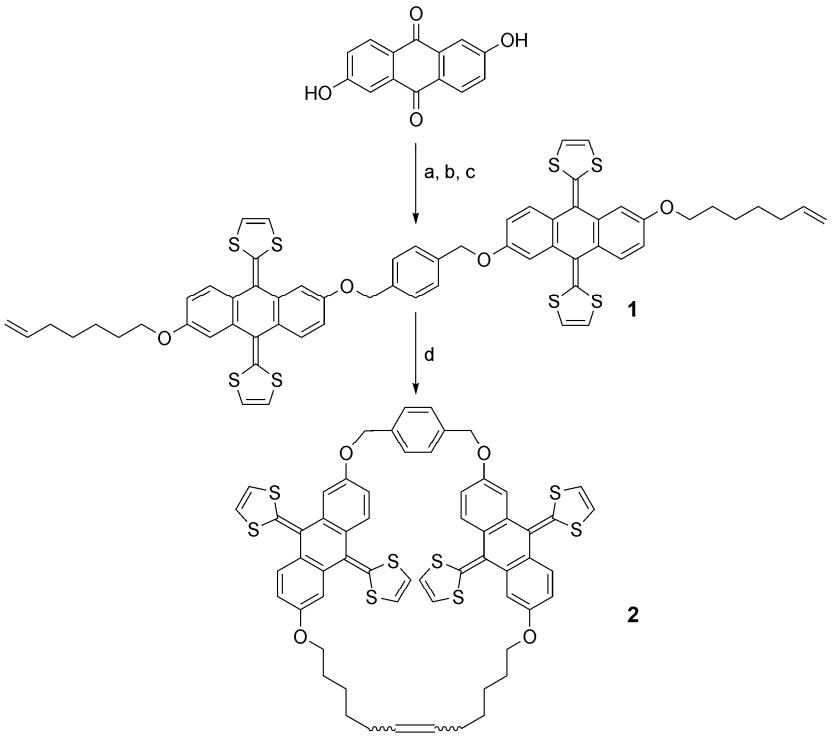

[a] Conditions: a) 7-bromo-1-heptene, K_2CO_3, DMF, reflux, 2 h; b) α,α'-*p*-dibromoxylene, K_2CO_3, DMF, 60 ºC, 4 h; c) dimethyl 1,3-dithiol-2-ylphosphonate, BuLi, THF, −78 ºC to r. t., 2 h; d) Grubb´s 1st generation catalyst, CH_2Cl_2, r. t., 2 h.

The design of the macrocyclic receptor conserves the basic features of the tweezers receptor, but including an alkyl linker with terminal alkenes to achieve macrocyclization through ring closing metathesis. Molecular mechanics showed that the most suitable spacer would be heptene, which showed flexible macrocyclic cavities of *ca.* 11-13 Å. Macrocycle **2** was synthesized in just four steps following Scheme 1, and obtained as a chromatographically inseparable mixture of *E/Z* isomers, which was used as such. The identity and purity of **2** and all synthetic intermediates were unambiguously established by standard spectroscopic and analytical techniques (see experimental section).

The binding constants of macrocycle **4.2** towards C_{60} and C_{70} were estimated through three independent UV-vis titrations at room temperature. In a typical experiment, to a solution of **4.2** (1.0×10^{-5} M, PhCl) aliquots of a solution of C_{60} or C_{70} ($3\text{-}4 \times 10^{-5}$ M, PhCl) were added until reaching 2-3 molar equivalents, working at constant concentration of host.

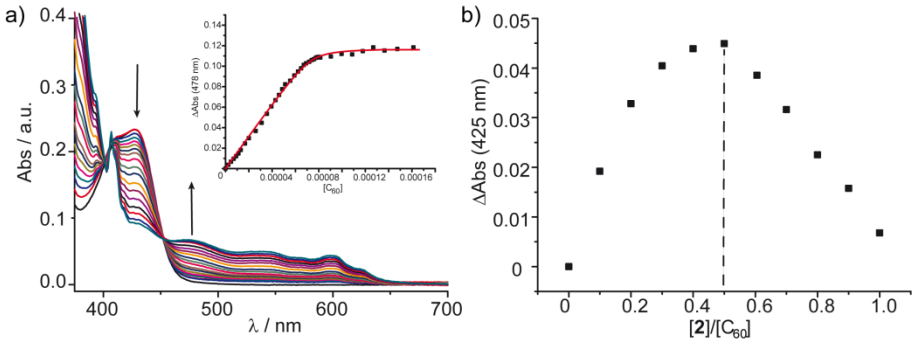

Figure 1. a) Spectral changes in a UV-vis titration experiment of **2** *vs.* C_{60} in PhCl at room temperature, and binding isotherm (inset, K_a = 1087200 M^{-1}, R^2 = 0.996). b) Job´s plot demonstrating the 1:1 stoichiometry.

A titration experiment between **4.2** and C_{60} is shown in Figure 1a. The spectral features are similar to what we had previously observed for exTTF tweezers.[11, 14] On increasing concentration of C_{60}, a significant decrease in the absorption at λ = 425 nm is observed, together with the appearance of a charge transfer band centered at 478 nm, with an isosbestic point at 450 nm. The expected 1:1 stoichiometry, suggested by the presence of the isosbestic point, was confirmed through continuous variation plots (see Figure 1b). In the case of C_{70} the spectral changes are less obvious due to spectral overlap. The binding constant of **4.2** towards C_{60} in chlorobenzene at room temperature was found to be of log K_a = 6.5 ± 0.5 (Specfit) or 6.1 ± 0.2 (Origin). This means an increase of three orders of magnitude with respect to our previously reported receptors,[11, 14] and one of the highest binding constants towards C_{60} reported in the literature,[1-3] illustrating the dramatic effect of preorganization. For comparison, the linear precursor **1** showed log K_a = 3.01 in PhCl at romm temperature (see figure 7). With regards to C_{70}, the binding constant is too high to be calculated precisely through UV-vis titrations (Utilizing Specfit we were able to approximate it as log K_a = 8.4 ± 2.5, see figure 8). With the aim of lowering the binding constant to a more reliable quantity, we changed to oDCB as solvent. However, despite both **4.2** and the fullerenes are soluble in oDCB, when we approached a 1:1 stoichiometry during the addition process the solution immediately turned turbid, precluding UV-vis measurements. The mixture of *E/Z* isomers and the flexibility of **4.2** prevented the formation of single crystals suitable for X-ray diffraction, so we investigated the geometry of the complexes through density functional theory (DFT) calculations (see computational details section). Figure 2 shows the structure of the complex of *Z*-**4.2** with C_{60} (BH&H/6-31G**).[17]

[17] The BH&H functional has been shown to provide good performance for supramolecular systems dominated by dispersion interactions, see: Y. Zhao and D. G. Truhlar, *J. Chem. Theory Comput.* **2006,** *3*, 289-300. The Z and E isomers define cavities of similar size.

Experimental Determination of Association Constants Involving Fullerenes

We consider that the correct determination of association constants is far from a trivial experimental technique. To arrive at chemically meaningful and quantitatively significant results we need to give attention to a variety of issues, from planning the titration to analysing the titration data. Here we will explain some necessary general considerations briefly, focused on the peculiarities of fullerenes as guest.

The objective of planning a titration experiment is to extract K_a from a series of spectroscopic measurements.

$$K_a = \frac{[HG]}{[H][G]}$$

To achieve this, we will generally prepare a solution of known concentration of host ($[H]_0$) and gradually increase the concentration of host–guest complex by adding aliquots of a solution of known concentration of guest ($[G]_0$). Then, we will analyse the variation in a given physical property that it is proportional to the concentration of the host–guest associate.

Planning and performing the titration. We need to consider the system we wish to study: host, guest, solvent and temperature. We need to consider the solubility of host, guest and complex in the selection of the solvent to prevent precipitation, and we need to consider the boiling point to prevent evaporation. The temperature has to be controlled since we need solvent and temperature data for each binding constant value.

The expected association constant determines the concentration we should choose for our titration experiment and the spectroscopic technique. Related with concentration we need to consider that we should add fullerene until saturation, or as close to saturation as possible, covering at least 70-80 % of the binding isotherm. A good starting point is a concentration of host equal or slightly higher than the reciprocal of the expected binding constant. We will use common sense and trial and error for that. With regard of the concentration of the guest (fullerene) we will select a concentration that allows us to get the saturation with the addition of a reasonably small volume of fullerene solution. It is worth noting that we use the host solution as solvent in the solution of the guest to prevent dilution factors.

The volume and number of aliquots that we will add will depend on the estimated binding constant and the number of data points that we consider reasonable. Finally we have to consider that we must repeat each titration experiment several times.

Spectroscopic method. The choice of the spectroscopic method depends on the chemical nature of host and guest and the concentration at which we are carrying out our titration (reciprocal to the expected binding constant). The sensitivity of ^{1}H NMR on a routine spectrometer will prevent measurements with concentrations smaller than 0.1 mM. That means that NMR is a good method for $K_a < 10^5\ M^{-1}$. UV-vis is suitable for concentration from mM to μM, then for $10^3 \leq K_a \leq 10^7 M^{-1}$. Fluorescence is the most sensitive of the three techniques and will allow us to carry put measurements at submicromolar concentrations, ideal for determination of $K_a > 10^6\ M^{-1}$. Since the changes in NMR signals are very weak upon complexation with fullerenes, the fullerenes are weak fluorophores, and the usual range of binding constants, UV-vis is often the spectroscopic method of choice.

Analysis. In the analysis of the data we have to observe carefully the shape of the binding isotherm. The typical shape is a hyperbole; for example we can identify if we have some cooperativity process if the binding isotherm is sigmoidal. In the changes in the absorption spectra the formation of isosbestic point indicates only one type of associate. In order to determine the stoichiometry we have to use the chemical common sense, and the continuous variation plot (Job's plot) method for the experimental determination. When the variation of a physical property is plotted versus the molar fraction of host, the maximum in the plot give us the stoichiometry of our complex. The method is more reliable if we work with the system fully saturated ($[H] >> K_a^{-1}$). Finally, after repeating the experiment, we can report the binding constant as the mean value of the experiments plus or minus the standard deviation.

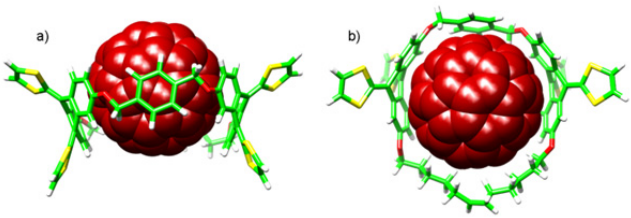

Figure 2. Side view (a) and top view (b) of the energy-minimized structure (BH&H/6-31G** level) of the *Z*-**2**·C_{60} associate.

DFT calculations confirm that **4.2** is a close to perfect fit for C_{60}, with both exTTFs, the aromatic xylylene linker, and the alkyl spacer closely wrapping the fullerene unit. BH&H/6-31+G** calculations including the basis set superposition error (BSSE) predict a binding energy of −24.1 kcal mol^{-1}, significantly higher than that calculated under the same computational conditions for the exTTF tweezers,[11, 12] in agreement with the experimental results.

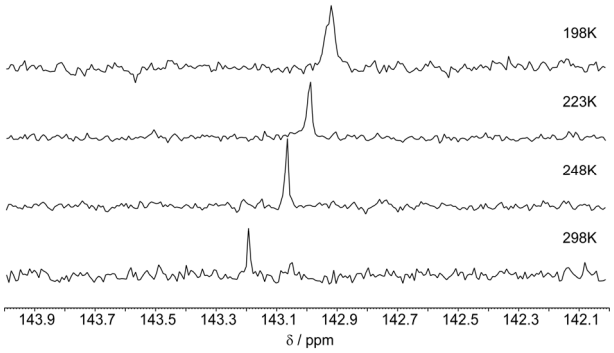

Figure 3. ^{13}C NMR (75 MHz) of a mixture of C_{60} and **4.2** (1.5:1) in toluene-d_8 at several temperatures.

The binding event was also investigated by ^{13}C NMR, which confirms the association of **4.2** with C_{60}. Figure 3 shows the variable temperature ^{13}C NMR spectra (75 MHz) of a mixture of C_{60} and **4.2** (1.5:1) in toluene-d_8. The spectra were run with sufficient scans to detect the signal of C_{60} only. Upon cooling, the signal is shifted upfield and broadened, as would be expected for the formation of the associate. The equilibrium of association continues to be rapid even at 198 K, although the significant broadening indicates that we were close to the temperature of coalescence.

4.1.3. Conclusions

In conclusion, we have described an exTTF-based macrocyclic receptor that associates C_{60} with binding constants three orders of magnitude higher than the previous examples of exTTF-based receptors,[11, 12, 14] nearly two orders of magnitude higher than those reported for metalloporphyrin tweezers,[18,19] and even superior to most of Aida´s porphyrin macrocycles, with the exception of the Rh(III) and Ir(III)[16] congeners. These results definitely consolidate exTTF as one of the most suitable fragments for the molecular recognition of fullerenes. The simplicity of the synthetic route to obtain **4.2** augurs well for its utilization in the construction of electroactive nanostructures.[20] This,

[18] A. Hosseini, S. Taylor, G. Accorsi, N. Armaroli, C. A. Reed and P. D. W. Boyd, *J. Am. Chem. Soc.* **2006,** *128*, 15903-15913.
[19] Z.-Q. Wu, X.-B. Shao, C. Li, J.-L. Hou, K. Wang, X.-K. Jiang and Z.-T. Li, *J. Am. Chem. Soc.* **2005,** *127*, 17460-17468.
[20] (a) G. Fernández, E. M. Pérez, L. Sánchez and N. Martín, *Angew. Chem. Int. Ed.* **2008,** *47*, 1094-1097; (b) G. Fernández, E. M. Pérez, L. Sánchez and N. Martín, *J. Am. Chem. Soc.* **2008,** *130*, 2410-2411; (c) G. Fernández, L. Sánchez, E. M. Pérez and N. Martín, *J. Am. Chem. Soc.* **2008,** *130*, 10674-10683.

together with the full structural optimization of the aromatic linker and the alkyl spacer, is the main objective of our future investigations.

4.1.4. Computational details

Theoretical calculations were carried out within the density functional theory (DFT) approach by using the D.02 revision of the Gaussian 03 suite of programs.[21] Geometry optimizations were performed making use of Becke's "half-and-half" functional, BH&H,[22] and the 6-31G** basis set.[23] The BH&H functional is an *ad hoc* mixture of exact Hartree-Fock (HF) and local density approximation (LDA) exchange, coupled with Lee, Yang, and Parr's (LYP) expression[24] for the correlation energy. The attractiveness of the BH&H functional to calculate supramolecular associations is that it successfully reproduces the results of highly-accurate post-HF methods for π-stacked complexes. [25, 26, 17, 27]Waller et al.[27] found that the BH&H functional provides a binding energy for the archetypal parallel-displaced benzene dimer in good agreement with the best available high-level computational methods. Truhlar et al. have recently reported a very comprehensive study of a large database of non-covalent interacting systems using different functionals and concluded that the BH&H functional gives good performance for dispersion-dominated interactions. A similar conclusion is stated by Hobza et al.[27b] in a very recent study on small peptides for which the interaction is dominated by dispersion forces. The different conformations of macrocycle **4.2** were also optimized using Becke's three-parameter B3LYP exchange-correlation functional[23] and the 6-31G** basis set. The B3LYP functional was not employed to calculate the supramolecular complexes because it fails in describing dispersion forces and does not properly account for stacking π–π interactions.[28]

Association binding energies were firstly obtained at the BH&H/6-31G** level by fully optimizing the geometry (intra- and intermolecular parameters) of the supramolecular complex. Binding energies were afterwards recalculated using the more extended 6-31+G** basis set,[29] which includes diffuse functions on the heavy atoms, and the 6-31G**-optimized geometries. The basis set superposition error (BSSE) was calculated using the counterpoise correction approach.[30] The BSSE is a spurious

[21] Gaussian 03, Revision C.02 Gaussian, Inc.: Wallingford CT, 2004.
[22] A. D. Becke, *J. Chem. Phys.* **1993,** *98*, 1372-1377.
[23] M. M. Francl, W. J. Pietro, W. J. Hehre, J. S. Binkley, M. S. Gordon, D. J. DeFrees and J. A. Pople, *J. Chem. Phys.* **1982,** *77*, 3654-3665.
[24] C. Lee, W. Yang and R. G. Parr, *Physical Review B* **1988,** *37*, 785-789.
[25] A. Robertazzi and J. A. Platts, *J. Phys. Chem. A* **2006,** *110*, 3992-4000.
[26] K. Gkionis, J. G. Hill, S. Oldfield and J. Platts, *J. Mol. Model.* **2009,** *15*, 1051-1060.
[27] (a) M. P. Waller, A. Robertazzi, J. A. Platts, D. E. Hibbs and P. A. Williams, *J. Comput. Chem.* **2006,** *27*, 491-504; (b) H. Valdes, K. Pluhackova, M. Pitonak, J. Rezac and P. Hobza, *PCCP* **2008,** *10*, 2747-2757.
[28] S. Tsuzuki and H. P. Luthi, *J. Chem. Phys.* **2001,** *114*, 3949-3957; Y. Zhao and D. G. Truhlar, *J. Chem. Theory Comput.* **2005,** *1*, 415-432.
[29] W. J. Hehre, L. Radom, P. v. R. Schleyer and J. Pople, *Ab initio Molecular Orbital Theory*. New York, 1986.
[30] S. F. Boys and F. Bernardi, *Mol. Phys.* **1970,** *19*, 553-566.

contribution to the interaction energy arising from the improved description of the molecular fragment A in the complex A•••B due to the assistance of the basis set located in fragment B, and vice versa. The counterpoise method corrects the interaction energy of the complex A•••B by computing the energies of the isolated fragments A and B with exactly the same basis set (both in number and location) as used to compute the complex A•••B.

Figure 4 sketches two energy-minimized structures calculated for the **4.2**•C_{60} associate at the BH&H/6-31G** level (structure A corresponds to that displayed in Figure 2 in the main text). Structures A and B in Figure 4 show a similar disposition of the exTTF moieties and the central xylylene unit around C_{60}, and mainly differ in the conformation of the alkyl chain that closes the macrocycle. Macrocycle **4.2** indeed presents a high flexibility due to the alkyl chain and to the relative orientation of the exTTF units, and multiple minima can be envisaged for the molecular associate.

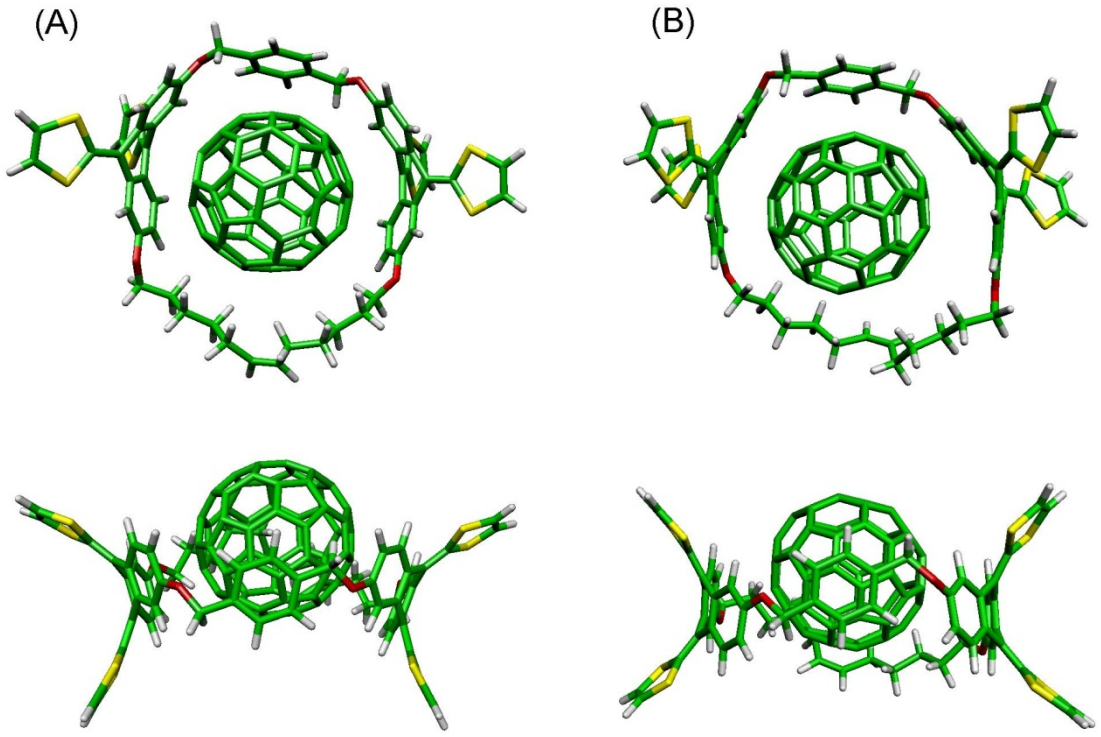

Figure 4. Top view (top) and side view (bottom) of two energy-minimized structures (A and B) calculated for the **4.2**•C_{60} associate at the BH&H/6-31G** level.

At the BH&H/6-31G** level, structure A is calculated to have a binding energy of –34.52 kcal/mol and is predicted to be more stable than structure B, for which a binding energy of –31.49 kcal/mol is obtained. The higher stability of structure A is due to the more closely wrapping of the fullerene unit by the exTTFs, the xylylene linker, and the alkyl chain. In structure A, the benzene rings of both the exTTF and the xylylene units are all oriented parallel to the fullerene surface and maximize the π–π interactions between the receptor and C_{60} (see Figure 4). This is not the case for structure B, for

which the benzene rings are tilted with respect to the C_{60} surface and the alkyl chain is less accomodated around C_{60}. When using the more extended 6-31+G** basis set, the value calculated for the association binding energy of structure A is –31.64 kcal/mol and diminishes to –24.13 kcal/mol when the correction for the BSSE (+7.51 kcal/mol) is added.

As mentioned above, macrocycle **4.2** presents a highly flexible structure due to the different conformations that the alkyl chain can adopt, and to the possible orientations of the exTTF units with respect to the central xylylene linker. Figure 5 sketches five energy-minimized conformations (M1 to M5) calculated for **4.2** at the BH&H/6-31G** level, although other conformational minima could be found. B3LYP/6-31G** calculations lead to similar minimum-energy conformations. The exTTF units always adopt a butterfly- or saddle-like structure, in which the central ring of the anthracene units folds into a boat conformation and the benzene and dithiole rings point to opposite directions. Structures M1 and M2 in Figure 5 present the same disposition of the exTTF units, with the dithiole rings pointing outwards of the macrocycle, and mainly differ in the conformation adopted by the alkyl chain. In structure M3 the exTTF units approach each other and the alkyl chain is completely folded. Structures M4 and M5 present a different orientation of the exTTF units, with one or the two exTTFs pointing inwards the macrocycle, and appear to be less adequate to host C_{60}. Indeed, the centre of the macrocycle is completely crowded in structure M5.

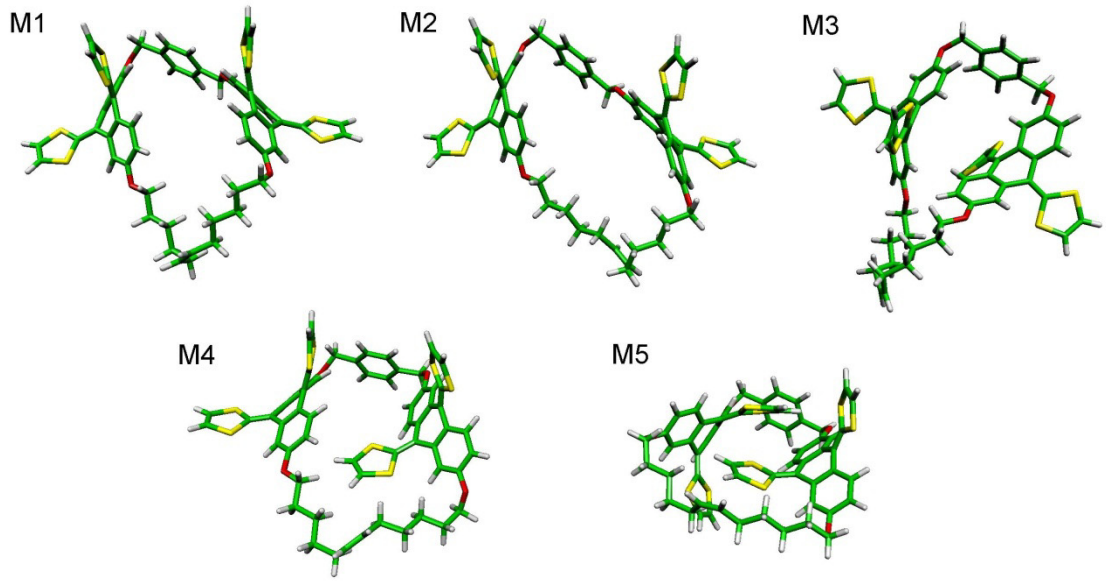

Figure 5. BH&H/6-31G**-optimized conformations calculated for macrocycle **4.2**.

At the B3LYP/6-31G** level, structures M1–M3 are predicted to be close in energy in a range of 3.24 kcal/mol and structures M4 and M5 are calculated to lie at higher energies (4.74 and 10.33 kcal/mol, respectively). The BH&H/6-31G** approach fails in

predicting the relative energy of these conformations since it obtains the crowded structure M5 as the most stable. Structures M1–M5 were also optimized in the presence of the solvent (chlorobenzene) making use of the polarized continuum model (PCM) approach.[31,32] At the B3LYP/6-31G** level, structure M1 is obtained to be the most stable and structures M2 and M3 lie very close in energy (0.60 and 3.38 kcal/mol, respectively). A mixture of conformations has therefore to be expected for macrocycle **4.2** in solution. Among these minimum-energy conformations, only some of them like M1 and M2 show geometries that can be easily reorganized to accommodate C_{60}. Indeed, optimization of **4.2** starting from the geometry it shows in structures A and B of the **4.2**•C_{60} associate leads to conformations M1 and M2, respectively.

Figure 6 displays the energy-minimized structures calculated for the **4.2**•C_{70} associate at the BH&H/6-31G** level. The structure was optimized starting from structure A of **4.2**•C_{60} and substituting C_{60} by C_{70}. When C_{70} is introduced horizontally with its long axis in the plain of the macrocycle, intermolecular interactions occur at too much short distances and C_{70} is moved out the cavity of the macrocycle (Figure 6 left). When C_{70} is introduced vertically (Figure 6 right), it stays inside the macrocycle and an association binding energy of –35.91 kcal/mol is computed at the BH&H/6-31G** level. This energy is slightly larger than that predicted for the **4.2**•C_{60} associate (–34.52 kcal/mol), in agreement with the higher association constant found experimentally for **4.2**•C_{70}. Association binding energies were calculated as the difference between the total energy of the complex and the sum of the total energies of the receptor and the fullerene. The energy used for the receptor was that computed for **4.2** using the optimized geometry it shows in the associate. We employed this energy instead of that calculated for the fully-relaxed macrocycle because the BH&H/6-31G** approach does not provide a correct description of the conformational behavior of **4.2**. When the energy of the fully-relaxed structure M1 is used, the binding energies calculated at the BH&H/6-31G** level for **4.2**•C_{60} and **4.2**•C_{70} decrease to –21.05 and –22.53 kcal/mol, respectively.

[31] (a) J. Tomasi and M. Persico, *Chem. Rev.* **1994,** *94*, 2027-2094; (b) C. S. Cramer and D. G. Truhlar, *Solvent Effects and Chemical Reactivity* Kluwer: Dordrecht, 1996.
[32] (a) S. Miertuš, E. Scrocco and J. Tomasi, *Chem. Phys.* **1981,** *55*, 117-129; (b) S. Miertuš and J. Tomasi, *Chem. Phys.* **1982,** *65*, 239-245; (c) M. Cossi, V. Barone, R. Cammi and J. Tomasi, *Chem. Phys. Lett.* **1996,** *255*, 327-335; (d) E. Cances, B. Mennucci and J. Tomasi, *J. Chem. Phys.* **1997,** *107*, 3032-3041; (e) V. Barone, M. Cossi and J. Tomasi, *J. Comput. Chem.* **1998,** *19*, 404-417; (f) M. Cossi, G. Scalmani, N. Rega and V. Barone, *J. Chem. Phys.* **2002,** *117*, 43-54.

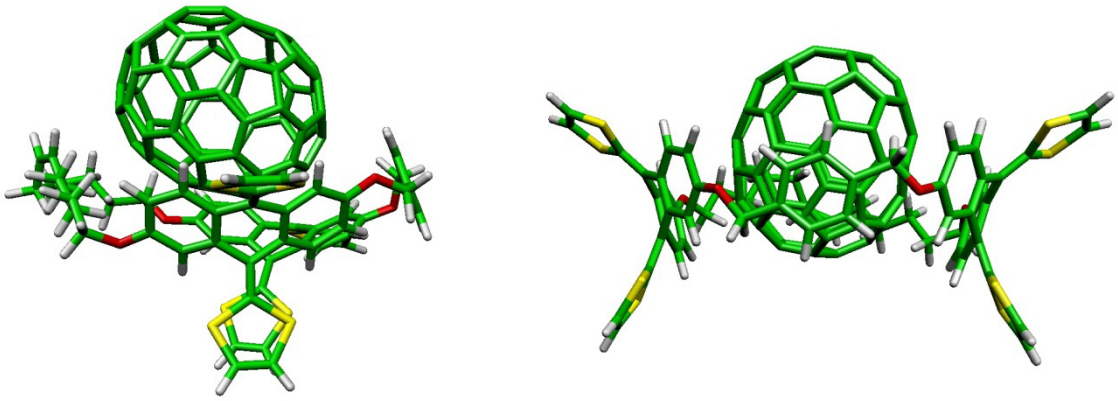

Figure 6. Energy-minimized structures calculated at the BH&H/6-31G** level for the **4.2**•C_{70} associate.

4.1.5. Experimental section

General. All solvents were dried according to standard procedures. Reagents were used as purchased. All air-sensitive reactions were carried out under argon atmosphere. Flash chromatography was performed using silica gel (Merck, Kieselgel 60, 230-240 mesh, or Scharlau 60, 230-240 mesh). Analytical thin layer chromatography (TLC) was performed using aluminium-coated Merck Kieselgel 60 F254 plates. Melting points were determined on a Gallenkamp apparatus. NMR spectra were recorded on a Bruker Avance 300 (^{1}H: 300 MHz; ^{13}C: 75 MHz) a Bruker Avance 500 (^{1}H: 500 MHz; ^{13}C: 125 MHz) or a Bruker AvanceIII 700 (^{1}H: 700 MHz; ^{13}C 175 MHz) spectrometers at 298 K, unless otherwise stated, using partially deuterated solvents as internal standards. Coupling constants (J) are denoted in Hz and chemical shifts (δ) in ppm. Multiplicities are denoted as follows: s = singlet, d = doublet, t = triplet, m = multiplet, b = broad. Electrospray ionization mass spectra (ESI-MS) and Matrix assisted Laser desorption ionization (coupled to a Time-of-Flight analyzer) experiments (MALDI-TOF) were recorded on a HP1100MSD spectrometer and a Bruker REFLEX spectrometer, respectively.

4.1.5.1. Synthesis and characterization

Monosubstituted anthraflavic acid derivative

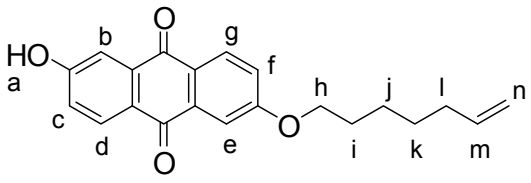

Chemical Formula: $C_{21}H_{20}O_4$
Molecular Weight: 336,38

Anthraflavic acid 3.33 g (12.5 mmol) was dissolved with sonication in 450 mL of dry DMF. Then, 1.73 g (12.5 mmol) of dry K_2CO_3, 2.21 g (12.5 mmol) of 7-bromo-1-

heptene, and a catalytic amount of NaI were added and the mixture heated to reflux for 2 h. The crude reaction was poured into ice-cold 1 M aqueous HCl, and filtrated. The solid was redissolved in CH_2Cl_2 and washed with water (2x), the organic fraction was dried over $MgSO_4$, the solvent evaporated, and the resulting product subjected to column chromatography (CH_2Cl_2 to CH_2Cl_2:CH_3OH 2%) to obtain the pure product as a light yellow solid in 47% yield.

Mp 80-82 ˚C; ^{1}H NMR (d_6-DMSO, 300 MHz) δ 11.02 (brs, 1H, H_a), 8.09 (d, J = 8.5 Hz, 1H, H_g), 8.06 (d, J = 8.1 Hz, 1H, H_d), 7.54 (d, J = 2.7 Hz, 1H, H_e), 7.48 (d, J = 2.7 Hz, 1H, H_b), 7.36 (dd, J = 2.7 Hz, J = 8.5 Hz, 1H, H_f), 7.20 (dd, J = 2.7 Hz, J = 8.1 Hz, 1H, H_c), 5.81 (m, 1H, H_m), 4.98 (m, 2H, H_n), 4.16 (t, J = 6.7 Hz, 2H, H_h), 2.04 (m, 2H, H_l), 1.77 (m, 2H, H_i), 1.44 (m, 4H, H_{j+k}). ^{13}C NMR (d_6-DMSO, 75 MHz) δ 182.26, 181.90, 164.33, 164.09, 139.53, 136.35, 130.71, 130.27, 127.20, 126.07, 121.94, 121.26, 115.68, 113.10, 111.48, 69.22, 33.98, 29.13, 28.81, 25.77. MS *m/z*: calcd. for $C_{21}H_{19}O_4$ [M-H$^+$] 335.1 found ESI (neg.) [M-H$^+$] 335.0.

Linear anthraquinone precursor

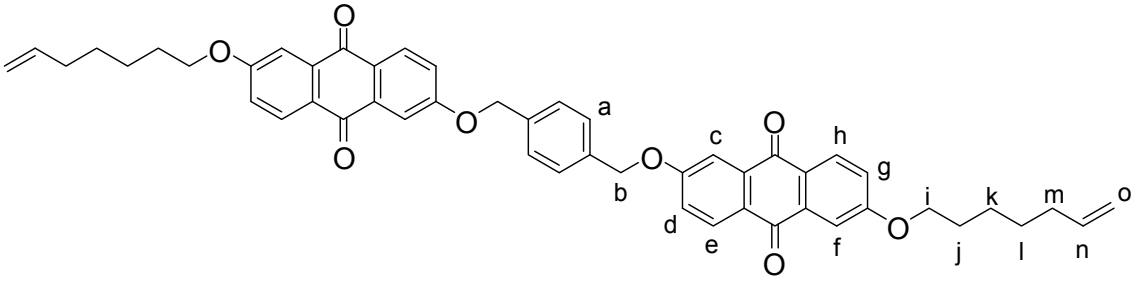

Chemical Formula: $C_{50}H_{46}O_8$
Molecular Weight: 774,90

1.23 g (8.91 mmol) of dry K_2CO_3, 1.17 g (4.46 mmol) of α–α´ dibromo-p-xylene, and a catalytic amount of sodium iodide were added to a solution of 2.69 g (8.0 mmol) of the monoalkylated anthraflavic acid in 20–25 mL of dry N,N-dimethylformamide. The solution was heated to 60 ºC for 4 h, and the resulting suspension was filtrated. The solid obtained was washed successively with methanol and diethylether to remove unreacted starting materials, to yield pure compounds without further purification (y = 67%). The insolubility of this compound at room temperature forced us to characterize it at 353 K in $C_2D_2Cl_4$.

Mp 275-278 ˚C; ^{1}H NMR ($C_2D_2Cl_4$, 500 MHz, 353 K) δ 8.28 (d, J = 8.3 Hz, 2H, H_h), 8.25 (d, J = 8.3 Hz, 2H, H_e), 7.86 (d, J = 2.6 Hz, 2H, H_f), 7.75 (d, J = 2.5 Hz, 2H, H_c), 7.56 (s, 4H, H_a), 7.37 (dd, J = 2.6 Hz, J = 8.3 Hz, 2H, H_g), 7.28 (dd, J = 2.5 Hz, J = 8.3 Hz, 2H, H_d), 5.89 (m, 2H, H_n), 5.32 (brs, 4H, H_b), 5.05 (m, 4H, H_o), 4.21 (t, J = 6.6 Hz, 4H, H_i), 2.16 (m, 4H, H_m), 1.91 (m, 4H, H_j), 1.55 (m, 8H, H_{k+l}). ^{13}C NMR ($C_2D_2Cl_4$, 125 MHz, 353 K) δ 181.85, 181.72, 164.02, 163.41, 138.46, 136.00, 135.90, 135.78, 129.56, 128.06, 127.66, 126.99, 120.91, 120.69, 120.21, 114.39, 111.35, 111.03, 70.24, 68.80,

33.26, 28.74, 28.39, 25.25. MS *m/z*: calcd. for $C_{50}H_{47}O_8$ [M+H$^+$] 775.32 found MALDI-TOF 775.32.

Linear exTTF precursor 4.1

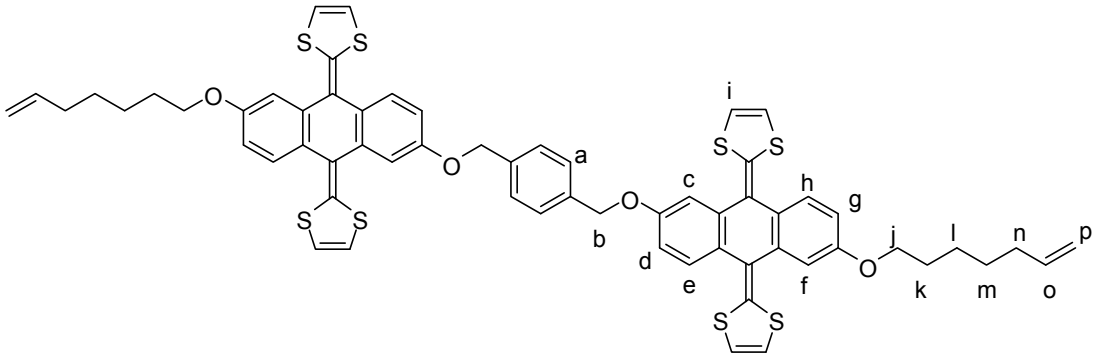

Chemical Formula: $C_{62}H_{54}O_4S_8$
Molecular Weight: 1119,61

A solution of dimethyl 1,3-dithiol-2-ylphosphonate 0.343 mg (1.62 mmol) in 5 mL of dry THF was cooled to –78 ºC, and then BuLi (0.85 mL, 2 M in hexane, 1.70 mmol) was added. The solution was left to stir at –78 ºC for 25 min, with appearance of a yellow precipitate. In the meantime, a suspension of 0.105 g of the anthraquinone precursor (0.135 mmol) in 5 mL of dry THF was dispersed with sonication for *ca.* 30 min. The resulting suspension was added to the phosphorous ylide suspension, and the cooling bath immediately removed. The mixture was allowed to warm to room temperature and left to stir for 2 h. The resulting deep red solution was quenched with CH_3OH, with precipitation of a yellow solid. The solid was filtrated, redissolved in CH_2Cl_2, and subjected to column chromatography (Hex:CH_2Cl_2 3:1 to Hex:CH_2Cl_2 2:1) to obtain the pure product as a bright yellow solid (y = 37%).

Mp 172–175 ˚C; ^{1}H NMR ($CDCl_3$, 500 MHz) δ 7.60 (d, J = 8.5 Hz, 2H, H_h), 7.57 (bd, 2H, H_e), 7.50 (s, 4H, H_a), 7.26 (bs, 2H, H_f), 7.22 (bs, 2H, H_c), 6.90 (bd, J = 8.5 Hz, 2H, H_g), 6.81 (bm, 2H, H_d), 6.23 (m, 8H, H_i), 5.87 (m, 2H, H_o), 5.17 (m, 4H, H_b), 5.01 (m, 4H, H_p), 4.03 (bt, 4H, H_j), 2.12 (m, 4H, H_n), 1.84 (m, 4H, H_k), 1.51 (m, 8H, H_{l+m}). ^{13}C NMR ($CDCl_3$, 125 MHz) δ 157.10, 156.57, 138.89, 137.04, 136.93, 136.79, 133.99, 133.80, 128.71, 128.26, 127.75, 126.12, 126.04, 122.05, 121.79, 117.16, 117.05, 114.47, 112.45, 112.37, 112.04, 111.97, 111.20, 111.15, 110.93, 110.90, 69.87, 68.12, 33.73, 29.15, 28.69, 25.70, 25.59. MS *m/z*: calcd. for $C_{62}H_{54}O_4S_8$ [M$^+$] 1118.18 found MALDI-TOF 1118.15.

Bis-exTTF macrocycle 4.2

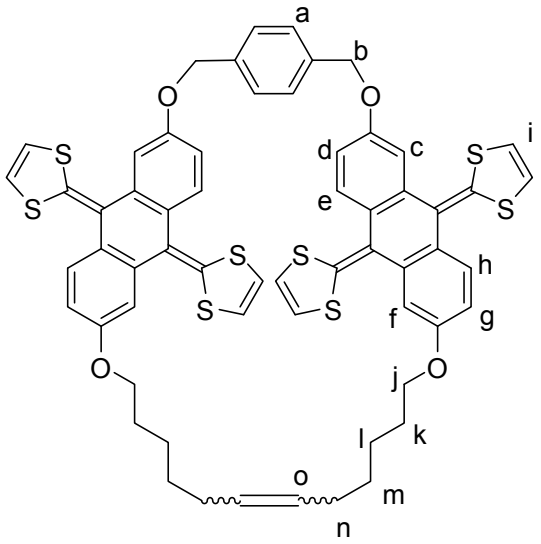

Chemical Formula: $C_{60}H_{50}O_4S_8$
Molecular Weight: 1091,557

A catalytic amount of Grubb´s 1st generation catalyst was added to a solution of the linear precursor **4.1** in dry and degassed CH_2Cl_2. The solution was stirred at room temperature and its progress monitored by TLC (Hex:CH_2Cl_2 2:1). The reaction proceeds spot to spot until it is close to completion, when unidentified polar spots start to appear on the TLC. The reaction is then stopped, filtered through a pad of Celite, the solvent evaporated under reduced pressure, and the crude subjected to column chromatography on silica gel (Hex:CH_2Cl_2 2:1) to yield the product as an inseparable mixture of *E/Z* isomers (y = 90%).

The product shows complicated ^{1}H NMR, consistent with an asymmetric molecule in several conformations in slow chemical exchange at NMR timescale. We have obtained a sufficiently well-resolved spectrum on a Bruker AvanceIII 700 MHz in chlorobenzene-d_5, and fully assigned it based on COSY and TOCSY experiments. Lettering corresponds to that shown above. No distinction between isomers or conformers has been made.

Mp 215–217 °C; ^{1}H NMR (chlorobenzene-d_5, 700 MHz, 298 K) δ (ppm) 7.64 (d, J = 8.4 Hz, 0.25H, H_h), 7.36 (d, J = 8.4 Hz, 0.75H, H_h), 7.31 (d, J = 8.4 Hz, 0.50H, H_e), 7.29 (d, J = 8.4 Hz, 0.50H, H_e),7.23 (s, 0.25H, H_f) 7.19 (d, J = 8.4 Hz, 0.75H, H_h), 7.16 (d, J = 8.4 Hz, 0.25H, H_h), 7.09 (d, J = 8.4 Hz, 0. 50H, H_e), 7.04 (s, 3H, H_a), 7.02 (s, 1H, H_a), 7.00 (d, J = 2.3 Hz, 0.50H, H_e), 6.99 (s, 0.50H, H_f), 6.98 (d, J = 2.3 Hz, 0.50H, H_f), 6.96 (d, J = 2.3 Hz, 0.75H, H_f), 6.88 (s, 0.25H, H_c), 6.86 (s, 0.25H, H_c), 6.85 (d, J = 2.3 Hz, 0.75H, H_c), 6.83 (m, 0.25H, H_c), 6.79 (dd, J = 8.3 Hz, J = 2.4 Hz, 0.25H, H_g), 6.77 (s, 0.25H, H_c), 6.66 (dd, J = 8.4 Hz, J = 2.4 Hz, 0.50H, H_g), 6.63 (s, 0.25H, H_c), 6.60 (dd, J = 8.4 Hz, J = 2.4 Hz, 1H, H_d), 6.51 (m, 1.5H, H_g), 6.33 (dd, J = 8.4 Hz, J = 2.3 Hz, 0.50H, H_d), 6.26 (dd, J = 8.5 Hz, J = 2.3 Hz, 0.50H, H_d), 5.63 (d, J = 6.6 Hz, 0.50H, H_i),

5.57 (m, 1H, H_i), 5.47 (m, 1H, H_i), 5.24 (d, J = 6.6 Hz, 0.50H, H_i), 5.19 (d, J = 6.6 Hz, 0.50H, H_i), 5.16 (m, 0.75H, H_o), 5.13 (m, 1.25H, H_o), 5.09 (d, J = 6.6 Hz, 0.5H, H_i), 4.98-4.87 (m, S12 4H, H_b), 3.59 (m, 4H, H_j), 1.79 (m, 4H, H_n), 1.44 (m, 4H, H_k), 1.19 (m, 8H, H_{l+m}). ^{13}C NMR (chlorobenzene-*d5*, 175 MHz, 298 K) δ (ppm) 157.52, 156.49, 156.25, 156.02, 138.90, 137.56, 137.49, 137.39, 137.31, 137.09, 136.95, 132.47, 130.89, 130.65, 127.28, 127.21, 127.10, 121.84, 121.43, 117.20, 117.09, 117.00, 116.93, 116.72, 116.66, 116.57, 114.31, 113.70, 112.83, 112.33, 111.89, 111.84, 111.76, 111.66, 111.39, 111.20, 111.01, 110.52, 69.21, 69.07, 68.23, 68.02, 37.91, 35.13, 34.55, 34.17, 33.21, 32.63, 32.51, 32.40, 31.44, 29.84, 29.63, 29.41, 29.14, 27.69, 27.23, 27.02, 25.38, 25.32. MS *m/z*: calcd. For $C_{60}H_{50}O_4S_8$ [M^+] 1090.1 found MALDI-TOF 1090.2 HRMS *m/z*: calcd. for $C_{60}H_{50}O_4S_8$ [M^+] 1090.1475 [M^{2+}] 545.0738 found ESI (pos.) 1090.1372; 545.0732.

4.1.5.2. Estimation of the binding constants through UV-vis titrations[33, 34]

Binding constants towards C_{60}:

In a typical experiment, we prepared stock solutions of the macrocyclic receptor **4.2** at a concentration of approximately 1×10^{-5} M. Those solutions were utilized as solvents in the C_{60} solution (1×10^{-4} M), to ensure working at constant concentration of host. Aliquots of the fullerene solution were added to the host solution and UV-vis spectra recorded at room temperature on a Cary UV-50 spectrophotometer. Determination of the binding constants towards C_{60} was carried out utilizing Specfit software and by non-linear least-squares analysis of the ΔAbs at both 425 nm and 478 nm against the concentration of the fullerene, utilizing OriginPro 7.5 (OriginLab corporation) and the binding isotherm:

$$\Delta_{abs} = \frac{\Delta_{max} \times (1 + K_a \times G + K_a \times H) - \sqrt{(1 + K_a \times G + K_a \times H)^2 - 4 \times K_a{}^2 \times H \times G)}}{2 \times K_a \times H}$$

In this case, plots of ΔAbs at 425 nm tend to overestimate the binding constants, so we have routinely utilized ΔAbs at 478 nm. Experiments were repeated three times. The value of log K_a of **4.2** vs C_{60} obtained through this method is 6.1 ± 0.2. An example of titration of **4.2** vs C_{60} and its fit for the binding isotherm are provided in the main text. The analysis of the spectral data utilizing Specfit software provided a value of log K_a = 6.5 ± 0.5, identical within the error limits.

Binding constants towards C_{70}:

In a typical experiment, we prepared stock solutions of the macrocyclic receptor **4.2** at a concentration of approximately 1×10^{-5}. Those solutions were utilized as solvents

[33] O. A. v. Lilienfeld and A. Tkatchenko, *J. Chem. Phys.* **2010,** *132*, 234109.
[34] S. Grimme, *J. Comput. Chem.* **2006,** *27*, 1787.

in the C_{70} solution (3.5×10^{-5} M), to ensure working at constant concentration of host. Aliquots of the fullerene solution were added to the host solution and UV-vis spectra recorded at room temperature on a Cary UV-50 spectrophotometer.

Due to the high degree of spectral overlap, analyses of the UV-vis data were performed utilizing Specfit software, which afforded a value of log $K_a = 8.4 \pm 2.5$.

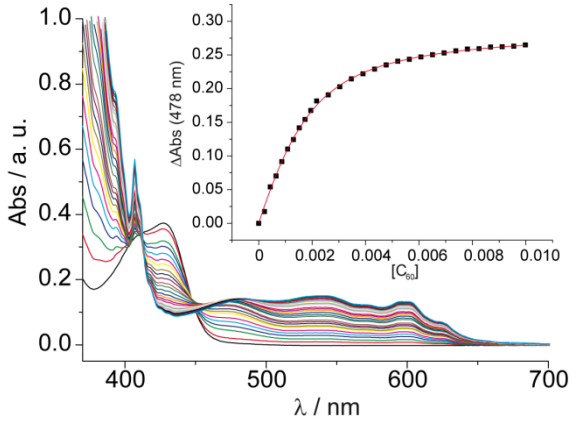

Figure 7. Spectral changes in a UV-vis titration experiment of the linear precursor **4.1** *vs.* C_{60} in PhCl at room temperature, and binding isotherm (inset, $K_a = 1271 \pm 101$ M^{-1}, $R^2 = 0.999$).

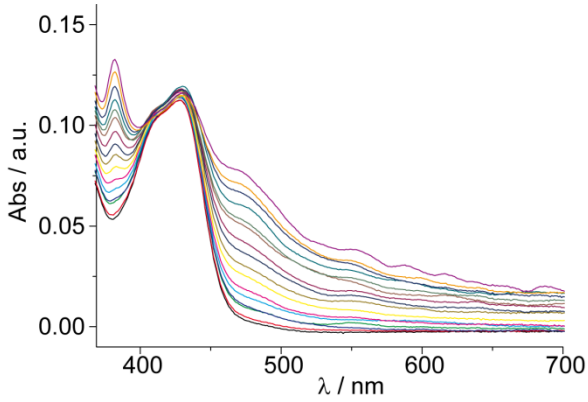

Figure 8. Spectral changes in a UV-vis titration experiment of **4.2** *vs.* C_{70} in PhCl at room temperature.

4.1.6. References

1. E. M. Pérez; N. Martín, Curves ahead: molecular receptors for fullerenes based on concave-convex complementarity. *Chem. Soc. Rev.* **2008,** *37*, 1512-1519.
2. K. Tashiro; T. Aida, Metalloporphyrin hosts for supramolecular chemistry of fullerenes. *Chem. Soc. Rev.* **2007,** *36*, 189-197.

3. T. Kawase; H. Kurata, Ball-, Bowl-, and Belt-Shaped Conjugated Systems and Their Complexing Abilities: Exploration of the Concave−Convex π−π Interaction. *Chem. Rev.* **2006,** *106*, 5250-5273.
4. J. W. Steed; P. C. Junk; J. L. Atwood; M. J. Barnes; C. L. Raston; R. S. Burkhalter, Ball and Socket Nanostructures: New Supramolecular Chemistry Based on Cyclotriveratrylene. *J. Am. Chem. Soc.* **1994,** *116*, 10346-10347.
5. E. Huerta; G. A. Metselaar; A. Fragoso; E. Santos; C. Bo; J. de Mendoza, Selective binding and easy separation of C_{70} by nanoscale self-assembled capsules. *Angew. Chem. Int. Ed.* **2007,** *46*, 202-205.
6. A. Sygula; F. R. Fronczek; R. Sygula; P. W. Rabideau; M. M. Olmstead, A Double Concave Hydrocarbon Buckycatcher. *J. Am. Chem. Soc.* **2007,** *129*, 3842-3843.
7. S. Mizyed; P. E. Georghiou; M. Bancu; B. Cuadra; A. K. Rai; P. Cheng; L. T. Scott, Embracing C_{60} with Multiarmed Geodesic Partners. *J. Am. Chem. Soc.* **2001,** *123*, 12770-12774.
8. T. Kawase; K. Tanaka; N. Shiono; Y. Seirai; M. Oda, Onion-Type Complexation Based on Carbon Nanorings and a Buckminsterfullerene. *Angew. Chem. Int. Ed.* **2004,** *43*, 1722-1724.
9. T. Kawase; K. Tanaka; Y. Seirai; N. Shiono; M. Oda, Complexation of Carbon Nanorings with Fullerenes: Supramolecular Dynamics and Structural Tuning for a Fullerene Sensor. *Angew. Chem. Int. Ed.* **2003,** *42*, 5597-5600.
10. T. Kawase; K. Tanaka; N. Fujiwara; H. R. Darabi; M. Oda, Complexation of a Carbon Nanoring with Fullerenes. *Angew. Chem. Int. Ed.* **2003,** *42*, 1624-1628.
11. S. S. Gayathri; M. Wielopolski; E. M. Pérez; G. Fernández; L. Sánchez; R. Viruela; E. Ortí; D. M. Guldi; N. Martín, Discrete supramolecular donor-acceptor complexes. *Angew. Chem. Int. Ed.* **2009,** *48*, 815-819.
12. E. M. Pérez; A. L. Capodilupo; G. Fernández; L. Sánchez; P. M. Viruela; R. Viruela; E. Ortí; M. Bietti; N. Martín, Weighting non-covalent forces in the molecular recognition of C_{60}. Relevance of concave-convex complementarity. *Chem. Commun.* **2008,** *0*, 4567-4569.
13. E. M. Pérez; M. Sierra; L. Sánchez; M. R. Torres; R. Viruela; P. M. Viruela; E. Ortí; N. Martín, Concave Tetrathiafulvalene-Type Donors as Supramolecular Partners for Fullerenes. *Angew. Chem. Int. Ed.* **2007,** *46*, 1847-1851.
14. E. M. Pérez; L. Sánchez; G. Fernández; N. Martín, exTTF as a Building Block for Fullerene Receptors. Unexpected Solvent-Dependent Positive Homotropic Cooperativity. *J. Am. Chem. Soc.* **2006,** *128*, 7172-7173.
15. J.-Y. Zheng; K. Tashiro; Y. Hirabayashi; K. Kinbara; K. Saigo; T. Aida; S. Sakamoto; K. Yamaguchi, Cyclic Dimers of Metalloporphyrins as Tunable Hosts for Fullerenes: A Remarkable Effect of Rhodium(III). *Angew. Chem. Int. Ed.* **2001,** *40*, 1857-1861.
16. M. Yanagisawa; K. Tashiro; M. Yamasaki; T. Aida, Hosting Fullerenes by Dynamic Bond Formation with an Iridium Porphyrin Cyclic Dimer: A "Chemical Friction" for Rotary Guest Motions. *J. Am. Chem. Soc.* **2007,** *129*, 11912-11913.
17. Y. Zhao; D. G. Truhlar, Density Functionals for Noncovalent Interaction Energies of Biological Importance. *J. Chem. Theory Comput.* **2006,** *3*, 289-300.
18. A. Hosseini; S. Taylor; G. Accorsi; N. Armaroli; C. A. Reed; P. D. W. Boyd, Calix[4]arene-Linked Bisporphyrin Hosts for Fullerenes: Binding Strength, Solvation Effects, and Porphyrin-Fullerene Charge Transfer Bands. *J. Am. Chem. Soc.* **2006,** *128*, 15903-15913.
19. Z.-Q. Wu; X.-B. Shao; C. Li; J.-L. Hou; K. Wang; X.-K. Jiang; Z.-T. Li, Hydrogen-Bonding-Driven Preorganized Zinc Porphyrin Receptors for Efficient Complexation of C_{60}, C_{70}, and C_{60} Derivatives. *J. Am. Chem. Soc.* **2005,** *127*, 17460-17468.
20. (a) G. Fernández; E. M. Pérez; L. Sánchez; N. Martín, Self-Organization of Electroactive Materials: A Head-to-Tail Donor–Acceptor Supramolecular Polymer. *Angew. Chem. Int. Ed.* **2008,** *47*, 1094-1097;(b) G. Fernández; E. M. Pérez; L. Sánchez; N. Martín, An Electroactive Dynamically Polydisperse Supramolecular Dendrimer. *J. Am. Chem. Soc.* **2008,** *130*, 2410-2411;(c) G. Fernández; L. Sánchez; E. M. Pérez; N. Martín, Large exTTF-Based Dendrimers. Self-Assembly and Peripheral Cooperative Multiencapsulation of C_{60}. *J. Am. Chem. Soc.* **2008,** *130*, 10674-10683.
21. Gaussian 03, Revision C.02 M. J. T. Frisch, G. W.; Schlegel, H. B.; Scuseria, G. E.; Robb, M. A.; Cheeseman, J. R.; Montgomery, Jr., J. A.; Vreven, T.; Kudin, K. N.; Burant, J. C.; Millam, J. M.; Iyengar, S. S.; Tomasi, J.; Barone, V.; Mennucci, B.; Cossi, M.; Scalmani, G.; Rega, N.; Petersson, G. A.; Nakatsuji, H.; Hada, M.; Ehara, M.; Toyota, K.; Fukuda, R.; Hasegawa, J.; Ishida, M.; Nakajima, T.; Honda, Y.; Kitao, O.; Nakai, H.; Klene, M.; Li, X.; Knox, J. E.; Hratchian, H. P.; Cross, J. B.; Bakken, V.; Adamo, C.; Jaramillo, J.; Gomperts, R.; Stratmann, R. E.; Yazyev, O.; Austin, A. J.; Cammi, R.;

Pomelli, C.; Ochterski, J. W.; Ayala, P. Y.; Morokuma, K.; Voth, G. A.; Salvador, P.; Dannenberg, J. J.; Zakrzewski, V. G.; Dapprich, S.; Daniels, A. D.; Strain, M. C.; Farkas, O.; Malick, D. K.; Rabuck, A. D.; Raghavachari, K.; Foresman, J. B.; Ortiz, J. V.; Cui, Q.; Baboul, A. G.; Clifford, S.; Cioslowski, J.; Stefanov, B. B.; Liu, G.; Liashenko, A.; Piskorz, P.; Komaromi, I.; Martin, R. L.; Fox, D. J.; Keith, T.; Al-Laham, M. A.; Peng, C. Y.; Nanayakkara, A.; Challacombe, M.; Gill, P. M. W.; Johnson, B.; Chen, W.; Wong, M. W.; Gonzalez, C.; and Pople, J. A., Gaussian, Inc.: Wallingford CT, 2004.

22. A. D. Becke, A new mixing of Hartree--Fock and local density-functional theories. *J. Chem. Phys.* **1993,** *98*, 1372-1377.

23. M. M. Francl; W. J. Pietro; W. J. Hehre; J. S. Binkley; M. S. Gordon; D. J. DeFrees; J. A. Pople, Self-consistent molecular orbital methods. XXIII. A polarization-type basis set for second-row elements. *J. Chem. Phys.* **1982,** *77*, 3654-3665.

24. C. Lee; W. Yang; R. G. Parr, Development of the Colle-Salvetti correlation-energy formula into a functional of the electron density. *Physical Review B* **1988,** *37*, 785-789.

25. A. Robertazzi; J. A. Platts, Gas-Phase DNA Oligonucleotide Structures. A QM/MM and Atoms in Molecules Study. *J. Phys. Chem. A* **2006,** *110*, 3992-4000.

26. K. Gkionis; J. G. Hill; S. Oldfield; J. Platts, Performance of Becke's half-and-half functional for non-covalent interactions: energetics, geometries and electron densities. *J. Mol. Model.* **2009,** *15*, 1051-1060.

27. (a) M. P. Waller; A. Robertazzi; J. A. Platts; D. E. Hibbs; P. A. Williams, Hybrid density functional theory for π-stacking interactions: Application to benzenes, pyridines, and DNA bases. *J. Comput. Chem.* **2006,** *27*, 491-504;(b) H. Valdes; K. Pluhackova; M. Pitonak; J. Rezac; P. Hobza, Benchmark database on isolated small peptides containing an aromatic side chain: comparison between wave function and density functional theory methods and empirical force field. *PCCP* **2008,** *10*, 2747-2757.

28. (a) S. Tsuzuki; H. P. Luthi, Interaction energies of van der Waals and hydrogen bonded systems calculated using density functional theory: Assessing the PW91 model. *J. Chem. Phys.* **2001,** *114*, 3949-3957;(b) Y. Zhao; D. G. Truhlar, Benchmark Databases for Nonbonded Interactions and Their Use To Test Density Functional Theory. *J. Chem. Theory Comput.* **2005,** *1*, 415-432.

29. W. J. Hehre; L. Radom; P. v. R. Schleyer; J. Pople, *Ab initio Molecular Orbital Theory*. New York, 1986.

30. S. F. Boys; F. Bernardi, The calculation of small molecular interactions by the differences of separate total energies. Some procedures with reduced errors. *Mol. Phys.* **1970,** *19*, 553-566.

31. (a) J. Tomasi; M. Persico, Molecular Interactions in Solution: An Overview of Methods Based on Continuous Distributions of the Solvent. *Chem. Rev.* **1994,** *94*, 2027-2094;(b) C. S. Cramer; D. G. Truhlar, *Solvent Effects and Chemical Reactivity* Kluwer: Dordrecht, 1996.

32. (a) S. Miertuš; E. Scrocco; J. Tomasi, Electrostatic interaction of a solute with a continuum. A direct utilizaion of AB initio molecular potentials for the prevision of solvent effects. *Chem. Phys.* **1981,** *55*, 117-129;(b) S. Miertuš; J. Tomasi, Approximate evaluations of the electrostatic free energy and internal energy changes in solution processes. *Chem. Phys.* **1982,** *65*, 239-245;(c) M. Cossi; V. Barone; R. Cammi; J. Tomasi, Ab initio study of solvated molecules: a new implementation of the polarizable continuum model. *Chem. Phys. Lett.* **1996,** *255*, 327-335;(d) E. Cances; B. Mennucci; J. Tomasi, A new integral equation formalism for the polarizable continuum model: Theoretical background and applications to isotropic and anisotropic dielectrics. *J. Chem. Phys.* **1997,** *107*, 3032-3041;(e) V. Barone; M. Cossi; J. Tomasi, Geometry optimization of molecular structures in solution by the polarizable continuum model. *J. Comput. Chem.* **1998,** *19*, 404-417;(f) M. Cossi; G. Scalmani; N. Rega; V. Barone, New developments in the polarizable continuum model for quantum mechanical and classical calculations on molecules in solution. *J. Chem. Phys.* **2002,** *117*, 43-54.

33. O. A. v. Lilienfeld; A. Tkatchenko, Two- and three-body interatomic dispersion energy contributions to binding in molecules and solids. *J. Chem. Phys.* **2010,** *132*, 234109.

34. S. Grimme, *J. Comput. Chem.* **2006,** *27*, 1787.

4.2. Balancing binding strength and charge transfer lifetime in supramolecular associates of fullerenes.

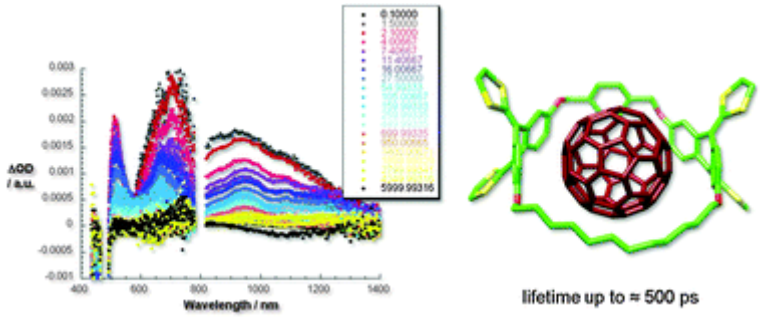

A macrocyclic exTTF host for fullerenes offers control over the electronic coupling between an electron donor and an acceptor, and stabilizes the charge separated state lifetimes into the range of 500 ps

Chem. Commun., **2011**, *47*, 7449–7451

4.2.1. Introduction

Investigation on the association of fullerenes by synthetic hosts started immediately after the former became available in gram quantities.[1] Among the various fullerene hosts described to date, macrocyclic structures have proven particularly effective in terms of both affinity and selectivity.[2] Following this strategy, some of us have recently reported macrocyclic bis-exTTF hosts (Figure 1) capable of associating C_{60} and/or C_{70} with affinities as high as micromolar.[3] These macrocyclic hosts have been designed as an evolution of our exTTF-tweezers.[4] Importantly, the alkyl linker provides the necessary means for preorganization and serves as a source of positive van der Waals interactions. To this end, among the macrocyclic hosts we have investigated, **4.2** reveals by far the best performance in terms of hosting C_{60}.[3a]

[1] (a) T. Kawase and H. Kurata, *Chem. Rev.* **2006,** *106*, 5250-5273; (b) K. Tashiro and T. Aida, *Chem. Soc. Rev.* **2007,** *36*, 189-197; (c) E. M. Pérez and N. Martín, *Chem. Soc. Rev.* **2008,** *37*, 1512-1519.
[2] (a) M. Yanagisawa, K. Tashiro, M. Yamasaki and T. Aida, *J. Am. Chem. Soc.* **2007,** *129*, 11912-11913; (b)G. n. Gil-Ramírez, S. D. Karlen, A. Shundo, K. Porfyrakis, Y. Ito, G. A. D. Briggs, J. J. L. Morton and H. L. Anderson, *Org. Lett.* **2010,** *12*, 3544-3547; (c) Y. Shoji, K. Tashiro and T. Aida, *J. Am. Chem. Soc.* **2010,** *132*, 5928-5929; (d) A. R. Mulholland, C. P. Woodward and S. J. Langford, *Chem. Commun.* **2011,** *47*, 1494-1496.
[3] (a) H. Isla, M. Gallego, E. M. Pérez, R. Viruela, E. Ortí and N. Martín, *J. Am. Chem. Soc.* **2010,** *132*, 1772-1773; (b) D. Canevet, M. Gallego, H. Isla, A. de Juan, E. M. Pérez and N. Martín, *J. Am. Chem. Soc.* **2011,** *133*, 3184-3190.
[4] (a) E. M. Pérez, L. Sánchez, G. Fernández and N. Martín, *J. Am. Chem. Soc.* **2006,** *128*, 7172-7173; (b) S. S. Gayathri, M. Wielopolski, E. M. Pérez, G. Fernández, L. Sánchez, R. Viruela, E. Ortí, D. M. Guldi and N. Martín, *Angew. Chem. Int. Ed.* **2009,** *48*, 815-819.

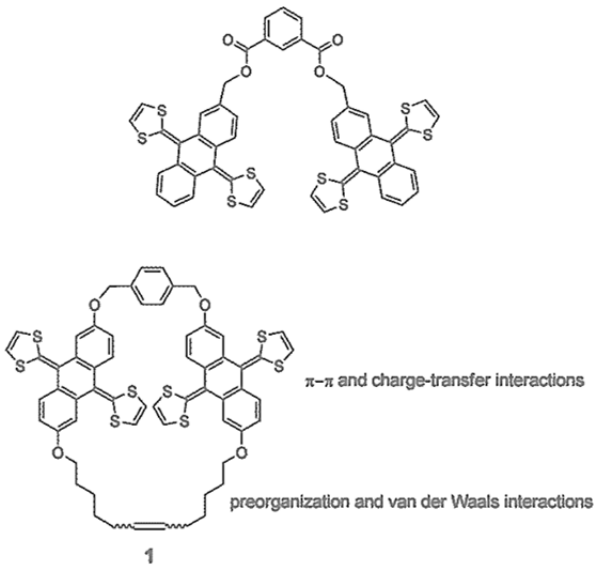

Figure 1 Structures of exTTF-tweezers and exTT-macrocycle **4.2.**

4.2.2. Results and discussion

We have previously demonstrated that upon light irradiation of our tweezers-like host-guest systems, fully charge-separated $C_{60}^{\bullet-}$ / $exTTF^{\bullet+}$ states are formed. These charge-separated states are short-lived, with lifetimes in the range of around 10 picoseconds.[4b] Such photoinduced electron transfer processes within exTTF/fullerene supramolecular species are poised for numerous applications, especially in the context of constructing more efficient optoelectronic devices[5] through self-assembly.[6] Here, we wish to report on the detailed investigations regarding the electron transfer chemistry in **4.2**•C_{60} and **4.2**•C_{70}.

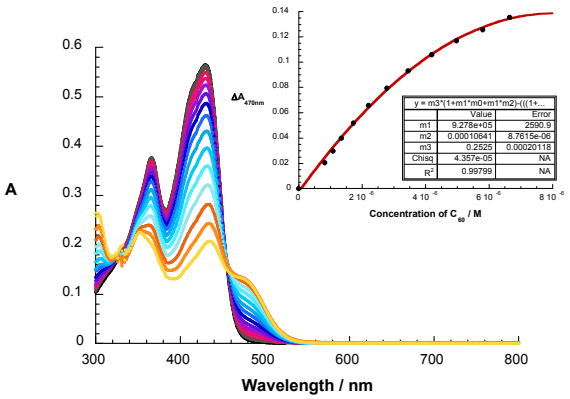

[5] (a) M. R. Wasielewski, *Chem. Rev.* **1992,** *92*, 435-61; F. D'Souza and O. Ito, *Coord. Chem. Rev.* **2005,** *249*, 1410-1422; (b) L. Sánchez, N. Martín and D. M. Guldi, *Angew. Chem. Int. Ed.* **2005,** *44*, 5374-5382; (c) M. R. Wasielewski, *J. Org. Chem.* **2006,** *71*, 5051-5066; (d) N. Martín, L. Sánchez, M. a. Á. Herranz, B. Illescas and D. M. Guldi, *Acc. Chem. Res.* **2007,** *40*, 1015-1024.

[6] (a) G. Fernández, E. M. Pérez, L. Sánchez and N. Martín, *Angew. Chem. Int. Ed.* **2008,** *47*, 1094-1097; (b) J. Santos, B. Grimm, B. M. Illescas, D. M. Guldi and N. Martín, *Chem. Commun.* **2008,** *0*, 5993-5995; (c) B. Grimm, J. Santos, B. M. Illescas, A. Muñoz, D. M. Guldi and N. Martín, *J. Am. Chem. Soc.* **2010,** *132*, 17387-17389.

Figure 2 Absorption spectra of **1** (1.56 x 10^{-5} M) in benzonitrile with variable concentrations of C_{60} (0; 3.36 x 10^{-7} M; 6.67 x 10^{-7} M; 9.96 x 10^{-7} M; 1.48 x 10^{-6} M; 1.96 x 10^{-6} M; 2.59 x 10^{-6} M; 3.22 x 10^{-6} M; 4.13 x 10^{-6} M; 5.28 x 10^{-6} M; 6.67 x 10^{-6} M; 8.28 x 10^{-6} M; 1.00 x 10^{-5} M; 1.2 x 10^{-5} M; 1.39 x 10^{-5} M and 1.60 x 10^{-5} M). C_{60} absorptions were subtracted. Inset: binding isotherm that displays the absorption changes at 470 nm as a function of C_{60} concentration.

Initially, we have employed absorption assays, in which approximately 2.0 x 10^{-5} M of **1** were titrated against variable concentrations of C_{60} or C_{70} (*i.e.* from 0 to 5.0 x 10^{-5} M). As a general feature, facilely formed charge transfer complexes —**4.2**•C_{60} or **4.2**•C_{70}— were seen to develop in a variety of solvents (i.e. toluene, chlorobenzene, and benzonitrile). For C_{60} in benzonitrile, the growth of a new broad transition at 475 nm goes hand in hand with the decrease of the exTTF absorption at 430 nm. Concomitantly, a low energy isosbestic point evolves around 460 nm. Relative to benzonitrile, hypsochromic shifts were noted in chlorobenzene and in toluene, where the maxima for the charge-transfer band are discernable at 470 and at 465 nm, respectively. The fact that the corresponding maxima tend to blue-shift with decreasing solvent polarity leads us to postulate a redistribution of charge density in the ground state, that is, from the electron donating exTTF to the electron accepting C_{60} or C_{70} to afford the corresponding $C_{60}^{\delta-}$ / $exTTF^{\delta+}$ or $C_{70}^{\delta-}$ / $exTTF^{\delta+}$. Throughout the solvent change the absorption maximum of exTTF is, however, not affected. For C_{70}, the maxima for the charge-transfer band were at 467 nm in chlorobenzene and 473 nm in benzonitrile.

In the next step, we subjected the absorption changes at 470 nm during the titration experiments to non-linear fitting functions assuming formation of the 1:1 complex.[3] K_a values of 4.2 x 10^4, 9.7 x 10^5, and 1.1 x 10^6 M^{-1} were calculated for the formation of **4.2**•C_{60} in toluene, chlorobenzene, and benzonitrile, respectively (see Figure 2). The corresponding **4.2**•C_{70} values were 5.6 x 10^5 M^{-1} in chlorobenzene and 5.8 x 10^5 M^{-1} in benzonitrile. These values are in good agreement with those obtained by global multivariable analysis.[3]

Figure 3, in which a complementary fluorescence assay is displayed, documents that even in the excited state mutual interactions prevail between the electron donating exTTF and the electron accepting C_{60} / C_{70}. As in the absorption assays, a new feature appears around 538 and 541 nm in the presence of variable C_{60} or C_{70} concentrations at the expense of the exTTF centered excited state features of **4.2**, which were seen to diminish around 470 nm. Again, we postulate that a charge transfer is responsible for the newly developing features. Notable is the mirror image between the charge transfer absorption and the charge transfer emission. For **4.2**•C_{60} and **4.2**•C_{70}, the $C_{60}^{\delta-}$ / $exTTF^{\delta+}$ and $C_{70}^{\delta-}$ / $exTTF^{\delta+}$ features are discernable in non-polar as well as polar solvents with emission quantum yields of about 10^{-3}. A substantial red shift of 30 nm accompanies the solvent change, which, in turn, infers a significant solvent stabilization of the charge

transfer state. For **4.2**•C_{70} the most prominent $C_{70}^{\delta-}$ / $exTTF^{\delta+}$ features are maxima at 515 nm in chlorobenzene, and 541 nm in benzonitrile.

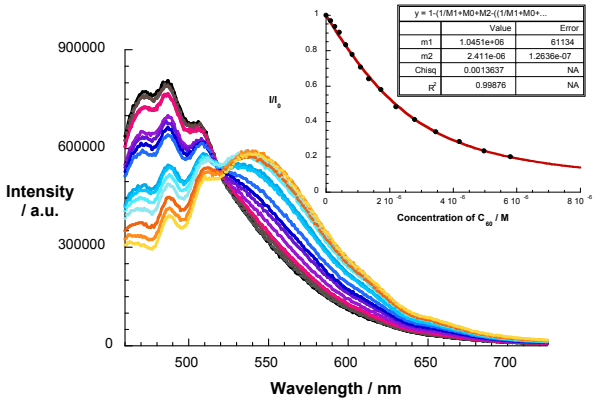

Figure 3 Emission spectra upon 450 nm excitation of a solution of **1** (1.56 x 10^{-5} M) in benzonitrile with variable concentrations of C_{60} (0; 3.36 x 10^{-7} M; 6.67 x 10^{-7} M; 9.96 x 10^{-7} M; 1.48 x 10^{-6} M; 1.96 x 10^{-6} M; 2.59 x 10^{-6} M; 3.22 x 10^{-6} M; 4.13 x 10^{-6} M; 5.28 x 10^{-6} M; 6.67 x 10^{-6} M; 8.28 x 10^{-6} M; 1.00 x 10^{-5} M; 1.2 x 10^{-5} M; 1.39 x 10^{-5} M and 1.60 x 10^{-5} M). Inset: plot of the normalized intensity I/I_0 at 462 nm versus concentration of C_{60} used to determine the association constant.

The exponential quenching of the steady-state fluorescence of **1** was further used to quantify the association between exTTF and C_{60} or between exTTF and C_{70}.[7] In particular, we have plotted the emission intensity gathered at 462 nm *versus* the concentration of C_{60} / C_{70} (Figure 3 inset). A nonlinear curve fitting allowed the association constants for the formation of **4.2**•C_{60} to be estimated as 5.1 x 10^4 (toluene) / 1.04 x 10^6 M^{-1} (benzonitrile) and 3.4 x 10^5 (chlorobenzene) and 3.8 x 10^6 M^{-1} for **4.2**•C_{70} (benzonitrile).

In the next step, with the help of femtosecond laser pulses at 387 nm the fate of localized exTTF and C_{60}/C_{70} singlet excited states were probed. In addition, 480 nm photoexcitation experiments were conducted to direct the excitation into the charge transfer state. Please note in this context the lack of ground state absorption of exTTF and C_{60} at the 480 nm excitation wavelength. Following the time evolution has emerged in our earlier work as a convenient approach to identify spectral features of the initial excited state and the resulting charge transfer products, and to determine absolute rate constants for their formation as well as their decay.[4b]

[7] (a) H.-J. Schneider, *Frontiers in supramolecular organic chemistry and photochemistry*. Wiley-VCH: Weinheim, 1991; (b) B. Valeur, *Molecular Fluorescence*. Wiley-VCH Verlag GmbH: 2001.

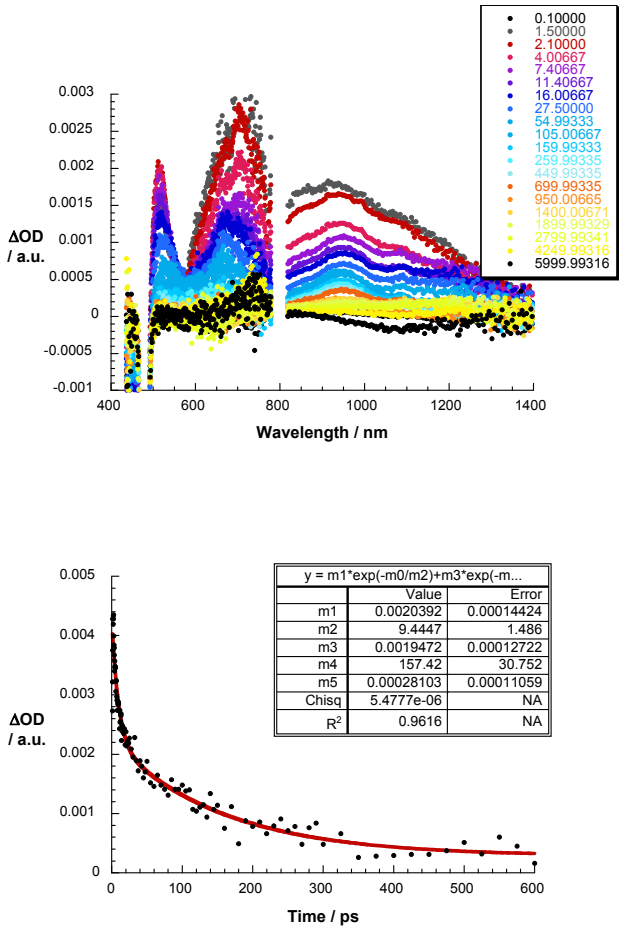

Figure 4 Upper part: differential absorption spectra (visible and near-infrared) obtained upon femtosecond flash photolysis (480 nm) of $1{\cdot}C_{60}$ in Ar-saturated benzonitrile with time delays between 0.1 and 6000 ps at room temperature. Lower part: time-absorption profile at 655 nm, reflecting the transformation of $C_{60}^{\delta-}$ / $exTTF^{\delta+}$ into the fully $C_{60}^{\bullet-}$ / $exTTF^{\bullet+}$ charge separated state and charge recombination kinetics.

In transient absorption measurements with **1** only one transient intermediate evolved. This excited state intermediate is centered on exTTF and appears simultaneously with the conclusion of the 387 nm laser pulse. Spectral characteristics of this very short-lived excited state (1.2 ps) are transient maxima around 465, 605, and 990 nm as well as transient bleaching at < 450 nm. The short lifetime is rationalized by the presence of the sulphur atoms, with a strong second-order vibronic spin-orbit coupling.[8]

The differential absorption changes, taken right after the excitation of C_{60}/C_{70} at 387 nm, show the instantaneous transformation of high lying singlet excited states into the lowest vibrational state of the associated singlet excited states. In particular, marked transitions develop in the near-infrared region with maxima at 960 nm for C_{60} and

[8] (a) A. Maciejewski and R. P. Steer, *Chem. Rev.* **1993,** *93*, 67-98; (b) H. Nishikawa, S. Kojima, T. Kodama, I. Ikemoto, S. Suzuki, K. Kikuchi, M. Fujitsuka, H. Luo, Y. Araki and O. Ito, *J. Phys. Chem. A* **2004,** *108*, 1881-1890.

860/1140 nm for C_{70}. These singlet excited state with energies of about 1.80 eV deactivate slowly via intersystem crossing to the energetically lower lying triplet excited state. The intersystem crossing lifetimes were determined from multi-wavelength analyses as 1.6 ns. The newly appearing band at 750 nm reflects the diagnostic signature of the triplet excited state of C_{60}, for which a lifetime of 45 μs has been determined. For C_{70}, the corresponding triplet excited state spectrum is dominated by a maximum at 950 nm.[9]

The differential absorption changes obtained upon photoexciting **4.2**•C_{60} in benzonitrile into the charge transfer features at 480 nm are gathered in Figure 4. The spectral features clearly reveal the instantaneous (i.e. > 1 ps) formation of photoexcited $C_{60}^{\delta-}$ / $exTTF^{\delta+}$ with features that include maxima at 540, 655, 950, and 1080 nm. The instantaneous appearance of the $C_{60}^{\delta-}$ / $exTTF^{\delta+}$ excited state further confirms the intimate interactions between C_{60} and exTTF in **4.2**•C_{60}. The $C_{60}^{\delta-}$ / **4.2**$^{\delta+}$ excited state is, however, short-lived and transforms within 6.7 ± 0.5 ps into a fully $C_{60}^{\bullet-}$ / $exTTF^{\bullet+}$ charge separated state. In this regard, the transient centering at around 665 nm is assigned to the one-electron oxidized radical cation of exTTF. This assignment is in accordance with previous studies conducted with photolytic and radiolytic techniques.[10] The one-electron reduced radical anion of C_{60}, on the other hand, shows up in the near-infrared (i.e. 1080 nm).[11] The charge separated state lifetimes, as determined from a multiwavelength analysis (i.e. decay at 665, 950, and 1080 nm), were 157 ± 31 ps. Products of the charge recombination are the energetically lower lying C_{60} singlet excited state (1.8 eV) and C_{60} triplet excited state (1.55 eV) as identified by maxima at 960 and 750 nm, respectively. In complementary experiments, chlorobenzene was probed as solvent. Essentially, the same spectral features of the $C_{60}^{\delta-}$ / **4.2**$^{\delta+}$ excited state were seen as they transform into the fully $C_{60}^{\bullet-}$ / **4.2**$^{\bullet+}$ charge separated state with kinetics of 9.0 ± 0.5 ps before charge recombination populates the C_{60} triplet excited state with 137 ± 11 ps. Longer lifetimes in benzonitrile —compared to chlorobenzene— are in line with dynamics that are placed in the normal region of the Marcus parabola. In other words, the large reorganization energy that exTTF reveals in electron transfer reactions is insufficiently compensated by the exceptionally small reorganization energy of C_{60}.[10,11] In addition, the low driving forces for the charge recombination (i.e. < 1.0 eV) prevent the processes to be beyond the thermodynamic maximum (Excitation, on the other hand, at 387 nm is the inception to transform the locally excited exTTF

[9] (a) N. M. Dimitrijevic and P. V. Kamat, *J. Phys. Chem.* **1992,** *96*, 4811-4814; (b) K. G. Thomas, V. Biju, D. M. Guldi, P. V. Kamat and M. V. George, *J. Phys. Chem. B* **1999,** *103*, 8864-8869; (c) D. M. Guldi and M. Prato, *Acc. Chem. Res.* **2000,** *33*, 695-703.

[10] (a) D. M. Guldi, L. Sánchez and N. Martín, *J. Phys. Chem. B* **2001,** *105*, 7139-7144; (b) A. E. Jones, C. A. Christensen, D. F. Perepichka, A. S. Batsanov, A. Beeby, P. J. Low, M. R. Bryce and A. W. Parker, *Chem. Eur. J.* **2001,** *7*, 973-978.

[11] (a) T. Kato, T. Kodama, T. Shida, T. Nakagawa, Y. Matsui, S. Suzuki, H. Shiromaru, K. Yamauchi and Y. Achiba, *Chem. Phys. Lett.* **1991,** *180*, 446-450; (b) D. M. Guldi, H. Hungerbuhler, E. Janata and K.-D. Asmus, *J. Chem. Soc., Chem. Commun.* **1993,** *0*, 84-86.

excited state into the same $C_{60}^{\bullet-}$ / **4.2**$^{\bullet+}$ charge separated state seen in the afore mentioned 480 nm excitation experiments).

Turning to the photoexcitation of **4.2**•C_{70}, the $C_{70}^{\delta-}$ / **4.2**$^{\delta+}$ features were seen to evolve in chlorobenzene with maxima at 540, 665, 860, and 1140 nm. Following its instantaneous formation, transformation to the corresponding $C_{70}^{\bullet-}$ / exTTF$^{\bullet+}$ charge-separated state takes over with 5.1 ± 1.5 ps. Evidence for the formation of the latter is based on the signatures of the one-electron-reduced radical anion of C_{70} at 880 and 1220 nm, in line with pulse radiolytic investigations,[12] and of one-electron oxidized radical cation of exTTF at 665 nm. A multi-wavelength analysis of the $C_{70}^{\bullet-}$ / **4.2**$^{\bullet+}$ features at 503, 665, 950, and 1200 nm helped to establish a lifetime of 371 ± 27 ps. In line with what has been seen for $C_{60}^{\bullet-}$ / **4.2**$^{\bullet+}$, studies in benzonitrile revealed an even longer lifetime of 482 ± 36 ps (Figure 5). Notable is that charge recombination in both solvents affords the C_{70} triplet excited state.

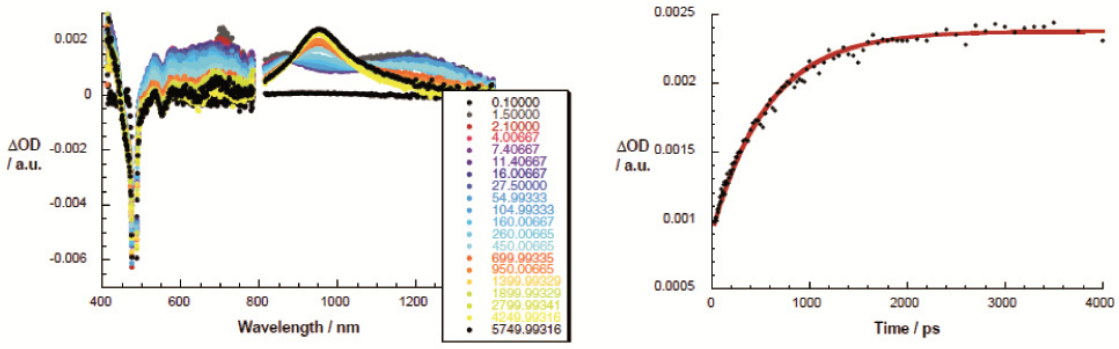

Figure 5. Upper part: differential absorption spectra (visible and near-infrared) obtained upon femtosecond flash photolysis (480 nm) of **4.2**·C_{70} in Ar-saturated benzonitrile with time delays between 0.1 and 5750 ps at room temperature. Lower part - time-absorption profile at 950 nm, reflecting the transformation of $C_{70}^{\delta-}$ / exTTF$^{\delta+}$ into the fully $C_{70}^{\bullet-}$ / exTTF$^{\bullet+}$ charge separated state and charge recombination kinetics yielding the triplet excited state of C_{70}.

4.2.3. Conclusions

In a nutshell, a macrocyclic exTTF host efficiently incorporates C_{60} or C_{70} with binding constants that range from 4.2 x 10^4 to 3.8 x 10^6 M^{-1}. The binding is driven in large by charge transfer interactions and, in turn, dominates the electronic ground state with the unambiguous formation of $C_{60}^{\delta-}$/**4.2**$^{\delta+}$ or $C_{70}^{\delta-}$/**4.2**$^{\delta+}$ charge transfer states. These charge transfer states reveal distinct absorption and emission features and transform in the excited state into a fully $C_{60}^{\bullet-}$/**4.2**$^{\bullet+}$ or $C_{70}^{\bullet-}$/**4.2**$^{\bullet+}$ charge separated states. Remarkable are the charge separated state lifetimes reaching into the 500 ps domain, which correlate with a weak electronic coupling between electron acceptor (*i.e.*

[12] D. M. Guldi, H. Hungerbuhler, M. Wilhelm and K.-D. Asmus, *J. Chem. Soc., Faraday Trans.* **1994,** *90*, 1391-1396.

C_{60} / C_{70}) and electron donor (i.e. exTTF). Support for this hypothesis comes from extinction coefficients of $C_{60}^{\delta-}$ / **4.2**$^{\delta+}$ in **4.2**•C_{60} relative to that seen in exTTF bis-crown ether•C_{60} with values of 4000 and 5500 $Lmol^{-1}cm^{-1}$, respectively (see Figure S4). In comparison to exTTF bis-crown ether and exTTF-tweezers,[4b, 6c] which feature lifetimes on the 10 to 50 ps time scale, the alkyl chain in **1** is key: it provides an alternative source for positive non-covalent interactions, and assures that C_{60} or C_{70} remains encapsulated by the macrocycle even despite weaker electronic coupling with the exTTF units.

4.2.4. Experimental section

General UV/Vis spectra were recorded with Varian Cary 50. Steady state fluorescence studies were carried out on a Fluoromax 3 (Horiba) instrument and all the spectra were corrected for the instrument response. The femtosecond transient absorption studies were performed with laser pulses (1Khz 150 fs pulse width) from an amplified Ti:Sapphire laser system (Model CPA 2101, Clark-MXR Inc.).

UV/Vis Titrations: Binding constants were evaluated by titrating a fixed concentration solution of **4.2** with variable amounts of fullerene C_{60} or C_{70} (from 0 to 2 x 10^{-5} M^{-1}) using toluene, chlorobenzene, or benzonitrile as solvent. The resulting solutions were measured by UV/Vis spectroscopy at room temperature. Some spectra were corrected by background substraction. ΔAbs of **4.2** at 470 nm was plotted against the total concentration of the fullerene. The resulting curve was fitted using Microcal Origin 7.5 software. The association constant K_S was evaluated using the equation:[13]

$$\Delta Abs = \Delta Abs_{max}(1 + K_s[C_{60}] + K_s[\mathbf{4.2}]_0) - ((1+ K_s[C_{60}] + K_s[\mathbf{4.2}]_0)^2 - 4\ K_s[C_{60}][\ \mathbf{4.2}]_0)^{1/2})/(2K_s[\mathbf{4.2}]_0)$$

Fluorescence titrations: Complementary fluorescence titration experiments were carried out in line with earlier work.[4b] The fluorescence of **4.2** was monitored while the variable amounts of fullerenes (C_{60} and C_{70}) were added. The gradual quenching at 462 nm was used to estimate the association constants K_s according to following equation:[7]

$$\frac{I_f}{I_0} = 1 - \frac{1}{2c_D}\left[\frac{1}{K_s} + c_0 + c_D - \sqrt{\left(\frac{1}{K_s} + c_0 + c_D\right)^2 - 4c_0c_D}\right]$$

References

1. (a) T. Kawase; H. Kurata, Ball-, Bowl-, and Belt-Shaped Conjugated Systems and Their Complexing Abilities: Exploration of the Concave−Convex π−π Interaction. *Chem. Rev.* **2006,** *106*, 5250-5273;(b) K. Tashiro; T. Aida, Metalloporphyrin hosts for supramolecular chemistry of fullerenes. *Chem. Soc. Rev.* **2007,** *36*, 189-197;(c) E. M. Pérez; N. Martín, Curves ahead: molecular receptors for fullerenes based on concave-convex complementarity. *Chem. Soc. Rev.* **2008,** *37*, 1512-1519.

[13] Pérez, Sánchez, Fernández and Martín; Z.-Q. Wu, X.-B. Shao, C. Li, J.-L. Hou, K. Wang, X.-K. Jiang and Z.-T. Li, *J. Am. Chem. Soc.* **2005,** *127*, 17460-17468.

2. (a) M. Yanagisawa; K. Tashiro; M. Yamasaki; T. Aida, Hosting Fullerenes by Dynamic Bond Formation with an Iridium Porphyrin Cyclic Dimer: A "Chemical Friction" for Rotary Guest Motions. *J. Am. Chem. Soc.* **2007,** *129*, 11912-11913;(b) G. n. Gil-Ramírez; S. D. Karlen; A. Shundo; K. Porfyrakis; Y. Ito; G. A. D. Briggs; J. J. L. Morton; H. L. Anderson, A Cyclic Porphyrin Trimer as a Receptor for Fullerenes. *Org. Lett.* **2010,** *12*, 3544-3547;(c) Y. Shoji; K. Tashiro; T. Aida, One-Pot Enantioselective Extraction of Chiral Fullerene C_{76} Using a Cyclic Host Carrying an Asymmetrically Distorted, Highly π-Basic Porphyrin Module. *J. Am. Chem. Soc.* **2010,** *132*, 5928-5929;(d) A. R. Mulholland; C. P. Woodward; S. J. Langford, Fullerene-templated synthesis of a cyclic porphyrin trimer using olefin metathesis. *Chem. Commun.* **2011,** *47*, 1494-1496.

3. (a) H. Isla; M. Gallego; E. M. Pérez; R. Viruela; E. Ortí; N. Martín, A Bis-exTTF Macrocyclic Receptor That Associates C_{60} with Micromolar Affinity. *J. Am. Chem. Soc.* **2010,** *132*, 1772-1773;(b) D. Canevet; M. Gallego; H. Isla; A. de Juan; E. M. Pérez; N. Martín, Macrocyclic hosts for fullerenes: extreme changes in binding abilities with small structural variations. *J. Am. Chem. Soc.* **2011,** *133*, 3184-3190.

4. (a) E. M. Pérez; L. Sánchez; G. Fernández; N. Martín, exTTF as a Building Block for Fullerene Receptors. Unexpected Solvent-Dependent Positive Homotropic Cooperativity. *J. Am. Chem. Soc.* **2006,** *128*, 7172-7173;(b) S. S. Gayathri; M. Wielopolski; E. M. Pérez; G. Fernández; L. Sánchez; R. Viruela; E. Ortí; D. M. Guldi; N. Martín, Discrete supramolecular donor-acceptor complexes. *Angew. Chem. Int. Ed.* **2009,** *48*, 815-819.

5. (a) M. R. Wasielewski, Photoinduced electron transfer in supramolecular systems for artificial photosynthesis. *Chem. Rev.* **1992,** *92*, 435-61;(b) F. D'Souza; O. Ito, Photoinduced electron transfer in supramolecular systems of fullerenes functionalized with ligands capable of binding to zinc porphyrins and zinc phthalocyanines. *Coord. Chem. Rev.* **2005,** *249*, 1410-1422;(c) L. Sánchez; N. Martín; D. M. Guldi, Hydrogen-Bonding Motifs in Fullerene Chemistry. *Angew. Chem. Int. Ed.* **2005,** *44*, 5374-5382;(d) M. R. Wasielewski, Energy, Charge, and Spin Transport in Molecules and Self-Assembled Nanostructures Inspired by Photosynthesis. *J. Org. Chem.* **2006,** *71*, 5051-5066;(e) N. Martín; L. Sánchez; M. a. Á. Herranz; B. Illescas; D. M. Guldi, Electronic Communication in Tetrathiafulvalene (TTF)/C_{60} Systems: Toward Molecular Solar Energy Conversion Materials? *Acc. Chem. Res.* **2007,** *40*, 1015-1024.

6. (a) G. Fernández; E. M. Pérez; L. Sánchez; N. Martín, Self-Organization of Electroactive Materials: A Head-to-Tail Donor–Acceptor Supramolecular Polymer. *Angew. Chem. Int. Ed.* **2008,** *47*, 1094-1097;(b) J. Santos; B. Grimm; B. M. Illescas; D. M. Guldi; N. Martín, Cooperativity between π–π and H-bonding interactions-a supramolecular complex formed by C_{60} and exTTF. *Chem. Commun.* **2008,** *0*, 5993-5995;(c) B. Grimm; J. Santos; B. M. Illescas; A. Muñoz; D. M. Guldi; N. Martín, A New exTTF-Crown Ether Platform To Associate Fullerenes: Cooperative n-π and π–π Effects. *J. Am. Chem. Soc.* **2010,** *132*, 17387-17389.

7. (a) H.-J. Schneider, *Frontiers in supramolecular organic chemistry and photochemistry*. Wiley-VCH: Weinheim, 1991;(b) B. Valeur, *Molecular Fluorescence*. Wiley-VCH Verlag GmbH: 2001.

8. (a) A. Maciejewski; R. P. Steer, The photophysics, physical photochemistry, and related spectroscopy of thiocarbonyls. *Chem. Rev.* **1993,** *93*, 67-98;(b) H. Nishikawa; S. Kojima; T. Kodama; I. Ikemoto; S. Suzuki; K. Kikuchi; M. Fujitsuka; H. Luo; Y. Araki; O. Ito, Photophysical Study of New Methanofullerene-TTF Dyads: An Obvious Intramolecular Charge Transfer in the Ground States. *J. Phys. Chem. A* **2004,** *108*, 1881-1890.

9. (a) N. M. Dimitrijevic; P. V. Kamat, Triplet excited state behavior of fullerenes: pulse radiolysis and laser flash photolysis of fullerenes (C60 and C70) in benzene. *J. Phys. Chem.* **1992,** *96*, 4811-4814;(b) K. G. Thomas; V. Biju; D. M. Guldi; P. V. Kamat; M. V. George, Photoinduced Charge Separation and Stabilization in Clusters of a Fullerene−Aniline Dyad. *J. Phys. Chem. B* **1999,** *103*, 8864-8869;(c) D. M. Guldi; M. Prato, Excited-State Properties of C_{60} Fullerene Derivatives. *Acc. Chem. Res.* **2000,** *33*, 695-703.

10. (a) D. M. Guldi; L. Sánchez; N. Martín, Formation and Characterization of the p-Radical Cation and Dication of p-Extended Tetrathiafulvalene Materials. *J. Phys. Chem. B* **2001,** *105*, 7139-7144;(b) A. E. Jones; C. A. Christensen; D. F. Perepichka; A. S. Batsanov; A. Beeby; P. J. Low; M. R. Bryce; A. W. Parker, Molecular saddles, part 6. Photochemistry of the π-extended 9,10-bis(1,3-dithiol-2-ylidene)-9,10-dihydroanthracene system: generation and characterization of the radical cation, dication, and derived products. *Chem. Eur. J.* **2001,** *7*, 973-978.

11. (a) T. Kato; T. Kodama; T. Shida; T. Nakagawa; Y. Matsui; S. Suzuki; H. Shiromaru; K. Yamauchi; Y. Achiba, Electronic absorption spectra of the radical anions and cations of fullerenes: C60 and C70. *Chem. Phys. Lett.* **1991,** *180*, 446-450;(b) D. M. Guldi; H. Hungerbuhler; E. Janata; K.-D.

Asmus, Radical-induced redox and addition reactions with C_{60} studied by pulse radiolysis. *J. Chem. Soc., Chem. Commun.* **1993,** *0*, 84-86.

12. D. M. Guldi; H. Hungerbuhler; M. Wilhelm; K.-D. Asmus, Pulse radiolytically induced redox and alkylation processes of C70. *J. Chem. Soc., Faraday Trans.* **1994,** *90*, 1391-1396.

13. Z.-Q. Wu; X.-B. Shao; C. Li; J.-L. Hou; K. Wang; X.-K. Jiang; Z.-T. Li, Hydrogen-Bonding-Driven Preorganized Zinc Porphyrin Receptors for Efficient Complexation of C_{60}, C_{70}, and C_{60} Derivatives. *J. Am. Chem. Soc.* **2005,** *127*, 17460-17468.

4.3. Macrocyclic hosts for fullerenes: extreme changes in binding abilities with small structural variations.

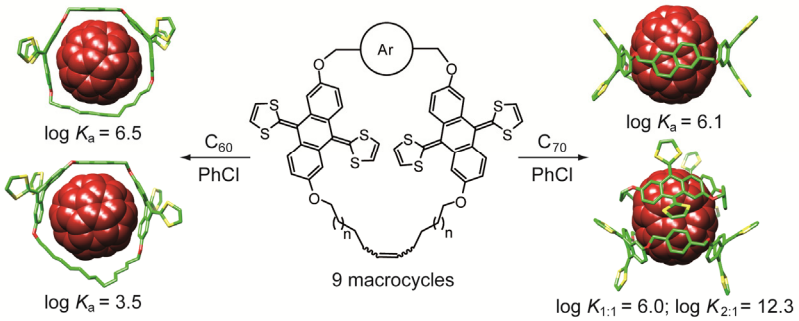

Exploiting the shape and electronic complementarity of C_{60} and C_{70} with π-extended derivatives of tetrathiafulvalene (exTTF), we have very recently reported a macrocyclic receptor featuring two exTTF recognizing units which forms 1:1 complexes with C_{60} with log K_a = 6.5 ± 0.5 in chlorobenzene at 298 K. This represents one of the highest binding constants towards C_{60} reported to date and a world-record for all-organic receptors. Here, we describe our efforts to fine-tune our macrocyclic bis-exTTF hosts to bind C_{60} and/or C_{70}, through structural variations. Based on preliminary molecular modeling, we have explored p-xylene, m-xylene and 2,6-dimethylnaphthalene as aromatic spacers between the two exTTF fragments and three alkene-terminated chains of different length to achieve macrocycles of different size through ring closing metathesis (RCM). Due to the structural simplicity of our design, all nine receptors could be accessed in a synthetically straightforward manner. A thorough investigation of the binding abilities of these nine receptors towards C_{60} and C_{70} has been carried out by means of UV-vis titrations. We have found that relatively small variations in the structure of the host lead to very significant changes in affinity towards the fullerene, and in some cases even in the stoichiometry of the associates. Our results highlight the peculiarities of fullerenes as guests in molecular recognition. The extreme stability of these associates in solution, and the unique combination of electronic and geometrical reciprocity of exTTF and fullerenes are the main features of this new family of macrocyclic hosts for fullerenes.

J. Am. Chem. Soc. **2011**, *133*, 3184–3190

4.3.1. Introduction

The search for molecular receptors for fullerenes was initiated soon after their discovery[1] with the pioneering work of the groups of Diederich, Ringsdorf and

[1] H. W. Kroto, J. R. Heath, S. C. O'Brien, R. F. Curl and R. E. Smalley, *Nature* **1985,** *318*, 162-163.

Wennerström.[2] The main motivations that have kept it as a very active area of research[3, 4, 5, 6] are the selective association of specific fullerenes to achieve their purification from complex mixtures[4j-l] and the construction of organized electroactive nanostructures by

[2] (a) T. Andersson, K. Nilsson, M. Sundahl, G. Westman and O. Wennerstrom, *J. Chem. Soc., Chem. Commun.* **1992,** *0*, 604-606; (b) J. Effing, U. Jonas, L. Jullien, T. Plesnivy, H. Ringsdorf, F. Diederich, C. Thilgen and D. Weinstein, *Angew. Chem., Int. Ed. Engl.* **1992,** *31*, 1599-1602.

[3] (a) P. D. W. Boyd and C. A. Reed, *Acc. Chem. Res.* **2004,** *38*, 235-242; (b) T. Kawase and H. Kurata, *Chem. Rev.* **2006,** *106*, 5250-5273; (c) K. Tashiro and T. Aida, *Chem. Soc. Rev.* **2007,** *36*, 189-197; (d) E. M. Pérez and N. Martín, *Chem. Soc. Rev.* **2008,** *37*, 1512-1519; (e) E. M. Pérez and N. Martín, *Pure Appl. Chem.* **2010,** *82*, 523-533.

[4] For recent examples, see: (a) J.-S. Marois, K. Cantin, A. Desmarais and J.-F. Morin, *Org. Lett.* **2008,** *10*, 33-36; (b) W. Xiao, D. Passerone, P. Ruffieux, K. Aiet-Mansour, O. Groening, E. Tosatti, J. S. Siegel and R. Fasel, *J. Am. Chem. Soc.* **2008,** *130*, 4767-4771; (c) A. Hosseini, S. Taylor, G. Accorsi, N. Armaroli, C. A. Reed and P. D. W. Boyd, *J. Am. Chem. Soc.* **2006,** *128*, 15903-15913; (d) E. M. Pérez, M. Sierra, L. Sánchez, M. R. Torres, R. Viruela, P. M. Viruela, E. Ortí and N. Martín, *Angew. Chem. Int. Ed.* **2007,** *46*, 1847-1851; (e) A. Sygula, F. R. Fronczek, R. Sygula, P. W. Rabideau and M. M. Olmstead, *J. Am. Chem. Soc.* **2007,** *129*, 3842-3843; (f) E. M. Pérez, L. Sánchez, G. Fernández and N. Martín, *J. Am. Chem. Soc.* **2006,** *128*, 7172-7173; (g) M. Yanagisawa, K. Tashiro, M. Yamasaki and T. Aida, *J. Am. Chem. Soc.* **2007,** *129*, 11912-11913; (h) J.-Y. Balandier, M. Chas, P. I. Dron, S. Goeb, D. Canevet, A. Belyasmine, M. Allain and M. Salle, *J. Org. Chem.* **2010,** *75*, 1589-1599; (i) J. U. Franco, J. C. Hammons, D. Rios and M. M. Olmstead, *Inorg. Chem. (Washington, DC, U. S.) FIELD Full Journal Title:Inorganic Chemistry (Washington, DC, United States)* **2010,** *49*, 5120-5125; (j) Y. Shoji, K. Tashiro and T. Aida, *J. Am. Chem. Soc.* **2010,** *132*, 5928-5929; (k) E. Huerta, E. Cequier and J. d. Mendoza, *Chem. Commun.* **2007,** *0*, 5016-5018; (l) E. Huerta, G. A. Metselaar, A. Fragoso, E. Santos, C. Bo and J. de Mendoza, *Angew. Chem. Int. Ed.* **2007,** *46*, 202-205; (m) Y. Shoji, K. Tashiro and T. Aida, *J. Am. Chem. Soc.* **2006,** *128*, 10690-10691; (n) S.-Q. Liu, D.-X. Wang, Q.-Y. Zheng and M.-X. Wang, *Chem. Commun.* **2007**, 3856-3858; (o) E.-X. Zhang, D.-X. Wang, Q.-Y. Zheng and M.-X. Wang, *Org. Lett.* **2008,** *10*, 2565-2568; (p) E. Huerta, H. Isla, E. M. Pérez, C. Bo, N. Martín and J. de Mendoza, *J. Am. Chem. Soc.* **2010,** *132*, 5351-5353; (q) E. M. Pérez, A. L. Capodilupo, G. Fernández, L. Sánchez, P. M. Viruela, R. Viruela, E. Ortí, M. Bietti and N. Martín, *Chem. Commun.* **2008,** *0*, 4567-4569.

[5] For a review on fullerene materials constructed by self- assembly, see: T. Nakanishi, *Chem. Commun.* **2010,** *46*, 3425-3436.

[6] For selected recent examples, see: (a) P. Xue, R. Lu, L. Zhao, D. Xu, X. Zhang, K. Li, Z. Song, X. Yang, M. Takafuji and H. Ihara, *Langmuir* **2010,** *26*, 6669-6675; (b) T. Haino, E. Hirai, Y. Fujiwara and K. Kashihara, *Angew. Chem. Int. Ed.* **2010,** *49*, 7899-7903; (c) X. Zhang and M. Takeuchi, *Angew. Chem. Int. Ed.* **2009,** *48*, 9646-9651; J. Wang, Y. Shen, S. Kessel, P. Fernandes, K. Yoshida, S. Yagai, D. G. Kurth, H. Mohwald and T. Nakanishi, *Angew. Chem. Int. Ed.* **2009,** *48*, 2166-2170; (d) F. D'Souza, E. Maligaspe, K. Ohkubo, M. E. Zandler, N. K. Subbaiyan and S. Fukuzumi, *J. Am. Chem. Soc.* **2009,** *131*, 8787-8797; (e) R. Tsunashima, S.-i. Noro, T. Akutagawa, T. Nakamura, H. Kawakami and K. Toma, *Chem. Eur. J.* **2008,** *14*, 8169-8176; (f) M. Schmittel, B. He and P. Mal, *Org. Lett.* **2008,** *10*, 2513-2516; (g) T. Nakanishi, T. Michinobu, K. Yoshida, N. Shirahata, K. Ariga, H. Mohwald and D. G. Kurth, *Adv. Mater.* **2008,** *20*, 443-446; (h) G. Fernández, L. Sánchez, E. M. Pérez and N. Martín, *J. Am. Chem. Soc.* **2008,** *130*, 10674-10683; (i) G. Fernández, E. M. Pérez, L. Sánchez and N. Martín, *J. Am. Chem. Soc.* **2008,** *130*, 2410-2411; (j) G. Fernández, E. M. Pérez, L. Sánchez and N. Martín, *Angew. Chem. Int. Ed.* **2008,** *47*, 1094-1097; (k) S. Barrau, T. Heiser, F. Richard, C. Brochon, C. Ngov, K. van de Wetering, G. Hadziioannou, D. V. Anokhin and D. A. Ivanov, *Macromolecules* **2008,** *41*, 2701-2710; (l) Y. Araki, R. Chitta, A. S. D. Sandanayaka, K. Langenwalter, S. Gadde, M. E. Zandler, O. Ito and F. D'Souza, *Journal of Physical Chemistry C* **2008,** *112*, 2222-2229; (m) Y.-W. Zhong, Y. Matsuo and E. Nakamura, *J. Am. Chem. Soc.* **2007,** *129*, 3052-3053; (n) S. Yoshimoto, E. Tsutsumi, R. Narita, Y. Murata, M. Murata, K. Fujiwara, K. Komatsu, O. Ito and K. Itaya, *J. Am. Chem. Soc.* **2007,** *129*, 4366-4376; (o) F. Wessendorf, J.-F. Gnichwitz, G. H. Sarova, K. Hager, U. Hartnagel, D. M. Guldi and A. Hirsch, *J. Am. Chem. Soc.* **2007,** *129*, 16057-16071; (p) U. Hahn, A. Gegout, C. Duhayon, Y. Coppel, A. Saquet and J.-F. Nierengarten, *Chem. Commun.* **2007**, 516-518; (q) D. Bonifazi, A. Kiebele, M. Stohr, F. Cheng, T. Jung, F. Diederich and H. Spillmann, *Adv. Funct. Mater.* **2007,** *17*, 1051-1062; (r) G.-B. Pan, X.-H. Cheng, S. Hoeger and W. Freyland, *J. Am. Chem. Soc.* **2006,** *128*, 4218-4219.

self-assembly.[5-6] In both cases the formation of associates with fullerenes of high stability in solution —that is, the construction of hosts that show large binding constants towards the fullerenes— is one of the main goals. To achieve this objective, a broad variety of molecular fragments capable of establishing positive non-covalent interactions with the outer surface of fullerenes have been explored. These include derivatives of calix[n]arenes,[7, 3d, 4n, 4o] cyclotriveratrylenes,[8, 4k, 4l] corannulenes,[9, 4e] cyclic paraphenyleneacetylenes,[10] π-extended tetrathiafulvalenes[4d, 4f, 4p, 4q] and, most frequently, porphyrins.[3c, 4g, 4m, 11]

Although the experimental results from different groups are sometimes difficult to compare due to the use of different methods to assess the binding constants and to the different solvents utilized, taking C_{60} as a reference fullerene guest, it is fair to say that obtaining hosts that show binding constants of log K_a = 5 or larger remains a major challenge. Aida´s bisporphyrin macrocycles —in which porphyrin units are connected via flexible alkyl spacers— constitute perhaps the most successful family of hosts for fullerenes to date.[3c, 4g, 4m, 11c, 11a, 11b, 11f] For example, the Zn(II) metalloporphyrin congener shows a log K_a = 5.8 towards C_{60}, while the free base shows log K_a = 5.9, both

[7] (a) K. Araki, K. Akao, A. Ikeda, T. Suzuki and S. Shinkai, *Tetrahedron Lett.* **1996,** *37*, 73-6; (b) C. L. Raston, J. L. Atwood, P. J. Nichols and I. B. N. Sudria, *Chem. Commun.* **1996,** *0*, 2615-2616; (c) T. Haino, M. Yanase and Y. Fukazawa, *Angew. Chem., Int. Ed. Engl.* **1997,** *36*, 259-260; T. Haino, M. Yanase and Y. Fukazawa, *Angew. Chem. Int. Ed.* **1998,** *37*, 997-998; (d) T. Haino, Y. Yamanaka, H. Araki and Y. Fukazawa, *Chem. Commun.* **2002,** *0*, 402-403; (e) T. Haino, Y. Matsumoto and Y. Fukazawa, *J. Am. Chem. Soc.* **2005,** *127*, 8936-8937; (f) T. Haino, C. Fukunaga and Y. Fukazawa, *Org. Lett.* **2006,** *8*, 3545-3548; (g) T. Haino, M. Yanase, C. Fukunaga and Y. Fukazawa, *Tetrahedron* **2006,** *62*, 2025-2035; (h) K. A. Nielsen, G. H. Sarova, L. Martín-Gomis, F. Fernández-Lázaro, P. C. Stein, L. Sanguinet, E. Levillain, J. L. Sessler, D. M. Guldi, A. Sastre-Santos and J. O. Jeppesen, *J. Am. Chem. Soc.* **2008,** *130*, 460-462; (i) J.-C. Wu, D.-X. Wang, Z.-T. Huang and M.-X. Wang, *Tetrahedron Lett.* **2009,** *50*, 7209-7212.

[8] (a) J. W. Steed, P. C. Junk, J. L. Atwood, M. J. Barnes, C. L. Raston and R. S. Burkhalter, *J. Am. Chem. Soc.* **1994,** *116*, 10346-10347; (b) J. L. Atwood, M. J. Barnes, M. G. Gardiner and C. L. Raston, *Chem. Commun.* **1996**, 1449-1450; (c) H. Matsubara, T. Shimura, A. Hasegawa, M. Semba, K. Asano and K. Yamamoto, *Chem. Lett.* **1998,** *27*, 1099-1100; (d) J.-F. Nierengarten, L. Oswald, J.-F. Eckert, J.-F. Nicoud and N. Armaroli, *Tetrahedron Lett.* **1999,** *40*, 5681-5684; (e) D. Felder, B. Heinrich, D. Guillon, J.-F. Nicoud and J.-F. Nierengarten, *Chem. Eur. J.* **2000,** *6*, 3501-3507; (f) Y. Rio and J.-F. Nierengarten, *Tetrahedron Lett.* **2002,** *43*, 4321-4324.

[9] (a) S. Mizyed, P. E. Georghiou, M. Bancu, B. Cuadra, A. K. Rai, P. Cheng and L. T. Scott, *J. Am. Chem. Soc.* **2001,** *123*, 12770-12774; (b) P. E. Georghiou, A. H. Tran, S. Mizyed, M. Bancu and L. T. Scott, *J. Org. Chem.* **2005,** *70*, 6158-6163; (c) C. Mueck-Lichtenfeld, S. Grimme, L. Kobryn and A. Sygula, *PCCP* **2010,** *12*, 7091-7097.

[10] (a) T. Kawase, K. Tanaka, Y. Seirai, N. Shiono and M. Oda, *Angew. Chem. Int. Ed.* **2003,** *42*, 5597-5600; (b) T. Kawase, N. Fujiwara, M. Tsutumi, M. Oda, Y. Maeda, T. Wakahara and T. Akasaka, *Angew. Chem. Int. Ed.* **2004,** *43*, 5060-5062; (c) T. Kawase, K. Tanaka, N. Shiono, Y. Seirai and M. Oda, *Angew. Chem. Int. Ed.* **2004,** *43*, 1722-1724; (d) T. Kawase and H. Kurata, *Chem. Rev.* **2006,** *106*, 5250-5273.

[11] (a) H. Sato, K. Tashiro, H. Shinmori, A. Osuka, Y. Murata, K. Komatsu and T. Aida, *J. Am. Chem. Soc.* **2005,** *127*, 13086-13087; (b) Y. Shoji, K. Tashiro and T. Aida, *J. Am. Chem. Soc.* **2004,** *126*, 6570-6571; (c) D. Sun, F. S. Tham, C. A. Reed, L. Chaker and P. D. W. Boyd, *J. Am. Chem. Soc.* **2002,** *124*, 6604-6612; (d) Y. Kubo, A. Sugasaki, M. Ikeda, K. Sugiyasu, K. Sonoda, A. Ikeda, M. Takeuchi and S. Shinkai, *Org. Lett.* **2002,** *4*, 925-928; (e) M. Ayabe, A. Ikeda, Y. Kubo, M. Takeuchi and S. Shinkai, *Angew. Chem. Int. Ed.* **2002,** *41*, 2790-2792; (f) J.-Y. Zheng, K. Tashiro, Y. Hirabayashi, K. Kinbara, K. Saigo, T. Aida, S. Sakamoto and K. Yamaguchi, *Angew. Chem. Int. Ed.* **2001,** *40*, 1857-1861.

in benzene at room temperature.[11f] The world-record in complex stability is the Ir(III) metalloporphyrin derivative which shows a log K_a = 8.1 for C_{60} in 1,2-dichlorobenzene (*o*-DCB) at room temperature.[4g,] It is noteworthy that in the latter case, the authors indicate that the supramolecular nature of the host-guest system is arguable, since iridium was found to bind a 6,6 junction of the fullerene in a η^2 fashion. Recently, a macrocycle featuring three porphyrins[12] and a "nanobarrel" formed by four porphyrin units[13] have been shown to bind C_{60} with log K_a = 6.2 and 5.7 respectively, both in toluene at room temperature.

4.3.2. Design and synthesis

We have very recently reported a macrocyclic receptor that associates C_{60} with log K_a = 6.5 ± 0.5 in PhCl at room temperature (***p*-xylmac12** in Chart 1).[14] The design of the macrocyclic host was based on our initial tweezers-like receptors, in which two exTTF units were connected through an isophthalic diester spacer. This simple receptor served as proof-of-principle for the utilization of exTTF as recognizing motif in the construction of hosts for fullerenes, and showed respectable affinities towards C_{60} considering its lack of preorganization (log K_a = 3.5 in PhCl at room temperature).[4f] To increase the degree of preorganization, we conserved all the basic traits of the exTTF tweezers, but included an alkyl linker with terminal alkenes to achieve macrocyclization through RCM. In the present study, we describe a collection of macrocyclic hosts with systematic structural modification of both the alkyl and aromatic spacers. Considering the precedents and preliminary molecular modelling, we decided to investigate *p*-xylene, *m*-xylene and 2,6-dimethylnaphthalene as aromatic spacers, and hexene, heptene and octene as alkyl spacers and precursors for RCM. The structures of the receptors synthesized are shown in Chart 1. The nomenclature utilized identifies the aromatic spacer and the length of the alkenyl spacers.

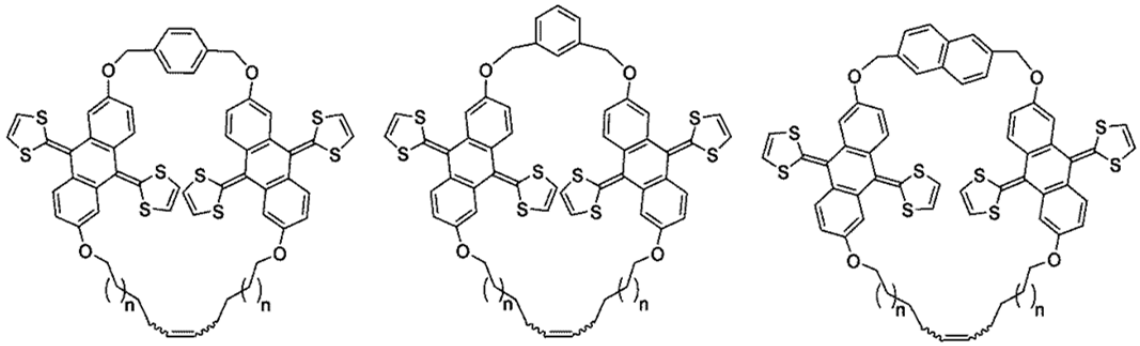

Chart 1. Chemical structures of the nine receptors.

[12] G. n. Gil-Ramírez, S. D. Karlen, A. Shundo, K. Porfyrakis, Y. Ito, G. A. D. Briggs, J. J. L. Morton and H. L. Anderson, *Org. Lett.* **2010,** *12*, 3544-3547.
[13] J. Song, N. Aratani, H. Shinokubo and A. Osuka, *J. Am. Chem. Soc.* **2010,** *132*, 16356–16357.
[14] H. Isla, M. Gallego, E. M. Pérez, R. Viruela, E. Ortí and N. Martín, *J. Am. Chem. Soc.* **2010,** *132*, 1772-1773.

The ***p*-xylmac** and ***m*-xylmac** families (n = 1-3) were synthesized following a procedure analogous to that reported for ***p*-xylmac12** (Scheme 1).[14] The synthesis starts with the Williamson etherification of anthraflavic acid with the corresponding bromoalkene under standard conditions, followed by dialkylation of either *para* or *meta*-α,α'-dibromoxylene with the remaining phenolic OH, which yielded linear tetraketone precursors. These were subjected to Horner-Wadsworth-Emmons olefination with dimethyl 1,3-dithiol-2-ylphosphonate, to afford the bis-exTTF linear precursors, which were finally treated with Grubb's 1st generation catalyst to obtain the desired macrocycles. The synthesis of the **naphmac** family follows the same procedure, but utilizing 2,6-bis(hydroxymethyl)naphthalene and a Mitsunobu protocol to obtain linear bis-anthraquinone precursors (Scheme 1). This was followed by olefination to form the exTTF derivatives and RCM to yield the macrocycles as a chromatographically inseparable mixture of *E/Z* isomers, which was used as such. The identity and purity of the nine macrocyclic hosts and all synthetic intermediates were unambiguously established by standard spectroscopic and analytical techniques (see experimental section for full experimental details and characterization).

Scheme 1. General scheme for the synthesis of the macrocyclic hosts.[a]

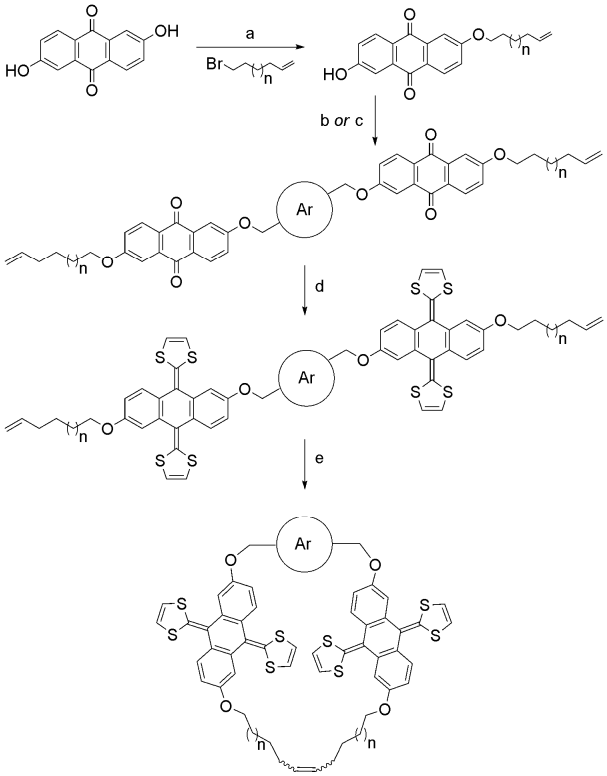

[a] Conditions: a) K_2CO_3, NaI (cat.), DMF, reflux; b) for ***p*-xylmac** and ***m*-xylmac** families: α,α'-*p*-dibromoxylene, or α,α'-*m*-dibromoxylene, K_2CO_3, NaI (cat.), DMF, 60 ºC; c) for **naphmac** family: 2,6-bis(hydroxymethyl)naphthalene, Ph_3P, diethyl azodicarboxylate, THF, reflux; d) dimethyl 1,3-dithiol-2-ylphosphonate, BuLi, THF, −78 ºC to r. t.; e) Grubb´s 1st generation catalyst, CH_2Cl_2, r. t.

4.3.3. Association of C_{60} and C_{70}.

Binding constants were estimated through UV-vis titrations. In a typical experiment, we prepared stock solutions of the macrocyclic receptor in PhCl at a concentration approximately equal to the reciprocal of the binding constant. Those solutions were utilized as solvents in the solution of fullerene, to ensure working at constant concentration of host. Aliquots of the fullerene solution were added to the host solution until reaching 3-4 molar equivalents, and UV-vis spectra recorded at room temperature on a Cary UV-50 or on a Shimadzu UV-3600 spectrophotometer equipped with a temperature control unit. Analysis of the UV-vis data to determine binding constants was carried out utilizing Specfit multivariable analysis software. Experiments were repeated three times. The values of the binding constants are reported in Table 1 and were calculated as the mean value of the three experiments, with the error estimated as the standard deviation.

Table 1. Logarithm of the calculated binding constants for the macrocyclic hosts towards C_{60} and C_{70}, as estimated from three separate UV-vis titration experiments in PhCl at 298 K.

	C_{60}	C_{70}
***p*-xylmac10**	4.3 ± 0.5	6.0 ± 0.4; 12.3 ± 0.6[a]
***p*-xylmac12**	6.5 ± 0.5	—[b]
***p*-xylmac14**	3.5 ± 0.6	5.9 ± 0.3
***m*-xylmac10**	4.0 ± 0.5	4.4 ± 0.4; 8.3 ± 0.5[a]
***m*-xylmac12**	4.8 ± 0.4	—[b]
***m*-xylmac14**	4.1 ± 0.4	5.4 ± 0.3
naphmac10	4.0 ± 0.2	4.7 ± 0.3
naphmac12	5.6 ± 0.6	5.6 ± 0.4
naphmac14	3.4 ± 0.1	6.1 ± 0.2

[a] First binding constant corresponds to log $K_{1:1}$ and second to log $K_{2:1}$. [b] Titration data did not provide satisfactory fits (see main text).

The changes in the absorption spectra during the titrations against C_{60} are very similar for all nine receptors. As representative examples, Figure 1 shows the evolution of the spectra of the best host of each series, ***p*-xylmac12**, ***m*-xylmac12** and **naphmac12** upon increasing C_{60} concentration. In all cases, we observe the decrease in absorption of the band at λ_{max} ~ 425-430 nm, and the appearance of a charge-transfer band at λ_{max} ~ 470-475 nm. An isosbestic point at around 450 nm is also clearly observable. These spectral changes distinctively indicate association of C_{60} inside the cavity of the macrocycle.[14] The relative intensity of the changes correlates very well with the calculated binding constants (see Table 1). For ***p*-xylmac12** (log K_a = 6.5 ± 0.5) and **naphmac12** (log K_a = 5.6 ± 0.6) both the decrease in the absorption of the exTTF and the increase in absorption of the charge-transfer band are significantly more marked than for ***m*-xylmac12** (log K_a = 4.8 ± 0.4).

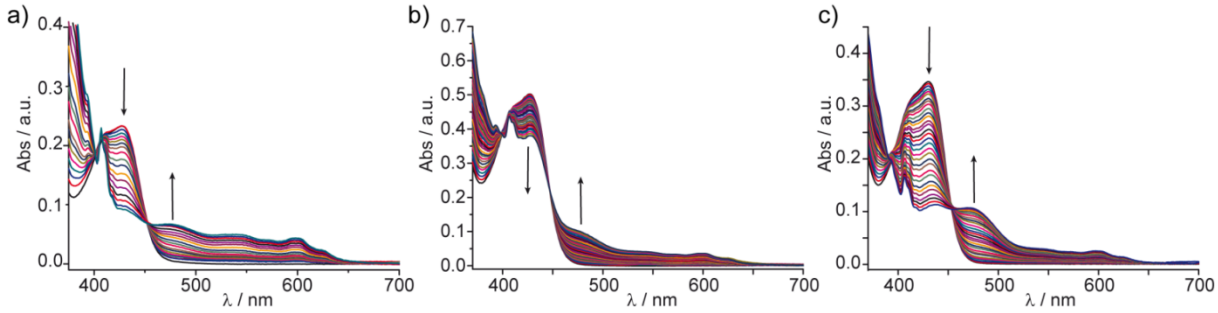

Figure 1. Spectral changes in UV-vis titration experiments of: a) ***p*-xylmac12** b) ***m*-xylmac12** and c) **naphmac12** against C_{60} in PhCl at 298 K.

The titration data versus C_{60} for all nine macrocycles was fitted successfully to a 1:1 binding mode,[15] yielding the binding constants summarized in Table 1. From the values of the binding constants, it is clearly apparent that the *m*-xylylene spacer is the least adequate of the aromatics, with *p*-xylylene producing the best host for C_{60}, and naphthalene in an intermediate position. With regards to the alkyl spacer, the C_{12} derivative consistently shows the highest binding constant, with a very significant increase with regards to C_{10} (too small) and C_{14} (too large). These results are qualitatively well reproduced by molecular mechanics calculations in the gas phase.[16]

[15] Continous variation plots to confirm the stoichiometries of the associates were also carried out. For the sake of brevity, only those indicating 2:1 stoichiometry are shown. The Job's plot of ***p*-xylmac12** vs.C_{60} can be seen in ref. 14.

[16] Minimizations were carried out utilizing the AMBER force field included in the HyperChem molecular modelling system. The AMBER force field was selected because it includes a term for van der Waals and electrostatic interactions. See: W. D. Cornell, P. Cieplak, C. I. Bayly, I. R. Gould, K. M. Merz, Jr., D. M. Ferguson, D. C. Spellmeyer, T. Fox, J. W. Caldwell and P. A. Kollman, *J. Am. Chem. Soc.* **1995,** *117*, 5179-97. In the case of ***p*-xylmac12**, we have previously reported calculations at the DFT (BH&H/6-31G**) level (see ref. 14). Due to the size of the collection of macrocycles, in this case we have resorted to less demanding molecular mechanics. The geometry optimization yields nearly identical results with both approaches. All optimizations were carried out with the *E* isomer of the corresponding macrocycle. We have previously shown that there is hardly any difference between the cavities of the *E* and *Z* macrocycles (see ref. 14).

Figure 2 shows the geometry optimized models for the ***p*-xylmac** series to illustrate this point.

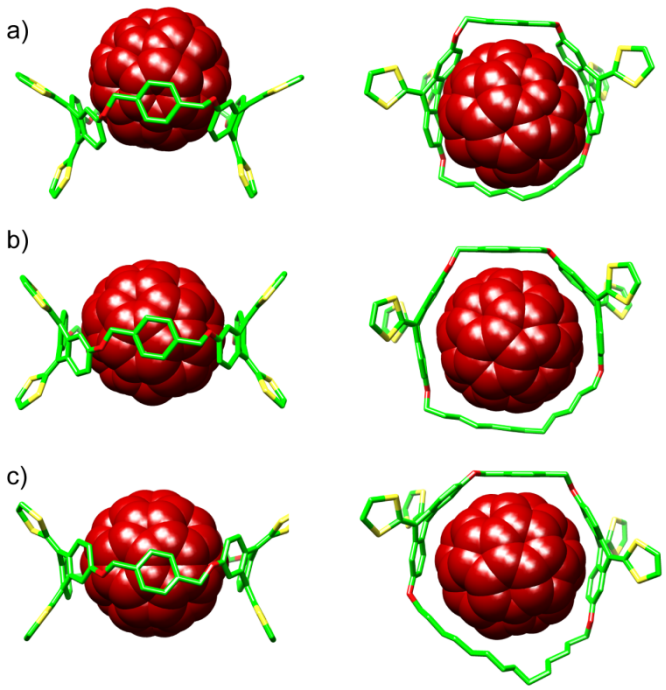

Figure 2. Side and top views of the energy-minimized (AMBER) models of the associates: a) ***p*-xylmac10**·C_{60}; b) ***p*-xylmac12**·C_{60}; c) ***p*-xylmac14**·C_{60}. The macrocycles are depicted in stick representation with carbon atoms in green, sulfurs in yellow, and oxygens in red. Hydrogen atoms are not shown for clarity. [60]fullerenes are depicted as space-filling models and coloured in dark red.

In ***p*-xylmac10**·C_{60} (Figure 2a) the macrocyclic cavity is too small to associate C_{60}, and the host adopts a bowl-type conformation, accommodating the fullerene above the plane of the macrocycle. In contrast, in ***p*-xylmac12**·C_{60} (Figure 2b) C_{60} fits perfectly inside the cavity of the macrocycle, with both exTTF units, the aromatic linker, and the alkyl spacer closely wrapping the fullerene unit. Finally, C_{60} fits loosely in ***p*-xylmac14**, so only part of the alkyl chain can approach the [60]fullerene and provide stabilizing van der Waals interactions.

The evolution of the spectra during the titrations against C_{70} is much less uniform across the different families of macrocycles attending to the aromatic spacer. The spectral changes in the **naphmac** series mirror what we have previously observed for exTTF-cyclotriveratrylene hosts,[4p] namely, during the first additions the absorbance at λ_{max} = 430 nm decreases, with the concomitant increase of a charge-transfer band centered at λ = 471 nm. As the concentration of C_{70} increases the spectral changes become difficult to trace due to spectral overlap. Figure 3 depicts the experimental results obtained in the titration of **naphmac14** *vs.* C_{70} (PhCl, 298 K). All three titrations

for **naphmac10**, **naphmac12** and **naphmac14** fitted successfully to a 1:1 binding model (see Figure 3 inset), yielding larger binding constants as the size of the macrocyclic cavity increases (see Figure 1), as could be expected. Thus, the most efficient binder for C_{70} was found to be **naphmac14**, with a remarkable binding constant of log $K_a = 6.1 \pm 0.2$.

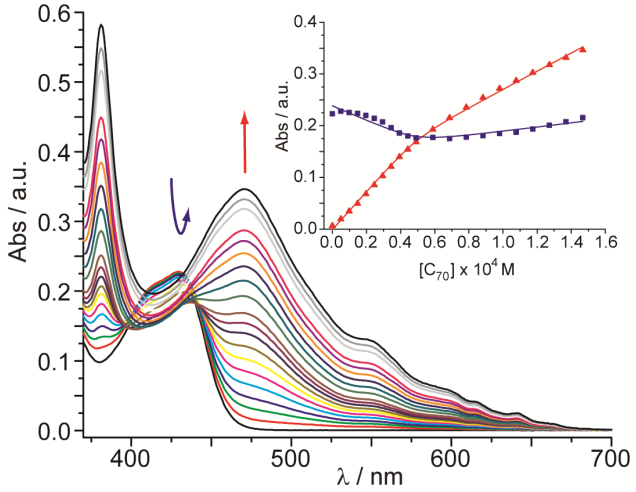

Figure 3. UV-vis spectra as recorded during the titration of **naphmac14** *vs.*C_{70} (PhCl, 298 K). Inset shows the binding isotherms at 430 nm (blue squares) and 471 nm (red triangles); solid lines represent the fits. For this particular experiment a log $K_a = 6.0$ was calculated.

On the other hand, the ***p*-xylmac** and ***m*-xylmac** families showed parallel trends, depending on the length of the alkyl spacer. The larger members of each series, ***p*-xylmac14** and ***m*-xylmac14** behaved similarly to the **naphmac** hosts, and analysis of their titration data was performed satisfactorily utilizing a 1:1 binding model, yielding binding constants of log $K_a = 5.9 \pm 0.3$ and 5.4 ± 0.3, for ***p*-xylmac14** and ***m*-xylmac14**, respectively.

Unexpectedly, the smaller macrocycles ***p*-xylmac10** and ***m*-xylmac10** showed singular spectroscopic changes during the titration experiments. Figure 4a shows the variations in the electronic absorption spectrum of ***p*-xylmac10** upon additions of 0.1 eq. aliquots of C_{70} in PhCl at 298 K. Although at first sight the general trends are similar to those we observed for **naphmac** hosts (see Figure 3), a closer look at the titration data offers major and informative differences. During the first three additions of the titration, where the concentration of the macrocycle is significantly larger than that of the [70]fullerene, two very well defined isosbestic points at $\lambda = 402$ and 432 nm can be noted (Figure 4b, inset). As the concentration of C_{70} increases these isosbestic points are lost, indicating the coexistence of more than one type of associates in solution. All these features point to the formation of complexes of both 2:1 and 1:1 host:guest stoichiometry, with the former prevailing in the early stages of the titration, and complexes of both stoichiometries being present in solution when the concentration of

C_{70} increases sufficiently. Indeed, the titration data did not provide satisfactory fits when assuming either a 1:1 or a 2:1 stoichiometry exclusively. On the contrary, the multivariable analysis software converged nicely when we utilized a model where both types of associates are presumed to exist in solution (Figure 4a, inset). The calculated binding constants for ***p*-xylmac10** were log $K_{1:1}$ = 6.0 ± 0.4 and log $K_{2:1}$ 12.3 ± 0.6, in agreement with both types of associates showing similar stability. Analogously, we estimated log $K_{1:1}$ = 4.4 ± 0.4 and log $K_{2:1}$ 8.3 ± 0.5 for ***m*-xylmac10**, which also shows smaller binding constants towards C_{70}, as was the case with C_{60}. Conclusive evidence for this model was provided by Job's plot analysis, which showed a broad maximum centered at molar fraction of 0.3-0.45 (Figure 4c), in an intermediate situation between 2:1 and 1:1, where the maxima would be located at 0.33 and 0.5, respectively.

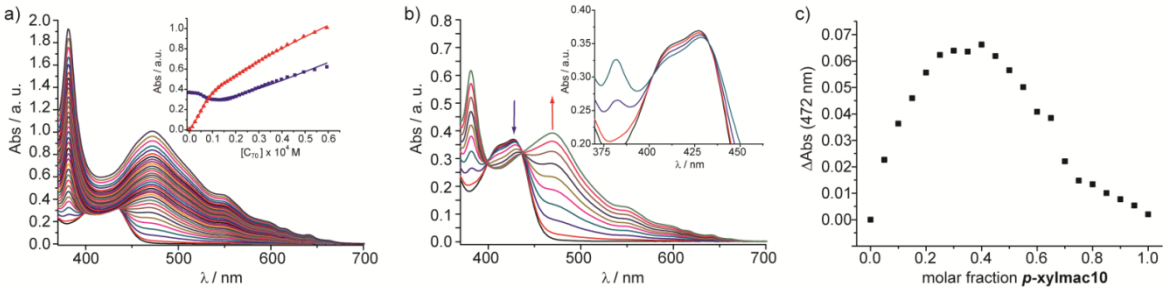

Figure 4. a) UV-vis spectra as recorded during the titration of ***p*-xylmac10** *vs.* C_{70} (PhCl, 298K). Inset shows the binding isotherms at 430 nm (blue squares) and 472 nm (red triangles), solid lines represent the fits. b) First ten additions, up to 1 eq. of C_{70}. Inset shows the first three additions. c) Job's plot ([***p*-xylmac10**] + [C_{70}] = 1.0 x 10^{-4} M).

Finally, ***p*-xylmac12** and ***m*-xylmac12** are apparently left in an intermediate situation between the C_{10} and C_{14} members, and, although association of C_{70} seems to take place considering the spectral changes, we could not achieve correct fitting of their titration data with any binding model. For instance, for ***m*-xylmac12** the best fit was obtained with a 1:1 model, and yielded a clearly over estimated binding constant of log K_a = 9.9 ± 2.6, with excessive error and less than modest fitting for the binding isotherms (Figure 5). Similarly, the best fit for the data corresponding to ***p*-xylmac12** *vs.* C_{70} affords log K_a = 8.4 ± 2.5.[14]

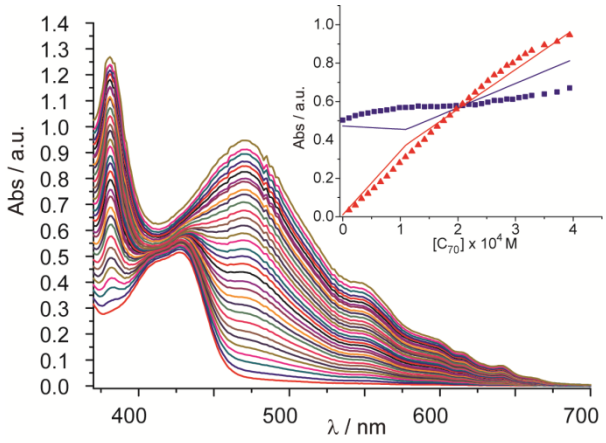

Figure 5. UV-vis spectra as recorded during the titration of ***p*-xylmac12** *vs.* C_{70} (PhCl, 298 K). Inset shows the binding isotherms at 430 nm (blue squares) and 471 nm (red triangles); solid lines represent the fits.

As with C_{60}, the experimental results can be rationalized in terms of a simple lock and key model through molecular mechanics calculations. The energy-minimized models of ***p*-xylmac10**·C_{70} and **naphmac10**·C_{70} are shown in Figure 6a and c. The cavity of ***p*-xylmac10** is too small to accommodate C_{70}, and leaves a significant part of its ellipsoidal surface exposed, so that it can be bound by another molecule of the host (Figure 6b) without steric congestion. On the other hand, the slight increase in size provided by the naphthalene spacer in **naphmac10** is sufficient to allow C_{70} to penetrate deeper into its cavity, stabilizing the 1:1 associate (Figure 6c and d). Meanwhile, **naphmac14** is the only macrocycle which is large enough to be capable of hosting C_{70} with its longer axis parallel to the plane of the macrocycle (Figure 6f). This provides an alternative to the perpendicular binding we observe for all other macrocycles, and can be responsible for the increase in stability.

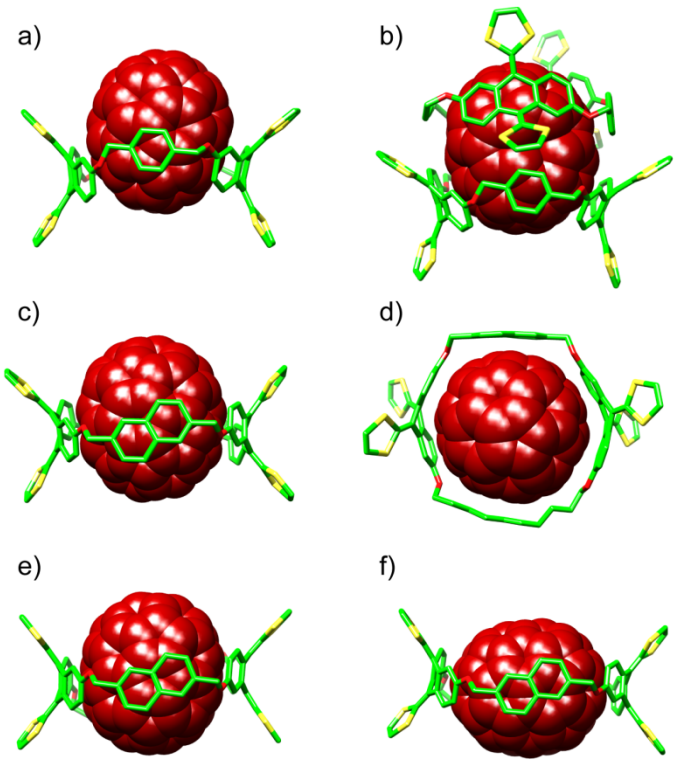

Figure 6. Energy-minimized (AMBER) models of the associates: a) ***p*-xylmac10**·C_{70}; b) ***p*-xylmac10**·C_{70}·***p*-xylmac10**; c) **naphmac10**·C_{70}, side view and d) top view; e) **naphmac14**·C_{70} with the guest perpendicular to the plane of the macrocycle; f) **naphmac14**·C_{70} with the guest parallel to the plane of the macrocycle. The macrocycles are depicted in stick representation with carbon atoms in green, sulfurs in yellow, and oxygens in red. Hydrogen atoms are not shown for clarity. [70]fullerenes are depicted as space-filling models and coloured in dark red.

To complete our understanding of the recognition process of these macrocyclic systems, and gain an insight into its thermodynamic nature, we carried out titrations at different temperatures (288, 298, 308 and 318 K) in PhCl. As model system, we chose the best binder of the family: ***p*-xylmac12** and C_{60} as a host. A plot of the natural logarithm of K_a *vs.* 1/T is shown in Figure 7. The data show a clear linear tendency, and was fitted to a straight line ($r^2 = 0.995$) with a slope of 19557 ± 1416 and an intercept of −51 ± 5. From these data, the standard enthalpy of association was calculated to be ΔH° = −163 ± 12 kJ mol^{-1} (−38 ± 3 kcal mol^{-1}) and ΔS° = −424 ± 42 J mol^{-1} (−101 ± 10 cal mol^{-1}). Thus, the association of fullerenes by our exTTF-based macrocyclic hosts is driven by strong enthalpic interactions. For comparison, the enthalpy value is approximately two to three times higher than that calculated for the association of C_{60} by calix[4]naphthalenes in toluene, which show a log K_a = 2.8.[17]

[17] S. Mizyed, P. E. Georghiou and M. Ashram, *J. Chem. Soc. Perk. Trans. 2* **2000,** *0*, 277-280.

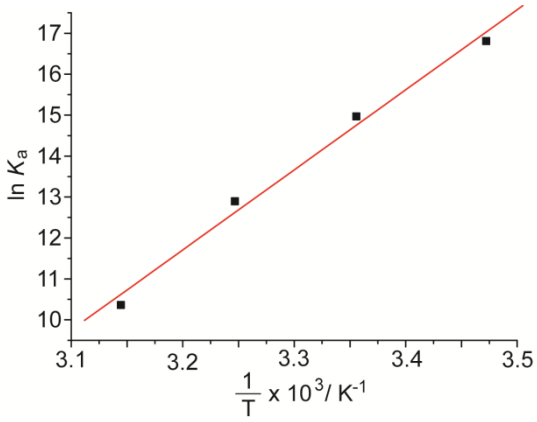

Figure 7. Plot of the natural logarithm of K_a *vs.* 1/T for the association of C_{60} with ***p*-xylmac12** in PhCl.

The appearance of a charge-transfer band during the titration suggests that electronic interactions between the fullerenes and our bis-exTTF macrocycles take place. These interactions in the ground state are also noticeable in cyclic voltammetry (CV) experiments. Though adsorption phenomena prevent a reliable measure of the oxidation potential of exTTF units, the cathodic part of the CV allowed us to draw interesting conclusions. Figure 8a shows the CVs of ***p*-xylmac12** (black), C_{60} (blue) and a mixture of both compounds (red). In the presence of macrocycle, the half-wave potentials associated with the reduction signals of [60]fullerene are clearly shifted, which definitely confirms an interaction in the ground state between the host and the guest, even though both positive and negative shifts were detected. Similar measurements (Figure 8b), performed with **naphmac14** and C_{70}, indicate a strong electronic communication in the complex with a half-wave potential shift as high as −150 mV for the fourth reduction of C_{70}.

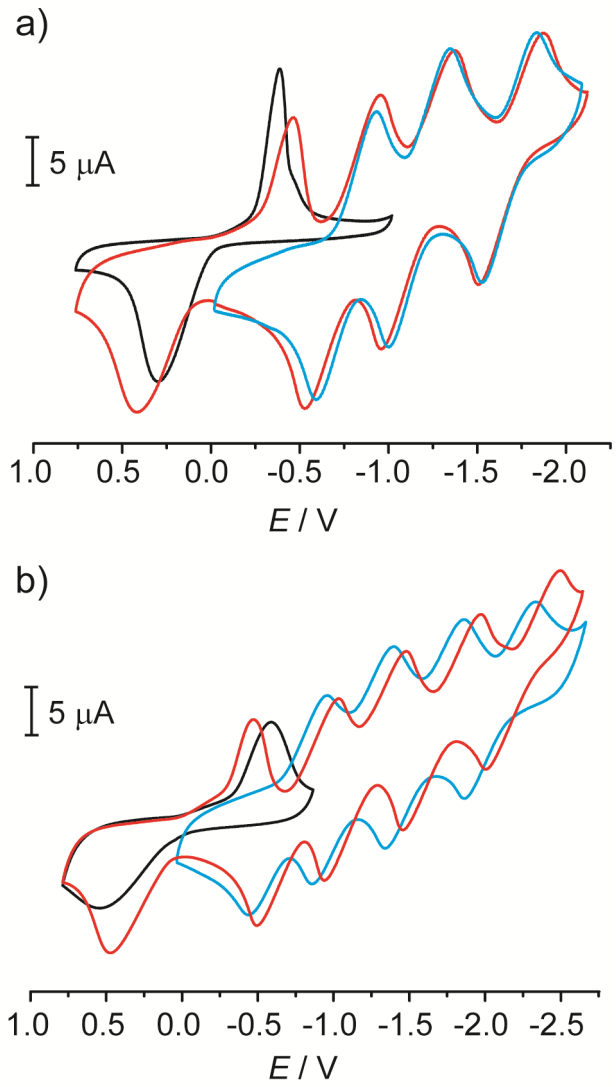

Figure 8. Cyclovoltammograms of a) ***p*-xylmac12** (black), C_{60} (blue), and ***p*-xylmac12**·C_{60} (red). b) **naphmac14** (black), C_{70} (blue) and **naphmac14**·C_{70} (red), in PhCl, Bu_4NClO_4 (0.1 M), v = 0.1 V s^{-1}, [fullerene] = [macrocycle] = 5 x 10^{-4} M. Potentials are indicated *vs.* the $Ag/AgNO_3$ redox couple.

To further investigate the influence of the electronic communication on the stability of the complexes, we carried out titrations in solvents of different polarities. In the more polar benzonitrile (ε_r = 25.2), where charge-transfer interactions should be favoured, we calculated a binding constant of log K_a = 7.5 ± 0.9. The increase in binding constant cannot be ascribed solely to stabilization of the complex through enhanced charge-transfer interactions, since the solubility of C_{60} in benzonitrile is 0.4 mg/mL. This is conclusively confirmed in the non-polar toluene (ε_r = 2.4), in which a decrease in binding constant to log K_a = 5.4 ± 0.9 was found. Considering the decrease in solubility

of C_{60} when moving from chlorobenzene (6.4 mg/mL) to toluene (2.4 mg/mL)[18] this is evidence of the contribution of the electronic interactions to the stabilization of the ***p*-xylmac12**·C_{60} associate, since a decrease in binding constant with increasing solubility is typically found.[4c] Such effect can be attributed to the solvation penalty associated with the formation of the supramolecular assembly. Since a significant portion of the molecular surfaces of both the receptor and the guest becomes unavailable for solvation upon complexation, the solvation penalty is more severe in solvents which solvate the separated entities more efficiently.

4.3.4. Conclusions

We have synthesized a collection of nine macrocycles bearing two units of exTTF as recognition elements for the fullerenes, connected through three different aromatic and alkyl spacers, and investigated their binding abilities towards C_{60} and C_{70}. It was found that ***p*-xylmac12** is the best binder for C_{60} with log K_a = 6.5 ± 0.5 for C_{60} in PhCl and log K_a = 7.5 ± 0.9 in benzonitrile. These values make ***p*-xylmac12** one of the most efficient receptors for C_{60} reported to date. With regards to C_{70}, **naphmac14** and ***p*-xylmac14** show log K_a = 6.1 ± 0.2 and 5.9 ± 0.3, respectively, in PhCl at 298 K. These are two of the very few examples of hosts capable of associating C_{70} with micromolar affinity.[4p, 19] From the general point of view of the design of hosts for fullerenes, our results show that relatively small structural variations in the receptor lead to large changes in binding affinities, and in, some cases, even stoichiometry. For example, while ***m*-xylmac14** forms 1:1 complexes with C_{70} with a respectable binding constant of log K_a = 5.4 ± 0.3, the smaller member ***m*-xylmac10** forms associates of both 1:1 and 2:1 stoichiometries, with log $K_{1:1}$ = 4.4 ± 0.4 and log $K_{2:1}$ 8.3 ± 0.5. With regards to C_{60}, an impressive change in binding constant of nearly three orders of magnitude is found when moving from ***p*-xylmac12** (log K_a = 6.5 ± 0.5) to ***p*-xylmac14** (log K_a = 3.5 ± 0.6). These differences underline the singularities of fullerenes as hosts in molecular recognition, and highlight the importance of fine-tuning the structure of the receptors. Remarkably, all our experimental results can be qualitatively explained with a simple lock and key model through undemanding molecular mechanics calculations.

In order to shed light on the driving force for binding, we have determined the thermodynamic parameters for the formation of ***p*-xylmac12**·C_{60}. To that end, we have carried out titrations at different temperatures (318, 308, 298 and 288 K). The positive slope of the ln K_a *vs.* 1/T indicates that association is driven by enthalpy. Indeed, we calculated a remarkably high ΔH° = −163 ± 12 kJ mol^{-1} (−38 ± 3 kcal mol^{-1}). The spectral features observed during the UV-vis titrations, cyclic voltammetry data, and titrations carried out in solvents of different polarity suggest that electronic interactions between the exTTF and C_{60} contribute significantly to the stabilization of the complex.

[18] K. N. Semenov, N. A. Charykov, V. A. Keskinov, A. K. Piartman, A. A. Blokhin and A. A. Kopyrin, *Journal of Chemical & Engineering Data* **2010,** *55*, 13-36.
[19] D. Pal, D. Goswami, S. K. Nayak, S. Chattopadhyay and S. Bhattacharya, *J. Phys. Chem. A* **2010,** *114*, 6776-6786.

In the near future, we plan to exploit the extreme stability of the bis-exTTF macrocycle-fullerene complexes, the lessons extracted from the structure-affinity relationships, and the relatively simple synthetic access to the macrocycles to construct chiral hosts for the enantioselective molecular recognition of the inherently chiral higher fullerenes.[4j, 4m]

4.3.5. Experimental section

4.3.5.1. Synthesis and characterization

General. All solvents were dried according to standard procedures. Reagents were used as purchased. All air-sensitive reactions were carried out under argon atmosphere. Flash chromatography was performed using silica gel (Merck, Kieselgel 60, 230-240 mesh, or Scharlau 60, 230-240 mesh). Analytical thin layer chromatographies (TLC) were performed using aluminium-coated Merck Kieselgel 60 F254 plates. Melting points were determined on a Gallenkamp apparatus. NMR spectra were recorded on a Bruker Avance 300 (^{1}H: 300 MHz; ^{13}C: 75 MHz), a Bruker Avance 500 (^{1}H: 500 MHz; ^{13}C: 125 MHz) spectrometers at 298 K, unless otherwise stated, using partially deuterated solvents as internal standards. Coupling constants (J) are denoted in Hz and chemical shifts (δ) in ppm. Multiplicities are denoted as follows: s = singlet, d = doublet, t = triplet, m = multiplet, b = broad. When necessary, NOESY or bidimensional ^{1}H-^{1}H experiments were executed for the assignations of protons. Electrospray ionization mass spectrometry (ESI-MS) and Matrix-assisted Laser desorption ionization (coupled to a Time-Of-Flight analyzer) experiments (MALDI-TOF) were recorded on a HP1100MSD spectrometer and a Bruker REFLEX spectrometer, respectively.

Monosubstituted anthraflavic acid derivatives.

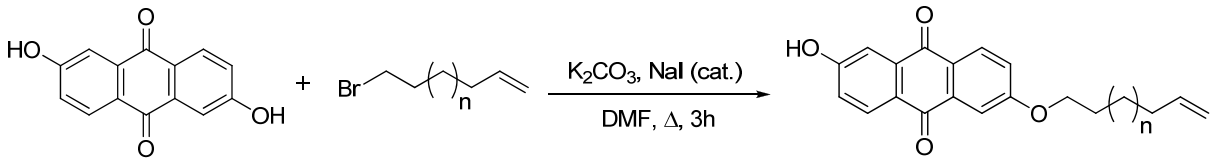

General procedure. Anthraflavic acid 94% (3.19 g - 12.5 mmol) was dispersed with sonication in dry DMF (450 mL). Then, dry K_2CO_3 (1.73 g - 12.5 mmol), the corresponding α-bromo-ω-alkene (12.5 mmol) and a catalytic amount of NaI were added and the mixture refluxed for three hours. The crude reaction was poured into ice-cold 1 M hydrochloric acid (1 L), and filtrated. The solid was redissolved in CH_2Cl_2 and washed with water (2 x 250 mL). The organic fraction was dried over $MgSO_4$, the solvent evaporated, and the corresponding residue subjected to column chromatography (CH_2Cl_2 to CH_2Cl_2:CH_3OH 2%) affording the pure product as a light yellow solid (**4.1a**: n = 1, y = 43%; **4.1b**: n = 2, y = 47%; **4.1c**: n = 3, y = 55%).

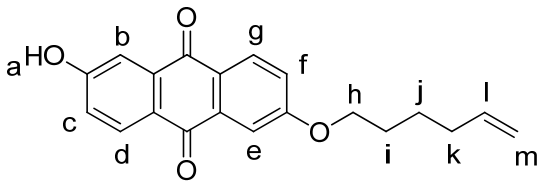

Compound 4.1a. ^{1}H NMR (d_6-DMSO, 300 MHz) δ 11.02 (s, 1H, H_a), 8.17 (d, J = 8.6 Hz, 1H, H_g), 8.13 (d, J = 8.4 Hz, 1H, H_d), 7.51 (d, J = 2.6 Hz, 1H, H_e), 7.46 (d, J = 2.6 Hz, 1H, H_b), 7.34 (dd, J = 8.6 Hz, J‘ = 2.6 Hz, 1H, H_f), 7.19 (dd, J = 8.4 Hz, J = 2.6 Hz, 1H, H_c), 5.83 (ddt, J = 17.1 Hz, J‘ = 10.3 Hz, J“ = 6.6 Hz, 1H, H_l), 5.08-4.95 (m, 2H, H_m), 4.16 (t, J = 6.4 Hz, 2H, H_h), 2.10 (m, 2H, H_k), 1.77 (m, 2H, H_i), 1.53 (m, 2H, H_j). ^{13}C NMR (d_6-DMSO, 75 MHz) δ 181.41, 181.04, 163.47, 163.23, 138.47, 135.40, 135.36, 129.84, 129.40, 126.36, 125.22, 121.08, 120.41, 115.00, 112.24, 110.64, 68.24, 32.77, 27.90, 24.59. MS *m/z*: calcd. for $C_{20}H_{17}O_4$ [M-H$^+$] 321.1 found ESI (neg.) 320.9.

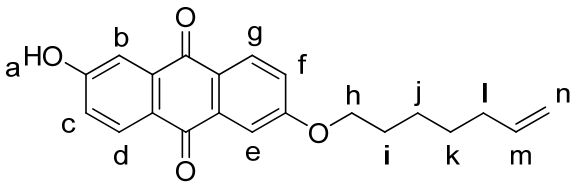

Compound 4.1b. ^{1}H NMR (d_6-DMSO, 300 MHz) δ 11.03 (s, 1H, H_a), 8.09 (d, J = 8.6 Hz, 1H, H_g), 8.06 (d, J = 8.6 Hz, 1H, H_d), 7.54 (d, J = 2.6 Hz, 1H, H_e), 7.48 (d, J = 2.5 Hz, 1H, H_b), 7.36 (dd, J = 8.7 Hz, J’ = 2.7 Hz, 1H, H_f), 7.20 (dd, J = 2.6 Hz, J’ = 8.6 Hz, 1H, H_c), 5.80 (ddt, J = 17.0 Hz, J’ = 10.2 Hz, J” = 6.6 Hz, 1H, H_m), 5.05-4.90 (m, 2H, H_n), 4.16 (t, J = 6.7 Hz, 2H, H_h), 2.03 (m, 2H, H_l), 1.76 (m, 2H, H_i), 1.49-1.30 (m, 4H, H_{j+k}). ^{13}C NMR (d_6-DMSO, 75 MHz) δ 182.26, 181.90, 164.33, 164.09, 139.53, 136.35, 130.71, 130.27, 127.20, 126.07, 121.94, 121.26, 115.68, 113.10, 111.48, 69.22, 33.98, 29.13, 28.81, 25.77. MS *m/z*: calcd. for $C_{21}H_{19}O_4$ [M-H$^+$] 335.1 found ESI (neg.) 335.0.

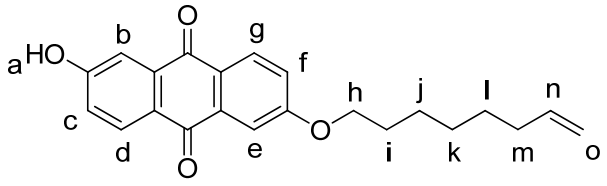

Compound 4.1c. ^{1}H NMR (d_6-DMSO, 300 MHz) δ 11.03 (s, 1H, H_a), 8.09 (d, J = 8.7 Hz, 1H, H_g), 8.06 (d, J = 8.7 Hz, 1H, H_d), 7.54 (d, J = 2.6 Hz, 1H, H_e), 7.48 (d, J = 2.7 Hz, 1H, H_b), 7.37 (dd, J = 8.7 Hz, J = 2.7 Hz, 1H, H_f), 7.20 (dd, J = 8.6 Hz, J = 2.6 Hz, 1H, H_c), 5.79 (ddt, J = 17.0 Hz, J’ = 10.2 Hz, J” = 6.6 Hz, 1H, H_n), 5.04-4.90 (m, 2H, H_o), 4.16 (t, J = 6.5 Hz, 2H, H_h), 2.03 (m, 2H, H_m), 1.76 (m, 2H, H_i), 1.49-1.30 (m, 6H, H_{j+k+l}). ^{13}C NMR (d_6-DMSO, 75 MHz) δ 182.22, 181.85, 164.29, 164.09, 139.62,

136.22, 136.15, 130.67, 130.22, 127.15, 126.02, 121.90, 121.19, 115.55, 113.08, 111.42, 69.21, 33.98, 29.25, 29.07, 26.07. MS *m/z*: calcd. for $C_{22}H_{21}O_4$ [M-H$^+$] 349.1 found ESI (neg.) 349.0.

General procedure for the bis-substitution of α, α'-dibromoxylenes.

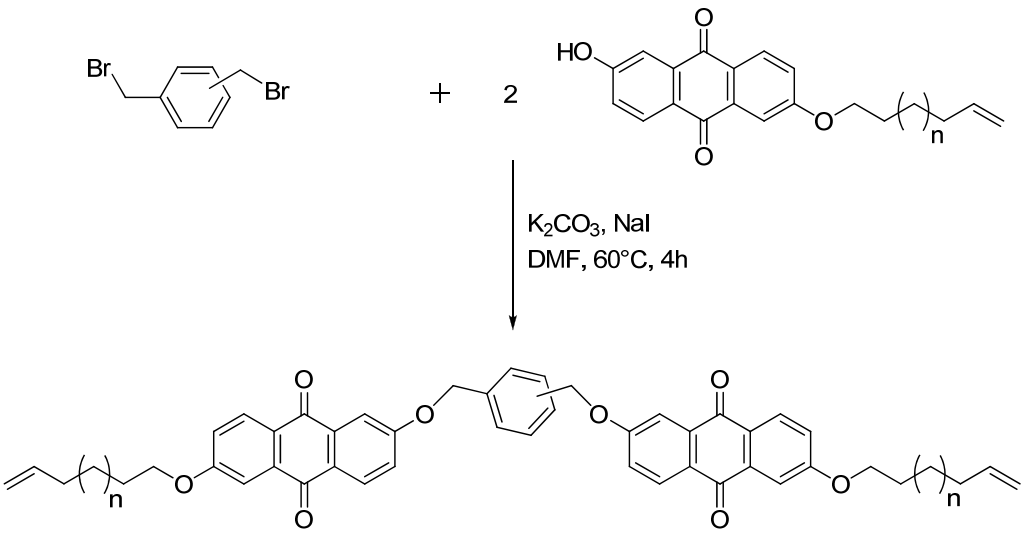

Dry K_2CO_3 (1.23 g - 8.91 mmol), α,α'-dibromoxylene (1.17 g – 4.0 mmol) and a catalytic amount of sodium iodide were added to a solution of monoalkylated anthraflavic acid **4.1a-c** (8.0 mmol – 2.0 eq.) in dry DMF (20-25 mL). The solution was heated to 60 ºC for 4-6 h, and the resulting suspension was filtrated. The corresponding solid was successively washed with methanol (30 mL) and diethyl ether (30 mL) to remove unreacted starting materials affording pure compounds without further purification (*p*-xylylene derivatives **4.2a**: n = 1, y = 74%; **4.2b**: n = 2, y = 67%; **4.2c**: n = 3, y = 54% - *m*-xylene derivatives **4.3a** : n = 1, y = 75%; **4.3b**: n = 2, 69%; **4.3c**: n = 3; 81%).

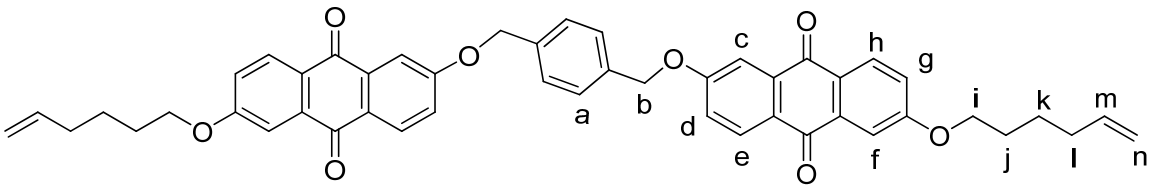

Compound 4.2a. ^{1}H NMR ($C_2D_2Cl_4$, 300 MHz, 383 K) δ 8.29 (d, J = 8.4 Hz, 2H, H_e), 8.28 (d, J = 8.4 Hz, 2H, H_h), 7.88 (d, J = 2.3 Hz, 2H, H_c), 7.77 (d, J = 2.3 Hz, 2H, H_f), 7.55 (s, 4H, H_a), 7.37 (dd, J = 8.4 Hz, J' = 2.5 Hz, 2H, H_d), 7.28 (dd, J = 8.4 Hz, J' = 2.5 Hz, 2H, H_g), 5.91 (ddt, J = 17.0 Hz, J' = 10.3 Hz, J' = 6.4 Hz, 2H, H_m), 5.33 (bs, 4H, H_b), 5.17-5.02 (m, 4H, H_n), 4.24 (t, J = 6.4 Hz, 4H, H_i), 2.21 (m, 4H, H_l), 1.94 (m,

4H, H_j), 1.68 (m, 4H, H_k). ^{13}C NMR could not be recorded given the insolubility of this compound. MS *m/z*: calcd. for $C_{48}H_{43}O_8$ [M+H$^+$] 747.30 found MALDI-TOF 747.16.

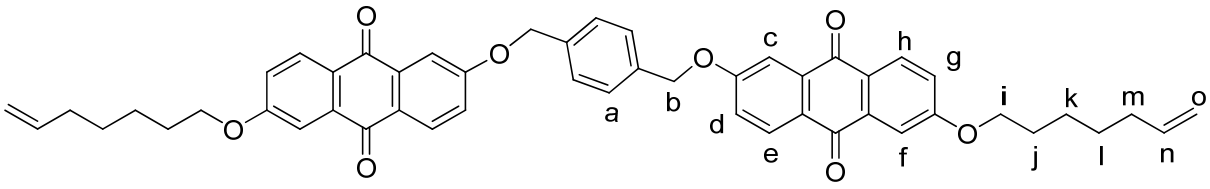

Compound 4.2b. ^1H NMR ($C_2D_2Cl_4$, 500 MHz, 353 K) δ 8.28 (d, J = 8.3 Hz, 2H, H_e), 8.25 (d, J = 8.3 Hz, 2H, H_h), 7.86 (d, J = 2.6 Hz, 2H, H_c), 7.75 (d, J = 2.5 Hz, 2H, H_f), 7.56 (s, 4H, H_a), 7.37 (dd, J = 2.6 Hz, J = 8.3 Hz, 2H, H_d), 7.28 (dd, J = 2.5 Hz, J = 8.3 Hz, 2H, H_g), 5.89 (m, 2H, H_n), 5.32 (brs, 4H, H_b), 5.05 (m, 4H, H_o), 4.21 (t, J = 6.6 Hz, 4H, H_i), 2.16 (m, 4H, H_m), 1.91 (m, 4H, H_j), 1.55 (m, 8H, H_{k+l}). ^{13}C NMR ($C_2D_2Cl_4$, 125 MHz, 353 K) δ 181.85, 181.72, 164.02, 163.41, 138.46, 136.00, 135.90, 135.78, 129.56, 128.06, 127.66, 126.99, 120.91, 120.69, 120.21, 114.39, 111.35, 111.03, 70.24, 68.80, 33.26, 28.74, 28.39, 25.25. MS *m/z*: calcd. for $C_{50}H_{47}O_8$ [M+H$^+$] 775.33 found MALDI-TOF 775.32.

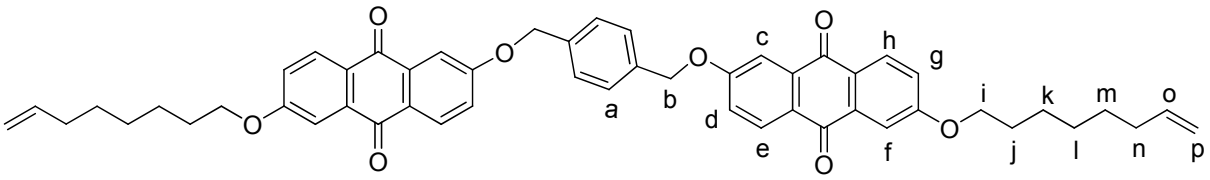

Compound 4.2c. ^1H NMR ($C_2D_2Cl_4$, 500 MHz, 353 K) δ 8.26 (bd, J = 7.8 Hz, 2H, H_e), 8.24 (bd, J = 8.6 Hz, 2H, H_h), 7.84 (bs, 2H, H_c), 7.74 (bs, 2H, H_f), 7.55 (bs, 4H, H_a), 7.35 (bd, J = 7.8 Hz, 2H, H_d), 7.26 (bd, J = 8.6 Hz, 2H, H_g), 5.87 (m, 2H, H_o), 5.31 (m, 4H, H_b), 5.05 (m, 4H, H_p), 4.19 (bt, 4H, H_i), 2.12 (m, 4H, H_n), 1.89 (m, 4H, H_j), 1.50 (m, 12H, H_{k+l+m}). ^{13}C NMR ($C_2D_2Cl_4$, 125 MHz, 353 K) δ 182.05, 181.91, 164.25, 163.61, 138.91, 136.22, 136.11, 135.65, 129.75, 128.87, 128.16, 127.75, 121.10, 120.90, 120.42, 114.39, 111.56, 111.24, 70.44, 69.06, 33.52, 29.04, 28.80, 28.74, 25.80. MS *m/z*: calcd. for $C_{52}H_{51}O_8$ [M+H$^+$] 803.36 found MALDI-TOF 803.34; calcd. for $C_{52}H_{50}O_8Na$ [M+Na$^+$] 824.34 found MALDI-TOF 824.35.

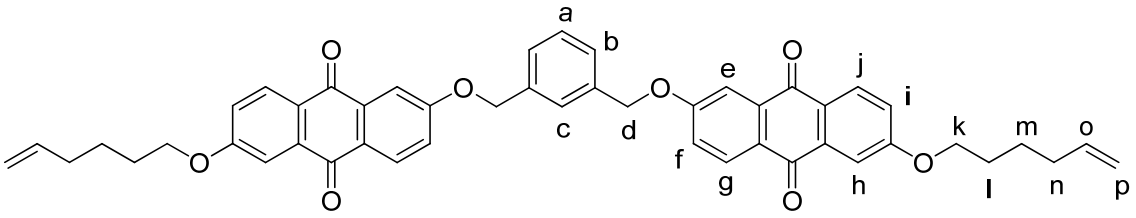

Compound 4.3a. ^{1}H NMR ($CDCl_3$, 300 MHz, 293 K) δ 8.23 (d, J = 8.6 Hz, 2H, H_g), 8.20 (d, J = 8.6 Hz, 2H, H_j), 7.79 (d, J = 2.6 Hz, 2H, H_e), 7.68 (d, J = 2.6 Hz, 2H, H_h), 7.58 (bs, 1H, H_a), 7.47 (m, 3H, H_{b+c}), 7.30 (dd, J = 8.7 Hz, J‘ = 2.7 Hz, 2H, H_f), 7.21 (dd, J = 8.7 Hz, J‘ = 2.6 Hz, 2H, H_i), 5.84 (ddt, J = 17.0 Hz, J‘ = 10.3 Hz, J“ = 6.7 Hz, 2H, H_o), 5.27 (s, 4H, H_d), 5.09-4.96 (m, 4H, H_p), 4.14 (t, J = 6.4 Hz, 4H, H_k), 2.15 (m, 4H, H_n), 1.87 (m, 4H, H_l), 1.61 (m, 4H, H_m). ^{13}C NMR ($CDCl_3$, 300 MHz) δ 182.18, 182.03, 163.95, 163.30, 138.27, 136.40, 135.81, 135.72, 129.72, 129.65, 129.20, 127.51, 127.39, 126.91, 126.56, 121.18, 120.95, 114.96, 110.87, 110.48, 70.21, 68.55, 33.33, 28.42, 25.17. MS *m/z*: calcd. for $C_{48}H_{43}O_8$ [M+H$^+$] 747.30 found MALDI-TOF 747.23.

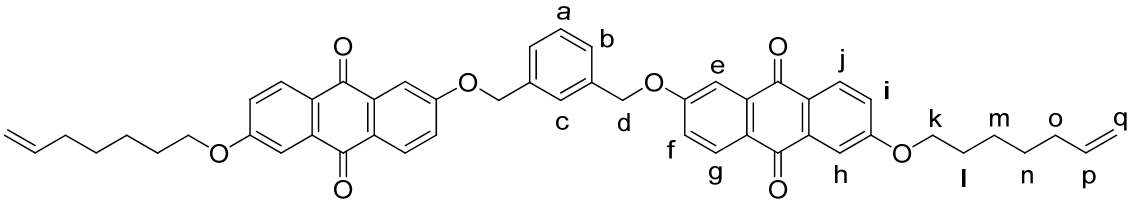

Compound 4.3b. ^{1}H NMR ($CDCl_3$, 300 MHz, 293 K) δ 8.22 (d, J = 9.2 Hz, 2H, H_g), 8.19 (d, J = 8.9 Hz, 2H, H_j), 7.78 (d, J = 2.6 Hz, 2H, H_e), 7.67 (d, J = 2.6 Hz, 2H, H_h), 7.57 (bs, 1H, H_a), 7.49 (m, 3H, H_{b+c}), 7.34 (dd, J = 8.7 Hz, J‘ = 2.6 Hz, 2H, H_f), 7.24 (dd, J = 8.7 Hz, J‘ = 2.6 Hz, 2H, H_i), 5.84 (ddt, J = 17.0 Hz, J‘ = 10.3 Hz, J“ = 6.7 Hz, 2H, H_p), 5.28 (s, 4H, H_d), 5.07-4.96 (m, 4H, H_q), 4.14 (t, J = 6.5 Hz, 4H, H_k), 2.10 (m, 4H, H_o), 1.86 (m, 4H, H_l), 1.49 (m, 8H, H_{m+n}). ^{13}C NMR ($CDCl_3$, 300 MHz) δ 182.23, 182.09, 164.04, 163.36, 138.71, 136.47, 135.88, 135.78, 129.78, 129.71, 129.26, 127.57, 127.46, 126.96, 126.62, 121.23, 121.00, 114.64, 110.93, 110.57, 70.28, 68.75, 33.68, 28.92, 28.61, 25.48. MS *m/z*: calcd. for $C_{50}H_{47}O_8$ [M+H$^+$] 775.33 found MALDI-TOF 775.26.

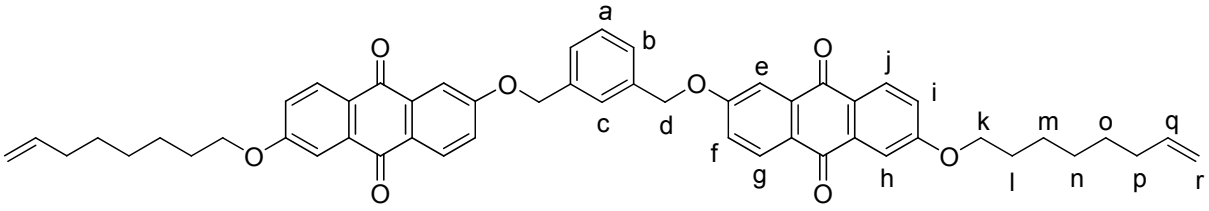

Compound 4.3c. ^{1}H NMR ($CDCl_3$, 300 MHz, 293 K) δ 8.22 (d, J = 8.8 Hz, 2H, H_g), 8.19 (d, J = 8.8 Hz, 2H, H_j), 7.78 (d, J = 2.6 Hz, 2H, H_e), 7.67 (d, J = 2.6 Hz, 2H, H_h), 7.57 (bs, 1H, H_a), 7.49 (m, 3H, $H_{b+c\ c}$), 7.34 (dd, J = 8.7 Hz, J‘ = 2.6 Hz, 2H, H_f), 7.24 (dd, J = 8.7 Hz, J‘ = 2.6 Hz, 2H, H_i), 5.84 (ddt, J = 17.0 Hz, J‘ = 10.2 Hz, J“ = 6.7 Hz, 2H, H_q), 5.28 (s, 4H, H_d), 5.06-4.94 (m, 4H, H_r), 4.13 (t, J = 6.5 Hz, 4H, H_k), 2.10 (m, 4H, H_p), 1.85 (m, 4H, H_l), 1.54-1.37 (m, 12H, H_{m+n+o}). ^{13}C NMR ($CDCl_3$, 300 MHz) δ

182.19, 182.03, 164.00, 163.30, 138.91, 136.40, 135.82, 135.71, 129.71, 129.64, 129.20, 127.50, 127.39, 126.88, 126.56, 121.16, 120.94, 114.36, 110.86, 110.50, 77.00, 70.21, 68.73, 53.41, 33.67, 28.95, 28.76, 25.78. MS *m/z*: calcd. for $C_{52}H_{51}O_8$ [M+H$^+$] 803.36 found MALDI-TOF 803.29.

General procedure for the Mitsunobu reaction:

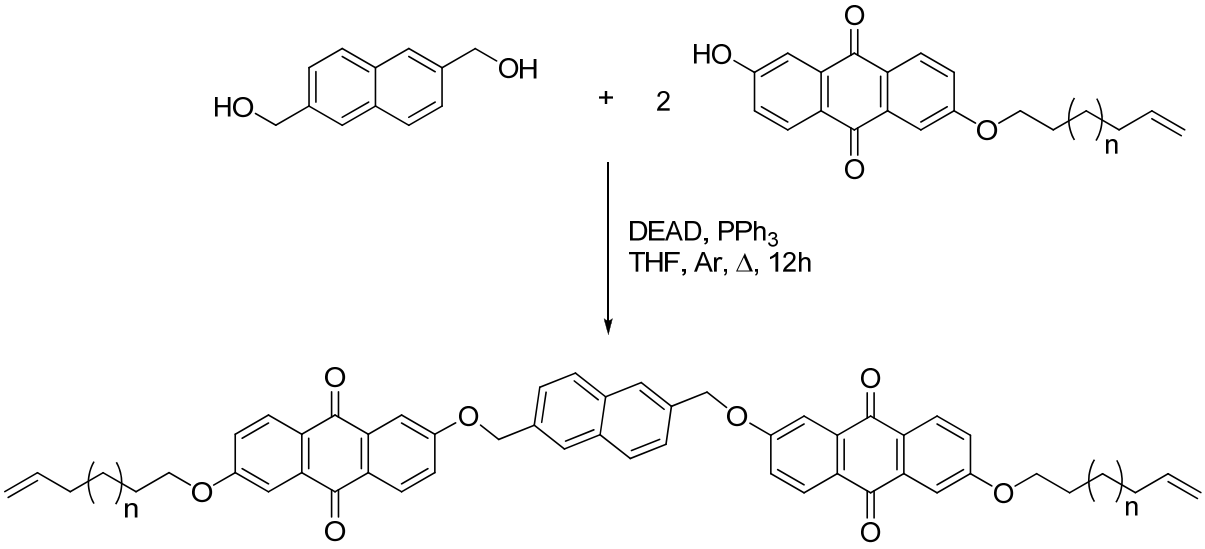

2,6-Bis(hydroxymethyl)naphthalene (56 mg – 0.3 mmol), triphenylphosphine (315 mg – 1.2 mmol) and the desired monosubstituted anthraflavic acid **4.1a-c** (0.6 mmol) were dissolved in freshly distilled THF (30 mL). Then, diethyl azodicarboxylate (209 mg – 1.2 mmol) was added dropwise under inert atmosphere and the mixture was refluxed for 12 hours. Afterwards, at room temperature, THF was cautiously removed after settling. The solid was rinsed with dichloromethane (30 mL) and pentane (30 mL) affording the pure desired compound (**4.4a**: n = 1, y = 65%; **4.4b**: n = 2, y = 68%, **4.4c**: n = 3, y = 69%). ^{13}C NMR could not be recorded given the low solubility of these derivatives even at high temperature.

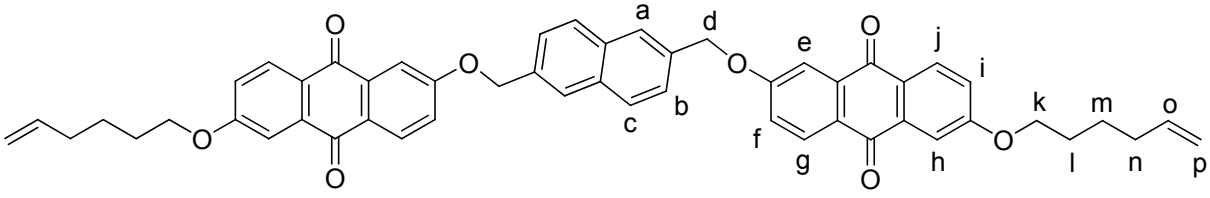

Compound 4.4a. ^{1}H NMR (300 MHz, $C_2D_2Cl_4$, 393 K) δ 8.31 (d, J = 8.3 Hz, 2H, H_g), 8.28 (d, J = 8.4 Hz, 2H, H_j), 7.97 (m, 6H, H_{a+c+e}), 7.79 (bs, 2H, H_h), 7.65 (bd, J = 8.4 Hz, 2H, H_b), 7.41 (dd, J = 8.4 Hz, J' = 2.0 Hz, 2H, H_f), 7.29 (bd, J = 8.6 Hz, 2H, H_i),

5.91 (m, 2H, H_o), 5.49 (s, 4H, H_d), 5.16-5.06 (m, 4H, H_p), 4.25 (t, J = 6.2 Hz, 4H, H_k), 2.24 (m, 4H, H_n), 1.95 (m, 4H, H_l), 1.69 (m, 4H, H_m). MS *m/z*: calcd. for $C_{52}H_{45}O_8$ [M+H$^+$] 797.31 found MALDI-TOF 797.32.

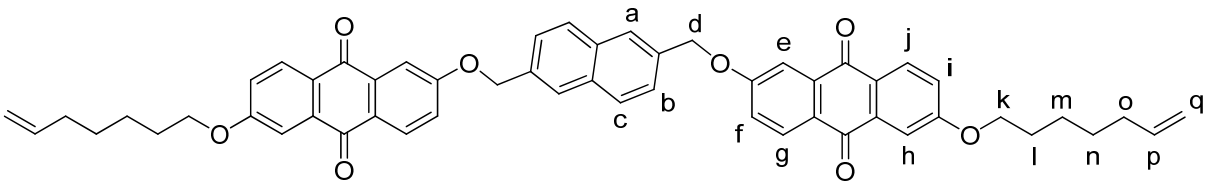

Compound 4.4b. ^{1}H NMR (300 MHz, $C_2D_2Cl_4$, 393 K) δ 8.30 (d, J = 8.5 Hz, 2H, H_g), 8.28 (d, J = 8.5 Hz, 2H, H_j), 7.96 (m, 6H, H_{a+c+e}), 7.79 (d, J = 2.6 Hz, 2H, H_h), 7.65 (dd, J = 8.4 Hz, J' = 1.2 Hz, 2H, H_b), 7.41 (dd, J = 8.6 Hz, J' = 2.7 Hz, 2H, H_f), 7.28 (dd, J = 8.6 Hz, J' = 2.7 Hz, 2H, H_i), 5.91 (ddt, J = 17.0 Hz, J' = 10.3 Hz, J" = 6.6 Hz, 2H, H_p), 5.49 (s, 4H, H_d), 5.13-5.02 (m, 4H, H_q), 4.24 (t, J = 6.5 Hz, 4H, H_k), 2.18 (m, 4H, H_o), 1.93 (m, 4H, H_l), 1.60 (m, 8H, H_{m+n}). MS *m/z*: calcd. for $C_{54}H_{49}O_8$ [M+H$^+$] 825.34 found MALDI-TOF 825.29.

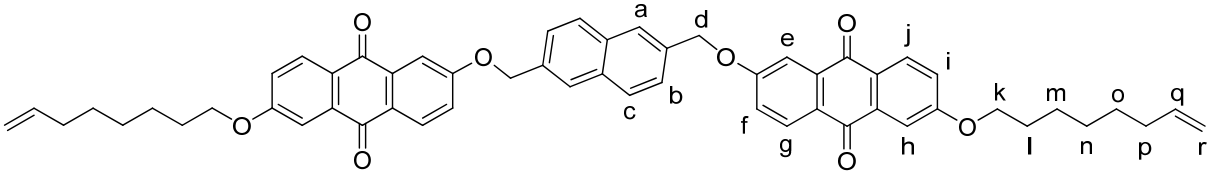

Compound 4.4c. ^{1}H NMR (300 MHz, $C_2D_2Cl_4$, 393 K) δ 8.30 (d, J = 8.5 Hz, 2H, H_g), 8.27 (d, J = 8.5 Hz, 2H, H_j), 7.98-7.94 (m, 6H, H_{a+c+e}), 7.77 (bs, 2H, H_h), 7.64 (bd, J = 8.4 Hz, 2H, H_b), 7.41 (bd, J = 8.6 Hz, 2H, H_f), 7.28 (bd, J = 8.6 Hz, 2H, H_i), 5.91 (bs, 2H, H_q), 5.49 (s, 4H, H_d), 5.12-4.97 (m, 4H, H_r), 4.23 (bt, 4H, H_k), 2.14 (m, 4H, H_p), 1.92 (m, 4H, H_l), 1.63-1.35 (m, 12H, H_{m+n+o}). MS *m/z*: calcd. for $C_{56}H_{53}O_8$ [M+H$^+$] 853.37 found MALDI-TOF 853.31.

General procedure for the Wittig-Horner reaction

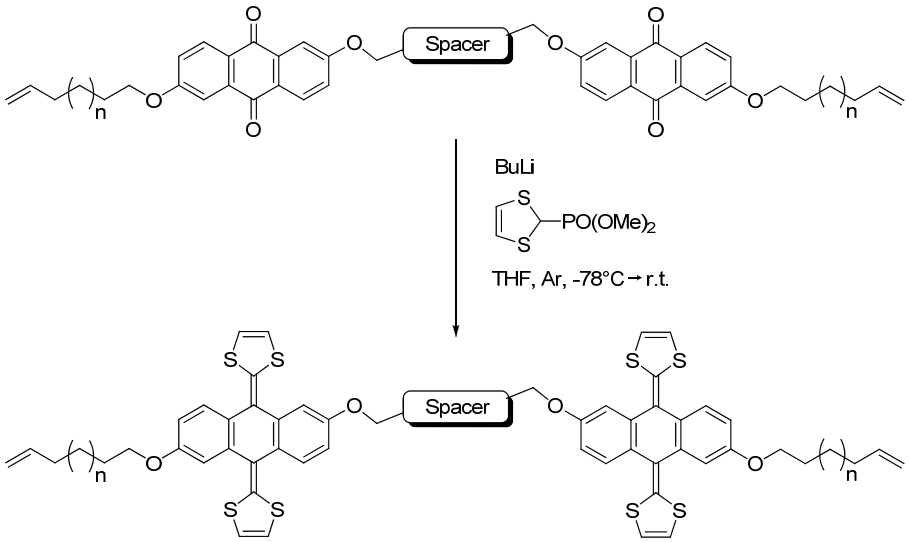

A solution of dimethyl 1,3-dithiol-2-ylphosphonate 0.343 mg (1.62 mmol) in 5 mL of dry THF was cooled to –78 ºC, and butyllithium 2.0 M in hexanes (0.85 mL, 1.70 mmol) was added. The solution was left to stir at –78 ºC for 30 min, with appearance of a precipitate. In the meantime, a suspension of anthraquinone precursor (0.135 mmol) in dry THF (5 mL) was sonicated for *ca.* 30 min. The resulting suspension was added to the phosphorous ylide suspension, and the cooling bath immediately removed. The mixture was allowed to warm to room temperature and left to stir for 2 h in the case of the *p*-xylylene and overnight with *m*-xylylene and naphthalene spacers. The resulting solution was quenched with methanol, with precipitation of a yellow solid. The solid was filtrated, redissolved in CH_2Cl_2, and subjected to column chromatography (CH_2Cl_2:Hexane 2:1 to 3:1) to obtain the pure product as a bright yellow solid.

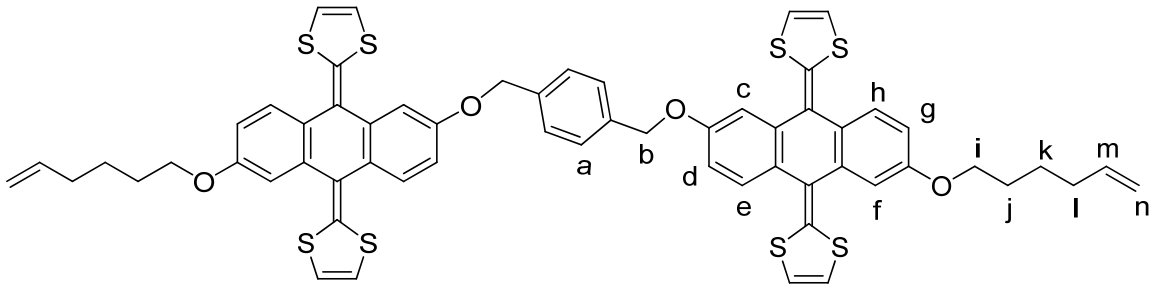

Compound 4.5a. ^{1}H NMR ($CDCl_3$, 500 MHz) δ 7.60 (d, J = 8.4 Hz, 2H, H_e), 7.56 (bd, 2H, H_h), 7.50 (s, 4H, H_a), 7.35 (bd, J = 7.8 Hz, 2H, H_c), 7.22 (bs, 2H, H_f), 6.90 (dd, J = 8.4 Hz, J = 2.4 Hz, 2H, H_d), 6.81 (bs, 2H, H_g), 6.23 (m, 8H, $H_{dithiole}$), 5.87 (m, 2H, H_m), 5.17 (m, 4H, H_b), 5.04 (m, 4H, H_n), 4.04 (bt, 4H, H_i), 2.17 (m, 4H, H_l), 1.85 (m, 4H, H_j), 1.61 (m, 6H, H_k + H_2O). ^{13}C NMR ($CDCl_3$, 125 MHz) δ 157.49, 156.99,

139.01, 137.45, 137.34, 137.20, 134.43, 134.22, 129.13, 128.70, 128.14, 126.53, 126.45, 122.46, 122.20, 117.55, 117.44, 115.15, 112.79, 112.44, 111.64, 111.35, 70.29, 68.41, 33.89, 29.16, 25.78. MS *m/z*: calcd. For $C_{60}H_{50}O_4S_8$ [M^+] 1090.15 found MALDI-TOF 1090.15.

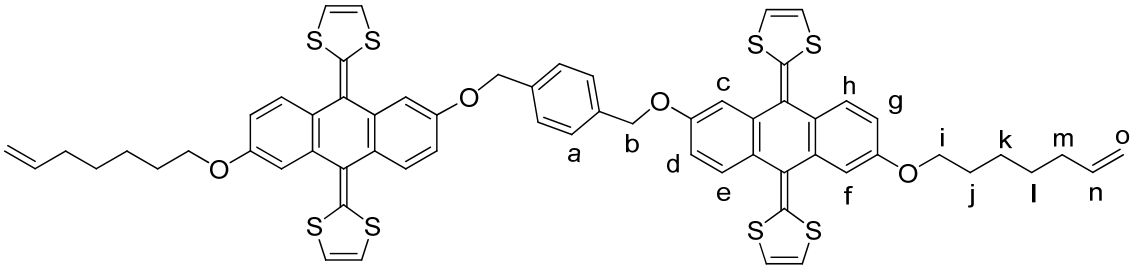

Compound 4.5b. ^{1}H NMR ($CDCl_3$, 500 MHz) δ 7.60 (d, J = 8.5 Hz, 2H, H_e), 7.57 (bd, 2H, H_h), 7.50 (s, 4H, H_a), 7.27 (bs, 2H, H_c), 7.22 (bs, 2H, H_f), 6.90 (bd, J = 8.5 Hz, 2H, H_d), 6.81 (bm, 2H, H_g), 6.23 (m, 8H, $H_{dithiole}$), 5.87 (m, 2H, H_n), 5.17 (m, 4H, H_b), 5.01 (m, 4H, H_o), 4.03 (bt, 4H, H_i), 2.12 (m, 4H, H_m), 1.84 (m, 4H, H_j), 1.51 (m, 8H, H_{k+l}). ^{13}C NMR ($CDCl_3$, 125 MHz) δ 157.10, 156.57, 138.89, 137.04, 136.93, 136.79, 133.99, 133.80, 128.71, 128.26, 127.75, 126.12, 126.04, 122.05, 121.79, 117.16, 117.05, 114.47, 112.45, 112.37, 112.04, 111.97, 111.20, 111.15, 110.93, 110.90, 69.87, 68.12, 33.73, 29.15, 28.69, 25.70, 25.59. MS *m/z*: calcd. for $C_{62}H_{54}O_4S_8$ [M+] 1118.18 found MALDI-TOF 1118.15.

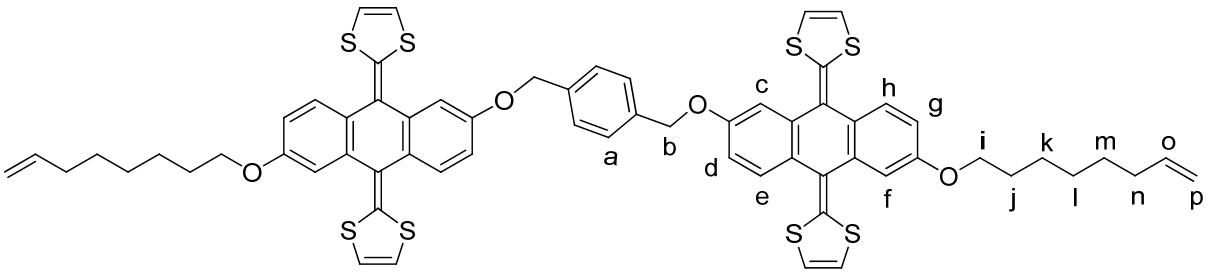

Compound 4.5c. ^{1}H NMR ($CDCl_3$, 500 MHz) δ 7.60 (d, J = 8.4 Hz, 2H, H_e), 7.56 (bd, J = 9.3 Hz, 2H, H_h), 7.50 (s, 4H, H_a), 7.24 (bs, 2H, H_c), 7.20 (bs, 2H, H_f), 6.91 (bd, J = 8.4 Hz, 2H, H_d), 6.81 (bm, 2H, H_g), 6.24 (m, 8H, $H_{dithiole}$), 5.85 (m, 2H, H_o), 5.17 (m, 4H, H_b), 5.00 (m, 4H, H_p), 4.03 (bt, 4H, H_i), 2.10 (m, 4H, H_n), 1.83 (m, 4H, H_j), 1.46 (m, 12H, H_{k+l+m}). ^{13}C NMR ($CDCl_3$, 125 MHz) δ 157.53, 156.99, 139.47, 137.46, 137.33, 137.20, 134.38, 134.19, 129.14, 128.66, 128.14, 126.53, 126.44, 122.48, 122.23, 117.54, 117.45, 114.70, 112.46, 111.64, 111.36, 70.30, 68.60, 34.14, 30.11, 29.65, 29.30, 29.26, 29.34. MS *m/z*: calcd. for $C_{64}H_{58}O_4S_8$ [M^+] 1146.21 found MALDI-TOF 1146.20.

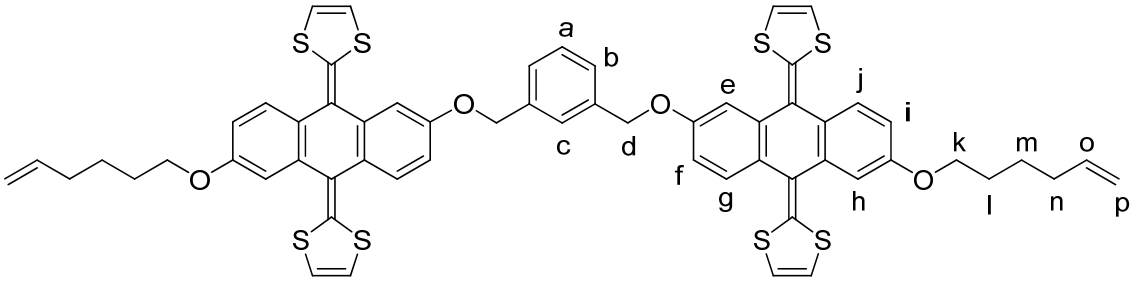

Compound 4.6a. ^{1}H NMR (300 MHz) : 7.57 (bs, 5H, H_{a+g+j}), 7.41 (bs, 3H, H_{b+c}), 7.27 (bs, 2H, H_e), 7.22 (bs, 2H, H_h), 6.87 (bd, J = 7.9 Hz, 2H, H_f), 6.80 (bd, J = 7.9 Hz, 2H, H_i), 6.30-6.15 (m, 8H, $H_{dithiole}$), 5.83 (m, 2H, H_o), 5.17 (s, 4H, H_d), 5.10-4.93 (m, 4H, H_p), 4.04 (bt, 4H, H_k), 2.14 (m, 4H, H_n), 1.84 (m, 4H, H_l), 1.60 (m, 4H, H_m). ^{13}C NMR (75 MHz):δ 157.03, 156.60, 138.56, 137.50, 136.98, 136.91, 133.96, 133.83, 128.91, 128.69, 128.25, 126.90, 126.40, 126.29, 126.07, 126.01, 121.99, 121.81, 117.19, 117.06, 117.00, 114.72, 112.35, 111.95, 111.28, 110.88, 70.02, 67.96, 33.45, 28.72, 25.33. MS *m/z*: calcd. for $C_{60}H_{50}O_4S_8$ [M^+] 1090.15 found MALDI-TOF 1090.03.

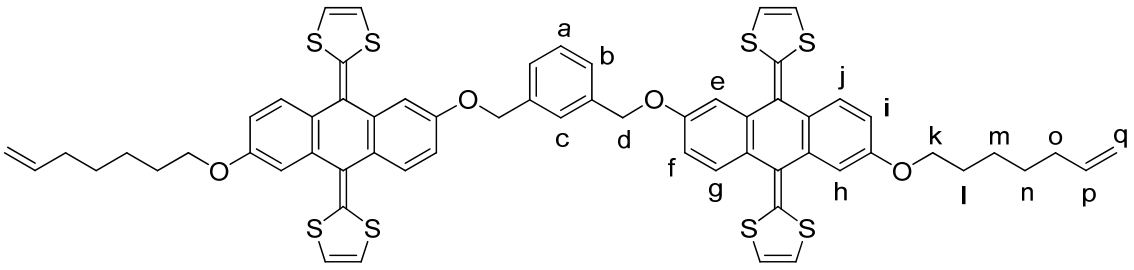

Compound 4.6b. ^{1}H NMR (300 MHz) δ 7.59-7.55 (m, 5H, H_{a+g+j}), 7.41 (m, 3H, H_{b+c}), 7.27 (d, J = 2.5 Hz, 2H, H_e), 7.20 (d, J = 2.5 Hz, 2H, H_h), 6.87 (dd, J = 8.6 Hz, J' = 2.5 Hz, 2H, H_f), 6.79 (dd, J = 8.5 Hz, J' = 2.5 Hz, 2H, H_i), 6.30-6.20 (m, 8H, $H_{dithiole}$), 5.83 (ddt, J = 17.0 Hz, J' = 10.2 Hz, J" = 6.7 Hz, 2H, H_p), 5.16 (s, 4H, H_d), 5.06-4.93 (m, 2H, H_q), 4.01 (t, J = 6.5 Hz, 4H, H_k), 2.09 (m, 4H, H_o), 1.82 (m, 4H, H_l), 1.48 (m, 8H, H_{m+n}). ^{13}C NMR (75 MHz) □ 157.05, 156.60, 138.84, 137.50, 136.99, 136.91, 133.93, 133.80, 128.92, 128.70, 128.23, 126.90, 126.40, 126.31, 126.08, 126.01, 122.01, 121.82, 117.19, 117.07, 117.00, 114.43, 112.36, 111.98, 111.28, 110.87, 70.02, 68.09, 33.70, 29.12, 28.66, 25.56. MS *m/z*: calcd. for $C_{62}H_{54}O_4S_8$ [M^+] 1118.18 found MALDI-TOF 1118.07.

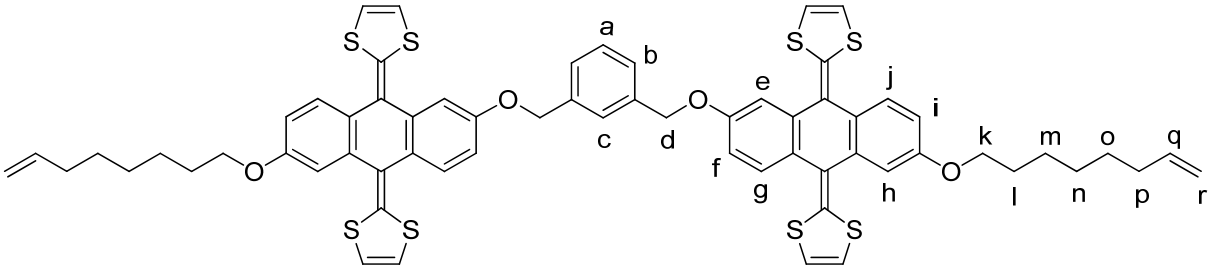

Compound 4.6c. ^{1}H NMR (300 MHz) δ 7.56 (m, 5H, H_{a+g+j}), 7.41 (m, 3H, H_{b+c}), 7.27 (d, J = 2.5 Hz, 2H, H_e), 7.20 (d, J = 2.5 Hz, 2H, H_h), 6.87 (dd, J = 8.6 Hz, J' = 2.5 Hz, H_f), 6.79 (dd, J = 8.6 Hz, J' = 2.5 Hz, 2H, H_i), 6.26 (m, 8H, $H_{dithiole}$), 5.82 (ddt, J = 17.0 Hz, J' = 10.2 Hz, J" = 6.7 Hz, 2H, H_q), 5.16 (s, 4H, H_d), 5.04-4.92 (m, 4H, H_r), 4.01 (t, J = 6.4 Hz, 4H, H_k), 2.07 (m, 4H, H_p), 1.81 (m, 4H, H_l), 1.54-1.36 (m, 12 H, H_{m+n+o}). ^{13}C NMR (75 MHz) δ 157.08, 156.60, 139.04, 137.50, 136.99, 136.90, 133.92, 133.79, 128.92, 128.70, 128.22, 126.90, 126.40, 126.28, 126.08, 126.00, 122.01, 121.84, 117.19, 117.07, 117.00, 114.27, 112.36, 111.98, 111.28, 110.88, 70.02, 68.15, 33.71, 29.21, 28.86, 28.83, 25.91. MS *m/z*: calcd. for $C_{64}H_{58}O_4S_8$ [M^+] 1146.21 found MALDI-TOF 1146.06.

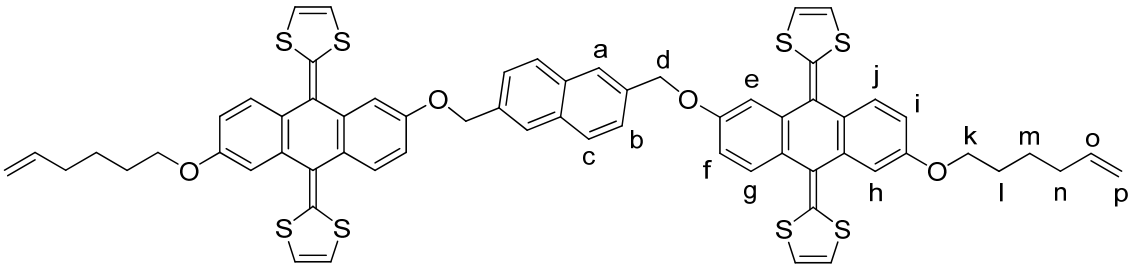

Compound 4.7a. ^{1}H NMR (300 MHz) δ 7.91 (bs, 2H, H_a), 7.88 (d, J = 8.4 Hz, 2H, H_c), 7.59-7.52 (m, 6H, H_{b+g+j}), 7.23 (d, J = 2.5 Hz, 2H, H_e), 7.19 (d, J = 2.5 Hz, 2H, H_h), 6.93 (dd, J = 8.5 Hz, J' = 2.4 Hz, 2H, H_f), 6.77 (dd, J = 8.5 Hz, J' = 1.9 Hz, 2H, H_i), 6.27 (s, 2H, $H_{dithiole}$), 6.25 (s, 2H, $H_{dithiole}$), 6.13 (m, 2H, $H_{dithiole}$), 5.94 (d, J = 6.7 Hz, 2H, $H_{dithiole}$), 5.84 (ddt, J = 16.8 Hz , J' = 10.2 Hz, J" = 6.7 Hz, 2H, H_o), 5.36 (d, J_{AB} = 12.3 Hz, 2H, H_d), 5.29 (d, J_{AB} = 12.3 Hz, 2H, $H_{d'}$), 5.07-4.95 (m, 4H, H_p), 4.01 (bt, 6.5 Hz, 4H, H_k), 2.13 (m, 4H, H_n), 1.81 (m, 4H, H_l), 1.59 (m, 4H, H_m). ^{13}C NMR (75 MHz) δ 157.02, 156.43, 138.56, 136.94, 136.87, 134.78, 134.11, 133.84, 133.71, 132.96, 128.69, 128.53, 128.25, 126.17, 126.07, 125.99, 125.51, 122.01, 121.61, 117.11, 117.04, 116.95, 114.71, 112.77 , 112.70 , 111.99, 111.28, 110.86, 70.24, 67.96, 33.45, 28.71, 25.33. MS *m/z*: calcd. for $C_{64}H_{52}O_4S_8$ [M^+] 1140.16 found MALDI-TOF 1140.07.

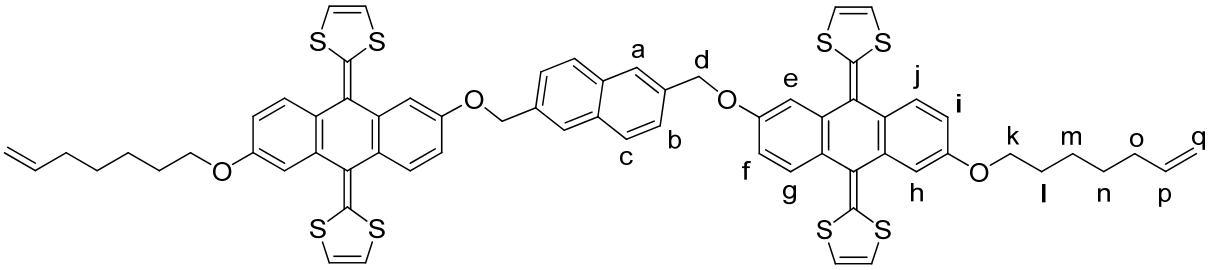

Compound 4.7b. ^{1}H NMR (300 MHz) δ 7.91 (s, 2H, H_a), 7.87 (d, J = 8.4 Hz, 2H, H_c), 7.60-7.50 (m, 6H, H_{b+g+j}), 7.23 (d, J = 2.5 Hz, 2H, H_e), 7.18 (d, J = 2.5 Hz, 2H, H_h), 6.93 (dd, J = 8.5 Hz, J' = 2.5 Hz, 2H, H_f), 6.77 (dd, J = 8.5 Hz, J' = 2.3 Hz, 2H, H_i), 6.27 (s, 2H, $H_{dithiole}$), 6.24 (s, 2H, $H_{dithiole}$), 6.14 (d, J = 6.2 Hz, 1H, $H_{dithiole}$), 6.12 (d, J = 6.6 Hz, 1H, $H_{dithiole}$), 5.94 (d, J = 6.7 Hz, 2H, $H_{dithiole}$), 5.82 (ddt, J = 17.0 Hz, J' = 10.2 Hz, J" = 6.7 Hz, 2H, H_p), 5.36 (d, J_{AB} = 12.8 Hz, 2H, H_d), 5.28 (d, J_{AB} = 12.8 Hz, 2H, $H_{d'}$), 5.05-4.93 (m, 4H, H_q), 4.00 (bt, J = 6.4 Hz, 4H, H_k), 2.09 (m, 4H, H_o), 1.81 (m, 4H, H_l), 1.48 (m, 8H, H_{m+n}). ^{13}C NMR (75 MHz) δ 157.04, 156.43, 138.84, 136.94, 136.86, 134.78, 134.09, 133.83, 133.73, 132.96, 128.69, 128.52, 128.23, 126.17, 126.07, 125.98, 125.51, 122.02, 121.62, 117.10, 117.04, 116.95, 114.43, 112.76, 112.73, 112.00, 111.28, 110.86, 70.23, 68.09, 33.69, 29.11, 28.65, 25.55. MS *m/z*: calcd. for $C_{66}H_{56}O_4S_8$ [M^+] 1168.19 found MALDI-TOF 1168.11.

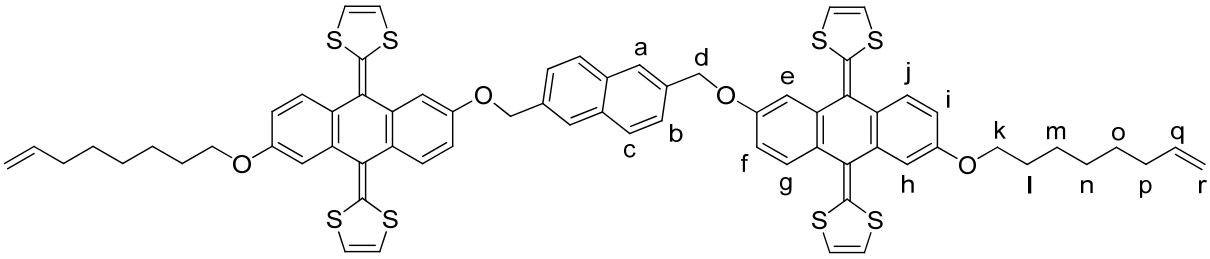

Compound 4.7c. ^{1}H NMR (300 MHz) δ 7.91 (s, 2H, H_a), 7.87 (d, J = 8.5 Hz, 2H, H_c), 7.59-7.52 (m, 6H, H_{b+g+j}), 7.23 (d, J = 2.5 Hz, 2H, H_e), 7.18 (d, J = 2.5 Hz, 2H, H_h), 6.92 (dd, J = 8.5 Hz, J' = 2.5 Hz, 2H, H_f), 6.77 (dd, J = 8.5 Hz, J' = 2.0 Hz, 2H, H_i), 6.26 (s, 2H, $H_{dithiole}$), 6.24 (s, 2H, $H_{dithiole}$), 6.13 (d, J = 6.2 Hz, 1H, $H_{dithiole}$), 6.12 (d, J = 6.6 Hz, 1H, $H_{dithiole}$), 5.94 (d, J = 6.7 Hz, 2H, $H_{dithiole}$), 5.82 (ddt, J = 17.0 Hz, J' = 10.2 Hz, J" = 6.7 Hz, 2H, H_q), 5.36 (d, J_{AB} = 12.5 Hz, 2H, H_d), 5.28 (d, J_{AB} = 12.5 Hz, 2H, $H_{d'}$), 5.03-4.92 (m, 4H, H_r), 4.00 (bt, J = 6.4 Hz, 4H, H_k), 2.06 (m, 4H, H_p), 1.80 (m, 4H, H_l), 1.49-1.36 (m, 12H, H_{m+n+o}). ^{13}C NMR (75 MHz) δ 157.06, 156.43, 139.04, 136.94, 136.86, 134.78, 134.08, 133.82, 133.72, 132.96, 128.69, 128.52, 128.21, 126.18, 126.07, 125.98, 125.51, 122.02, 121.63, 117.10, 117.04, 116.95, 114.26, 112.75, 112.72, 112.00, 111.28, 110.87, 70.23, 68.14, 33.71, 29.21, 28.86, 28.82, 25.90. MS *m/z*: calcd. for $C_{68}H_{60}O_4S_8$ [M^+] 1196.23 found MALDI-TOF 1196.15.

General procedure for the metathesis reaction

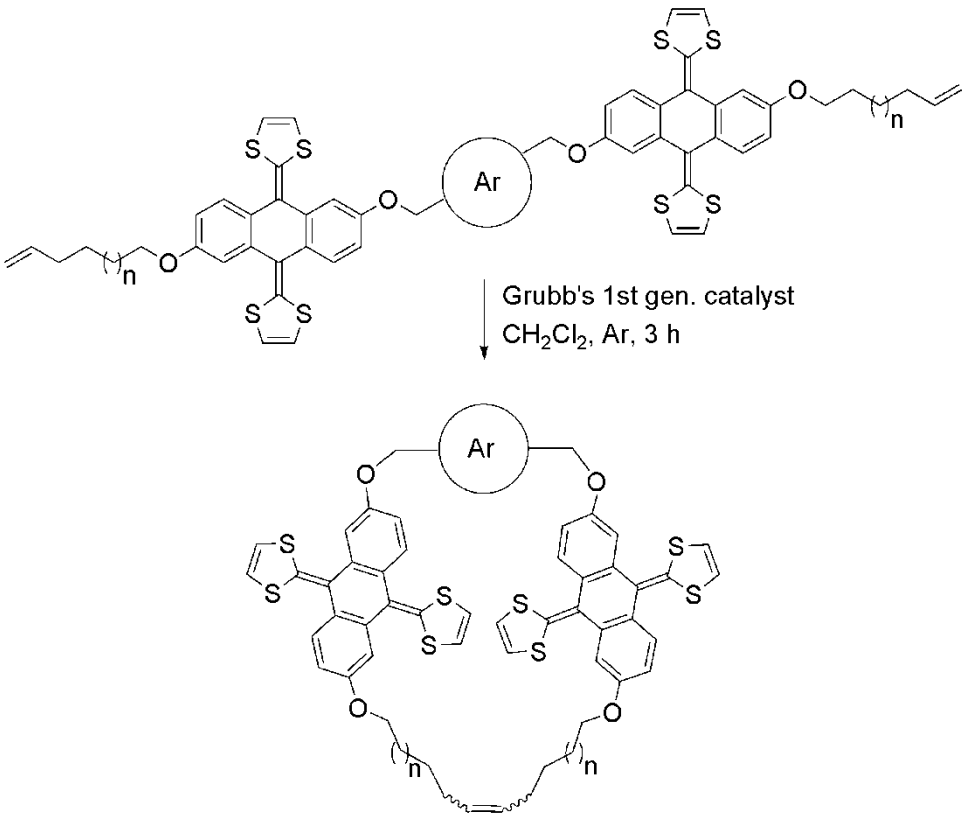

A 10^{-4} M solution of bis(exTTF) **5-7** was prepared in dichloromethane and was degassed by nitrogen bubbling during 30 minutes. Then, a catalytic amount of benzylidene-bis(tricyclohexylphosphine)-dichlororuthenium was introduced and the mixture was stirred for three hours at room temperature. The mixture was filtered on celite and concentrated in vacuo. The desired macrocycles were finally isolated by silica gel chromatography (eluent: CH_2Cl_2/Hexane: 2/1 to 3/1). Most products show moderate solubility and complicated ^{1}H NMR, consistent with an asymmetric molecule in several conformations in slow chemical exchange at NMR timescale (see H. Isla *et al., J. Am. Chem. Soc.* **2010**, *132*, 1772–1773). Their identity and purity was unambiguously established by ^{1}H NMR and HRMS.

p-Xylmac10 (n = 1). Yield: 90%; ^{1}H NMR (DMSO-d_6, 300 MHz, 298 K) δ 7.39- 7.29 (m, 2H), 7.30- 7.18 (m, 4H), 6.93- 6.84 (m, 1H), 6.84- 6.63 (m, 7H), 6.61- 6.50 (m, 4H), 6.34- 6.26 (m, 1.5H), 6.10- 6.01 (m, 1.5H), 6.00- 5.84 (m, 1H), 5.33- 4.95 (m, 8H), 3.95- 3.76 (m, 1.5H), 3.76- 3.55 (m, 1H), 3.43- 3.25 (m, 1.5H), 1.99- 1.80 (m, 4H), 1.59- 1.42 (m, 4H), 1.39- 1.26 (m, 4H) ppm. MS *m/z*: calcd. for $C_{58}H_{46}O_4S_8$ [M^+] 1062.11618 found HR-ESI 1062.11522.

p-Xylmac12 (n = 2). See H. Isla *et al., J. Am. Chem. Soc.* **2010**, *132*, 1772–1773.

p-Xylmac14 (n = 3). Yield: 94%; ^{1}H NMR ($CDCl_3$, 300 MHz, 298 K) δ 7.78-7.69 (m, 0.75H), 7.60- 7.36 (m, 6.25 H), 7.15-7.08 (m, 1H), 7.04- 7.71 (m, 6H), 6.47-6.13 (5H), 5.78-5.70 (m, 1H), 5.51-5.03 (m, 8H), 4.32-3.40 (m, 6H), 2.39-1.93 (m, 6H), 1.88-1.65 (m, 6H), 1.55-1.37 (m, 8H) ppm.: MS *m/z*: calcd. for $C_{62}H_{54}O_4S_8$ [M^+] 1118.17878 found HR-ESI 1118.17500.

m-Xylmac10 (n = 1). Yield: 97 %; ^{1}H NMR (300 MHz) δ 7.49-7.27 (m, 8H), 7.13-7.04 (m, 4H), 6.73 (m, 2H), 6.64 (m, 2H), 6.25-5.91 (m, 8H, H), 5.42 (bs, 2H), 5.24 (d, J = 14.0 Hz, 2H), 5.15 (d, J = 14.0 Hz, 2H), 4.01-3.73 (m, 4H), 2.06 (m, 4H), 1.75 (m, 4H), 1.55 (m, 4H). MS *m/z*: calcd. for $C_{58}H_{46}O_4S_8$ [M^+] 1062.11618 found HR-ESI 1062.11653.

m-Xylmac12 (n = 2). Yield: 96 %; ^{1}H NMR (300 MHz) δ 7.48-7.30 (m, 8H), 7.14-7.06 (m, 4H), 6.75-6.59 (m, 4H), 6.24-5.96 (m, 8H), 5.37 (m, 2H), 5.21 (bs, 4H), 3.99 (m, 4H), 2.02 (m, 4H), 1.78 (m, 4H), 1.59 (m, 8H). MS *m/z*: calcd. for $C_{60}H_{50}O_4S_8$ [M^+] 1090.14748 found HR-ESI 1090.15096.

m-Xylmac14 (n = 3). Yield: 98 %; ^{1}H NMR (300 MHz) δ 7.50-7.29 (m, 8H), 7.14 (m, 4H), 6.78-6.59 (m, 4H), 6.23-6.00 (m, 8H), 5.35 (bs, 2H), 5.20 (s, 4H), 3.98 (m, 4H), 1.99 (m, 4H), 1.77 (m, 4H), 1.47-1.19 (m, 12H). MS *m/z*: calcd. for $C_{62}H_{54}O_4S_8$ [M^+] 1118.17878 found HR-ESI 1118.17634.

Naphmac10 (n = 1). Yield: 94 %; ^{1}H NMR (300 MHz) δ 7.83-7.75 (m, 3H), 7.56-7.30 (m, 6H), 7.06 (m, 2H), 6.95-6.82 (m, 3H), 6.69 (m, 1H), 6.61-6.57 (m, 1H), 6.25-6.12 (m, 4H), 5.65-4.96 (m, 9H), 4.00-3.79 (m, 4H), 2.01 (m, 4H), 1.74 (m, 4H), 1.42 (m, 4H). MS *m/z*: calcd. for $C_{62}H_{48}O_4S_8$ [M^+] 1112.13183 found HR-ESI 1112.13672.

Naphmac12 (n = 2). Yield: 86 %; ^{1}H NMR (300 MHz) δ 7.81-7.75 (m, 3H), 7.54-7.32 (m, 6H), 7.05-7.00 (m, 2H), 6.93-6.75 (m, 3H), 6.70 (m, 2H), 6.52 (m, 2H), 6.22 (m, 3H), 5.55-5.27 (m, 6H), 5.20-4.85 (m, 3H), 4.03-3.71 (m, 4H), 2.08 (m, 4H), 1.74 (m, 4H), 1.57 (m, 8H). MS *m/z*: calcd. for $C_{64}H_{52}O_4S_8$ [M^+] 1140.16313 and HR-ESI 1140.16644.

Naphmac14 (n = 3). Yield: 90 %; ^{1}H NMR (300 MHz) δ 7.83-7.75 (m, 3H), 7.61-7.30 (m, 6H), 7.07 (m, 2H), 6.95-6.82 (m, 3H), 6.69 (d, J = 8.8 Hz, 2H), 6.59 (d, J = 8.8 Hz, 2H), 6.25-6.10 (m, 3H), 5.65-4.93 (m, 9H), 4.02-3.76 (m, 4H), 2.01 (m, 4H), 1.75 (m, 4H), 1.50-1.23 (m, 12H). MS *m/z*: calcd. for $C_{66}H_{56}O_4S_8$ [M^+] 1168.19443 found HR-ESI 1168.19727.

4.3.5.2. Analysis of the UV-vis titration data

As described in the main text, the analysis of the UV-vis titration data was performed utilizing Specfit global analysis software. We have previously shown (see *J. Am. Chem. Soc.* **2010**, *132*, 1772–1773) that this method provides satisfactory results for our experiments, comparable to those obtained by non-linear least-squares analysis of the ΔAbs at both 425 nm and 478 nm against the concentration of the fullerene, utilizing OriginPro 7.5 (OriginLab corporation) and the binding isotherm:

$$\Delta_{abs} = \frac{\Delta_{max} \times (1 + K_a \times G + K_a \times H) - \sqrt{(1 + K_a \times G + K_a \times H)^2 - 4 \times K_a{}^2 \times H \times G)}}{2 \times K_a \times H}$$

We find that analysis with Specfit software provides several advantages: It analyses all wavelengths of the titration spectra without making any assumption (the above equation assumes significant excess of guest), and produces simulated spectra for host, guest and host-guest species. As indication of satisfactory fitting, we examined both the binding isotherms at key wavelengths (see main text) and the sensibleness of the simulated spectra. For instance, we eliminated fits that predicted spectra with negative absorbance or excessive molar absorptivities. We also considered the correct reproduction of the wavelengths of isosbestic points. An example for each guest is given below.

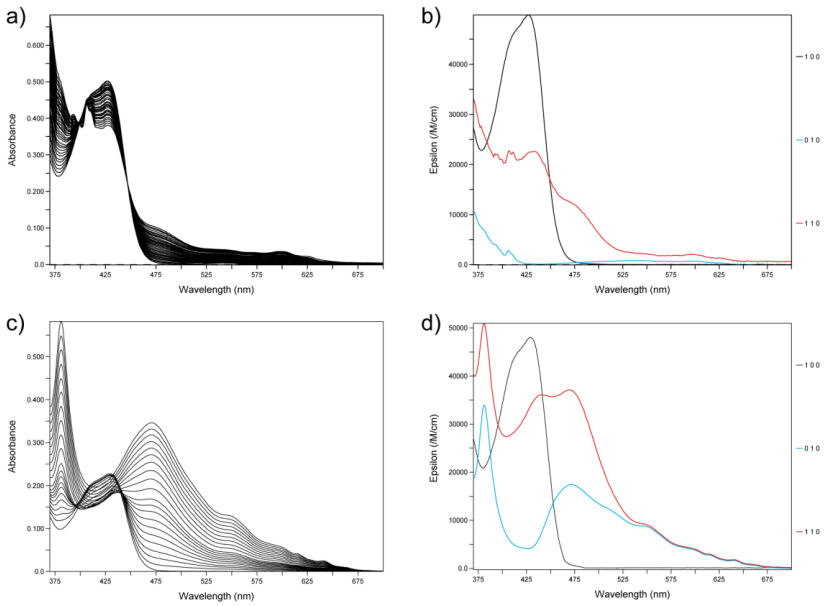

Figure 9. a) Titration data for ***m*-xylmac12** vs C_{60} and b) simulated spectra of host (100), guest (010), and host-guest complex (110) for log K_a = 4.5. c) Titration data for **naphmac14** vs C_{70} and b) simulated spectra of host (100), guest (010), and host-guest complex (110) for log K_a = 6.0.

4.3.5.3. Cyclic voltammetry measurements

Cyclic voltammograms were acquired using a three-electrode cell equipped with a glassy carbon working electrode (Ø = 3 mm), a platinum wire as a counter-electrode, an $Ag/AgNO_3$ reference on a Autolab potentiostat. Before the acquisition, solutions were systematically degassed by bubbling argon for five minutes. The constancy of the reference electrode potential was also checked by measuring the oxidation potential of a ferrocene solution before and after the different studies.

4.3.6. References

1. H. W. Kroto; J. R. Heath; S. C. O'Brien; R. F. Curl; R. E. Smalley, C_{60}: Buckminsterfullerene. *Nature* **1985,** *318*, 162-163.

2. (a) T. Andersson; K. Nilsson; M. Sundahl; G. Westman; O. Wennerstrom, C_{60} embedded in [gamma]-cyclodextrin: a water-soluble fullerene. *J. Chem. Soc., Chem. Commun.* **1992,** *0*, 604-606;(b) J. Effing; U. Jonas; L. Jullien; T. Plesnivy; H. Ringsdorf; F. Diederich; C. Thilgen; D. Weinstein, C_{60} and C_{70} in a Basket? – Investigations of Mono- and Multilayers from Azacrown Compounds and Fullerenes. *Angew. Chem., Int. Ed. Engl.* **1992,** *31*, 1599-1602.

3. (a) P. D. W. Boyd; C. A. Reed, Fullerene−Porphyrin Constructs. *Acc. Chem. Res.* **2004,** *38*, 235-242;(b) T. Kawase; H. Kurata, Ball-, Bowl-, and Belt-Shaped Conjugated Systems and Their Complexing Abilities: Exploration of the Concave-Convex p-p Interaction. *Chem. Rev.* **2006,** *106*, 5250-5273;(c) K. Tashiro; T. Aida, Metalloporphyrin hosts for supramolecular chemistry of fullerenes. *Chem. Soc. Rev.* **2007,** *36*, 189-197;(d) E. M. Pérez; N. Martín, Curves ahead: molecular receptors for fullerenes based on concave-convex complementarity. *Chem. Soc. Rev.* **2008,** *37*, 1512-1519;(e) E. M. Pérez; N. Martín, Molecular tweezers for fullerenes. *Pure Appl. Chem.* **2010,** *82*, 523-533.

4. (a) J.-S. Marois; K. Cantin; A. Desmarais; J.-F. Morin, [3]Rotaxane-Porphyrin Conjugate as a Novel Supramolecular Host for Fullerenes. *Org. Lett.* **2008,** *10*, 33-36;(b) W. Xiao; D. Passerone; P. Ruffieux; K. Aiet-Mansour; O. Groening; E. Tosatti; J. S. Siegel; R. Fasel, C_{60}/Corannulene on Cu(110): A Surface-Supported Bistable Buckybowl-Buckyball Host-Guest System. *J. Am. Chem. Soc.* **2008,** *130*, 4767-4771;(c) A. Hosseini; S. Taylor; G. Accorsi; N. Armaroli; C. A. Reed; P. D. W. Boyd, Calix[4]arene-Linked Bisporphyrin Hosts for Fullerenes: Binding Strength, Solvation Effects, and Porphyrin-Fullerene Charge Transfer Bands. *J. Am. Chem. Soc.* **2006,** *128*, 15903-15913;(d) E. M. Pérez; M. Sierra; L. Sánchez; M. R. Torres; R. Viruela; P. M. Viruela; E. Ortí; N. Martín, Concave Tetrathiafulvalene-Type Donors as Supramolecular Partners for Fullerenes. *Angew. Chem. Int. Ed.* **2007,** *46*, 1847-1851;(e) A. Sygula; F. R. Fronczek; R. Sygula; P. W. Rabideau; M. M. Olmstead, A Double Concave Hydrocarbon Buckycatcher. *J. Am. Chem. Soc.* **2007,** *129*, 3842-3843;(f) E. M. Pérez; L. Sánchez; G. Fernández; N. Martín, exTTF as a Building Block for Fullerene Receptors. Unexpected Solvent-Dependent Positive Homotropic Cooperativity. *J. Am. Chem. Soc.* **2006,** *128*, 7172-7173;(g) M. Yanagisawa; K. Tashiro; M. Yamasaki; T. Aida, Hosting Fullerenes by Dynamic Bond Formation with an Iridium Porphyrin Cyclic Dimer: A "Chemical Friction" for Rotary Guest Motions. *J. Am. Chem. Soc.* **2007,** *129*, 11912-11913;(h) J.-Y. Balandier; M. Chas; P. I. Dron; S. Goeb; D. Canevet; A. Belyasmine; M. Allain; M. Salle, N-Aryl pyrrolo-tetrathiafulvalene based ligands: synthesis and metal coordination. *J. Org. Chem.* **2010,** *75*, 1589-1599;(i) J. U. Franco; J. C. Hammons; D. Rios; M. M. Olmstead, New Tetraazaannulene Hosts for Fullerenes. *Inorg. Chem. (Washington, DC, U. S.) FIELD Full Journal Title:Inorganic Chemistry (Washington, DC, United States)* **2010,** *49*, 5120-5125;(j) Y. Shoji; K. Tashiro; T. Aida, One-Pot Enantioselective Extraction of Chiral Fullerene C_{76} Using a Cyclic Host Carrying an Asymmetrically Distorted, Highly π-Basic Porphyrin Module. *J. Am. Chem. Soc.* **2010,** *132*, 5928-5929;(k) E. Huerta; E. Cequier; J. d. Mendoza, Preferential separation of fullerene[84] from fullerene mixtures by encapsulation. *Chem. Commun.* **2007,** *0*, 5016-5018;(l) E. Huerta; G. A. Metselaar; A. Fragoso; E. Santos; C. Bo; J. de Mendoza, Selective binding and easy separation of C_{70} by nanoscale self-assembled capsules. *Angew. Chem. Int. Ed.* **2007,** *46*, 202-205;(m) Y. Shoji; K. Tashiro; T. Aida, Sensing of Chiral Fullerenes by a Cyclic Host with an Asymmetrically Distorted π-Electronic Component. *J. Am. Chem. Soc.* **2006,** *128*, 10690-10691;(n) S.-Q. Liu; D.-X. Wang; Q.-Y. Zheng; M.-X. Wang, Synthesis and structure of nitrogen bridged calix[5]- and -[10]-pyridines and their complexation with fullerenes. *Chem. Commun.* **2007**, 3856-3858;(o) E.-X. Zhang; D.-X. Wang; Q.-Y. Zheng; M.-X. Wang, Synthesis of Large Macrocyclic

Azacalix[n]pyridines (n = 6 - 9) and Their Complexation with Fullerenes C_{60} and C_{70}. *Org. Lett.* **2008,** *10*, 2565-2568;(p) E. Huerta; H. Isla; E. M. Pérez; C. Bo; N. Martín; J. de Mendoza, Tripodal exTTF-CTV Hosts for Fullerenes. *J. Am. Chem. Soc.* **2010,** *132*, 5351-5353;(q) E. M. Pérez; A. L. Capodilupo; G. Fernández; L. Sánchez; P. M. Viruela; R. Viruela; E. Ortí; M. Bietti; N. Martín, Weighting non-covalent forces in the molecular recognition of C_{60}. Relevance of concave-convex complementarity. *Chem. Commun.* **2008,** *0*, 4567-4569.

5. T. Nakanishi, Supramolecular soft and hard materials based on self-assembly algorithms of alkyl-conjugated fullerenes. *Chem. Commun.* **2010,** *46*, 3425-3436.

6. (a) P. Xue; R. Lu; L. Zhao; D. Xu; X. Zhang; K. Li; Z. Song; X. Yang; M. Takafuji; H. Ihara, Hybrid Self-Assembly of a Ï€ Gelator and Fullerene Derivative with Photoinduced Electron Transfer for Photocurrent Generation. *Langmuir* **2010,** *26*, 6669-6675;(b) T. Haino; E. Hirai; Y. Fujiwara; K. Kashihara, Supramolecular Cross-Linking of [60]Fullerene-Tagged Polyphenylacetylene by the Host–Guest Interaction of Calix[5]arene and [60]Fullerene. *Angew. Chem. Int. Ed.* **2010,** *49*, 7899-7903;(c) X. Zhang; M. Takeuchi, Controlled Fabrication of Fullerene C_{60} into Microspheres of Nanoplates through Porphyrin-Polymer-Assisted Self-Assembly. *Angew. Chem. Int. Ed.* **2009,** *48*, 9646-9651;(d) J. Wang; Y. Shen; S. Kessel; P. Fernandes; K. Yoshida; S. Yagai; D. G. Kurth; H. Mohwald; T. Nakanishi, Self-assembly made durable: water-repellent materials formed by cross-linking fullerene derivatives. *Angew. Chem. Int. Ed.* **2009,** *48*, 2166-2170;(e) F. D'Souza; E. Maligaspe; K. Ohkubo; M. E. Zandler; N. K. Subbaiyan; S. Fukuzumi, Photosynthetic Reaction Center Mimicry: Low Reorganization Energy Driven Charge Stabilization in Self-Assembled Cofacial Zinc Phthalocyanine Dimer-Fullerene Conjugate. *J. Am. Chem. Soc.* **2009,** *131*, 8787-8797;(f) R. Tsunashima; S.-i. Noro; T. Akutagawa; T. Nakamura; H. Kawakami; K. Toma, Fullerene nanowires: self-assembled structures of a low-molecular-weight organogelator fabricated by the Langmuir-Blodgett method. *Chem. Eur. J.* **2008,** *14*, 8169-8176;(g) M. Schmittel; B. He; P. Mal, Supramolecular Multicomponent Self-Assembly of Shape-Adaptive Nanoprisms: Wrapping up C_{60} with Three Porphyrin Units. *Org. Lett.* **2008,** *10*, 2513-2516;(h) T. Nakanishi; T. Michinobu; K. Yoshida; N. Shirahata; K. Ariga; H. Mohwald; D. G. Kurth, Nanocarbon superhydrophobic surfaces created from fullerene-based hierarchical supramolecular assemblies. *Adv. Mater.* **2008,** *20*, 443-446;(i) G. Fernández; L. Sánchez; E. M. Pérez; N. Martín, Large exTTF-Based Dendrimers. Self-Assembly and Peripheral Cooperative Multiencapsulation of C_{60}. *J. Am. Chem. Soc.* **2008,** *130*, 10674-10683;(j) G. Fernández; E. M. Pérez; L. Sánchez; N. Martín, An Electroactive Dynamically Polydisperse Supramolecular Dendrimer. *J. Am. Chem. Soc.* **2008,** *130*, 2410-2411;(k) G. Fernández; E. M. Pérez; L. Sánchez; N. Martín, Self-Organization of Electroactive Materials: A Head-to-Tail Donor–Acceptor Supramolecular Polymer. *Angew. Chem. Int. Ed.* **2008,** *47*, 1094-1097;(l) S. Barrau; T. Heiser; F. Richard; C. Brochon; C. Ngov; K. van de Wetering; G. Hadziioannou; D. V. Anokhin; D. A. Ivanov, Self-Assembling of Novel Fullerene-Grafted Donor-Acceptor Rod-Coil Block Copolymers. *Macromolecules* **2008,** *41*, 2701-2710;(m) Y. Araki; R. Chitta; A. S. D. Sandanayaka; K. Langenwalter; S. Gadde; M. E. Zandler; O. Ito; F. D'Souza, Self-Assembled Supramolecular Ferrocene-Fullerene Dyads and Triad: Formation and Photoinduced Electron Transfer. *Journal of Physical Chemistry C* **2008,** *112*, 2222-2229;(n) Y.-W. Zhong; Y. Matsuo; E. Nakamura, Lamellar Assembly of Conical Molecules Possessing a Fullerene Apex in Crystals and Liquid Crystals. *J. Am. Chem. Soc.* **2007,** *129*, 3052-3053;(o) S. Yoshimoto; E. Tsutsumi; R. Narita; Y. Murata; M. Murata; K. Fujiwara; K. Komatsu; O. Ito; K. Itaya, Epitaxial Supramolecular Assembly of Fullerenes Formed by Using a Coronene Template on a Au(111) Surface in Solution. *J. Am. Chem. Soc.* **2007,** *129*, 4366-4376;(p) F. Wessendorf; J.-F. Gnichwitz; G. H. Sarova; K. Hager; U. Hartnagel; D. M. Guldi; A. Hirsch, Implementation of a Hamilton-receptor-based hydrogen-bonding motif toward a new electron donor-acceptor prototype: electron versus energy transfer. *J. Am. Chem. Soc.* **2007,** *129*, 16057-16071;(q) U. Hahn; A. Gegout; C. Duhayon; Y. Coppel; A. Saquet; J.-F. Nierengarten, Self-assembly of fullerene-rich nanostructures with a stannoxane core. *Chem. Commun.* **2007**, 516-518;(r) D. Bonifazi; A. Kiebele; M. Stohr; F. Cheng; T. Jung; F. Diederich; H. Spillmann, Supramolecular nanostructuring of silver surfaces via self-assembly of [60]fullerene and porphyrin modules. *Adv. Funct. Mater.* **2007,** *17*, 1051-1062;(s) G.-B. Pan; X.-H. Cheng; S. Hoeger; W. Freyland, 2D Supramolecular Structures of a Shape-Persistent Macrocycle and Co-deposition with Fullerene on HOPG. *J. Am. Chem. Soc.* **2006,** *128*, 4218-4219.

7. (a) K. Araki; K. Akao; A. Ikeda; T. Suzuki; S. Shinkai, Molecular design of calixarene-based host molecules for inclusion of C_{60} in solution. *Tetrahedron Lett.* **1996,** *37*, 73-6;(b) C. L. Raston; J. L. Atwood; P. J. Nichols; I. B. N. Sudria, Supramolecular encapsulation of aggregates of C_{60}. *Chem. Commun.* **1996,** *0*, 2615-2616;(c) T. Haino; M. Yanase; Y. Fukazawa, New Supramolecular Complex of C_{60} Based on Calix[5]arene—Its Structure in the Crystal and in Solution. *Angew. Chem., Int. Ed. Engl.* **1997,** *36*, 259-260;(d) T. Haino; M. Yanase; Y. Fukazawa, Fullerenes Enclosed in Bridged Calix[5]arenes. *Angew. Chem. Int. Ed.* **1998,** *37*, 997-998;(e) T. Haino; Y. Yamanaka; H. Araki; Y. Fukazawa, Metal-induced regulation

of fullerene complexation with double-calix[5]arene. *Chem. Commun.* **2002,** *0*, 402-403;(f) T. Haino; Y. Matsumoto; Y. Fukazawa, Supramolecular Nano Networks Formed by Molecular-Recognition-Directed Self-Assembly of Ditopic Calix[5]arene and Dumbbell [60]Fullerene. *J. Am. Chem. Soc.* **2005,** *127*, 8936-8937;(g) T. Haino; C. Fukunaga; Y. Fukazawa, A New Calix[5]arene-Based Container: Selective Extraction of Higher Fullerenes. *Org. Lett.* **2006,** *8*, 3545-3548;(h) T. Haino; M. Yanase; C. Fukunaga; Y. Fukazawa, Fullerene encapsulation with calix[5]arenes. *Tetrahedron* **2006,** *62*, 2025-2035;(i) K. A. Nielsen; G. H. Sarova; L. Martín-Gomis; F. Fernández-Lázaro; P. C. Stein; L. Sanguinet; E. Levillain; J. L. Sessler; D. M. Guldi; A. Sastre-Santos; J. O. Jeppesen, Chloride Anion Controlled Molecular "Switching". Binding of 2,5,7-Trinitro-9-dicyanomethylenefluorene-C_{60} by Tetrathiafulvalene Calix[4]pyrrole and Photophysical Generation of Two Different Charge-Separated States. *J. Am. Chem. Soc.* **2008,** *130*, 460-462;(j) J.-C. Wu; D.-X. Wang; Z.-T. Huang; M.-X. Wang, A [2+3] fragment coupling approach to N,O-bridged calix[1]arene[4]pyridines and their complexation with C_{60}. *Tetrahedron Lett.* **2009,** *50*, 7209-7212.

8. (a) J. W. Steed; P. C. Junk; J. L. Atwood; M. J. Barnes; C. L. Raston; R. S. Burkhalter, Ball and Socket Nanostructures: New Supramolecular Chemistry Based on Cyclotriveratrylene. *J. Am. Chem. Soc.* **1994,** *116*, 10346-10347;(b) J. L. Atwood; M. J. Barnes; M. G. Gardiner; C. L. Raston, Cyclotriveratrylene polarization assisted aggregation of C_{60}. *Chem. Commun.* **1996**, 1449-1450;(c) H. Matsubara; T. Shimura; A. Hasegawa; M. Semba; K. Asano; K. Yamamoto, Syntheses of Novel Fullerene Tweezers and Their Supramolecular Inclusion Complex of C_{60}. *Chem. Lett.* **1998,** *27*, 1099-1100;(d) J.-F. Nierengarten; L. Oswald; J.-F. Eckert; J.-F. Nicoud; N. Armaroli, Complexation of fullerenes with dendritic cyclotriveratrylene derivatives. *Tetrahedron Lett.* **1999,** *40*, 5681-5684;(e) D. Felder; B. Heinrich; D. Guillon; J.-F. Nicoud; J.-F. Nierengarten, A Liquid Crystalline Supramolecular Complex of C_{60} with a Cyclotriveratrylene Derivative. *Chem. Eur. J.* **2000,** *6*, 3501-3507;(f) Y. Rio; J.-F. Nierengarten, Water soluble supramolecular cyclotriveratrylene–[60]fullerene complexes with potential for biological applications. *Tetrahedron Lett.* **2002,** *43*, 4321-4324.

9. (a) S. Mizyed; P. E. Georghiou; M. Bancu; B. Cuadra; A. K. Rai; P. Cheng; L. T. Scott, Embracing C_{60} with Multiarmed Geodesic Partners. *J. Am. Chem. Soc.* **2001,** *123*, 12770-12774;(b) P. E. Georghiou; A. H. Tran; S. Mizyed; M. Bancu; L. T. Scott, Concave Polyarenes with Sulfide-Linked Flaps and Tentacles: New Electron-Rich Hosts for Fullerenes. *J. Org. Chem.* **2005,** *70*, 6158-6163;(c) C. Mueck-Lichtenfeld; S. Grimme; L. Kobryn; A. Sygula, Inclusion complexes of buckycatcher with C_{60} and C_{70}. *PCCP* **2010,** *12*, 7091-7097.

10. (a) T. Kawase; K. Tanaka; Y. Seirai; N. Shiono; M. Oda, Complexation of Carbon Nanorings with Fullerenes: Supramolecular Dynamics and Structural Tuning for a Fullerene Sensor. *Angew. Chem. Int. Ed.* **2003,** *42*, 5597-5600;(b) T. Kawase; N. Fujiwara; M. Tsutumi; M. Oda; Y. Maeda; T. Wakahara; T. Akasaka, Supramolecular Dynamics of Cyclic [6]Paraphenyleneacetylene Complexes with [60]- and [70]Fullerene Derivatives: Electronic and Structural Effects on Complexation. *Angew. Chem. Int. Ed.* **2004,** *43*, 5060-5062;(c) T. Kawase; K. Tanaka; N. Shiono; Y. Seirai; M. Oda, Onion-Type Complexation Based on Carbon Nanorings and a Buckminsterfullerene. *Angew. Chem. Int. Ed.* **2004,** *43*, 1722-1724;(d) T. Kawase; H. Kurata, Ball-, Bowl-, and Belt-Shaped Conjugated Systems and Their Complexing Abilities: Exploration of the Concave−Convex π−π Interaction. *Chem. Rev.* **2006,** *106*, 5250-5273.

11. (a) H. Sato; K. Tashiro; H. Shinmori; A. Osuka; Y. Murata; K. Komatsu; T. Aida, Positive Heterotropic Cooperativity for Selective Guest Binding via Electronic Communications through a Fused Zinc Porphyrin Array. *J. Am. Chem. Soc.* **2005,** *127*, 13086-13087;(b) Y. Shoji; K. Tashiro; T. Aida, Selective Extraction of Higher Fullerenes Using Cyclic Dimers of Zinc Porphyrins. *J. Am. Chem. Soc.* **2004,** *126*, 6570-6571;(c) D. Sun; F. S. Tham; C. A. Reed; L. Chaker; P. D. W. Boyd, Supramolecular Fullerene-Porphyrin Chemistry. Fullerene Complexation by Metalated \"Jaws Porphyrin\" Hosts. *J. Am. Chem. Soc.* **2002,** *124*, 6604-6612;(d) Y. Kubo; A. Sugasaki; M. Ikeda; K. Sugiyasu; K. Sonoda; A. Ikeda; M. Takeuchi; S. Shinkai, Cooperative C60 Binding to a Porphyrin Tetramer Arranged around a p-Terphenyl Axis in 1:2 Host-Guest Stoichiometry. *Org. Lett.* **2002,** *4*, 925-928;(e) M. Ayabe; A. Ikeda; Y. Kubo; M. Takeuchi; S. Shinkai, A dendritic porphyrin receptor for C_{60} which features a profound positive allosteric effect. *Angew. Chem. Int. Ed.* **2002,** *41*, 2790-2792;(f) J.-Y. Zheng; K. Tashiro; Y. Hirabayashi; K. Kinbara; K. Saigo; T. Aida; S. Sakamoto; K. Yamaguchi, Cyclic dimers of metalloporphyrins as tunable hosts for fullerenes: a remarkable effect of rhodium(III). *Angew. Chem. Int. Ed.* **2001,** *40*, 1857-1861.

12. G. n. Gil-Ramírez; S. D. Karlen; A. Shundo; K. Porfyrakis; Y. Ito; G. A. D. Briggs; J. J. L. Morton; H. L. Anderson, A Cyclic Porphyrin Trimer as a Receptor for Fullerenes. *Org. Lett.* **2010,** *12*, 3544-3547.

13. J. Song; N. Aratani; H. Shinokubo; A. Osuka, A Porphyrin Nanobarrel That Encapsulates C_{60}. *J. Am. Chem. Soc.* **2010,** *132*, 16356–16357.

14. H. Isla; M. Gallego; E. M. Pérez; R. Viruela; E. Ortí; N. Martín, A Bis-exTTF Macrocyclic Receptor That Associates C_{60} with Micromolar Affinity. *J. Am. Chem. Soc.* **2010,** *132*, 1772-1773.

15. Continous variation plots to confirm the stoichiometries of the associates were also carried out. For the sake of brevity, only those indicating 2:1 stoichiometry are shown. The Job's plot of ***p*-xylmac12** vs.C_{60} can bee seen in ref. 14.

16. W. D. Cornell; P. Cieplak; C. I. Bayly; I. R. Gould; K. M. Merz, Jr.; D. M. Ferguson; D. C. Spellmeyer; T. Fox; J. W. Caldwell; P. A. Kollman, A Second Generation Force Field for the Simulation of Proteins, Nucleic Acids, and Organic Molecules. *J. Am. Chem. Soc.* **1995,** *117*, 5179-97.

17. S. Mizyed; P. E. Georghiou; M. Ashram, Thermodynamic study of the complexes of calix[4]naphthalenes with [60]fullerene in different solvents. *J. Chem. Soc. Perk. Trans. 2* **2000,** *0*, 277-280.

18. K. N. Semenov; N. A. Charykov; V. A. Keskinov; A. K. Piartman; A. A. Blokhin; A. A. Kopyrin, Solubility of Light Fullerenes in Organic Solvents. *Journal of Chemical & Engineering Data* **2010,** *55*, 13-36.

19. D. Pal; D. Goswami; S. K. Nayak; S. Chattopadhyay; S. Bhattacharya, Spectroscopic and Theoretical Insights into the Origin of Fullerene-Calix[4]pyrrole Interaction. *J. Phys. Chem. A* **2010,** *114*, 6776-6786.

5. Tripodal exTTF-CTV Hosts for Fullerenes

Elisa Huerta, Helena Isla, Emilio M. Pérez, Carles Bo, Nazario Martín, and Javier de Mendoza, *J. Am. Chem. Soc.* **2010**, *132*, 5351-5353

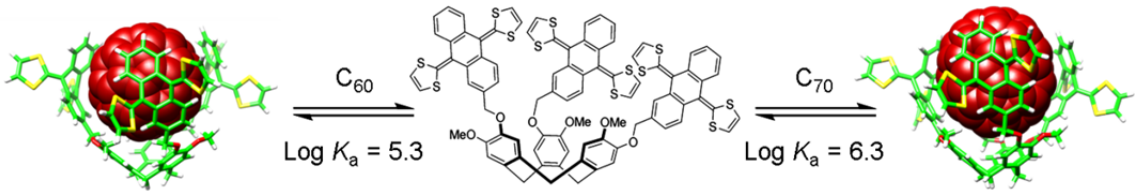

A receptor for fullerenes featuring three exTTF units linked to a CTV scaffold is described. The exTTF-CTV host forms remarkably stable complexes with both C_{60} (log K_a = 5.3 ± 0.2) and C_{70} (log K_a = 6.3 ± 0.6). Light-induced ESR spectra demonstrate that intracomplex PET processes take place in solution.

J. Am. Chem. Soc. **2010**, *132*, 5351–5353

5.1. Introduction

Since the early 1990s, cyclotriveratrylene (CTV) derivatives have been shown to form "ball and socket" complexes with C_{60}.[1] Recently, some of us have reported hydrogen bonded self-assembled capsules that associate higher fullerenes (C_{70} and C_{84}) with increased affinity and selectivity over C_{60}.[2] In our capsules, two CTV scaffolds endowed with three 2-ureido-4[1*H*]-pyrimidinone subunits selfassemble into dimeric capsules in the presence of the appropriate fullerene host and can be used to purify C_{70} and C_{84}[2c] from complex fullerene mixtures (fullerites) without chromatography. Although other receptors for fullerenes based on calixarenes,[3] calixpyrroles,[4] corannulenes,[5] or tribenzotriquinacenes[6] have been employed as scaffolds, relatively

[1] J. W. Steed, P. C. Junk, J. L. Atwood, M. J. Barnes, C. L. Raston and R. S. Burkhalter, *J. Am. Chem. Soc.* **1994,** *116*, 10346-10347.
[2] (a) E. Huerta, E. Cequier and J. d. Mendoza, *Chem. Commun.* **2007,** *0*, 5016-5018; (b) E. Huerta, G. A. Metselaar, A. Fragoso, E. Santos, C. Bo and J. de Mendoza, *Angew. Chem. Int. Ed.* **2007,** *46*, 202-205; (c) J. d. Mendoza, E. Huerta and G. A. Metselaar US 2008/0025904 A1, 2008.
[3] (a) J. L. Atwood, L. J. Barbour, P. J. Nichols, C. L. Raston and C. A. Sandoval, *Chem. Eur. J.* **1999,** *5*, 990-996; (b) A. Hosseini, S. Taylor, G. Accorsi, N. Armaroli, C. A. Reed and P. D. W. Boyd, *J. Am. Chem. Soc.* **2006,** *128*, 15903-15913.
[4] (a) K. A. Nielsen, L. Martín-Gomis, G. H. Sarova, L. Sanguinet, D. E. Gross, F. Fernández-Lázaro, P. C. Stein, E. Levillain, J. L. Sessler, D. M. Guldi, A. Sastre-Santos and J. O. Jeppesen, *Tetrahedron* **2008,** *64*, 8449-8463; (b) K. A. Nielsen, G. H. Sarova, L. Martín-Gomis, F. Fernández-Lázaro, P. C. Stein, L. Sanguinet, E. Levillain, J. L. Sessler, D. M. Guldi, A. Sastre-Santos and J. O. Jeppesen, *J. Am. Chem. Soc.* **2008,** *130*, 460-462.
[5] (a) S. Mizyed, P. E. Georghiou, M. Bancu, B. Cuadra, A. K. Rai, P. Cheng and L. T. Scott, *J. Am. Chem. Soc.* **2001,** *123*, 12770-12774; (b) P. E. Georghiou, A. H. Tran, S. Mizyed, M. Bancu and L. T. Scott, *J. Org. Chem.* **2005,** *70*, 6158-6163.
[6] P. E. Georghiou, L. N. Dawe, H.-A. Tran, J. Strube, B. Neumann, H.-G. Stammler and D. Kuck, *J. Org. Chem.* **2008,** *73*, 9040-9047.

few examples of hosts in which CTV is combined with other recognition motifs have been reported.[7] On the other hand, we have reported that the concave aromatic surface of 2-[9-(1,3-dithiol-2-ylidene)anthracen-10(9*H*)-ylidene]-1,3-dithiole (exTTF) can be exploited for the molecular recognition of C_{60}. Even with relatively simple tweezer-like designs, the exTTF-based receptors form complexes with C_{60} with a binding constant of log K_a = 3.5 in chlorobenzene at room temperature.[8] Later, we have optimized the design of our exTTF-based receptors by making use of bis-exTTF macrocyclic structures, to achieve an improvement of 3 orders of magnitude in the binding constants.[9]

5.2. Results and discussion

We reasoned an alternative strategy to obtain efficient exTTF based receptors for fullerenes would be to increase the number of exTTF units in the host. Considering the precedents outlined above, we designed and synthesized host **exTTF-CTV**, in which three exTTF subunits are linked to a CTV scaffold through short ether linkages. The concave surfaces of both the CTV and the exTTF subunits should nicely wrap around the entrapped fullerene guest. The **exTTF-CTV** host was readily synthesized from known fragments v*ia* a simple Mitsunobu coupling (Scheme 1). Its purity and identity were unambiguously established by HPLC-MS, ^{1}H and ^{13}C NMR, and UV-vis.

Scheme 1. Synthesis of **exTTF-CTV**

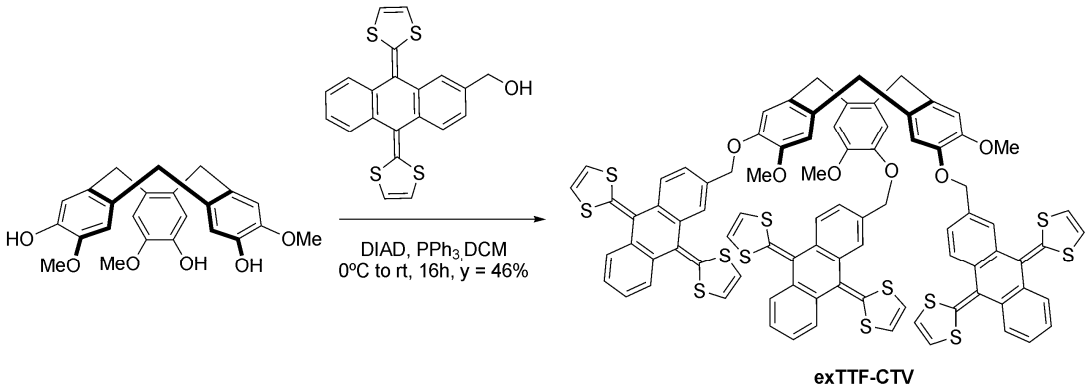

An early indication of the ability of **exTTF-CTV** to bind fullerenes came from the MALDI-TOF spectrum (negative mode, pyrene matrix). When 1:1 mixtures of **exTTF-CTV** and either C_{60} or C_{70} were analyzed, peaks at *m*/*z* 2306.3 and 2426.2,

[7] (a) H. Matsubara, T. Shimura, A. Hasegawa, M. Semba, K. Asano and K. Yamamoto, *Chem. Lett.* **1998,** *27*, 1099-1100; (b) M. J. Hardie, P. D. Godfrey and C. L. Raston, *Chem. Eur. J.* **1999,** *5*, 1828-1833; (c) J. F. Nierengarten, *Fullerenes, Nanotubes and Carbon Nanostructures* **2005,** *13*, 229-242.

[8] (a) E. M. Pérez, L. Sánchez, G. Fernández and N. Martín, *J. Am. Chem. Soc.* **2006,** *128*, 7172-7173; (b) E. M. Pérez, A. L. Capodilupo, G. Fernández, L. Sánchez, P. M. Viruela, R. Viruela, E. Ortí, M. Bietti and N. Martín, *Chem. Commun.* **2008,** *0*, 4567-4569; (c) E. M. Perez and N. Martin, *Chem. Soc. Rev.* **2008,** *37*, 1512-1519; (d) S. S. Gayathri, M. Wielopolski, E. M. Pérez, G. Fernández, L. Sánchez, R. Viruela, E. Ortí, D. M. Guldi and N. Martín, *Angew. Chem. Int. Ed.* **2009,** *48*, 815-819.

[9] H. Isla, M. Gallego, E. M. Pérez, R. Viruela, E. Ortí and N. Martín, *J. Am. Chem. Soc.* **2010,** *132*, 1772-1773.

corresponding to C_{60}@**exTTF-CTV** (calcd 2306.1) and C_{70}@**exTTF-CTV** (calcd 2426.1) respectively were clearly observed. No peaks corresponding to aggregates of other stoichiometries were found. The 1:1 complexes in solution were confirmed by a UV-vis Job's plot analysis (see Figure 2).

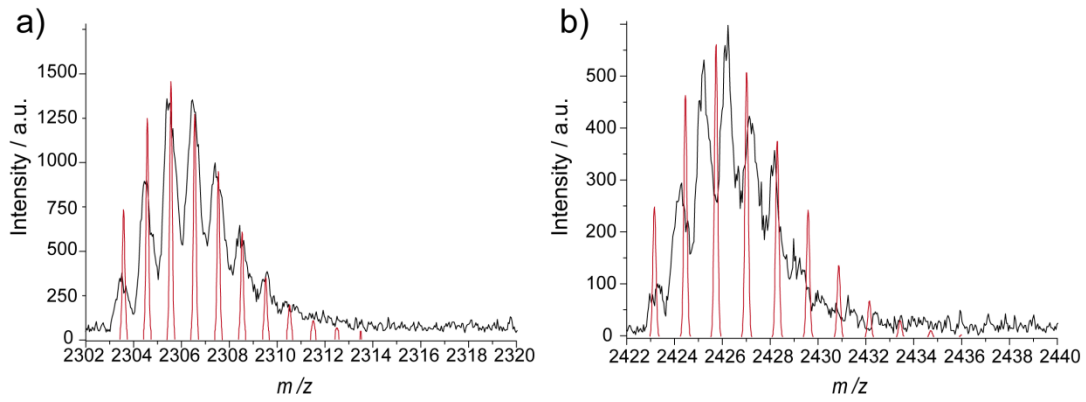

Figure 1. Simulated (red) and found (MALDI-TOF, black) isotopic pattern for (a) C_{60}@**exTTF-CTV** and (b) C_{70}@**exTTF-CTV**.

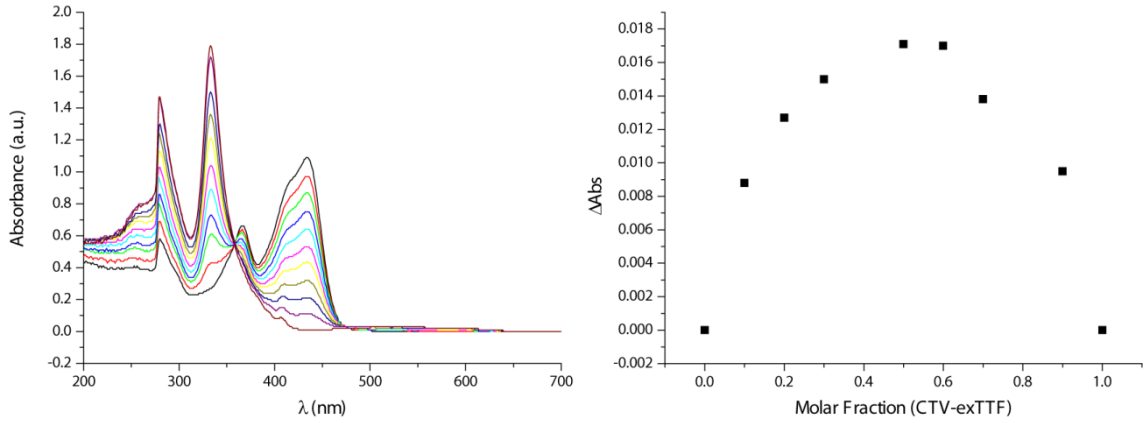

Figure 2: Job's Plot for complex C_{60}@**exTTF-CTV**. [**exTTF-CTV**] = [C_{60}] = 0.3 mM in chlorobenzene (λ = 436 nm).

The host shows rather complex ^{1}H NMR spectra (500 MHz) at room temperature in $CDCl_3/CS_2$ (2:5 v/v) or in d^8-toluene, indicative of the coexistence of several stable conformations in solution, in slow chemical exchange. Indeed, splitting and sharpening of most signals were observed upon cooling, in both solvents. Similarly, heating caused the spectrum to significantly simplify at 378 K in d^8-toluene, although without matching with a C_3 symmetric molecule. However, the spectrum displays a single set of broad signals at room temperature in d^5-chlorobenzene, which is fully resolved at 353 K. The binding event produced slight, though reproducible changes in the ^{1}H NMR of **exTTF-CTV**. Additionally, the C_{60} ^{13}C NMR signal was shifted upfield and broadened in C_{60}@**exTTF-CTV** (Figure 3), both processes being strengthened upon cooling.

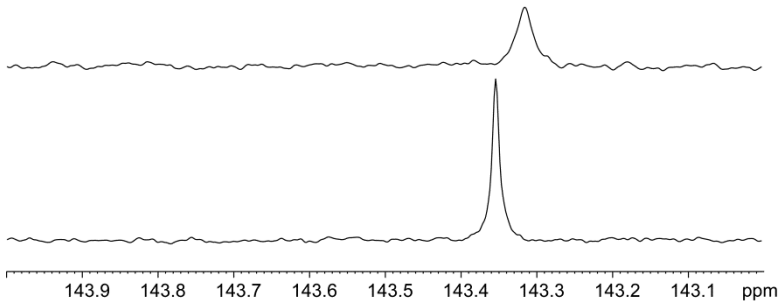

Figure 3. ^{13}C NMR (d^5-chlorobenzene, 125 MHz, 25ºC) of C_{60}@**exTTF-CTV** (top) and C_{60} (bottom).

The stability of the complexes was estimated through three independent UV-vis titrations. In a typical experiment, 0.1 equiv aliquots of the fullerene were added (up to 3.3 equiv) to a constant concentration of the **exTTF-CTV** host (10^{-4} M, chlorobenzene).

Upon addition of either C_{60} or C_{70} a significant decrease in intensity of the exTTF band at λ_{max}) 434 nm was observed (Figure 4), accompanied by the emergence of an intense charge-transfer band centered at λ = 478 nm for C_{60} and at λ = 472 nm for C_{70}. During the early steps of the titration (after addition of 1-1.2 equiv of guest), well-defined isosbestic points at 452 nm (C_{60}) and 445 nm (C_{70}) were observed. The changes in the electronic absorption spectra are fully consistent with those found for our previously reported tweezer-like exTTF receptors[8-9] and constitute the typical signature of the exTTF-fullerene interaction.[10]

Analysis of the UV-vis data was carried out with both Specfit and Origin software, in the latter case fitting the data to the equation currently employed by us[8-9] and by others[11] (see figure 5). An association constant toward C_{60} of log *K*a = 5.3 ± 0.2 was obtained. With regard to C_{70}, analysis of the titration data produced a binding constant of log *K*a = 6.3 ± 0.6, 10-fold higher than that found for C_{60}. The values of the binding constants are among the highest reported to date for a nonmetalloporphyrin containing host and comparable to those reported by the groups of Boyd, Reed, and Armaroli for bisporphyrin tweezers[3b] and by Aida for bisporphyrin cages,[12] with the exception of the Rh (III)[12a] and Ir(III)[12c] metalloporphyrin derivatives.

[10] In fact, these changes correspond to the (partial) formation of the exTTF radical cation, see: D. M. Guldi, L. Sánchez and N. Martín, *J. Phys. Chem. B* **2001,** *105*, 7139-7144; A. E. Jones, C. A. Christensen, D. F. Perepichka, A. S. Batsanov, A. Beeby, P. J. Low, M. R. Bryce and A. W. Parker, *Chem. Eur. J.* **2001,** *7*, 973-978.

[11] C. A. Schalley, Introduction. In *Analytical Methods in Supramolecular Chemistry*, Wiley-VCH Verlag GmbH & Co. KGaA: 2007; pp 1-16.

[12] (a) J.-Y. Zheng, K. Tashiro, Y. Hirabayashi, K. Kinbara, K. Saigo, T. Aida, S. Sakamoto and K. Yamaguchi, *Angew. Chem. Int. Ed.* **2001,** *40*, 1857-1861; (b) K. Tashiro and T. Aida, *Chem. Soc. Rev.* **2007,** *36*, 189-197; (c) M. Yanagisawa, K. Tashiro, M. Yamasaki and T. Aida, *J. Am. Chem. Soc.* **2007,** *129*, 11912-11913.

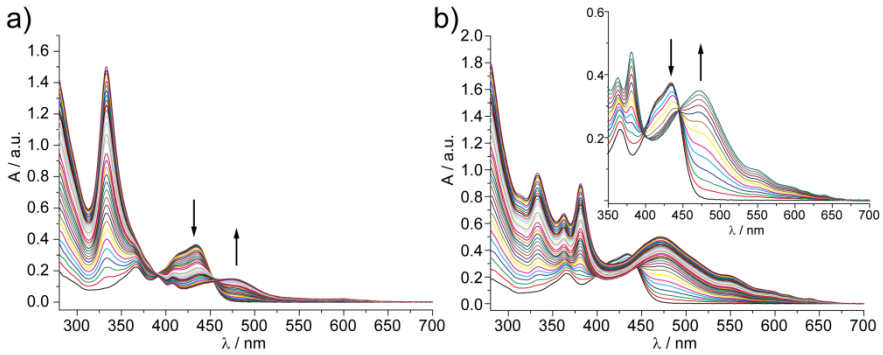

Figure 4. UV-vis spectra as recorded during the titration of (a) **exTTFCTV** vs C_{60} and (b) **exTTF-CTV** vs C_{70} (inset shows the first 12 additions), PhCl, 298 K.

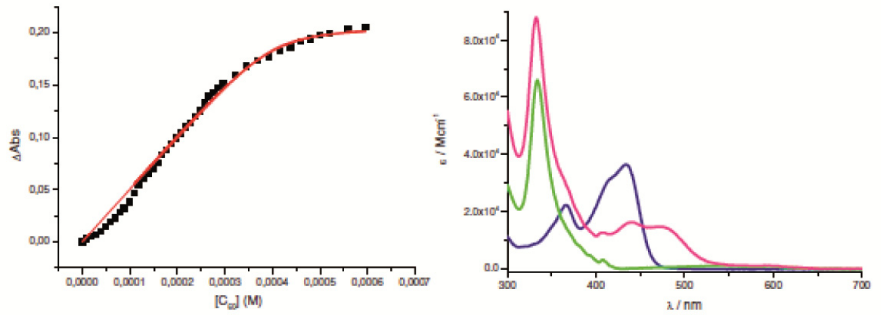

Figure 5. Binding isotherm (left) and calculated ε (right, pink) for the C_{60}@**exTTF-CTV**.

The electrochemical characterization of **exTTF-CTV** and its fullerene complexes was carried out by cyclic voltammetry of 10^{-5} M solutions in chlorobenzene/acetonitrile (5:1 v/v) (0.1 M of Bu_4NClO_4 as electrolyte, glassy carbon as working electrode, Pt wire as counter electrode, Ag/AgCl as reference electrode, scan rates: 25, 50, 100, and 200 mV/s). The voltammogram of **exTTFCTV** displays the characteristic electrochemically irreversible oxidation of exTTF at 0.36 V, with a weak shoulder at 0.74 V, most probably due to weak adsorption processes. Upon complexation with either fullerene, we observed a significant shift of the oxidation potential to 0.54 V. With respect to the reduction waves of the fullerenes we observed the first four reduction processes for C_{60}, C_{70}, and their complexes. The changes to the first and second reduction potential upon complexation are approximately 10-50 mV, while the third reduction process is affected to a greater extent, up to 100 mV in the case of C_{70}@**exTTF-CTV**.

Table 1. Redox Potentials (V vs Ag/Ag+) of **exTTF-CTV**, C_{60}, C_{70}, and their complexes

	E^1_{red}	E^2_{red}	E^3_{red}	E^4_{red}	E^1_{ox}
exTTF-CTV	-	-	-	-	0.36
C_{60}	-0.50	-0.92	-1.41	-1.87	-
C_{60}@exTTF-CTV	-0.49	-0.91	-1.37	-	0.54
C_{70}	-0.51	-0.92	-1.37	-1.77	-
C_{70}@exTTF-CTV	-0.48	-0.87	-1.27	-1.74	0.54

The structure and properties of the complexes were determined computationally by using DFT methods as implemented in the ADF v.2008 package.[13] Full geometry optimizations were carried at the BP86/DZP level, while final energies were evaluated by singlepoint calculations at the BP86/TZP and BH&H/TZ2P levels. Despite the intrinsic limitations of pure DFT methods for evaluating nonbonding interaction energies, we found recently that this hybrid method was suitable to evaluate the interaction strength of these species in the gas phase.[8b, 8d, 9, 14] As predicted by our initial modeling, the calculated structures show that the fullerenes dwell deep into the cavity of the **exTTF-CTV** host, with the CTV serving as both a bowl-shaped recognition element and as a preorganizing scaffold for the exTTF subunits, which wrap almost completely around the surface of the fullerenes. Host deformation energies, calculated as the difference between the energy of the host in the complex and the energy of the free **exTTF-CTV** structure at both the BP86/ TZP and BH&H/TZ2P levels, gave convergent results. **exTTF-CTV** requires 7-9 kcal mol^{-1} to adapt to C_{60}, whereas less deformation, namely 1.5-2.5 kcal mol^{-1}, is needed to form the complex with C_{70}. The average angle between the centroids of two consecutive aromatic rings in the CTV and the linking methylene carbon in the C_{60}@**exTTF-CTV** complex is 113.6° and slightly larger (114.0°) for C_{70}@exTTF-CTV. The curvature of the exTTF units is also dependent on the guest. The average angle between the planes defined by the two aromatic rings of

[13](a) E. J. Baerends, D. E. Ellis and P. Ros, *Chem. Phys.* **1973,** *2*, 41-51; (b) E. J. Baerends and P. Ros, *Chem. Phys.* **1973,** *2*, 52-9; (c) S. H. Vosko, L. Wilk and M. Nusair, *Can. J. Phys.* **1980,** *58*, 1200-11; A. D. Becke, *Phys. Rev. A* **1986,** *33*, 2786-2788; (d) M. Levy and J. P. Perdew, *J. Chem. Phys.* **1986,** *84*, 4519-4523; (d) A. D. Becke, *Phys. Rev. A* **1988,** *38*, 3098-3100; (e) P. M. Boerrigter, G. Te Velde and E. J. Baerends, *Int. J. Quantum Chem* **1988,** *33*, 87-113; (f) G. Te Velde and E. J. Baerends, *J. Comput. Phys.* **1992,** *99*, 84-98; (g) C. F. Guerra, J. G. Snijders, G. Te Velde and E. J. Baerends, *Theor. Chem. Acc.* **1998,** *99*, 391-403.

[14] For a comprehensive comparative study of the performance of different DFT functionals for the evaluation of the supramolecular systems, see: Y. Zhao and D. G. Truhlar, *J. Chem. Theory Comput.* **2006,** *3*, 289-300. The authors demonstrate that BH&H is reliable for system dominated by dispersion interactions, such as ours.

each exTTF subunit is 49.9° for C_{60}@**exTTF-CTV** and 52.0° for C_{70}@**exTTF-CTV**. The energy release to build up the complex starting from the two isolated units computed at the BH&H level nicely correlates with the binding constants reported above and with those of related systems.[8-9] For C_{70}@**exTTF-CTV**, the interaction energy is -22.1 kcal mol^{-1}, while for C_{60}@**exTTF-CTV** we evaluated -15.0 kcal mol^{-1}. These values also agree with the tiny amount of charge transferred from host to the fullerene (0.31 for C_{70}, 0.25 for C_{60}) when forming the complex. TDDFT calculations (BP86, DZP) were carried out to shed light on the electronic absorption spectra. The charge transfer band is quite accurately reproduced by the calculations, with a calculated λ_{max} = 498 nm (observed = 478 nm) for a C_{60} complex and λ_{max} = 484 nm (observed = 472 nm) for a C_{70} complex (see the computational details section).

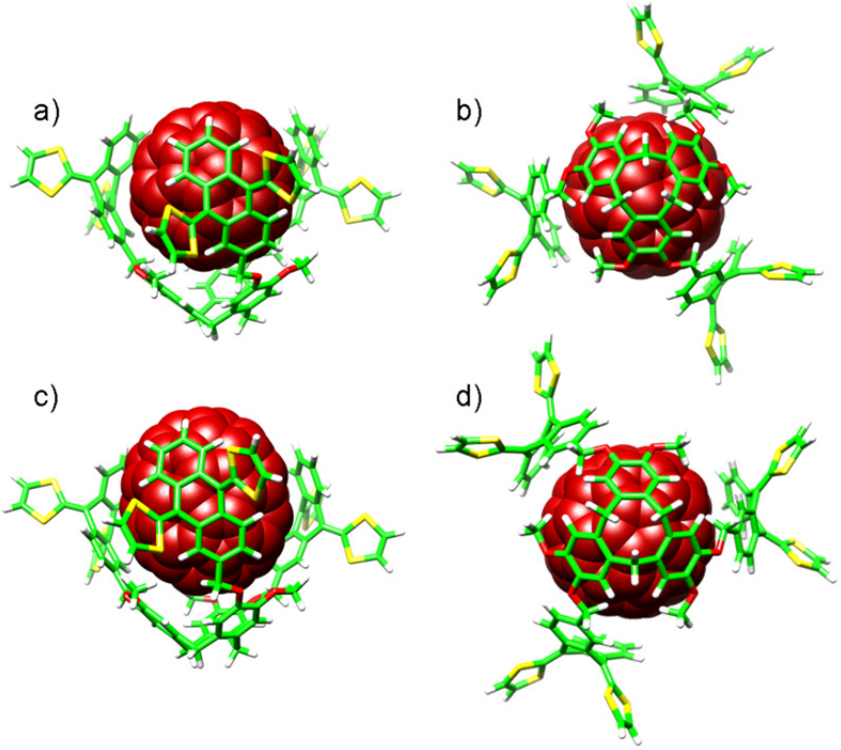

Figure 6. Energy-minimized structures (DFT) of (a) C_{60}@**exTTF-CTV** side view, (b) C_{60}@**exTTF-CTV** top view, (c) C_{70}@**exTTF-CTV** side view, and (d) C_{70}@**exTTF-CTV** top view.

Besides the very high binding constants, one of the most significant features of the C_{60}@**exTTF-CTV** complex is the combination of shape and electronic complementarity between **exTTF** and C_{60}. We have previously shown that photoinduced electron transfer (PET) from the electron donor exTTF to the electron acceptor C_{60} occurs readily in our tweezer-like receptors.[8d] This is also the case for the C_{60}@**exTTF-CTV** complex, as demonstrated by preliminary light-induced electron spin resonance (LESR) measurements at 298 K (Figure 7). When a 1:1 mixture of C_{60} and **exTTF-CTV** in deareated PhCl - ESR silent in the dark- was irradiated with a broad-band Hg lamp, a clearly visible, albeit weak signal (g = 2.0014; ΔH = 5.9 G) was

observed,[15] which increases in intensity with irradiation time and decreases rapidly upon switching the lamp off. To unambiguously establish the PET origin of this ESR signal, control LESR experiments were carried out with both C_{60} and **exTTF-CTV** separately, which remained ESR silent under light irradiation.

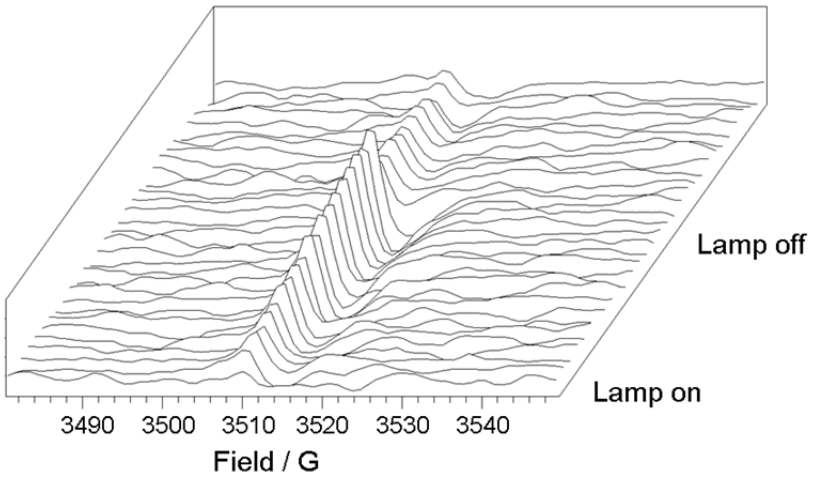

Figure 7. ESR spectra of C_{60}@**exTTF-CTV** (PhCl, 298 K) taken at 45 s intervals. The sample was irradiated with a broad-band Hg lamp.

5.3. Conclusion

In summary, **exTTF-CTV** features the combination of two concave recognition fragments, resulting in a very effective association of both C_{60} and C_{70}, with binding constants comparable to the strongest reported in the literature for metalloporphyrin-based receptors, and superior to any other receptors containing only purely organic fragments. Taking into account the successful application of our previous receptors -with binding constants 2 orders of magnitude weaker- to the construction of nanostructured electroactive materials[16] and the relatively simple synthetic route that gives access to **exTTF-CTV**, we will focus our future research on the utilization of this new host-guest system to similar goals. Finally, given the chiral nature of the CTV central scaffold, the enantioselective recognition of the D_2-isomers of higher fullerenes C_{76} and C_{84} constitutes current pursuit in our laboratories.[17]

5.4. Computational details

[15] (a) S. Fukuzumi, H. Mori, T. Suenobu, H. Imahori, X. Gao and K. M. Kadish, *J. Phys. Chem. A* **2000,** *104*, 10688-10694; (b) D. F. Perepichka, M. R. Bryce, I. F. Perepichka, S. B. Lyubchik, C. A. Christensen, N. Godbert, A. S. Batsanov, E. Levillain, E. J. L. McInnes and J. P. Zhao, *J. Am. Chem. Soc.* **2002,** *124*, 14227-14238.

[16] (a) G. Fernández, E. M. Pérez, L. Sánchez and N. Martín, *Angew. Chem. Int. Ed.* **2008,** *47*, 1094-1097; (b) G. Fernández, E. M. Pérez, L. Sánchez and N. Martín, *J. Am. Chem. Soc.* **2008,** *130*, 2410-2411; (c) G. Fernández, L. Sánchez, E. M. Pérez and N. Martín, *J. Am. Chem. Soc.* **2008,** *130*, 10674-10683; (d) D. Canevet, M. Salle, G. Zhang, D. Zhang and D. Zhu, *Chem. Commun.* **2009**, 2245-2269; (e) E. M. Pérez, B. M. Illescas, M. A. Herranz and N. Martín, *New J. Chem.* **2009,** *33*, 228-234.

[17] Y. Shoji, K. Tashiro and T. Aida, *J. Am. Chem. Soc.* **2006,** *128*, 10690-10691.

DFT Calculations

A theoretical study of the complexes was carried out using a density functional theory (DFT) approach. Calculations to show the electrostatic potential distribution of the fullerenes C_{60} and C_{70} and **exTTF-CTV** receptor were obtained from minimized structures. The electrostatic potential mapped onto an electronic charge density isosurface of the molecules is shown so that, from most negative values to most positive values, the range of colours is red, orange, yellow, green, light blue, dark blue, where green regions are the most neutral ones. Figure S 8 shows the mapping of the electrostatic potential for C_{60} (left) and C_{70} (right) fullerenes. In the representation, the whole surface is mostly positive, especially in the centre of the pentagonal and hexagonal rings.

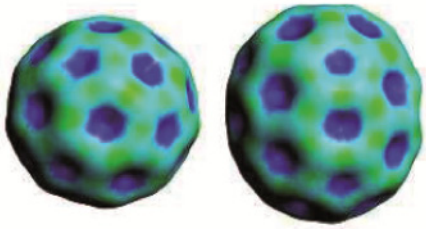

Figure 8. Mapping of the electrostatic potential onto an electron density isosurface of C_{60} and C_{70} (BP86/DZP).

In case of **exTTF-CTV** (Figure 9), the entire molecule is mostly negative (red) and the most negative regions are found in the aromatic surfaces of cyclotriveratrylene moiety as well as in the anthracene-like part in exTTF moiety (see inner and side views in Figure 9). This means that there is not only a perfect match between the concave shape of the receptor and the convex surface of the fullerene, but also an electronic match as the more negative electrostatic potential inside the cavity attracts the positive electrostatic potential of the fullerene.

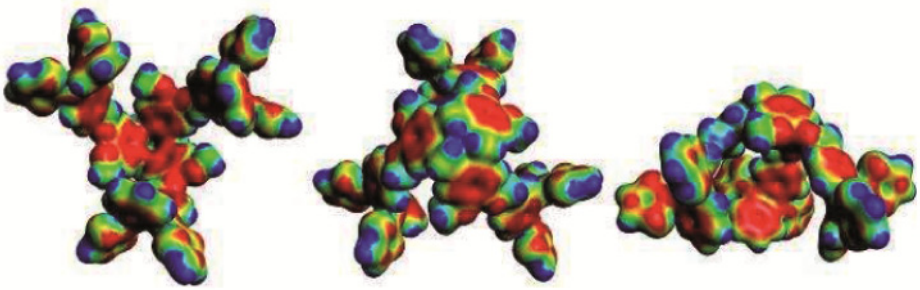

Figure 9. Mapping of the electrostatic potential onto an electron density isosurface of empty receptor (BP86/DZP). From left to right: inner, outer and side views**.**

In the complexes (Figure 10), the electrostatic potential for fullerenes is no longer as positive as in the case of free fullerenes, which suggest that either charge transfer or strong polarization occurred upon complexation.

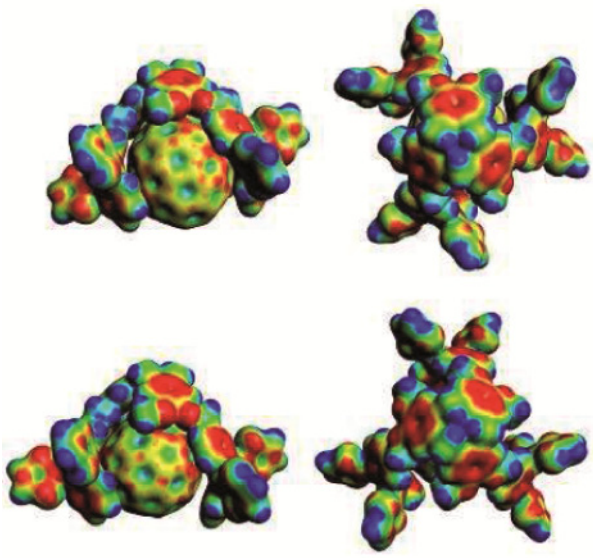

Figure 10. Mapping of the electrostatic potential onto an electron density isosurface of the complexes (BP86/DZP) C_{70}@**exTTF-CTV** (top) and C_{60}@**exTTF-CTV** (bottom) in the ground state.

Indeed, analysis of the Mulliken atomic charges indicates clearly that the receptor and the fullerene moieties in the complex are slightly positively and negatively charged, respectively, so charge transfer from the host to the guest. Note that the value is larger for C_{70} (0.31) than for C_{60} (0.25).

5.5. Experimental section

Materials and Experimental Methods:

All chemicals were purchased from commercial sources and used without further purification. Solvents were dried and distilled using conventional methods or using a Solvent Purification System (SPS).NMR spectra were performed on Bruker Avance 400 (^{1}H: 400 MHz, ^{13}C: 100 MHz) or Bruker Avance 500 (^{1}H: 500 MHz, ^{13}C: 125 MHz) Ultrashield spectrometers. Deuterated solvents used are indicated in each case. Chemical shifts (δ) are expressed in ppm, and are referred to the residual peak of the solvent. High performance liquid chromatography (HPLC) analyses were carried out on an Agilent Technologies Serie 1100 apparatus using a reverse phased C18 Sunfire column (4.6x150mm, 5μm) from Waters, with UV-diode array and mass detectors. The mobile phase used was acetonitrile 100% at 25 °C. HPLC grade solvents were purchased from Scharlab and Carlo Erba and were used with no further purification**.** Mass analysis was performed in Waters LCT Premier (ESI or APCI mode), and Bruker MALDI-TOF spectrometers. UV titrations were done in a Shimadzu UV-2401PC UV-Vis spectrophotometer with a thermostated (7–60 ºC) sample holder (optical range from 190 to 1100 nm). Thin layer chromatography (TLC) was performed on Alugram Sil G-25/UV254-coated aluminium sheets (Macherey-Nagel) with detection by UV at 254 nm. Electrochemistry was carried out in a PARSTAT 2273 potentiostat from Princeton Applied Research with 2 A as maximum current and 1fA of resolution. HPLC or high

purity solvents were used to prepare the solutions, which were bubbled with argon 5 minutes before each measurement. To avoid sample concentration, the argon flow was passed through a reservoir flask containing the solvent mixture which was placed before the working cell. Working electrode was glassy carbon; counter electrode was Pt wire and reference electrode was Ag/AgCl. Working electrode was polished between each measurement with 3μm silica. Pt wire was also cleaned between each measurement with a mixture of sulphuric acid and hydrogen peroxide, then water and methanol, and dried in an oven. The CW-EPR spectra were obtained at room temperature on a Bruker EMX 10/12 spectrometer at X band (9.84 GHz) with the ER4123D dielectric resonator, using a 4.0 mm outer-diameter quartz tube (Norell, Landisville, NJ, USA) for liquid solutions. Solutions were freeze-thaw deareated prior to measurements. The UV irradiation in situ EPR measurements was carried out with a high pressure mercury lamp (Bruker, UV Irradiation System, ER 202 UV). The distance between the lamp and the sample was 60 cm. Instrumental settings were as follows: center field = 3365 G; sweep width = 1000 G; microwave power = 12.6 mW: modulation amplitude = 1,00 G; modulation frequency = 100 kHz; receiver gain = 105; time constant = 163.84 ms; sweep time = 41.94 s; resolution in x = 1024 points; number of scans = 1.

Synthesis of exTTF-CTV

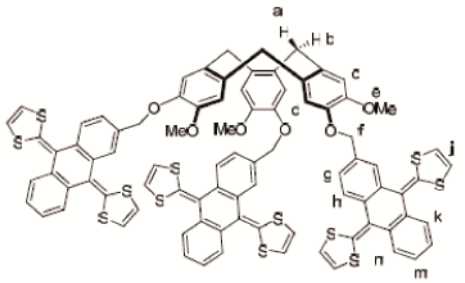

CTV triphenol[18] (25 mg, 0.061 mmol), exTTF methylene alcohol[19] (88 mg, 0.214 mmol) and PPh_3 (57 mg, 0.214 mmol) were mixed together, solved in dry CH_2Cl_2 into a round bottom flask and stirred at 0ºC. DIAD (44 μl, 0.214 mmol) was then added and the mixture was allowed to room temperature and stirred 4 days. Solvent was taken up and the residue was purified by flash chromatography in $CHCl_3$/MeOH (1%). **exTTF-CTV** was isolated as a yellow solid in a 46% yield (45 mg). ^{1}H NMR (500 MHz, chlorobenzene-d^5, 353 K) δ (ppm): 8.09 (bs, 3H, H_i); 7.97 (s, 6H, H_k + H_n); 7.93 (d, *J = 8.2 Hz*, 3H, H_h); 7.53 (bd, *J = 8.2 Hz,* 3H, H_g); 7.44 (hidden under solvent signal – used HH COSY, 6H, .H_l + H_m); 7.31 (s, 3H, H_c); 7.12 (s, 3H, H_d); 6.06 (m, 12H, H_j); 5.36 (m, 6H, H_f); 4.92 (d, J =14.0 Hz, 3H, H_a); 3.84 (s, 9H, H_e); 3.73 (d, J = 14.0 Hz, 3H, H_b). HPLC-MS analysis: Sunfire C18, MeCN, 1 mL/min, λ=254 nm, 95% purity. APCI(+) MS: m/z 1584.1 $[M]^+$ (100%).; ESI(+) MS: m/z 1548.2 $[M]^+$ (10%), 792.7 $[M]^{2+}$ (100%). MALDI-TOF MS: 1584.2 $[M]^+$ (100%).

[18] G. Vériot, J.-P. Dutasta, G. Matouzenko and A. Collet, *Tetrahedron* **1995,** *51*, 389-400.
[19] G. J. Marshallsay and M. R. Bryce, *J. Org. Chem.* **1994,** *59*, 6847-6849.

5.6. References

1. J. W. Steed; P. C. Junk; J. L. Atwood; M. J. Barnes; C. L. Raston; R. S. Burkhalter, Ball and Socket Nanostructures: New Supramolecular Chemistry Based on Cyclotriveratrylene. *J. Am. Chem. Soc.* **1994,** *116*, 10346-10347.

2. (a) E. Huerta; E. Cequier; J. d. Mendoza, Preferential separation of fullerene[84] from fullerene mixtures by encapsulation. *Chem. Commun.* **2007,** *0*, 5016-5018;(b) E. Huerta; G. A. Metselaar; A. Fragoso; E. Santos; C. Bo; J. de Mendoza, Selective binding and easy separation of C_{70} by nanoscale self-assembled capsules. *Angew. Chem. Int. Ed.* **2007,** *46*, 202-205;(c) J. d. Mendoza; E. Huerta; G. A. Metselaar US 2008/0025904 A1, 2008.

3. (a) J. L. Atwood; L. J. Barbour; P. J. Nichols; C. L. Raston; C. A. Sandoval, Symmetry-aligned supramolecular encapsulation of C_{60}: [C_{60} .cntnd. $(L)_2$], L = p-Benzylcalix[5]arene or p-benzylhexahomooxacalix[3]arene. *Chem. Eur. J.* **1999,** *5*, 990-996;(b) A. Hosseini; S. Taylor; G. Accorsi; N. Armaroli; C. A. Reed; P. D. W. Boyd, Calix[4]arene-Linked Bisporphyrin Hosts for Fullerenes: Binding Strength, Solvation Effects, and Porphyrin-Fullerene Charge Transfer Bands. *J. Am. Chem. Soc.* **2006,** *128*, 15903-15913.

4. (a) K. A. Nielsen; L. Martín-Gomis; G. H. Sarova; L. Sanguinet; D. E. Gross; F. Fernández-Lázaro; P. C. Stein; E. Levillain; J. L. Sessler; D. M. Guldi; A. Sastre-Santos; J. O. Jeppesen, Binding studies of tetrathiafulvalene-calix[4]pyrroles with electron-deficient guests. *Tetrahedron* **2008,** *64*, 8449-8463;(b) K. A. Nielsen; G. H. Sarova; L. Martín-Gomis; F. Fernández-Lázaro; P. C. Stein; L. Sanguinet; E. Levillain; J. L. Sessler; D. M. Guldi; A. Sastre-Santos; J. O. Jeppesen, Chloride Anion Controlled Molecular "Switching". Binding of 2,5,7-Trinitro-9-dicyanomethylenefluorene-C_{60} by Tetrathiafulvalene Calix[4]pyrrole and Photophysical Generation of Two Different Charge-Separated States. *J. Am. Chem. Soc.* **2008,** *130*, 460-462.

5. (a) S. Mizyed; P. E. Georghiou; M. Bancu; B. Cuadra; A. K. Rai; P. Cheng; L. T. Scott, Embracing C_{60} with Multiarmed Geodesic Partners. *J. Am. Chem. Soc.* **2001,** *123*, 12770-12774;(b) P. E. Georghiou; A. H. Tran; S. Mizyed; M. Bancu; L. T. Scott, Concave Polyarenes with Sulfide-Linked Flaps and Tentacles: New Electron-Rich Hosts for Fullerenes. *J. Org. Chem.* **2005,** *70*, 6158-6163.

6. P. E. Georghiou; L. N. Dawe; H.-A. Tran; J. Strube; B. Neumann; H.-G. Stammler; D. Kuck, C3v-Symmetrical Tribenzotriquinacenes as Hosts for C_{60} and C_{70} in Solution and in the Solid State. *J. Org. Chem.* **2008,** *73*, 9040-9047.

7. (a) H. Matsubara; T. Shimura; A. Hasegawa; M. Semba; K. Asano; K. Yamamoto, Syntheses of Novel Fullerene Tweezers and Their Supramolecular Inclusion Complex of C_{60}. *Chem. Lett.* **1998,** *27*, 1099-1100;(b) M. J. Hardie; P. D. Godfrey; C. L. Raston, Self-assembly of grid and helical hydrogen-bonded arrays incorporating bowl-shaped receptor sites that bind globular molecules. *Chem. Eur. J.* **1999,** *5*, 1828-1833;(c) J. F. Nierengarten, Supramolecular Encapsulation of [60]Fullerene with Dendritic Cyclotriveratrylene Derivatives. *Fullerenes, Nanotubes and Carbon Nanostructures* **2005,** *13*, 229-242.

8. (a) E. M. Pérez; L. Sánchez; G. Fernández; N. Martín, exTTF as a Building Block for Fullerene Receptors. Unexpected Solvent-Dependent Positive Homotropic Cooperativity. *J. Am. Chem. Soc.* **2006,** *128*, 7172-7173;(b) E. M. Pérez; A. L. Capodilupo; G. Fernández; L. Sánchez; P. M. Viruela; R. Viruela; E. Ortí; M. Bietti; N. Martín, Weighting non-covalent forces in the molecular recognition of C_{60}. Relevance of concave-convex complementarity. *Chem. Commun.* **2008,** *0*, 4567-4569;(c) E. M. Perez; N. Martin, Curves ahead: molecular receptors for fullerenes based on concave-convex complementarity. *Chem. Soc. Rev.* **2008,** *37*, 1512-1519;(d) S. S. Gayathri; M. Wielopolski; E. M. Pérez; G. Fernández; L. Sánchez; R. Viruela; E. Ortí; D. M. Guldi; N. Martín, Discrete supramolecular donor-acceptor complexes. *Angew. Chem. Int. Ed.* **2009,** *48*, 815-819.

9. H. Isla; M. Gallego; E. M. Pérez; R. Viruela; E. Ortí; N. Martín, A Bis-exTTF Macrocyclic Receptor That Associates C_{60} with Micromolar Affinity. *J. Am. Chem. Soc.* **2010,** *132*, 1772-1773.

10. (a) D. M. Guldi; L. Sánchez; N. Martín, Formation and Characterization of the p-Radical Cation and Dication of p-Extended Tetrathiafulvalene Materials. *J. Phys. Chem. B* **2001,** *105*, 7139-7144;(b) A. E. Jones; C. A. Christensen; D. F. Perepichka; A. S. Batsanov; A. Beeby; P. J. Low; M. R. Bryce; A. W. Parker, Molecular saddles, part 6. Photochemistry of the π-extended 9,10-bis(1,3-dithiol-2-ylidene)-9,10-dihydroanthracene system: generation and characterization of the radical cation, dication, and derived products. *Chem. Eur. J.* **2001,** *7*, 973-978.

11. C. A. Schalley, Introduction. In *Analytical Methods in Supramolecular Chemistry*, Wiley-VCH Verlag GmbH & Co. KGaA: 2007; pp 1-16.
12. (a) J.-Y. Zheng; K. Tashiro; Y. Hirabayashi; K. Kinbara; K. Saigo; T. Aida; S. Sakamoto; K. Yamaguchi, Cyclic Dimers of Metalloporphyrins as Tunable Hosts for Fullerenes: A Remarkable Effect of Rhodium(III). *Angew. Chem. Int. Ed.* **2001,** *40*, 1857-1861;(b) K. Tashiro; T. Aida, Metalloporphyrin hosts for supramolecular chemistry of fullerenes. *Chem. Soc. Rev.* **2007,** *36*, 189-197;(c) M. Yanagisawa; K. Tashiro; M. Yamasaki; T. Aida, Hosting Fullerenes by Dynamic Bond Formation with an Iridium Porphyrin Cyclic Dimer: A "Chemical Friction" for Rotary Guest Motions. *J. Am. Chem. Soc.* **2007,** *129*, 11912-11913.
13. (a) E. J. Baerends; D. E. Ellis; P. Ros, Self-consistent molecular Hartree-Fock-Slater calculations. I. Computational procedure. *Chem. Phys.* **1973,** *2*, 41-51;(b) E. J. Baerends; P. Ros, Self-consistent molecular Hartree-Fock-Slater calculations. II. Effect of exchange scaling in some small molecules. *Chem. Phys.* **1973,** *2*, 52-9;(c) S. H. Vosko; L. Wilk; M. Nusair, Accurate spin-dependent electron liquid correlation energies for local spin density calculations: a critical analysis. *Can. J. Phys.* **1980,** *58*, 1200-11;(d) A. D. Becke, Completely numerical calculations on diatomic molecules in the local-density approximation. *Phys. Rev. A* **1986,** *33*, 2786-2788;(e) M. Levy; J. P. Perdew, Success of quantum mechanical approximations for molecular geometries and electron--nuclear attraction expectation values: Gift of the Coulomb potential? *J. Chem. Phys.* **1986,** *84*, 4519-4523;(f) A. D. Becke, Density-functional exchange-energy approximation with correct asymptotic behavior. *Phys. Rev. A* **1988,** *38*, 3098-3100;(g) P. M. Boerrigter; G. Te Velde; E. J. Baerends, Three-dimensional numerical integration for electronic structure calculations. *Int. J. Quantum Chem* **1988,** *33*, 87-113;(h) G. Te Velde; E. J. Baerends, Numerical integration for polyatomic systems. *J. Comput. Phys.* **1992,** *99*, 84-98;(i) C. F. Guerra; J. G. Snijders; G. Te Velde; E. J. Baerends, Towards an order-N DFT method. *Theor. Chem. Acc.* **1998,** *99*, 391-403.
14. Y. Zhao; D. G. Truhlar, Density Functionals for Noncovalent Interaction Energies of Biological Importance. *J. Chem. Theory Comput.* **2006,** *3*, 289-300.
15. (a) S. Fukuzumi; H. Mori; T. Suenobu; H. Imahori; X. Gao; K. M. Kadish, Effects of Lowering Symmetry on the ESR Spectra of Radical Anions of Fullerene Derivatives and the Reduction Potentials. *J. Phys. Chem. A* **2000,** *104*, 10688-10694;(b) D. F. Perepichka; M. R. Bryce; I. F. Perepichka; S. B. Lyubchik; C. A. Christensen; N. Godbert; A. S. Batsanov; E. Levillain; E. J. L. McInnes; J. P. Zhao, A (π-Extended Tetrathiafulvalene)-Fluorene Conjugate. Unusual Electrochemistry and Charge Transfer Properties: The First Observation of a Covalent D2+-s-A.bul.- Redox State. *J. Am. Chem. Soc.* **2002,** *124*, 14227-14238.
16. (a) G. Fernández; E. M. Pérez; L. Sánchez; N. Martín, Self-Organization of Electroactive Materials: A Head-to-Tail Donor–Acceptor Supramolecular Polymer. *Angew. Chem. Int. Ed.* **2008,** *47*, 1094-1097;(b) G. Fernández; E. M. Pérez; L. Sánchez; N. Martín, An Electroactive Dynamically Polydisperse Supramolecular Dendrimer. *J. Am. Chem. Soc.* **2008,** *130*, 2410-2411;(c) G. Fernández; L. Sánchez; E. M. Pérez; N. Martín, Large exTTF-Based Dendrimers. Self-Assembly and Peripheral Cooperative Multiencapsulation of C_{60}. *J. Am. Chem. Soc.* **2008,** *130*, 10674-10683;(d) D. Canevet; M. Salle; G. Zhang; D. Zhang; D. Zhu, Tetrathiafulvalene (TTF) derivatives: key building-blocks for switchable processes. *Chem. Commun.* **2009**, 2245-2269;(e) E. M. Pérez; B. M. Illescas; M. A. Herranz; N. Martín, Supramolecular chemistry of π-extended analogues of TTF and carbon nanostructures. *New J. Chem.* **2009,** *33*, 228-234.
17. Y. Shoji; K. Tashiro; T. Aida, Sensing of Chiral Fullerenes by a Cyclic Host with an Asymmetrically Distorted π-Electronic Component. *J. Am. Chem. Soc.* **2006,** *128*, 10690-10691.
18. G. Vériot; J.-P. Dutasta; G. Matouzenko; A. Collet, Synthesis of C3-cyclotriveratrylene ligands for iron(II) and iron(III) coordination. *Tetrahedron* **1995,** *51*, 389-400.
19. G. J. Marshallsay; M. R. Bryce, *J. Org. Chem.* **1994,** *59*, 6847-6849.

5. Tripodal exTTF- CTV host for fullerenes

6. exTTF-capped gold nanoparticles as receptors

Roberto Cao Jr., Helena Isla, Roberto Cao, Emilio M. Pérez, Nazario Martín *Chem. Sci.* **2011**, *2*, 1384-1388

Fulvio G. Brunetti, Helena Isla, Juan Aragó, Enrique Ortí, Emilio M. Pérez, Nazario Martín, *Chem. Eur. J.* **2013**, DOI: 10.1002/chem.201301102

6.1. exTTF-capped gold nanoparticles as multivalent receptors for C_{60}

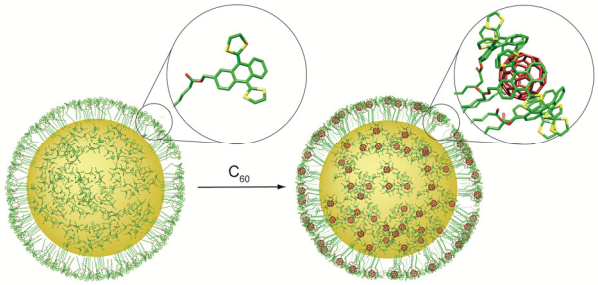

We report the synthesis and C_{60} binding abilities of gold nanoparticles capped with p-extended tetrathiafulvalene (exTTFAuNPs). The exTTFAuNPs show a strong tendency to aggregate both in solution and in the solid state through multiple weak exTTF-exTTF interactions. A thorough collection of experiments demonstrates that upon addition of C_{60}, stable noncovalent exTTFAuNP•C_{60} associates are formed, with concomitant partial disaggregation of the nanoparticles.

Chem. Sci. **2011**, *2*, 1384-1388

6.1.1. Introduction

Framed within the search for new materials for energy conversion, there is a growing interest in the exploration of noncovalent associates of electroactive molecules.[1,2] With regards to electron donors, the supramolecular properties of tetrathiafulvalene have been thoroughly explored,[3] while the noncovalent chemistry

[1] For recent reviews, see: (a) L. Zang, Y. K. Che and J. S. Moore, *Acc. Chem. Res.* **2008,** *41*, 1596-1608; (b) F. D'Souza and O. Ito, *Chem. Commun.* **2009**, 4913-4928; (c) E. M. Pérez, B. M. Illescas, M. A. Herranz and N. Martín, *New J. Chem.* **2009,** *33*, 228-234; (d) H. Liu, J. Xu, Y. Li and Y. Li, *Acc. Chem. Res.* **2010,** *43*, 1496-1508; E. M. Pérez, *Pure Appl. Chem.* **2011,** *83*, 201-211.

[2] For selected recent examples, see: (a) F. D'Souza, E. Maligaspe, K. Ohkubo, M. E. Zandler, N. K. Subbaiyan and S. Fukuzumi, *J. Am. Chem. Soc.* **2009,** *131*, 8787-8797; (b) X. Feng, V. Marcon, W. Pisula, M. R. Hansen, J. Kirkpatrick, F. Grozema, D. Andrienko, K. Kremer and K. Muellen, *Nature Materials* **2009,** *8*, 421-426; (c) X. Feng, W. Pisula, T. Kudernac, D. Wu, L. Zhi, S. De Feyter and K. Muellen, *J. Am. Chem. Soc.* **2009,** *131*, 4439-4448; (d) J. M. Mativetsky, M. Kastler, R. C. Savage, D. Gentilini, M. Palma, W. Pisula, K. Muellen and P. Samori, *Adv. Funct. Mater.* **2009,** *19*, 2486-2494; (e) L. Welte, A. Calzolari, R. Di Felice, F. Zamora and J. Gómez-Herrero, *Nature Nanotechnology* **2010,** *5*, 110-115; (f) G. Bottari, D. Olea, C. Gomez-Navarro, F. Zamora, J. Gómez-Herrero and T. Torres, *Angew. Chem. Int. Ed.* **2008,** *47*, 2026-2031.

[3] (a) J. L. Segura and N. Martín, *Angew. Chem. Int. Ed.* **2001,** *40*, 1372-1409; (b) M. M. S. Abdel-Mottaleb, E. Gomar-Nadal, M. Surin, H. Uji-i, W. Mamdouh, J. Veciana, V. Lemaur, C. Rovira, J.

of its π-extended analogue 9,10-di(1,3-dithiol-2-ylidene)-9,10-dihydroanthracene (exTTF) had hardly been investigated. Building on the design of the first receptors for fullerene based on exTTF,[4] our group has contributed to this area with the investigation of the supramolecular associates between π-extended tetrathiafulvalenes and fullerenes,[4, 5, 6] Thus far, we have reported the construction of linear[6d] and hyperbranched[6c] supramolecular polymers, covalent dendrimers capable of associating multiple units of fullerene,[6b] and fully electron acceptor variants of the former two.[6a] Based on the example of the covalent dendrimers, we reasoned we could increase the number of fullerene binding sites and significantly reduce the synthetic effort by utilizing gold nanoparticles as scaffolds. This approach has been successfully utilized in the construction of multivalent receptors for numerous analytes.[7] Moreover, the attachment of electroactive molecules to gold nanoparticles has received considerable attention, especially in the case of porphyrins,[8] but to date,

---

Cornil, R. Lazzaroni, D. B. Amabilino, S. De Feyter and F. C. De Schryver, *J. Mater. Chem.* **2005,** *15*, 4601-4615; (c) D. Canevet, M. Salle, G. Zhang, D. Zhang and D. Zhu, *Chem. Commun.* **2009**, 2245-2269.

[4] (a) E. M. Pérez, L. Sánchez, G. Fernández and N. Martín, *J. Am. Chem. Soc.* **2006,** *128*, 7172-7173; (b) E. M. Pérez, A. L. Capodilupo, G. Fernández, L. Sánchez, P. M. Viruela, R. Viruela, E. Ortí, M. Bietti and N. Martín, *Chem. Commun.* **2008,** 4567-4569; (c) S. S. Gayathri, M. Wielopolski, E. M. Pérez, G. Fernández, L. Sánchez, R. Viruela, E. Ortí, D. M. Guldi and N. Martín, *Angew. Chem. Int. Ed.* **2009,** *48*, 815-819.

[5] (a) D. Canevet, M. Gallego, H. Isla, A. de Juan, E. M. Pérez and N. Martín, *J. Am. Chem. Soc.* **2011,** *133*, 3184-3190; (b) H. Isla, M. Gallego, E. M. Pérez, R. Viruela, E. Ortí and N. Martín, *J. Am. Chem. Soc.* **2010,** *132*, 1772-1773; (c) E. Huerta, H. Isla, E. M. Pérez, C. Bo, N. Martín and J. de Mendoza, *J. Am. Chem. Soc.* **2010,** *132*, 5351-5353; (d) B. Grimm, J. Santos, B. M. Illescas, A. Muñoz, D. M. Guldi and N. Martín, *J. Am. Chem. Soc.* **2010,** *132*, 17387-17389; (e) J. Santos, B. Grimm, B. M. Illescas, D. M. Guldi and N. Martín, *Chem. Commun.* **2008,** 5993-5995; (f) E. M. Pérez and N. Martín, *Chem. Soc. Rev.* **2008,** *37*, 1512-1519; (g) E. M. Pérez, M. Sierra, L. Sánchez, M. R. Torres, R. Viruela, P. M. Viruela, E. Ortí and N. Martín, *Angew. Chem. Int. Ed.* **2007,** *46*, 1847-1851.

[6] (a) J. Santos, E. M. Pérez, B. M. Illescas and N. Martín, *Chem.--Asian J.* **2011,** *6*, 1848-1853; (b) G. Fernández, L. Sánchez, E. M. Pérez and N. Martín, *J. Am. Chem. Soc.* **2008,** *130*, 10674-10683; (c) G. Fernández, E. M. Pérez, L. Sánchez and N. Martín, *J. Am. Chem. Soc.* **2008,** *130*, 2410-2411; (d) G. Fernández, E. M. Pérez, L. Sánchez and N. Martín, *Angew. Chem. Int. Ed.* **2008,** *47*, 1094-1097.

[7] (a) N. Kanayama, T. Takarada and M. Maeda, *Chem. Commun.* **2011,** *47*, 2077-2079; (b) R. Cao and B. Li, *Chem. Commun.* **2011,** *47*, 2865-2867; (c) Z. Zhu, C. Wu, H. Liu, Y. Zou, X. Zhang, H. Kang, C. J. Yang and W. Tan, *Angew. Chem. Int. Ed.* **2010,** *49*, 1052-1056, S1052/1-S1052/4; (d) X. Xu, W. L. Daniel, W. Wei and C. A. Mirkin, *Small* **2010,** *6*, 623-626; (e) X. Li, J. Wang, L. Sun and Z. Wang, *Chem. Commun.* **2010,** *46*, 988-990; (f) Y. Jiang, H. Zhao, Y. Lin, N. Zhu, Y. Ma and L. Mao, *Angew. Chem. Int. Ed.* **2010,** *49*, 4800-4804; (g) D. A. Giljohann, D. S. Seferos, W. L. Daniel, M. D. Massich, P. C. Patel and C. A. Mirkin, *Angew. Chem. Int. Ed.* **2010,** *49*, 3280-3294; (h) D. Feng, Y. Zhang, W. Shi, X. Li and H. Ma, *Chem. Commun.* **2010,** *46*, 9203-9205; (i) U. H. F. Bunz and V. M. Rotello, *Angew. Chem. Int. Ed.* **2010,** *49*, 3268-3279.

[8] (a) J. Ohyama, Y. Hitomi, Y. Higuchi, M. Shinagawa, H. Mukai, M. Kodera, K. Teramura, T. Shishido and T. Tanaka, *Chem. Commun.* **2008**, 6300-6302; (b) M. Kanehara, H. Takahashi and T. Teranishi, *Angew. Chem. Int. Ed.* **2008,** *47*, 307-310; (c) T. Akiyama, M. Nakada, N. Terasaki and S. Yamada, *Chem. Commun.* **2006**, 395-397; (d) H. Imahori, A. Fujimoto, S. Kang, H. Hotta, K. Yoshida, T. Umeyama, Y. Matano, S. Isoda, M. Isosomppi, N. V. Tkachenko and H. Lemmetyinen, *Chem. Eur. J.* **2005,** *11*, 7265-7275; (e) H. Imahori, A. Fujimoto, S. Kang, H. Hotta, K. Yoshida, T. Umeyama, Y. Matano and S. Isoda, *Adv. Mater.* **2005,** *17*, 1727-1730; (f) T. Hasobe, H. Imahori, P. V. Kamat, T. K. Ahn, S. K. Kim, D. Kim, A. Fujimoto, T. Hirakawa and S. Fukuzumi, *J. Am. Chem. Soc.* **2005,** *127*, 1216-1228.

Gold Nanoparticles

Hystory. Nanotechnology is a fairly new science, but it is possible that the first examples of "soluble" gold appeared as early as the 5th or 4th century B.C. in Egypt and China. These ancient civilizations used colloidal gold for aesthetic and curative purposes. A thoroughly documented example of early nanotechnology is medieval stained glass. They were the first nanotechnologists, as they trapped gold nanoparticles in the 'glass matrix' in order to generate the ruby red colour in the windows. For example the colouring material made by precipitation of gold in a tin chloride solution is called "purple of Cassius". The description of the process is attributed to Andreas Cassius in his treatise *De Auro* (1685), although it was known before. Egyptian manuscripts from the Greco-Roman era make reference to it.

Southern Germany, 1695-1700, Museumslandschaft Hessen, Kassel, Germany.

Synthesis. The citrate reduction of $HAuCl_4$ in water has been the most popular method for the synthesis of AuNP, for a long time. This method was introduced by Turkevitch in 1951 and reported in 1973 by Frens to obtain AuNP of prechosen size via their controlled formation, for example controlling the ratio between reducing/stabilizing agents. Other technique is the two-phase synthesis and stabilization by thiols (Brust-Schiffrin method), transferring the $AuCl_4^-$ using a phase-transfer agent and reducing it with $NaBH_4$ in the presence of thiols. A wide variety of ligands are used to stabilize the NP besides thiols. There are techniques that use microemulsions, reversed micelles, surfactants, membranes and polyelectrolytes to maintain a favourable microenviroment for the synthesis. Another strategy is the seeding growth. The modulation of different variables in the technique of synthesis allows for the control of size and shape. Physical methods as photochemistry, sonochemistry, radiolysis and thermolysis can also be used to control the reduction of $HAuCl_4$.

Optical properties. The optical properties of gold are dramatically modified when the size of the metallic particle is reduced to a few nanometres. The surface plasmon resonance (SPR) band appears corresponding to an interaction between matter and the electromagnetic field of light and its resulting behaviour is completely different from the bulk metal one. The electric field of incident light induces coherent collective oscillation of conduction band electrons with respective to the positively charged metallic core. This dipolar oscillation is resonant with the incoming light at a specific frequency that depends on particle size and shape. This quantum size effect appears when the size of the particle is of the same order than the de Broglie wavelength of the valence electrons. In the case of AuNP the SPR give rise to the plasmon resonance band near 530 nm in 5-20 nm-diameter range.

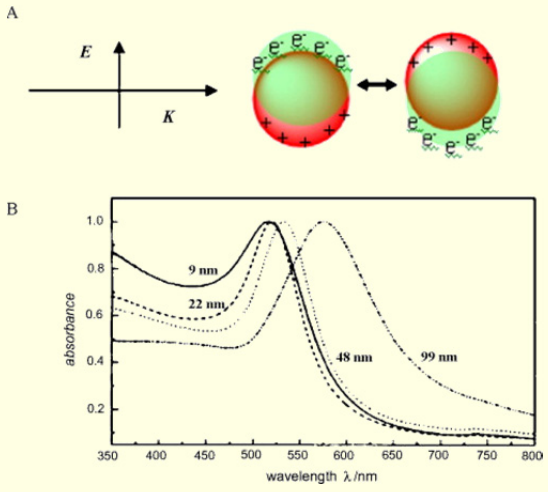

A) Schematic illustration of surface plasmon resonance in nanoparticles

B) SPR bands in absorption spectra of gold nanoparticles in different sizes

TTF and its derivatives have played a secondary role.[9]

Here we present the synthesis, characterization, and supramolecular properties of gold nanoparticles densely functionalised with exTTF.

6.1.2. Results and discussion

It has been shown that gold nanoparticles (AuNPs) functionalized with porphyrins through alkanethiole spacers bind fullerenes in solution, with the AuNP acting as a linker between the two necessary porphyrin units.[8d] Taking this into account, we designed and synthesised exTTF-capped AuNPs (exTTFAuNPs) according to Scheme 1. Firstly, we prepared AuNPs by reduction of $AuCl_3$ with sodium citrate in water, following the classic protocol described by Frens.[10] Separately, we prepared the exTTF ester of mercaptoundecanoic acid (MUA-exTTF) by condensation of readily available exTTF-CH_2OH and MUA in CH_2Cl_2 with *N*-(3-dimethylaminopropyl)-*N*′-ethylcarbodiimide hydrochloride as coupling reagent and 4-dimethylaminopyridine as base and catalyst. To obtain the exTTFAuNPs we performed a liquid-liquid extraction, with the MUA-exTTF dissolved in chlorobenzene as organic phase and the citrate-capped AuNPs in aqueous solution. This mixture was stirred vigorously for two hours or until complete decoloration of the red aqueous phase. The golden-green organic phase was centrifuged with CH_2Cl_2 to precipitate the exTTFAuNPs, which were further washed several times with CH_2Cl_2 and CH_3OH to remove excess organic ligand (for experimental details, see experimental section). The exTTFAuNPs thus obtained show a diameter of 7.4 ± 1.0 nm, as calculated from statistical analysis of transmission electron microscopy (TEM) images (Figure 1).

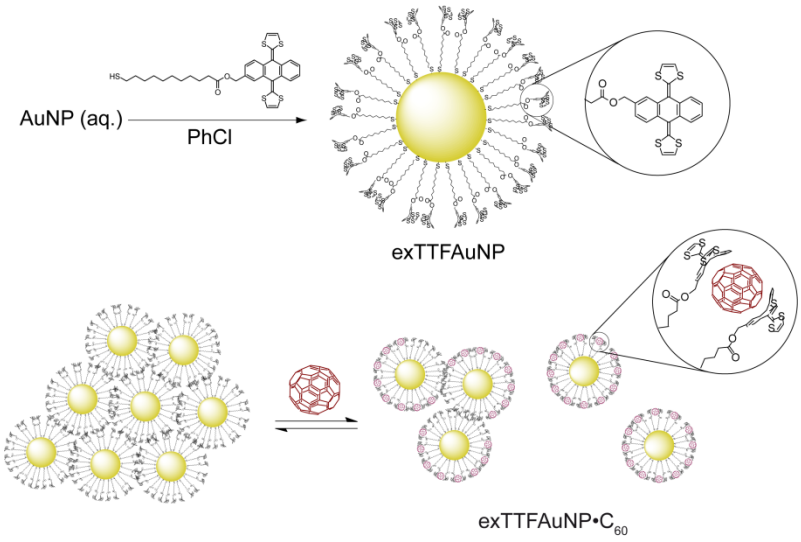

[9] (a) G. Zhang, D. Zhang, X. Zhao, X. Ai, J. Zhang and D. Zhu, *Chem. Eur. J.* **2006,** *12*, 1067-1073; (b) W.-J. Guo, J. Dai, D.-Q. Zhang, Q.-Y. Zhu and G.-Q. Bian, *Inorg. Chem. Commun.* **2005,** *8*, 994-997; (c) J. Dai, L. Guo, Y. Jiang, Q.-Y. Zhu, R.-A. Gu, D.-x. Jia and W.-J. Guo, *J. Nanosci. Nanotechnol.* **2005,** *5*, 474-478; (d) H. Nakai, M. Yoshihara and H. Fujihara, *Langmuir* **1999,** *15*, 8574-8576.
[10] G. Frens, *Nature* **1973,** *241*, 20-2.

Scheme 1. Synthesis of exTTFAuNPs and representation of their aggregation and partial disaggregation upon binding of [60]fullerene.

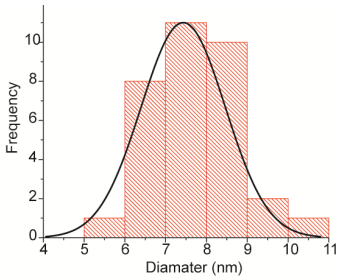

Figure 1. Statistical analysis of the diameter of the exTTFAuNPs.

The electronic absorption spectrum of the exTTFAuNPs (chlorobenzene, 298 K) shows a band at λ ~ 450 nm in a region in which the spectrum of MUA-AuNPs shows a minimum (Figure 2). We attribute this absorption to the exTTF chromophore (λ_{max} = 434 nm). Besides this, an intense and broad absorption band at λ ~ 590 nm, characteristic of AuNPs forming aggregates[11] (Figures 2 and 3) is also found. We had previously observed the same tendency to self-associate in the case of covalent dendrimers featuring numerous exTTF units in their outer shell.[6b] In the case of the dendrimers, upon addition of C_{60} the weak exTTF···exTTF interactions were readily substituted with the energetically more favorable exTTF···C_{60},[4-6,12] which allowed for the recognition of multiple units of C_{60}. This is also the case for the exTTFAuNPs, as shown in Figure 3. Upon addition of C_{60} (chlorobenzene, 0.52 mM), we observed depletion of the band at λ ~ 450 nm, which is the signature of the exTTF·C_{60} recognition event.[4,5] Besides this, we observed a decrease in intensity and a slight hypsochromic shift in the plasmon resonance band (λ ~ 590 nm), indicating partial disaggregation of the nanoparticles. In order to confirm this last observation a computational simulation was carried out (see computational details section).[13] Briefly, the optical response of aggregated nanoparticles was described using a simplified model composed by three aligned gold nanoparticles in which one of them was set to increase its distance from the other two. Our computational model confirms that an increase in the distance between the nanoparticles leads to a decrease in the intensity and a blue shift of the plasmon band (Figure 9, computational details), as observed experimentally.

---

[11] U. Kreibig and L. Genzel, *Surf. Sci.* **1985,** *156, Part 2*, 678-700.

[12] For other examples of supramolecular systems based on the exTTF-C_{60} interaction, see: (a) X. Yang, G. Zhang, D. Zhang and D. Zhu, *Langmuir* **2010,** *26*, 11720-11725; (b) X. Yang, G. Zhang, D. Zhang, J. Xiang, G. Yang and D. Zhu, *Soft Matter* **2011,** *7*, 3592-3598.

[13](a) F. J. García de Abajo and A. Howie, *Phys. Rev. Lett.* **1998,** *80*, 5180-5183; (b) F. J. García de Abajo and A. Howie, *Physical Review B* **2002,** *65*, 115418; (c) V. Myroshnychenko, E. Carbó-Argibay, I. Pastoriza-Santos, J. Pérez-Juste, L. M. Liz-Marzán and F. J. García de Abajo, *Adv. Mater.* **2008,** *20*, 4288-4293; (d) V. Myroshnychenko, J. Rodriguez-Fernandez, I. Pastoriza-Santos, A. M. Funston, C. Novo, P. Mulvaney, L. M. Liz-Marzan and F. J. Garcia de Abajo, *Chem. Soc. Rev.* **2008,** *37*, 1792-1805.

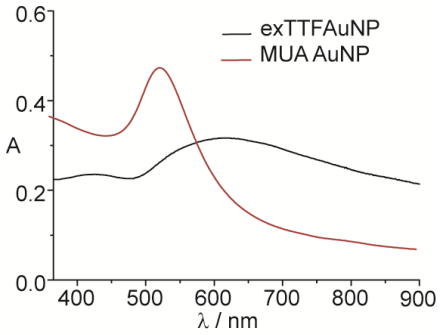

Figure 2. UV-vis spectra of exTTFAuNPs and MUAAuNP in oDCB at room temperature.

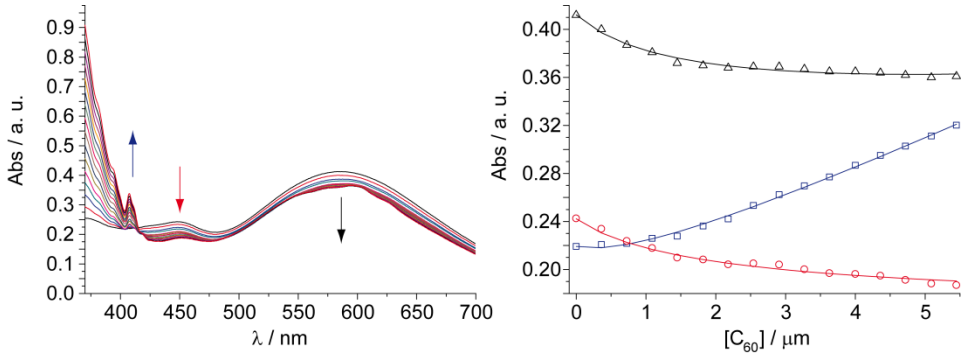

Figure 3. Left: changes in the UV-vis spectrum (chlorobenzene, 298 K) of exTTFAuNPs with increasing concentration of C_{60}. Right: binding isotherms for a 5:1 exTTF:C_{60} model at 406 nm (blue), 449 nm (red) and 587 nm (black); empty squares, circles and triangles are experimental data, solid lines correspond to the fit for a binding constant log $\beta_{5:1} = 22.5 \pm 0.1$.

The absence of tight isosbestic points is in agreement with the coexistence of several species of different stoichiometry during the titration, as was expected. The quantitative analysis of such complex titration data is not straightforward. Firstly, we calculated the molar concentration of exTTF chromophores in the solution of the nanoparticles considering the absorbance at 450 nm and the molar absorptivity of exTTF. Secondly, in order to get an idea of the possible exTTF:C_{60} stoichiometry of the associates, we carried out continuous variation plots, which resulted in several poorly defined maxima. This disappointing result is due to the tendency of Job's plots to fail when more than one type of complexes are present in solution.[14] Thus, we resorted to molecular mechanics calculations (AMBER),[15] which indicated that up to five units of MUA-exTTF can surround C_{60} without steric congestion (Figure

[14] P. Thordarson, *Chem. Soc. Rev.* **2011,** *40*, 1305-1323.
[15] Minimizations were carried out utilizing AMBER force field included in the HyperChem molecular modelling system. The AMBER force field was selected because it includes a term for Van der Waals and electrostatic interactions. See: W. D. Cornell, P. Cieplak, C. I. Bayly, I. R. Gould, K. M. Merz, Jr., D. M. Ferguson, D. C. Spellmeyer, T. Fox, J. W. Caldwell and P. A. Kollman, *J. Am. Chem. Soc.* **1995,** *117*, 5179-97.

4). Indeed, the UV-vis titration data (Figure 3) fitted successfully to either a 5:1 or a 4:1 exTTF:C_{60} binding models utilizing global multivariable analysis software, while fitting to other reasonable models (2:1, 3:1, and 6:1) was unsuccessful (Figure 5). The analysis yielded binding constants of log $\beta_{5:1}$ = 22.5 ± 0.1 or log $\beta_{4:1}$ = 17.9 ± 0.1. Assuming all exTTF-C_{60} binding events present the same binding constant, both of these values correspond to a log $K_{1:1}$ = 4.5, indicative of a very strong multivalent effect. For comparison, our original tweezers-like hosts show a binding constant one order of magnitude smaller, despite featuring two units of exTTF (log K_a = 3.5).[4a] Only highly preorganized macrocyclic bis-exTTF receptors show binding constants comparable to the exTTFAuNPs (log K_a 4-6.5).[5a] In fact, we have not observed spectroscopic evidence of binding C_{60} for a single unit of exTTF in the absence of the gold nanoparticle scaffold,[4a] unless other cooperative forces are also present.[5d, 5e]

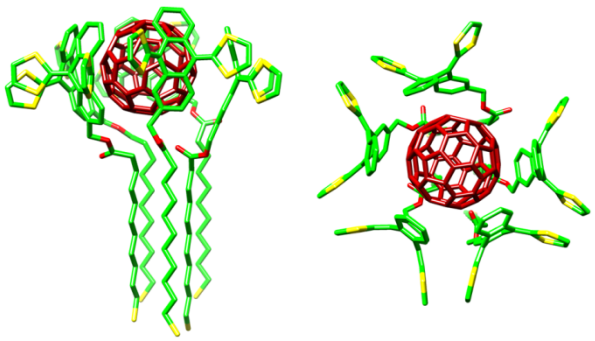

Figure 4. Side and top views of the energy-minimized (AMBER) model of the associate with five units of MUA-exTTF surrounding C_{60}. Carbon atoms are depicted in green, sulfurs in yellow and oxygens in red. Hydrogens are omitted for clarity. C_{60} is depicted in dark red.

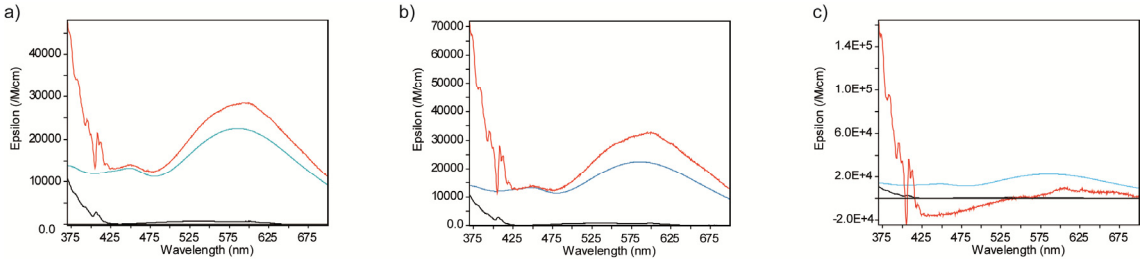

Figure 5. Simulated spectra (Specfit) for the exTTFAuNP·C_{60} associate (red) for a) 2:1 binding model; b) 3:1 binding model; and c) 6:1 bonding model. The spectra of exTTFAuNPs (blue) and C_{60} (black) are determined experimentally and introduced as data for the fit. As indication of the satisfactory fitting, we examined both the binding isotherms at key wavelengths (as in figure 3) and the sensibleness of the simulated spectra. Note that in a) and b) the trends during the titrations experiment (decrease in absorption of the bands at λ = 450 and 590 nm) are not reproduced, while in the 6:1 model in c) produces a chemically meaningless strong negative absorption.

The multivalent effect

The valency of a particle is the number of connections of the same kind that it can form with other particles through ligand-receptor interactions. Multivalent interactions are essential in the mediation of biological processes. For example carbohydrate-protein interactions that govern many biological processes are characterized by a low affinity compensated in nature by multivalency. Multivalent interactions tend to be much stronger than the sum of the corresponding monovalent ones. Although this binding enhancement is well-demonstrated, the contributions of enthalpy and entropy are still unclear.

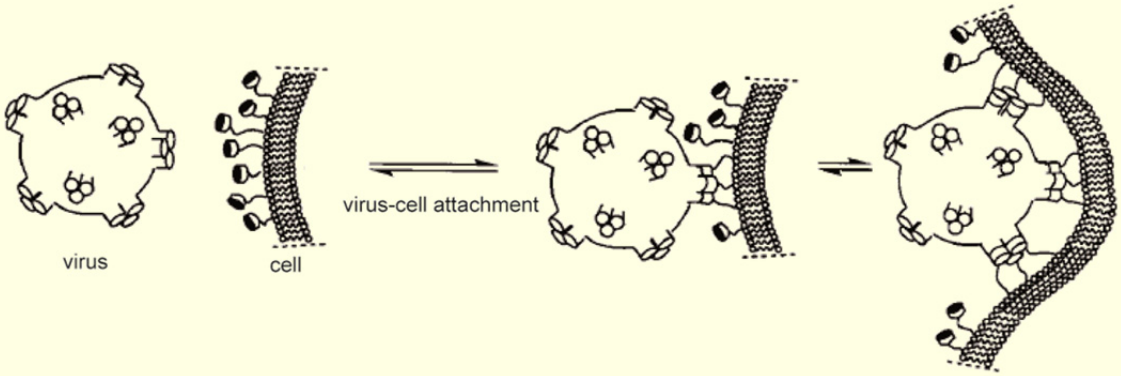

Graphic representation of the attachment of influenza virus to a cell surface. Only a few of the hemagglutinin trimers and SA groups are represented; neither is to scale.

Viruses attach to the cell membrane via multivalent interacions:

Attachment of a virus to its host is the first step to viral infection, and involves the simultaneous association of multiple molecules on the surface of the virus with multiple molecules on the surface of its host cell. The influenza virus attaches to cells by multiple simultaneous interaction of trimeric hemagglutinin (HA) with sialic acid (SA) on the cell. There is an estimation of the avidity between a strain of influenza and erythrocyte surface with a lower limit of K_N^{poly} of 10^{13} M^{-1}. Since the association constant between single molecules SA and HA is $K^{mono} \sim 10^3$ M^{-1}, this interaction is clearly multivalent.

Organic molecules as multivalent inhibitors of viral infection

The study of multivalency may provide new targets and new strategies for the design of pharmaceutical agents. One important strategy is the competitive inhibition. Different structural analogues of SA can be used as inhibitors. For example there are multivalent ligands as polyacrylamide with SA-containing side chains with very high binding constants with HA on the surface of influenza virus, and these inhibitors are remarkably better than monomeric SA (*Angew. Chem. Int. Ed.* **1998**, 37, 2754).

As a recent example, water-soluble glycofullerenes based on a hexakis-adduct of [60]fullerene have been used to interact with lectins in a multivalent manner (*Chem. Commun.* **2010**, 46, 3860; *Chem.-Eur. J.* **2011**, 17, 766). The activity of glycodendrofullerenes with 36 mannoses in its periphery as antiviral agents has been investigated in an Ebola pseudotyped infection model with very promising data (IC_{50} around 0.3 μM) (*Biomacromolecules* **2013**, 14, 431).

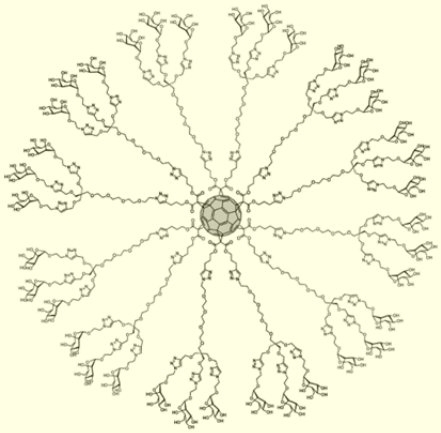

Fourier transform infrared spectroscopy (FTIR) of samples of exTTFAuNPs and exTTFAuNP•C_{60} also provided evidence of complexation/dissaggregation. Most characteristic signals of the exTTF fragment are significantly shifted (8-4 cm^{-1}) upon complexation, and a remarkable sharpening of the signal corresponding to the substituted benzene ring (735 cm^{-1}) is also observed. Meanwhile the $F_{1u}(3)$ and $F_{1u}(4)$ modes of C_{60} in the exTTFAuNP•C_{60} appear at 1180 and 1428 cm^{-1}, respectively (Figure 6), in good agreement with data reported for complexes of C_{60} with TTF-type donors.[16]

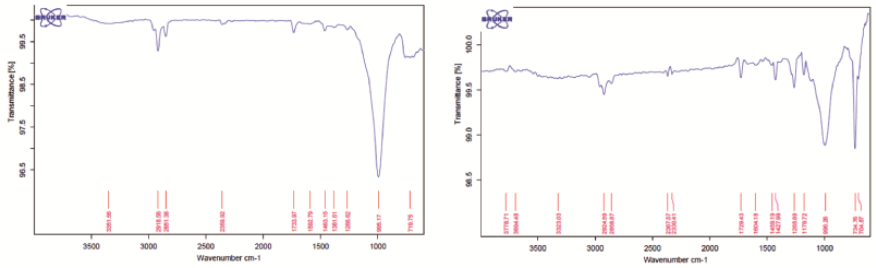

Figure 6. Fourier Transform Infrared (FTIR) spectra of exTTFAuNPs (left) and exTTFAuNP·C_{60} (right).

Exploration under atomic force microscopy (AFM, tapping mode, air) confirmed the proposed scenario (Figure 7). Images of a dropcast of a saturated solution of the exTTFAuNPs in 1,2-dichlorobenzene on freshly exfoliated mica, showed exclusively large (ca. 0.5-1μm) clusters of nanoparticles of approximately 100 nm in height (i.e. 10-15 exTTFAuNP layers) separated by large void areas. Neither smaller clusters nor single exTTFAuNPs were observed. When the same solution was incubated with C_{60} for two hours before deposition, AFM revealed large areas of fullerene precipitate (1-5 nm, Figure 7c and d), together with clusters of nanoparticles of 50-100 nm in height (i, Figure 7c and d), and abundant smaller aggregates of exTTFAuNP•C_{60} comprising approximately 2-3 layers of nanoparticles (15-25 nm, ii, Figure 7c and d).

[16] D. V. Konarev, R. N. Lyubovskaya, N. y. V. Drichko, E. I. Yudanova, Y. M. Shul'ga, A. L. Litvinov, V. N. Semkin and B. P. Tarasov, *J. Mater. Chem.* **2000,** *10*, 803-818.

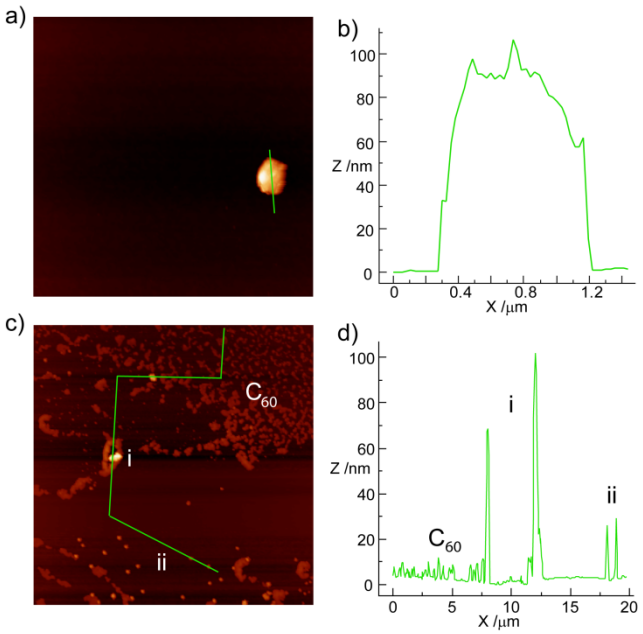

Figure 7. AFM imaging of a) dropcast of a saturated solution of exTTFAuNPs in 1,2-dichlorobenzene, showing a cluster of nanoparticles and c) dropcast of a saturated solution of exTTFAuNPs incubated with C_{60} for 2h prior to dropcasting. b) and d) show profiles along the green lines in a) and c), respectively.

TEM imaging was also consistent with the UV-vis data and AFM pictures (Figure 8). Pristine exTTFAuNPs are heavily aggregated, forming large clusters of nanoparticles in very close contact, as shown in Figure 8a. After incubation with C_{60}, however, the size of the clusters is reduced, and the relative distance between the nanoparticles increased, to the point that some single exTTFAuNP•C_{60} are observed (Figure 8c).

Energy dispersive X-ray spectroscopy (EDX) of the TEM micrographs is also in agreement with the binding event. In the case of pristine exTTFAuNPs (Figure 8b), besides the signature signals of the copper grid, we observed peaks at a 2.2, 9.7 and 11.5 keV, corresponding to gold, and at 0.2 keV, corresponding to carbon. The sulfur peak is most likely too weak to be detected or overlapped with the intense Au peak at 2.2 keV. As for the exTTFAuNP•C_{60} spectrum, the main features are identical, but the relative intensity of the carbon signal compared to the most prominent gold peak is approximately 0.7, compared to 0.3 in exTTFAuNPs, in accordance with a high loading of C_{60}.

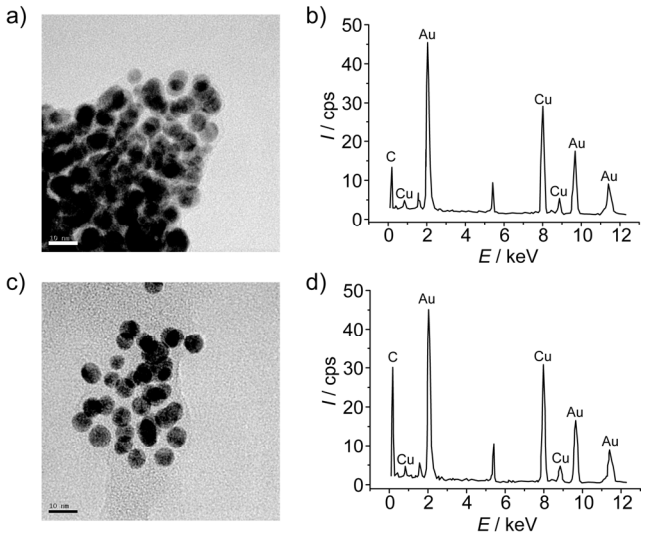

Figure 8. a) TEM micrograph of exTTFAuNPs and b) its EDX spectrum. c) TEM micrograph of exTTFAuNP•C_{60} and d) its EDX spectrum. Scale bars on the micrographs represent 10 nm.

Finally, we have also carried out cyclic voltammetry (CV) measurements of exTTFAuNPs, exTTFAuNP•C_{60} and C_{60} to investigate the influence of the binding event on the electronic properties of the elecroactive units. Measurements were carried out in chlorobenzene containing 0.1 M Bu_4NPF_6 under argon atmosphere. A glassy carbon was used as working electrode, $Ag/AgNO_3$ as the reference electrode, and a platinum wire as the counter. Ferrocene (Fc) was added as an internal reference. Table 1 shows the results of the CV experiments.

Table 1. Cyclic voltammetry data in chlorobenzene (0.1 M Bu_4NPF_6). Potentials in V vs. Fc/Fc^+.

	E_{ox} [a]	$E^{1/2}_{red,1}$	$E^{1/2}_{red,2}$	$E^{1/2}_{red,3}$
exTTFAuNPs	0.386	-	-	-
exTTFAuNP•C_{60}	- [b]	−1.183	−1.584	−2.059
C_{60}	-	−1.155	−1.544	−2.037

[a] Peak potential; [b] Broad oxidation wave.

The CV of exTTFAuNPs shows a single oxidation process at a peak potential of 0.386 V, with marked absorption and desorption processes dominating the anodic part of the voltammogram and preventing determination of the back-wave potential. Upon addition of C_{60}, the oxidation wave is significantly broadened, and three quasi-

reversible reduction processes involving the carbon cage are detected. These reductions appear at half-wave potentials of −1.183, −1.584, and −2.059 V. For comparison, the cyclic voltammetry of C_{60} under identical experimental conditions showed similar reduction processes, although at less negative potential values. Typically, the reductions show a cathodic shift of ~ 30 mV in exTTFAuNP•C_{60} compared to C_{60} (see Table 1). Remarkably, all three waves are affected to a similar extent, indicating that the fullerene unit remains associated upon the first and second reduction processes. These results are in line with those we have reported previously for other exTTF-based hosts for fullerenes.[4,5]

6.1.3. Conclusions

In summary, we have presented the synthesis and fullerene binding abilities of the first exTTF-capped gold nanoparticles. The synthesis of the exTTFAuNPs was carried out following standard and preparative straightforward protocols, both for the gold nanoparticles and the organic addend. The exTTFAuNPs are heavily aggregated through multiple weak van der Waals interactions between the exTTF units, as shown by UV-vis, AFM and TEM. These weak exTTF-exTTF interactions are readily substituted in solution with the stronger exTTF-C_{60}. Indeed, a thorough collection of experiments demonstrates that the exTTFAuNPs are capable of associating C_{60} both in solution (UV-vis, CV) and in the solid state (FTIR, AFM, TEM, EDX), and that binding occurs with concomitant partial disaggregation of the nanoparticles. Quantitative analysis of the UV-vis titration data was performed utilizing global multivariable analysis software, and shows that the exTTFAuNP•C_{60} associates are extremely stable, with log $\beta_{5:1}$ = 22.5 ± 0.1, and show a very strong multivalent effect. The exTTFAuNP•C_{60} supramolecular associate represents a synthetically more accessible alternative to the large exTTF dendrimers we have reported previously.[6b] Such nanostructured donor-acceptor composites hold promise for their application in photovoltaic devices. The investigation of this possibility will be the subject of our future research.

6.1.4. Computational details.

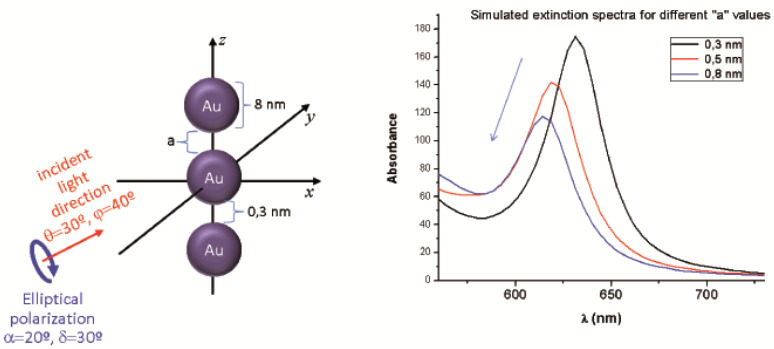

Figure 9. Model for the computational simulation of the impact of the disaggregation process on their UV-vis spectra, and results of the simulation.

We present here the study of the optical response of aggregated nanoparticles using a simplified model composed of three aligned gold nanoparticles in which one of them was set to increase its distance from the other two. For three dimensional ensembles the extinction band of coupled free electron oscilation will be broader as in case of Figure 3 (main text). It can also be observed that the decrease in intensity of the band is more significant than its blue shift. In case of three dimensional ensembles, in which the coupled electron resonating band is very broad, during a partial disaggregation process, the decrease in intensity of the band should be more noticeable than the hypsochromic shift, as experimentally observed

6.1.5. Experimental section

General All solvents were dried according to standard procedures. Reagents were used as purchased. All air-sensitive reactions were carried out under argon atmosphere. Flash chromatography was performed using silica gel (Merck, Kieselgel 60, 230-240 mesh, or Scharlau 60, 230-240 mesh). Analytical thin layer chromatographies (TLC) were performed using aluminium-coated Merck Kieselgel 60 F254 plates. NMR spectra were recorded on a Bruker Avance 300 (^{1}H: 300 MHz; ^{13}C: 75 MHz) spectrometer at 298 K, unless otherwise stated, using partially deuterated solvents as internal standards. Coupling constants (J) are denoted in Hz and chemical shifts (δ) in ppm. Multiplicities are denoted as follows: s = singlet, d = doublet, t = triplet, m = multiplet, b = broad. Matrix-assisted Laser desorption ionization (coupled to a Time-Of-Flight analyzer) spectrometry was carried out on a Bruker REFLEX spectrometer.

Synthesis of exTTF-MUA: 100 mg of exTTF-CH_2OH (0.24 mmol), 64 mg of MUA (0.29 mmol) and 58 mg of 4-dimethylaminopyridine (0.48 mmol) were dissolved in 30 mL of dry CH_2Cl_2 under argon atmosphere. Then 69 mg of *N*-(3-Dimethylaminopropyl)-*N*′-ethylcarbodiimide hydrochloride (0.36 mmol) were added in small portions. The reaction mixture was stirred at room temperature for 3 h, then diluted with 30 mL CH_2Cl_2, and washed successively with 1 M HCl (aq.), and 1 M $NaHCO_3$ (aq.). The combined organic layers were collected and the solvent removed under reduced pressure. The crude product was purified by column chromatography on silica gel (CH_2Cl_2) to afford exTTF-MUA in 76% yield.

^{1}H NMR ($CDCl_3$) δ 7.74- 7.66 (4H, m, Ar-H), 7.33- 7.24 (3H, m, Ar-H), 6.29 (4H, bs,S-CH-CH-S), 4.75 (2H, s, CH_2-O), 2.96- 2.83 (4H, m, CH_2-CH_2-COOR), 2.60- 2.48 (4H, m,alkyl), 2.39 (2H, t, J = 7.5 Hz, CH_2-SH), 1.72- 1.54 (10 H, m, alkyl) ppm. ^{13}C NMR ($CDCl_3$) δ 174.1, 136.1, 135.7, 135.4, 135.2, 134.2, 130.1, 128.1, 126.8, 126.4, 126.1, 125.5, 125.3, 125.1, 117.7, 117.6, 117.5, 34.8, 34.4, 29.8, 29.7, 29.6, 29.4, 28.8, 27.0, 26.1, 25.4, 25.0, 19.4 ppm. MS *m/z*: calcd. for $C_{32}H_{34}O_2S_5$ [M^+] 610.1 found (MALDI-TOF) 609.9.

Synthesis of exTTF-capped gold nanoparticles: 220 mg of sodium citrate dihydrate (0.748 mol) were dissolved in 200 mL of milliQ water, and the solution

heated to reflux. When the solution is boiling vividly, 10 μL of $AuCl_3$•HCl (30%) were added. After a few seconds, the solution turns deep red colour, and the solution is kept at reflux for 40-60 min, and then allowed to cool to room temperature. To this aqueous solution, a solution of 26 mg of exTTF-MUA (42 mmol) in 50 mL of chlorobenzene was added. The corresponding biphasic mixture was stirred vigorously for approximately 1h or until complete decoloration of the aqueous phase. The golden-green organic phase was separated and distributed in centrifuge tubes which were topped up with CH_2Cl_2 and subjected to centrifugation (6000 rpm, 10 min) to precipitate the nanoparticles. The yellow supernatant was decanted and further washes with CH_2Cl_2 (3x) and CH_3OH (3x) were carried out to remove excess exTTF-MUA and other organic impurities. The exTTFAuNPs were obtained as a black powder and used as such.

6.1.6. References

1. (a) L. Zang; Y. K. Che; J. S. Moore, One-Dimensional Self-Assembly of Planar π-Conjugated Molecules: Adaptable Building Blocks for Organic Nanodevices. *Acc. Chem. Res.* **2008,** *41*, 1596-1608;(b) F. D'Souza; O. Ito, Supramolecular donor-acceptor hybrids of porphyrins/phthalocyanines with fullerenes/carbon nanotubes: electron transfer, sensing, switching, and catalytic applications. *Chem. Commun.* **2009**, 4913-4928;(c) E. M. Pérez; B. M. Illescas; M. A. Herranz; N. Martín, Supramolecular chemistry of π-extended analogues of TTF and carbon nanostructures. *New J. Chem.* **2009,** *33*, 228-234;(d) H. Liu; J. Xu; Y. Li; Y. Li, Aggregate Nanostructures of Organic Molecular Materials. *Acc. Chem. Res.* **2010,** *43*, 1496-1508;(e) E. M. Pérez, Energy, supramolecular chemistry, fullerenes, and the sky. *Pure Appl. Chem.* **2011,** *83*, 201-211.

2. (a) F. D'Souza; E. Maligaspe; K. Ohkubo; M. E. Zandler; N. K. Subbaiyan; S. Fukuzumi, Photosynthetic Reaction Center Mimicry: Low Reorganization Energy Driven Charge Stabilization in Self-Assembled Cofacial Zinc Phthalocyanine Dimer-Fullerene Conjugate. *J. Am. Chem. Soc.* **2009,** *131*, 8787-8797;(b) X. Feng; V. Marcon; W. Pisula; M. R. Hansen; J. Kirkpatrick; F. Grozema; D. Andrienko; K. Kremer; K. Muellen, Towards high charge-carrier mobilities by rational design of the shape and periphery of discotics. *Nature Materials* **2009,** *8*, 421-426;(c) X. Feng; W. Pisula; T. Kudernac; D. Wu; L. Zhi; S. De Feyter; K. Muellen, Controlled Self-Assembly of C3-Symmetric Hexa-peri-hexabenzocoronenes with Alternating Hydrophilic and Hydrophobic Substituents in Solution, in the Bulk, and on a Surface. *J. Am. Chem. Soc.* **2009,** *131*, 4439-4448;(d) J. M. Mativetsky; M. Kastler; R. C. Savage; D. Gentilini; M. Palma; W. Pisula; K. Muellen; P. Samori, Self-Assembly of a Donor-Acceptor Dyad Across Multiple Length Scales: Functional Architectures for Organic Electronics. *Adv. Funct. Mater.* **2009,** *19*, 2486-2494;(e) L. Welte; A. Calzolari; R. Di Felice; F. Zamora; J. Gómez-Herrero, Highly conductive self-assembled nanoribbons of coordination polymers. *Nature Nanotechnology* **2010,** *5*, 110-115;(f) G. Bottari; D. Olea; C. Gomez-Navarro; F. Zamora; J. Gómez-Herrero; T. Torres, Highly conductive supramolecular nanostructures of a covalently linked phthalocyanine-C60 fullerene conjugate. *Angew. Chem. Int. Ed.* **2008,** *47*, 2026-2031.

3. (a) J. L. Segura; N. Martín, New Concepts in Tetrathiafulvalene Chemistry. *Angew. Chem. Int. Ed.* **2001,** *40*, 1372-1409;(b) M. M. S. Abdel-Mottaleb; E. Gomar-Nadal; M. Surin; H. Uji-i; W. Mamdouh; J. Veciana; V. Lemaur; C. Rovira; J. Cornil; R. Lazzaroni; D. B. Amabilino; S. De Feyter; F. C. De Schryver, Self-assembly of tetrathiafulvalene derivatives at a liquid/solid interface-compositional and constitutional influence on supramolecular ordering. *J. Mater. Chem.* **2005,** *15*, 4601-4615;(c) D. Canevet; M. Salle; G. Zhang; D. Zhang; D. Zhu, Tetrathiafulvalene (TTF) derivatives: key building-blocks for switchable processes. *Chem. Commun.* **2009**, 2245-2269.

4. (a) E. M. Pérez; L. Sánchez; G. Fernández; N. Martín, exTTF as a Building Block for Fullerene Receptors. Unexpected Solvent-Dependent Positive Homotropic Cooperativity. *J. Am. Chem. Soc.* **2006,** *128*, 7172-7173;(b) E. M. Pérez; A. L. Capodilupo; G. Fernández; L. Sánchez; P. M. Viruela; R. Viruela; E. Ortí; M. Bietti; N. Martín, Weighting non-covalent forces in the molecular recognition of C_{60}. Relevance of concave-convex complementarity. *Chem. Commun.* **2008,** *0*, 4567-4569;(c) S. S. Gayathri;

M. Wielopolski; E. M. Pérez; G. Fernández; L. Sánchez; R. Viruela; E. Ortí; D. M. Guldi; N. Martín, Discrete supramolecular donor-acceptor complexes. *Angew. Chem. Int. Ed.* **2009,** *48*, 815-819.

5. (a) D. Canevet; M. Gallego; H. Isla; A. de Juan; E. M. Pérez; N. Martín, Macrocyclic hosts for fullerenes: extreme changes in binding abilities with small structural variations. *J. Am. Chem. Soc.* **2011,** *133*, 3184-3190;(b) H. Isla; M. Gallego; E. M. Pérez; R. Viruela; E. Ortí; N. Martín, A Bis-exTTF Macrocyclic Receptor That Associates C_{60} with Micromolar Affinity. *J. Am. Chem. Soc.* **2010,** *132*, 1772-1773;(c) E. Huerta; H. Isla; E. M. Pérez; C. Bo; N. Martín; J. de Mendoza, Tripodal exTTF-CTV Hosts for Fullerenes. *J. Am. Chem. Soc.* **2010,** *132*, 5351-5353;(d) B. Grimm; J. Santos; B. M. Illescas; A. Muñoz; D. M. Guldi; N. Martín, A New exTTF-Crown Ether Platform To Associate Fullerenes: Cooperative n-π and π–π Effects. *J. Am. Chem. Soc.* **2010,** *132*, 17387-17389;(e) J. Santos; B. Grimm; B. M. Illescas; D. M. Guldi; N. Martín, Cooperativity between π–π and H-bonding interactions-a supramolecular complex formed by C_{60} and exTTF. *Chem. Commun.* **2008,** *0*, 5993-5995;(f) E. M. Pérez; N. Martín, Curves ahead: molecular receptors for fullerenes based on concave-convex complementarity. *Chem. Soc. Rev.* **2008,** *37*, 1512-1519;(g) E. M. Pérez; M. Sierra; L. Sánchez; M. R. Torres; R. Viruela; P. M. Viruela; E. Ortí; N. Martín, Concave Tetrathiafulvalene-Type Donors as Supramolecular Partners for Fullerenes. *Angew. Chem. Int. Ed.* **2007,** *46*, 1847-1851.

6. (a) J. Santos; E. M. Pérez; B. M. Illescas; N. Martín, Linear and Hyperbranched Electron-Acceptor Supramolecular Oligomers. *Chem.--Asian J.* **2011,** *6*, 1848-1853;(b) G. Fernández; L. Sánchez; E. M. Pérez; N. Martín, Large exTTF-Based Dendrimers. Self-Assembly and Peripheral Cooperative Multiencapsulation of C_{60}. *J. Am. Chem. Soc.* **2008,** *130*, 10674-10683;(c) G. Fernández; E. M. Pérez; L. Sánchez; N. Martín, An Electroactive Dynamically Polydisperse Supramolecular Dendrimer. *J. Am. Chem. Soc.* **2008,** *130*, 2410-2411;(d) G. Fernández; E. M. Pérez; L. Sánchez; N. Martín, Self-Organization of Electroactive Materials: A Head-to-Tail Donor–Acceptor Supramolecular Polymer. *Angew. Chem. Int. Ed.* **2008,** *47*, 1094-1097.

7. (a) N. Kanayama; T. Takarada; M. Maeda, Rapid naked-eye detection of mercury ions based on non-crosslinking aggregation of double-stranded DNA-carrying gold nanoparticles. *Chem. Commun.* **2011,** *47*, 2077-2079;(b) R. Cao; B. Li, A simple and sensitive method for visual detection of heparin using positively-charged gold nanoparticles as colorimetric probes. *Chem. Commun.* **2011,** *47*, 2865-2867;(c) Z. Zhu; C. Wu; H. Liu; Y. Zou; X. Zhang; H. Kang; C. J. Yang; W. Tan, An Aptamer Cross-Linked Hydrogel as a Colorimetric Platform for Visual Detection. *Angew. Chem. Int. Ed.* **2010,** *49*, 1052-1056, S1052/1-S1052/4;(d) X. Xu; W. L. Daniel; W. Wei; C. A. Mirkin, Colorimetric Cu^{2+} Detection Using DNA-Modified Gold-Nanoparticle Aggregates as Probes and Click Chemistry. *Small* **2010,** *6*, 623-626;(e) X. Li; J. Wang; L. Sun; Z. Wang, Gold nanoparticle-based colorimetric assay for selective detection of aluminum cation on living cellular surfaces. *Chem. Commun.* **2010,** *46*, 988-990;(f) Y. Jiang; H. Zhao; Y. Lin; N. Zhu; Y. Ma; L. Mao, Colorimetric Detection of Glucose in Rat Brain Using Gold Nanoparticles. *Angew. Chem. Int. Ed.* **2010,** *49*, 4800-4804;(g) D. A. Giljohann; D. S. Seferos; W. L. Daniel; M. D. Massich; P. C. Patel; C. A. Mirkin, Gold Nanoparticles for Biology and Medicine. *Angew. Chem. Int. Ed.* **2010,** *49*, 3280-3294;(h) D. Feng; Y. Zhang; W. Shi; X. Li; H. Ma, A simple and sensitive method for visual detection of phosgene based on the aggregation of gold nanoparticles. *Chem. Commun.* **2010,** *46*, 9203-9205;(i) U. H. F. Bunz; V. M. Rotello, Gold Nanoparticle-Fluorophore Complexes: Sensitive and Discerning "Noses" for Biosystems Sensing. *Angew. Chem. Int. Ed.* **2010,** *49*, 3268-3279.

8. (a) J. Ohyama; Y. Hitomi; Y. Higuchi; M. Shinagawa; H. Mukai; M. Kodera; K. Teramura; T. Shishido; T. Tanaka, One-phase synthesis of small gold nanoparticles coated by a horizontal porphyrin monolayer. *Chem. Commun.* **2008**, 6300-6302;(b) M. Kanehara; H. Takahashi; T. Teranishi, Gold(0) porphyrins on gold nanoparticles. *Angew. Chem. Int. Ed.* **2008,** *47*, 307-310;(c) T. Akiyama; M. Nakada; N. Terasaki; S. Yamada, Photocurrent enhancement in a porphyrin-gold nanoparticle nanostructure assisted by localized plasmon excitation. *Chem. Commun.* **2006**, 395-397;(d) H. Imahori; A. Fujimoto; S. Kang; H. Hotta; K. Yoshida; T. Umeyama; Y. Matano; S. Isoda; M. Isosomppi; N. V. Tkachenko; H. Lemmetyinen, Host-guest interactions in the supramolecular incorporation of fullerenes into tailored holes on porphyrin-modified gold nanoparticles in molecular photovoltaics. *Chem. Eur. J.* **2005,** *11*, 7265-7275;(e) H. Imahori; A. Fujimoto; S. Kang; H. Hotta; K. Yoshida; T. Umeyama; Y. Matano; S. Isoda, Molecular photoelectrochemical devices: Supramolecular incorporation of C60 molecules into tailored holes on porphyrin-modified gold nanoclusters. *Adv. Mater.* **2005,** *17*, 1727-1730;(f) T. Hasobe; H. Imahori; P. V. Kamat; T. K. Ahn; S. K. Kim; D. Kim; A. Fujimoto; T. Hirakawa; S. Fukuzumi, Photovoltaic Cells Using Composite Nanoclusters of Porphyrins and Fullerenes with Gold Nanoparticles. *J. Am. Chem. Soc.* **2005,** *127*, 1216-1228.

9. (a) G. Zhang; D. Zhang; X. Zhao; X. Ai; J. Zhang; D. Zhu, Assembly of a tetrathiafulvalene-anthracene dyad on the surfaces of gold nanoparticles: tuning the excited-state properties of the anthracene unit in the dyad. *Chem. Eur. J.* **2006,** *12*, 1067-1073;(b) W.-J. Guo; J. Dai; D.-Q. Zhang; Q.-Y. Zhu; G.-Q. Bian, Redox active gold nanoparticles modified with tetrathiafulvalene derivative via direct sulfur bridge. *Inorg. Chem. Commun.* **2005,** *8*, 994-997;(c) J. Dai; L. Guo; Y. Jiang; Q.-Y. Zhu; R.-A. Gu; D.-x. Jia; W.-J. Guo, Preparation of gold nanoparticles modified with tetrathiafulvalene via direct sulfur bridge. *J. Nanosci. Nanotechnol.* **2005,** *5*, 474-478;(d) H. Nakai; M. Yoshihara; H. Fujihara, New electroactive tetrathiafulvalene-derivatized gold nanoparticles and their remarkably stable nanoparticle films on electrodes. *Langmuir* **1999,** *15*, 8574-8576.

10. G. Frens, Controlled nucleation for the regulation of the particle size in monodisperse gold suspensions. *Nature* **1973,** *241*, 20-2.

11. U. Kreibig; L. Genzel, Optical absorption of small metallic particles. *Surf. Sci.* **1985,** *156, Part 2*, 678-700.

12. (a) X. Yang; G. Zhang; D. Zhang; D. Zhu, A New ex-TTF-Based Organogelator: Formation of Organogels and Tuning with Fullerene. *Langmuir* **2010,** *26*, 11720-11725;(b) X. Yang; G. Zhang; D. Zhang; J. Xiang; G. Yang; D. Zhu, Self-assembly of a new C_{60} compound with a L-glutamid-derived lipid unit: formation of organogels and hierarchically structured spherical particles. *Soft Matter* **2011,** *7*, 3592-3598.

13. (a) F. J. García de Abajo; A. Howie, Relativistic Electron Energy Loss and Electron-Induced Photon Emission in Inhomogeneous Dielectrics. *Phys. Rev. Lett.* **1998,** *80*, 5180-5183;(b) F. J. García de Abajo; A. Howie, Retarded field calculation of electron energy loss in inhomogeneous dielectrics. *Physical Review B* **2002,** *65*, 115418;(c) V. Myroshnychenko; E. Carbó-Argibay; I. Pastoriza-Santos; J. Pérez-Juste; L. M. Liz-Marzán; F. J. García de Abajo, Modeling the Optical Response of Highly Faceted Metal Nanoparticles with a Fully 3D Boundary Element Method. *Adv. Mater.* **2008,** *20*, 4288-4293;(d) V. Myroshnychenko; J. Rodriguez-Fernandez; I. Pastoriza-Santos; A. M. Funston; C. Novo; P. Mulvaney; L. M. Liz-Marzan; F. J. Garcia de Abajo, Modelling the optical response of gold nanoparticles. *Chem. Soc. Rev.* **2008,** *37*, 1792-1805.

14. P. Thordarson, Determining association constants from titration experiments in supramolecular chemistry. *Chem. Soc. Rev.* **2011,** *40*, 1305-1323.

15. W. D. Cornell; P. Cieplak; C. I. Bayly; I. R. Gould; K. M. Merz, Jr.; D. M. Ferguson; D. C. Spellmeyer; T. Fox; J. W. Caldwell; P. A. Kollman, A Second Generation Force Field for the Simulation of Proteins, Nucleic Acids, and Organic Molecules. *J. Am. Chem. Soc.* **1995,** *117*, 5179-97.

16. D. V. Konarev; R. N. Lyubovskaya; N. y. V. Drichko; E. I. Yudanova; Y. M. Shul'ga; A. L. Litvinov; V. N. Semkin; B. P. Tarasov, Donor-acceptor complexes of fullerene C60 with organic and organometallic donors. *J. Mater. Chem.* **2000,** *10*, 803-818.

6.2. Exploiting multivalent nanoparticles for the supramolecular functionalization of graphene with a non-planar recognition motif.

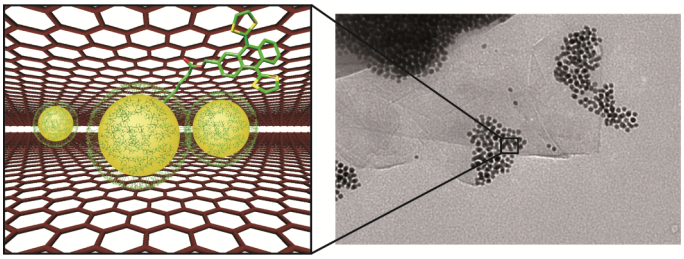

Mismatched, yet attracted to each other: The supramolecular modification of planar graphene with the geometrically mismatched exTTF molecule is demonstrated. The exTTF-graphene interaction is amplified through a multivalent effect, utilizing gold nanoparticles as scaffolds. The resulting graphene-exTTFAuNP conjugates form sandwich-type nanostructures.

Chem. Eur. J. **2013**, DOI: 10.1002/chem.201301102

6.2.1. Introduction

Monolayer graphene is a 2-D lattice of carbon atoms arranged in a honeycomb structure.[1] More generally, few layer graphene (FLG) can be viewed as less than 10 layers of graphite. The extraordinary structural and physical properties of graphene have rightly made it the object of a very intense multidisciplinary research effort, in which physics has so far played the leading role.[2] In particular, its electronic properties have been the focus of a significant number of investigations.[3] In comparison, the chemistry of graphene is not so well developed.[4] From the synthetic point of view, important breakthroughs include the synthesis of graphene through sublimation of Si from SiC,[5] chemical vapour deposition (CVD) of gaseous carbon sources on metal catalysts,[6]

---

[1] (a) A. K. Geim and K. S. Novoselov, *Nat Mater* **2007,** *6*, 183-191; (b) M. J. Allen, V. C. Tung and R. B. Kaner, *Chem. Rev.* **2010,** *110*, 132-145.

[2] (a) A. K. Geim, *Angew. Chem. Int. Ed.* **2011,** *50*, 6966-6985; (b) K. S. Novoselov, *Angew. Chem. Int. Ed.* **2011,** *50*, 6986-7002.

[3] (a) C. N. R. Rao, A. K. Sood, K. S. Subrahmanyam and A. Govindaraj, *Angew. Chem. Int. Ed.* **2009,** *48*, 7752-7777; (b) P. Avouris, *Nano Lett.* **2010,** *10*, 4285-4294; S. Pang, Y. Hernández, X. Feng and K. Muellen, *Adv. Mater.* **2011,** *23*, 2779-2795; (c) E. Bekyarova, S. Sarkar, F. Wang, M. E. Itkis, I. Kalinina, X. Tian and R. C. Haddon, *Acc. Chem. Res.* **2013,** *46*, 65-76.

[4] (a) Z. Sun, D. K. James and J. M. Tour, *J. Phys. Chem. Lett.* **2011,** *2*, 2425-2432; (b) Y. Chen, B. Zhang, G. Liu, X. Zhuang and E.-T. Kang, *Chem. Soc. Rev.* **2012,** *41*, 4688-4707; (c) C. K. Chua and M. Pumera, *Chem. Soc. Rev.* **2013,** *42*, 3222-3233; (d) J. Park and M. Yan, *Acc. Chem. Res.* **2013,** *46*, 181-189; (e) M. Quintana, E. Vázquez and M. Prato, *Acc. Chem. Res.* **2013,** *46*, 138-148; (f) L. Rodríguez-Pérez, M. A. Herranz and N. Martín, *Chem. Commun.* **2013,** *49*, 3721-3735.

[5] K. V. Emtsev, A. Bostwick, K. Horn, J. Jobst, G. L. Kellogg, L. Ley, J. L. McChesney, T. Ohta, S. A. Reshanov, J. Roehrl, E. Rotenberg, A. K. Schmid, D. Waldmann, H. B. Weber and T. Seyller, *Nat. Mater.* **2009,** *8*, 203-207.

[6] (a) A. L. Vázquez de Parga, F. Calleja, B. Borca, M. C. G. Passeggi, Jr., J. J. Hinarejos, F. Guinea and R. Miranda, *Phys. Rev. Lett.* **2008,** *100*, 056807/1-056807/4; (b) K. S. Kim, Y. Zhao, H. Jang, S. Y. Lee, J. M. Kim, K. S. Kim, J.-H. Ahn, P. Kim, J.-Y. Choi and B. H. Hong, *Nature* **2009,** *457*, 706-710; (c) X.

reduction of graphene oxide (RGO),[7] "unzipping" of carbon nanotubes to produce graphene nanoribbons,[8] and the synthesis of monodisperse nanographenes (or large polycyclic aromatic hydrocarbons, PAHs).[9] Recently, the synthesis of graphene from inexpensive carbon sources through CVD has been described.[10]

The toolbox of reactions for the chemical manipulation of graphene is more limited.[4a, 4d, 4e] The covalent modification of graphene's basal planes through its reaction with aryl diazonium salts[11] and 1,3-dipoles[4e, 12] has been reported. With regard to its noncovalent or supramolecular modification, the interaction of graphene with surfactants[13] and planar aromatic moieties, including PAHs,[14] pyrene,[15] tetracyano-*p*-quinodimethane,[16] and phthalocyanines,[17] has been described.

We have previously exploited the concave geometry of 9,10-di(1,3-dithiol-2-ylidene)-9,10-dihydroanthracene (exTTF) to synthesize hosts for fullerenes[18] and a variety of fullerene-exTTF self-assembled nanostructures profiting from the concave-convex complementarity of the systems.[19] In the field of molecular recognition of

---

Li, W. Cai, J. An, S. Kim, J. Nah, D. Yang, R. Piner, A. Velamakanni, I. Jung, E. Tutuc, S. K. Banerjee, L. Colombo and R. S. Ruoff, *Science* **2009,** *324*, 1312-1314.

[7] D. R. Dreyer, S. Park, C. W. Bielawski and R. S. Ruoff, *Chem. Soc. Rev.* **2010,** *39*, 228-240.

[8] D. V. Kosynkin, A. L. Higginbotham, A. Sinitskii, J. R. Lomeda, A. Dimiev, B. K. Price and J. M. Tour, *Nature* **2009,** *458*, 872-876.

[9] (a) P. Samori, N. Severin, C. D. Simpson, K. Müllen and J. P. Rabe, *J. Am. Chem. Soc.* **2002,** *124*, 9454-9457; (b) M. Kastler, J. Schmidt, W. Pisula, D. Sebastiani and K. Müllen, *J. Am. Chem. Soc.* **2006,** *128*, 9526-9534; (c) K. Müllen and J. P. Rabe, *Acc. Chem. Res.* **2008,** *41*, 511-520.

[10] G. Ruan, Z. Sun, Z. Peng and J. M. Tour, *ACS Nano* **2011,** *5*, 7601-7607.

[11] (a) J. R. Lomeda, C. D. Doyle, D. V. Kosynkin, W.-F. Hwang and J. M. Tour, *J. Am. Chem. Soc.* **2008,** *130*, 16201-16206; (b) E. Bekyarova, M. E. Itkis, P. Ramesh, C. Berger, M. Sprinkle, W. A. de Heer and R. C. Haddon, *J. Am. Chem. Soc.* **2009,** *131*, 1336-1337; (c) G. L. C. Paulus, Q. H. Wang and M. S. Strano, *Acc. Chem. Res.* **2013,** *46*, 160-170.

[12] M. Quintana, K. Spyrou, M. Grzelczak, W. R. Browne, P. Rudolf and M. Prato, *ACS Nano* **2010,** *4*, 3527-3533; M. Quintana, A. Montellano, A. E. del Rio Castillo, G. Van Tendeloo, C. Bittencourt and M. Prato, *Chem. Commun.* **2011,** *47*, 9330-9332.

[13] M. Lotya, Y. Hernández, P. J. King, R. J. Smith, V. Nicolosi, L. S. Karlsson, F. M. Blighe, S. De, Z. Wang, I. T. McGovern, G. S. Duesberg and J. N. Coleman, *J. Am. Chem. Soc.* **2009,** *131*, 3611-3620.

[14] Q. Su, S. Pang, V. Alijani, C. Li, X. Feng and K. Muellen, *Adv. Mater.* **2009,** *21*, 3191-3195.

[15] J. A. Mann, J. Rodríguez-López, H. D. Abruña and W. R. Dichtel, *J. Am. Chem. Soc.* **2011**.

[16] (a) S. Barja, M. Garnica, J. J. Hinarejos, A. L. Vázquez de Parga, N. Martín and R. Miranda, *Chem. Commun.* **2010,** *46*, 8198-8200; (b) M. Garnica, D. Stradi, S. Barja, F. Calleja, C. Díaz, M. Alcamí, N. Martín, A. L. Vazquez de Parga, F. Martín and R. Miranda, *Nature Physics* **2013**.

[17] J. Malig, N. Jux, D. Kiessling, J.-J. Cid, P. Vázquez, T. Torres and D. M. Guldi, *Angew. Chem. Int. Ed.* **2011,** *50*, 3561-3565, S3561/1-S3561/15.

[18] (a) E. M. Pérez, L. Sánchez, G. Fernández and N. Martín, *J. Am. Chem. Soc.* **2006,** *128*, 7172-7173; (b) E. M. Pérez, A. L. Capodilupo, G. Fernández, L. Sánchez, P. M. Viruela, R. Viruela, E. Ortí, M. Bietti and N. Martín, *Chem. Commun.* **2008**, 4567-4569; (c) S. S. Gayathri, M. Wielopolski, E. M. Pérez, G. Fernández, L. Sánchez, R. Viruela, E. Ortí, D. M. Guldi and N. Martín, *Angew. Chem. Int. Ed.* **2009,** *48*, 815-819; (d) E. Huerta, H. Isla, E. M. Pérez, C. Bo, N. Martín and J. de Mendoza, *J. Am. Chem. Soc.* **2010,** *132*, 5351-5353; (e) H. Isla, M. Gallego, E. M. Pérez, R. Viruela, E. Ortí and N. Martín, *J. Am. Chem. Soc.* **2010,** *132*, 1772-1773; (f) D. Canevet, M. Gallego, H. Isla, A. de Juan, E. M. Pérez and N. Martín, *J. Am. Chem. Soc.* **2011,** *133*, 3184-3190; (g) B. Grimm, H. Isla, E. M. Pérez, N. Martín and D. M. Guldi, *Chem. Commun.* **2011,** *47*, 7449-7451.

[19] (a) G. Fernández, E. M. Pérez, L. Sánchez and N. Martín, *Angew. Chem. Int. Ed.* **2008,** *47*, 1094-1097; (b) G. Fernández, E. M. Pérez, L. Sánchez and N. Martín, *J. Am. Chem. Soc.* **2008,** *130*, 2410-2411; (c)

fullerenes, there are numerous examples of hosts that exploit planar aromatic moieties (particularly porphyrins) to recognize the convex surface of the fullerene guests, despite the planar-convex mismatch.[20] The same is true for the supramolecular chemistry of carbon nanotubes, where pyrene is by far the most widely used recognition motif.[21] Inspired by this fact, we contemplated the possibility that exTTF could establish positive noncovalent interactions with planar graphene, regardless of its biconcave geometry.[22] So far, it has not been established whether planarity is a *sine qua non* condition for the structure of recognition motifs for graphene. In this article we demonstrate that this is not the case, by proving the noncovalent modification of graphene with a nonplanar recognition motif like exTTF.

6.2.2. Results and Discussion

To explore the interaction between exTTF and planar graphene, we firstly carried out density functional theory (DFT) calculations on an exTTF-graphene model, in which the exTTF unit is placed in different orientations with respect to a PAH graphene-like molecule including 31 benzene rings ($C_{84}H_{24}$). Calculations were performed using the revPBE0-D3 functional,[23] which is able to capture the dispersion effects and is one of the best functionals to accurately describe supramolecular complexes governed by π-π interactions (see the Computational details section).[24] Figure 1 displays the minimum-energy structures (**1**–**5**) calculated for the exTTF-graphene supramolecular interaction at the revPBE0-D3/cc-pVDZ level. More detailed pictures about the orientation of exTTF with respect to the graphene sheet are given in Figures 9-13 in the Computational details section. In structures **1** and **2** the interaction of the exTTF fragment with graphene mainly occurs through the concave anthracene backbone, whereas in structure **3** the interaction takes place through the concave dithiol face. Structures **1** and **2** are mainly determined by π–π interactions, whereas structure **3** involves close CH-π interactions (~2.7 Å) between the terminal hydrogen atoms of the dithiole rings and the graphene sheet. The exTTF molecule can also interact with the graphene sheet through a benzene ring and the sulfur atoms (structure **4**), or through a dithiol ring (structure **5**). Structures **4** and **5** imply a mixture of π–π and CH-π interactions. All optimized structures **1**–**5** show close intermolecular distances in the 3.1–4.0 Å range (see Figures 9-13), which are the structural signature of positive noncovalent

---

G. Fernández, L. Sánchez, E. M. Pérez and N. Martín, *J. Am. Chem. Soc.* **2008,** *130*, 10674-10683; (d) J. Santos, E. M. Pérez, B. M. Illescas and N. Martín, *Chem.--Asian J.* **2011,** *6*, 1848-1853.

[20] (a) K. Tashiro and T. Aida, *Chem. Soc. Rev.* **2007,** *36*, 189-197; (b) E. M. Pérez and N. Martín, *Chem. Soc. Rev.* **2008,** *37*, 1512-1519; (c) D. Canevet, E. M. Pérez and N. Martín, *Angew. Chem. Int. Ed.* **2011,** *50*, 9248-9259.

[21] (a) N. Nakashima, Y. Tomonari and H. Murakami, *Chem. Lett.* **2002**, 638-639; (b) M. Á. Herranz, C. Ehli, S. Campidelli, M. Gutiérrez, G. L. Hug, K. Ohkubo, S. Fukuzumi, M. Prato, N. Martín and D. M. Guldi, *J. Am. Chem. Soc.* **2007,** *130*, 66-73.

[22] S. P. Economopoulos, G. Rotas, Y. Miyata, H. Shinohara and N. Tagmatarchis, *ACS Nano* **2010,** *4*, 7499-7507.

[23] Y. Zhang and W. Yang, *Phys. Rev. Lett.* **1998,** *80*, 890-890; S. Grimme, J. Antony, S. Ehrlich and H. Krieg, *J. Chem. Phys.* **2010,** *132*, 154104-19.

[24] W. Hujo and S. Grimme, *J. Chem. Theory Comput.* **2011,** *7*, 3866-3871.

interactions. Remarkably, despite the electron donor character of exTTF, our calculations predict negligible contributions from charge-transfer interactions (< 0.005e).

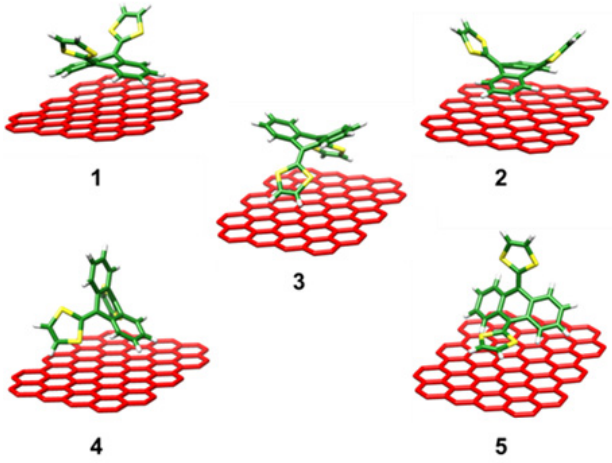

Figure 1. Minimum-energy structures computed for the exTTF-graphene models (1–5) at the revPBE0-D3/cc-pVDZ level. Carbon atoms of exTTF are depicted in green, sulfur in yellow and hydrogen in white. Carbon atoms of the graphene sheet are depicted in red and hydrogen atoms have been omitted for clarity

To estimate the association binding energies of the exTTF-graphene models **1**–**5**, single-point energy calculations were performed on the previously-optimized structures using the revPBE0-D3 functional and the more extended triple-ζ cc-pVTZ basis set (see Computational details section). Table 1 collects the binding energies calculated for structures **1**–**5**. Structures **4** and **5** are found to be the most stable with association binding energies of –22.2 and –25.2 kcal mol^{-1}, respectively. Structures **1**–**3** also exhibit significant association binding energies ranging from –16.8 to –20.7 kcal mol^{-1}. To discard possible undesirable terminal effects due to the limited size of the PAH used to model the graphene sheet, an exTTF-graphene model based on structure **1** with a larger PAH ($C_{104}H_{28}$) was also calculated (Figure 14). The association binding energy for the larger exTTF-graphene model is –19.3 kcal mol^{-1}, which is similar to that obtained for structure **1** (–19.0 kcal mol^{-1}). These results confirm that the size of the PAH ($C_{84}H_{24}$) used to model the graphene sheet is appropriate to compute the association binding energies between exTTF and graphene. To investigate the influence of the nonplanar geometry of exTTF on the supramolecular association with graphene, the interaction of the graphene sheet with a planar π-conjugated motif like anthracene (the central backbone of exTTF) was also computed in an eclipsed-like disposition similar to structure **1** (Figure 15). The association binding energy computed at the revPBE0-D3/cc-pVTZ level for this anthracene-graphene model is –20.4 kcal mol^{-1}, which is higher than that computed for its homologous structure **1** but is significant smaller than those computed for structures **4** and **5** (Table 1). The remarkable increase of the association binding energies for structure **4** and **5** with respect to the anthracene-graphene model clearly reveals that the planarity of the π-conjugated motif does not

necessarily favor a stronger supramolecular association with a graphene sheet. For instance, despite the concave-planar mismatch, the exTTF system can orientate in different ways to interact strongly with a graphene sheet.

Table 1. Association binding energies computed for the exTTF-graphene structures 1–5 at the revPBE0-D3/cc-pVTZ level.

Structure	ΔE (kcal mol^{-1})
1	–19.0
2	–20.7
3	–16.8
4	–22.2
5	–25.2

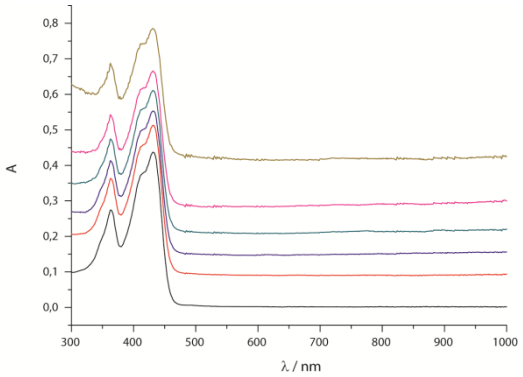

Figure 2. UV-vis spectra of exTTF (1 mL, 2.5 × 10^{-5} M, chlorobenzene, rt) upon addition of few layers graphene (chlorobenzene, same suspension utilized in Figure 3, 5 μL additions).

Experimentally (UV-vis titration, Figure 2), we found that a single unit of exTTF does not produce detectable interactions with graphene,[18a] so we decided to employ a multivalent approach to amplify it, in which gold nanoparticles would serve as a scaffold to present multiple units of exTTF to the surface of graphene. Multivalent interactions are often much stronger than the corresponding sum of the monovalent ones, a strategy that nature has exploited in multiple recognition events, for example in the recognition of polysaccharides by lectins.[25] Besides, gold nanoparticles can be

[25] (a) J. D. Badjic, A. Nelson, S. J. Cantrill, W. B. Turnbull and J. F. Stoddart, *Acc. Chem. Res.* **2005,** *38*, 723-732; (b) C. Fasting, C. A. Schalley, M. Weber, O. Seitz, S. Hecht, B. Koksch, J. Dernedde, C. Graf, E.-W. Knapp and R. Haag, *Angew. Chem. Int. Ed.* **2012,** *51*, 10472-10498; (c) J. Luczkowiak, A. Muñoz, M. Sánchez-Navarro, R. Ribeiro-Viana, A. Ginieis, B. M. Illescas, N. Martín, R. Delgado and J. Rojo, *Biomacromolecules* **2013,** *14*, 431-437.

utilized to track the interaction through UV-vis spectroscopy and transmission electron microscopy (TEM).[12] We have recently reported the synthesis of gold nanoparticles capped with multiple units of exTTF.[26] In the batch utilized for these experiments, the exTTF gold nanoparticles (exTTFAuNPs, Figure 3) showed an average diameter of 7.1 ± 0.9 nm from TEM analysis, with 567 ± 41 exTTF units/nanoparticle. As a control, we also synthesized nanoparticles capped with the ethyl ester of mercaptoundecanoic acid (ethylAuNPs, Figure 3). The nanoparticles were characterized by UV-vis, FTIR, TEM, atomic force microscopy (AFM) and thermogravimetric analysis (TGA). For full experimental details and characterization, see experimental section.

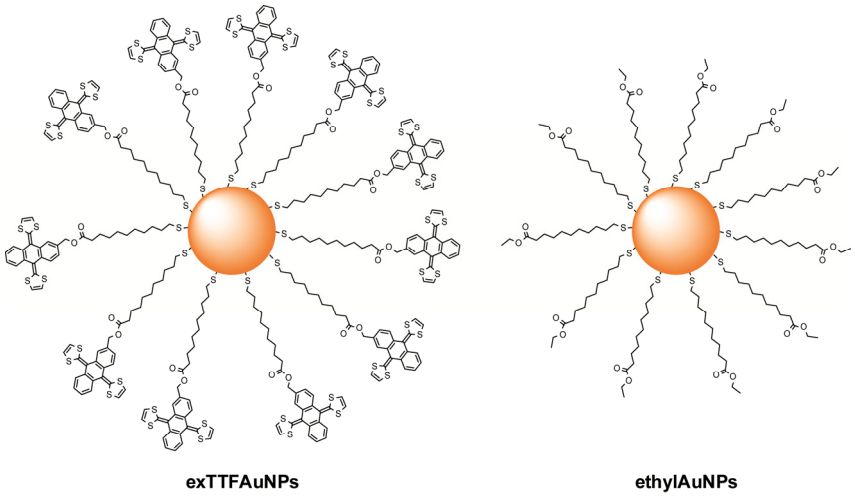

Figure 3. Structures of exTTFAuNPs and ethylAuNPs.

Complete removal of the oxygen-containing moieties in RGO is problematic.[7] To avoid interactions that might arise from residual oxygenated moieties, we decided to obtain FLG from exfoliation of graphite, following a procedure previously described by Coleman et al.[27] Typical TEM micrographs and the Raman spectrum of the obtained FLG are shown in Figure 17. The images and spectroscopy data are consistent with ≤4 layer graphene. In particular, the G' band requires five lorentzians of ~24 cm^{-1} full width at half maximum (FWHM) to be fitted, indicative of 3 layer graphene.[28]

In order to investigate the interaction between exTTFAuNPs and FLG in solution, we carried out a UV-vis titration. To a solution of 1 mL of exTTFAuNPs in chlorobenzene, we added aliquots of 5 μL of a suspension of FLG in chlorobenzene. The resulting mixtures were sonicated for 15 min to allow for complete mixing prior to registration of their spectra.[29] The results are shown in Figure 4a. Upon addition of FLG to the solution

[26] R. Cao, Jr., H. Isla, R. Cao, E. M. Pérez and N. Martín, *Chem. Sci.* **2011,** *2*, 1384-1388.
[27] (a) Y. Hernández, V. Nicolosi, M. Lotya, F. M. Blighe, Z. Sun, S. De, I. T. McGovern, B. Holland, M. Byrne, Y. K. Gun'Ko, J. J. Boland, P. Niraj, G. Duesberg, S. Krishnamurthy, R. Goodhue, J. Hutchison, V. Scardaci, A. C. Ferrari and J. N. Coleman, *Nat Nano* **2008,** *3*, 563-568; (b) J. N. Coleman, *Acc. Chem. Res.* **2013,** *46*, 14-22.
[28] L. M. Malard, M. A. Pimenta, G. Dresselhaus and M. S. Dresselhaus, *Phys. Rep.* **2009,** *473*, 51-87.
[29] It is known that chlorobenzene can generate chlorine radicals upon sonication (see K. R. Moonoosawmy and P. Kruse, *J. Am. Chem. Soc.* **2008,** *130*, 13417-13424.). We have carried out spectra

of exTTFAuNPs, significant changes are observed in their UV-vis spectrum, which point to a substantial exTTFAuNP-graphene interaction. In particular, we observed a decrease in intensity of the band at λ = 437 nm, assigned to the exTTF chromophore, and depletion of the plasmon band at λ = 564 nm, accompanied by an increase of the featureless absorption in the 700-1000 nm region, due to the absorption of FLG. These changes occur with the formation of a pseudo-isosbestic point at approximately 650 nm. We have previously found similar changes in the association of fullerene by exTTFAuNPs.[26] In particular, the decrease in the absorbance of exTTF at 437 nm is the spectroscopic signature of the binding event in our exTTF hosts upon association with fullerene guests.[18] The decrease in intensity of the plasmon resonance band can be ascribed to a change in the state of aggregation of the nanoparticles and/or to a change in the dielectric function of the media surrounding them upon association.[26 , 30]

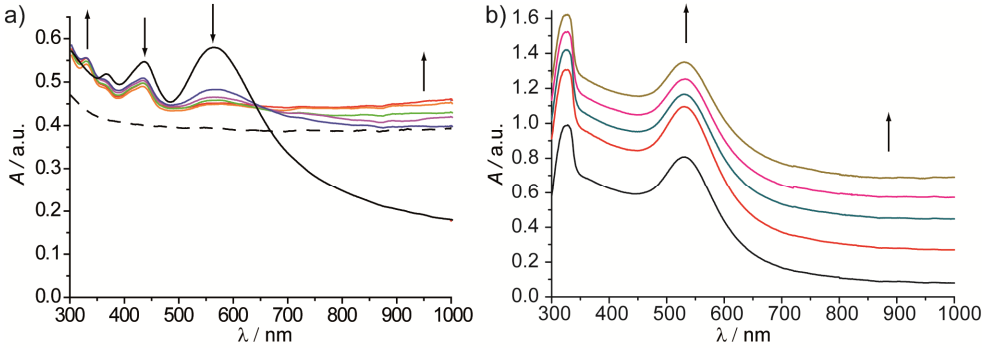

Figure 4. a) Solid lines: UV-vis spectra obtained during the titration of exTTFAuNPs (ca. 0.33 mg/mL, 1 mL, chlorobenzene, r.t.) with aliquots of 5 μL (0-25 μL) of a suspension of FLG (ca. 1 mg/mL, chlorobenzene, r.t.). Dashed line: UV-vis spectrum of an aliquot of 25 μL of FLG in chlorobenzene dissolved in 1 mL of chlorobenzene. b) UV-vis spectra obtained during the titration of ethylAuNPs (0.5 mg/mL, 1 mL chlorobenzene, r.t.) with aliquots of 5 μL (0-25 μL) of a suspension of FLG (ca. 1 mg/mL, chlorobenzene, r.t.).

When the same titration experiment was carried out with ethylAuNPs, the spectra obtained were approximately the arithmetic addition of the spectra of ethylAuNPs and FLG (Figure 4b). This is an indication of the absence of interactions between ethylAuNPs and graphene which confirms the specificity of the exTTF-graphene assembly.

To visualize the association, an aliquot of the final solution of the UV-vis titration experiment was drop-casted onto a carbon-coated copper TEM grid. Examples of the typical micrographs obtained are shown in Figures 5a-d and Figure 20 in the Experimental section. The basal planes of graphene are heavily functionalized with

---

of exTTFAuNPs after sonication under experimental conditions (15, 30 and 45 min.) to prove that no chemical reaction due to the presence of radicals originated from chlorobenzene takes place. Therefore the changes can be safely attributed to the interaction of FLG (Figure 18 in experimental section).

[30] M. A. García, *J. Phys. D: Appl. Phys.* **2011,** *44*, 283001.

exTTFAuNPs, which are concentrated in regions with a higher number of graphene layers (Figure 5a and b). A close examination of the micrographs suggests that the nanoparticles are localized between layers of graphene (Figure 5c and d), a situation in which the exTTFAuNPs-graphene noncovalent interactions are maximized. We observed neither free exTTFAuNPs nor unfunctionalized FLG flakes, suggesting a very strong binding event. In contrast, and in agreement with the UV-vis experiments, TEM scrutiny of an analogous mixture of ethylAuNPs and FLG revealed a random distribution of nanoparticles on the graphene flakes and outside of them (Figure 5e, f and figure 21 in the Experimental section).

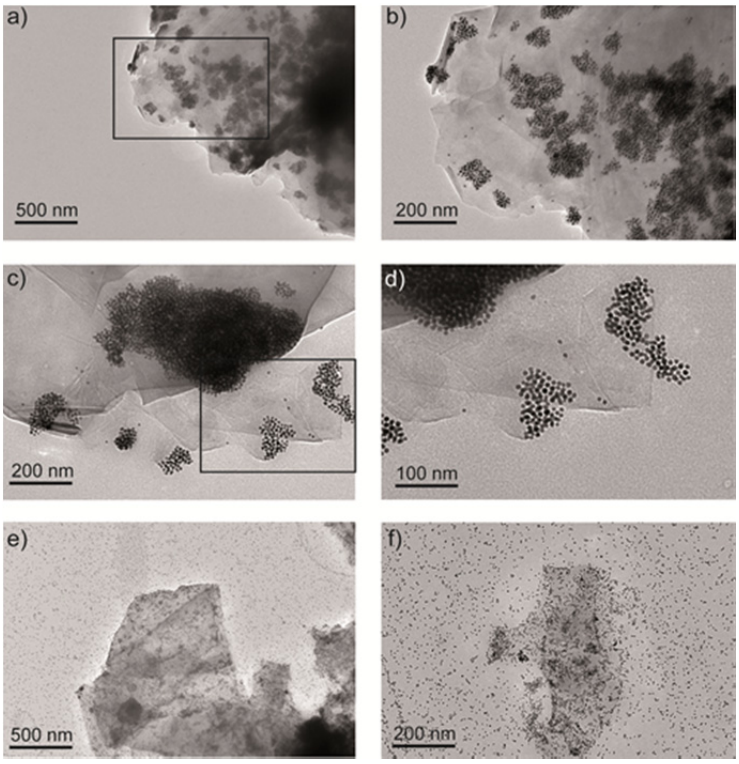

Figure 5. a-d) TEM micrographs of exTTFAuNPs-FLG associates. b) and d) are higher magnification images of the regions marked with a black rectangle in a) and c) respectively. e-f) TEM micrographs of a mixture of ethylAuNPs and FLG.

Raman and energy-dispersive X-ray diffraction spectroscopies (EDX) also support the functionalization. In the Raman spectrum of the exTTFAuNPs-FLG associate, besides the D, G and G' bands of the graphitic material, signals at 2800–3000 and ~1470 cm^{-1} corresponding to the alkyl moieties in the exTTFAuNPs were observed (Figure 6a). We also observed a shift towards higher wavenumbers in the G band of 4 cm^{-1}, compared to pristine FLG (Figure 6b). These changes are consistent with the supramolecular modification of FLG through weak dispersion-type interactions,[31] without significant charge-transfer,[14] as predicted by theory. Remarkably, the G' band

[31] S. K. Samanta, K. S. Subrahmanyam, S. Bhattacharya and C. N. R. Rao, *Chem. Eur. J.* **2012,** *18*, 2890-2901.

still demands six lorentzians of FWHM = 24 cm^{-1} to be fitted correctly, proving that there is little or no graphitization of the sample during the titration experiments.

EDX shows the presence of a significant amount of gold (Figure 6c), which was confirmed to be confined to the exTTFAuNPs through STEM with EDX elemental distribution (Figure 7). All these data are fully consistent with the supramolecular functionalization.

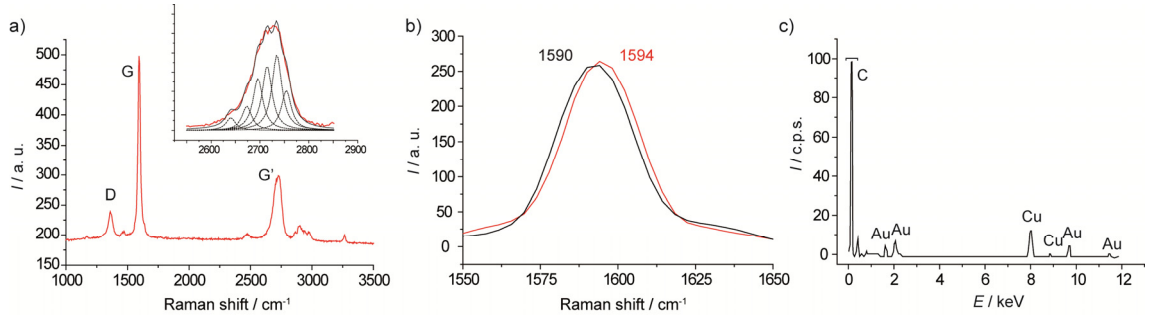

Figure 6. a) Raman spectra ($\lambda_{exc.}$ = 532 nm, 0.8 mW, 100x optical lens) of the exTTFAuNPs-FLG associate. Inset shows the fit of the G' band to six lorentzians of FWHM = 24 cm^{-1}. b) Zoom in on the G band of FLG (black) and exTTFAuNPs-FLG (red). c) EDX spectrum of the exTTFAuNPs-FLG associate.

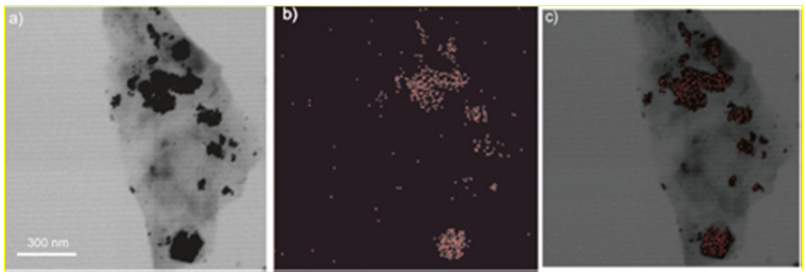

Figure 7. a) STEM micrograph of the exTTFAuNPs-FLG associate; b) elemental distribution (EDX) of Au in the same image and c) combined images.

To determine if the exTTFAuNPs are placed in between or on top of graphene layers, we carried out scanning electron (SEM) and atomic force microscopy (AFM). SEM of the as obtained FLG revealed flakes composed of several layers of graphene, as expected (Figure 17 in the Experimental section). Figure 8a and b show SEM imaging at different beam potentials (5, 10 kV) of a flake of exTTFAuNPs-FLG. The surface of FLG is mostly clean, with a few nanoparticle clusters scattered on it. On the contrary, where graphene has folded over, several clusters of exTTFAuNPs can be seen (marked with a white circle in Figure 8a and b). Upon doubling the intensity of the beam potential, these clusters become more visible, proving that they are placed between the graphene layers.

Likewise, investigation under AFM revealed FLG flakes of heights 12-50 nm, with fundamentally clean flat surfaces (Figure 8c and d). Luckily, one of the flakes presented a hole in which the presence of several exTTFAuNPs was evident. A closer inspection

of this area is shown in Figure 8d. The topographic profile along the white line depicted in Figure 8d reveals a step of –11 nm, consistent with two layers of FLG separated by one layer of exTTFAuNPs, followed by an increase in height of approximately 23 nm, revealing the presence of a conglomerate of nanoparticles. These findings are concordant with the formation of graphene-exTTFAuNPs-graphene sandwich-type nanostructures. The prevalence of this type of structure can be reasoned in terms of its thermodynamic stability compared to a situation where the exTTFAuNPs would lay on top of graphene. In the sandwich-type structure the exTTF-graphene interactions are maximized, whereas the latter would leave many possible exTTF-graphene interaction points unsatisfied.

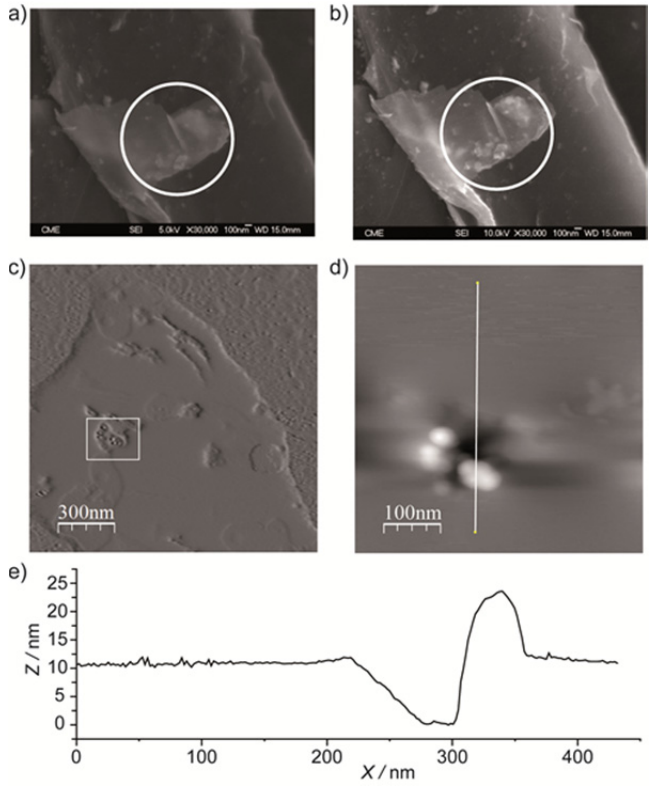

Figure 8. a) SEM micrograph of exTTFAuNPs-functionalized FLG at beam potential 5.0 kV. b) SEM micrograph of exTTFAuNPs-functionalized FLG at double intensity in the beam potential 10.0 kV. c) AFM phase image of a FLG flake. d) Higher magnification AFM topographic image of the area in the white rectangle in c). e) Profile along the white line in d).

6.2.3. Conclusion

In conclusion, we have found that the biconcave exTTF molecule serves as an efficient recognition motif for graphene, allowing for its noncovalent modification despite the geometric disparity. The positive exTTF-graphene interaction is supported by DFT calculations, which indicate that it is based on π–π and CH-π interactions, with no contribution from charge-transfer. These findings were corroborated by Raman spectroscopy. The magnitude of the exTTF-graphene interaction is similar to that of a

similar but planar molecule, anthracene, proving that planarity is not a prerequisite for the structure of supramolecular partners for graphene. Similar convex-planar mismatched supramolecular pairs are frequent in the noncovalent chemistry of fullerenes and carbon nanotubes,[20-21] but had not been observed previously for graphene.

The use of gold nanoparticles as scaffold to present multiple units of exTTF to the surface of graphene allowed us to magnify the exTTF-graphene interaction through a multivalent effect. The properties of the gold nanoparticles were also exploited to track the recognition event. Scrutiny under TEM, Raman, STEM, SEM and AFM of the exTTFAuNPs-graphene associates strongly suggests that these are graphene-exTTFAuNPs-graphene sandwich-type nanostructures.

Our findings expand the number of possible recognition motifs for graphene to a great extent. The changes to the electronic properties of graphene brought about by its noncovalent modification with the electron donor exTTF and their possible applications will be the subject of our future investigations.

6.2.4. Computational details

All calculations were carried out within the density functional theory (DFT) approach by using the 2.9 release of the ORCA program package.[32] Geometry optimizations of the exTTF, the graphene model sheet and the supramolecular exTTF-graphene complexes **1**–**5** were carried out with the revPBE0-D3 functional[23a] and the cc-pVDZ basis set.[33] No symmetry constrains were imposed during the optimization process. The -D3 term in the revPBE0 functional denotes the approach originally developed by Grimme and co-workers to calculate the dispersion energy between two weakly overlapping systems in a post-self consistent field fashion.[23b] The -D3 approximation as well as its -D2 predecessor[34] have been successfully employed in many supramolecular complexes of widespread interest.[35] Since the three-body interaction energy can be significant for large molecular systems,[36] the three-body dispersion contribution was calculated and added to the former pair wise two-body contribution as proposed by Grimme and co-workers.[23b] The choice of the exchange-correlation functional revPBE0 is justified by its excellent performance with respect to the very popular S22[37] and S66[38] non-covalent interaction databases[24] as well as for other related applications.[39] The "resolution of identity" (RI)[40] and "chain of spheres"

[32] F. Neese, *Wiley Interdisciplinary Reviews: Computational Molecular Science* **2012,** *2*, 73-78.
[33] J. T. H. Dunning, *J. Chem. Phys.* **1989,** *90*, 1007-1023.
[34] S. Grimme, *J. Comput. Chem.* **2006,** *27*, 1787.
[35] M. P. Waller, H. Kruse, C. Muck-Lichtenfeld and S. Grimme, *Chem. Soc. Rev.* **2012,** *41*, 3119-3128.
[36] O. A. v. Lilienfeld and A. Tkatchenko, *J. Chem. Phys.* **2010,** *132*, 234109.
[37] P. Jurecka, J. Sponer, J. Cerny and P. Hobza, *PCCP* **2006,** *8*, 1985-1993.
[38] J. Řezáč, K. E. Riley and P. Hobza, *J. Chem. Theory Comput.* **2011,** *7*, 2427-2438.
[39](a) A. Tkatchenko and O. A. von Lilienfeld, *Physical Review B* **2008,** *78*, 045116; (b) F. Goltl and J. Hafner, *J. Chem. Phys.* **2011,** *134*, 064102; (c) S. Grimme, W. Hujo and B. Kirchner, *PCCP* **2012,** *14*, 4875-4883; (d) M. K. Rana, H. S. Koh, J. Hwang and D. J. Siegel, *J. Phys. Chem. C* **2012,** *116*, 16957-16968.
[40] K. Eichkorn, O. Treutler, H. Öhm, M. Häser and R. Ahlrichs, *Chem. Phys. Lett.* **1995,** *240*, 283-290.

(COSX)[41] techniques, for the Coulomb and exchange integrals, respectively, were used to alleviate the computational cost of the more demanding steps. The corresponding auxiliary basis sets[42] are taken from the ORCA libraries.

On the optimized structures, single-energy calculations at the revPBE0-D3/cc-pVTZ level were performed to compute the association binding energies. The association binding energies were calculated as $\Delta E = E_{\text{exTTF-graphene}} - E_{\text{graphene}} - E_{\text{exTTF}}$, where $E_{\text{exTTF-graphene}}$, E_{graphene} and E_{exTTF} stand for the energy of the exTTF-graphene model, the PAH graphene-like molecule and the exTTF unit, respectively. The basis set superposition error (BSSE) was not corrected because the more extended cc-pVTZ basis set was employed. Within the DFT framework in combination with the Grimme's dispersion correction, the cc-pVTZ basis set has proven to be large enough to provide binding energies in supramolecular donor-acceptor complexes with a small basis set superposition error (BSSE).[43]

Figures 9-13 display the optimized geometries calculated for the exTTF-graphene structures **1**–**5** at the revPBE0-D3/cc-pVDZ level. In structure **1**, the central anthracene backbone of exTTF is placed atop the PAH molecule ($C_{84}H_{24}$) in an eclipsed-like disposition (Figure 9). This structure is mainly dominated by π-π interactions with short carbon-carbon (C···C) intermolecular contacts in the 3.15–4.10 Å range. Close carbon-hydrogen (C···H) intermolecular distances (~2.9–3.2 Å) are also predicted. Structure **2** is very similar to structure **1,** but the exTTF unit is now rotated by 90 degrees (Figure 10). Short C···C intermolecular contacts in the 3.12–3.95 Å range are also found for this structure. In both structures **1** and **2**, the anthracene core of exTTF is significantly planarized with respect to isolated exTTF to maximize the interaction with the graphene sheet. The value calculated for the angle between the planes defined by the lateral benzene rings of the anthracene unit increases from 133º in isolated exTTF to 153º and 148º in structures **1** and **2**, respectively. In structure **3**, the interaction between the exTTF molecule and the graphene sheet takes place through the dithiol rings with close intermolecular C···C and sulfur-carbon (S···C) distances in the 3.36–5.69 Å range (Figure 11). The shortest intermolecular distances correspond to the C···H contacts that are around 2.66 Å. Therefore, the interaction in structure **3** stems from a mixing of π-π and CH-π contributions. In contrast to structures **1** and **2**, exTTF in structure **3** maintains the same folding than that found for isolated exTTF. The exTTF molecule can also adopt different orientations to interact with the graphene sheet by a peripheral benzene ring and the sulfur atoms (structure **4**, Figure 12), and by a dithiol ring (structure **5**, Figure 13). Similar to structure **3**, structures **4** and **5** also imply a mixing of π-π and CH-π interactions with many short intermolecular C···C, S···C and C···H contacts. In both structures, the exTTF moiety hardly undergoes changes in its conformation.

[41] F. Neese, F. Wennmohs, A. Hansen and U. Becker, *Chem. Phys.* **2009,** *356*, 98-109.
[42] K. Eichkorn, F. Weigend, O. Treutler and R. Ahlrichs, *Theor. Chem. Acc.* **1997,** *97*, 119-124.
[43] J. Aragó, J. C. Sancho-García, E. Ortí and D. Beljonne, *J. Chem. Theory Comput.* **2011,** *7*, 2068-2077.

Figure 14 displays the minimum-energy geometries computed at revPBE0-D3/cc-pVDZ for structure **1** and for a larger exTTF-graphene model based on structure **1**, where the size of the PAH graphene-like molecule has been increased ($C_{104}H_{28}$). The association binding energies calculated at the revPBE0-D3/cc-pVTZ level for both structures are almost equal (–19.0 and –19.3 kcal mol^{-1}, respectively), which confirms that the size of the PAH molecule used to model the graphene sheet is appropriate to provide an estimation of the association binding energy between exTTF and graphene.

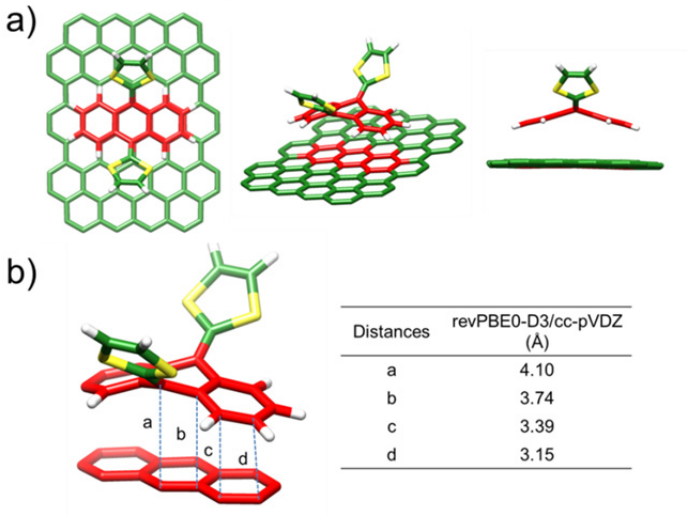

Distances	revPBE0-D3/cc-pVDZ (Å)
a	4.10
b	3.74
c	3.39
d	3.15

Figure 9. a) Top and side views of the minimum-energy geometry computed for exTTF-graphene structure **1** at the revPBE0-D3/cc-pVDZ level. The intermolecular interacting regions of exTTF and graphene are colored in red. b) Magnification of the interacting region with the most representative intermolecular distances collected in the table.

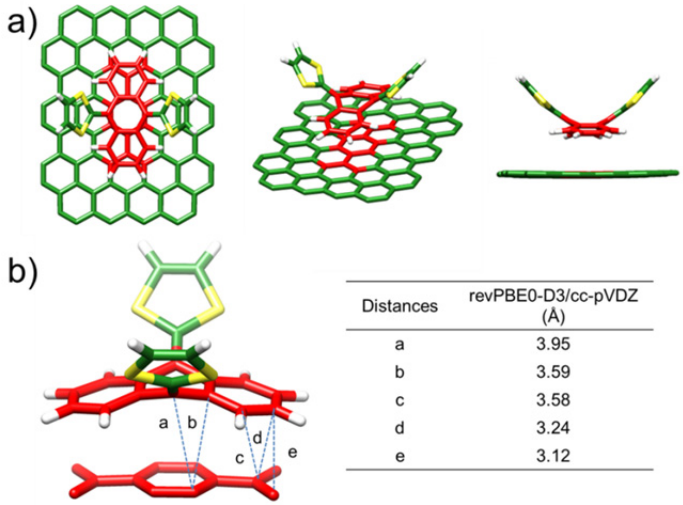

Distances	revPBE0-D3/cc-pVDZ (Å)
a	3.95
b	3.59
c	3.58
d	3.24
e	3.12

Figure 10. a) Top and side views of the minimum-energy geometry computed for exTTF-graphene structure **2** at the revPBE0-D3/cc-pVDZ level. The intermolecular interacting regions of exTTF and graphene are colored in red. b) Magnification of the

interacting region with the most representative intermolecular distances collected in the table.

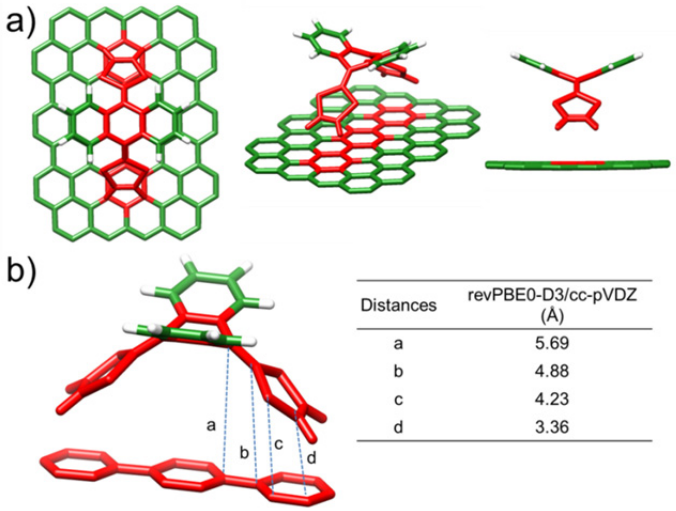

Distances	revPBE0-D3/cc-pVDZ (Å)
a	5.69
b	4.88
c	4.23
d	3.36

Figure 11. a) Top and side views of the minimum-energy geometry computed for exTTF-graphene structure **3** at the revPBE0-D3/cc-pVDZ level. The intermolecular interacting regions of exTTF and graphene are colored in red. b) Magnification of the interacting region with the most representative intermolecular distances collected in the table.

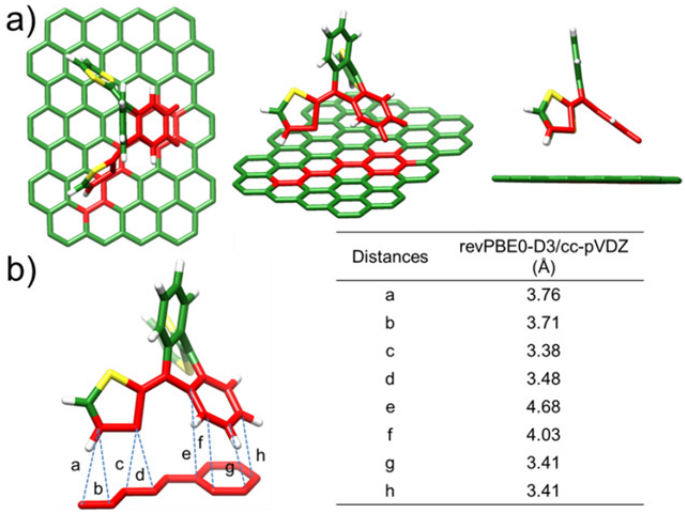

Distances	revPBE0-D3/cc-pVDZ (Å)
a	3.76
b	3.71
c	3.38
d	3.48
e	4.68
f	4.03
g	3.41
h	3.41

Figure 12. a) Top and side views of the minimum-energy geometry computed for exTTF-graphene structure **4** at the revPBE0-D3/cc-pVDZ level. The intermolecular interacting regions of exTTF and graphene are colored in red. b) Magnification of the interacting region with the most representative intermolecular distances collected in the table.

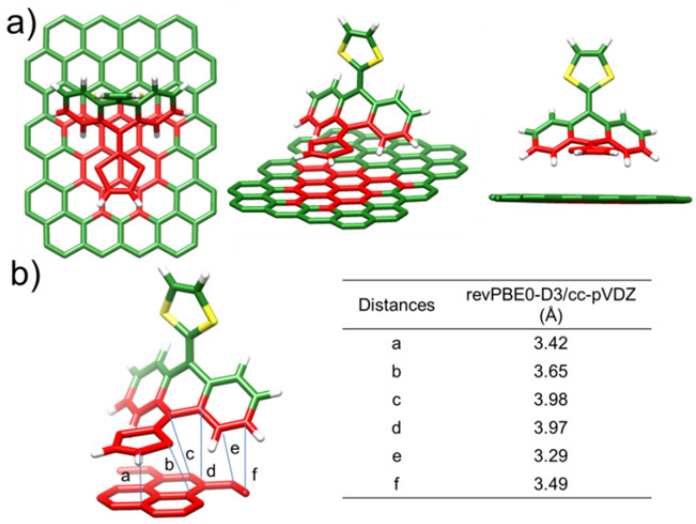

Distances	revPBE0-D3/cc-pVDZ (Å)
a	3.42
b	3.65
c	3.98
d	3.97
e	3.29
f	3.49

Figure 13. a) Top and side views of the minimum-energy geometry computed for exTTF-graphene structure **5** at the revPBE0-D3/cc-pVDZ level. The intermolecular interacting regions of exTTF and graphene are colored in red. b) Magnification of the interacting region with the most representative intermolecular distances collected in the table.

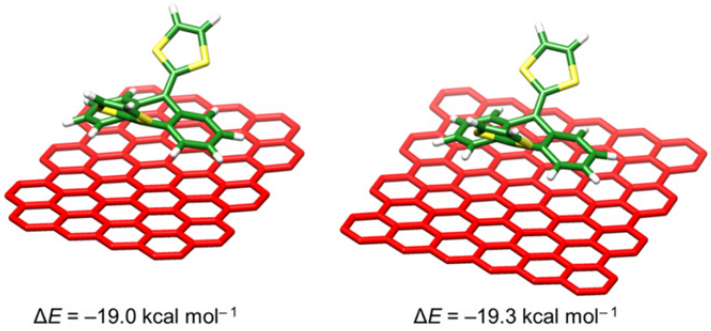

Figure 14. Minimum-energy geometries computed at the revPBE0-D3/cc-pVDZ level for structure **1** and for a larger exTTF-graphene model based on **1** where the size of the graphene sheet has been increased from $C_{84}H_{24}$ to $C_{104}H_{28}$. The association binding energies (ΔE) are calculated at the revPBE0-D3/cc-pVTZ level.

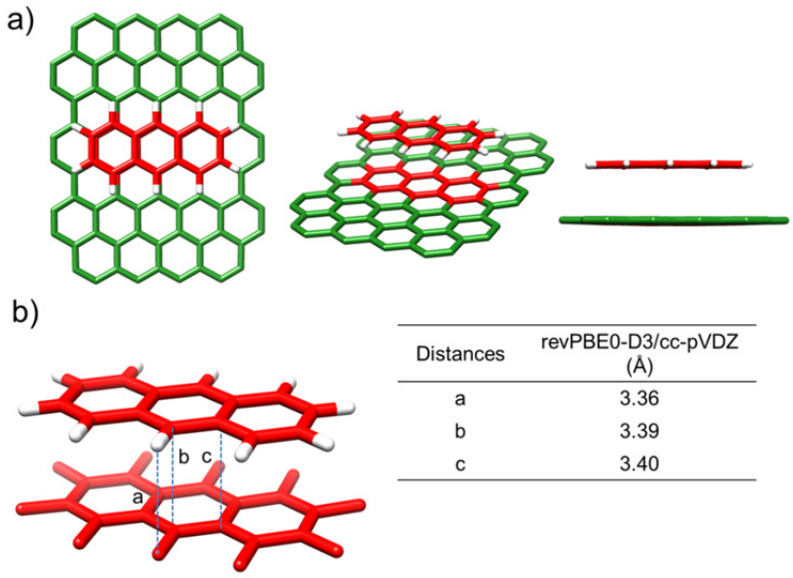

Distances	revPBE0-D3/cc-pVDZ (Å)
a	3.36
b	3.39
c	3.40

Figure 15. a) Top and side views of the minimum-energy geometry computed for anthracene-graphene at the revPBE0-D3/cc-pVDZ level. The intermolecular interacting regions of anthracene and graphene are colored in red. b) Magnification of the interacting region with the most representative intermolecular distances collected in the table.

6.2.5. Experimental section

General. All solvents were dried according to standard procedures. Reagents were used as purchased. All air-sensitive reactions were carried out under argon atmosphere. Flash chromatography was performed using silica gel (Merck, Kieselgel 60, 230-240 mesh, or Scharlau 60, 230-240 mesh). Analytical thin layer chromatographies (TLC) were performed using aluminium-coated Merck Kieselgel 60 F254 plates. NMR spectra were recorded on a Bruker Avance 300 (^{1}H: 300 MHz; ^{13}C: 75 MHz) spectrometer at 298 K, unless otherwise stated, using partially deuterated solvents as internal standards. Coupling constants (*J*) are denoted in Hz and chemical shifts (δ) in ppm. Multiplicities are denoted as follows: s = singlet, d = doublet, t = triplet, m = multiplet, b = broad. Matrix-assisted Laser desorption ionization (coupled to a Time-Of-Flight analyzer) spectrometry was carried out on a Bruker REFLEX spectrometer. Thermogravimetric analyses were realized in a TGA G 500 from TA Instruments (10 ºC/min, under N_2 atmosphere). UV-vis spectra were carried out with a UV-VIS-NIR Spectrophotometer Shimazdu UV-3600 and a UV-Visible Spectrophotometer Varian Cary 50-Scan. TEM images were acquired on a JEOL-JEM 2100 microscope. SEM images were acquired on a JEOL-JSM 6335F. AFM images were acquired on a Nanoscope IIIa microscope equipped with Veeco TESP-SS tips. Raman spectra were acquired on a WITec Confocal Raman Microscope alpha300 R.

Preparation of few layers graphene from Fisher graphite powder (batch 1089145) as reported by Coleman et al. (*Nat. Nano* **2008**, *3*, 563).

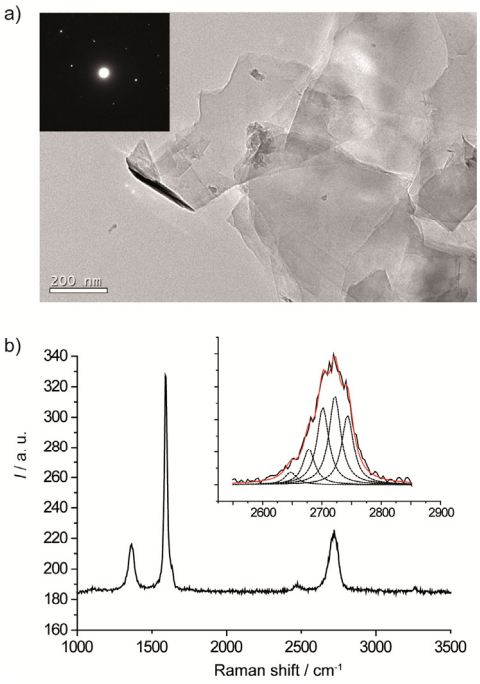

Figure 16. a) TEM micrograph and diffraction pattern of as-obtained FLG. b) Raman spectrum of FLG, showing the fit of the G' band to 5 lorenztians of 24 cm^{-1} FWHM.

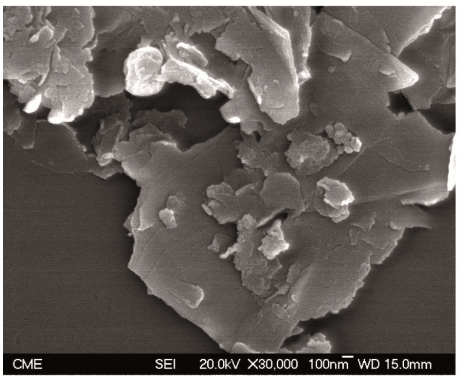

Figure 17. Typical SEM micrograph of as-obtained FLG.

Synthesis of exTTF-MUA: 100 mg of exTTF-CH_2OH (0.24 mmol), 64 mg of MUA (0.29 mmol) and 58 mg of 4-dimethylaminopyridine (0.48 mmol) were dissolved in 30 mL of dry CH2Cl2 under argon atmosphere. Then 69 mg of *N*-(3-dimethylaminopropyl)-*N*′-ethylcarbodiimide hydrochloride (0.36 mmol) were added in small portions. The reaction mixture was stirred at room temperature for 3 h, then diluted with 30 mL CH_2Cl_2, and washed successively with 1 M HCl (aq.) and saturated $NaHCO_3$ (aq.). The combined organic layers were collected and the solvent removed under reduced pressure. The crude product was purified by column chromatography on silica gel (CH_2Cl_2) to afford exTTF-MUA as an orange solid in 76% yield.

^{1}H NMR ($CDCl_3$) δ 7.74–7.66 (4H, m, Ar-H), 7.33–7.24 (3H, m, Ar-H), 6.29 (4H, bs,S-CH-CH-S), 4.75 (2H, s, CH_2-O), 2.96–2.83 (4H, m, CH_2-CH_2-COOR), 2.60–2.48 (4H, m,alkyl), 2.39 (2H, t, J = 7.5 Hz, CH_2-SH), 1.72–1.54 (10 H, m, alkyl) ppm. ^{13}C NMR ($CDCl_3$) δ 174.1, 136.1, 135.7, 135.4, 135.2, 134.2, 130.1, 128.1, 126.8, 126.4, 126.1, 125.5, 125.3, 125.1, 117.7, 117.6, 117.5, 34.8, 34.4, 29.8, 29.7, 29.6, 29.4, 28.8, 27.0, 26.1, 25.4, 25.0, 19.4 ppm. MS *m/z*: calcd. for $C_{32}H_{34}O_2S_5$ [M+] 610.1 found (MALDI-TOF) 609.9.

Synthesis of ethyl 11-mercaptoundecanoate: The synthesis was carried out as in *Chem. Commun.,* **2009**, 5874. 67 mg of MUA (0.31 mmol) was added to a flask with 20 mL of ethanol. Then 0.1 mL of concentrated sulfuric acid was slowly added and the mixture refluxed for 2 hours. The solvent was evaporated under reduced pressure and the crude reaction was diluted with 20 mL of CH_2Cl_2, and washed successively with saturated $NaHCO_3$ aqueous solution (2 × 15 mL) and water (2 × 15 mL). The organic layers were dried over $MgSO_4$ and evaporated to yield 66 mg (87%) of the compound as a white solid. ^{1}H NMR ($CDCl_3$) δ 4.13 (2H, c, J = 7.2 Hz, O−CH_2−CH_3), 2.68 (2H, t, J = 7.5 Hz, HS−CH_2−CH_2), 2.29 (2H, t, J = 7.5 Hz, CH_2−CH_2−CO), 1.64 (4H, m, CH_2−CH_2−CH_2), 1.44–1.22 (15H, m, CH_3 + 6 alkyl) ppm.

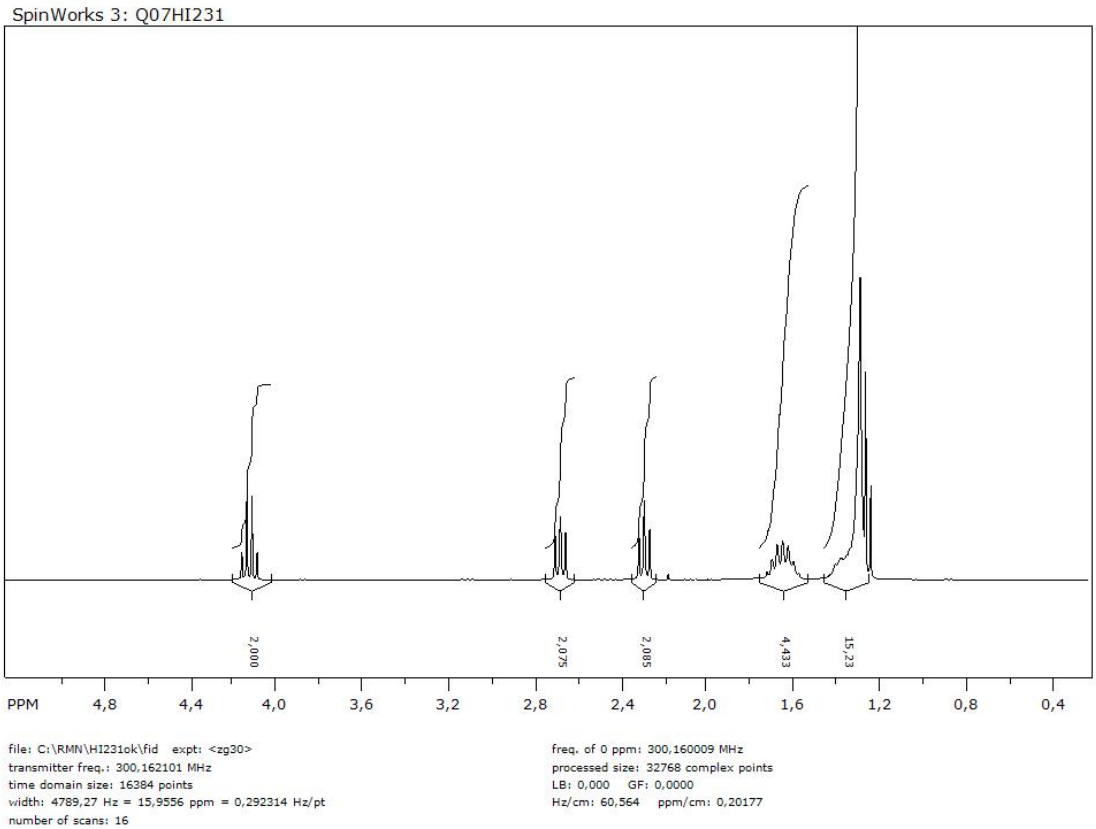

Synthesis and characterization of capped gold nanoparticles. The synthesis of both capped gold nanoparticles, exTTFAuNPs (with exTTFMUA ester) and

ethylAuNPs (with ethylMUA ester) was carried out as reported in *Chem. Sci.* **2011**, 1384.

exTTFAuNPs FTIR (KBr, cm^{-1}): 647, 793, 1100, 1164, 1455, 1510, 1547, 1733, 2851, 2921, 3070. UV-vis (PhCl, 298 K) λ_{max} : 367, 436, 563 nm.

ethylAuNPs FTIR : (neat, cm^{-1}): 700, 756, 802, 1029, 1091, 1244, 1373, 1449, 1736, 2854, 2923. UV-vis (PhCl/MeOH 10%, 298 K) λ_{max} : 531, 327 nm.

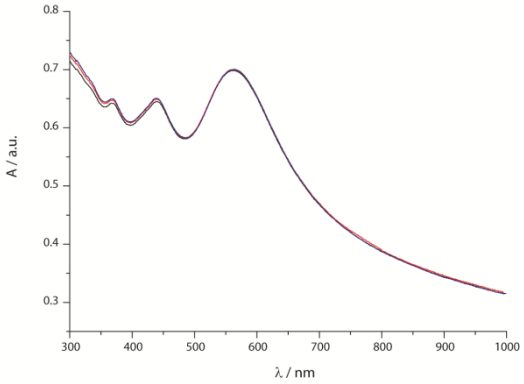

Figure 18. UV-vis spectra of exTTFAuNPs in chlorobenzene upon 15 min (black), 30 min (red) and 45 min (blue) sonication.

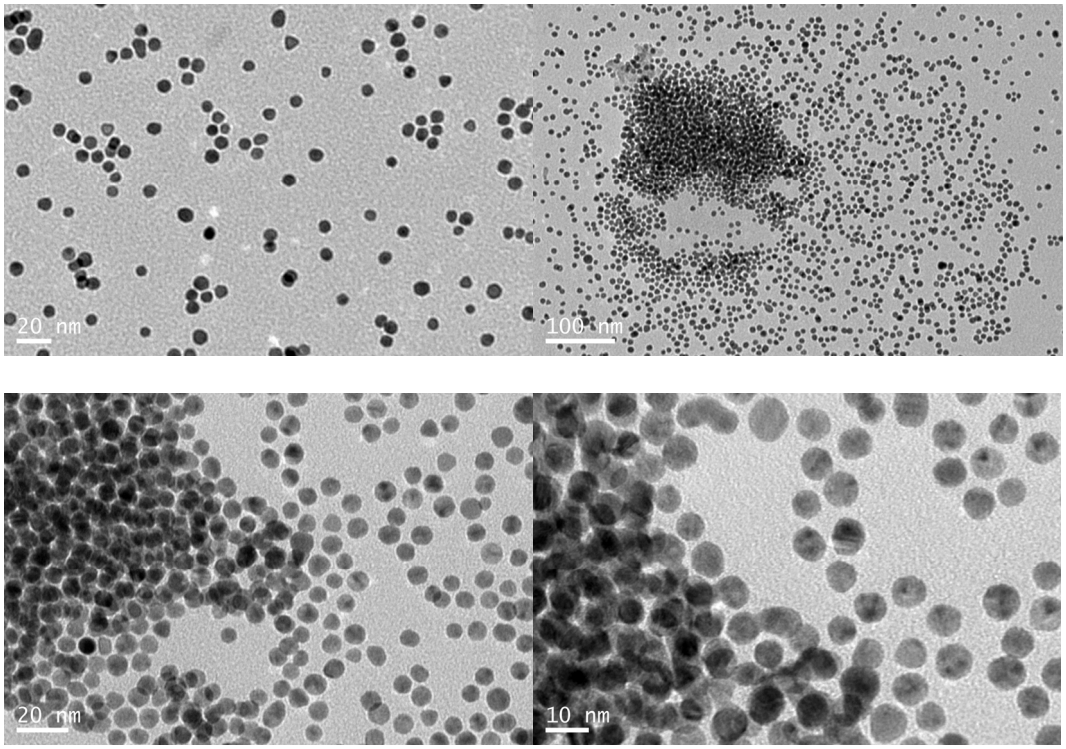

Figure 19. TEM micrographs of ethylAuNPs.

Additional TEM micrographs of AuNPs with FLG

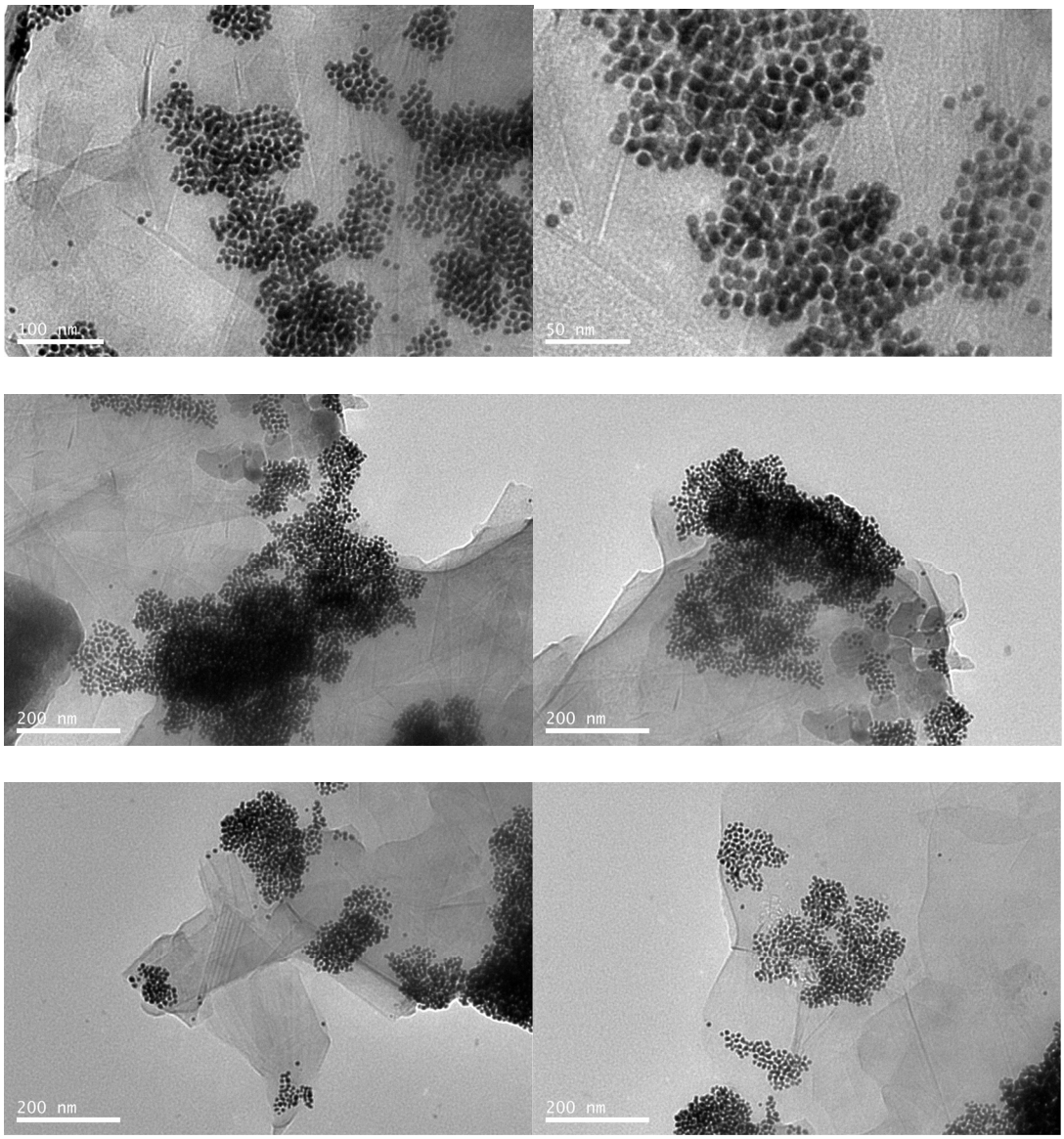

Figure 20. TEM micrographs of exTTFAuNPs-FLG associates from the solution utilized in the titration depicted in Figure 4a.

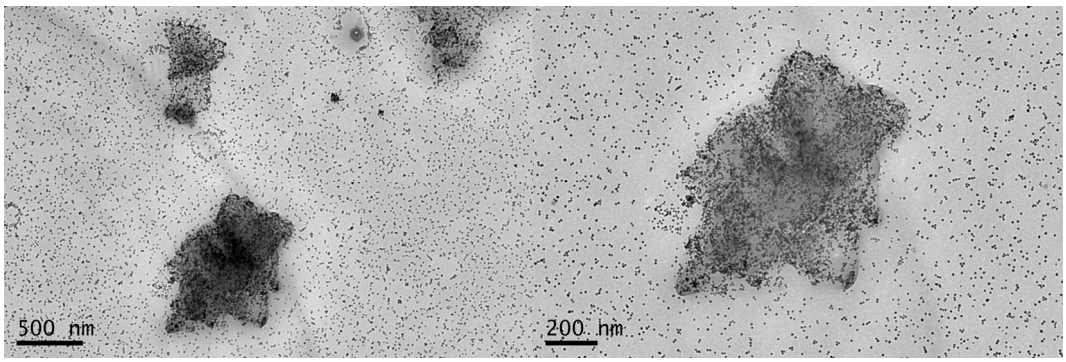

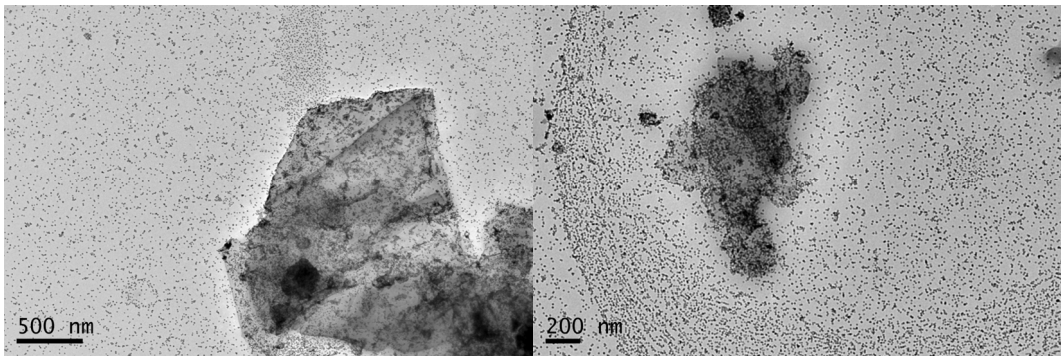

Figure 21. TEM micrographs of ethylAuNPs with FLG, from the solution utilized in the titration depicted in Figure 4b.

6.2.6. References

1. (a) A. K. Geim; K. S. Novoselov, The rise of graphene. *Nat Mater* **2007,** *6*, 183-191;(b) M. J. Allen; V. C. Tung; R. B. Kaner, Honeycomb Carbon: A Review of Graphene. *Chem. Rev.* **2010,** *110*, 132-145.
2. (a) A. K. Geim, Random Walk to Graphene (Nobel Lecture). *Angew. Chem. Int. Ed.* **2011,** *50*, 6966-6985;(b) K. S. Novoselov, Graphene: Materials in the Flatland (Nobel Lecture). *Angew. Chem. Int. Ed.* **2011,** *50*, 6986-7002.
3. (a) C. N. R. Rao; A. K. Sood; K. S. Subrahmanyam; A. Govindaraj, Graphene: The New Two-Dimensional Nanomaterial. *Angew. Chem. Int. Ed.* **2009,** *48*, 7752-7777;(b) P. Avouris, Graphene: Electronic and Photonic Properties and Devices. *Nano Lett.* **2010,** *10*, 4285-4294;(c) S. Pang; Y. Hernández; X. Feng; K. Muellen, Graphene as Transparent Electrode Material for Organic Electronics. *Adv. Mater.* **2011,** *23*, 2779-2795;(d) E. Bekyarova; S. Sarkar; F. Wang; M. E. Itkis; I. Kalinina; X. Tian; R. C. Haddon, Effect of Covalent Chemistry on the Electronic Structure and Properties of Carbon Nanotubes and Graphene. *Acc. Chem. Res.* **2013,** *46*, 65-76.
4. (a) Z. Sun; D. K. James; J. M. Tour, Graphene Chemistry: Synthesis and Manipulation. *J. Phys. Chem. Lett.* **2011,** *2*, 2425-2432;(b) Y. Chen; B. Zhang; G. Liu; X. Zhuang; E.-T. Kang, Graphene and its derivatives: switching ON and OFF. *Chem. Soc. Rev.* **2012,** *41*, 4688-4707;(c) C. K. Chua; M. Pumera, Covalent chemistry on graphene. *Chem. Soc. Rev.* **2013,** *42*, 3222-3233;(d) J. Park; M. Yan, Covalent Functionalization of Graphene with Reactive Intermediates. *Acc. Chem. Res.* **2013,** *46*, 181-189;(e) M. Quintana; E. Vázquez; M. Prato, Organic Functionalization of Graphene in Dispersions. *Acc. Chem. Res.* **2013,** *46*, 138-148;(f) L. Rodríguez-Pérez; M. A. Herranz; N. Martín, The chemistry of pristine graphene. *Chem. Commun.* **2013,** *49*, 3721-3735.
5. K. V. Emtsev; A. Bostwick; K. Horn; J. Jobst; G. L. Kellogg; L. Ley; J. L. McChesney; T. Ohta; S. A. Reshanov; J. Roehrl; E. Rotenberg; A. K. Schmid; D. Waldmann; H. B. Weber; T. Seyller, Towards wafer-size graphene layers by atmospheric pressure graphitization of silicon carbide. *Nat. Mater.* **2009,** *8*, 203-207.
6. (a) A. L. Vázquez de Parga; F. Calleja; B. Borca; M. C. G. Passeggi, Jr.; J. J. Hinarejos; F. Guinea; R. Miranda, Periodically rippled graphene. Growth and spatially resolved electronic structure. *Phys. Rev. Lett.* **2008,** *100*, 056807/1-056807/4;(b) K. S. Kim; Y. Zhao; H. Jang; S. Y. Lee; J. M. Kim; K. S. Kim; J.-H. Ahn; P. Kim; J.-Y. Choi; B. H. Hong, Large-scale pattern growth of graphene films for stretchable transparent electrodes. *Nature* **2009,** *457*, 706-710;(c) X. Li; W. Cai; J. An; S. Kim; J. Nah; D. Yang; R. Piner; A. Velamakanni; I. Jung; E. Tutuc; S. K. Banerjee; L. Colombo; R. S. Ruoff, Large-Area Synthesis of High-Quality and Uniform Graphene Films on Copper Foils. *Science* **2009,** *324*, 1312-1314.
7. D. R. Dreyer; S. Park; C. W. Bielawski; R. S. Ruoff, The chemistry of graphene oxide. *Chem. Soc. Rev.* **2010,** *39*, 228-240.
8. D. V. Kosynkin; A. L. Higginbotham; A. Sinitskii; J. R. Lomeda; A. Dimiev; B. K. Price; J. M. Tour, Longitudinal unzipping of carbon nanotubes to form graphene nanoribbons. *Nature* **2009,** *458*, 872-876.

9. (a) P. Samori; N. Severin; C. D. Simpson; K. Müllen; J. P. Rabe, Epitaxial Composite Layers of Electron Donors and Acceptors from Very Large Polycyclic Aromatic Hydrocarbons. *J. Am. Chem. Soc.* **2002,** *124*, 9454-9457;(b) M. Kastler; J. Schmidt; W. Pisula; D. Sebastiani; K. Müllen, From Armchair to Zigzag Peripheries in Nanographenes. *J. Am. Chem. Soc.* **2006,** *128*, 9526-9534;(c) K. Müllen; J. P. Rabe, Nanographenes as active components of single-molecule electronics and how a scanning tunneling microscope puts them to work. *Acc. Chem. Res.* **2008,** *41*, 511-520.

10. G. Ruan; Z. Sun; Z. Peng; J. M. Tour, Growth of graphene from food, insects, and waste. *ACS Nano* **2011,** *5*, 7601-7607.

11. (a) J. R. Lomeda; C. D. Doyle; D. V. Kosynkin; W.-F. Hwang; J. M. Tour, Diazonium Functionalization of Surfactant-Wrapped Chemically Converted Graphene Sheets. *J. Am. Chem. Soc.* **2008,** *130*, 16201-16206;(b) E. Bekyarova; M. E. Itkis; P. Ramesh; C. Berger; M. Sprinkle; W. A. de Heer; R. C. Haddon, Chemical Modification of Epitaxial Graphene: Spontaneous Grafting of Aryl Groups. *J. Am. Chem. Soc.* **2009,** *131*, 1336-1337;(c) G. L. C. Paulus; Q. H. Wang; M. S. Strano, Covalent Electron Transfer Chemistry of Graphene with Diazonium Salts. *Acc. Chem. Res.* **2013,** *46*, 160-170.

12. (a) M. Quintana; K. Spyrou; M. Grzelczak; W. R. Browne; P. Rudolf; M. Prato, Functionalization of Graphene via 1,3-Dipolar Cycloaddition. *ACS Nano* **2010,** *4*, 3527-3533;(b) M. Quintana; A. Montellano; A. E. del Rio Castillo; G. Van Tendeloo; C. Bittencourt; M. Prato, Selective organic functionalization of graphene bulk or graphene edges. *Chem. Commun.* **2011,** *47*, 9330-9332.

13. M. Lotya; Y. Hernández; P. J. King; R. J. Smith; V. Nicolosi; L. S. Karlsson; F. M. Blighe; S. De; Z. Wang; I. T. McGovern; G. S. Duesberg; J. N. Coleman, Liquid Phase Production of Graphene by Exfoliation of Graphite in Surfactant/Water Solutions. *J. Am. Chem. Soc.* **2009,** *131*, 3611-3620.

14. Q. Su; S. Pang; V. Alijani; C. Li; X. Feng; K. Muellen, Composites of Graphene with Large Aromatic Molecules. *Adv. Mater.* **2009,** *21*, 3191-3195.

15. J. A. Mann; J. Rodríguez-López; H. D. Abruña; W. R. Dichtel, Multivalent Binding Motifs for the Noncovalent Functionalization of Graphene. *J. Am. Chem. Soc.* **2011**.

16. (a) S. Barja; M. Garnica; J. J. Hinarejos; A. L. Vázquez de Parga; N. Martín; R. Miranda, Self-organization of electron acceptor molecules on graphene. *Chem. Commun.* **2010,** *46*, 8198-8200;(b) M. Garnica; D. Stradi; S. Barja; F. Calleja; C. Díaz; M. Alcamí; N. Martín; A. L. Vazquez de Parga; F. Martín; R. Miranda, *Nature Physics* **2013**.

17. J. Malig; N. Jux; D. Kiessling; J.-J. Cid; P. Vázquez; T. Torres; D. M. Guldi, Towards Tunable Graphene/Phthalocyanine-PPV Hybrid Systems. *Angew. Chem. Int. Ed.* **2011,** *50*, 3561-3565, S3561/1-S3561/15.

18. (a) E. M. Pérez; L. Sánchez; G. Fernández; N. Martín, exTTF as a Building Block for Fullerene Receptors. Unexpected Solvent-Dependent Positive Homotropic Cooperativity. *J. Am. Chem. Soc.* **2006,** *128*, 7172-7173;(b) E. M. Pérez; A. L. Capodilupo; G. Fernández; L. Sánchez; P. M. Viruela; R. Viruela; E. Ortí; M. Bietti; N. Martín, Weighting non-covalent forces in the molecular recognition of C_{60}. Relevance of concave-convex complementarity. *Chem. Commun.* **2008,** *0*, 4567-4569;(c) S. S. Gayathri; M. Wielopolski; E. M. Pérez; G. Fernández; L. Sánchez; R. Viruela; E. Ortí; D. M. Guldi; N. Martín, Discrete supramolecular donor-acceptor complexes. *Angew. Chem. Int. Ed.* **2009,** *48*, 815-819;(d) E. Huerta; H. Isla; E. M. Pérez; C. Bo; N. Martín; J. de Mendoza, Tripodal exTTF-CTV Hosts for Fullerenes. *J. Am. Chem. Soc.* **2010,** *132*, 5351-5353;(e) H. Isla; M. Gallego; E. M. Pérez; R. Viruela; E. Ortí; N. Martín, A Bis-exTTF Macrocyclic Receptor That Associates C_{60} with Micromolar Affinity. *J. Am. Chem. Soc.* **2010,** *132*, 1772-1773;(f) D. Canevet; M. Gallego; H. Isla; A. de Juan; E. M. Pérez; N. Martín, Macrocyclic hosts for fullerenes: extreme changes in binding abilities with small structural variations. *J. Am. Chem. Soc.* **2011,** *133*, 3184-3190;(g) B. Grimm; H. Isla; E. M. Pérez; N. Martín; D. M. Guldi, Balancing binding strength and charge transfer lifetime in supramolecular associates of fullerenes. *Chem. Commun.* **2011,** *47*, 7449-7451.

19. (a) G. Fernández; E. M. Pérez; L. Sánchez; N. Martín, Self-Organization of Electroactive Materials: A Head-to-Tail Donor–Acceptor Supramolecular Polymer. *Angew. Chem. Int. Ed.* **2008,** *47*, 1094-1097;(b) G. Fernández; E. M. Pérez; L. Sánchez; N. Martín, An Electroactive Dynamically Polydisperse Supramolecular Dendrimer. *J. Am. Chem. Soc.* **2008,** *130*, 2410-2411;(c) G. Fernández; L. Sánchez; E. M. Pérez; N. Martín, Large exTTF-Based Dendrimers. Self-Assembly and Peripheral Cooperative Multiencapsulation of C_{60}. *J. Am. Chem. Soc.* **2008,** *130*, 10674-10683;(d) J. Santos; E. M. Pérez; B. M. Illescas; N. Martín, Linear and Hyperbranched Electron-Acceptor Supramolecular Oligomers. *Chem.--Asian J.* **2011,** *6*, 1848-1853.

20. (a) K. Tashiro; T. Aida, Metalloporphyrin hosts for supramolecular chemistry of fullerenes. *Chem. Soc. Rev.* **2007,** *36*, 189-197;(b) E. M. Pérez; N. Martín, Curves ahead: molecular receptors for fullerenes based on concave-convex complementarity. *Chem. Soc. Rev.* **2008,** *37*, 1512-1519;(c) D. Canevet; E. M. Pérez; N. Martín, Wraparound Hosts for Fullerenes: Tailored Macrocycles and Cages. *Angew. Chem. Int. Ed.* **2011,** *50*, 9248-9259.

21. (a) N. Nakashima; Y. Tomonari; H. Murakami, Water-soluble single-walled carbon nanotubes via noncovalent sidewall-functionalization with a pyrene-carrying ammonium ion. *Chem. Lett.* **2002**, 638-639;(b) M. Á. Herranz; C. Ehli; S. Campidelli; M. Gutiérrez; G. L. Hug; K. Ohkubo; S. Fukuzumi; M. Prato; N. Martín; D. M. Guldi, Spectroscopic Characterization of Photolytically Generated Radical Ion Pairs in Single-Wall Carbon Nanotubes Bearing Surface-Immobilized Tetrathiafulvalenes. *J. Am. Chem. Soc.* **2007,** *130*, 66-73.

22. S. P. Economopoulos; G. Rotas; Y. Miyata; H. Shinohara; N. Tagmatarchis, Exfoliation and Chemical Modification Using Microwave Irradiation Affording Highly Functionalized Graphene. *ACS Nano* **2010,** *4*, 7499-7507.

23. (a) Y. Zhang; W. Yang, Comment on "Generalized Gradient Approximation Made Simple". *Phys. Rev. Lett.* **1998,** *80*, 890-890;(b) S. Grimme; J. Antony; S. Ehrlich; H. Krieg, A consistent and accurate ab initio parametrization of density functional dispersion correction (DFT-D) for the 94 elements H-Pu. *J. Chem. Phys.* **2010,** *132*, 154104-19.

24. W. Hujo; S. Grimme, Performance of the van der Waals Density Functional VV10 and (hybrid)GGA Variants for Thermochemistry and Noncovalent Interactions. *J. Chem. Theory Comput.* **2011,** *7*, 3866-3871.

25. (a) J. D. Badjic; A. Nelson; S. J. Cantrill; W. B. Turnbull; J. F. Stoddart, Multivalency and Cooperativity in Supramolecular Chemistry. *Acc. Chem. Res.* **2005,** *38*, 723-732;(b) C. Fasting; C. A. Schalley; M. Weber; O. Seitz; S. Hecht; B. Koksch; J. Dernedde; C. Graf; E.-W. Knapp; R. Haag, Multivalency as a Chemical Organization and Action Principle. *Angew. Chem. Int. Ed.* **2012,** *51*, 10472-10498;(c) J. Luczkowiak; A. Muñoz; M. Sánchez-Navarro; R. Ribeiro-Viana; A. Ginieis; B. M. Illescas; N. Martín; R. Delgado; J. Rojo, Glycofullerenes Inhibit Viral Infection. *Biomacromolecules* **2013,** *14*, 431-437.

26. R. Cao, Jr.; H. Isla; R. Cao; E. M. Pérez; N. Martín, exTTF-capped gold nanoparticles as multivalent receptors for C_{60}. *Chem. Sci.* **2011,** *2*, 1384-1388.

27. (a) Y. Hernández; V. Nicolosi; M. Lotya; F. M. Blighe; Z. Sun; S. De; I. T. McGovern; B. Holland; M. Byrne; Y. K. Gun'Ko; J. J. Boland; P. Niraj; G. Duesberg; S. Krishnamurthy; R. Goodhue; J. Hutchison; V. Scardaci; A. C. Ferrari; J. N. Coleman, High-yield production of graphene by liquid-phase exfoliation of graphite. *Nat Nano* **2008,** *3*, 563-568;(b) J. N. Coleman, Liquid exfoliation of defect-free graphene. *Acc. Chem. Res.* **2013,** *46*, 14-22.

28. L. M. Malard; M. A. Pimenta; G. Dresselhaus; M. S. Dresselhaus, Raman spectroscopy in graphene. *Phys. Rep.* **2009,** *473*, 51-87.

29. K. R. Moonoosawmy; P. Kruse, To Dope or Not To Dope: The Effect of Sonicating Single-Wall Carbon Nanotubes in Common Laboratory Solvents on Their Electronic Structure. *J. Am. Chem. Soc.* **2008,** *130*, 13417-13424.

30. M. A. García, Surface plasmons in metallic nanoparticles: fundamentals and applications. *J. Phys. D: Appl. Phys.* **2011,** *44*, 283001.

31. S. K. Samanta; K. S. Subrahmanyam; S. Bhattacharya; C. N. R. Rao, Composites of Graphene and Other Nanocarbons with Organogelators Assembled through Supramolecular Interactions. *Chem. Eur. J.* **2012,** *18*, 2890-2901.

32. F. Neese, The ORCA program system. *Wiley Interdisciplinary Reviews: Computational Molecular Science* **2012,** *2*, 73-78.

33. J. T. H. Dunning, Gaussian basis sets for use in correlated molecular calculations. I. The atoms boron through neon and hydrogen. *J. Chem. Phys.* **1989,** *90*, 1007-1023.

34. S. Grimme, *J. Comput. Chem.* **2006,** *27*, 1787.

35. M. P. Waller; H. Kruse; C. Muck-Lichtenfeld; S. Grimme, Investigating inclusion complexes using quantum chemical methods. *Chem. Soc. Rev.* **2012,** *41*, 3119-3128.

36. O. A. v. Lilienfeld; A. Tkatchenko, Two- and three-body interatomic dispersion energy contributions to binding in molecules and solids. *J. Chem. Phys.* **2010,** *132*, 234109.

37. P. Jurecka; J. Sponer; J. Cerny; P. Hobza, Benchmark database of accurate (MP2 and CCSD(T) complete basis set limit) interaction energies of small model complexes, DNA base pairs, and amino acid pairs. *PCCP* **2006,** *8*, 1985-1993.
38. J. Řezáč; K. E. Riley; P. Hobza, S66: A Well-balanced Database of Benchmark Interaction Energies Relevant to Biomolecular Structures. *J. Chem. Theory Comput.* **2011,** *7*, 2427-2438.
39. (a) A. Tkatchenko; O. A. von Lilienfeld, Popular Kohn-Sham density functionals strongly overestimate many-body interactions in van der Waals systems. *Physical Review B* **2008,** *78*, 045116;(b) F. Goltl; J. Hafner, Alkane adsorption in Na-exchanged chabazite: The influence of dispersion forces. *J. Chem. Phys.* **2011,** *134*, 064102;(c) S. Grimme; W. Hujo; B. Kirchner, Performance of dispersion-corrected density functional theory for the interactions in ionic liquids. *PCCP* **2012,** *14*, 4875-4883;(d) M. K. Rana; H. S. Koh; J. Hwang; D. J. Siegel, Comparing van der Waals Density Functionals for CO2 Adsorption in Metal Organic Frameworks. *J. Phys. Chem. C* **2012,** *116*, 16957-16968.
40. K. Eichkorn; O. Treutler; H. Öhm; M. Häser; R. Ahlrichs, Auxiliary basis sets to approximate Coulomb potentials. *Chem. Phys. Lett.* **1995,** *240*, 283-290.
41. F. Neese; F. Wennmohs; A. Hansen; U. Becker, Efficient, approximate and parallel Hartree–Fock and hybrid DFT calculations. A 'chain-of-spheres' algorithm for the Hartree–Fock exchange. *Chem. Phys.* **2009,** *356*, 98-109.
42. K. Eichkorn; F. Weigend; O. Treutler; R. Ahlrichs, Auxiliary basis sets for main row atoms and transition metals and their use to approximate Coulomb potentials. *Theor. Chem. Acc.* **1997,** *97*, 119-124.
43. J. Aragó; J. C. Sancho-García; E. Ortí; D. Beljonne, Ab Initio Modeling of Donor-Acceptor Interactions and Charge-Transfer Excitations in Molecular Complexes: The Case of Terthiophene-Tetracyanoquinodimethane. *J. Chem. Theory Comput.* **2011,** *7*, 2068-2077.

7. Bowl-shape electron donors with absorptions in the visible range of the solar spectrum and their supramolecular assemblies with C_{60}

Helena Isla, Bruno Grimm, Emilio M. Pérez, M. Rosario Torres, M. Ángeles Herranz, Rafael Viruela, Juan Aragó, Enrique Ortí, Dirk M. Guldi and Nazario Martín, *Chem. Sci.*, **2012**, *3*, 498-508

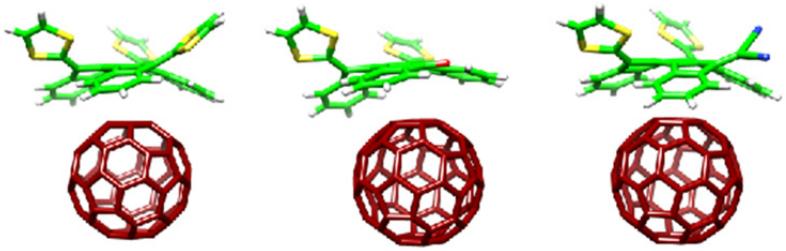

*We describe the synthesis, electronic, optical, and photophysical properties of a family of three electron-donor bowl-shaped organic molecules that absorb light in the whole range of the visible spectrum (up to 800 nm in one case), and associate C_{60} in solution with binding constants in the range of 10^4–10^2 M^{-1} as measured from both UV-vis and fluorescence titrations in several solvents. These molecules are π-extended derivatives of tetrathiafulvalene, based on a truxene core to which two or three units of dithiole are covalently attached. The inclusion of the bulky dithiole groups is responsible for their bowl-shape geometry, which allows them to associate with C_{60}, and their electron donor character. The symmetric derivative **7.1**, with three dithiole units, absorbs light in the 370–520 nm range. Exchanging one of the dithiole groups by an electron withdrawing group, ketone (**7.2**) and dicyanomethylene (**7.3**), results in an intramolecular push-pull effect that expands the absorption to nearly 700 nm in the case of **7.2**, and up to 800 nm in the case of **7.3**. Transient absorption measurements, supported by spectroelectrochemical and radiolytical experiments, reveal that upon photoexcitation of the **7.1**·C_{60} associate the fully charge-separated state **7.1**$^{\bullet+}$·$C_{60}^{\bullet-}$ is generated, with lifetimes of hundreds of picoseconds. Molecular-level understanding of the electronic and supramolecular properties of **7.1**–**7.3** is provided by density functional theory calculations.*

Chem. Sci., **2012**, *3*, 498–50

7.1. Introduction

The molecule-by-molecule manipulation of matter constitutes the basis for the "bottom-up" approach in nanoscience. In principle, such manipulation can be achieved by two different strategies. One is based on physics and chemistry, in which the properties of materials arise from the design, synthesis, and engineering of novel molecular structures. The other one is directly inspired by nature, in which new properties emerge from the evolution and self-selection of ensembles of a preexisting collection of molecular fragments. The self-assembly of judiciously designed molecular

components —based on the dynamic nature of noncovalent interactions— bridges the gap between them and has already allowed the creation of structurally well-defined nanostructures.[1] In the context of new materials for improved organic photovoltaics, the self-assembly of electroactive molecular fragments has attracted a great deal of attention in the recent years.[2] Owing to their widespread use as electron acceptors in organic electronics,[3] the majority of these research efforts have focused on the supramolecular organization of fullerenes and fullerene-containing molecules.[4,5]

---

[1] For recent reviews, see: (a) M. Numata and S. Shinkai, *Chem. Commun.* **2011,** *47*, 1961-1975; (b) J. J. Davis, G. A. Orlowski, H. Rahman and P. D. Beer, *Chem. Commun.* **2010,** *46*, 54-63; (c) S. F. M. van Dongen, H.-P. M. de Hoog, R. J. R. W. Peters, M. Nallani, R. J. M. Nolte and J. C. M. van Hest, *Chem. Rev.* **2009,** *109*, 6212-6274; (d) D. B. Amabilino, *Chem. Soc. Rev.* **2009,** *38*, 669-670; (e) J. K. Klosterman, Y. Yamauchi and M. Fujita, *Chem. Soc. Rev.* **2009,** *38*, 1714-1725; (f) C. C. Lee, C. Grenier, E. W. Meijer and A. P. H. J. Schenning, *Chem. Soc. Rev.* **2009,** *38*, 671-683; (g) K. M. Mullen and P. D. Beer, *Chem. Soc. Rev.* **2009,** *38*, 1701-1713.

[2] (a) M. Á. Herranz, C. Ehli, S. Campidelli, M. Gutiérrez, G. L. Hug, K. Ohkubo, S. Fukuzumi, M. Prato, N. Martín and D. M. Guldi, *J. Am. Chem. Soc.* **2008,** *130*, 66-73; (b) N. Crivillers, M. Mas-Torrent, J. Vidal-Gancedo, J. Veciana and C. Rovira, *J. Am. Chem. Soc.* **2008,** *130*, 5499-5506; (c) C. Ehli, C. Oelsner, D. M. Guldi, A. Mateo-Alonso, M. Prato, C. Schmidt, C. Backes, F. Hauke and A. Hirsch, *Nature Chemistry* **2009,** *1*, 243-249; (d) D. Gonzalez-Rodriguez, E. Carbonell, D. M. Guldi and T. Torres, *Angew. Chem. Int. Ed.* **2009,** *48*, 8032-8036; (e) S. Schlundt, G. Kuzmanich, F. Spaenig, G. d. M. Rojas, C. Kovacs, M. A. Garcia-Garibay, D. M. Guldi and A. Hirsch, *Chem. Eur. J.* **2009,** *15*, 12223-12233; (f) F. Silvestri, I. López-Duarte, W. Seitz, L. Beverina, M. V. Martínez-Díaz, T. J. Marks, D. M. Guldi, G. A. Pagani and T. Torres, *Chem. Commun.* **2009**, 4500-4502; (g) A. A. Gorodetsky, C.-Y. Chiu, T. Schiros, M. Palma, M. Cox, Z. Jia, W. Sattler, I. Kymissis, M. Steigerwald and C. Nuckolls, *Angew. Chem. Int. Ed.* **2010,** *49*, 7909-7912; (h) Y. Rio, W. Seitz, A. Gouloumis, P. Vazquez, J. L. Sessler, D. M. Guldi and T. Torres, *Chem. Eur. J.* **2010,** *16*, 1929-1940; (i) W. Seitz, A. J. Jimenez, E. Carbonell, B. Grimm, M. S. Rodriguez-Morgade, D. M. Guldi and T. Torres, *Chem. Commun.* **2010,** *46*, 127-129; (j) J. Tremblay Noah, A. Gorodetsky Alon, P. Cox Marshall, T. Schiros, B. Kim, R. Steiner, Z. Bullard, A. Sattler, W.-Y. So, Y. Itoh, F. Toney Michael, H. Ogasawara, P. Ramirez Arthur, I. Kymissis, L. Steigerwald Michael and C. Nuckolls, *ChemPhysChem* **2010,** *11*, 799-803; (k) F. Würthner and K. Meerholz, *Chem. Eur. J.* **2010,** *16*, 9366-9373; (l) C.-Y. Chiu, B. Kim, A. A. Gorodetsky, W. Sattler, S. Wei, A. Sattler, M. Steigerwald and C. Nuckolls, *Chem. Sci.* **2011,** *2*, 1480-1486; (m) J. K. Sprafke, S. D. Stranks, J. H. Warner, R. J. Nicholas and H. L. Anderson, *Angew. Chem. Int. Ed.* **2011,** *50*, 2313-2316; (n) A. C. Whalley, K. N. Plunkett, A. A. Gorodetsky, C. L. Schenck, C.-Y. Chiu, M. L. Steigerwald and C. Nuckolls, *Chem. Sci.* **2011,** *2*, 132-135.

[3] (a) N. Martín, *Chem. Commun.* **2006,** 2093-2104; (b) D. M. Guldi, B. M. Illescas, C. M. Atienza, M. Wielopolski and N. Martín, *Chem. Soc. Rev.* **2009,** *38*, 1587-1597.

[4] For reviews, see: (a) A. Hirsch, *Pure Appl. Chem.* **2008,** *80*, 571-587; (b) E. M. Pérez and N. Martín, *Chem. Soc. Rev.* **2008,** *37*, 1512-1519; (c) F. D'Souza and O. Ito, *Chem. Commun.* **2009**, 4913-4928; (d) E. M. Pérez, *Pure Appl. Chem.* **2011,** *83*, 201-211.

[5] For recent examples, see: (a) G. Fernández, E. M. Pérez, L. Sánchez and N. Martín, *Angew. Chem. Int. Ed.* **2008,** *47*, 1094-1097; (b) G. Fernández, E. M. Pérez, L. Sánchez and N. Martín, *J. Am. Chem. Soc.* **2008,** *130*, 2410-2411; (c) G. Fernández, L. Sánchez, E. M. Pérez and N. Martín, *J. Am. Chem. Soc.* **2008,** *130*, 10674-10683; (d) R. D. Kennedy, A. L. Ayzner, D. D. Wanger, C. T. Day, M. Halim, S. I. Khan, S. H. Tolbert, B. J. Schwartz and Y. Rubin, *J. Am. Chem. Soc.* **2008,** *130*, 17290-17292; (e) E. M. Pérez, A. L. Capodilupo, G. Fernández, L. Sánchez, P. M. Viruela, R. Viruela, E. Ortí, M. Bietti and N. Martín, *Chem. Commun.* **2008,** 4567-4569; (f) F. D'Souza, E. Maligaspe, K. Ohkubo, M. E. Zandler, N. K. Subbaiyan and S. Fukuzumi, *J. Am. Chem. Soc.* **2009,** *131*, 8787-8797; (g) K. S. Iyer, M. Saunders, T. Becker, C. W. Evans and C. L. Raston, *J. Am. Chem. Soc.* **2009,** *131*, 16338-16339; (h) A. Kira, T. Umeyama, Y. Matano, K. Yoshida, S. Isoda, J. K. Park, D. Kim and H. Imahori, *J. Am. Chem. Soc.* **2009,** *131*, 3198-3200; (i) J. M. MacLeod, O. Ivasenko, C. Fu, T. Taerum, F. Rosei and D. F. Perepichka, *J. Am. Chem. Soc.* **2009,** *131*, 16844-16850; (j) C. Reiriz, R. J. Brea, R. Arranz, J. L. Carrascosa, A. Garibotti, B. Manning, J. M. Valpuesta, R. Eritja, L. Castedo and J. R. Granja, *J. Am. Chem. Soc.* **2009,** *131*, 11335-11337; (k) J. Wang, Y. Shen, S. Kessel, P. Fernandes, K. Yoshida, S. Yagai, D. G. Kurth, H.

With the long term goal of constructing self-assembled nanosized optoelectronic devices, we have recently reported on a supramolecular donor-acceptor hybrid comprised of truxene-tetrathiafulvalenes (truxTTF), in which three dithiole units are covalently linked to a truxene core, as electron donors and C_{60} or C_{70} as electron acceptors.[6] Investigation of the solid state structure of truxTTF revealed that all of three dithiole units are present in all-*cis* configuration, forcing the truxene core to deviate from planarity and to adopt a bowl-shape geometry. The latter complements perfectly the convex surface of fullerenes. We have shown that truxTTFs exhibit good electron donating abilities, donating up to five electrons, self-assemble with fullerenes with binding constants of $K_a = (1.2 \pm 0.3) \times 10^3$ M^{-1} and $(8.0 \pm 1.5) \times 10^3$ M^{-1} for C_{60} and C_{70}, respectively, in $CDCl_3/CS_2$ (1:1), and absorb light efficiently in the visible region with extinction coefficients as high as 30.000 M^{-1} cm^{-1}. Although this represents already a significant red-shift with respect to conventional TTF and its derivatives, in order to utilize them in organic photovoltaic devices it would be desirable to obtain truxTTF-like molecules that would absorb even further in the red, while maintaining the electron donor abilities and the supramolecular properties of the parent truxTTFs.

Here, we present the design, synthesis, optical, and electrochemical properties of two new truxTTF-type derivatives with improved light absorption properties. We also report the detailed electronic, optical, and photophysical characterization of the parent truxTTF and these two new derivatives as well as their supramolecular assemblies with C_{60}. Experimental trends are rationalized with the help of density functional theory (DFT) calculations.

7.2. Results and discussion

7.2.1. Design and synthesis

In the case of truxTTF **7.1** (Scheme 1), time-dependent density functional theory (TDDFT) calculations predicted that the lowest-energy absorption, which maximizes at 450 nm, is due to a multiple of electronic transitions that originate from one-electron excitations among the HOMO–1, HOMO and LUMO, LUMO+1 molecular orbitals.[6] In particular, excitations from the degenerate HOMO to the degenerate LUMO give rise to four excited electronic states calculated at 2.57, 2.77 (degenerate state), and 2.83 eV above the ground state. While the transition to the first excited state has no intensity (oscillator strength $f = 0.00$), the transitions to the degenerate state are quite intense ($f = 0.33$), and the transition to the fourth excited state has a medium intensity ($f = 0.12$). The couple of transitions calculated at 2.77 eV (447 nm) are therefore responsible for

---

Mohwald and T. Nakanishi, *Angew. Chem. Int. Ed.* **2009,** *48*, 2166-2170; (l) X. Zhang and M. Takeuchi, *Angew. Chem. Int. Ed.* **2009,** *48*, 9646-9651; (m) M. Dante, C. Yang, B. Walker, F. Wudl and T.-Q. Nguyen, *Adv. Mater.* **2010,** *22*, 1835-1839; (n) D. Canevet, M. Gallego, H. Isla, A. de Juan, E. M. Pérez and N. Martín, *J. Am. Chem. Soc.* **2011,** *133*, 3184-3190; (o) R. Cao, Jr., H. Isla, R. Cao, E. M. Pérez and N. Martín, *Chem. Sci.* **2011,** *2*, 1384-1388; (p) B. Grimm, H. Isla, E. M. Pérez, N. Martín and D. M. Guldi, *Chem. Commun.* **2011,** *47*, 7449-7451.

[6] E. M. Pérez, M. Sierra, L. Sánchez, M. R. Torres, R. Viruela, P. M. Viruela, E. Ortí and N. Martín, *Angew. Chem. Int. Ed.* **2007,** *46*, 1847-1851.

the absorption maximum observed at 450 nm. Based on this, we reasoned we could lower the energy of the LUMO and LUMO+1 orbitals by covalently attaching electron withdrawing groups to the truxene core. Considering we wished to maintain the electron donating and supramolecular properties of the parent truxTTF, we established molecules **7.2** and **7.3** as synthetic targets (Scheme 1). In **7.2**, we have replaced one of the dithiole units by a moderately electron withdrawing ketone group, while in **7.3** we have substituted the ketone by the stronger electron acceptor dicyanomethylene group. We expected **7.2** and **7.3** to show a significant bathochromic shift with respect to **7.1** as a result of the push-pull effects between the electron donor dithioles and the electron acceptor groups.

A key feature of **7.1**, **7.2**, and **7.3** is that they can all be obtained easily from truxenone. Since truxenone is commercially available only in limited quantities and at relatively high price, we decided to synthesize truxenone from indandione by acid-catalyzed condensation. Initially, we followed the procedure described by Twieg and co-workers[7] that is, utilizing methanesulfonic acid as catalyst / solvent and heating the sample to 110 ºC for approximately 4 hours. We found this procedure to be perfectly reproducible and obtained pure truxenone on the multigram scale. Nevertheless, in order to reduce the reaction time and to increase the yield, we decided to attempt the methanesulfonic catalyzed reaction under microwave irradiation.[8] In Table 1 the reaction times and isolated yields of truxenone are summarized. As is shown, the yield of the reaction increases with decreasing time. Under optimized conditions, just 5 seconds of microwave irradiation is sufficient to obtain a 77 % yield of truxenone, equivalent to that obtained with standard heating in 4 hours, a three-thousand fold improvement in reaction time. The reaction is scalable up to the gram scale.

[7] L. Sanguinet, J. C. Williams, Z. Yang, R. J. Twieg, G. Mao, K. D. Singer, G. Wiggers and R. G. Petschek, *Chem. Mater.* **2006,** *18*, 4259-4269.

[8] (a) P. Lidstrom, J. Tierney, B. Wathey and J. Westman, *Tetrahedron* **2001,** *57*, 9225-9283; (b) D. Obermayer, B. Gutmann and C. O. Kappe, *Angew. Chem. Int. Ed.* **2009,** *48*, 8321-8324.

Table 1 Optimization of the synthesis of truxenone under microwave irradiation.[a]

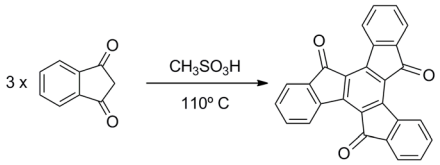

Method	Time (seconds)	Yield
Thermal	14400	78 %
Microwave	60	32 %
Microwave	30	62 %
Microwave	15	71 %
Microwave	5	77 %

[a] See the Experimental section for experimental details.

Attaching three (**7.1**) or two (**7.2** and **7.3**) dithioles by Horner-Wadsworth-Emmons olefination under stoichiometric control gives direct access to **7.1** and **7.2** (Scheme 1). Knoevenagel condensation of **7.2** with malononitrile yielded **7.3**. Remarkably, the alternative reaction sequence, in which the Knoevenagel condensation was carried out before the Horner-Wadsworth-Emmons reaction, did not produce any of the desired products.

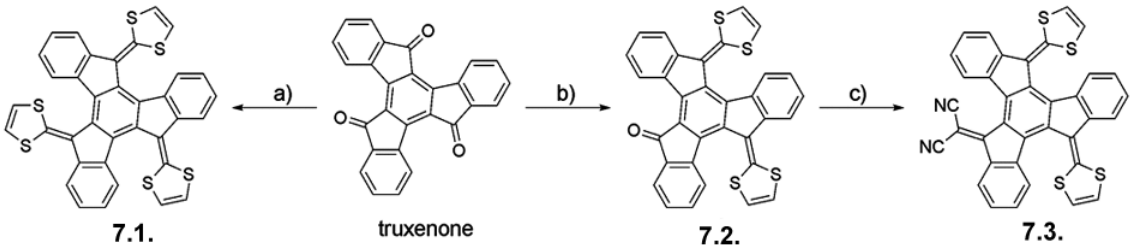

Scheme 1 Synthesis of compounds **7.1**, **7.2**, and **7.3**. Reagents and conditions: a) dimethyl 1,3-dithiol-2-ylphosphonate (exc. 3 equiv.), BuLi, THF, −78 ºC to r. t., 2 h, *y* = 67 %; b) dimethyl 1,3-dithiol-2-ylphosphonate (0.7 equiv.), BuLi, THF, −78 ºC to r. t., 2 h, *y* = 37 %; c) malononitrile, $TiCl_4$, pyridine, PhCl, r.t., 3 h, *y* = 28 %.

7.2.2. Molecular Structure

Crystals of **7.2** of sufficient quality for X-ray analysis were obtained by slow evaporation of a semisaturated solution of **7.2** in $CHCl_3$. Its solid state structure is shown in Figure 1. In analogy to **7.1**,[6] the incorporation of two dithiole units results in the distortion of the planar aromatic core, which adopts a concave shape. To alleviate

the steric interactions, the peripheral benzene rings fold down and the dithiole rings point outside the curved surface (Figure 1). The concave aromatic cavity is found to be shallower for **7.2**, due to the presence of the sterically non-demanding ketone group. In the case of **7.1**, which exhibits a C_3 molecular symmetry, the peripheral benzene rings form an angle of 23.7º with the central benzene ring. For **7.2**, the angles between the plane defined by the central aromatic ring and those defined by the benzene rings containing C1 and C2, C8 and C9, and C14 and C15 are 15.8, 0.20, and 26.2º, respectively. Attachment of dithioles on either side of the prochiral truxenone produces a racemic mixture of *P, P, P/M, M, M* enantiomers for both **7.2** and **7.3**. Following the numbering depicted in Figure 1 allows an easy visualization of the helices. In Figure 1b, the C1-C2-C3-C4-C5-C6-S7 series forms an *M*-helix, while in Figure 1d the equivalent series gives rise to a *P*-helix. As can be seen in Figure 1a for **7.2**, even the relatively planar C8-C9-C10-C11-C12-O13 environment presents helical chirality.

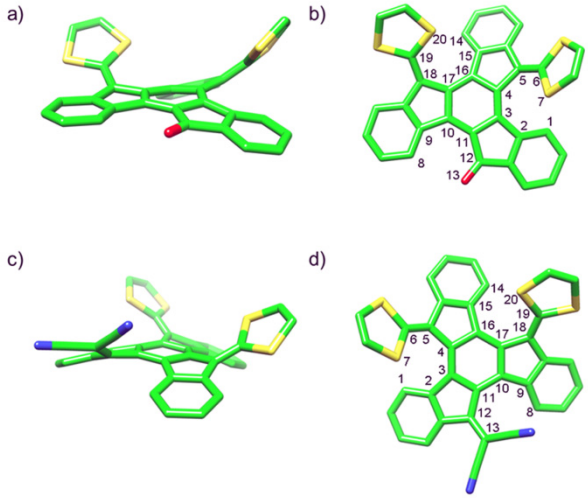

Figure 1 a) X-ray crystal structure of (*M*, *M*, *M*) **7.2**, side view and b) top view. c) Energy-minimized (B3LYP/6-31G**) structure of (*P, P, P*) **7.3**, side view and d) top view. Carbon atoms are shown in green, sulfur in yellow, oxygen in red, and nitrogen in blue. Hydrogen atoms have been omitted for clarity.

Unfortunately, we were unable to produce single crystals of **7.3**. Nevertheless, comparison between the crystal structures of **7.1** and **7.2** and their optimized geometries computed at the B3LYP/6-31G** level confirms that calculations are highly reliable to predict the structure of this kind of compounds. For instance, the theoretical value calculated for the angle between the central and the peripheral benzene rings for isolated **7.1** (21.5º) is very close to the solid-state X-ray value (23.7º). The B3LYP/6-31G**-optimized geometry calculated for **7.3** is shown in Figure 1c and d. The dicyanomethylene group has a comparable steric demand to the dithiole rings, and the truxene core in **7.3** adopts a bowl shape with a concave cavity similar to that of **7.1**. The angles calculated between the plane defined by the central aromatic ring and those defined by the benzene rings containing C1 and C2, C8 and C9, and C14 and C15 have values of 21.1, 20.4, and 21.6º, respectively, which are all similar to that computed for

7.1 (21.5º).

7.2.3. Electronic properties

The redox behaviour of **7.1**, **7.2**, and **7.3** was investigated through cyclic voltammetry (CV) in THF containing 0.1 M $TBAPF_6$ under an argon atmosphere. Glassy carbon was used as the working electrode, $Ag/AgNO_3$ as the reference electrode, and a platinum wire as the counter electrode. Ferrocene was added as an internal reference. The results are summarized in Figure 2. Under these experimental conditions, the CV of **7.1** shows two quasi-reversible oxidation processes at half-wave potentials of 0.254 and 0.415 V, and a third oxidation wave at a half-wave potentials of 0.560 V. **7.2** and **7.3** show two quasi-reversible oxidation waves at half-wave potentials of 0.355 and 0.499 V for **7.2** and 0.404 and 0.515 V for **7.3**. These results confirm that **7.2** and **7.3** preserve the electron-donor ability of the parent **7.1**, although the oxidation potentials are slightly anodically-shifted due to the presence of the electron withdrawing ketone and dicyanomethylene groups, respectively. In agreement with the relative electron withdrawing abilities of ketone and dicyanomethylene, both oxidation processes occur at lower potentials in **7.2** compared to **7.3**.

The cathodic part of the CVs of **7.2** and **7.3** shows up to five reduction processes. However, we only expected a single reduction process due to the presence of the ketone or dicyanomethylene group. For comparison, the CV of truxenone was also recorded under the same experimental conditions (Figure 2). Truxenone shows four reduction processes, the first three of which occur at −1.392, −1.910, and −2.375 V half-wave potentials, and the fourth process at a −2.572 V cathodic peak potential. Considering this and the strong tendency of truxenone, **7.2**, and **7.3** to absorb on the electrode, we postulate that a small local concentration of truxenone might be formed during the measurements in the close proximity of the electrode, giving rise to most of the reduction processes observed for **7.2** and **7.3**. Nevertheless, TLC analysis showed that both **7.2** and **7.3** remain pure after CV measurements, so if truxenone is formed during the electrochemical measurements it must be in relatively small amounts, perhaps at high local concentrations in the proximity of the electrode. In this respect, it is important to note that truxenone is hardly soluble in THF, but nevertheless provides relatively intense reduction signals in the CV. A more detailed electrochemical study of compounds **7.2** and **7.3** will be carried out to unambiguously test this hypothesis, but is out of the scope of the present work.

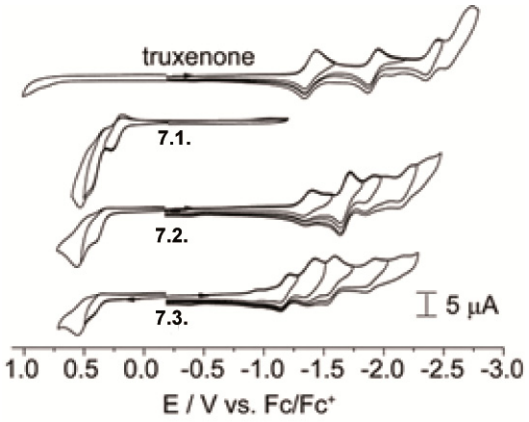

Figure 2 Cyclic voltammograms of truxenone, **7.1**, **7.2**, and **7.3** in THF, 0.1 M $TBAPF_6$, with a scan rate of 0.1 V s^{-1}.

Figure 3b sketches the atomic orbital (AO) composition calculated for the highest-occupied (HOMO–1 and HOMO) and lowest unoccupied (LUMO and LUMO+1) molecular orbitals of **7.2**. Similar MO topologies are found for **7.3** (Figure 3c). The HOMO and HOMO–1 spread over the dithiole environments and appear close in energy and well separated from the HOMO–2. The first two electrons are respectively extracted from the HOMO and HOMO–1 and lead to a triplet state open-shell dication species that is calculated to be slightly more stable (**7.2**: 0.05 eV, **7.3**: 0.06 eV) than the singlet-state closed-shell species, in which the two electrons are extracted from the HOMO. The lower energies predicted for the HOMO and HOMO–1 of **7.2** (–4.96 and –5.12 eV) and **7.3** (–5.13 and –5.28 eV) compared to **7.1** (–4.72 eV), for which the HOMO and HOMO–1 are degenerate, support the anodic shift observed for the first two oxidation potentials in passing from **7.1** to **7.3**.

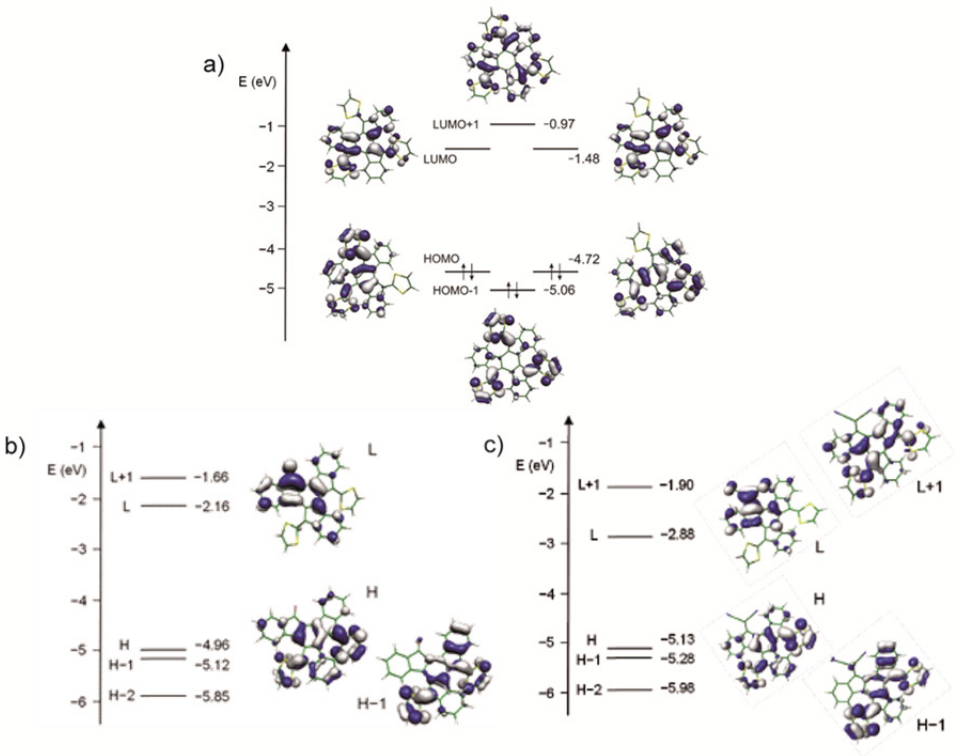

Figure 3 Electron density contours (0.03 e bohr^{-3}) and energies calculated for the HOMOs and LUMOs of a) **7.1** (both the HOMO and the LUMO are doubly degenerate due to the *C*3 symmetry of the molecule.); b) **7.2**; and c) **7.3** at the B3LYP/6-31G** level. H and L denote HOMO and LUMO, respectively.

In contrast to the HOMO, the LUMO is mainly localized in the environment of the ketone (**7.2**) and dicyanomethylene (**7.3**) groups and is separated by 0.5 (**7.2**) and 1.0 eV (**7.3**) from the LUMO+1 (see figure 3b-c). Only one electron is therefore expected to be extracted in the reduction process at low cathodic potentials. Compared to truxenone, for which the LUMO is doubly degenerate (C_{3h} symmetry) and is calculated at –2.78 eV, the LUMO of **7.2** is computed at –2.16 eV, significantly higher in energy. This indicates that the first reduction wave observed in the CV of **7.2** at –1.370 V —almost the same value recorded for truxenone (–1.392 V)— corresponds to the reduction of truxenone, as suggested above, and that the reduction of **7.2** is associated with the more intense wave registered at –1.674 V (see Figure 2). For **7.3**, the LUMO is calculated to be lower in energy (–2.88 eV) in good agreement with the less negative value measured for the first reduction potential (–1.184 V). The electron affinities calculated for truxenone (1.60 eV), **7.2** (1.11 eV), and **7.3** (1.83 eV) also support the lower and higher electron acceptor ability predicted for compounds **7.2** and **7.3**, respectively.

The electronic absorption spectra of **7.1**, **7.2**, and **7.3** in a variety of solvents are gathered in Figure 4. The absorption of **7.2** and **7.3** spans over nearly all the visible region, a significant improvement with regards to **7.1**. Notable, the spectrum of **7.2** resembles that of **7.1**, but with the addition of a low intensity absorption that is centered at ~550 nm and that spreads to ~655 nm in CH_2Cl_2 and up to 695 nm in CH_3OH. The relatively modest extinction coefficients of ~6000 M^{-1} cm^{-1} in, for example, CH_2Cl_2 as

well as the solvent effect point to a charge transfer transition. The spectrum of **7.2** is nearly invariable with concentration, which allows us to tentatively assign this band to an intramolecular charge-transfer process from the electron donating dithioles to the electron withdrawing ketone. TDDFT calculations (vide infra) confirm this assignment.

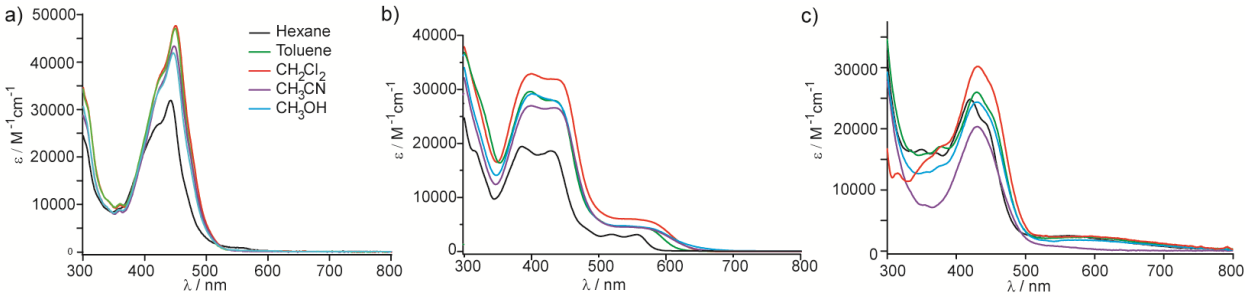

Figure 4 UV-vis spectra of compounds **7.1** (a), **7.2** (b), and **7.3** (c) recorded at 298 K in hexane (black), toluene (green), dichloromethane (red), acetonitrile (purple) and methanol (light blue).

The electronic absorption spectra of **7.3** show similar features (Figure 4c). Here, the main absorption band is centered at 430 nm and is narrower than that of **7.2**. A charge-transfer band is also present in **7.3**, although its absorption coefficient is ~2400 M^{-1} cm^{-1} in CH_2Cl_2 even lower than that noted for **7.2**. On the other hand, it spreads over a wider range of wavelengths, absorbing all the way to 800 nm. In this particular case the solvent effect is much less evident.

To investigate the nature of the electronic transitions that give rise to the absorption bands observed in the electronic spectra, the lowest-energy singlet excited states (S_n) were calculated using the time-dependent DFT (TDDFT) approach. B3LYP/6-31G** calculations predict that the low-energy absorption band observed for **7.2** at ~550 nm is due to electronic transitions to the first two excited singlets, S_1 and S_2, calculated at 2.23 eV (555 nm) and 2.45 eV (505 nm) with small oscillator strengths (f = 0.04 and 0.02, respectively). The experimental band exhibits indeed a double peak structure with maxima at 557 and 519 nm in good correlation with the theoretical prediction. The S_1 and S_2 states originate from HOMO→LUMO and HOMO–1→LUMO one-electron excitations, respectively, and imply an electron density transfer from the dithiole moieties, where the HOMO and HOMO–1 reside, to the ketone, where the LUMO is mainly located (Figure 3). Similar results are obtained for **7.3**, for which the HOMO→LUMO (S_1) and HOMO–1→LUMO (S_2) transitions also imply an intramolecular charge transfer and are calculated at lower energies (S_1: 1.75 eV, 709 nm, S_2: 1.98 eV, 628 nm) and with lower intensities (f = 0.01 and 0.03) in agreement with the experimental observations. Calculations therefore confirm the charge-transfer nature of the low-energy absorption bands. When calculated in the presence of a polar solvent (CH_2Cl_2), the electronic transitions to the S_1 and S_2 states undergo a bathochromic shift, as observed experimentally, and are calculated at 602 (f = 0.06) and 546 nm (f = 0.02), respectively, for **7.2**.

The intense absorption band observed around 400 nm for **7.2** and **7.3** is equivalent in nature to that observed for **7.1** around 450 nm. It is associated to a group of intense electronic transitions mainly originating from HOMO–1 and HOMO → LUMO+1 and LUMO+2 monoexcitations. For **7.2**, the most intense transitions are computed at 2.87 eV (432 nm, f = 0.08), 2.99 eV (415 nm, f = 0.17), 3.29 eV (376 nm, f = 0.46), and 3.40 eV (364 nm, f = 0.13) explaining the two-peak structure observed experimentally (Figure 4b) with maxima at 429 and 385 nm in hexane solutions. These transitions imply some electronic density transfer from the dithiole rings to the rest of the molecule and shift slightly to higher wavelengths when calculated in polar solvents in agreement with experiment. For instance, the most intense transition calculated for **7.2** at 376 nm in gas phase shifts to 392 nm in CH_2Cl_2.

7.2.4. Supramolecular association of C_{60}

Preliminary evidence for the ability of **7.1**, **7.2**, and **7.3** to bind C_{60} was obtained in the gas phase through MALDI-TOF spectrometry. In all three cases, a distinctive peak for either **7.1**·C_{60}, **7.2**·C_{60}, or **7.3**·C_{60} was found in the spectra. No aggregates of other stoichiometries were found, suggesting that both **7.2** and **7.3** bind C_{60} in a 1:1 manner, as has already been demonstrated to be the case for **7.1**.[6]

In solution, the first insight into electronic interactions came from absorption assays, that is, by titrating a constant concentration of **7.1** (~10^{-5} M) in toluene, ortho-dichlorobenzene, and benzonitrile with variable concentrations of pristine C_{60} (0−10^{-5} M). A representative example is shown for toluene in Figure 5. Incremental addition of C_{60} (i.e., 0 to 4 × 10^{-5} M), while keeping the concentration of **7.1** constant at 2 × 10^{-5} M, resulted in a notable decrease of the **7.1**-centered transition in the 400 to 500 nm range, an increase of C_{60}-centered transitions in the 300 to 400 nm range with a 335 nm maximum, and the formation of new features in the 500 to 700 nm range. Notable is that when staying within equimolar conditions isosbestic points at 402 / 496 (toluene), 410 / 496 (ortho-dichlorobenzene), and 401 / 496 nm (benzonitrile) attest to a clean transformation of truxene into what we tentatively assign as a **7.1**·C_{60} complex. To characterize the mutually interacting constituents, the intrinsic absorptions of C_{60} were subtracted (Figure 5b). Once this is done, maxima in two different spectral regions are evident: one around 430 nm and one in the 550 to 600 nm range. It is especially the latter that red-shifts in solvents with increasing polarity, with maxima at 569, 579, and 589 nm in toluene, ortho-dichlorobenzene, and benzonitrile, respectively. The rather strong impact that the solvent polarity imposes on the new features suggests an intermolecular charge-transfer character.

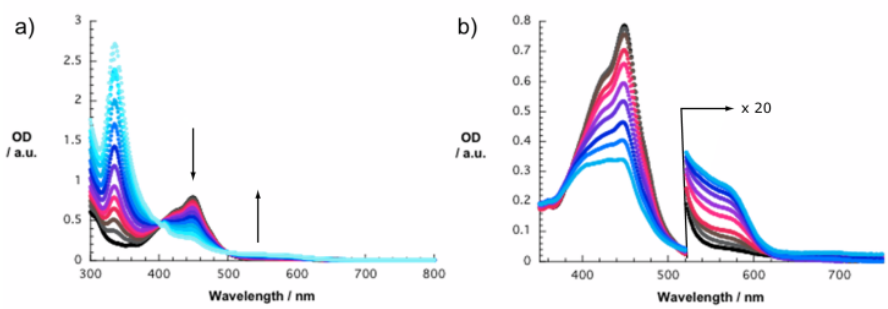

Figure 5 a) Absorption spectra of **7.1** (1.72×10^{-5} M) in toluene with variable concentrations of C_{60} (0, 2.21×10^{-6} M, 4.41×10^{-6} M, 6.55×10^{-6} M, 8.65×10^{-6} M, 1.07×10^{-5} M, 1.47×10^{-5} M, 1.86×10^{-5} M, 2.23×10^{-5} M, 2.76×10^{-5} M, 3.27×10^{-5} M, 3.75×10^{-5} M, and 4.21×10^{-5} M). b) Same spectra, after subtraction of the absorption of C_{60}.

Next, the spectral changes that were noted throughout the absorption titration assays were used to quantify the binding constant of **7.1** with C_{60}. In this regard, plots of the absorption changes at the **7.1** absorption maximum (i.e., 430 nm) versus different concentrations of C_{60} (from 0 to 1.6×10^{-5} M) allowed performing least-square analyses that disclosed binding constants of $1.3 \pm 0.5 \times 10^4$ M^{-1} in toluene, $1.6 \pm 0.6 \times 10^4$ M^{-1} in benzonitrile, and $1.1 \pm 0.3 \times 10^4$ M^{-1} in ortho-dichlorobenzene. Interestingly, reasonable fits were only obtained when the non-linear fitting was subjected to 1:1 stoichiometries for all three solutions, as suggested by the MALDI-TOF experiments.

Additionally, the formation of **7.1**·C_{60} was probed by cyclic voltammetry and square wave voltammetry. On one hand, C_{60} was titrated with variable concentrations of **7.1** to result in relative ratios of 4:1, 3:1, and 2:1. Here, all of the detectable reduction process, that is, formation of $C_{60}^{\bullet-}$ (−0.89 V), C_{60}^{2-} (−1.27 V), C_{60}^{3-} (−1.72 V), and C_{60}^{4-} (−2.2 V), rendered more energetic in the presence of **7.1**. Taking, for example, the first reduction of C_{60}, the potentials changed in the square wave voltammetric investigations from −0.89 V vs. Fc/Fc^+ to −0.93 (4:1), −0.94 (3:1), and −0.95 V (2:1). A similar trend is seen in the cyclic voltammetric experiments. On the other hand, the oxidation of **7.1** at 0.62 V vs. Fc/Fc^+ shifts to 0.63 V at a **7.1**:C_{60} ratio of 2.5:1, to 0.64 V at 1.5:1, and to 0.65 V at 1:1. Again, these trends are indicative for a partial redistribution of electron density, namely from the electron donating **7.1** to the electron accepting C_{60}.

The intermolecular charge-transfer assumption was further corroborated in complementary emission assays, where intermolecular charge-transfer features develop in the 500 to 800 nm range. Notable is the broad and featureless but weak fluorescence of **7.1** that centers around 500 nm. C_{60}, on the other hand, is known to emit in the 600 to 700 nm range with again low quantum yields (2.0×10^{-4}). In fluorescence titration assays with **7.1** ($\sim 10^{-5}$), we note that in the presence of variable C_{60} concentrations ($0-10^{-5}$ M) additional features emerge. In toluene, for example, a new maximum develops with a quantum yield of $3.5 \pm 0.5 \times 10^{-4}$ at 620 nm regardless of the excitation wavelength (Figure 6a). Unambiguous evidence for the charge-transfer hypothesis came

from appreciably shifted maxima, like in the absorption spectra, when the fluorescence spectra were recorded in ortho-dichlorobenzene (maximum at 650 nm) or benzonitrile (maximum at 675 nm, Figure 6b). In terms of correlating the charge-transfer emission with the charge-transfer absorption, a decisive excitation spectrum of the 675 nm emission maximum in benzonitrile was recorded. The fact that an excellent agreement between the absorption and the excitation spectrum was reached confirms our hypothesis. However, at concentrations exceeding a 1:1 stoichiometry the intensity of the charge-transfer emission starts to decrease in any of the solvents investigated although the isosbestic points were used to photoexcite the mixtures of **7.1** and C_{60}. This speaks undoubtedly for a 1:1 complex, which was furthermore substantiated by a Job's plot analysis. From the decay of the emission of **7.1** and the growth of the charge-transfer emission we derived binding constants of $3.4 \pm 0.2 \times 10^4$ M^{-1} in toluene (Figure 6a, inset) and $6.8 \pm 0.3 \times 10^4$ M^{-1} in benzonitrile.

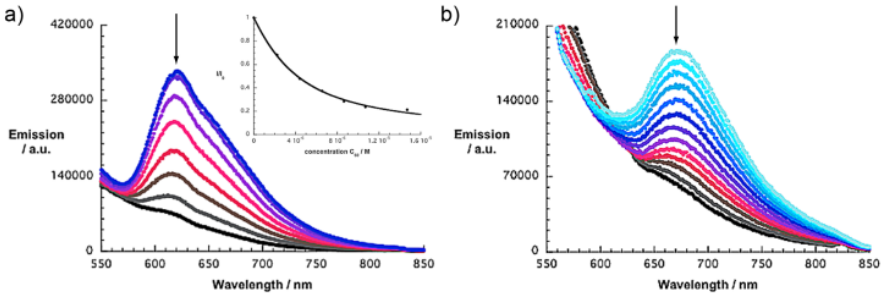

Figure 6 a) Emission spectra upon 406 nm excitation of a dilute toluene solution of **7.1** (1.72×10^{-5} M) with variable concentrations of C_{60} (0, 2.23×10^{-6} M, 4.41×10^{-6} M, 6.55×10^{-6} M, 8.65×10^{-6} M, 1.07×10^{-5} M, 1.47×10^{-5} M, and 1.86×10^{-5} M); inset: plot of the normalized intensity I/I_0 at 550 nm versus concentration of C_{60} used to determine the association constant. b) Emission spectra upon 490 nm excitation of a dilute benzonitrile solution of **7.1** (1.39×10^{-5} M) with variable concentrations of C_{60} (0, 6.09×10^{-7} M, 1.21×10^{-6} M, 1.79×10^{-6} M, 3.21×10^{-6} M, 4.56×10^{-6} M, 6.47×10^{-6} M, 8.26×10^{-6} M, 1.05×10^{-5} M, 1.25×10^{-5} M, 1.53×10^{-5} M, 1.77×10^{-5} M, 2.07×10^{-5} M, 2.32×10^{-5} M, 2.55×10^{-5} M, 2.75×10^{-5} M, and 2.92×10^{-5} M).

With the help of the charge-transfer absorption ($\lambda_{absorption}$) and emission ($\lambda_{emission}$), the internal (λ_V) and solvent reorganization energy (λ_S) of **7.1**·C_{60} were assessed via ($\lambda_{absorption} - \lambda_{emission}$)/2) and ($-\lambda_{emission} - \Delta G_{CR}$), respectively. ΔG_{CR} reflects the thermodynamic driving force for the charge recombination and is essentially the sum of the reduction and oxidation potentials. Small λ_V values of 0.11 ± 0.02 eV result in toluene, ortho-dichlorobenzene, and benzonitrile, and a λ_S value of 0.37 V was determined in ortho-dichlorobenzene. In turn, we obtain a total reorganization energy for the **7.1**·C_{60} complex in ortho-dichlorobenzene of 0.48 eV. Considering that the underlying self-organization must be enthalpy driven, this value is remarkably small.

When adding C_{60} up to 4.6×10^{-5} M to a 1.3×10^{-5} M solution of **7.2** in either toluene or benzonitrile we note an appreciable decrease of the **7.2**-centered transition in

the 400 to 500 nm range, an increase of the C_{60}-centered transitions in the 300 to 400 nm range with a 335 nm maximum, a development of isosbestic points at 395 / 498 nm in toluene and at 395 / 502 nm in benzonitrile, and changes in the 500 to 800 nm range, which is dominated by intramolecular charge-transfer characteristics. An example is presented in Figure 7a. Essentially the same trends emerged for **7.3** (see Figure 8). Here, the exact positions of the isosbestic points are 409 / 480 / 635 nm in toluene and 408 / 495 / 635 nm in benzonitrile. Upon subtracting the C_{60}-centered absorptions, rather broad absorption features are discernable with 572 and 584 nm in toluene and benzonitrile, respectively. Implicit in this trend is a transformation of the intramolecular charge transfer in **7.2** and in **7.3** into an intermolecular charge transfer in **7.2**·C_{60} and in **7.3**·C_{60}. With the aforementioned absorption changes in hand we determined the binding constants in toluene to be: 2.5 ± 0.1 × 10^3 M^{-1} and 1.9 ± 0.1 × 10^2 M^{-1} for **7.2**·C_{60} and **7.3**·C_{60}, respectively.

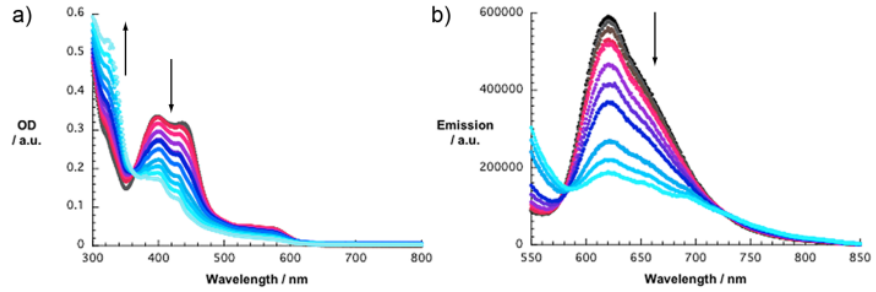

Figure 7 a) Absorption spectra of **7.2** (1.26 × 10^{-5} M) in toluene with variable concentrations of C_{60} (0, 2.04 × 10^{-6} M, 4.03 × 10^{-6} M, 6.59 × 10^{-6} M, 9.65 × 10^{-6} M, 1.26 × 10^{-5} M, 1.67 × 10^{-5} M, 2.06 × 10^{-5} M, 2.43 × 10^{-5} M, 2.77 × 10^{-5} M, 3.19 × 10^{-5} M, 3.95 × 10^{-5} M, and 4.61 × 10^{-5} M). C_{60} absorptions were subtracted. b) Emission spectra upon 395 nm excitation of a dilute toluene solution of **7.2** (1.26 × 10^{-5} M) with variable concentrations of C_{60} (0, 2.04 × 10^{-6} M, 4.03 × 10^{-6} M, 6.59 × 10^{-6} M, 9.65 × 10^{-6} M, 1.26 × 10^{-5} M, 1.67 × 10^{-5} M, 2.06 × 10^{-5} M, 2.43 × 10^{-5} M, 2.77 × 10^{-5} M, 3.19 × 10^{-5} M, 3.95 × 10^{-5} M, and 4.61 × 10^{-5} M).

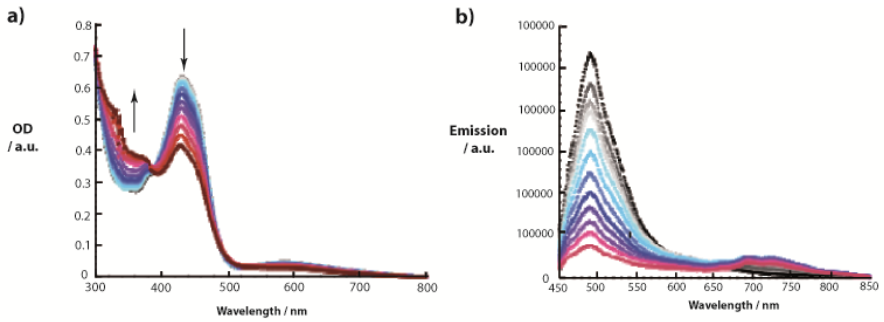

Figure 8 a) Absorption spectra of **7.3** (1.84 x 10^{-5}M) in toluene with variable concentrations of C_{60} (0; 2.96 x 10^{-6}M; 5.78 x 10^{-6}M; 8.47 x 10^{-6}M; 1.10 x 10^{-5}M; 1.58 x 10^{-5}M; 2.02 x 10^{-5}M; 2.62 x 10^{-5}M; 3.15 x 10^{-5}M; 3.77 x 10^{-5}M; 4.31 x 10^{-5}M and 5.20 x 10-5M). C_{60} absorptions were subtracted. b) Emission spectra upon 350 nm excitation of a dilute toluene solution of **7.3** (1.84 x 10^{-5}M) with variable concentrations

of C_{60} (0; 2.96 x 10^{-6}M; 5.78 x 10^{-6}M; 8.47 x 10^{-6}M; 1.10 x 10^{-5}M; 1.58 x 10^{-5}M; 2.02 x 10^{-5}M; 2.62 x 10^{-5}M; 3.15 x 10^{-5}M; 3.77 x 10^{-5}M; 4.31 x 10^{-5}M and 5.20 x 10^{-5}M).

In emission experiments, **7.2** and **7.3** show **7.1**-type emissions, which are seen in the 450 to 600 nm range, and charge-transfer emissions, which occur between 600 and 800 nm. In toluene, for example, a strong 620 nm charge-transfer emission maximum evolves for **7.2**, while in benzonitrile the emission maximum shifts to 677 nm. Much weaker are the emissions for **7.3,** approximately ten times weaker than that of **7.2**, however with nearly the same maxima (i.e., 615 nm in toluene).

Adding C_{60} in the range from 0 to 4.6 × 10^{-5} M to **7.2** and exciting the resulting **7.2**·C_{60} at the 400 nm isosbestic point leads to the gradual quenching of the intramolecular charge-transfer emission (Figure 7b). Simultaneous with the quenching, a new emissive transition starts to grow at, for example, 490 nm in benzonitrile. In toluene, however, it is impossible to derive the exact location of the new maximum as it seems to coalesce with the **7.2**-centered features. In the corresponding **7.3**·C_{60}, the intermolecular charge-transfer emissions, which are located at 488 nm in toluene and at 490 nm in benzonitrile, evolve at the expense of the intramolecular charge-transfer emission.

To visualize the association of compounds **7.1**–**7.3** with C_{60}, the interaction of these systems was theoretically investigated. Calculations were performed at the DFT level making use of the BH&H and M06-2X functionals. The BH&H functional successfully reproduces the results of highly accurate post-HF methods for π-stacked complexes,[9] for which the interactions are dominated by dispersion forces, and has recently been applied to the study of supramolecular complexes involving fullerenes.[10] The M06-2X functional has also been used to investigate fullerene molecular associations,[11] and has recently been shown to provide correct descriptions of noncovalent interactions in supramolecular donor-acceptor complexes involving π-conjugated systems.[12]

Figure 8 shows the BH&H/6-31G** minimum-energy structures calculated for the **7.1**·C_{60}, **7.2**·C_{60}, and **7.3**·C_{60}. The concave form adopted by the truxene moiety perfectly matches the convex surface of C_{60}. In all three cases, the central benzene ring of the

[9](a) A. Robertazzi and J. A. Platts, *J. Phys. Chem. A* **2006,** *110*, 3992-4000; (b) M. P. Waller, A. Robertazzi, J. A. Platts, D. E. Hibbs and P. A. Williams, *J. Comput. Chem.* **2006,** *27*, 491-504; (c) Y. Zhao and D. G. Truhlar, *J. Chem. Theory Comput.* **2006,** *3*, 289-300; (d) H. Valdes, K. Pluhackova, M. Pitonak, J. Rezac and P. Hobza, *PCCP* **2008,** *10*, 2747-2757; (e) K. Gkionis, J. G. Hill, S. Oldfield and J. Platts, *J. Mol. Model.* **2009,** *15*, 1051-1060.

[10] (a) S. S. Gayathri, M. Wielopolski, E. M. Pérez, G. Fernández, L. Sánchez, R. Viruela, E. Ortí, D. M. Guldi and N. Martín, *Angew. Chem. Int. Ed.* **2009,** *48*, 815-819; (b) H. Isla, M. Gallego, E. M. Pérez, R. Viruela, E. Ortí and N. Martín, *J. Am. Chem. Soc.* **2010,** *132*, 1772-1773.

[11] (a) Y. Zhao and D. G. Truhlar, *PCCP* **2008,** *10*, 2813-2818; (b) L. Feng, Z. Slanina, S. Sato, K. Yoza, T. Tsuchiya, N. Mizorogi, T. Akasaka, S. Nagase, N. Martín and D. M. Guldi, *Angew. Chem. Int. Ed.* **2011,** *50*, 5909-5912.

[12] (a) J. Aragó, J. C. Sancho-García, E. Ortí and D. Beljonne, *J. Chem. Theory Comput.* **2011,** *7*, 2068-2077; (b) G. Sini, J. S. Sears and J.-L. Brédas, *J. Chem. Theory Comput.* **2011,** *7*, 602-609.

truxene core stacks on one benzene ring of C_{60} and gives rise to an almost parallel complex. For **7.1**·C_{60} and **7.3**·C_{60}, the benzene rings of the truxene and C_{60} fragments are twisted by approximately 20 and 25º relative to each other (Figure 8b) and their centroids are at a distance of 3.34 and 3.30 Å, respectively. For **7.2**·C_{60}, the C_{60} fragment is displaced along the direction involving the ketone environment that is more planar, but the distance between the benzene centroids (3.35 Å) remains similar. These distances are considerably shorter than those reported for the benzene dimer in parallel (3.9 Å) and parallel-displaced (3.6 Å) configurations.[13] In addition to the interaction of the central benzene ring, the peripheral benzene rings of the truxene moiety show many intermolecular contacts in the 3.4–3.9 Å range with the C_{60} guest for the three complexes. To maximize the interactions that greatly contribute to stabilize the complex, the truxene core increases its folding with respect to the isolated **7.1**–**7.3** compounds to better wrap C_{60}. For instance, the peripheral benzene rings form an average angle of 24.6º with the central benzene ring in **7.1**·C_{60}, which is significantly larger than that calculated at the BH&H/6-31G** level for isolated **7.1** (20.1º). The folding is even greater for **7.3**·C_{60}, since the average angle changes from 20.0º for **7.3** to 25.6º for **7.3**·C_{60}. For **7.2**, the angles between the plane defined by the central aromatic ring and those defined by the benzene rings containing C1 and C2, C8 and C9, and C14 and C15 are 14.1, 7.3, and 23.1º for isolated **7.2**, respectively, and increase to 20.2, 14.0, and 27.2º for **7.2**·C_{60}. The M06-2X functional leads to very similar optimized structures and to identical geometrical trends. For instance, the folding angles predicted at the M06-2X/6-31G** level for the peripheral benzene rings of the truxene core (**7.1**·C_{60}: 27.0º; **7.2**·C_{60}: 21.1, 16.7, and 29.6º; and **7.3**·C_{60}: 27.9º) are only slightly larger than the BH&H/6-31G** values discussed above and follow the same trend.

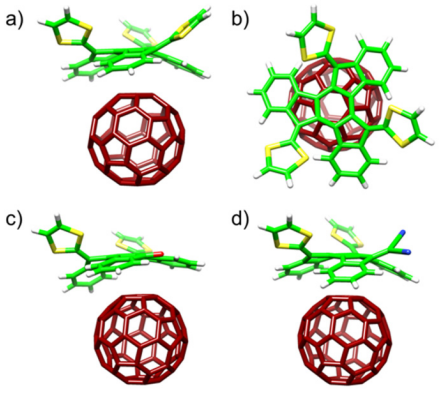

Figure 8 Energy-minimized BH&H/6-31G** structures calculated for complexes **7.1**·C_{60}, side view (a) and top view (b), **7.2**·C_{60} (c), and **7.3**·C_{60} (d). The structures show the stack between the central benzene ring of the truxene core and one of the hexagonal rings of C_{60}.

[13] (a) M. O. Sinnokrot, E. F. Valeev and C. D. Sherrill, *J. Am. Chem. Soc.* **2002,** *124*, 10887-10893; (b) M. O. Sinnokrot and C. D. Sherrill, *J. Phys. Chem. A* **2004,** *108*, 10200-10207; (c) T. Sato, T. Tsuneda and K. Hirao, *J. Chem. Phys.* **2005,** *123*, 104307-10.

Table 2 Association binding energies (kcal mol^{-1}) calculated for the **7.1**·C_{60}, **7.2**·C_{60}, and **7.3**·C_{60} complexes.[a]

Method	**7.1**·C_{60}	**7.2**·C_{60}	**7.3**·C_{60}
BH&H/6-31G**	–8.70 (–14.25)	–7.05 (–12.50)	–7.84 (–13.75)
BH&H/cc-pVTZ[b]	–10.88 (–12.32)	–9.06 (–10.50)	–9.98 (–11.50)
M06-2X/6-31G**	–11.82 (–17.73)	–10.07 (–15.32)	–11.51 (–17.15)
M06-2X/cc-pVTZ[c]	–15.31 (–17.01)	–13.18 (–14.70)	–14.60 (–16.19)

[a]Association binding energies are calculated as the difference between the total energy of the complex and the sum of the total energies of the receptor and C_{60} Energies are corrected for BSSE using the counterpoise method (counterpoise-uncorrected values are given within parentheses). [b]Single-point energy calculations on the BH&H/6-31G** optimized geometries. [c]Single-point energy calculations on the M06-2X/6-31G** optimized geometries.

Table 2 collects the association binding energies calculated for the **7.1**·C_{60}, **7.2**·C_{60}, and **7.3**·C_{60} complexes using both the BH&H and M06-2X functionals and including the counterpoise (CP) correction for the basis set superposition error (BSSE). Binding energies were computed both using the 6-31G** basis set and the more extended cc-pVTZ basis set. The extension of the basis set drastically reduces the BSSE from 5.3–5.9 kcal mol^{-1} when using the split-valence "double-ζ" 6-31G** basis set to only 1.5–1.6 kcal mol^{-1} when employing the "triple-ζ" cc-pVTZ basis set. The counterpoise-corrected BH&H/cc-pVTZ binding energies are –10.88, –9.06, and –9.98 kcal mol^{-1} for **7.1**·C_{60}, **7.2**·C_{60}, and **7.3**·C_{60}, respectively. The M06-2X/cc-pVTZ approach yields higher binding energies of –15.31, –13.18, and –14.60 kcal mol^{-1} because the M06-2X functional is especially designed to deal with noncovalent interactions. Both theoretical approaches therefore provide the same trend for the complex stability **7.1**·C_{60} > **7.3**·C_{60} > **7.2**·C_{60}. This trend is in contrast with experimental data based on optical absorption and fluorescence measurements and with the increase of the electron-acceptor character along the series **7.1** < **7.2** < **7.3**. Complex **7.3**·C_{60} is predicted to be more stable than complex **7.2**·C_{60} because host **7.3**, despite the higher acceptor character of the $C(CN)_2$ group it incorporates, wraps more effectively the convex surface of C_{60} (Figure 8c and d). The lower stability of **7.2**·C_{60} is therefore attributed to the less concave structure of the truxene moiety in host **7.2**. The difference between experimental and theoretical trends most likely arises from the fact that the experimental data are collected in solution, whereas the theoretical data are obtained in gas phase.

Figure 9 displays the frontier MOs calculated at the B3LYP/6-31G** level for complex **7.2**·C_{60}. The HOMO and HOMO–1 are located on the host and correspond to the HOMO and HOMO–1 of **7.2** (Figure 3b). The LUMO, LUMO+1, and LUMO+2 are

located on the guest and correspond to the triple degenerate LUMO of C_{60}. Similar MO topologies are found for complex **7.1**·C_{60}, for which the HOMO–2 is also located on the dithiole moieties, and **7.3**·C_{60}. The electronic communication between the host and the guest in the ground state is evidenced by the shift to lower energies of the HOMOs located on the truxene core (e.g., **7.1**: –4.72 eV, **7.1**·C_{60} –4.77 eV) and to higher energies of the LUMOs located on C_{60} (C_{60}: –3.23 eV, **7.1**·C_{60} –2.79 eV, **7.2**·C_{60} –2.89 eV, **7.3**·C_{60} –3.03 eV,), in agreement with the above-mentioned electrochemical trends, and also by the small charge transfer of 0.047e (**7.1**·C_{60}), 0.037e (**7.2**·C_{60}), and 0.036e (**7.3**·C_{60}) that takes place from the truxene unit to C_{60}.

The topology of the frontier MOs supports the intermolecular charge-transfer nature suggested above for the lowest-energy absorption bands observed in the electronic spectra of complexes **7.1**·C_{60}, **7.2**·C_{60}, and **7.3**·C_{60}. Time-dependent DFT calculations performed at the B3LYP/6-31G** level indeed confirm that the lowest-energy excited singlet states (9 states for **7.1**·C_{60} and 6 states for **7.2**·C_{60} and **7.3**·C_{60}) involve electron excitations from the HOMO–1 and HOMO (HOMO–2, HOMO–1, and HOMO for **7.1**·C_{60}) to the LUMO, LUMO+1, and LUMO+2 and imply a charge transfer from the truxTTF-type receptors to C_{60}, thereby affording truxTTF$^{\delta+}$–$C_{60}^{\delta-}$.

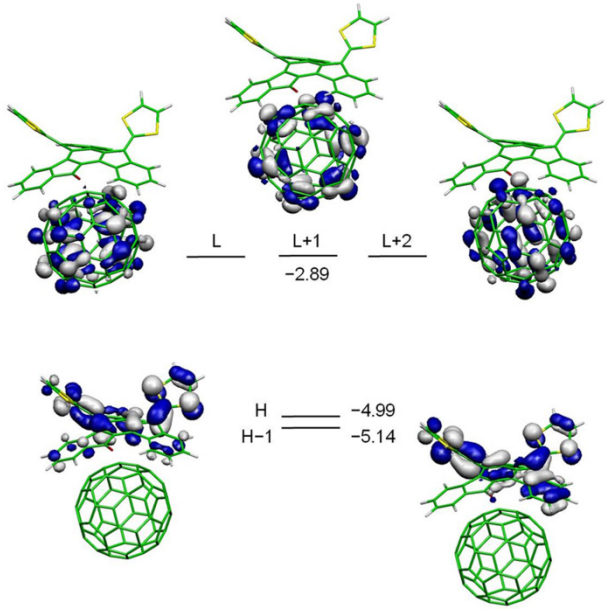

Figure 9 Electron density contours (0.03 e bohr^{-3}) and energies (eV) calculated for the HOMOs and LUMOs of **7.2**·C_{60} at the B3LYP/6-31G** level. H and L denote HOMO and LUMO, respectively.

Besides the ground-state / excited-state interactions, we turned to transient absorption measurements to unravel the processes following photoexcitation. Immediately commencing with the 387 nm excitation, a new transient develops in **7.1** (Figure 10). Characteristics of the latter are a marked maximum in the visible at 540 nm and a broad, featureless transition that spans all throughout the near-infrared. In addition, marked ground-state bleaching maximizes at 450 nm. Notable is that this excited state decays

rapidly, like in other sulfur-rich electron donors (i.e., TTF, exTTF, etc.), with a lifetime of only 0.97 ps. The short lifetime is rationalized by the presence of the sulfur atoms, with a strong second-order vibronic spin-orbit coupling, as it transforms into a much weaker absorbing state, for which a maximum is detected at 620 nm.

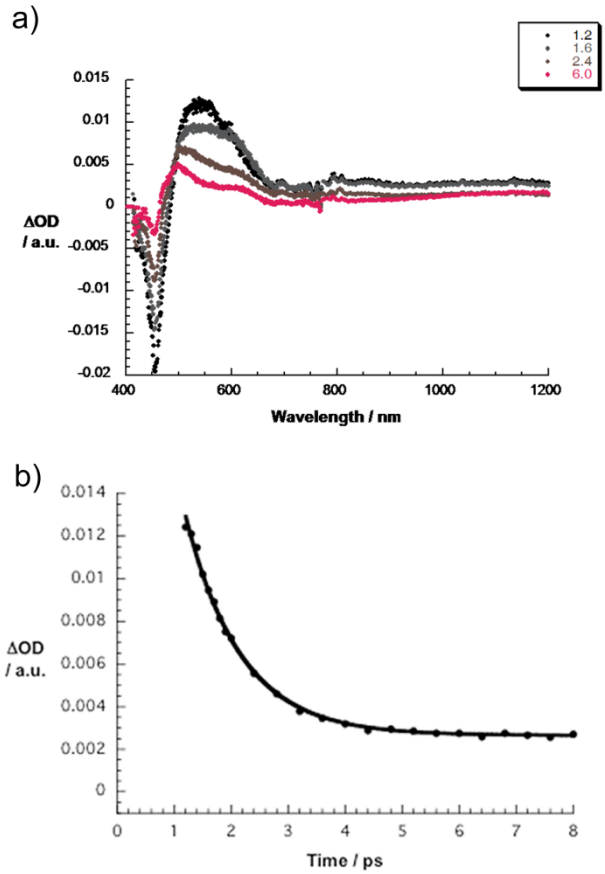

Figure 10 a) Differential absorption spectra (visible and near-infrared) obtained upon femtosecond flash photolysis (387 nm) of **7.1** in Ar-saturated benzonitrile with time delays between 1.2 and 6.0 ps at room temperature, see legend for time evolution. b) Time-absorption profile at 550 nm reflecting the excited-state deactivation process of **7.1**.

For C_{60}, the singlet and triplet excited states include transient maxima at 960 and 750 nm, respectively. The former reflects the singlet excited state (1.80 eV) that decays within 1.6 ns via intersystem crossing to the energetically low-lying triplet excited state. A multiwavelength analysis led to a triplet excited-state lifetime of 45 µs.

In **7.1**·C_{60}, 387 nm excitation generates instantaneously the singlet excited state of **7.1** as well as that of C_{60} as evidenced by fingerprint absorptions at 530 and 970 nm (vide supra). In benzonitrile, at time delays of around 3 ps, new features develop in the visible at 525 / 615 nm and in the near-infrared at 1095 nm (Figure 11). These resemble those seen in spectroelectrochemical and radiolytical experiments dealing with the oxidation of **7.1** at 525 / 615 nm (Figure 12) and the reduction of C_{60} at 1080 nm. In other words, a charge-separated state, **7.1**$^{\bullet+}$ / $C_{60}^{\bullet-}$, evolves from the locally excited states. From

multiwavelength analyses, a lifetime of 225 ± 10 ps was derived in benzonitrile. In ortho-dichlorobenzene, on the other hand, the lifetime was significantly shorter with values of 165 ± 25 ps. In going beyond 600 ps (i.e., 3000 ps), only **7.1**- and/or C_{60}-centered excited-state features are seen. These are likely to evolve from uncomplexed **7.1** and/or C_{60} rather than being formed as a product of charge recombination. The same conclusion stems from nanosecond experiments that were performed with 355 nm excitation, where simply the long-lived C_{60} triplet excited state with its maximum absorption at 750 nm came across.

Complementary experiments with 550 nm excitation, which correlates with the wavelength of the charge-transfer absorption, resulted into the spontaneous formation of the excited charge-transfer state. The latter transforms instantaneously into the charge-separated state, namely 525 / 615 nm maxima of the one-electron oxidized **7.1** and a 1080 maximum of the one-electron reduced C_{60}. In terms of charge-separated state lifetimes the same values were seen as those seen upon excitation of either **7.1** or C_{60} (vide supra).

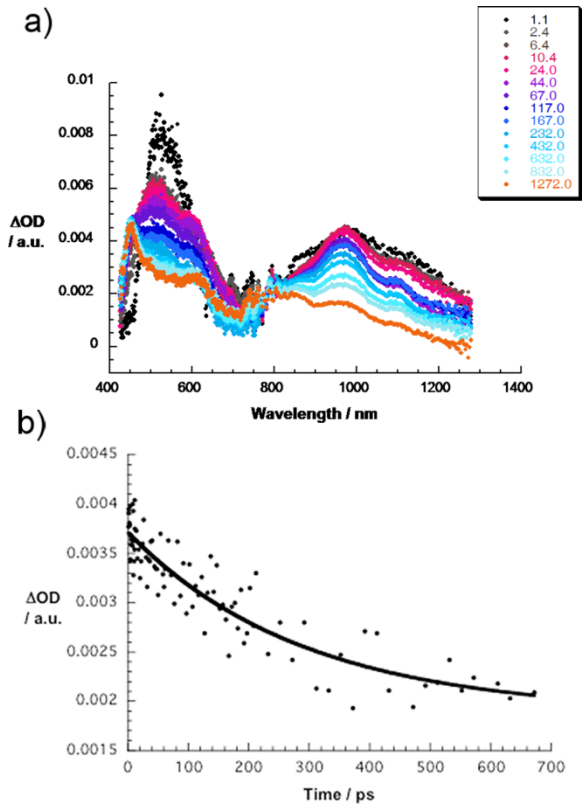

Figure 11 a) Differential absorption spectra (visible and near-infrared) obtained upon femtosecond flash photolysis (387 nm) of **7.1**·C_{60} in Ar-saturated benzonitrile with time delays between 1.1 and 1272 ps at room temperature. b) Time-absorption profile at 1090 nm reflecting the charge-separated state and charge recombination kinetics.

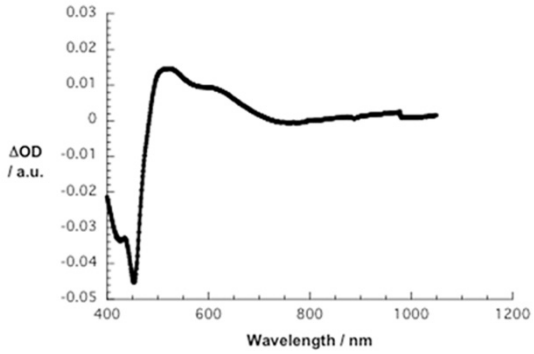

Figure 12 Differential absorption changes following electrochemical oxidation of **7.1** in ortho-dichlorobenzene at a potential of +0.65 V versus Fc/Fc^+.

Finally, we turned our attention to transient absorption measurements with **7.2**, **7.3**, **7.2**·C_{60}, and **7.3**·C_{60}. When exciting **7.2** and **7.3** in toluene, shortly after the conclusion of the 387 nm laser pulse, excited-state maxima at 511 nm for **7.2** and at 530 nm for **7.3** developed together with ground-state bleaching at 440 nm for **7.2** and at 450 nm for **7.3**. At longer time delays these features fade and transform into new broad transient absorption bands that span over the entire visible range of the solar spectrum. Interestingly, the early excited-state features of **7.2** and **7.3** reveal substantially longer lifetimes (59.7 ± 1.2 ps for **7.3** and 32.8 ± 0.6 ps for **7.2**) when compared to **7.1**, as obtained from multiwavelength analyses of the aforementioned transients.

Upon photoexciting **7.2** and **7.3** in the presence of C_{60} various transients evolved in the differential transient absorption spectra. On one hand, broad transient bands that can be ascribed to the singlet excited states of **7.2** and **7.3** emerge at 508 and 517 nm shortly after the 387 nm laser pulse. On the other hand, transients that maximize at 960 and 750 nm relate to the singlet and triplet excited state features of C_{60}, respectively, and relate to each other by means of intersystem crossing. However, transient features as they may correspond to charge separated states in **7.2**·C_{60} and **7.3**·C_{60} (i.e., radical cations of **7.2** or **7.3** at 525 / 615 nm and radical anion of C_{60} at 1080 nm) are masked by the prominent features of locally excited states of free, uncomplexed **7.2**, **7.3**, and C_{60}. Such a hypothesis is in sound agreement with the absorption assays that give rise to rather weak binding between **7.2** and **7.3**, on one hand, and C_{60}, on the other hand.

7.3. Conclusions

In this work, we have presented a family of synthetically accessible bowl-shaped truxene derivatives as electron donor partners that self-assemble with C_{60} in a controlled fashion and show enhanced light-absorption properties expanding the whole visible range. All derivatives have been synthesized from truxenone, which was easily and rapidly obtained in multigram quantities through a modification of the method reported by Sanguinet et al.[7] The condensation of indandione catalyzed by methanesulphonic acid proceeded smoothly in just 5 seconds under microwave irradiation to yield truxenone in excess of 70 % yield.

Derivative **7.1**, in which three dithiole units are covalently attached to a truxene core, shows good electron donor-abilities, with a first oxidation process at half-wave potential of 0.254 V vs Fc/Fc^+. It also absorbs light efficiently in the visible region, with a strong absorption band ($\varepsilon \sim 30.000\ M^{-1}\ cm^{-1}$) spanning the 350–520 nm range and centered at 450 nm. Finally, the steric demand of the dithiole groups forces the truxene core to deviate from planarity, adopting a bowl-shape configuration that allows it to associate C_{60} in solution, forming 1:1 complexes of respectable stability in several solvents ($K_a \sim 10^4\ M^{-1}$).

With the aim of improving the light-absorption abilities of **7.1**, we have also synthesized derivatives **7.2** and **7.3**, in which one of the dithiole units was replaced by a ketone or a dicyanomethylene electron withdrawing groups, respectively. With this structural modification, we expected to create a push-pull intramolecular effect that would result in a significant bathochromic shift of the electronic absorption spectra of **7.2** and **7.3**. This is indeed the case: **7.2** absorbs all the way to 695 nm, while **7.3** reaches the 800 nm, although with modest absorption coefficients. Meanwhile, the presence of the two dithiole groups ensures that both the electron donor and the C_{60} binding abilities are not severely affected compared to **7.1**. For instance, **7.2** associates C_{60} with a K_a of $2.5 \pm 0.1 \times 10^3\ M^{-1}$ in toluene at room temperature.

Theoretical calculations performed at the DFT level show that derivatives **7.2** and **7.3** preserve the concave bowl-shape structure of compound **7.1**, and explain the effect that the introduction of the ketone and dicyanomethylene groups has on the electron donor and electron acceptor abilities of these compounds. TDDFT calculations support the intramolecular charge-transfer nature of the low-energy absorption bands recorded for **7.2** and **7.3** in the visible-NIR range and correctly describe the bathochromic shift they experiment with solvent polarity. DFT calculations also help to visualize the association of compounds **7.1**–**7.3** with C_{60}. The concave form adopted by the truxene moiety perfectly matches the convex surface of C_{60}. In the supramolecular associates, the peripheral benzene rings of the truxene core increase their folding with respect to the isolated compounds to better wrap C_{60}. The lowest-energy excited singlet states of the associates imply an intermolecular charge transfer from the truxTTF-type receptors to C_{60}, thereby affording $truxTTF^{\delta+}$–$C_{60}^{\delta-}$.

Upon photoexcitation at 387 nm of **7.1**, a short-lived excited state (0.97 ps) is formed which is characterized by a transient absorption at 540 nm and marked ground-state bleaching at 450 nm in benzonitrile. Similarly, **7.2**, and **7.3**, show transient absorptions at 511 nm and 530 nm, and bleaching at 440 nm and 450 nm, respectively. These excited states show markedly longer lifetimes compared to **7.1**, namely 23.8 ps in the case of **7.2**, and 59.7 ps in the case of **7.3**. Transient absorption measurements, supported by spectroelectrochemical and radiolytical experiments, reveal that upon photoexcitation of the **7.1**·C_{60} associate a fully charge-separated state $\mathbf{7.1}^{\bullet+}\cdot C_{60}^{\bullet-}$ is generated, with lifetimes of hundreds of picoseconds (225 ps in benzonitrile and 165 ps in ortho-dichlorobenzene).

We believe the molecular and supramolecular properties of **7.1**–**7.3** make them a valuable addition to the armamentarium of electron donor molecules that will serve as materials for the development of improved organic photovoltaic devices. This will be the focus of our future investigations.

7.4. Computational details

Theoretical calculations were carried out within the density functional theory (DFT) approach by using the A.02 revision of the Gaussian 09 program package.[14] Geometry optimizations of compounds **7.1**−**7.3** were performed with Becke's three-parameter B3LYP exchange functional[15] and the 6-31G** basis set.[16] Dications were calculated both as singlet-state closed-shell species and as triplet-state open-shell species using for the latter spin-unrestricted UB3LYP wave functions. Open-shell anions were also computed using the UB3LYP approach. Molecular orbitals were plotted using Molekel 4.3.[17] Vertical electronic transition energies to the lowest-energy 50 excited states were computed at the B3LYP/6-31G** level using the time-dependent DFT (TDDFT) approach and the optimized ground-state molecular geometries. The vertical excitation energies were also calculated using the hybrid PBE0 functional.[18] The PBE0 functional led to slightly higher energies (~0.1 eV) for the excited states and to an identical description of the electronic spectra. TDDFT calculations were also performed in the presence of the solvent to study the influence of solvent polarity on the electronic absorption spectrum. Solvent effects were considered within the SCRF (self-consistent reaction field) theory using the polarized continuum model (PCM)[19] approach to model the interaction with the solvent. The PCM model considers the solvent as a continuous medium with a dielectric constant ε, and represents the solute by means of a cavity built with a number of interlaced spheres.[20] The solvents considered were CH_2Cl_2 (ε = 8.93) and CH_3CN (ε = 36.64). TDDFT calculations in the presence of the solvent led to a description of the electronic absorption spectra identical to that obtained for the isolated molecule and confirm the charge transfer nature of the S_1 and S_2 excited states.

---

[14] Gaussian 09, Revision A.02 Wallingford CT, 2009.Gaussian 09, Revision A.02 Wallingford CT, 2009.

[15] (a) C. Lee, W. Yang and R. G. Parr, *Physical Review B* **1988,** *37*, 785-789; (b) A. D. Becke, *J. Chem. Phys.* **1993,** *98*, 5648-5652.

[16] M. M. Francl, W. J. Pietro, W. J. Hehre, J. S. Binkley, M. S. Gordon, D. J. DeFrees and J. A. Pople, *J. Chem. Phys.* **1982,** *77*, 3654-3665.

[17] S. Portmann and H. P. thi, *CHIMIA International Journal for Chemistry* **2000,** *54*, 766-770; MOLEKEL 4.3 Manno, Switzerland, 2002.

[18] (a) C. Adamo and V. Barone, *J. Chem. Phys.* **1999,** *110*, 6158-6170; (b) M. Ernzerhof and G. E. Scuseria, *J. Chem. Phys.* **1999,** *110*, 5029-5036.

[19] J. Tomasi and M. Persico, *Chem. Rev.* **1994,** *94*, 2027-2094; C. S. Cramer and D. G. Truhlar, *Solvent Effects and Chemical Reactivity* Kluwer: Dordrecht, 1996.

[20] (a) S. Miertuš, E. Scrocco and J. Tomasi, *Chem. Phys.* **1981,** *55*, 117-129; (b) S. Miertuš and J. Tomasi, *Chem. Phys.* **1982,** *65*, 239-245; (c) M. Cossi, V. Barone, R. Cammi and J. Tomasi, *Chem. Phys. Lett.* **1996,** *255*, 327-335; (d) E. Cances, B. Mennucci and J. Tomasi, *J. Chem. Phys.* **1997,** *107*, 3032-3041; (e) V. Barone, M. Cossi and J. Tomasi, *J. Comput. Chem.* **1998,** *19*, 404-417; (f) M. Cossi, G. Scalmani, N. Rega and V. Barone, *J. Chem. Phys.* **2002,** *117*, 43-54.

Calculations on supramolecular complexes of compounds **7.1**−**7.3** with C_{60} were performed making use of Becke's "half-and-half" (BH&H) functional[21] and of the hybrid meta M06-2X functional developed by Truhlar et al.[22] The BH&H functional is an *ad hoc* mixture of exact Hartree-Fock (HF) and local density approximation (LDA) exchange, coupled with Lee, Yang, and Parr's (LYP) expression[15a] for the correlation energy. It has been found to provide binding energies for the archetypal parallel-displaced benzene dimer in good agreement with the best available high-level computational methods,[9a, 9b] and to show good performance for dispersion-dominated systems.[9c-e] The M06-2X functional has been especially designed to deal with noncovalent interactions. The B3LYP functional was not employed to calculate the supramolecular complexes because it fails in describing dispersion forces and does not properly account for stacking π-π interactions.[23]

Association binding energies were firstly obtained at the BH&H/6-31G** and M06-2X/6-31G** levels by fully optimizing the geometry (intra- and intermolecular parameters) of the supramolecular complex. Binding energies were afterwards recalculated using the more extended cc-pVTZ basis set,[24] and the 6- 31G**-optimized geometries. The basis set superposition error (BSSE) was computed using the counterpoise correction approach.[25] The BSSE is a spurious contribution to the interaction energy arising from the improved description of the molecular fragment A in the complex A•••B due to the assistance of the basis set located in fragment B, and vice versa. The counterpoise method corrects the interaction energy of the complex A•••B by computing the energies of the isolated fragments A and B with exactly the same basis set (both in number and location) as used to compute the complex A•••B.

The association binding energies were also calculated at the M06-2X/6-31G** level in the presence of the solvent (toluene) using the PCM approach and fully reoptimizing the geometry of the supramolecular complex. The solvent reduces the binding energies calculated for complexes **7.1**·C_{60}, **7.2**·C_{60}, and **7.3**·C_{60} to – 8.71, –6.76, and –7.98 kcal mol–1, respectively, thus preserving the relative stability predicted in gas phase (–17.73, –15.32, and –17.15 kcal mol–1, respectively). Therefore, the theoretical ordering predicted for the association binding energy (**7.1**·C_{60} > **7.3**·C_{60} > **7.2**·C_{60}) do not reproduce the experimental ordering deduced from absorption and fluorescence data for the binding constant (**7.1**·C_{60} > **7.2**·C_{60} > **7.3**·$_{C60.}$). The main limitation of the PCM approach is that it defines the solvent as a continuum polar medium and does not take properly into account the discrete interactions between the solvent and the solute molecules. A more elaborated model is therefore needed to correctly describe the formation of the supramolecular complexes in the presence of the solvent.

[21] A. D. Becke, *J. Chem. Phys.* **1993,** *98*, 1372-1377.
[22] Y. Zhao and D. G. Truhlar, *Theor Chem Account* **2008,** *120*, 215-241.
[23] (a) S. Tsuzuki and H. P. Luthi, *J. Chem. Phys.* **2001,** *114*, 3949-3957; (b) Y. Zhao and D. G. Truhlar, *J. Chem. Theory Comput.* **2005,** *1*, 415-432.
[24] J. T. H. Dunning, *J. Chem. Phys.* **1989,** *90*, 1007-1023.
[25] S. F. Boys and F. Bernardi, *Mol. Phys.* **1970,** *19*, 553-566.

7.5. Experimental section

General. All solvents were dried according to standard procedures. Reagents were used as purchased. All air-sensitive reactions were carried out under argon atmosphere. Flash chromatography was performed using silica gel (Merck, Kieselgel 60, 230-240 mesh, or Scharlau 60, 230-240 mesh). Analytical thin layer chromatography (TLC) was performed using aluminium-coated Merck Kieselgel 60 F254 plates. Melting points were determined on a Gallenkamp apparatus. NMR spectra were recorded on a Bruker Avance 300 (^{1}H: 300 MHz; ^{13}C: 75 MHz) a Bruker Avance 500 (^{1}H: 500 MHz; ^{13}C: 125 MHz) or a Bruker AvanceIII 700 (^{1}H: 700 MHz; ^{13}C 175 MHz) spectrometers at 298 K, unless otherwise stated, using partially deuterated solvents as internal standards. Coupling constants (J) are denoted in Hz and chemical shifts (δ) in ppm. Multiplicities are denoted as follows: s = singlet, d = doublet, t = triplet, m = multiplet, b = broad. Electrospray ionization mass spectra (ESI-MS) and Matrix assisted Laser desorption ionization (coupled to a Time-of-Flight analyzer) experiments (MALDI-TOF) were recorded on a HP1100MSD spectrometer and a Bruker REFLEX spectrometer, respectively. UV/Vis spectra were recorded with Varian Cary 50. Steady state fluorescence studies were carried out on a Fluoromax 3 (Horiba) instrument and all the Electronic Supplementary Material (ESI) for spectra were corrected for the instrument response. The femtosecond transient absorption studies were performed with laser pulses (1Khz 150 fs pulse width) from an amplified Ti:Sapphire laser system (Model CPA 2101, Clark-MXR Inc.). Mass spectra were recorded with a HP 5989A spectrometer. Cyclic voltammograms were acquired using a three-electrode cell equipped with a glassy carbon working electrode (Ø = 3 mm), a platinum wire as a counter-electrode, an $Ag/AgNO_3$ reference on an Autolab potentiostat. Before the acquisition, solutions were systematically degassed by bubbling argon for five minutes.

Synthesis and characterization

Truxenone

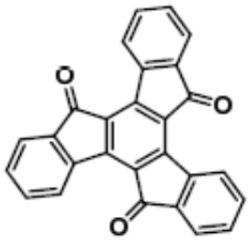

Chemical Formula: $C_{27}H_{12}O_3$
Molecular Weight: 384.38

1.0g of 1,3 indandione (6.8 mmol) were dissolved in 16 mL of methanesulfonic acid, and the solution placed in an standard microwave 30 mL vial equipped with a magnetic stirrer bar. This solution was heated to 110 ºC in an Anton Paar Monowave 300 microwave synthesis reactor utilizing the "as fast as possible" heating mode with stirring, and a hold temperature time of 5 seconds. The resulting suspension was poured into 10 mL of water and filtered. The solid was successively washed with copious amounts of water and methanol, then recrystallized from propylene carbonate and from picoline, and finally washed with diethyl ether and dried, to obtain 0.675 g (1.7 mmol, y = 77 %) of truxenone. This compound showed identical analytical and spectroscopic data to those reported in L. Sanguinet, J. C. Williams, Z. Yang, R. J. Twieg, G. Mao, K. D. Singer, G. Wiggers and R. G. Petschek, *Chem. Mater.*, 2006, **7.18**, 4259.

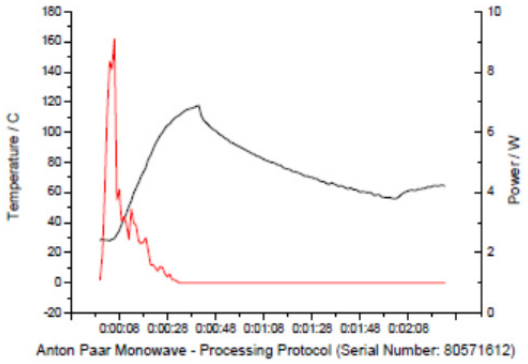

Compound 7.2

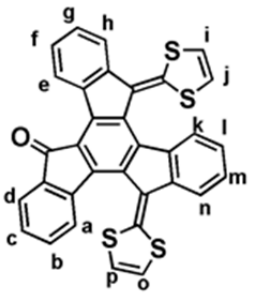

Chemical Formula: $C_{33}H_{16}OS_4$
Molecular Weight: 604.79

A solution of dimethyl 1,3-dithiol-2-ylphosphonate 1.10 g (5.2 mmol) in 10 mL of dry THF was cooled to –78 ºC, and then BuLi (2.6 mL, 2 M in hexane, 5.2 mmol) was added. The solution was left to stir at –78 ºC for 15-20 min, with appearance of a yellow precipitate. In the meantime, a suspension of 1.0 g of the truxenone precursor (2.6 mmol) in 30 mL of dry THF was dispersed with sonication for *ca.* 30 min. The resulting suspension was added to the phosphorous ylide suspension, and the cooling bath immediately removed. The mixture was allowed to warm to room temperature and left to stir for 2 h. The solvent was taken up and the residue was purified by column chromatography (SiO_2, Hexane: Dichloromethane 2:1). After purification 0.54 g (y = 37%) of the pure product was obtained as a black solid.

^{1}H NMR (DMSO) δ 9.39 (1H, d, J = 7.6 Hz, a), 7.81 (2H, d, J = 7.6 Hz, e + k), 7,70-7.51 (4H, m, f + g + l + m), 7.45 (2H, t, J = 7.6 Hz, b + c), 7.39-7.25 (5H, m, i + j + o + p + h/n), 7.12 (1H, d, J = 7.6 Hz, d), 7.04 (1H, d, J = 7.6 Hz, h/n) ppm. ^{13}C NMR (DMSO) δ 194.2, 146.1, 144.2, 144.0, 142.3, 141.7, 136.8, 135.9, 135.7, 135.2, 135.0, 134.9, 134.8, 133.5, 133.3, 129.8, 128.9, 128.5, 128.4, 127.9, 127.3, 126.7, 126.1, 125.4, 124.1, 123.7, 123.5, 122.6, 122.5, 121.0, 120.2, 120.1 ppm. MS-ESI (neg.) m/z 554.8 [M-H$^+$]. IR = 3068, 2923, 2854, 1698, 1602, 1570, 1541, 1494, 747 cm^{-1}. UV (CH_2Cl_2, 298 K) λ_{max} (log ε): 274.06 (4.64), 402.02 (4.46), 537.02 (3.67)

Compound 7.3

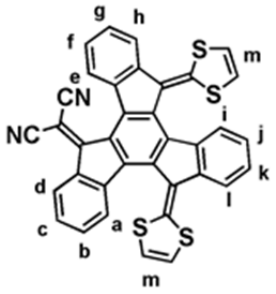

Chemical Formula: $C_{36}H_{16}N_2S_4$
Molecular Weight: 604.79

A mixture of 25 mg of **7.2** (0.045 mmol) and 8.9 mg (0.135 mmol) of malononitrile in 15 mL of chlorobenzene was treated by ultrasound irradiation for 30 minutes.Then were added 0.015 mL of $TiCl_4$ (0.135 mmol) and 0.02 mL of pyridine (0.225 mmol) successively to catalyze the reaction. The reaction mixture was stirring at room temperature for 2 hours. The solvent was removed under vacuum conditions and the crude was purified by column chromatography (SiO_2 Hexane:Dichloromethane 2:1). After purification 7.5 mg (y = 28%) of pure product was obtained as deep green solid and 10 mg (y = 40%) of pure **7.2** was retrieved.

^{1}H NMR($CDCl_3$) δ 8.28 (1H, d, J = 8.2 Hz, a); 7.86-7.77 (3H, m, e + h + l); 7.52 (1H, td, J = 7.6 y 1.2 Hz, f /g); 7.51 (1H, td , J = 7.6 y 1.2 Hz, f/g); 7.46 (1H, dd, J = 7.6 y 1.0 Hz, d); 7.39 (1H, td, J = 7.7 y 1.1 Hz, j/k); 7.38 (1H, td, J = 7.7 y 1.1 Hz, j/k); 7.30-7.23 (2H, m, b + c); 6.92 (1H, bd, J = 7.7 Hz, i); 6.88- 6.73 (4H, m, m) ppm. ^{13}CRMN ($CDCl_3$) δ: 142.7, 142.3, 142.2, 141.6, 137.8, 135.8, 135.3, 133.0, 129.3, 128.7, 128.0, 127.8, 127.3, 125.5, 125.1, 124.8, 123.0, 122.3, 121.8, 119.1, 119.0, 114.8 ppm. MS-ESI m/z= 627.0 $[M+Na]^+$. IR = 2923, 2852, 2222(ν_{CN}), 1596, 1541, 1499, 1464, 769 cm^{-1}. UV–Vis (CH_2Cl_2, 298 K) λ_{max} (log ε): 430.97 (4.48), 594.02 (3.38).

7.6. References

1. (a) M. Numata; S. Shinkai, Supramolecular wrapping chemistry' by helix-forming polysaccharides: a powerful strategy for generating diverse polymeric nano-architectures. *Chem. Commun.* **2011,** *47*, 1961-1975;(b) J. J. Davis; G. A. Orlowski; H. Rahman; P. D. Beer, Mechanically interlocked and switchable molecules at surfaces. *Chem. Commun.* **2010,** *46*, 54-63;(c) S. F. M. van Dongen; H.-P. M. de Hoog; R. J. R. W. Peters; M. Nallani; R. J. M. Nolte; J. C. M. van Hest, Biohybrid Polymer Capsules. *Chem. Rev.* **2009,** *109*, 6212-6274;(d) D. B. Amabilino, Chiral nanoscale systems: preparation, structure, properties and function. *Chem. Soc. Rev.* **2009,** *38*, 669-670;(e) J. K. Klosterman; Y. Yamauchi; M. Fujita, Engineering discrete stacks of aromatic molecules. *Chem. Soc. Rev.* **2009,** *38*, 1714-1725;(f) C. C. Lee; C. Grenier; E. W. Meijer; A. P. H. J. Schenning, Preparation and characterization of helical self-assembled nanofibers. *Chem. Soc. Rev.* **2009,** *38*, 671-683;(g) K. M. Mullen; P. D. Beer, Sulfate anion templation of macrocycles, capsules, interpenetrated and interlocked structures. *Chem. Soc. Rev.* **2009,** *38*, 1701-1713.

2. (a) M. Á. Herranz; C. Ehli; S. Campidelli; M. Gutiérrez; G. L. Hug; K. Ohkubo; S. Fukuzumi; M. Prato; N. Martín; D. M. Guldi, Spectroscopic Characterization of Photolytically Generated Radical Ion Pairs in Single-Wall Carbon Nanotubes Bearing Surface-Immobilized Tetrathiafulvalenes. *J. Am. Chem. Soc.* **2008,** *130*, 66-73;(b) N. Crivillers; M. Mas-Torrent; J. Vidal-Gancedo; J. Veciana; C. Rovira, Self-Assembled Monolayers of Electroactive Polychlorotriphenylmethyl Radicals on Au(111). *J. Am. Chem. Soc.* **2008,** *130*, 5499-5506;(c) C. Ehli; C. Oelsner; D. M. Guldi; A. Mateo-Alonso; M. Prato; C. Schmidt; C. Backes; F. Hauke; A. Hirsch, Manipulating single-wall carbon nanotubes by chemical doping and charge transfer with perylene dyes. *Nature Chemistry* **2009,** *1*, 243-249;(d) D. Gonzalez-Rodriguez; E. Carbonell; D. M. Guldi; T. Torres, Modulating Electronic Interactions between Closely Spaced Complementary π Surfaces with Different Outcomes: Regio- and Diastereomerically Pure Subphthalocyanine-C_{60} Tris Adducts. *Angew. Chem. Int. Ed.* **2009,** *48*, 8032-8036;(e) S. Schlundt; G. Kuzmanich; F. Spaenig; G. d. M. Rojas; C. Kovacs; M. A. Garcia-Garibay; D. M. Guldi; A. Hirsch, Dendritic Porphyrin-Fullerene Conjugates: Efficient Light-Harvesting and Charge-Transfer Events. *Chem. Eur. J.* **2009,** *15*, 12223-12233;(f) F. Silvestri; I. López-Duarte; W. Seitz; L. Beverina; M. V. Martínez-Díaz; T. J. Marks; D. M. Guldi; G. A. Pagani; T. Torres, A squaraine-phthalocyanine ensemble:

towards molecular panchromatic sensitizers in solar cells. *Chem. Commun.* **2009**, 4500-4502;(g) A. A. Gorodetsky; C.-Y. Chiu; T. Schiros; M. Palma; M. Cox; Z. Jia; W. Sattler; I. Kymissis; M. Steigerwald; C. Nuckolls, Reticulated Heterojunctions for Photovoltaic Devices. *Angew. Chem. Int. Ed.* **2010,** *49*, 7909-7912;(h) Y. Rio; W. Seitz; A. Gouloumis; P. Vazquez; J. L. Sessler; D. M. Guldi; T. Torres, A Panchromatic Supramolecular Fullerene-Based Donor-Acceptor Assembly Derived from a Peripherally Substituted Bodipy-Zinc Phthalocyanine Dyad. *Chem. Eur. J.* **2010,** *16*, 1929-1940;(i) W. Seitz; A. J. Jimenez; E. Carbonell; B. Grimm; M. S. Rodriguez-Morgade; D. M. Guldi; T. Torres, Synthesis and photophysical properties of a hydrogen-bonded phthalocyanine-perylenediimide assembly. *Chem. Commun.* **2010,** *46*, 127-129;(j) J. Tremblay Noah; A. Gorodetsky Alon; P. Cox Marshall; T. Schiros; B. Kim; R. Steiner; Z. Bullard; A. Sattler; W.-Y. So; Y. Itoh; F. Toney Michael; H. Ogasawara; P. Ramirez Arthur; I. Kymissis; L. Steigerwald Michael; C. Nuckolls, Photovoltaic universal joints: ball-and-socket interfaces in molecular photovoltaic cells. *ChemPhysChem* **2010,** *11*, 799-803;(k) F. Würthner; K. Meerholz, Systems Chemistry Approach in Organic Photovoltaics. *Chem. Eur. J.* **2010,** *16*, 9366-9373;(l) C.-Y. Chiu; B. Kim; A. A. Gorodetsky; W. Sattler; S. Wei; A. Sattler; M. Steigerwald; C. Nuckolls, Shape-shifting in contorted dibenzotetrathienocoronenes. *Chem. Sci.* **2011,** *2*, 1480-1486;(m) J. K. Sprafke; S. D. Stranks; J. H. Warner; R. J. Nicholas; H. L. Anderson, Noncovalent Binding of Carbon Nanotubes by Porphyrin Oligomers. *Angew. Chem. Int. Ed.* **2011,** *50*, 2313-2316;(n) A. C. Whalley; K. N. Plunkett; A. A. Gorodetsky; C. L. Schenck; C.-Y. Chiu; M. L. Steigerwald; C. Nuckolls, Bending contorted hexabenzocoronene into a bowl. *Chem. Sci.* **2011,** *2*, 132-135.

3. (a) N. Martín, New challenges in fullerene chemistry. *Chem. Commun.* **2006,** *0*, 2093-2104;(b) D. M. Guldi; B. M. Illescas; C. M. Atienza; M. Wielopolski; N. Martín, Fullerene for organic electronics. *Chem. Soc. Rev.* **2009,** *38*, 1587-1597.

4. (a) A. Hirsch, Amphiphilic architectures based on fullerene and calixarene platforms: from buckysomes to shape-persistent micelles. *Pure Appl. Chem.* **2008,** *80*, 571-587;(b) E. M. Pérez; N. Martín, Curves ahead: molecular receptors for fullerenes based on concave-convex complementarity. *Chem. Soc. Rev.* **2008,** *37*, 1512-1519;(c) F. D'Souza; O. Ito, Supramolecular donor-acceptor hybrids of porphyrins/phthalocyanines with fullerenes/carbon nanotubes: electron transfer, sensing, switching, and catalytic applications. *Chem. Commun.* **2009**, 4913-4928;(d) E. M. Pérez, Energy, supramolecular chemistry, fullerenes, and the sky. *Pure Appl. Chem.* **2011,** *83*, 201-211.

5. (a) G. Fernández; E. M. Pérez; L. Sánchez; N. Martín, Self-Organization of Electroactive Materials: A Head-to-Tail Donor–Acceptor Supramolecular Polymer. *Angew. Chem. Int. Ed.* **2008,** *47*, 1094-1097;(b) G. Fernández; E. M. Pérez; L. Sánchez; N. Martín, An Electroactive Dynamically Polydisperse Supramolecular Dendrimer. *J. Am. Chem. Soc.* **2008,** *130*, 2410-2411;(c) G. Fernández; L. Sánchez; E. M. Pérez; N. Martín, Large exTTF-Based Dendrimers. Self-Assembly and Peripheral Cooperative Multiencapsulation of C_{60}. *J. Am. Chem. Soc.* **2008,** *130*, 10674-10683;(d) R. D. Kennedy; A. L. Ayzner; D. D. Wanger; C. T. Day; M. Halim; S. I. Khan; S. H. Tolbert; B. J. Schwartz; Y. Rubin, Self-Assembling Fullerenes for Improved Bulk-Heterojunction Photovoltaic Devices. *J. Am. Chem. Soc.* **2008,** *130*, 17290-17292;(e) E. M. Pérez; A. L. Capodilupo; G. Fernández; L. Sánchez; P. M. Viruela; R. Viruela; E. Ortí; M. Bietti; N. Martín, Weighting non-covalent forces in the molecular recognition of C_{60}. Relevance of concave-convex complementarity. *Chem. Commun.* **2008,** *0*, 4567-4569;(f) F. D'Souza; E. Maligaspe; K. Ohkubo; M. E. Zandler; N. K. Subbaiyan; S. Fukuzumi, Photosynthetic Reaction Center Mimicry: Low Reorganization Energy Driven Charge Stabilization in Self-Assembled Cofacial Zinc Phthalocyanine Dimer-Fullerene Conjugate. *J. Am. Chem. Soc.* **2009,** *131*, 8787-8797;(g) K. S. Iyer; M. Saunders; T. Becker; C. W. Evans; C. L. Raston, Nanorings of Self-Assembled Fullerene C_{70} as Templating Nanoreactors. *J. Am. Chem. Soc.* **2009,** *131*, 16338-16339;(h) A. Kira; T. Umeyama; Y. Matano; K. Yoshida; S. Isoda; J. K. Park; D. Kim; H. Imahori, Supramolecular donor-acceptor heterojunctions by vectorial stepwise assembly of porphyrins and coordination-bonded fullerene arrays for photocurrent generation. *J. Am. Chem. Soc.* **2009,** *131*, 3198-3200;(i) J. M. MacLeod; O. Ivasenko; C. Fu; T. Taerum; F. Rosei; D. F. Perepichka, Supramolecular Ordering in Oligothiophene-Fullerene Monolayers. *J. Am. Chem. Soc.* **2009,** *131*, 16844-16850;(j) C. Reiriz; R. J. Brea; R. Arranz; J. L. Carrascosa; A. Garibotti; B. Manning; J. M. Valpuesta; R. Eritja; L. Castedo; J. R. Granja, α,γ-Peptide nanotube templating of one-dimensional parallel fullerene arrangements. *J. Am. Chem. Soc.* **2009,** *131*, 11335-11337;(k) J. Wang; Y. Shen; S. Kessel; P. Fernandes; K. Yoshida; S. Yagai; D. G. Kurth; H. Mohwald; T. Nakanishi, Self-assembly made durable: water-repellent materials formed by cross-linking fullerene derivatives. *Angew. Chem. Int. Ed.* **2009,** *48*, 2166-2170;(l) X. Zhang; M. Takeuchi, Controlled Fabrication of Fullerene C_{60} into Microspheres of Nanoplates through Porphyrin-Polymer-Assisted Self-

Assembly. *Angew. Chem. Int. Ed.* **2009,** *48*, 9646-9651;(m) M. Dante; C. Yang; B. Walker; F. Wudl; T.-Q. Nguyen, Self-Assembly and Charge-Transport Properties of a Polythiophene-Fullerene Triblock Copolymer. *Adv. Mater.* **2010,** *22*, 1835-1839;(n) D. Canevet; M. Gallego; H. Isla; A. de Juan; E. M. Pérez; N. Martín, Macrocyclic hosts for fullerenes: extreme changes in binding abilities with small structural variations. *J. Am. Chem. Soc.* **2011,** *133*, 3184-3190;(o) R. Cao, Jr.; H. Isla; R. Cao; E. M. Pérez; N. Martín, exTTF-capped gold nanoparticles as multivalent receptors for C_{60}. *Chem. Sci.* **2011,** *2*, 1384-1388;(p) B. Grimm; H. Isla; E. M. Pérez; N. Martín; D. M. Guldi, Balancing binding strength and charge transfer lifetime in supramolecular associates of fullerenes. *Chem. Commun.* **2011,** *47*, 7449-7451.

6. E. M. Pérez; M. Sierra; L. Sánchez; M. R. Torres; R. Viruela; P. M. Viruela; E. Ortí; N. Martín, Concave Tetrathiafulvalene-Type Donors as Supramolecular Partners for Fullerenes. *Angew. Chem. Int. Ed.* **2007,** *46*, 1847-1851.

7. L. Sanguinet; J. C. Williams; Z. Yang; R. J. Twieg; G. Mao; K. D. Singer; G. Wiggers; R. G. Petschek, Synthesis and Characterization of New Truxenones for Nonlinear Optical Applications. *Chem. Mater.* **2006,** *18*, 4259-4269.

8. (a) P. Lidstrom; J. Tierney; B. Wathey; J. Westman, Microwave assisted organic synthesis: a review. *Tetrahedron* **2001,** *57*, 9225-9283;(b) D. Obermayer; B. Gutmann; C. O. Kappe, Microwave Chemistry in Silicon Carbide Reaction Vials: Separating Thermal from Nonthermal Effects. *Angew. Chem. Int. Ed.* **2009,** *48*, 8321-8324.

9. (a) A. Robertazzi; J. A. Platts, Gas-Phase DNA Oligonucleotide Structures. A QM/MM and Atoms in Molecules Study. *J. Phys. Chem. A* **2006,** *110*, 3992-4000;(b) M. P. Waller; A. Robertazzi; J. A. Platts; D. E. Hibbs; P. A. Williams, Hybrid density functional theory for π-stacking interactions: Application to benzenes, pyridines, and DNA bases. *J. Comput. Chem.* **2006,** *27*, 491-504;(c) Y. Zhao; D. G. Truhlar, Density Functionals for Noncovalent Interaction Energies of Biological Importance. *J. Chem. Theory Comput.* **2006,** *3*, 289-300;(d) H. Valdes; K. Pluhackova; M. Pitonak; J. Rezac; P. Hobza, Benchmark database on isolated small peptides containing an aromatic side chain: comparison between wave function and density functional theory methods and empirical force field. *PCCP* **2008,** *10*, 2747-2757;(e) K. Gkionis; J. G. Hill; S. Oldfield; J. Platts, Performance of Becke's half-and-half functional for non-covalent interactions: energetics, geometries and electron densities. *J. Mol. Model.* **2009,** *15*, 1051-1060.

10. (a) S. S. Gayathri; M. Wielopolski; E. M. Pérez; G. Fernández; L. Sánchez; R. Viruela; E. Ortí; D. M. Guldi; N. Martín, Discrete supramolecular donor-acceptor complexes. *Angew. Chem. Int. Ed.* **2009,** *48*, 815-819;(b) H. Isla; M. Gallego; E. M. Pérez; R. Viruela; E. Ortí; N. Martín, A Bis-exTTF Macrocyclic Receptor That Associates C_{60} with Micromolar Affinity. *J. Am. Chem. Soc.* **2010,** *132*, 1772-1773.

11. (a) Y. Zhao; D. G. Truhlar, Computational characterization and modeling of buckyball tweezers: density functional study of concave-convex π***π interactions. *PCCP* **2008,** *10*, 2813-2818;(b) L. Feng; Z. Slanina; S. Sato; K. Yoza; T. Tsuchiya; N. Mizorogi; T. Akasaka; S. Nagase; N. Martín; D. M. Guldi, Covalently Linked Porphyrin–La@C_{82} Hybrids: Structural Elucidation and Investigation of Intramolecular Interactions. *Angew. Chem. Int. Ed.* **2011,** *50*, 5909-5912.

12. (a) J. Aragó; J. C. Sancho-García; E. Ortí; D. Beljonne, Ab Initio Modeling of Donor–Acceptor Interactions and Charge-Transfer Excitations in Molecular Complexes: The Case of Terthiophene–Tetracyanoquinodimethane. *J. Chem. Theory Comput.* **2011,** *7*, 2068-2077;(b) G. Sini; J. S. Sears; J.-L. Brédas, Evaluating the Performance of DFT Functionals in Assessing the Interaction Energy and Ground-State Charge Transfer of Donor/Acceptor Complexes: Tetrathiafulvalene−Tetracyanoquinodimethane (TTF−TCNQ) as a Model Case. *J. Chem. Theory Comput.* **2011,** *7*, 602-609.

13. (a) M. O. Sinnokrot; E. F. Valeev; C. D. Sherrill, Estimates of the Ab Initio Limit for π–π Interactions: The Benzene Dimer. *J. Am. Chem. Soc.* **2002,** *124*, 10887-10893;(b) M. O. Sinnokrot; C. D. Sherrill, Highly Accurate Coupled Cluster Potential Energy Curves for the Benzene Dimer: Sandwich, T-Shaped, and Parallel-Displaced Configurations. *J. Phys. Chem. A* **2004,** *108*, 10200-10207;(c) T. Sato; T. Tsuneda; K. Hirao, A density-functional study on pi-aromatic interaction: Benzene dimer and naphthalene dimer. *J. Chem. Phys.* **2005,** *123*, 104307-10.

14. Gaussian 09, Revision A.02 M. J. T. Frisch, G. W.; Schlegel, H. B.; Scuseria, G. E.; Robb,; J. R. S. M. A.; Cheeseman, G.; Barone, V.; Mennucci, B.; Petersson, G. A.; Nakatsuji, H.;; M. L. Caricato, X.; Hratchian, H. P.; Izmaylov, A. F.; Bloino, J.; Zheng, G.; Sonnenberg, J. L.;; M. E. Hada, M.; Toyota, K.; Fukuda, R.; Hasegawa, J.; Ishida, M.; Nakajima, T.; Honda, Y.;; O. N. Kitao, H.; Vreven, T.; Montgomery, Jr., J. A.; Peralta, J. E.; Ogliaro, F.; Bearpark,V;; J. J. B. Heyd, E.; Kudin, K. N.;

Staroverov, V. N.; Kobayashi, R.; Normand, J.;; K. R. Raghavachari, A.; Burant, J. C.; Iyengar, S. S.; Tomasi, J.; Cossi, M.; Rega, N.;; J. M. K. Millam, M.; Knox, J. E.; Cross, J. B.; Bakken, V.; Adamo, C.; Jaramillo, J.;; R. S. Gomperts, R. E.; Yazyev, O.; Austin, A. J.; Cammi, R.; Pomelli, C.; Ochterski, J.; R. L. M. W.; Martin, K.; Zakrzewski, V. G.; Voth, G. A.; Salvador, P.; Dannenberg, J. J.;; S. D. Dapprich, A. D.; Farkas, O.; Foresman, J. B.; Ortiz, J. V.; Cioslowski, J.; Fox, D. J., Wallingford CT, 2009.

15. (a) C. Lee; W. Yang; R. G. Parr, Development of the Colle-Salvetti correlation-energy formula into a functional of the electron density. *Physical Review B* **1988,** *37*, 785-789;(b) A. D. Becke, Density-functional thermochemistry. III. The role of exact exchange. *J. Chem. Phys.* **1993,** *98*, 5648-5652.

16. M. M. Francl; W. J. Pietro; W. J. Hehre; J. S. Binkley; M. S. Gordon; D. J. DeFrees; J. A. Pople, Self-consistent molecular orbital methods. XXIII. A polarization-type basis set for second-row elements. *J. Chem. Phys.* **1982,** *77*, 3654-3665.

17. (a) S. Portmann; H. P. thi, MOLEKEL: An Interactive Molecular Graphics Tool. *CHIMIA International Journal for Chemistry* **2000,** *54*, 766-770;(b) MOLEKEL 4.3 P. Flukiger; H. P. Lüthi; S. Portmann; J. Weber, Manno, Switzerland, 2002.

18. (a) C. Adamo; V. Barone, Toward reliable density functional methods without adjustable parameters: The PBE0 model. *J. Chem. Phys.* **1999,** *110*, 6158-6170;(b) M. Ernzerhof; G. E. Scuseria, Assessment of the Perdew--Burke--Ernzerhof exchange-correlation functional. *J. Chem. Phys.* **1999,** *110*, 5029-5036.

19. (a) J. Tomasi; M. Persico, Molecular Interactions in Solution: An Overview of Methods Based on Continuous Distributions of the Solvent. *Chem. Rev.* **1994,** *94*, 2027-2094;(b) C. S. Cramer; D. G. Truhlar, *Solvent Effects and Chemical Reactivity* Kluwer: Dordrecht, 1996.

20. (a) S. Miertuš; E. Scrocco; J. Tomasi, Electrostatic interaction of a solute with a continuum. A direct utilizaion of AB initio molecular potentials for the prevision of solvent effects. *Chem. Phys.* **1981,** *55*, 117-129;(b) S. Miertuš; J. Tomasi, Approximate evaluations of the electrostatic free energy and internal energy changes in solution processes. *Chem. Phys.* **1982,** *65*, 239-245;(c) M. Cossi; V. Barone; R. Cammi; J. Tomasi, Ab initio study of solvated molecules: a new implementation of the polarizable continuum model. *Chem. Phys. Lett.* **1996,** *255*, 327-335;(d) E. Cances; B. Mennucci; J. Tomasi, A new integral equation formalism for the polarizable continuum model: Theoretical background and applications to isotropic and anisotropic dielectrics. *J. Chem. Phys.* **1997,** *107*, 3032-3041;(e) V. Barone; M. Cossi; J. Tomasi, Geometry optimization of molecular structures in solution by the polarizable continuum model. *J. Comput. Chem.* **1998,** *19*, 404-417;(f) M. Cossi; G. Scalmani; N. Rega; V. Barone, New developments in the polarizable continuum model for quantum mechanical and classical calculations on molecules in solution. *J. Chem. Phys.* **2002,** *117*, 43-54.

21. A. D. Becke, A new mixing of Hartree--Fock and local density-functional theories. *J. Chem. Phys.* **1993,** *98*, 1372-1377.

22. Y. Zhao; D. G. Truhlar, The M06 suite of density functionals for main group thermochemistry, thermochemical kinetics, noncovalent interactions, excited states, and transition elements: two new functionals and systematic testing of four M06-class functionals and 12 other functionals. *Theor Chem Account* **2008,** *120*, 215-241.

23. (a) S. Tsuzuki; H. P. Luthi, Interaction energies of van der Waals and hydrogen bonded systems calculated using density functional theory: Assessing the PW91 model. *J. Chem. Phys.* **2001,** *114*, 3949-3957;(b) Y. Zhao; D. G. Truhlar, Benchmark Databases for Nonbonded Interactions and Their Use To Test Density Functional Theory. *J. Chem. Theory Comput.* **2005,** *1*, 415-432.

24. J. T. H. Dunning, Gaussian basis sets for use in correlated molecular calculations. I. The atoms boron through neon and hydrogen. *J. Chem. Phys.* **1989,** *90*, 1007-1023.

25. S. F. Boys; F. Bernardi, The calculation of small molecular interactions by the differences of separate total energies. Some procedures with reduced errors. *Mol. Phys.* **1970,** *19*, 553-566.

7. TruxTTF receptors for C_{60}

8. GENERAL DISCUSSION

8.1. Binding abilities

The common method to study the stability of the complexes in all cases was the estimation of the binding constants through several independent UV-vis titrations. We have found some similarities in the study of the association event of our exTTF-based receptors (chart 1) with fullerenes and even with FLG. The band assigned to exTTF chromophores centred around 430-450 nm decreases in intensity with an increase of C_{60}-centered transitions in the 300-400 range when the complex with [60]fullerene is formed (Figure 1). In the case of C_{70} the changes are similar but more difficult to trace due to the spectral overlap (Figure 2).

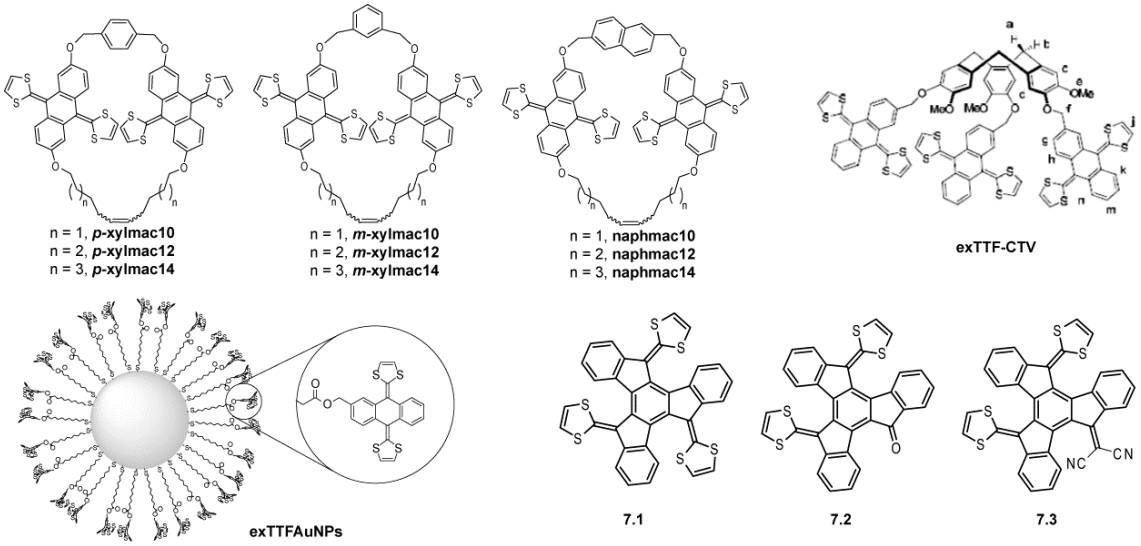

Chart 1. Chemical structures of the different receptors.

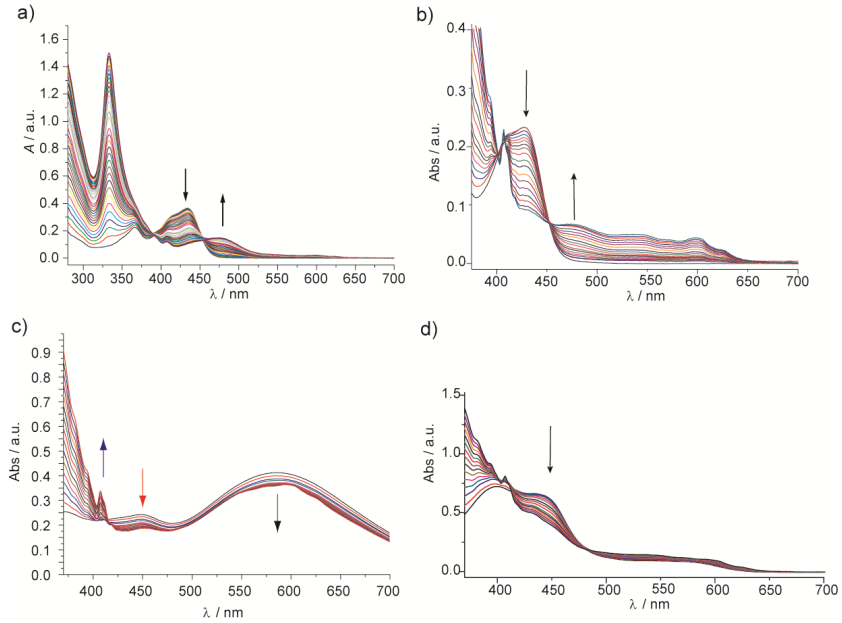

Figure 1. UV-vis titrations with C_{60} of the exTTF-based receptors a) **exTTF-CTV**, b) bis-exTTF macrocycle ***p*-xylmac12**, c) **exTTFAuNPs**, and d) **7.2**.

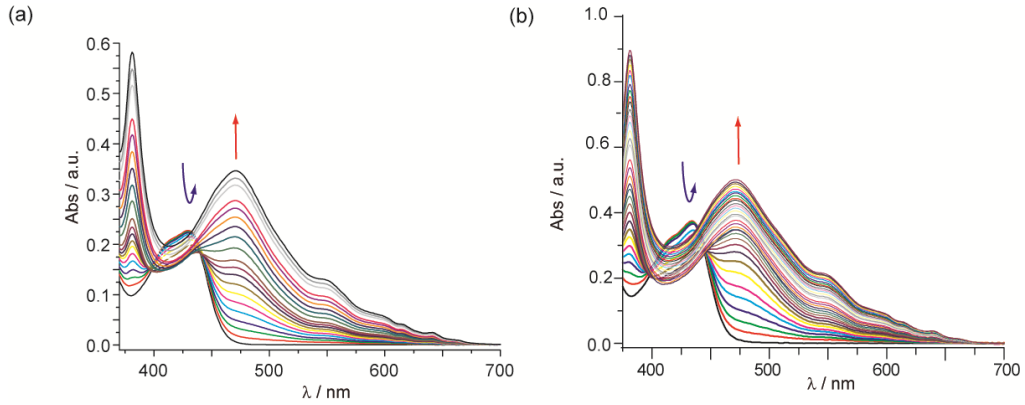

Figure 2. UV-vis spectra as recorded during the titration of (a) **naphmac14** and (b) **exTTF-CTV** *vs* C_{70} in chlorobenzene at room temperature.

Besides this quantitative approach, different experiments in solution were carried out to study the association events qualitatively. The use of NMR spectroscopy is useful for the observation of the equilibrium between the bound and unbound species. In the cases of ***p*-xylmac12** and **exTTF-CTV** ^{13}C NMR experiments were carried out to explore that equilibrium. In both cases the spectra of a mixture of host and guest at different temperatures were recorded, and the signal corresponding to C_{60} was shifted and broadened upon cooling (Figure 3). The significant broadening indicates that we are closer to the temperature of coalescence but the equilibrium remains rapid even at low temperature. We can also observe the difference in the C_{60} signal in ^{13}C NMR if we compare the signal of C_{60} alone and C_{60} in the presence of the **exTTF-CTV** receptor. In this case we can also observe that the signal is shifted and broadened in presence of the receptor, indicating the coexistence of free C_{60} and C_{60} in the complex.

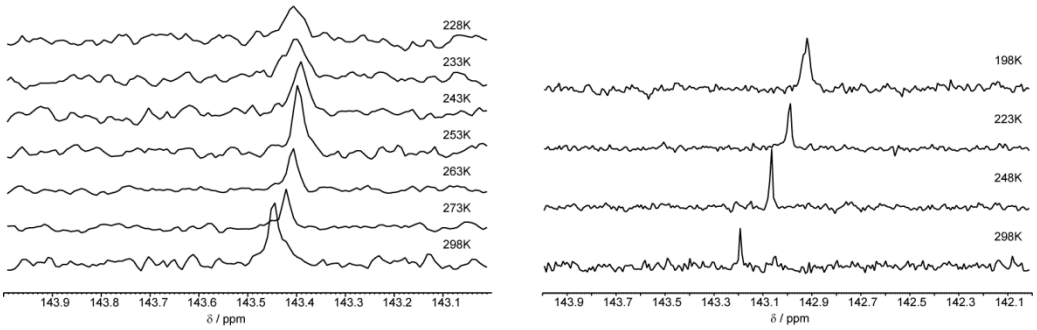

Figure 3. ^{13}C NMR spectra (75 MHz) of a mixture of C_{60} and receptors **exTTF-CTV** (left, chlorobenzene-d_5) and ***p*-xylmac12** (right, toluene-d_8) at several temperatures.

In the study of the binding abilities of truxTTF-based receptors and the **exTTF-CTV** receptor with fullerenes we considered the results of mass spectrometry of 1:1 mixtures of fullerene and each receptor as an early indication of their binding ability in the gas phase (Figure 4). In all cases peaks corresponding to C_{60}·**exTTF-CTV** (found 2306.3, calcd. 2306.1), C_{70}·**exTTF-CTV** (found 2426.2, calcd. 2426.1 , C_{60}·**7.1** (found 1362.9, calcd. 1363.0), C_{60}·**7.2** (found 1326.1, calcd. 1325.0) and C_{60}·**7.3** (found 1276.0, calcd.

1277.0) were clearly observed and no peaks corresponding to other stoichiometries were found. The 1:1 complexes were confirmed in solution by UV-vis Job's plot analyses.

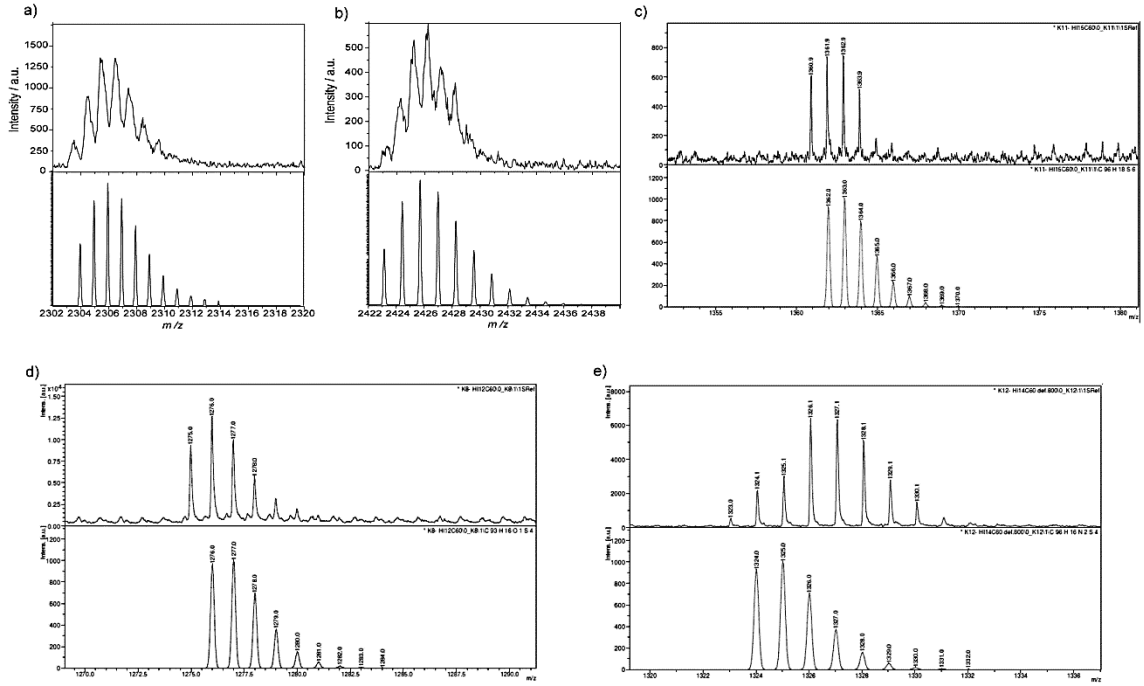

Figure 4. Simulated (down) and found (up) isotopic pattern for a) C_{60}·**exTTF-CTV**, b) C_{70}·**exTTF-CTV**, c) C_{60}·**7.1**, d) C_{60}·**7.2** and e) C_{60}·**7.3**.

In the design of bis-exTTF macrocyclic receptors we relied on the macrocyclic effect. With only four reaction steps we synthesized a macrocyclic host (***p*-xylmac12**) with a binding constant three orders of magnitude higher than the previous tweezers like receptors (from log K_a = 3.5 to log K_a = 6.5, both in chlorobenzene at room temperature). A similar difference was observed between the linear precursor of the macrocycle and the closed analogue. The examination of the binding abilities of our collection of nine receptors towards C_{60} and C_{70} showed that relatively small changes in structure were sometimes accompanied by dramatic changes in the association constant, and sometimes even in the stoichiometry of the binding event. We can find differences such as log K_a = 3.5 for ***p*-xylmac14** while log K_a = 6.5 for ***p*-xylmac12**, both with C_{60} in chlorobenzene at room temperature. The preorganization had been also the cause for fullerene discrimination in some hosts, for example **naphmac14** features log K_a = 3.4 with C_{60} and log K_a = 6.1 with C_{70} (figure 2a), 500-fold higher.

Working at constant concentration of the hosts gives us the opportunity to value the spectral changes before the analysis of the data. This preliminary valuation corresponds very well with the final binding constants quantitatively obtained. In the case of bis-exTTF macrocycles we can take a close look to the characteristic band of C_{60} around 600 nm and consider the amount of fullerene necessary to achieve the decrease of the exTTF chromophores band at 430 nm. If we compare three UV-vis titration of one family we can see the progression as shown in figure 5.

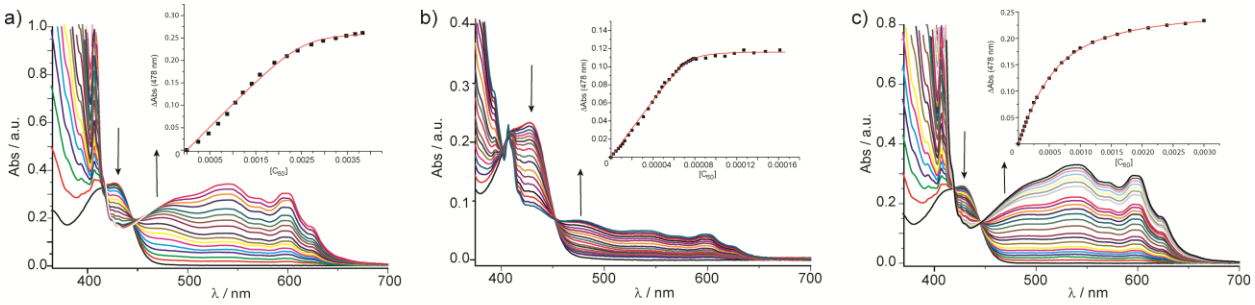

Figure 5. UV-vis titrations with C_{60} of the bis-exTTF macrocycles a) ***p*-xylmac10**, b) ***p*-xylmac12**, and c) ***p*- xylmac14** in chlorobenzene at 298 K. Inset shows the binding isotherms.

The values of the binding constant with C_{60} that correspond to the receptors titrated in figure 5 are log K_a = 4.3 for ***p*-xylmac10**, log K_a = 6.5 for ***p*-xylmac12**, and log K_a = 3.5 for ***p*-xylmac14**. We can observe qualitatively that more C_{60} has to be added to ***p*-xylmac10** and ***p*-xylmac14** compared with ***p*-xylmac12** to obtain significant spectral changes around 430 nm, where the band corresponding to the exTTF chromophores is placed.

In the case of **exTTF-CTV** receptor, we increased the number of recognition units to three, and linked them through a preorganized although flexible scaffold such as cyclotriveratrylene. This design allowed very stable complexes with log K_a = 5.3 with [60]fullerene, and 10-fold higher, log K_a = 6.3 with [70]fullerene. The chiral nature of central CTV scaffold opened up the possibility of selective association of chiral fullerenes. The chiral nature of the CTV unit and the reasonably flexible cavity of **exTTF-CTV** encouraged us to investigate the possibility of utilizing it in the chiral recognition of the inherently chiral higher fullerenes. When we tried to study the association event with C_{76} and C_{84} we found an unexpected and extreme selectivity for C_{60} and C_{70} over higher fullerenes in **exTTF-CTV** receptor (unpublished results). This receptor that forms such stable complexes with the smaller fullerenes, showed negligible binding constants (log K_a < 2) towards C_{76} and C_{84}. These surprising results demonstrate the need for a deeper understanding of the eccentric features of the fullerenes as guests in supramolecular chemistry.

After the thorough investigation of the binding abilities of bis-exTTF macrocycles and exTTF-CTV receptors with different fullerenes, we can conclude that the relationship between structure of host and guest and binding affinity is more critical than we anticipated in the case of fullerenes. Although preorganization can result in a significant increase in the binding constant, as we saw in the case of cyclodimeric porphyrins of Aida's group, a certain conformational flexibility in the linker parts of the host molecule is essential to drive association.

The main objective of the design of **exTTFAuNPs** was to achieve multivalent effect. The use of gold nanoparticles (AuNP) as structural unit for our recognition motif allowed us to construct a multivalent receptor with a very simple synthetic method. We

prepared an organic addend with an exTTF unit, and with a simple liquid-liquid extraction of citrate-capped AuNPs in aqueous solution and our recognition motif (MUA-exTTF) in chlorobenzene we are able to prepare AuNPs with more than 500 exTTF recognition units (**exTTFAuNP**). Analysis of the UV-vis titrations indicated a 5:1 stoichiometry, with five exTTF units wrapping the fullerene, and a binding constant of log $\beta_{5:1}$ = 22.5 ± 0.1 in chlorobenzene at room temperature. This value of the binding constant corresponds to a binding constant of log $K_{1:1}$ = 4.5 for each exTTF unit assuming that all exTTF-C_{60} binding events present the same binding constant. This value is very large compared with the log K_a = 3.5 for the tweezers-like receptors that correspond to a binding constant log $K_{1:1}$ = 1.75 for each exTTF unit. We can also compare these values with the corresponding in the case of **exTTF-CTV** receptor, where the analogous value is log $K_{1:1}$ = 1.76, very similar to the value obtained with two units. Therefore, we did not get multivalent effect with only three exTTF units in **exTTF-CTV**, but we achieved an important multivalent effect in the **exTTFAuNPs**, where a high number of binding sites are exposed to the host.

The increase of the aromatic surface in the receptor was the strategy followed for the construction of the first truxTTF receptor. A new π-extended TTF derivative was synthesized with three 1,3-dithiole moieties decorating the truxene core, truxTTF (**7.1**). Here, we considered the design of new bowl-shaped receptors based on truxTTF, with improved light absorption properties, with the long term goal of constructing self-assembled nanosized optoelectronic devices. Considering we wished to maintain the electron donating and supramolecular properties of the parent **7.1**, we preserved two dithiole rings and replaced one of the dithiole units by an electron-withdrawing group (**7.2** and **7.3**). Related with the binding abilities, **7.2** receptor preserves an affinity toward fullerenes similar to that of the parent truxTTF, with a log K_a = 3.4 in toluene at room temperature. Host **7.3**, on the other hand, shows a significant decrease, to log K_a = 2.3, we postulate due to its more withdrawing character when compared to truxTTF and **7.2**.

8.2. Optical and photophysical properties

The absorption of light in the visible range is also an important feature of the receptors when we think of possible applications in optoelectronic devices. Bis-exTTF macrocycles and exTTF-CTV receptors feature very similar electronic absorption spectra, with the characteristic band with very high absorption coefficients corresponding to exTTF chromophores centred at 430 nm approximately. TDDFT calculations predict that this absorption band observed around 430 nm in exTTF derivatives is as a result of the electronic transition to the first excited state. The electronic transition corresponds to the promotion of one electron from the HOMO to the LUMO, thus implies some electron-density transfer from the dithiole rings, on which the HOMO is mainly located, to the anthracene units, on which the LUMO mainly spreads (Figure 6a). In the case of **exTTFAuNPs**, the band assigned to the exTTF chromophores is centred at 450 nm, and the absorption continues in the visible

range with a strong and broad band. In this case we achieved the extension of absorption because of the plasmon resonance band ($\lambda \sim 590$ nm) of the gold nanoparticles. The surface plasmon resonance (SPR) band corresponds to an interaction between matter and the electromagnetic field of light, giving rise to a quantum size effect. This quantum size effect appears when the size of the particle is of the same order than the de Broglie wavelength of the valence electrons- in gold nanoparticles in 5-20 nm range- and is modified with aggregation-disagreggation processes.

In the case of the truxTTF receptors the extension of the light absorption in the visible was one of the main objectives in the design. Besides conserving similar binding abilities towards fullerenes, we obtained a significant bathocromic shift with respect to **7.1** as a result of the push-pull effects between the electron-donor dithioles and the electron-acceptor groups. To investigate the nature of the electronic transitions that give rise to the absorption bands observed in the electronic spectra, the lowest-energy singlet excited states (S_n) were calculated using the time-dependent density functional theory (TD-DFT) approach. Thanks to the calculations we know the transitions implied in the absorption bands and the prediction of the intensities corresponds to the experimental data. In the case of truxTTF **7.1** TDDFT calculations predict that the experimental band around 450 nm is as a result of a group of electronic transitions from HOMO and HOMO-1 to LUMO and LUMO+1 (Figure 6b). This group of transitions also implies some electronic-density transfer from the dithiole rings, on which HOMO and HOMO-1 are mainly located, to the truxene core, on which LUMO and LUMO +1 mainly spread. When we move to **7.2** and **7.3** the absorption spans over nearly all the visible region. In these cases the experimental evidences and TDDFT calculations confirm the assignment of the bands to an intramolecular charge-transfer process. The absorption in **7.2** and **7.3** is due to electronic transitions to the first two excited singlets S1 and S2, which originate from HOMO→LUMO and HOMO-1→LUMO one-electron excitations, and imply an intramolecular charge transfer from dithiole rings to the acceptor groups, where the LUMO are mainly located.

With the understanding of the processes involved in the absorption of light, we are able to fine-tune these important electronic properties. This fact open the way to the design of new organic molecules with the appropriate absorption abilities that are necessary if we think in the construction of photoelectronic devices.

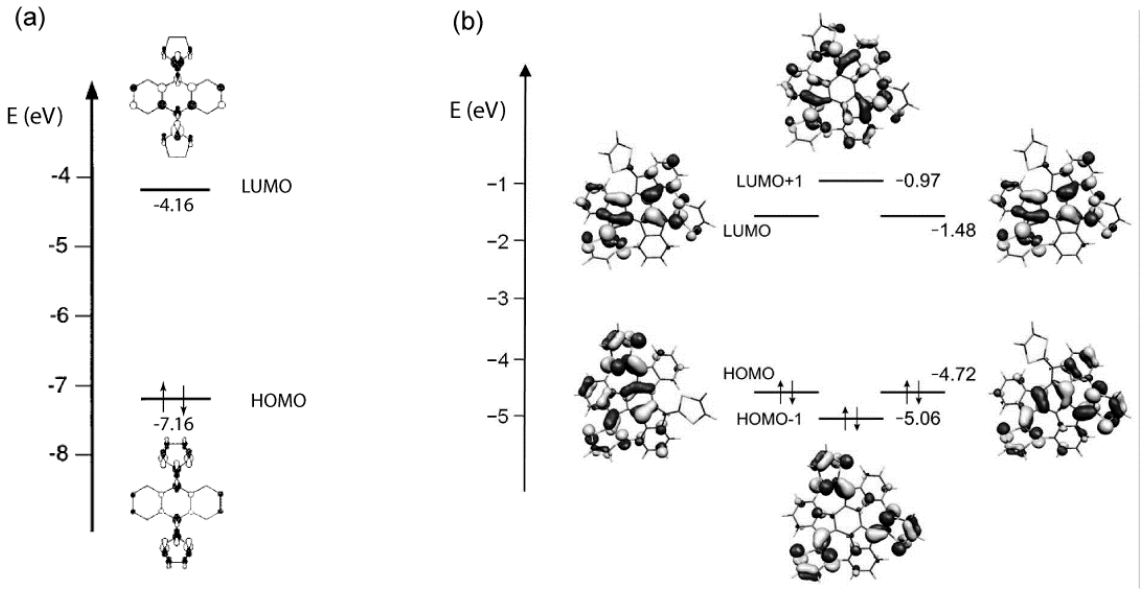

Figure 6. a) Molecular orbital diagram correlating the energies and atomic orbital (AO) compositions of the HOMO and LUMO calculated for exTTF at the VEH level (*J. Org. Chem.* **1998,** *63*, 1268); b) Electron density contours (0.03 e bohr^{-3}) and energies calculated for the HOMOs and LUMOs of truxTTF at the B3LYP/6-31G** level.

The processes that take place in the receptors and complexes upon excitation are known thanks to the study of their photophysical properties in solution. These studies include the analysis of the data of the emission spectra upon excitation and the differential absorption spectra upon femtosecond flash photolysis (figure 7).

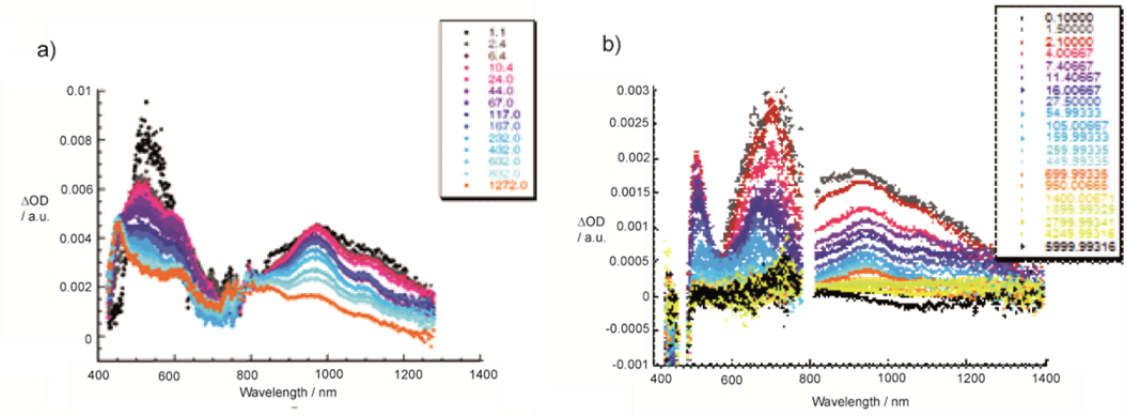

Figure 7. Differential absorption spectra obtained upon femtosecond laser photolysis (a) (387 nm) of **7.1**·C_{60} in Ar-saturated benzonitrile with time delays between 1.1 and 1272 ps at room temperature; (b) (480 nm) of ***p*-xylmac12**·C_{60} in Ar-saturated benzonitrile with time delays between 0.1 and 6000 ps at room temperature.

We have photophysical studies of our previous tweezers-like receptor, truxTTF receptors and ***p*-xylmac12** macrocyclic receptor. In the case of our starting point, tweezers-like receptor, the analysis of the differential absorption spectra conclude that the pristine exTTF-tweezers have a short lived 1.2 ps excited state after irradiation with

laser pulse (387 nm). When irradiated in the presence of fullerene, the spectroscopic features reveal the instantaneous formation of a fully charge-separated state with a lifetime of 12.7 ps in benzonitrile and 5.8 ps in *o*-dichlorobenzene with the singlet ground state being the product of this charge recombination. The lifetimes of the excited state of the receptors upon photoexcitation with a laser pulse at 387 nm are very similar in the cases of **7.1** and ***p*-xylmac12**, being 0.97 ps and 1.2 ps respectively. These short lived excited states are rationalized by the presence of sulphur atoms. In the case of the truxTTF receptors **7.2** and **7.3** the lifetimes are longer, 32.8 ± 0.6 ps and 59.7 ± 1.2 ps respectively.

More worth noting are the differences found in the lifetimes of the charge-separated states when the receptors were irradiated in the presence of fullerenes. In the case of receptor **7.1** the irradiation results in a charge-separated state that evolves from the locally excited states, with lifetimes of 225 ± 10 ps in benzonitrile and 165 ± 25 ps in *o*-dichlorobenzene. In the case of the ***p*-xylmac12** bis-exTTF macrocycle, these transient absorption measurements were carried out in the presence of [60] and [70]fullerenes. The laser pulse irradiation of the ***p*-xylmac12** and C_{60} provokes the short-lived $C_{60}^{\delta-}$/***p*-xylmac12**$^{\delta+}$ excited state that transforms within 6.7 ± 0.5 ps in benzonitrile and 9.0 ± 0.5 ps in chlorobenzene into a fully charge-separated state with a lifetime of 157 ± 31 ps in benzonitrile and 137 ± 11 ps in chlorobenzene. In the case of the irradiation of ***p*-xylmac12** in the presence of C_{70} the formed excited state $C_{70}^{\delta-}$/***p*-xylmac12**$^{\delta+}$ has a lifetime of 5.1 ± 1.5 ps and transforms in the charge-separated state $C_{70}^{\bullet-}$/***p*-xylmac12**$^{\bullet+}$, which has lifetimes of 482 ± 36 ps in benzonitrile and 371 ± 27 ps in chlorobenzene.

As remarkable data, the lifetimes of the charge-separated states upon excitation of the new complexes are, in all cases, at least one order of magnitude larger than those found for the complexes of fullerene with the previous exTTF tweezers-like receptors. It can be rationalized by the extension of the aromatic core in receptor **7.1** and it seems that the alkyl chain is key in the lifetimes of charge-separated state in ***p*-xylmac12**.

9. CONCLUSIONS

i) The design and synthesis of new exTTF-based receptors has been achieved by increasing the number of recognition units. We have increased the number of exTTF to three in the exTTF-CTV receptor, by making use of a CTV scaffold that also provides some preorganization. We have increased the number of exTTF moieties up to 500 units with a very simple synthetic method by using gold nanoparticles as a scaffold. A very significant multivalent effect was observed with this kind of receptor.

ii) We have synthesized highly preorganized macrocyclic receptors. A thorough structure-affinity investigation was carried out, by varying both the aromatic and the alkenyl spacers, and revealed that very small changes in structure lead to remarkable changes in the binding abilities of the receptors.

iii) The increase of the aromatic surface of the recognition unit resulted in the design and synthesis of a family of truxTTF receptors, with two or three dithiole rings, that are able to associate fullerene with 1:1 stoichiometry. The change of one of the dithiole rings by an electron withdrawing group causes enhanced absorption properties in the visible range.

iv) The investigation of the stability of the complexes was successfully carried out and quantified by means of UV-vis titrations. The analysis of the data provides some of the larger binding constants for fullerenes with all organic receptors. We have corroborated the association event with fluorescence titrations, mass spectrometry, NMR spectroscopy and microscopic techniques in the case of exTTFAuNPs.

v) Theoretical calculations have helped the understanding of the structural properties of the receptors and complexes; they have also been instrumental, in combination with voltammetry measurements, in the study of their electronic properties and, in combination with other spectroscopic techniques, in the investigation of their photophysical properties.

vi) We have achieved the supramolecular modification of FLG with our non-planar recognition motif exTTF, proving that planarity is not a prerequisite for the association with graphene layers.

1. INTRODUCTION

Fullerenes are molecular allotropes of carbon built up of fused pentagonal and hexagonal rings. [60]fullerene was discovered by H. W. Kroto, R. F. Curl, and R. E. Smalley in 1985.[1] The C_{60} molecule was named buckminsterfullerene after the American architect R. Buckminster Fuller, whose geodesic dome is constructed on the same structural principles. H. W. Kroto, R. F. Curl, and R. E. Smalley were awarded with the Nobel Prize of Chemistry in 1996 for the discovery of fullerenes.[2] The first important breakthrough in fullerene science occurred in 1990, when the astrophysicist Wolfgang Krätschmer and Donald Huffman prepared fullerene C_{60} for the first time in multigram amounts, [3] thus making it available for the scientific community. The study of the supramolecular chemistry of fullerenes started immediately after macroscopic quantities of fullerene C_{60} became available.

The peculiar electronic properties in of fullerenes make them attractive from the photophysical point of view. Photophysical properties has been previously reported and reviewed.[4] Some of the main properties, which make the fullerenes interesting for different applications, are the following:

- It is a good electron acceptor.[4c, 5, 6]
- Its LUMO allows for the reversible addition of up to 6 electrons.
- It has a low reorganization energy.
- It is relatively inert.

Upon light irradiation and in the presence of oxygen, C_{60} generates excited singlet molecular oxygen with high efficiency by bimolecular quenching,[4a, 7]. The photogeneration of singlet oxygen, a highly reactive species, could allow for the development of C_{60}-based photodynamic therapy agents.[8] Moreover, the fact that C_{60} is

[1] H. W. Kroto, J. R. Heath, S. C. O'Brien, R. F. Curl and R. E. Smalley, *Nature* **1985,** *318*, 162-163.
[2] (a) R. F. Curl, *Angew. Chem., Int. Ed. Engl.* **1997,** *36*, 1566-1576; (b) H. Kroto, *Angew. Chem., Int. Ed. Engl.* **1997,** *36*, 1578-1593; R. E. Smalley, *Angew. Chem., Int. Ed. Engl.* **1997,** *36*, 1594-1601.
[3] W. Kratschmer, L. D. Lamb, K. Fostiropoulos and D. R. Huffman, *Nature* **1990,** *347*, 354-358.
[4](a) J. W. Arbogast, A. P. Darmanyan, C. S. Foote, F. N. Diederich, R. L. Whetten, Y. Rubin, M. M. Alvarez and S. J. Anz, *J. Phys. Chem.* **1991,** *95*, 11-12; (b) T. W. Ebbesen, K. Tanigaki and S. Kuroshima, *Chem. Phys. Lett.* **1991,** *181*, 501-504; (c) D. M. Guldi and M. Prato, *Acc. Chem. Res.* **2000,** *33*, 695-703.
[5] K. M. Kadish and R. S. Ruoff, *Fullerenes: Chemistry, Physics, and Technology*. Wiley: 2000.
[6] (a) N. Martín, L. Sánchez, B. Illescas and I. Pérez, *Chem. Rev.* **1998,** *98*, 2527-2548; (b) H. Imahori and Y. Sakata, *Eur. J. Org. Chem.* **1999,** *1999*, 2445-2457; (c) D. M. Guldi, *Chem. Commun.* **2000,** *0*, 321-327.
[7] R. R. Hung and J. J. Grabowski, *J. Phys. Chem.* **1991,** *95*, 6073-6075.
[8] T. Da Ros and M. Prato, *Chem. Commun.* **1999,** *0*, 663-669.

relatively inert under mild conditions, has made functionalized fullerenes potential candidates for a variety of medicinal applications.[9]

The triply-degenerate low-lying LUMO in fullerene allows for the reversible addition of up to six electrons.[5] Remarkably, small reorganization energies are associated with the reduction of C_{60} and its derivatives. Under optimal conditions, small reorganization energies lead to optimal charge-separation kinetics, and a deceleration of charge-recombination rates. That is, charge recombination in these systems occurs more slowly than photoelectron transfer which results in the generation of relatively long-lived charge-separated states. These properties have led to the synthesis of a large number of donor-acceptor arrays containing fullerene, which have been proposed as models for photosynthesis and as energy storage systems.[5, 6b, 10]

One of the most active research areas in fullerene chemistry is the design of a wide variety of donor-acceptor systems, acting as artificial photosynthetic centres, and the study of their photoinduced electron transfer processes. Photoinduced electron transfer is a fundamental process in Nature since it governs photosynthesis in plants and bacteria. The human being needs to face the energy problem, and designing new molecular materials capable to harvest and transform solar energy into chemical or electrical power represents one of the more promising alternatives. Owing to the unique photophysical and electrochemical features of fullerene C_{60}, is the electron acceptor of choice for most organic photovoltaic devices.

The covalent linkage of electron donors to fullerene has been the most studied approach, forming dyads, triads, etc. A wide variety of electron donors have been covalently linked to fullerenes, such as porphyrins,[10c, 11] organometallic compounds such as ferrocenes[12] or Ru^{II}bipyridine,[13] carotenes,[14] aniline derivatives,[15] π-conjugated oligomers,[16] phthalocyanines,[17] and tetrathiafulvalenes.[18]

---

[9] Kadish and Ruoff; A. W. Jensen, S. R. Wilson and D. I. Schuster, *Biorg. Med. Chem.* **1996,** *4*, 767-779.
[10] (a) H. Imahori and Y. Sakata, *Adv. Mater.* **1997,** *9*, 537-546; (b) D. Gust, T. A. Moore and A. L. Moore, *Acc. Chem. Res.* **2000,** *34*, 40-48; (c) D. M. Guldi, *Chem. Soc. Rev.* **2002,** *31*, 22-36.
[11] H. Imahori, *J. Phys. Chem. B* **2004,** *108*, 6130-6143.
[12] (a) D. M. Guldi, M. Maggini, G. Scorrano and M. Prato, *J. Am. Chem. Soc.* **1997,** *119*, 974-980; (b) M. Fujitsuka, N. Tsuboya, R. Hamasaki, M. Ito, S. Onodera, O. Ito and Y. Yamamoto, *J. Phys. Chem. A* **2003,** *107*, 1452-1458; (c) D. M. Guldi, C. Luo, N. A. Kotov, T. D. Ros, S. Bosi and M. Prato, *J. Phys. Chem. B* **2003,** *107*, 7293-7298.
[13] (a) D. M. Guldi, M. Maggini, E. Menna, G. Scorrano, P. Ceroni, M. Marcaccio, F. Paolucci and S. Roffia, *Chem. Eur. J.* **2001,** *7*, 1597-1605; (b) J.-F. Nierengarten, N. Armaroli, G. Accorsi, Y. Rio and J.-F. Eckert, *Chem. Eur. J.* **2003,** *9*, 36-41.
[14] S. N. Smirnov, P. A. Liddell, I. V. Vlassiouk, A. Teslja, D. Kuciauskas, C. L. Braun, A. L. Moore, T. A. Moore and D. Gust, *J. Phys. Chem. A* **2003,** *107*, 7567-7573.
[15] (a) R. M. Williams, J. M. Zwier and J. W. Verhoeven, *J. Am. Chem. Soc.* **1995,** *117*, 4093-4099; (b) K. G. Thomas, V. Biju, D. M. Guldi, P. V. Kamat and M. V. George, *J. Phys. Chem. B* **1999,** *103*, 8864-8869.
[16] (a) D. M. Guldi, C. Luo, A. Swartz, R. Gómez, J. L. Segura, N. Martín, C. Brabec and N. S. Sariciftci, *J. Org. Chem.* **2002,** *67*, 1141-1152; (b) D. M. Guldi, A. Swartz, C. Luo, R. Gómez, J. L. Segura and N. Martín, *J. Am. Chem. Soc.* **2002,** *124*, 10875-10886; (c) J. L. Segura, N. Martín and D. M. Guldi, *Chem. Soc. Rev.* **2005,** *34*, 31-47; (d) C. M. Atienza, G. Fernández, L. Sánchez, N. Martín, I. S. Dantas, M. M.

Our group has reported a vast variety of dyads containing fullerene as electron acceptor and TTF derivatives as electron donors.[19] Unlike other electron donors, tetrathiafulvalene TTF and π-extended TTF become aromatic upon oxidation. The aromatization affords thermodynamically stable radical-cationic and dicationic species at relatively low oxidation potentials.[20] This is a crucial factor in the stabilization of the photogenerated radical ion pairs, which could help improve efficiencies in possible devices. Besides this, TTF derivatives feature some of highest hole mobilities for solution-processed materials.[21]

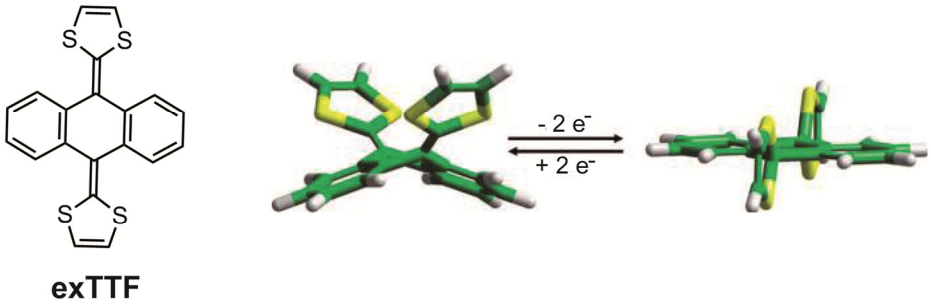

Figure 1. Structure of exTTF, and geometry of the ground state (left) and dicationic state (right) of exTTF.[18]

Three main facts prompted the evolution of the next strategy, the supramolecular chemistry of fullerenes: i) the arrangement of the donor-acceptor couples in the photosynthetic reaction centre[22] is based on non-covalent interactions; ii) photoinduced electron transfer between a donor and C_{60} can take place through space; iii) the

---

Wienk, R. A. J. Janssen, G. M. A. Rahman and D. M. Guldi, *Chem. Commun.* **2006,** 514-516; (e) G. Fernández, L. Sánchez, D. Veldman, M. M. Wienk, C. Atienza, D. M. Guldi, R. A. J. Janssen and N. Martín, *J. Org. Chem.* **2008,** *73*, 3189-3196.

[17] M. Antonietta Loi, P. Denk, H. Hoppe, H. Neugebauer, C. Winder, D. Meissner, C. Brabec, N. Serdar Sariciftci, A. Gouloumis, P. Vazquez and T. Torres, *J. Mater. Chem.* **2003,** *13*, 700-704.

[18] N. Martín, L. Sánchez, M. a. Á. Herranz, B. Illescas and D. M. Guldi, *Acc. Chem. Res.* **2007,** *40*, 1015-1024.

[19] (a) N. Martín, L. Sánchez, C. Seoane, R. Andreu, J. Garín and J. Orduna, *Tetrahedron Lett.* **1996,** *37*, 5979-5982; (b) N. Martín, L. Sánchez, M. A. Herranz and D. M. Guldi, *J. Phys. Chem. A* **2000,** *104*, 4648-4657; (c) M. C. Díaz, M. A. Herranz, B. M. Illescas, N. Martín, N. Godbert, M. R. Bryce, C. Luo, A. Swartz, G. Anderson and D. M. Guldi, *J. Org. Chem.* **2003,** *68*, 7711-7721.

[20] (a) Y. Yamashita, Y. Kobayashi and T. Miyashi, *Angew. Chem., Int. Ed. Engl.* **1989,** *28*, 1052-1053; (b) M. R. Bryce, A. J. Moore, M. Hasan, G. J. Ashwell, A. T. Fraser, W. Clegg, M. B. Hursthouse and A. I. Karaulov, *Angew. Chem., Int. Ed. Engl.* **1990,** *29*, 1450-1452; (c) N. Martín, L. Sánchez, C. Seoane, E. Ortí, P. M. Viruela and R. Viruela, *J. Org. Chem.* **1998,** *63*, 1268-1279; (d) C. A. Christensen, A. S. Batsanov and M. R. Bryce, *J. Am. Chem. Soc.* **2006,** *128*, 10484-10490.

[21] (a) N. Gautier, F. Dumur, V. Lloveras, J. Vidal-Gancedo, J. Veciana, C. Rovira and P. Hudhomme, *Angew. Chem. Int. Ed.* **2003,** *42*, 2765-2768; (b) M. Mas-Torrent, P. Hadley, S. T. Bromley, X. Ribas, J. Tarrés, M. Mas, E. Molins, J. Veciana and C. Rovira, *J. Am. Chem. Soc.* **2004,** *126*, 8546-8553.

[22] (a) W. Khlbrandt and D. N. Wang, *Nature* **1991,** *350*, 130-134; (b) G. McDermott, S. M. Prince, A. A. Freer, A. M. Hawthornthwaite-Lawless, M. Z. Papiz, R. J. Cogdell and N. W. Isaacs, *Nature* **1995,** *374*, 517-521.

nanometric organization of p- and n-type materials in photovoltaic devices is expected to facilitate charge mobility, preventing recombination.[23]

Generally speaking, the search for receptors for fullerenes is fuelled mainly by the interest in finding new, simpler methods for the purification from fullerite, and in the control of the nanometric organization of electroactive materials, since it could increase the efficiency of the photovoltaic devices.[24]

Designing receptors for a specific guest is a challenging topic in supramolecular chemistry.[25, 26] In order to build receptors for fullerenes we have evaluate the peculiar features of this guest. Fullerenes behave as a polyene without further functionality, which prevents the utilization of directional forces such as hydrogen bonds. On the other hand, its spherical geometry implies a very high surface/volume ratio, which facilitates the use of dispersion-type forces, such as π–π stacking, van der Waals, and solvophobic interactions. Since dispersion forces depend directly on surface area, the basic strategy to optimize noncovalent interactions is to increase the surface of the receptor in short contact with the fullerene guest.[27]

In the development of supramolecular chemistry of fullerenes in the group we have chosen exTTF as recognition unit. exTTF is an electron donor absorbs light effectively in the visible range. The concave shape of exTTF, as we can see in the solid-state structure (Figure 1), and its electronic complementarity, indicates it could establish charge-transfer, π–π and Van der Waals interactions with the convex surface of fullerene, making it a promising candidate as a recognition motif for fullerenes.

Although theoretical calculations indicate that one single molecule of exTTF could associate with C_{60}, this does not happen experimentally. The next step in the design of a receptor for fullerenes was to increase the number of the recognition units in the receptor, concluding in these simple tweezers composed of two exTTF units linked by an aromatic spacer (figure 2).[28] The association event was studied by means of UV-visible titrations. The analysis of the data, fitting these changes to a 1:1 binding isotherm, afforded a log K_a = 3.5 in chlorobenzene at room temperature, which is a good complexation result taking into account the lack of preorganization of the receptor.

[23] C.-H. Huang, N. D. McClenaghan, A. Kuhn, J. W. Hofstraat and D. M. Bassani, *Org. Lett.* **2005,** *7*, 3409-3412.
[24] (a) P. M. Beaujuge and J. M. J. Fréchet, *J. Am. Chem. Soc.* **2011,** *133*, 20009-20029; (b) Y.-H. Chen, L.-Y. Lin, C.-W. Lu, F. Lin, Z.-Y. Huang, H.-W. Lin, P.-H. Wang, Y.-H. Liu, K.-T. Wong, J. Wen, D. J. Miller and S. B. Darling, *J. Am. Chem. Soc.* **2012,** *134*, 13616-13623.
[25] L. R. MacGillivray and J. L. Atwood, *Angew. Chem. Int. Ed.* **1999,** *38*, 1018-1033.
[26] D. Canevet, E. M. Pérez and N. Martín, *Angew. Chem. Int. Ed.* **2011,** *50*, 9248-9259.
[27] E. M. Pérez and N. Martín, *Chem. Soc. Rev.* **2008,** *37*, 1512-1519.
[28] E. M. Pérez, L. Sánchez, G. Fernández and N. Martín, *J. Am. Chem. Soc.* **2006,** *128*, 7172-7173.

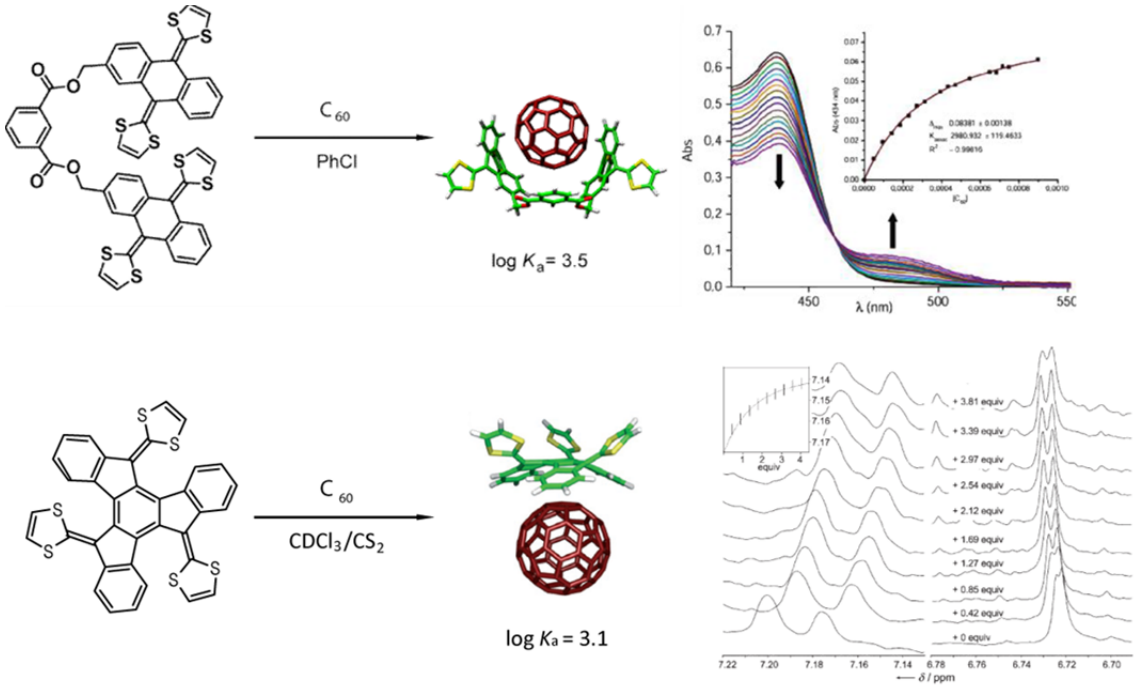

Figure 2. Upper part) Structure of tweezers-like receptor and model of complex upon addition of C_{60} (left); Absorption spectral changes of the receptor (chlorobenzene, 298 K, 2.31 x 10^{-5} M) upon addition of fullerene (chlorobenzene, 298 K, 4.05 x 10^{-3} M). Inset shows the fit of ΔAbs (434 nm) to a 1:1 binding isotherm (rigth). Below part) Structure of truxTTF receptor and model of complex upon addition of C_{60} (left); Partial 1H NMR spectra of truxTTF (300 MHz, 298 K, $CDCl_3/CS_2$) upon addition of fullerene. Inset shows the fit of the chemical shift of the aromatic protons to a 1:1 binding isotherm (rigth).

Part of the work described in this thesis is based on the previously reported concave tetrathiafulvalene-type donor truxene TTF (truxTTF).[29] Following the seminal work with tetrathiafulvalene, derivatives in which the 1,3-dithiole moieties are connected to a π-conjugated core have been studied. In this case truxene is the selected π-conjugated core to which three dithiol moieties were covalently connected. The extended delocalized π-system of truxene results in a shift of the absorption spectra towards the visible range, and at the same provides a large aromatic surface to establish favorable noncovalent interactions. To accommodate the dithiole rings, the truxene moiety breaks down its planar structure and adopts an all-*cis* sphere-like geometry with the three dithiole rings protruding outside. The association event was studied by means of ^{1}H NMR titration. The analysis of the data afforded log K_a = 3.1 in a mixture of chloroform and carbon disulfide at room temperature.

[29] E. M. Pérez, M. Sierra, L. Sánchez, M. R. Torres, R. Viruela, P. M. Viruela, E. Ortí and N. Martín, *Angew. Chem. Int. Ed.* **2007,** *46*, 1847-1851.

2. OBJECTIVES

The present thesis addresses one main objective: **to design and synthesize new exTTF-based receptors for fullerenes with high affinity**. Within this main objective, we will follow three different strategies:

i) to increase the number of recognition units.
ii) to include preorganization in the design of the receptors.
iii) to expand the π-surface and the number of dithiole rings of the recognition motif.

As part of the study of the properties of these new hosts we will investigate:

iv) the binding events in solution, through UV-vis, fluorescence and NMR titrations; in the gas phase, through mass spectrometry; and in the solid state, through X-ray crystallography and microscopic techniques.
v) the structural, electronic and photophysical properties of the receptors and the supramolecular associates, through a combination of theory and spectroscopy.
vi) the structure-affinity relationships, that is, how changes in the structure of the receptors affect the binding constant towards fullerenes.
vii) the association of some of the receptors to other nanoforms of carbon, in particular graphene.

3. RESULTS

We will summarize here the articles that make up the main chapters of the present thesis.

3.1. Bis exTTF macrocyclic receptors.

Exploiting the shape and electronic complementarity of [60] and [70] fullerene with π-extended derivatives of tetrathiafulvalene (exTTF), we have reported a family of exTTF-based macrocyclic receptors. In this chapter we will describe the articles related with this project

3.1.1. A bis-exTTF macrocyclic receptor that associates C_{60} with micromolar affinity

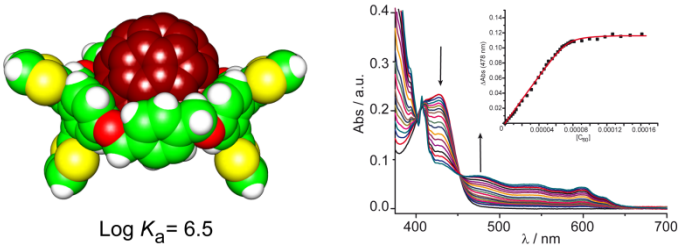

The design of this new bis-exTTF macrocyclic receptor is based in our previous tweezers-like receptor but using an aromatic and alkyl spacers. In this case we have made use of the macrocyclic effect to increase the preorganization in the host. The binding abilities with C_{60} and C_{70} were investigated through UV-vis titrations and the analysis of the data result in a binding constant of log K_a = 6.5 in chlorobenzene at room temperature. This represents an improvement of three orders of magnitude with respect to the previous examples of exTTF-based receptors, and one of the highest binding constants towards C_{60} reported to date.

Helena Isla, María Gallego, Emilio M. Pérez, Rafael Viruela, Enrique Ortí and Nazario Martín *J. Am. Chem. Soc*. **2010**, *132*, 1772–1773

3.1.2. Macrocyclic hosts for fullerenes: extreme changes in binding abilities with small structural variations

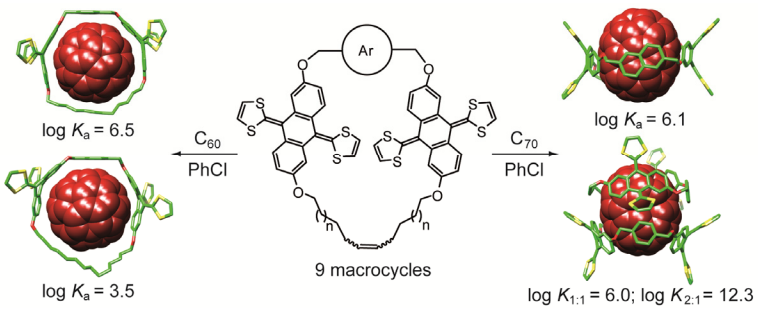

In this work we describe our efforts to fine-tune our macrocyclic bis-exTTF hosts to bind C_{60} and/or C_{70}, through structural variations. Based on preliminary molecular modeling, we have explored *p*-xylene, *m*-xylene and 2,6-dimethylnaphthalene as aromatic spacers between the two exTTF fragments and three alkene-terminated alkyl chains of different length to achieve macrocycles of different size through ring closing metathesis (RCM). Due to the structural simplicity of our design, all nine receptors could be accessed in a synthetically straightforward manner. A thorough investigation of the binding abilities of these nine receptors towards C_{60} and C_{70} has been carried out by means of UV-vis titrations. We have found that relatively small variations in the structure of the host lead to very significant changes in affinity towards the fullerene, and in some cases even in the stoichiometry of the associates. Our results highlight the peculiarities of fullerenes as guests in molecular recognition. We have found evidence of association and electronic communication also in CV experiments. The extreme stability of these associates in solution, and the unique combination of electronic and geometrical reciprocity of exTTF and fullerenes are the main features of this new family of macrocyclic hosts for fullerenes.

David Canevet, María Gallego, Helena Isla, Alberto de Juan, Emilio M. Pérez and Nazario Martín *J. Am. Chem. Soc.* ***2011****, 133, 3184–3190*

3.1.3. Balancing binding strength and charge transfer lifetime in supramolecular associates of fullerenes.

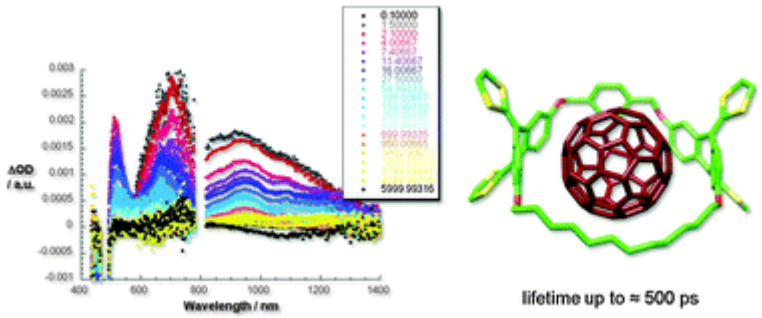

Photophysical studies on the first bis-exTTF macrocycle receptor were carried out. The absorption and fluorescence titrations confirmed the association abilities of the receptor in different solvents. The behaviour of the system upon irradiation was also investigated. A contribution to the stability of the complex from charge transfer in the ground state was postulated, which upon photoirradiation lead to a fully charge-separated state. Transient absorption measurements indicate that the charge separated state showed lifetimes reaching into the 500 ps.

Bruno Grimm, Helena Isla, Emilio M Pérez, Nazario Martín and Dirk M. Guldi *Chem. Commun.,* **2011***, 47,* 7449-7451

3.2. Tripodal exTTF-CTV Hosts for Fullerenes

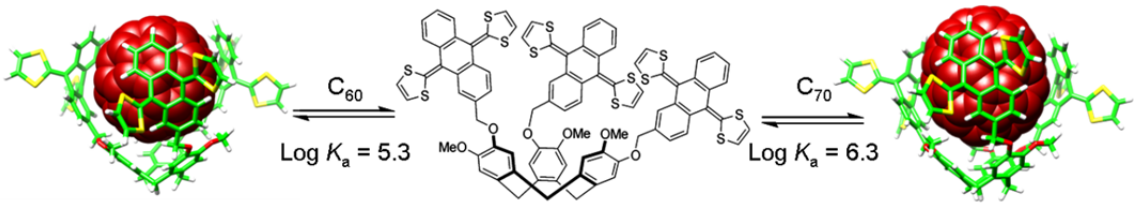

We reasoned an alternative strategy to obtain efficient exTTF-based receptors for fullerenes would be to increase the number of exTTF units in the host. We have made use of the association abilities of cyclotriveratrylenes (CTV) derivatives and exTTF units to nicely wrap fullerenes. Three exTTF units were linked to a CTV scaffols *via* Mitsunobu coupling in the synthesis of this new receptor. The association abilities with [60] and [70]fullerenes were investigated through UV-vis titrations and the analysis of the data indicate that exTTF-CTV host forms remarkably stable complexes with both C_{60} (log K_a = 5.3 ± 0.2) and C_{70} (log K_a = 6.3 ± 0.6). Evidence of association were also found in CV and NMR experiments in solution, and in the gas phase by mass spectrometry. Light-induced ESR spectra demonstrate that intracomplex PET processes take place in solution.

Elisa Huerta, Helena Isla, Emilio M. Pérez, Carles Bo, Nazario Martín and Javier de Mendoza *J. Am. Chem. Soc.* **2010**, *132*, 5351–5353

3.3. exTTF-capped gold nanoparticles as multivalent receptors.

Making use of the multivalent effect we have achieved new high affinity exTTF-based receptors for fullerenes and few layers graphene (FLG, material composed by <10 layers of graphene). The use of gold nanoparticles as support allowed the synthesis of the multivalent receptor by a very simple synthetic method. In this chapter we will describe the articles related with this receptor.

3.3.1. exTTF-capped gold nanoparticles as multivalent receptors for C_{60}

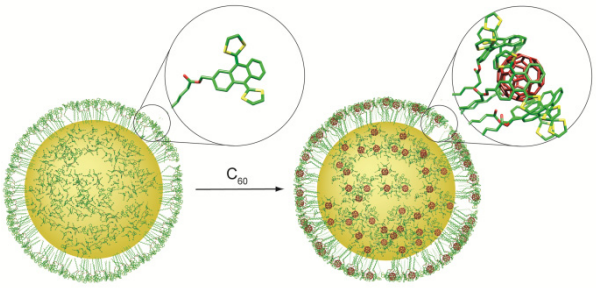

With a simple liquid-liquid extraction process we achieved exTTF-capped gold nanoparticles that show a diameter around 7 nm and are capped by approximately 500 units of exTTF. The exTTFAuNPs tend to aggregate through multiple weak exTTF-exTTF interactions in solution and in the solid state. A thorough collection of experiments demonstrates that upon addition of [60]fullerene these weak forces are

substituted with the stronger exTTF-C_{60} interactions. The binding event with concomitant partial disaggregation of the nanoparticles has been studied in solution (UV-vis , CV) and in the solid state (FTIR, AFM, TEM, EDX). The analysis of the data obtained by UV-vis titrations indicated 4:1 and 5:1 as possible exTTF:C_{60} stoichiometries with log $\beta_{5:1}$ = 22.5 (chlorobenzene, room temperature). Assuming all exTTF-C_{60} binding events present the same value, that corresponds to log $K_{1:1}$ = 4.5, indicative of a very strong multivalent effect.

Roberto Cao Jr., Helena Isla, Roberto Cao, Emilio M. Pérez and Nazario Martín *Chem. Sci.* **2011**, *2*, 1384-1388

3.3.2. Exploiting multivalent nanoparticles for the supramolecular functionalization of graphene with a non-planar recognition motif.

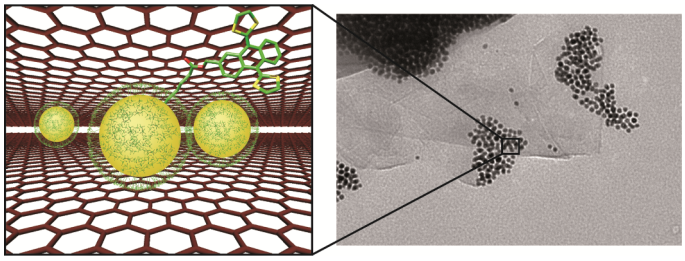

The main objective of this work was to apply the binding abilities of the exTTFAuNPs to the supramolecular modification of planar graphene or few layers graphene (FLG). Quantifying the binding constant is impossible but UV-vis titrations were performed by adding FLG suspension to an exTTFAuNPs solution in chlorobenzene. The titrations gave rise to the typical spectroscopic changes that we observed previously in the titrations against [60]fullerene. The final solution was drop-casted in different supports to visualize the association by microscopic techniques. The micrographs obtained in TEM show that the basal planes of the graphene are heavily functionalized with exTTFAuNPs, which are concentrated in areas with a higher number of graphene layers. The scrutiny of micrographs and AFM images suggest a sandwich-type nanostructure with the nanoparticles placed between the graphene layers. This work, supported by DFT calculations, show that planarity is not a prerequisite for recognition motifs for graphene.

Fulvio G. Brunetti, Helena Isla, Juan Aragó, Enrique Ortí, Emilio M. Pérez and Nazario Martín *Chem. Eur. J.* **2013**, DOI: 10.1002/chem.201301102

3.4. Bowl-shape electron donors with absorptions in the visible range of the solar spectrum and their supramolecular assemblies with C_{60}

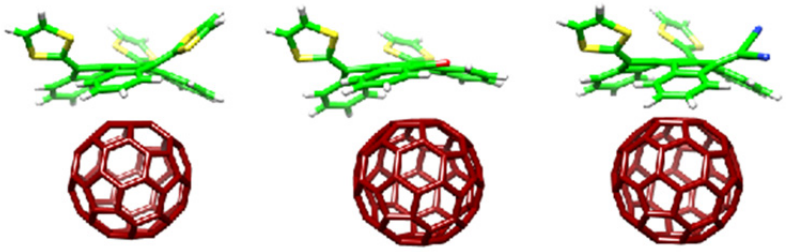

We describe the synthesis, electronic, optical, and photophysical properties of a family of three electron-donor bowl-shaped organic molecules that absorb light in the whole range of the visible spectrum (up to 800 nm in one case), and associate C_{60} in solution with binding constants in the range of 10^4–10^2 M^{-1} as measured from both UV-vis and fluorescence titrations in several solvents. These molecules are π-extended derivatives of tetrathiafulvalene, based on a truxene core to which two or three units of dithiole are covalently attached. The inclusion of the bulky dithiole groups is responsible for their bowl-shape geometry, which allows them to associate C_{60}, and their electron donor character. The symmetric derivative **7.1**, with three dithiole units, absorbs light in the 370–520 nm range. Exchanging one of the dithiole groups by an electron withdrawing group, ketone (**7.2**) or a dicyanomethylene (**7.3**), results in an intramolecular push-pull effect that expands the absorption to nearly 700 nm in the case of **7.2**, and up to 800 nm in the case of **7.3**. Transient absorption measurements, supported by spectroelectrochemical and radiolytical experiments, reveal that upon photoexcitation of the **7.1**·C_{60} associate the fully charge-separated state **7.1**$^{\bullet+}$·$C_{60}^{\bullet-}$ is generated, with lifetimes of hundreds of picoseconds. Molecular-level understanding of the electronic and supramolecular properties of **7.1**–**7.3** is provided by density functional theory calculations.

Helena Isla, Bruno Grimm, Emilio M. Pérez, M. Rosario Torres, M. Ángeles Herranz, Rafael Viruela, Juan Aragó, Enrique Ortí, Dirk M. Guldi and

Nazario Martín *Chem. Sci*., **2012**, *3*, 498–508

4. CONCLUSIONS

i) The design and synthesis of new exTTF-based receptors has been achieved by increasing the number of recognition units. We have increased the number of exTTF to three in exTTF-CTV receptor, by making use of a CTV scaffold that allows us some kind of preorganization. We have increased the number of exTTF moieties up to 500 units with a very simple synthetic method by using gold nanoparticles as scaffold. We have got a great multivalent effect with this kind of receptor.

ii) The strategy of the use of preorganized receptors has been followed in the design and synthesis of a family of bis-exTTF macrocyclic receptors. The study of these receptors shows us the importance of the macrocyclic effect.

iii) The increase of the aromatic surface of the recognition unit results in the design and synthesis of a family of truxTTF receptors, with two or three dithiole rings, that are able to associate fullerene with 1:1 stoichiometry. The change of one of the dithiole ring by a withdrawing group causes enhanced absorption properties in the visible range.

iv) The investigation of the stability of the formed complexes with fullerenes was successfully carried out and quantified by means of UV-vis titrations. The analysis of the data provides some of the larger binding constants for fullerenes with all organic receptors. We have corroborated the association event with fluorescence and NMR spectroscopy. The formation of the complexes was also evidenced by mass spectrometry in the gas phase and by microscopic techniques in the case of exTTFAuNPs as receptor.

v) Theoretical calculations have helped in the understanding of structural properties of the receptors and complexes; also have participated in combination with voltammetry measurements in the study of the electronic properties and in combination with other spectroscopic techniques in the investigation of the photophysical properties.

vi) We can conclude, after the study of all these systems, that small variation in the structure of the host or the guest causes very significant changes in the stability of the complexes, even in the stoichiometry.

vii) We have achieved the supramolecular modification of FLG with our non-planar recognition motif exTTF, proving that planarity is not a prerequisite for the association with graphene layers.

References

1. H. W. Kroto; J. R. Heath; S. C. O'Brien; R. F. Curl; R. E. Smalley, C_{60}: Buckminsterfullerene. *Nature* **1985,** *318*, 162-163.

2. (a) R. F. Curl, Dawn of Fullerenes: Conjecture and Experiment (Nobel Lecture). *Angew. Chem., Int. Ed. Engl.* **1997,** *36*, 1566-1576;(b) H. Kroto, Symmetry, Space, Stars, and C60 (Nobel Lecture). *Angew. Chem., Int. Ed. Engl.* **1997,** *36*, 1578-1593;(c) R. E. Smalley, Discovering the Fullerenes (Nobel Lecture). *Angew. Chem., Int. Ed. Engl.* **1997,** *36*, 1594-1601.

3. W. Kratschmer; L. D. Lamb; K. Fostiropoulos; D. R. Huffman, Solid C_{60}: a new form of carbon. *Nature* **1990,** *347*, 354-358.

4. (a) J. W. Arbogast; A. P. Darmanyan; C. S. Foote; F. N. Diederich; R. L. Whetten; Y. Rubin; M. M. Alvarez; S. J. Anz, Photophysical properties of sixty atom carbon molecule (C_{60}). *J. Phys. Chem.* **1991,** *95*, 11-12;(b) T. W. Ebbesen; K. Tanigaki; S. Kuroshima, Excited-state properties of C_{60}. *Chem.*

Phys. Lett. **1991,** *181*, 501-504;(c) D. M. Guldi; M. Prato, Excited-State Properties of C_{60} Fullerene Derivatives. *Acc. Chem. Res.* **2000,** *33*, 695-703.

5. K. M. Kadish; R. S. Ruoff, *Fullerenes: Chemistry, Physics, and Technology*. Wiley: 2000.

6. (a) N. Martín; L. Sánchez; B. Illescas; I. Pérez, C_{60}-Based Electroactive Organofullerenes. *Chem. Rev.* **1998,** *98*, 2527-2548;(b) H. Imahori; Y. Sakata, Fullerenes as Novel Acceptors in Photosynthetic Electron Transfer. *Eur. J. Org. Chem.* **1999,** *1999*, 2445-2457;(c) D. M. Guldi, Fullerenes: three dimensional electron acceptor materials. *Chem. Commun.* **2000,** *0*, 321-327.

7. R. R. Hung; J. J. Grabowski, A precise determination of the triplet energy of carbon (C_{60}) by photoacoustic calorimetry. *J. Phys. Chem.* **1991,** *95*, 6073-6075.

8. T. Da Ros; M. Prato, Medicinal chemistry with fullerenes and fullerene derivatives. *Chem. Commun.* **1999,** *0*, 663-669.

9. A. W. Jensen; S. R. Wilson; D. I. Schuster, Biological applications of fullerenes. *Biorg. Med. Chem.* **1996,** *4*, 767-779.

10. (a) H. Imahori; Y. Sakata, Donor-Linked Fullerenes: Photoinduced electron transfer and its potential application. *Adv. Mater.* **1997,** *9*, 537-546;(b) D. Gust; T. A. Moore; A. L. Moore, Mimicking Photosynthetic Solar Energy Transduction. *Acc. Chem. Res.* **2000,** *34*, 40-48;(c) D. M. Guldi, Fullerene-porphyrin architectures; photosynthetic antenna and reaction center models. *Chem. Soc. Rev.* **2002,** *31*, 22-36.

11. H. Imahori, Giant Multiporphyrin Arrays as Artificial Light-Harvesting Antennas. *J. Phys. Chem. B* **2004,** *108*, 6130-6143.

12. (a) D. M. Guldi; M. Maggini; G. Scorrano; M. Prato, Intramolecular Electron Transfer in Fullerene/Ferrocene Based Donor−Bridge−Acceptor Dyads. *J. Am. Chem. Soc.* **1997,** *119*, 974-980;(b) M. Fujitsuka; N. Tsuboya; R. Hamasaki; M. Ito; S. Onodera; O. Ito; Y. Yamamoto, Solvent Polarity Dependence of Photoinduced Charge Separation and Recombination Processes of Ferrocene−C60 Dyads. *J. Phys. Chem. A* **2003,** *107*, 1452-1458;(c) D. M. Guldi; C. Luo; N. A. Kotov; T. D. Ros; S. Bosi; M. Prato, Zwitterionic Acceptor Moieties: Small Reorganization Energy and Unique Stabilization of Charge Transfer Products†. *J. Phys. Chem. B* **2003,** *107*, 7293-7298.

13. (a) D. M. Guldi; M. Maggini; E. Menna; G. Scorrano; P. Ceroni; M. Marcaccio; F. Paolucci; S. Roffia, A Photosensitizer Dinuclear Ruthenium Complex: Intramolecular Energy Transfer to a Covalently Linked Fullerene Acceptor. *Chem. Eur. J.* **2001,** *7*, 1597-1605;(b) J.-F. Nierengarten; N. Armaroli; G. Accorsi; Y. Rio; J.-F. Eckert, [60]Fullerene: A Versatile Photoactive Core for Dendrimer Chemistry. *Chem. Eur. J.* **2003,** *9*, 36-41.

14. S. N. Smirnov; P. A. Liddell; I. V. Vlassiouk; A. Teslja; D. Kuciauskas; C. L. Braun; A. L. Moore; T. A. Moore; D. Gust, Characterization of the Giant Transient Dipole Generated by Photoinduced Electron Transfer in a Carotene−Porphyrin−Fullerene Molecular Triad. *J. Phys. Chem. A* **2003,** *107*, 7567-7573.

15. (a) R. M. Williams; J. M. Zwier; J. W. Verhoeven, Photoinduced Intramolecular Electron Transfer in a Bridged C_{60} (Acceptor)-Aniline (Donor) System; Photophysical Properties of the First "Active" Fullerene Diad. *J. Am. Chem. Soc.* **1995,** *117*, 4093-4099;(b) K. G. Thomas; V. Biju; D. M. Guldi; P. V. Kamat; M. V. George, Photoinduced Charge Separation and Stabilization in Clusters of a Fullerene−Aniline Dyad. *J. Phys. Chem. B* **1999,** *103*, 8864-8869.

16. (a) D. M. Guldi; C. Luo; A. Swartz; R. Gómez; J. L. Segura; N. Martín; C. Brabec; N. S. Sariciftci, Molecular Engineering of C_{60}-Based Conjugated Oligomer Ensembles: Modulating the Competition between Photoinduced Energy and Electron Transfer Processes. *J. Org. Chem.* **2002,** *67*, 1141-1152;(b) D. M. Guldi; A. Swartz; C. Luo; R. Gómez; J. L. Segura; N. Martín, Rigid Dendritic Donor−Acceptor Ensembles: Control over Energy and Electron Transduction. *J. Am. Chem. Soc.* **2002,** *124*, 10875-10886;(c) J. L. Segura; N. Martín; D. M. Guldi, Materials for organic solar cells: the C_{60}/π-conjugated oligomer approach. *Chem. Soc. Rev.* **2005,** *34*, 31-47;(d) C. M. Atienza; G. Fernández; L. Sánchez; N. Martín; I. S. Dantas; M. M. Wienk; R. A. J. Janssen; G. M. A. Rahman; D. M. Guldi, Light harvesting tetrafullerene nanoarray for organic solar cells. *Chem. Commun.* **2006,** *0*, 514-516;(e) G. Fernández; L. Sánchez; D. Veldman; M. M. Wienk; C. Atienza; D. M. Guldi; R. A. J. Janssen; N. Martín, Tetrafullerene Conjugates for All-Organic Photovoltaics. *J. Org. Chem.* **2008,** *73*, 3189-3196.

17. M. Antonietta Loi; P. Denk; H. Hoppe; H. Neugebauer; C. Winder; D. Meissner; C. Brabec; N. Serdar Sariciftci; A. Gouloumis; P. Vazquez; T. Torres, Long-lived photoinduced charge separation for solar cell applications in phthalocyanine-fulleropyrrolidine dyad thin films. *J. Mater. Chem.* **2003,** *13*, 700-704.

18. N. Martín; L. Sánchez; M. a. Á. Herranz; B. Illescas; D. M. Guldi, Electronic Communication in Tetrathiafulvalene (TTF)/C_{60} Systems: Toward Molecular Solar Energy Conversion Materials? *Acc. Chem. Res.* **2007,** *40*, 1015-1024.

19. (a) N. Martín; L. Sánchez; C. Seoane; R. Andreu; J. Garín; J. Orduna, Semiconducting charge transfer complexes from [60]Fullerene-tetrathiafulvalene (C_{60}-TTF) systems. *Tetrahedron Lett.* **1996,** *37*, 5979-5982;(b) N. Martín; L. Sánchez; M. A. Herranz; D. M. Guldi, Evidence for Two Separate One-Electron Transfer Events in Excited Fulleropyrrolidine Dyads Containing Tetrathiafulvalene (TTF). *J. Phys. Chem. A* **2000,** *104*, 4648-4657;(c) M. C. Díaz; M. A. Herranz; B. M. Illescas; N. Martín; N. Godbert; M. R. Bryce; C. Luo; A. Swartz; G. Anderson; D. M. Guldi, Probing Charge Separation in Structurally Different C_{60}/exTTF Ensembles. *J. Org. Chem.* **2003,** *68*, 7711-7721.

20. (a) Y. Yamashita; Y. Kobayashi; T. Miyashi, p-Quinodimethane Analogues of Tetrathiafulvalene. *Angew. Chem., Int. Ed. Engl.* **1989,** *28*, 1052-1053;(b) M. R. Bryce; A. J. Moore; M. Hasan; G. J. Ashwell; A. T. Fraser; W. Clegg; M. B. Hursthouse; A. I. Karaulov, Electrical and Magnetic Properties and X-Ray Structure of a Highly Conductive 4:1 Complex of Tetracyanoquinodimethane and a Tetrathiafulvalene Derivative. *Angew. Chem., Int. Ed. Engl.* **1990,** *29*, 1450-1452;(c) N. Martín; L. Sánchez; C. Seoane; E. Ortí; P. M. Viruela; R. Viruela, Synthesis, Properties, and Theoretical Characterization of Largely π-Extended Tetrathiafulvalene Derivatives with Quinonoid Structures. *J. Org. Chem.* **1998,** *63*, 1268-1279;(d) C. A. Christensen; A. S. Batsanov; M. R. Bryce, Extreme Conformational Constraints in π-Extended Tetrathiafulvalenes: Unusual Topologies and Redox Behavior of Doubly and Triply Bridged Cyclophanes. *J. Am. Chem. Soc.* **2006,** *128*, 10484-10490.

21. (a) N. Gautier; F. Dumur; V. Lloveras; J. Vidal-Gancedo; J. Veciana; C. Rovira; P. Hudhomme, Intramolecular Electron Transfer Mediated by a Tetrathiafulvalene Bridge in a Purely Organic Mixed-Valence System. *Angew. Chem. Int. Ed.* **2003,** *42*, 2765-2768;(b) M. Mas-Torrent; P. Hadley; S. T. Bromley; X. Ribas; J. Tarrés; M. Mas; E. Molins; J. Veciana; C. Rovira, Correlation between Crystal Structure and Mobility in Organic Field-Effect Transistors Based on Single Crystals of Tetrathiafulvalene Derivatives. *J. Am. Chem. Soc.* **2004,** *126*, 8546-8553.

22. (a) W. Khlbrandt; D. N. Wang, Three-dimensional structure of plant light-harvesting complex determined by electron crystallography. *Nature* **1991,** *350*, 130-134;(b) G. McDermott; S. M. Prince; A. A. Freer; A. M. Hawthornthwaite-Lawless; M. Z. Papiz; R. J. Cogdell; N. W. Isaacs, Crystal structure of an integral membrane light-harvesting complex from photosynthetic bacteria. *Nature* **1995,** *374*, 517-521.

23. C.-H. Huang; N. D. McClenaghan; A. Kuhn; J. W. Hofstraat; D. M. Bassani, Enhanced Photovoltaic Response in Hydrogen-Bonded All-Organic Devices. *Org. Lett.* **2005,** *7*, 3409-3412.

24. (a) P. M. Beaujuge; J. M. J. Fréchet, Molecular Design and Ordering Effects in π-Functional Materials for Transistor and Solar Cell Applications. *J. Am. Chem. Soc.* **2011,** *133*, 20009-20029;(b) Y.-H. Chen; L.-Y. Lin; C.-W. Lu; F. Lin; Z.-Y. Huang; H.-W. Lin; P.-H. Wang; Y.-H. Liu; K.-T. Wong; J. Wen; D. J. Miller; S. B. Darling, Vacuum-Deposited Small-Molecule Organic Solar Cells with High Power Conversion Efficiencies by Judicious Molecular Design and Device Optimization. *J. Am. Chem. Soc.* **2012,** *134*, 13616-13623.

25. L. R. MacGillivray; J. L. Atwood, Structural Classification and General Principles for the Design of Spherical Molecular Hosts. *Angew. Chem. Int. Ed.* **1999,** *38*, 1018-1033.

26. D. Canevet; E. M. Pérez; N. Martín, Wraparound Hosts for Fullerenes: Tailored Macrocycles and Cages. *Angew. Chem. Int. Ed.* **2011,** *50*, 9248-9259.

27. E. M. Pérez; N. Martín, Curves ahead: molecular receptors for fullerenes based on concave-convex complementarity. *Chem. Soc. Rev.* **2008,** *37*, 1512-1519.

28. E. M. Pérez; L. Sánchez; G. Fernández; N. Martín, exTTF as a Building Block for Fullerene Receptors. Unexpected Solvent-Dependent Positive Homotropic Cooperativity. *J. Am. Chem. Soc.* **2006,** *128*, 7172-7173.

29. E. M. Pérez; M. Sierra; L. Sánchez; M. R. Torres; R. Viruela; P. M. Viruela; E. Ortí; N. Martín, Concave Tetrathiafulvalene-Type Donors as Supramolecular Partners for Fullerenes. *Angew. Chem. Int. Ed.* **2007,** *46*, 1847-1851.

1. INTRODUCCIÓN

Los fullerenos son alótropos moleculares de carbono formados por anillos hexagonales y pentagonales fusionados, siendo los anillos pentagonales los que les otorgan su característica curvatura. El fullereno C_{60} fue descubierto por H. W. Kroto, R. F. Curl, y R. E. Smalley en 1985.[1] Esta molécula fue llamada Buckminsterfullereno en honor al arquitecto y genio americano R. Buckminster Fuller, cuyas cúpulas geodésicas fueron diseñadas bajo los mismos principios estructurales (figura 1). El [60]fullereno está compuesto por 60 átomos de carbono unidos covalentemente mediante enlaces dobles y sencillos formando 12 anillos pentagonales y 20 hexagonales- una estructura que recuerda a la de un balón de fútbol.

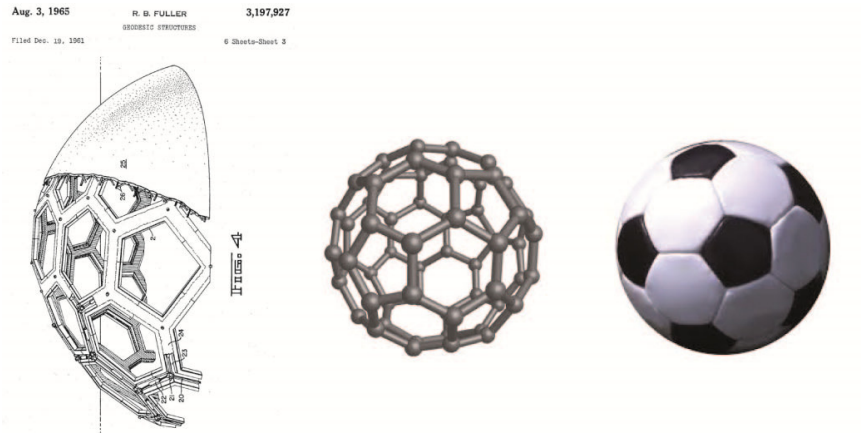

Figura 1. De izquierda a derecha: Una de las figuras de la patente de 1961 de Buckminster Fuller sobre la cúpula geodésica[2], estructura del fullereno C_{60} y un balón de fútbol.

La química supramolecular de fullerenos comenzó a desarrollarse en cuanto cantidades macroscópicas del mismo comenzaron a estar disponibles.[3] Las peculiares propiedades del fullereno, tanto electrónicas como fotofísicas,[4] le hacen un interesante sustrato también para la química supramolecular. Algunas de las propiedades más importantes que hacen al fullereno interesante para distintas aplicaciones son las siguientes:

- Es un buen aceptor de electrones.[4c, 5, 6]

[1] H. W. Kroto, J. R. Heath, S. C. O'Brien, R. F. Curl and R. E. Smalley, *Nature* **1985,** *318*, 162-163.
[2] R.Buckminster Fuller GEODESIC STRUCTURES (OCR). US 3197927, 1965.
[3] W. Kratschmer, L. D. Lamb, K. Fostiropoulos and D. R. Huffman, *Nature* **1990,** *347*, 354-358.
[4] (a) J. W. Arbogast, A. P. Darmanyan, C. S. Foote, F. N. Diederich, R. L. Whetten, Y. Rubin, M. M. Alvarez and S. J. Anz, *J. Phys. Chem.* **1991,** *95*, 11-12; (b) T. W. Ebbesen, K. Tanigaki and S. Kuroshima, *Chem. Phys. Lett.* **1991,** *181*, 501-504; (c) D. M. Guldi and M. Prato, *Acc. Chem. Res.* **2000,** *33*, 695-703.
[5] K. M. Kadish and R. S. Ruoff, *Fullerenes: Chemistry, Physics, and Technology*. Wiley: 2000.
[6] (a) N. Martín, L. Sánchez, B. Illescas and I. Pérez, *Chem. Rev.* **1998,** *98*, 2527-2548; (b) H. Imahori and Y. Sakata, *Eur. J. Org. Chem.* **1999,** *1999*, 2445-2457; (c) D. M. Guldi, *Chem. Commun.* **2000,** *0*, 321-327.

- Su LUMO permite la incorporación reversible de hasta 6 electrones.
- Tiene una baja energía de reorganización.
- Es relativamente inerte.

El LUMO triplemente degenerado y bajo en energía del fullereno le permite aceptar hasta 6 electrones de forma reversible.[5] Estas propiedades han hecho posible la síntesis de multitud de sistemas dador-aceptor en los que el fullereno funciona como aceptor. En condiciones adecuadas, la baja energía de reorganización del fullereno es responsable de cinéticas de separación de carga óptimas, y de una deceleración de la velocidad de recombinación de cargas. Esto quiere decir que la recombinación de carga en estos sistemas ocurre más despacio que la transferencia fotoelectrónica, dando lugar a estados de separación de carga con tiempos de vida relativamente largos. Gracias a esto sistemas dador-aceptor que contengan fullereno han sido propuestos como modelos fotosintéticos y como sistemas de almacenamiento de energía.[5, 6b, 7]

El comportamiento del fullereno una vez es fotoexcitado le convierte en un aceptor de electrones atractivo para dispositivos capaces de usar la energía lumínica para convertirla en energía química útil. Por otra parte, una vez fotoexcitado en presencia de oxígeno es capaz de formar fácilmente el estado excitado oxígeno singlete,[4a, 8] una especie muy reactiva. Esta capacidad de generar oxígeno singlete hace del fullereno un gran candidato para el desarrollo de nuevos agentes para terapia fotodinámica.[9] Además el hecho de ser relativamente inerte en condiciones suaves hacen de los derivados de fullereno grandes candidatos para el uso en diversas aplicaciones médicas.[10]

La transferencia electrónica fotoinducida es un proceso fundamental en la naturaleza que permite la fotosíntesis en plantas y bacterias. El ser humano necesita enfrentarse en este momento a la crisis energética en la que se encuentra, y la alternativa de desarrollar sistemas que mimeticen a la naturaleza para transformar la energía lumínica en energía química útil o electricidad se presenta como una opción prometedora. El fullereno es elegido actualmente como uno de los aceptores de electrones más adecuados en la construcción de células solares orgánicas debido a sus únicas propiedades tanto optoelectrónicas como fotofísicas. Se ha estudiado ampliamente la transferencia electrónica fotoinducida desde dadores de electrones adecuados a fullerenos.

Dentro del campo de investigación de los fullereneos, una de las líneas más activas de investigación corresponde al diseño de sistemas dador-aceptor que actúan como centros fotosintéticos artificiales. La unión covalente de dadores de electrones a fullerenos ha sido la estrategia más ampliamente usada, formando díadas, tríadas, etc. Una gran variedad de dadores de electrones han sido unidos covalentemente al fullereno

[7] (a) H. Imahori and Y. Sakata, *Adv. Mater.* **1997,** *9*, 537-546; (b) D. Gust, T. A. Moore and A. L. Moore, *Acc. Chem. Res.* **2000,** *34*, 40-48; (c) D. M. Guldi, *Chem. Soc. Rev.* **2002,** *31*, 22-36.
[8] R. R. Hung and J. J. Grabowski, *J. Phys. Chem.* **1991,** *95*, 6073-6075.
[9] T. Da Ros and M. Prato, *Chem. Commun.* **1999,** *0*, 663-669.
[10] Kadish and Ruoff; A. W. Jensen, S. R. Wilson and D. I. Schuster, *Biorg. Med. Chem.* **1996,** *4*, 767-779.

con este propósito, tales como porfirinas,[7c, 11] compuestos organometálicos como el ferroceno[12] o complejos de Ru(II), [13] carotenos, [14] derivados de anilina, [15] oligómeros π-conjugados, [16] ftalocianinas[17] y tetratiafulvalenos.[18]

En nuestro grupo se han desarrollado un gran número de díadas basadas en fullereno y derivados de tetratiafulvaleno (TTF). A diferencia de otros dadores de electrones el TTF y su derivado π-extendido exTTF se vuelven aromáticos tras su oxidación (figura 2). Esta aromatización permite llegar a especies catiónicas y dicatiónicas termodinámicamente estables a potenciales de oxidación relativamente bajos.[19] Esto es un factor crucial para la estabilidad de los pares de radicales iónicos fotogenerados, uno de los objetivos para mejorar las eficiencias en los posibles dispositivos. Además de esto, los derivados de TTF poseen una de las mayores movilidades de huecos en materiales procesados desde disolución.[20]

[11] H. Imahori, *J. Phys. Chem. B* **2004,** *108*, 6130-6143.
[12] (a) D. M. Guldi, M. Maggini, G. Scorrano and M. Prato, *J. Am. Chem. Soc.* **1997,** *119*, 974-980; (b) M. Fujitsuka, N. Tsuboya, R. Hamasaki, M. Ito, S. Onodera, O. Ito and Y. Yamamoto, *J. Phys. Chem. A* **2003,** *107*, 1452-1458; (c) D. M. Guldi, C. Luo, N. A. Kotov, T. D. Ros, S. Bosi and M. Prato, *J. Phys. Chem. B* **2003,** *107*, 7293-7298.
[13] (a) D. M. Guldi, M. Maggini, E. Menna, G. Scorrano, P. Ceroni, M. Marcaccio, F. Paolucci and S. Roffia, *Chem. Eur. J.* **2001,** *7*, 1597-1605; (b) J.-F. Nierengarten, N. Armaroli, G. Accorsi, Y. Rio and J.-F. Eckert, *Chem. Eur. J.* **2003,** *9*, 36-41.
[14] S. N. Smirnov, P. A. Liddell, I. V. Vlassiouk, A. Teslja, D. Kuciauskas, C. L. Braun, A. L. Moore, T. A. Moore and D. Gust, *J. Phys. Chem. A* **2003,** *107*, 7567-7573.
[15] (a) R. M. Williams, J. M. Zwier and J. W. Verhoeven, *J. Am. Chem. Soc.* **1995,** *117*, 4093-4099; (b) K. G. Thomas, V. Biju, D. M. Guldi, P. V. Kamat and M. V. George, *J. Phys. Chem. B* **1999,** *103*, 8864-8869.
[16] (a) D. M. Guldi, C. Luo, A. Swartz, R. Gómez, J. L. Segura, N. Martín, C. Brabec and N. S. Sariciftci, *J. Org. Chem.* **2002,** *67*, 1141-1152; (b) D. M. Guldi, A. Swartz, C. Luo, R. Gómez, J. L. Segura and N. Martín, *J. Am. Chem. Soc.* **2002,** *124*, 10875-10886; (c) J. L. Segura, N. Martín and D. M. Guldi, *Chem. Soc. Rev.* **2005,** *34*, 31-47; (d) C. M. Atienza, G. Fernández, L. Sánchez, N. Martín, I. S. Dantas, M. M. Wienk, R. A. J. Janssen, G. M. A. Rahman and D. M. Guldi, *Chem. Commun.* **2006,** *0*, 514-516; (e) G. Fernández, L. Sánchez, D. Veldman, M. M. Wienk, C. Atienza, D. M. Guldi, R. A. J. Janssen and N. Martín, *J. Org. Chem.* **2008,** *73*, 3189-3196.
[17] M. Antonietta Loi, P. Denk, H. Hoppe, H. Neugebauer, C. Winder, D. Meissner, C. Brabec, N. Serdar Sariciftci, A. Gouloumis, P. Vazquez and T. Torres, *J. Mater. Chem.* **2003,** *13*, 700-704.
[18] N. Martín, L. Sánchez, M. a. Á. Herranz, B. Illescas and D. M. Guldi, *Acc. Chem. Res.* **2007,** *40*, 1015-1024.
[19] (a) Y. Yamashita, Y. Kobayashi and T. Miyashi, *Angew. Chem., Int. Ed. Engl.* **1989,** *28*, 1052-1053; (b) M. R. Bryce, A. J. Moore, M. Hasan, G. J. Ashwell, A. T. Fraser, W. Clegg, M. B. Hursthouse and A. I. Karaulov, *Angew. Chem., Int. Ed. Engl.* **1990,** *29*, 1450-1452; (c) N. Martín, L. Sánchez, C. Seoane, E. Ortí, P. M. Viruela and R. Viruela, *J. Org. Chem.* **1998,** *63*, 1268-1279; (d) C. A. Christensen, A. S. Batsanov and M. R. Bryce, *J. Am. Chem. Soc.* **2006,** *128*, 10484-10490.
[20] (a) N. Gautier, F. Dumur, V. Lloveras, J. Vidal-Gancedo, J. Veciana, C. Rovira and P. Hudhomme, *Angew. Chem. Int. Ed.* **2003,** *42*, 2765-2768; (b) M. Mas-Torrent, P. Hadley, S. T. Bromley, X. Ribas, J. Tarrés, M. Mas, E. Molins, J. Veciana and C. Rovira, *J. Am. Chem. Soc.* **2004,** *126*, 8546-8553.

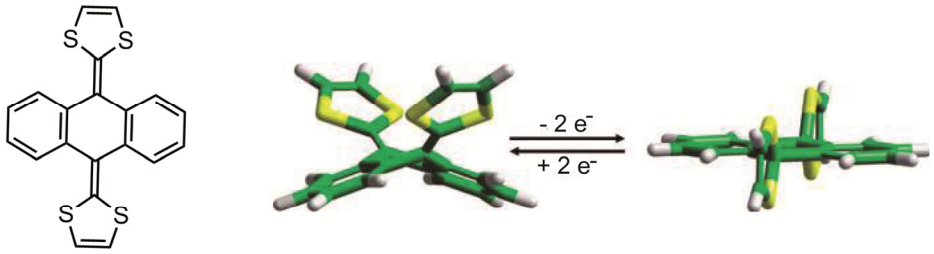

Figura 2. Estructura de la molécula exTTF, y geometría de la especie en estado fundamental (izquierda) y de la especie dicatiónica $exTTF^{2+}$ (derecha).

Los factores que impulsaron al cambio de estrategia basado en la química supramolecular de fullerenos son los siguientes: i) la relación entre dador y aceptor en el centro de reacción fotosintético se lleva a cabo mediante interacciones no covalentes;[21] ii) la transferencia electrónica fotoinducida entre un dador y el fullereno puede darse a través del espacio; iii) se espera que la organización nanométrica de los materiales tipo n y tipo p en los dispositivos facilite la movilidad de carga, previniendo así la recombinación.[22]

Por tanto, la búsqueda de receptores para fullereno es incentivada principalmente por dos razones: la búsqueda de nuevos y simples métodos de purficación de los distintos fullerenos desde mezclas complejas de fullerita, y la formación de sistemas nanoestructurados que involucren al fullereno con la intención de mejorar las eficiencias de posibles dispositivos fotovoltaicos.

Tanto para su purificación como para la elaboración de sistemas electroactivos nanoestructurados nuestro principal objetivo es conseguir unos complejos con fullereno con la mayor estabilidad posible. El diseño de receptores específicos para fullereno nos obliga a tener en cuenta las peculiares propiedades de nuestro sustrato. Dado que el fullereno se comporta como un polieno sin funcionalidad no podemos usar interacciones supramoleculares direccionales como puentes de hidrógeno. Sin embargo, su superficie esférica, con la mayor relación superficie/volumen posible nos indica que debemos usar las interacciones de tipo dispersivo, que dependen del área de interacción, como π–π, Van der Waals y solvofóbicas.

En el desarrollo de la química supramolecular de fullerenos llevado a cabo en el grupo se elige la unidad de exTTF como principal unidad de reconocimiento de fullerenos. El exTTF es una molécula dadora, con una fuerte absorción en el visible y con una geometría cóncava que le permitiría abarcar la superficie convexa del fullereno. Para la elaboración de este trabajo se toman como antecedentes más importantes los

[21] (a) W. Khlbrandt and D. N. Wang, *Nature* **1991,** *350*, 130-134; (b) G. McDermott, S. M. Prince, A. A. Freer, A. M. Hawthornthwaite-Lawless, M. Z. Papiz, R. J. Cogdell and N. W. Isaacs, *Nature* **1995,** *374*, 517-521.
[22] C.-H. Huang, N. D. McClenaghan, A. Kuhn, J. W. Hofstraat and D. M. Bassani, *Org. Lett.* **2005,** *7*, 3409-3412.

receptores pinza-exTTF[23] anteriormente publicadas por el grupo y los receptores truxTTF[24] en los que un esqueleto de truxeno se ocupa de ampliar la parte aromática y cóncava del receptor (figura 3).

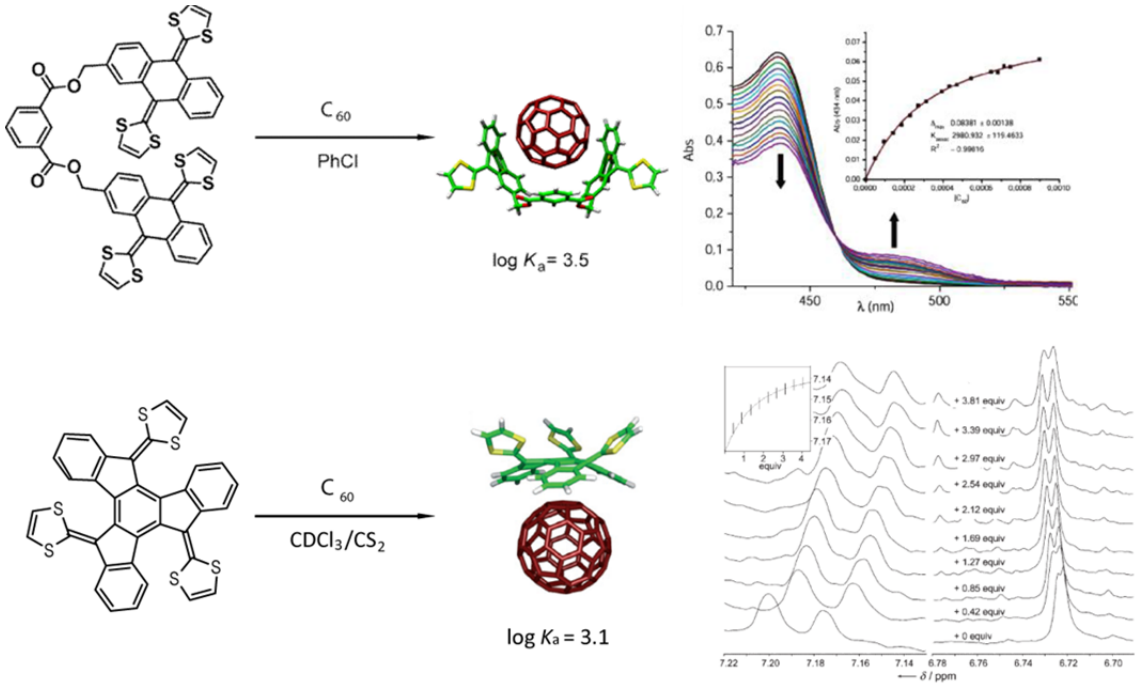

Figura 3. Arriba: Estructura del receptor pinza-exTTF y modelo del complejo tras la asociación de C_{60}. A la derecha se muestra la valoración UV-vis del mismo en clorobenceno a temperatura ambiente, insertada se muestra la isoterma de enlace. Abajo: Estructura del receptor truxTTF y modelo del complejo tras la asociación de C_{60}. A la derecha se muestran los cambios en el espectro parcial de ^{1}H RMN en cloroformo deuterado/disulfuro de carbono a temperatura ambiente, insertada se muestra la isoterma de enlace.

Las propiedades complementarias de la unidad de exTTF respecto al fullereno le hacen un candidato idóneo para la asociación de fullereno. Sin embargo, experimentalmente observamos que una única unidad de exTTF no es suficiente para asociar fullereno. La estrategia que se siguió entonces fue el diseño de estas sencillas pinzas en las que dos unidades de exTTF se unen mediante un espaciador aromático. Con este diseño se logra una asociación respetable con el fullereno C_{60} si tenemos en cuenta su falta de preorganización.

Un nuevo derivado del tetratiafulvaleno, el truxeno TTF (truxTTF), se diseña con la idea de conseguir una unidad de reconocimiento suficiente por sí sola para asociar fullereno. Se elige un esqueleto aromático de truxeno en el que se unen tres anillos 1,3-ditiol. Con este diseño se pretende extender la absorción en el visible gracias a su

[23] E. M. Pérez, L. Sánchez, G. Fernández and N. Martín, *J. Am. Chem. Soc.* **2006,** *128*, 7172-7173.
[24] E. M. Pérez, M. Sierra, L. Sánchez, M. R. Torres, R. Viruela, P. M. Viruela, E. Ortí and N. Martín, *Angew. Chem. Int. Ed.* **2007,** *46*, 1847-1851.

esqueleto conjugado. Las repulsiones provocadas entre los anillos de ditiol y el esqueleto de truxeno le hacen tomar una geometría cóncava que se adapta muy bien a la superficie convexa del fullereno. También con este receptor se consigue la asociación con fullerenos C_{60} y C_{70}.

2. OBJETIVOS

La presente tesis tiene como objetivo principal el diseño y síntesis de nuevos receptores basados en exTTF con gran afinidad con los fullerenos. Para conseguir este objetivo principal seguiremos diferentes estrategias:

i) Incrementar el número de unidades de reconocimiento.

ii) Aumentar la preorganización en el diseño de los receptores.

iii) Expandir la superficie aromática y el número de anillos de ditiol en el motivo de reconocimiento

Como parte del estudio de las propiedades de estos nuevos receptores investigaremos:

iv) El proceso de asociación en disolución, a través de valoraciones UV-vis, fluorescencia y RMN; en fase gas, a través de espectrometría de masas; en fase sólida, a través de cristalografía rayos-X y técnicas microscópicas.

v) Las propiedades estructurales, electrónicas y fotofísicas de los receptores y los complejos supramoleculares, a través de una combinación de técnicas espectroscópicas y cálculos teóricos.

vi) Las relaciones entre estructura y afinidad, esto quiere decir cómo afectan los cambios estructurales de los receptores a la capacidad de asociación de fullerenos.

vii) La asociación de alguno de los receptores con otras nanoformas del carbono, en concreto con el grafeno.

3. RESULTADOS

Se resumen aquí los siete artículos que conforman los capítulos centrales de la presente tesis.

3.1. Bis exTTF macrocyclic receptors

Explotando la complementareidad geométrica y electrónica de C_{60} y C_{70} con derivados π-extendidos del tetratiafulvaleno (exTTF), hemos descrito una familia de receptores macrocíclicos basados en unidades de exTTF. En este capítulos se recogen los artículos relacionados con este proyecto.

3.1.1. A bis-exTTF macrocyclic receptor that associates C_{60} with micromolar affinity

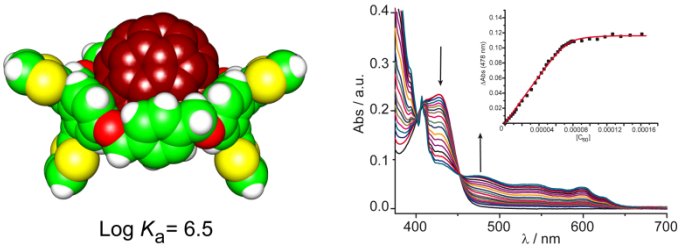

El diseño de este nuevo receptor bis-exTTF con dos unidades de exTTF como principales unidades de reconocimiento de fullerenos demuestra la importancia de la preorganización, y en concreto del efecto macrociclo. Se describe un receptor macrocíclico basado en dos unidades de exTTF conectadas mediante un espaciador aromático y otro alquenílico. Las propiedades de asociación de este macrociclo fueron estudiadas mediante valoraciones UV-vis con [60] y [70]fullereno, resultando en datos que muestran que asocia C_{60} y C_{70} con una constante de asociación de log K_a = 6.5 en clorobenceno a temperatura ambiente. Esto representa una mejora de tres órdenes de magnitud con respecto a los ejemplos previos de receptores basados en exTTF, y una de las mayores constantes de asociación con C_{60} descritas hasta la fecha.

Helena Isla, María Gallego, Emilio M. Pérez, Rafael Viruela, Enrique Ortí y Nazario Martín *J. Am. Chem. Soc*. **2010**, *132*, 1772–1773

3.1.2. Macrocyclic hosts for fullerenes: extreme changes in binding abilities with small structural variations

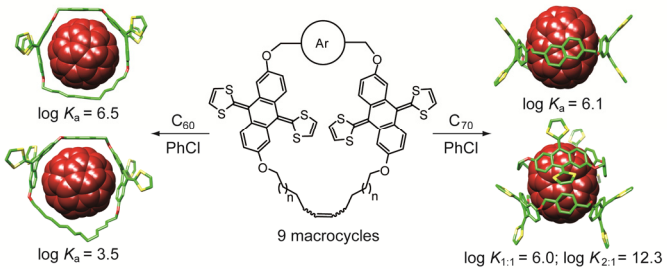

En este trabajo describimos nuestros esfuerzos por ajustar nuestros receptores macrocíclicos para asociar C_{60} y/o C_{70}, a través de variaciones estructurales. Basados en la modelización molecular preliminar, hemos probado el *p*-xileno, *m*-xileno y 2,6-dimetilnaftaleno como espaciadores aromáticos entre los dos fragmentos de exTTF y tres cadenas de distinta longitud terminadas en alqueno para obtener macrociclos de distinto tamaño a través de la metátesis de cierre de anillo (RCM). Gracias a la simplicidad de nuestro diseño, los nueve receptores son de fácil acceso sintético. Se ha llevado a cabo una investigación minuciosa de las capacidades de asociación de C_{60} y C_{70} por medio de valoraciones UV-vis. Hemos encontrado que relativamente pequeñas variaciones en la estructura del receptor suponen cambios significativos en la afinidad por los fullerenos, incluso en algunos casos en la estequiometría de los complejos.

Nuestros resultados resaltan la peculiaridad del fullereno como sustrato en el reconocimiento molecular. La extrema estabilidad de estos complejos en disolución, así como la única combinación de complementariedad electrónica y geométrica entre exTTF y fullerenos son las principales características de esta nueva familia de receptores macrocíclicos para fullerenos.

David Canevet, María Gallego, Helena Isla, Alberto de Juan, Emilio M. Pérez y Nazario Martín *J. Am. Chem. Soc*. **2011**, *133*, 3184–3190

3.1.3. Balancing binding strength and charge transfer lifetime in supramolecular associates of fullerenes

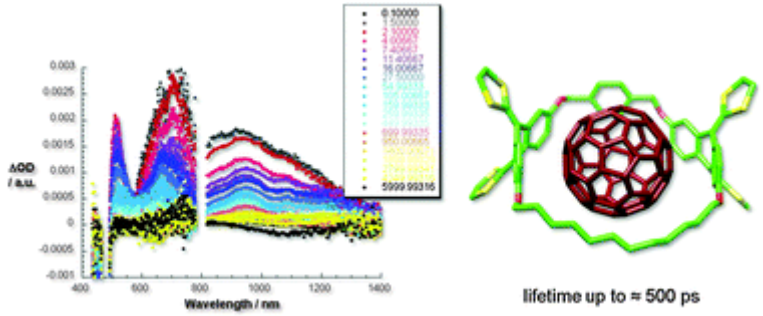

Se llevaron a cabo estudios fotofísicos del primer receptor bis-exTTF macrocíclico descrito. Además de corroborar los estudios de asociación con C_{60} y C_{70} mediante valoraciones de fluorescencia y absorción en distintos disolventes, se estudió también el comportamiento del complejo tras irradiación con luz. La transferencia de carga en el complejo fue comprobada y el estudio de las medidas de absorción transitoria indica que tras la irradiación se produce un proceso de transferencia electrónica fotoinducida (PET) que da lugar a la formación de especies con separación de cargas con unos tiempos de vida en el rango de los 500 ps.

Bruno Grimm, Helena Isla, Emilio M Pérez, Nazario Martín y Dirk M. Guldi *Chem. Commun.,* **2011***, 47,* 7449-7451

3.2. Tripodal exTTF-CTV Hosts for Fullerenes

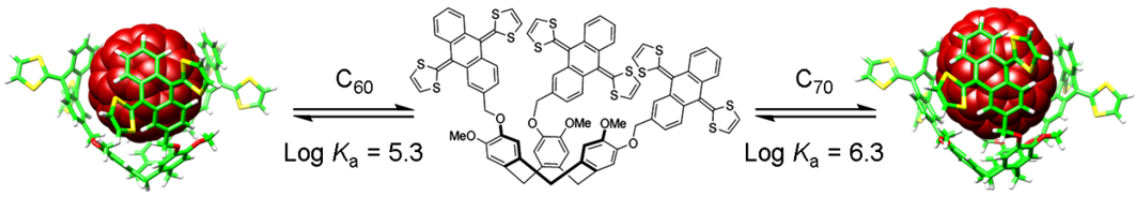

Para el diseño de un nuevo receptor para fullerenos se tuvieron en cuenta las capacidades de asociación de fullerenos de las unidades de ciclotriveratrileno (CTV) y exTTF. Se aumentaron las unidades de exTTF en el receptor respecto a receptores basados en unidades de exTTF previamente descritos, y la unidad de CTV ha sido empleada como esqueleto, incrementando también la preorganización del receptor. Se

describe por lo tanto un receptor para fullerenos compuesto por tres unidades de exTTF unidas covalentemente a un esqueleto de ciclotriveratrileno (CTV) mediante un acoplamiento de Mitsunobu. El receptor exTTF-CTV forma complejos muy estables tanto con C_{60} (log K_a = 5.3 ± 0.2) como con C_{70} (log K_a = 6.3 ± 0.6). Las constantes de asociación fueron calculadas mediante el análisis de los datos obtenidos en los cambios en el espectro UV-vis del receptor durante la valoración con fullerenos. Otras pruebas de asociación fueron también encontradas en la electroquímica del receptor en presencia del fullereno, en distintos experimentos de resonancia magnética nuclear y en fase gas en los experimentos MALDI-TOF de mezclas de fullerenos y receptor.

Elisa Huerta, Helena Isla, Emilio M. Pérez, Carles Bo, Nazario Martín y Javier de Mendoza *J. Am. Chem. Soc.* **2010**, *132*, 5351–5353

3.3. exTTF-capped gold nanoparticles as multivalent receptors.

Haciendo uso del efecto multivalente se han conseguido nuevos receptores basados en unidades de exTTF con gran afinidad por el [60]fullereno y grafeno mediante un proceso sintético muy sencillo. En este capítulo se resumen los artículos que se basan en este receptor.

3.3.1. exTTF-capped gold nanoparticles as multivalent receptors for C_{60}

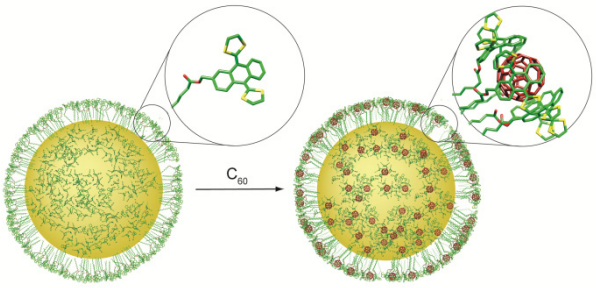

La estrategia seguida en el diseño de este receptor ha sido el incremento de unidades de reconocimiento, exTTF. Con el recubrimiento de nanopartículas de oro (AuNP) en un sencillo proceso de transferencia de fase se consiguen AuNPs con un tamaño alrededor de los 7 nm que contienen un número aproximado de 500 unidades de exTTF. Las exTTFAuNPs muestran una fuerte tendencia a agregar en disolución y en estado sólido por medio de múltiples interacciones débiles exTTF-exTTF. Una minuciosa colección de experimentos demuestra que tras la adición de C_{60}, se forman asociaciones estables no covalentes exTTFAuNP•C_{60}, con la simultánea desagregación de las nanopartículas. El estudio de los datos tomados en las valoraciones UV-vis de estas nanopartículas con [60]fullereno conducen a estequiometrías exTTF:C_{60} de entre 4:1 y 5:1 con log $\beta_{5:1}$ = 22.5, lo que suponiendo una capacidad de asociación regular equivale a constantes de asociación log $K_{1:1}$ = 4.5 para cada unidad de exTTF. Estos valores son superiores incluso a la constante de asociación de las pinzas-exTTF previamente

publicadas que contenían dos unidades de reconocimiento cada una, haciendo evidente el fuerte efecto multivalente conseguido.

Roberto Cao Jr., Helena Isla, Roberto Cao, Emilio M. Pérez y Nazario Martín *Chem. Sci.* **2011**, *2*, 1384-1388

3.3.2. Exploiting multivalent nanoparticles for the supramolecular functionalization of graphene with a non-planar recognition motif.

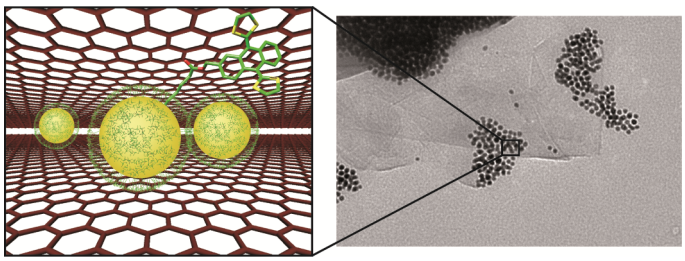

El principal objetivo de este trabajo es aplicar la capacidad de asociación de estas nanopartículas exTTFAuNPs en la modificación supramolecular de la superficie plana del grafeno. El grafeno de pocas capas (FLG) fue obtenido mediante exfoliación de grafito en disolventes orgánicos adecuados. Aunque no es posible la cuantificación de la constante de asociación se realizaron valoraciones UV-vis de las nanopartículas con la adición de alícuotas de una suspensión de FLG, que dieron lugar a los cambios espectrales típicos que encontramos previamente en la interacción exTTFAuNP-fullereno. Las imágenes obtenidas con distintas técnicas de microscopía demuestran la colocación de las nanopartículas en el grafeno y sugieren la formación de una estructura de tipo sándwich. En esta estructura las exTTFAuNPs se colocan entre capas de grafeno maximizando así el número de interacciones posibles, lo cual es razonable en términos de estabilidad termodinámica. Este trabajo, corroborado por los cálculos teóricos, demuestra que la planaridad no es un requisito imprescindible en la asociación del grafeno, ampliando así las posibilidades en la química supramolecular de este material.

Fulvio G. Brunetti, Helena Isla, Juan Aragó, Enrique Ortí, Emilio M. Pérez y Nazario Martín *Chem. Eur. J.* **2013**, DOI: 10.1002/chem.201301102

3.4. Bowl-shape electron donors with absorptions in the visible range of the solar spectrum and their supramolecular assemblies with C_{60}

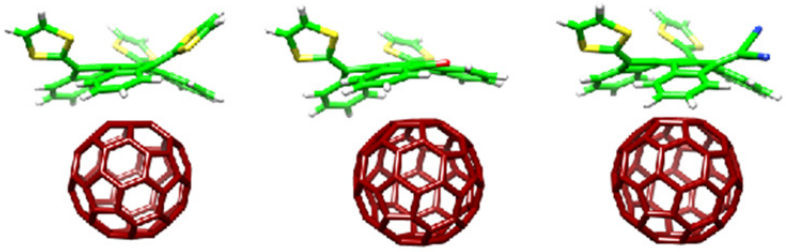

Se describe la síntesis y propiedades electrónicas, ópticas y fotofísicas de tres moléculas orgánicas electrodadoras con forma cóncava que absorben luz en todo el rango del espectro visible (hasta 800 nm en uno de los casos), y asocian C_{60} en disolución con constantes de asociación en el rango de 10^4-10^2 M^{-1} medidas mediante valoraciones UV-vis y de fluorescencia en varios disolventes. Éstas son derivados π-extendidos de tetratiafulvaleno, basadas en un esqueleto de truxeno al que se unen covalentemente dos o tres unidades de ditiol. La inclusión de los voluminosos grupos ditiol es la responsable de su carácter electrodador, y de su geometría cóncava, que les permite la asociación con C_{60}. El derivado simétrico **7.1** (truxTTF en figura 3), con tres unidades de ditiol, absorbe luz en el rango de 370-520 nm. Intercambiando uno de los grupos ditiol por un grupo electroaceptor, cetona (**7.2**) o dicianometileno (**7.3**), resulta en un efecto push-pull intramolecular que expande la absorción a cerca de 700 nm en el caso de **7.2**, y hasta los 800 nm en el caso de **7.3**. Medidas de absorción transitoria, apoyadas por experimentos espectroelectroquímicos y radiolíticos, revelan que tras la fotoexcitación del complejo **7.1**·C_{60} se genera el estado de total separación de cargas **7.1**$^{\bullet+}$·$C_{60}^{\bullet-}$, con tiempos de vida de cientos de picosegundos. La comprensión de las propiedades electrónicas y supramoleculares en **7.1-3** es proporcionada por los cálculos realizados mediante la teoría de densidad de funcional (DFT).

Helena Isla, Bruno Grimm, Emilio M. Pérez, M. Rosario Torres, M. Ángeles Herranz, Rafael Viruela, Juan Aragó, Enrique Ortí, Dirk M. Guldi y Nazario Martín *Chem. Sci*., **2012**, *3*, 498–508

4. CONCLUSIONES

- Se han diseñado, sintetizado, caracterizado y estudiado las propiedades de receptores basados en unidades de exTTF que asocian fullerenos con gran afinidad siguiendo estrategias de aumento de unidades de reconocimiento, preorganización, y extensión de la parte aromática de la unidad de reconocimiento.

- Mediante la estrategia de aumento de unidades de reconocimiento se ha llegado al receptor exTTF-CTV, con tres unidades de exTTF y un esqueleto de CTV que aporta cierto grado de preorganización. Se ha potenciado esta estrategia con el uso de nanopartículas de oro como soporte, permitiendo un fácil acceso a

receptores que constan de aproximadamente 500 unidades de exTTF y muestran un gran efecto multivalente.

- Con una mayor preorganización se elabora una colección de receptores bis-exTTF macrocíclicos que demuestran la importancia del efecto macrociclo con tres órdenes de magnitud de diferencia respecto a las constantes de asociación de análogos acíclicos.

- Incrementando la superficie aromática de la unidad de exTTF se elaboran receptores basados en un esqueleto de truxeno que mantienen las propiedades de asociación con una mejora en las propiedades de absorción de luz que se extiende en casi todo el visible.

- Las propiedades de asociación de los distintos receptores sintetizados fueron estudiadas mediante distintas técnicas espectroscópicas en disolución (UV-vis, RMN, fluorescencia), en fase gas (espectrometría de masas) y en fase sólida (distintas técnicas microscópicas). Todas las técnicas concluyen interacción entre receptor y huésped, y el tratamiento de los datos en software de análisis multivariable de las valoraciones espectroscópicas nos ha permitido cuantificar estos eventos de asociación mediante el cálculo de constantes de asociación. Éste cálculo se ha realizado principalmente con los datos de valoraciones UV-vis.

- Las propiedades electrónicas, estructurales y fotofísicas de los distintos compuestos así como de los complejos supramoleculares se han estudiado mediante una combinación de cálculos teóricos y medidas espectroscópicas. Las voltamperometrías cíclicas junto con los cálculos muestran distinta comunicación electrónica entre receptores y huéspedes. Las medidas fotofísicas nos han facilitado datos del comportamiento de los distintos receptores y complejos tras irradiación con luz.

- El estudio del sistema formado por nuestro receptor multivalente exTTFAuNPs junto con FLG nos permite concluir que la planaridad no es un requisito imprescindible para la modificación supramolecular de esta nanoforma del carbono plana.

- Pequeñas variaciones estructurales en los receptores causan cambios significantes en la afinidad por los fullerenos, observando incluso cambios en la estequiometría.

- Los resultados expuestos en la presente tesis consolidan a los derivados π-extendidos del TTF como uno de los fragmentos más adecuados para el reconocimiento molecular de fullerenos y abre la posibilidad a los receptores no-planos para el reconocimiento del grafeno.

Referencias

1. H. W. Kroto; J. R. Heath; S. C. O'Brien; R. F. Curl; R. E. Smalley, C_{60}: Buckminsterfullerene. *Nature* **1985,** *318*, 162-163.
2. R.Buckminster Fuller GEODESIC STRUCTURES (OCR). US 3197927, 1965.
3. W. Kratschmer; L. D. Lamb; K. Fostiropoulos; D. R. Huffman, Solid C_{60}: a new form of carbon. *Nature* **1990,** *347*, 354-358.
4. (a) J. W. Arbogast; A. P. Darmanyan; C. S. Foote; F. N. Diederich; R. L. Whetten; Y. Rubin; M. M. Alvarez; S. J. Anz, Photophysical properties of sixty atom carbon molecule (C_{60}). *J. Phys. Chem.* **1991,** *95*, 11-12;(b) T. W. Ebbesen; K. Tanigaki; S. Kuroshima, Excited-state properties of C_{60}. *Chem. Phys. Lett.* **1991,** *181*, 501-504;(c) D. M. Guldi; M. Prato, Excited-State Properties of C_{60} Fullerene Derivatives. *Acc. Chem. Res.* **2000,** *33*, 695-703.
5. K. M. Kadish; R. S. Ruoff, *Fullerenes: Chemistry, Physics, and Technology*. Wiley: 2000.
6. (a) N. Martín; L. Sánchez; B. Illescas; I. Pérez, C_{60}-Based Electroactive Organofullerenes. *Chem. Rev.* **1998,** *98*, 2527-2548;(b) H. Imahori; Y. Sakata, Fullerenes as Novel Acceptors in Photosynthetic Electron Transfer. *Eur. J. Org. Chem.* **1999,** *1999*, 2445-2457;(c) D. M. Guldi, Fullerenes: three dimensional electron acceptor materials. *Chem. Commun.* **2000,** *0*, 321-327.
7. (a) H. Imahori; Y. Sakata, Donor-Linked Fullerenes: Photoinduced electron transfer and its potential application. *Adv. Mater.* **1997,** *9*, 537-546;(b) D. Gust; T. A. Moore; A. L. Moore, Mimicking Photosynthetic Solar Energy Transduction. *Acc. Chem. Res.* **2000,** *34*, 40-48;(c) D. M. Guldi, Fullerene-porphyrin architectures; photosynthetic antenna and reaction center models. *Chem. Soc. Rev.* **2002,** *31*, 22-36.
8. R. R. Hung; J. J. Grabowski, A precise determination of the triplet energy of carbon (C_{60}) by photoacoustic calorimetry. *J. Phys. Chem.* **1991,** *95*, 6073-6075.
9. T. Da Ros; M. Prato, Medicinal chemistry with fullerenes and fullerene derivatives. *Chem. Commun.* **1999,** *0*, 663-669.
10. A. W. Jensen; S. R. Wilson; D. I. Schuster, Biological applications of fullerenes. *Biorg. Med. Chem.* **1996,** *4*, 767-779.
11. H. Imahori, Giant Multiporphyrin Arrays as Artificial Light-Harvesting Antennas. *J. Phys. Chem. B* **2004,** *108*, 6130-6143.
12. (a) D. M. Guldi; M. Maggini; G. Scorrano; M. Prato, Intramolecular Electron Transfer in Fullerene/Ferrocene Based Donor−Bridge−Acceptor Dyads. *J. Am. Chem. Soc.* **1997,** *119*, 974-980;(b) M. Fujitsuka; N. Tsuboya; R. Hamasaki; M. Ito; S. Onodera; O. Ito; Y. Yamamoto, Solvent Polarity Dependence of Photoinduced Charge Separation and Recombination Processes of Ferrocene−C60 Dyads. *J. Phys. Chem. A* **2003,** *107*, 1452-1458;(c) D. M. Guldi; C. Luo; N. A. Kotov; T. D. Ros; S. Bosi; M. Prato, Zwitterionic Acceptor Moieties: Small Reorganization Energy and Unique Stabilization of Charge Transfer Products†. *J. Phys. Chem. B* **2003,** *107*, 7293-7298.
13. (a) D. M. Guldi; M. Maggini; E. Menna; G. Scorrano; P. Ceroni; M. Marcaccio; F. Paolucci; S. Roffia, A Photosensitizer Dinuclear Ruthenium Complex: Intramolecular Energy Transfer to a Covalently Linked Fullerene Acceptor. *Chem. Eur. J.* **2001,** *7*, 1597-1605;(b) J.-F. Nierengarten; N. Armaroli; G. Accorsi; Y. Rio; J.-F. Eckert, [60]Fullerene: A Versatile Photoactive Core for Dendrimer Chemistry. *Chem. Eur. J.* **2003,** *9*, 36-41.
14. S. N. Smirnov; P. A. Liddell; I. V. Vlassiouk; A. Teslja; D. Kuciauskas; C. L. Braun; A. L. Moore; T. A. Moore; D. Gust, Characterization of the Giant Transient Dipole Generated by Photoinduced Electron Transfer in a Carotene−Porphyrin−Fullerene Molecular Triad. *J. Phys. Chem. A* **2003,** *107*, 7567-7573.
15. (a) R. M. Williams; J. M. Zwier; J. W. Verhoeven, Photoinduced Intramolecular Electron Transfer in a Bridged C_{60} (Acceptor)-Aniline (Donor) System; Photophysical Properties of the First "Active" Fullerene Diad. *J. Am. Chem. Soc.* **1995,** *117*, 4093-4099;(b) K. G. Thomas; V. Biju; D. M. Guldi; P. V. Kamat; M. V. George, Photoinduced Charge Separation and Stabilization in Clusters of a Fullerene−Aniline Dyad. *J. Phys. Chem. B* **1999,** *103*, 8864-8869.
16. (a) D. M. Guldi; C. Luo; A. Swartz; R. Gómez; J. L. Segura; N. Martín; C. Brabec; N. S. Sariciftci, Molecular Engineering of C_{60}-Based Conjugated Oligomer Ensembles: Modulating the Competition between Photoinduced Energy and Electron Transfer Processes. *J. Org. Chem.* **2002,** *67*,

1141-1152;(b) D. M. Guldi; A. Swartz; C. Luo; R. Gómez; J. L. Segura; N. Martín, Rigid Dendritic Donor−Acceptor Ensembles: Control over Energy and Electron Transduction. *J. Am. Chem. Soc.* **2002,** *124*, 10875-10886;(c) J. L. Segura; N. Martín; D. M. Guldi, Materials for organic solar cells: the C_{60}/π-conjugated oligomer approach. *Chem. Soc. Rev.* **2005,** *34*, 31-47;(d) C. M. Atienza; G. Fernández; L. Sánchez; N. Martín; I. S. Dantas; M. M. Wienk; R. A. J. Janssen; G. M. A. Rahman; D. M. Guldi, Light harvesting tetrafullerene nanoarray for organic solar cells. *Chem. Commun.* **2006,** *0*, 514-516;(e) G. Fernández; L. Sánchez; D. Veldman; M. M. Wienk; C. Atienza; D. M. Guldi; R. A. J. Janssen; N. Martín, Tetrafullerene Conjugates for All-Organic Photovoltaics. *J. Org. Chem.* **2008,** *73*, 3189-3196.

17. M. Antonietta Loi; P. Denk; H. Hoppe; H. Neugebauer; C. Winder; D. Meissner; C. Brabec; N. Serdar Sariciftci; A. Gouloumis; P. Vazquez; T. Torres, Long-lived photoinduced charge separation for solar cell applications in phthalocyanine-fulleropyrrolidine dyad thin films. *J. Mater. Chem.* **2003,** *13*, 700-704.

18. N. Martín; L. Sánchez; M. a. Á. Herranz; B. Illescas; D. M. Guldi, Electronic Communication in Tetrathiafulvalene (TTF)/C_{60} Systems: Toward Molecular Solar Energy Conversion Materials? *Acc. Chem. Res.* **2007,** *40*, 1015-1024.

19. (a) Y. Yamashita; Y. Kobayashi; T. Miyashi, p-Quinodimethane Analogues of Tetrathiafulvalene. *Angew. Chem., Int. Ed. Engl.* **1989,** *28*, 1052-1053;(b) M. R. Bryce; A. J. Moore; M. Hasan; G. J. Ashwell; A. T. Fraser; W. Clegg; M. B. Hursthouse; A. I. Karaulov, Electrical and Magnetic Properties and X-Ray Structure of a Highly Conductive 4:1 Complex of Tetracyanoquinodimethane and a Tetrathiafulvalene Derivative. *Angew. Chem., Int. Ed. Engl.* **1990,** *29*, 1450-1452;(c) N. Martín; L. Sánchez; C. Seoane; E. Ortí; P. M. Viruela; R. Viruela, Synthesis, Properties, and Theoretical Characterization of Largely π-Extended Tetrathiafulvalene Derivatives with Quinonoid Structures. *J. Org. Chem.* **1998,** *63*, 1268-1279;(d) C. A. Christensen; A. S. Batsanov; M. R. Bryce, Extreme Conformational Constraints in π-Extended Tetrathiafulvalenes: Unusual Topologies and Redox Behavior of Doubly and Triply Bridged Cyclophanes. *J. Am. Chem. Soc.* **2006,** *128*, 10484-10490.

20. (a) N. Gautier; F. Dumur; V. Lloveras; J. Vidal-Gancedo; J. Veciana; C. Rovira; P. Hudhomme, Intramolecular Electron Transfer Mediated by a Tetrathiafulvalene Bridge in a Purely Organic Mixed-Valence System. *Angew. Chem. Int. Ed.* **2003,** *42*, 2765-2768;(b) M. Mas-Torrent; P. Hadley; S. T. Bromley; X. Ribas; J. Tarrés; M. Mas; E. Molins; J. Veciana; C. Rovira, Correlation between Crystal Structure and Mobility in Organic Field-Effect Transistors Based on Single Crystals of Tetrathiafulvalene Derivatives. *J. Am. Chem. Soc.* **2004,** *126*, 8546-8553.

21. (a) W. Khlbrandt; D. N. Wang, Three-dimensional structure of plant light-harvesting complex determined by electron crystallography. *Nature* **1991,** *350*, 130-134;(b) G. McDermott; S. M. Prince; A. A. Freer; A. M. Hawthornthwaite-Lawless; M. Z. Papiz; R. J. Cogdell; N. W. Isaacs, Crystal structure of an integral membrane light-harvesting complex from photosynthetic bacteria. *Nature* **1995,** *374*, 517-521.

22. C.-H. Huang; N. D. McClenaghan; A. Kuhn; J. W. Hofstraat; D. M. Bassani, Enhanced Photovoltaic Response in Hydrogen-Bonded All-Organic Devices. *Org. Lett.* **2005,** *7*, 3409-3412.

23. E. M. Pérez; L. Sánchez; G. Fernández; N. Martín, exTTF as a Building Block for Fullerene Receptors. Unexpected Solvent-Dependent Positive Homotropic Cooperativity. *J. Am. Chem. Soc.* **2006,** *128*, 7172-7173.

24. E. M. Pérez; M. Sierra; L. Sánchez; M. R. Torres; R. Viruela; P. M. Viruela; E. Ortí; N. Martín, Concave Tetrathiafulvalene-Type Donors as Supramolecular Partners for Fullerenes. *Angew. Chem. Int. Ed.* **2007,** *46*, 1847-1851.